Lecture Notes in Engineering

Edited by C. A. Brebbia and S. A. Orszag

33

P. Thoft-Christensen (Editor)

Reliability and Optimization of Structural Systems

Proceedings of the First IFIP WG 7.5 Working Conference
Aalborg, Denmark, May 6-8, 1987

Springer-Verlag

Lecture Notes in Engineering

Edited by C. A. Brebbia and S. A. Orszag

33

P. Thoft-Christensen (Editor)

Reliability and Optimization of Structural Systems

Proceedings of the First IFIP WG 7.5 Working Conference
Aalborg, Denmark, May 6-8, 1987

Springer-Verlag
Berlin Heidelberg New York
London Paris Tokyo

Editor
P. Thoft-Christensen
Institute of Building Technology
and Structural Engineering
The University of Aalborg
Sohngardsholmvej 57
DK-9000 Aalborg
Denmark

ISBN-13:978-3-540-18570-3 e-ISBN-13:978-3-642-83279-6
DOI: 10.1007/978-3-642-83279-6

Library of Congress Cataloging-in-Publication Data
IFIP WG 7.5 Working Conference (1st : 1987 : Aalborg, Denmark)
Reliability and optimization of structural systems :
proceedings of the First IFIP WG 7.5 Working Conference,
Aalborg, Denmark, May 6-8, 1987 / P. Thoft-Christensen, editor.
p. cm. – (Lecture notes in engineering ; 33)
Includes indexes.
ISBN-13:978-3-540-18570-3 (U.S.)
1. Structural design – Mathematical models – Congresses.
2. Mathematical optimization – Congresses.
3. Reliability (Engineering) – Congresses.
I. Thoft-Christensen, Palle,
II. Title.
III. Series.
TA658.2.I38 1987 624.1'771 – dc 19 87-28646

2161/3020-543210

PREFACE

The Proceedings contain 28 papers presented at the 1st Working Conference on »Reliability and Optimization of Structural Systems», Aalborg, Denmark, May 6 - 8, 1987. The Working Conference was organized by the IFIP Working Group 7.5. The Proceedings also include 4 papers which were submitted, but for various reasons not presented at the Working Conference. The Working Conference was attended by 50 participants from 18 countries.

The Conference was the first scientific meeting of the new IFIP Working Group 7.5 on »Reliability and Optimization of Structural Systems». The purpose of the Working Group 7.5 is

- to promote modern structural system optimization and reliability theory,
- to advance international cooperation in the field of structural system optimization and reliability theory,
- to stimulate research, development and application of structural system optimization and reliability theory,
- to further the dissemination and exchange of information on reliability and optimization of structural system optimization and reliability theory,
- to encourage education in structural system optimization and reliability theory.

At present the members of the Working Group are:

A. H. S. Ang, USA
G. Augusti, Italy
M. J. Baker, United Kingdom
P. Bjerager, Denmark
A. Der Kiureghian, USA
O. Ditlevsen, Denmark
M. R. Gorman, USA
M. Grimmelt, Germany F. R.
N. C. Lind, Canada
H. O. Madsen, Norway
F. Moses, USA
Y. Murotsu, Japan
R. Rackwitz, Germany F. R.
P. Thoft-Christensen, Denmark (Chairman)

Members of the organizing committee are:

M. J. Baker, United Kingdom
H. O. Madsen, Norway
Y. Murotsu, Japan
R. Rackwitz, Germany F. R.
P. Thoft-Christensen, Denmark (Conference Director)

The Conference was financially supported by

IFIP
DANFIP
The University of Aalborg.

I would like to thank the organizing committee members for their valuable help in organizing the Working Conference, and all the authors for preparing papers for the Proceedings. Special thanks to Mrs. Kirsten Aakjær, University of Aalborg, for her efficient work as Conference Secretary before, during and after the institute.

August 1987

P. Thoft-Christensen

CONTENTS

* Not presented at the Conference.

* Not presented at the Conference.

ON THE APPLICATION OF A NONLINEAR FINITE ELEMENT FORMULATION IN STRUCTURAL SYSTEMS RELIABILITY

J. Amdahl & B. Leira
SINTEF, Division of Structural Engineering, Trondheim, Norway
and
Yu-Lin Wu
Division of Marine Structures
The Norwegian Institute of Technology, Trondheim, Norway

ABSTRACT

An attempt is made to combine methods for advanced progressive collapse analysis with a probabilistic formulation of load and resistance variables. A brief description is first given of a nonlinear computer program intended for progressive collapse analysis of space frame structures. The basic idea behind the program is to use only one finite element per physical element in the structure.

Plastic interaction functions for stress resultants serve as local failure functions of the system. The basic variables are the external load parameters and the yield stresses of the members. A dominant failure path is found by load incrementation, where the direction in the load space is governed by the current smallest distance to the failure surface. The associated failure probability and bounds for system reliability are found by means of first order reliability methods. The use of the method is illustrated in numerical examples.

1 INTRODUCTION

Design of a structure according to a specific code commonly involves checking of individual structural members. However, most structures are redundant in the sense that collapse of the first single element merely causes the load to be redistributed. The system structural reliability may then be far different from individual member reliability. Efficient and accurate methods for evaluation of the system reliability will then be needed to form the basis for development of more rational codes.

System structural reliability has been subject to considerable research effort during the last decade. Two mainstreams of analysis can be idenfified. The failure mode approach is based on ways in which the structure can fail, whereas the stable configuration approach is based on ways the structure can survive.

The probabilistic analysis corresponding to the former involves computation of the probability content of a union of intersections between sets. The latter approach leads correspondingly to the intersection of unions, see e.g. Refs. [1, 2, 3, 4].

Estimation of system reliability on the basis of system failure modes has been considered by several authors. Simple but most useful bounds were derived by Cornell, [5], applying the failure probabilities of each mode separately. As these bounds frequently are too wide, closer bounds obtained by taking correlation between failure modes into account were introduced e.g. by Ditlevsen, [6], Ang and Ma, [7], Stevenson and Moses, [8],and Vanmarkcke, [9]. The bounds presented in [6] have been extensively applied in the literature. Madsen, [10], discusses first vs. second order reliability analysis of series structural systems based on these bounds.

Prior to evaluation of system failure probability, identification of the failure modes must be performed. Commonly, the most dominant modes in a stochastic sense are sought, as the total number of modes can be very large. An incremental method for this purpose was presented by Moses et. al, [11, 12, 13, 14]. A method based on a secant stiffness formulation, also including a probabilistic algorithm, was introduced by Murotsu et. al. [15, 16, 17, 18, 19, 20]. Application of this method to reliability analysis of offshore structures has been conducted by Crohas et. al., [21, 22]. Guenard, [23], also studied offshore structures by a similar method.

An alternative strategy for performing the branch and bound operations as described by Murotsu has been adopted by Thoft-Christensen et. al., [24]. This so-called β-unzipping method has been applied by Baadshaug et. al., [25], for evaluation of reliability of jacket platform structures.

Ang and Ma, [26], proposed a different method for determination of the most probable failure modes by using mathematical programming based on the basic failure modes of the structure. Klingmüller, [27], applied a procedure based on the principle of virtual work and mathematical programming algorithms.

It seems that realistic models for structural behaviour is difficult to incorporate in the search procedcures for identification of dominant failure modes. One possible solution would be a Monte Carlo type of approach, see e.g. [28, 29]. However, this will lead to numerous structural analyses, which constitute the most expensive part of the reliability determination. Alternative methods have been developed by Kam et. al., [30], for nonlinear structures with deterministic

strength. Similar simplified analyses based on mean values of random structural strength parameters are described by Lin el. al., [31]. Methods based on extension of Moses' method have been proposed by Melchers and Tang, [32, 33]. Recently, a consistent formulation has been outlined by Gollwitzer and Rackwitz, [34], also including instabilities.

Brittle structural behaviour has been included by several of the authors referred to above, see e.g. Refs. [14, 16, 24, 26]. Consideration of this topic has also been given by Giannini et.al., [35], Bjerager, [36].

Although there has been significant achievements with respect to techniques for reliability assessment as such, the representation of structural behaviour is still very simple and idealized. To enhance the acceptance of reliability analysis there is a strong need for applying structural behaviour models with which the designers are familiar.

In this paper, a method for identification of the most significant failure modes for nonlinear structures is outlined, based on a statistical representation of both external load and random strength. Instability failure is represented in a uniform way by progressive inclusion of internal hinges in the structural finite element model. The basis of the method is an incremental formulation of the equilibrium equations.

2 NONLINEAR STRUCTURAL ANALYSIS FORMULATION FOR SPACE FRAMES

For a thorough description of the computer program USFOS it is referred to [37, 38]. In the following only the basic concepts are reviewed.

The main idea behind USFOS is to represent each physical element by one finite element as shown in Figure 1. This facilitates that input models from conventional linear analysis can be used with minor modifications.

The basic finite element is the spatial beam element with 12 degrees of freedom. As stress and strain measures the stress resultants and the corresponding displacements are used.

The coupling between axial and lateral displacements is automatically taken care of by including large deflection effects in the strain expression on local element level (von Karman theory).

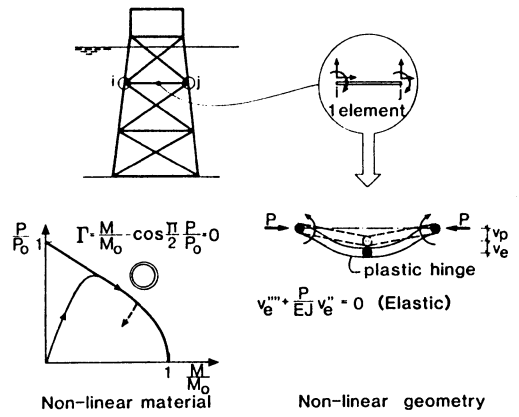

Figure 1. USFOS - basic concepts

In the elastic range equilibrium equations and incremental equations can be derived from the first and second variation of the potential energy. An important feature with the method is the choice of interpolation functions. These satisfy exactly the differential equation for a beam under axial force and lateral bending and yield trigonometric functions for compression and exponential (hyberbolic) functions for tension. This facilitates closed form solutions for all integrations in the equilibrium and incremental equations.

The modelling of plasticity uses stress resultants as basic parameters. The capacity of a cross-section is expressed by an interaction equation

$$\Gamma\ (\sigma_y,\ S_i) = 0 \qquad i = 1 \ldots 6 \qquad (1)$$

where σ_y = yield stress, S_i, denotes a stress resultant. If a cross-section reaches the plastic state defined by Eq. (1) a hinge is introduced. Elastic and plastic displacements are separated. The plastic deformations are concentrated to the plastic hinges whereas the beam remains elastic between hinges. The next step is to introduce the normality criterion for the incremental plastic displacements and the consistency criterion for the incremental stress resultants.

The latter criterion states that the stress state lies on the interaction sur-

face during plastic deformation. From this, the elastoplastic stiffness matrix for a beam element with local large deflection effects is obtained.

Plastic hinges can be introduced at beam ends or at midspan. In case of a plastic hinge at midspan, the element is divided into two subelements for which the elasto-plastic stiffness matrices are calculated separately. Subsequently, the midnode is eliminated by static condensation and the original element is again the basic element.

The solution technique is based upon incremental loading with updating of the local element coordinate system and incremental stiffness matrix at each step, (updated Lagrangian technique). Equilibrium iterations may optionally be performed, but experience so far shows that acceptable accuracy is obtained with pure incrementation in most cases.

The increment size is scaled automatically when plastification occurs so that the failure surface at the new hinge is not exceeded.

The concept of plastic interaction formulas is very attractive. New cross-sectional types are easily made available by implementing the appropriate interaction formulaes. At present the program offers tubular, circular, rectangular and I-profiles. Concrete sections are also being implemented.

Thin-walled members are often not able to attain their theoretical plastic capacity or only maintain this for a limited amount of plastic deformation. This loss of strength may for instance be induced by wall shear buckling of deep girders or local wall buckling on the compression side of tubes. The present formulation allows these important effects to be taken into account in an approximate manner by modification of the plastic interaction formulaes. Similarly, damages as dents in tubulars have been modelled by reducing the plastic interaction formulaes [39].

Numerical studies have shown that the program is able to predict with acceptable accuracy the large displacement behaviour of simple beam-columns as well as beams with membrane action with only one model element [38]. The program has also been compared successfully with alternative nonlinear finite element programs and experiments with planar and spatial frames [40].

3 FAILURE MODE IDENTIFICATION

The yield hinge concept used in USFOS is convenient also in the context of structural reliability. It is natural to define the event "failure" as the occurence of a yield hinge. In this way "buckling" of a member is no longer a failure event as such, but is the result of the formation of a sufficient number of yield hinges. This formulation is very attractive because the post-collapse behaviour for a given element is fully determined by the yield stress. The stress resultants are namely forced to follow the yield surface. As far as the yield stress is constant the "brittleness" problem, i.e. unloading of buckling members, is circumvented. Unfortunately, this condition is generally not met because in the more advanced calculations the variability of the yield stresses will be considered as well.

In the subsequent derivation it is assumed that the yield stresses and the external load parameters constitute the set of basic random variables.

Taking the occurrence of a yield hinge as the failure criterion, the associated failure surface is given by Eq. (1). However, whereas the yield stress of a cross-section is a basic random variable the stress resultants are dependent on the external load parameters. Thus, the failure function given by Eq. (1) should rather be formulated as

$$\Gamma(\sigma_y, R_i) = 0 \qquad i = 1 \ldots n \tag{2}$$

where R_i = independent external load parameter. Contrary to Eq. (1) no closed form solution of Eq. (2) exists for general nonlinear problems. However, incremental relationships are available. They may be used to establish an approximate failure function.

Assume that the external loads have been incremented up to a value R_l^*, corresponding to a stress resultant state S_i^*. Linearizing abuot this point there is obtained

$$S_i = S_i^* + \Delta S_i = S_i^* + \frac{\delta S_i}{\delta v_j} \frac{\partial v_j}{\partial r_k} \frac{\partial r_k}{\delta R_l} \Delta R_l = S_i^* + b_{il}(R_l - R_l^*) \tag{3}$$

where v_j, r_k denote local and global degree of freedom, respectively. Einstein's summation convention is adopted. b_{il} represents the increment in stress resultant S_i due to an increment of external load R_l, and is given by

$$b_{il} = k_{ij}\ t_{jk}\ F_{kl} \tag{4}$$

where k_{ij} = tangential element stiffness, t_{jk} = current transformation between local and global degree of freedom, F_{kl} = elements of the inverted system stiffness matrix. Introducing the reduced variates

$$R_l' = \frac{R_l - \bar{R}_l}{\sigma_{R_l}} \tag{5}$$

where $\bar{R}_l$, σ_{R_l} = mean value and standard deviation of R_l, Eq. (3) can also be formulated as

$$S_i = \bar{S}_i + \sigma_{R_l} b_{il} R_l' \tag{6}$$

where the current mean value, $\bar{S}_i$, is defined as

$$\bar{S}_i = S_i^* + b_{il}(\bar{R}_l - R_l^*) \tag{7}$$

Eq. (7) may be substituted into Eq. (1), which now becomes

$$\Gamma(\sigma_y + \sigma_{\sigma_y} \cdot \sigma_y',\ \bar{S}_i + \sigma_{R_l} b_{il} R_l') = 0 \qquad i=1 \ldots. 6, \quad l=1 \ldots. n \tag{8}$$

where σ_{σ_y} is the standard deviation and σ_y' is the reduced variate of the yield stress.

For convenience, it is here assumed that all variables are uncorrelated and normally distributed. Otherwise this should be accomplished by means of the Rosenblatt-tranformation.

In this way an analytical approximation of the failure function in terms of the true random variables has been established. Eq. (8) may be used to find the most probable failure point by the algorithm proposed by Rackwitz /41/. The failure point is exact provided that the linearization of the load effect is carried out on the failure point. (Possible deviation from the true load-load effect path during pure incrementation is disregarded in this context.)

The incrementation is carried out in the load parameter space. A fundamental assumption is related to the incremental direction. This is selected so as to coincide with the current smallest distance to the failure surface for all

potential yield hinge locations. This gives the following direction cosines

$$\alpha_{R_l}^{*} = \frac{\left(\frac{\partial \Gamma}{\partial R_l'}\right)^{*}}{\left(\left(\frac{\partial \Gamma}{\partial \sigma_y'}\right)^2 + \frac{\partial \Gamma}{\partial R_i'}\frac{\partial \Gamma}{\partial R_i'}\right)^{1/2}_{*}} \qquad l=1 \ldots n \qquad (9)$$

where the derivatives are evaluated at the failure point (σ_y^*, R_l^*).

Due to the nonlinearities the direction varies during load incrementation. Hence, the loading up to the first failure point is carried out in several steps.

After failure a yield hinge is introduced with yield stress equal to the failure point value. The effect of yield stress pertubations can still be taken into account in the subsequent calculations. At a hinge, the increments in yield stress and stress resultants must obey the consistency criterion

$$\Delta\Gamma = \frac{\partial \Gamma}{\partial \sigma_y}\Delta\sigma_y + \frac{\partial \Gamma}{\partial S_i}\Delta S_i = 0 \qquad (10)$$

Introducing the element stiffness equations and the normality criterion for the plastic displacement, the following relationship is obtained

$$\Delta S_i + \Delta S_i^{eq} = k_{ij}\Delta v_j \qquad (11)$$

where the (elasto-plastic) incremental stiffness reads

$$k_{ij} = \left(k_{ij}^{e} - k_{ik}^{e}\frac{\partial \Gamma}{\partial S_k}\frac{\delta \Gamma}{\delta S_l}k_{lj}^{e} \Big/ \frac{\delta \Gamma}{\partial S_m}k_{mn}\frac{\partial \Gamma}{\partial S_n}\right)\Delta v_j \qquad (12)$$

k_{ij}^{e} = elastic incremental stiffness. Thus, it comes out that an increment of the yield stress gives equivalent nodal forces

$$\Delta S_i^{eq} = \left(k_{ij}^{e}\frac{\partial \Gamma}{\partial S_j}\frac{\partial \Gamma}{\partial \sigma_y} \Big/ \frac{\partial \Gamma}{\partial S_m}k_{mn}\frac{\partial \Gamma}{\partial S_n}\right)\Delta\sigma_y \qquad (13)$$

This yields in turn equivalent nodal loads

$$\Delta R_m^{eq} = t_{im}\Delta S_i^{eq} = e_m\Delta\sigma_y \qquad m = 1 \ldots 6 \qquad (14)$$

The procedure is analogous to the approach adopted by Murotsu et al. /15-20/, but is now formulated for incremental loading.

With (p-1) failed hinges the failure function of the p'th hinge can be written as

$$\Gamma(\sigma_{yp} + \sigma_{\sigma_{yp}} \sigma'_{yp},\ \bar{S}_i + \sigma_{\sigma_{yr}}\ b_{im}\ e_{mr}\sigma'_{yr} + \sigma_{R_l} b_{il} R'_l) = 0 \tag{15}$$

where

$$\bar{S}_i = \bar{S}_i^* + b_{im}e_{mr}(\bar{\sigma}_{yr}-\sigma_{yr}^*) + b_{il}(\bar{R}_l-R_l^*) \tag{16}$$

$$r = 1 \ldots p-1,\ l = 1 \ldots n$$

Thus, a failure mode is identified by incrementation of the external loads. At each step the shortest distance to the failure surface of all potential yield hinges is identified in the space of uncorrellated and normalized variables. If the yield hinges are some distance apart in the load space the step is scaled and the incrementation direction is recalculated along with updating of yield stresses of existing hinges. This process is continued until global collapse is detected, whereby the most probable failure mode is determined. Other failure modes can be identified by means of some branching algorithm.

4 EVALUATION OF SYSTEMS RELIABILITY

For each of the failure modes identified by the algorithm outlined in Section 3, a final failure function of the type specified by equation (15) is produced. However, the sequence of hinges formed during the analysis must also be considered. Denoting by Γ_k^i the failure function obtained for mode i after formation of the k'th hinge, the system probability of failure can be approximated by

$$P_f \approx P\{ \bigcup_{i=1,\ 2 \ldots 1} \ \bigcap_{k=1,\ 2 \ldots m(i)} (\Gamma_k^i \leq 0)\} \tag{17}$$

The intersection is taken over all the m(i) events of hinges forming for mode number i, and the union is over the total number, 1, of failure modes.

Typically, Equation (17) will yield a lower bound on the system probability of failure, due to some failure modes being left out. If the linearization points for structural load/load-effect relations needed for computation of each Γ_k^i are located too far away from the failure points, however, this property could be invalidated in some cases.

Evaluation of the probability of intersection events of the type

$$P\{\bigcap_{k=1,\,2,\,\ldots.\,m(i)} \{\Gamma_k^i \leq 0\}\} \tag{18}$$

can be accomplished e.g. by linearizing each failure function at the respective design points in normalized space, see Hohenbichler and Rackwitz [42]. (Note that this linearization is not the same as linearization of the structural stiffness properties that was discussed above.) An equivalent event with a linear boundary and the same probability of occurrence as (18) can then be obtained, also possessing the same sensitivity with respect to the independent standard normal variables.

Computation of the probability of the union event in (17) is thus greatly facilitated. For most purposes, the Ditlevsen bounds, [6], can be employed. These require simply evaluation of the probability of pairwise intersections of the equivalent events in in addition to those in (18).

Alternatively, the intersection probabilities can be computed by second order methods or more advanced first-order methods based on joint linearization points, see e.g. Karamchandani, [43], for a review.

An upper bound for the system probability of failure can be obtained e.g. by truncating each failure sequence after a specific small number of hinges has formed. The applicability of this bound, however, depends on the specific structure being studied.

5 ILLUSTRATIVE EXAMPLES

Example 1

The effect of linearization of stiffness properties on estimation of the design point is considered first. Assume that the plastic interaction between axial force N and bending moment M for a cross-section is given by the function

$$\Gamma = N^2 + M + C - 1 = 0 \tag{19}$$

where C is a capacity factor.

The stress resultants are related to the external load R by

$$N = R \tag{20}$$

$$M = R^2 \tag{21}$$

The basic random variables R and C are uncorrelated and standard normally distributed.

For this simple example the analytic failure function is found from Eqs. (19-21)

$$\Gamma = 2R^2 + C - 1 = 0 \tag{22}$$

The corresponding failure point is R = 0.612 and C = 0.25.

Applying the incremental approach and linearizing about N*, M*, R* there is obtained

$$N = R \tag{23}$$

$$M = 2R^* R - (R^*)^2 \tag{24}$$

By substitution of Eqs. (23-24) into Eq. (19) there follows

$$\Gamma = R^2 + 2R^* R - (R^*)^2 + C - 1 \tag{25}$$

The most probable failure point depends now on the linearization point R*. This is shown in Table 1.

Table 1 Failure point vs. linearization point

Linearization point R*	Safety index β	Failure point R	C
0	0.866	0.707	0.500
0.3	0.704	0.618	0.336
0.612	0.662	0.612	0.25

Thus, the failure function based on the linearized expression gives the exact result provided that the linearization is performed on the true failure surface. In practice, the linearization is to be performed at some distance. However, by applying relatively small load increments in the neighbourhood of the failure point quite accurate results are obtained.

Example 2

Consider the portal frame shown in Figure 2. It possesses the same key parameters as the structure studied by Gollwitzer and Rackwitz in Ref. /34/, but the actual dimensions are not known and have to be assumed. Plastic hinges can occur at nodes 2, 3 and 4. The basic random variables are two independent, normally distributed load parameters P_1 and P_2.

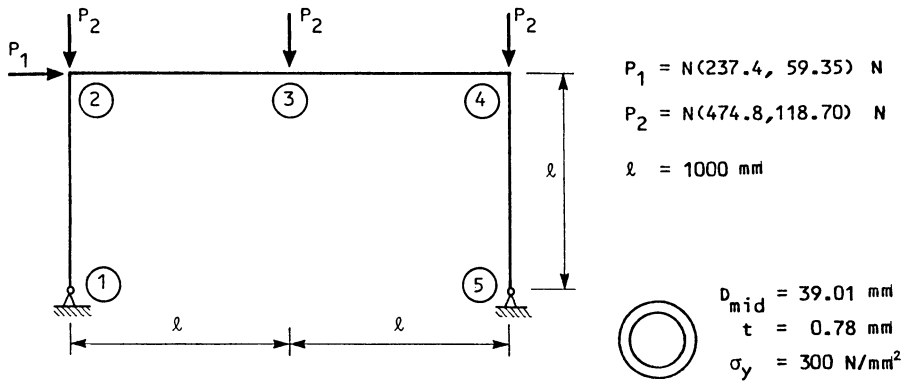

Figure 2 Portal frame

Reliability indeces for all the limit states corresponding to a failure mode approach are listed in Table 2. The limit states, which are categorized into initial failure limit states and collapse limit states, are plotted in the load parameter space in Figure 3 and Figure 4.

Because the loads are incremented up to the most likely failure point on the limit state surface, the formation of plastic hinges has to be controlled. For example, from Figure 3 it is observed that the most likely failure point associated with failure of node 3 lies in the failure domain governed by initial failure of node 4. Hence, the formation of a hinge at node 4 has to be suppressed in this case.

In Table 3 the incrementation procedure for failure sequence 3-4 is listed. It appears that the linearization point approaches the most likely failure point, which shows that the process converges.

The possibility of multiple, local, most likely failure points corresponding to different quadrants of the failure surface is also considered. However, the calculations indicate that only one of the associated β-indeces is small enough

to be taken into account.

It is noted that the improvement due to second order assessment of component reliability based on Equation 8 or Equation 15 is insignificant in the present example.

The system reliability is calculated on the basis of the following model of a series system of parallel subsystems.

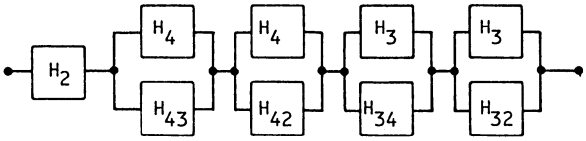

The limit state H_2 represents an incomplete failure path, but it is anyway of little significance.

By a first order analysis the system probability of failure is assessed to $P_f = 0.79 \cdot 10^{-4}$. This is fairly close to the value predicted by Gollwitzer and Rackwitz, namely $P_f = 0.7 \cdot 10^{-4}$. The largest contribution comes from failure sequence 3-4.

TABLE 2 Reliability indeces

Failure sequence	Hyperplane no.	Safety index β	Failure point P_1	Failure point P_2
4	H_4	2.86	366	697
3	H_3	5.42	241	1118
2	H_2	8.88	737	138
4,3	H_{43}	3.78	359	852
4,2	H_{42}	4.30	416	840
3,4	H_{34}	4.43	361	938
3,2	H_{32}	8.60	-41	1332

TABLE 3 Load history corresponding to failure sequence 4,3

Increment No.	Linearization point P_1	P_2	Safety index β	Failure point P_1^*	P_2^*
	0	0	3.98	426	760
1	250	446	3.02	376	702
2	350	650	2.87	366	696
3	366	696	2.86	366	697
	366	696	3.97	371	863
4	369	796	3.81	362	853
5	362	853	3.78	359	852

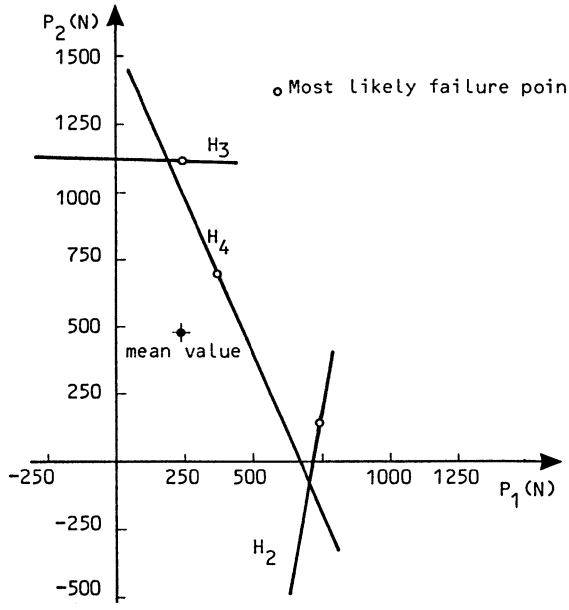

Figure 3 Limit states of initial failure in load space

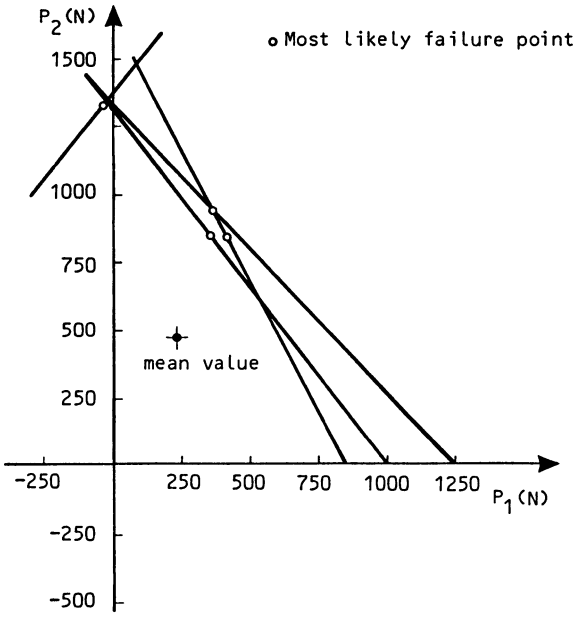

Figure 4 Limit states of collapse in load space

6 CONCLUSIONS

A new method for identification of stochastically dominant failure modes of space frame structures has been described. It is based upon an efficient nonlinear finite element formulation where the material nonlinearity is modelled by means of yield hinges. The yield stresses and external load parameters are considered to be the basic random variables. The direction of load increments in the load space is determined on the basis of the shortest distance to the failure surface for all potential yield hinges.

The attractiveness of the method is that it combines acknowledged reliability formats with an advanced physical representation of the structural behaviour in the large defelction range. The concept of cross-sectional interaction functions, which are used as failure functions, are well known for those working with conventional design methods.

6 REFERENCES

1 Augusti, G. and Baratta, A.: Limit Analysis of Structures with Stochastic Strength Variations, Journ. Structural Mechanics, Vol. 1, No. 1, 1972, pp. 43-62.

2 Bjerager, P. and Gravesen, S.: Lower Bound Reliability Analysis of Plastic Structures. In: Probabilistic Methods in the Mechanics of Solids and Structures, ed. Eggwertz and Lind, Springer Verlag, Berlin, 1984.

3 Ditlevsen, O. and Bjerager, P.: Reliability of Highly Redundant Plastic Structures, Journ. Eng. Mech. Div., ASCE, Vol 110, No. 5, 1984, pp. 671-693.

4 Bennett, R.M. and Ang, A.H. - S.: Formulations of Structural System Reliability, Journ. Eng. Mech. Div., Vol 112, No. 11, November 1986, pp. 1135-1151.

5 Cornell, C.A.: Bounds on the Reliability of Structural Systems, Journal of the Struct. Div., Proc. of the ASCE, 91, ST-1, 1967, pp. 171-200.

6 Ditlevsen, O.: Narrow Reliability Bounds for Structural Systems, Journal of Structural Mechanics, 7, 1979, pp. 435-451.

7 Ang, A.H.-S. and Ma, H.F.: On the Reliability Analysis of Framed Structures, Proc. of ASCE Speciality Conf. of Probabilistic Mechanics and Structural Reliability, Tucson, 1979, pp. 109-11.

8 Stevenson, J.D, and Moses, F.: Reliability Analysis of Frame Structures, Journal of the Struct. Div., ASCE, 96, ST-11, 1972, pp. 2409-2427.

9 Vanmarcke, E.H.: Matrix Formulation of Reliability Analysis and Reliability - Based Design, Computers and Structures, 3, 1973, pp. 757-770.

10 Madsen, H. O.: First Order vs. Second Order Reliability Analysis of Series Structures, Structural Safety, 2 (1985), pp. 207-214.

11 Moses, F.: Reliability of Structural Systems, Proc. ASCE, Vol 100, ST9, Sept. 1974.

12 Moses, F.: System Reliability Developments in Structural Engineering, Structural Safety, 1, 1982.

13 Moses, F. and Stahl, B.: Reliability Analysis Format for Offshore Structures, Paper OTC 3046, Proc. Offshore Technology Conf., Houston, May, 1978.

14 Moses, F. and Rashedi, M.R.: The Application of System Reliability to Structural Safety, Proc. Fourth ICASP Conf., Florence, 1983.

15 Murotsu, Y., Okada, H., Yonezawa, M. and Taguchi, K.: Reliability Assessment of Redundant Structure, in Moan, T. and Shinozuka, M. (Eds.): Structural Safety and Reliability, Elsevier, 1981, pp. 315-329.

16 Murotsu, Y.: Reliability Analysis of Frame Structure through Automatic Generation of Failure Modes, in Thoft-Christensen, P. (Ed.): Reliability Theory and its Application in Structural and Soil Mechanics, Martinus Nijhof, 1982, pp. 525-540.

17 Murotsu, Y., Okada, H., Yonezawa, M. and Kishi, M.: Identification of Stochastically Dominant Failure Modes in Frame Structure, Proc. 4th ICASP Conf., Florence, 1983.

18 Murotsu, Y., Okada, H., Yonezawa, M., Grimmelt, M. and Taguchi, K.: Automatic Generation of Stochastically Dominant Modes of Structural Failure in Frame Structure, Structural Safety, 2, 1984.

19 Murotsu, Y., Okada, H., Matsuzaki, S.: Reliability Analysis of Frame Structure under Combined Load Effects, in Konishi, I., Ang, A.H-S. and Shinozuka, M. (Eds.): Structural Safety and Reliability, IASSAR, 1985.

20 Murotsu, Y., Okada, H., Matzuzaki, S. and Katsura, S.: Reliability Assessment of Marine Structures, Proc. 5th OMAE Conf., Tokyo, 1986.

21 Crohas, H., Tai, A., Hachemi-Safai, V. and Barnouin, B.: Reliability of Offshore Structures under Extreme Environmental Loading, OTC Conf. Paper 4826, Houston, 1984.

22 Crohas, H., Tai, A., Hachemi-Safai, V. and Barnouin, B.: Dominant Collapse Modes of Jacket Platforms Under the Design Extreme Loading.

23 Guenard, Y. F.: Application of System Reliability Analysis to Offshore Structures, Report No. 71, The John A. Blume Earthquake Engineering Center, Department of Civil Engineering, Stanford University, November, 1984.

24 Thoft - Christensen, P. and Murotsu, Y.: Application of Structural Systems Reliability Theory, Springer-Verlag, Berlin, Heidelberg, 1986.

25 Baadshaug, O. and Bach-Garsmo, O.: System Reliability Analysis of a Jacket Structure. In: Structural Safety and Reliability, ed. Konishi, I., Ang, A.H.-S. and Shinozuka, M., IASSAR, 1985.

26 Ang, A.H.-S. and Ma, H.F.: On the Reliability of Structural Systems, in Structural Safety and Reliability, ed. Moan, T. and Shinozuka, M., Elsevier, 1981.

27 Klingmüller, O.: Redundancy of Structures and Probability of Failure, in Structural Safety and Reliability, ed. Moan, T. and Shinozuka, M., Elsevier, 1981.

28 Angusti, G., Baratta, A. and Casciati, F.: Probabilistic Methods in Structural Engineering, Chapman and Hall, 1984.

29 Edwards, G.E., Heidweiller, A., Kerstens, J. and Vrouwenvelder, A.: Methodologies for Limit State Reliability Analysis of Offshore Jacket Platforms, in: Behaviour of Offshore Structures, ed. Battjes, J.A., Proceedings of the 4th Boss Conference, Delft, Netherlands, 1985.

30 Kam, T.Y., Corotis, R.B. and Rossow, E.C.: Reliability of Nonlinear Framed Structures, Journal of Structural Engineering, Vol. 109, No 7, July, 1983.

31 Lin, T.S. and Corotis, R.B.: Reliability of Ductile Systems with Random Strengths, Journal of Structural Engineering, Vol. 111, No. 6, June, 1985.

32 Melchers, R.E. and Tang, I.K.: Failure Modes in Complex Stochastic Systems, in Structural Safety and Reliability, ed. Konishi, I., Ang, A.H.-S. and Shinozuka, M., IASSAR, 1985.

33 Melchers, R.E. and Tang, L. K..: Dominant Failure Modes in Stochastic Structural Systems, Structural Safety,

34 Gollwitzer, S. and Rackwitz, R.: First-order System Reliability of Structural Systems, in Konishi, I., Ang, A.H.-S. and Shinozuka, M. (eds): Structural Safety and Reliability, IASSAR, 1985.

35 Giannini, R., Giuffre, A. and Pinto, P.E.: Reliability of Systems with Brittle Elements, Proc. Fourth ICASP Conf., Florence, 1983.

36 Bjerager, P.: Reliability Analysis of Brittle Structural Systems, in: Structural Safety and Reliability, ed. Konishi, I., Ang, A.H.-S. and Shinozuka, M., IASSAR, 1985.

37 Søreide, T.H. and Amdahl, J.: USFOS - A Computer Program for Ultimate Strength Analysis of Framed Offshore Structures.

38 Søreide, T.H., Amdahl, J., Granli, T. and Astrup, O.C.: Collapse Analysis of Framed Offshore Structures, OTC 5302, 1986.

39 Taby, J.: Residual Strength of Damaged Tubulars. Final Report. SINTEF Report STF71 A86068, Trondheim 1986.

40 Søreide, T.H., Amdahl, J. and Rembar, H.: The Idealized Structural Unit Method of Space Tubular Frames. Int. Conf. on Steel and Aluminum Structures, Cardiff, 1987.

41 Rackwitz, R.: Practical Probabilistic Approach to Design, Bulletin 112, Comité European du Beten, Paris, France, 1976.

42 Hohenbichler, M. and Rackwitz, R.: First Order Concepts in System Reliability, Structural Safety, 1, 1983.

43 Karamchandani, A.: Structural System Reliability Analysis Methods, Department of Civil Engineering, Stanford University, February, 1987.

FATIGUE LIFE ESTIMATION UNDER RANDOM OVERLOADS

R. Arone
Israel Institute of Metals, Technion
R&D Foundation, Technion City, Haifa 32000, Israel

ABSTRACT

A stochastic approach to fatigue crack growth under random overload sequences, superimposed on a base-line cyclic load is described. The approach consists in presentation of the delay time due to retardation effect associated with the overload peaks as a purely discontinuous Markov process. A numerical procedure based on the Kolmogarav-Feller integrodifferential equation is used to determine the probability of failure. Proposed model accounts for fracture occurrence either under an overload or under the base-line cyclic load.

1. INTRODUCTION

One of the main difficulties in evaluating fatigue crack growth in metallic structural components under random loading is associated with the interaction effects leading to retardation, acceleration and interrupted retardation phenomenon [1-14]. For instance, sharp overload peaks cause strong retardation effect which could significantly influence the fatigue life of the component [1,4-7]. While such overloads are generally rare, their influence is quite significant. In recent period several probabilistic models has been proposed for description of the fatigue crack behaviour under random sequences of overload peaks [15-18]. Presentation of the loading process as a superposition of a base-line constant-amplitude cyclic load and random sequences of overload peaks permitted relatively simple stochastic description of the fatigue crack behaviour [17,18]. In what follows further development of the model described in [17,18] is given.

2. MODEL

As in the earlier works [17,18] a superposition of random overload sequences on a base-line constant-amplitude cyclic load is considered

(Fig. 1a), overload peaks being generally random in time and magnitude.

It is assumed that each individual overload contributes little to crack length but delays crack growth; the higher the overload stress, the longer the delay. The individual delay interval Δt_d associated with the given overload is determined as the difference of the times t_a required for the crack to traverse the zone affected by the overload, and t_ℓ required for it to traverse the same distance in the absence of an overload ($\Delta t_d = t_a - t_\ell$, see Fig. 1b).

The individual delay interval is a function of the overload stress σ_o crack length ℓ, the maximum (σ_{max}) and minimum (σ_{min}) base-line stresses, material parameters and so on.

With the base-line stresses and material characteristics as parameters, the delay interval as a function of σ_o and ℓ can be given in the general form:

$$\Delta t_d = f_1(\sigma_o, \ell) \tag{1}$$

We assume that the expression for the stress intensity factor and the crack propagation law are known

$$K_1 = \sigma f_2(\ell) \tag{2a}$$

$$\frac{d\ell}{dt} = f_3(\Delta K) = f_3(\Delta\sigma f_2(\ell)) \tag{2b}$$

where K-the stress intensity factor, σ the applied stress, ℓ crack length, and ΔK and $\Delta\sigma$ - the stress intensity and stress ranges of the base-line load respectively.

Integration of equation (2b) yields the time-dependence of crack length

$$\ell = f_4(t) \tag{3}$$

Accordingly, the individual delay interval can be presented in terms of the crack growth time, namely, equation (1) can be written as

$$\Delta t_d = f_1(\sigma_o, \ell) = f_1(\sigma_o, f_4(t)) = f_5(t) \tag{4}$$

We subdivide the time interval of crack growth (0,t) into two sub-

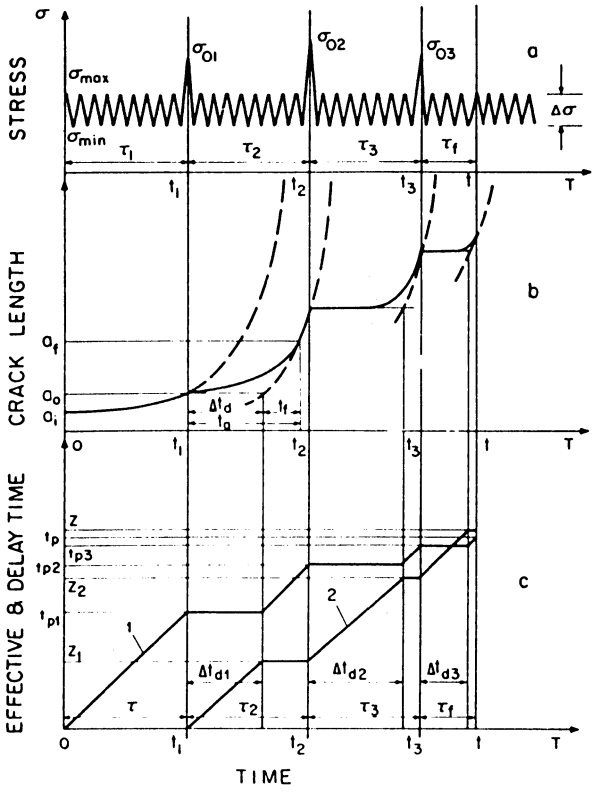

Fig. 1: Schematic representation of crack retardation process:
Overload moments designated t_1, $t_2 \ldots t_i$
Interoverload times designated $\tau_1 \tau_2 \ldots \tau_i$
Delay intervals designated $\Delta t_{d1}, \Delta t_{d2} \ldots \Delta t_{di+1}$
(τ_f - time interval between last overload and observation moment t)
(a) - Base-line constant-amplitude cyclic load with superimposed random overloads.
(b) - Time dependence of crack length. (Dashed line supposed crack growth behaviour in the absence of overloads).
(c) - Effective (curve 1) and delay (curve 2) times.

intervals: effective time t_e and total delay time t_d (see Fig. 1c).

$$t=t_e+t_d \tag{5}$$

The total delay time, being the sum of the individual delay intervals, represents that part of the total time which is "lost" in terms of crack growth; thus, effective time is that of active crack growth under the base-line load as if no overloads occur.

Combination of equations (4) and (5) yields

$$\Delta t_d=f_s(\sigma_o,t_e)=f_s(\sigma_o,(t-t_d)) \tag{6}$$

which indicates that at an arbitrary moment of observation t the individual delay interval depends on the total delay time at that moment, irrespective of the history of the process.

Considering the total delay time as a random process due to the random nature of the overload moments, material parameters and so on, and using the Markov property implied by equation (6), stochastic model representing the delay process as a purely dicontinuous Markov process was developed [17,18]. It was assumed that individual delay intervals can be considered as jumps in the delay process, for which transition probabilities are obtainable from the Kolmogorov-Feller integro-differential equations [19]:

$$\frac{\partial F(t_o,x;t,y)}{\partial t}=-qF(t_o;x;t,y)+q\int_{\Omega}P(t,z,y)d_zF(t_o,x;t,z) \tag{7a}$$

$$t_o<t \quad z\in\Omega$$

$$p=q\cdot\Delta t+0(\Delta t) \tag{7b}$$

where $F(t_o,x;t,y)$ is the transition probability, (i.e., the probability of the total delay time t_d being less than Y at moment t, provided that at moment $t_o<t$ $t_d=x$); p - the probability of overload occurrence during time interval Δt (approximately equal to the base-line cycle time), q - the overload intensity, and $P(t,z,y)$ - the conditional probability distribution function, defining the probability of t_d being less than Y subject to the overload occurring at moment t and just before the overload $t_d=Z$.

In the first version of the model [17] it was assumed, by virtue of infrequency of the overloads, that the individual delay intervals are smaller than the interoverload times. In such a case, bearing in mind equation (6)

$$P(t,Z,y)=P\{Z+f_s(\sigma_o,t-t_d)<y\} \tag{8}$$

At the starting moment $t_o=0$ and $x=0$, and the initial condition can be formulated as

$$\lim_{t\to 0} F(0,0;t,y)=F(0,Y)=E(0,Y)=\begin{cases} 0 \text{ for } Y\leq 0 \\ 1 \text{ for } Y>0 \end{cases} \tag{9}$$

where for simplicity

$$F(0,0;t,y)=F(t,y) \tag{10}$$

Equation (7a) can be solved numerically by a simple step-by-step procedure, with equation (9) stating the initial condition [17].

The first version of the model may be nonconservative at high values of the overload intensity parameter q (high frequency of occurrence) since in that case interoverload times may be comparable to or even shorter than the individual delay intervals.

The second conservative version of the model [18] preserves conservativeness of the reliability assessment even at high values of q. According to this version each individual delay interval equals Δt_d as per equation (6) only when it is less than the interoverload time τ. Otherwise, the value of t_d is truncated so as to equate the individual delay interval to τ. By this means overlapping of individual intervals is eliminated. This leads in turn to some underestimation of the total delay time and imparts conservativeness to the reliability assessment.

The dissimilarity between the two versions manifests itself in the structure of the conditional probability function P(t,z,y). Since in the second version individual delay interval $\hat{\Delta t}_d$ is identified with the smaller of two random values $(\Delta t_d, \tau)$, the function has the structure

$$P(t,z,y)=P_1+P_2-P_1P_2 \tag{11a}$$

for

$$\hat{\Delta t}_a = \min\{\Delta t_a, \tau\} \tag{11b}$$

where P_1 is determined by equation (8), and

$$P_2 = P\{\tau < y - Z\} = F_\tau(Y - Z) \tag{12}$$

$F_\tau(\cdot)$ being the probability distribution function of the inter-over load time. Thus, using P(t,Z,y) from equation (8), or for high q - equation (11a), the whole array of transitional probabilities F(t,y) can be determined by simple step-by-step procedure embodied in equations (7a) and (9).

We define reliability as the probability of nonfailure within a given time interval (0,T). Failure occurs if one of the following two events takes place during (0,T): (a) a crack growing under the base-line load reaches critical length for maximum base-line stress σ_{max}, and (b) at least one of the overloads has stress magnitude σ_o sufficient for the current crack length to become critical, thus causing unstable fracture.

According to equation (2a), the critical crack length for a given stress magnitude is obtainable from equation

$$\ell_i = f_2^{-1}\left(\frac{K_{IC}}{\sigma_i}\right) \;;\; i = 0,1 \tag{13}$$

where $f_2^{-1}(\cdot)$ is the inverse of $f_2(\cdot)$, K_{IC} - the fracture toughness of the material the index 0 refers to an overload and 1 - to the base-line load. Recalling equation (4) the critical time required for the crack to reach critical length is obtainable as follows

$$t_i = f_4^{-1}(\ell_i) \;;\; i=0,1 \tag{14}$$

Failure does not take place when the following two events coincide

$$\{\text{Sup } t_p < t_1;\ t \in (0,T)\} \tag{15a}$$

$$\{\text{for none of the overloads } t_p \geq t_o;\ t \in (0,T)\} \tag{15b}$$

As was shown previously [17,18] the probability of the first event is

$$P\{Supt_p<t_1;\ t\in(0,T)\}=P\{t-t_d<t_1\}=1-F(T,T-t_1) \tag{16}$$

Let us now consider inequality (15b). An overload causes failure when the following two events coincide: (1) an overload occurs, and (2) its random magnitude σ_o is critical for the current crack length. The probability of the first event according to equation (7b) is $q\Delta t$. Combination of equations (13) and (14) yields the following expression for critical time as function of the overload stress σ_o:

$$t_o=f_4^{-1}(f_2^{-1}(\frac{K_{IC}}{\sigma_o}))=f_6(\frac{K_{IC}}{\sigma_o}) \tag{17}$$

If the probability density function $\omega_1(\sigma_o)$ of σ_o is known its counterpart for t_o ($\omega_2(t_o)$) is obtainable with the aid of equation (17). Accordingly, the probability of σ_o being critical can be given in terms of the effective and critical times

$$P\{t_p\geq t_o\}=\int_{t_0min}^{t_0max} P\{t-t_d\geq x\,/\,t_o=x\}\omega_2(t_o)dt_o \tag{18}$$

Equation (18) can be rewritten as

$$P\{t_p\geq t_o\}=\int_{t_0min}^{t_0max} F(t,t-t_o)\omega_2(t_o)dt_o \tag{19}$$

and the probability of an overload causing fracture (or, to coin a term, of its being "damaging") can be found as the product

$$\phi(t)=(q\cdot\Delta t)\cdot\int_{t_0min}^{t_0max} F(t,t-t_o)\omega_2(t_o)dt_o \tag{20a}$$

or

$$\phi(t)=q_1(t)\cdot\Delta t \tag{20b}$$

where $q_1(t)$ is the time-dependent intensity of damaging overloads:

$$q_1(t)=q\int_{t_o\min}^{t_o\max} F(t,t-t_o)\,\omega_2(t_o)dt_o \qquad (20c)$$

Thus, for Poisson flow of overloads, the probability of nonoccurrence of a damaging overload during the time interval (0,T) is

$$P_d=\exp\left(-\int_0^T q_1(t)dt\right) \qquad (21)$$

Reverting now to equations (15a,b) and bearing in mind equations (16) and (21) the probability of nonfailure during the time interval (0,T), or in other words the reliability can be formulated as follows

$$R=(1-F(T,T-t_1))\cdot\exp\left(-\int_0^T q_1(t)dt\right) \qquad (22a)$$

and if the overloads do not cause retardation,

$$R=(1-E(t_1,T))\cdot\exp\left(-\int_0^T q_1(t)dt\right) \qquad (22b)$$

where $E(t_1,T)=\begin{cases}0 & \text{if } T<t_1\\ 1 & \text{if } T\geq t_1\end{cases}$

Here it should be borne in mind that for $Y\leq 0$ $F(t,Y)\equiv 0$.

REFERENCES

1. J. Schijve, Observations on the reduction of fatigue crack growth propagation under variable-amplitude loading. Fatigue Crack Growth Under Spectrum Loads. ASTM STP 595, 3-25 (1976).
2. R.I. Stephens, D.K. Chen and W.B. Hom, Fatigue crack growth with negative stress ratio following single overloads in 2024-23 and 7057 T6 aluminium alloys. Fatigue Crack Growth Under Spectrum Loads, ASTM STP 595, 27037 (1976).
3. W.X. Alzos, A.C. Skat and B.M. Hillberry. Effect of single overload/underload cycles on fatigue crack propagation. Fatigue Crack Growth Under Spectrum Loads. ASTM STP 595, 41-56 (1976).
4. P.J. Bernard, T.C. Lindey and C.E. Richards, Mechanisms of overload retardation during fatigue crack propagation. Fatigue Crack Growth Under Spectrum Loads. ASTM 595, 78-96 (1976).
5. W.J. Mills, R.W. Hertzberg and R. Roberts, Load interaction effects on fatigue crack growth in A514F steel alloy. Cyclic Stress-Strain and Plastic Deformation Aspects of Fatigue Crack Growth, ASTM STP 637, 192-208 (1977).

6. R.I. Stephens, E.S. Sheets and G.O. Njus. Fatigue crack growth and life prediction in man-tan steel subjected to a single and intermittent tensile overloads. Cyclic Strain and Plastic Deformation Aspects of Fatigue Crack Growth. ASTM STP 637, 176-191 (1977).
7. C. Bathias and M. Vancorn. Mechanisms of overload effect on fatigue crack propagation in aluminium alloys. Engng Fracture Mech. 10, 409-424 (1978).
8. D. Brock and S.H. Smith. The prediction of fatigue crack growth under flight-by flight loading. Engng Fracture Mech. 11, 12-141 (1979).
9. S.G. Druce, C.J. Beevers and E.F. Walker. Fatigue crack growth retardation following load reductions in a plain C.M. Steel. Engng Fracture Mech. 11, 385-395 (1976).
10. J.H. Underwood and J.A. Kapp. Benefits of overload for fatigue cracking at notch. Fracture Mechanics: Thirteenth Conference, ASTM STP 743, 43-62 (1981).
11. T.K. Brog, J.W. Jones and C.S. Was. Fatigue crack growth retardation in Inconel 600. Engng Fracture Mech. 20, 313-320 (1984).
12. H.D. Dill and C.R. Saff, Analysis of crack growth following compressive high loads based on crack surface displacements and contact analysis. Stress Strain and Plastic Deformation Aspects of Fatigue Crack Growth, ASTM STP 637, 141-152 (1972).
13. T.D. Gray and J.P. Gallagher, Predicting fatigue crack retardation following a single overload using a modified Weeler model, Mechanics of Crack Growth, ASTM STP 590, 331-344 (1976).
14. S. Suresh, Micromechanism of fatigue crack growth retardation following overloads. Engng Fracture Mech, 18, 577-599 (1983).
15. R. Arone, Fatigue crack growth under random overloads superimposed on constant-amplitude cyclic loading, Engng Fracture Mech., 24, 223-232 (1986).
16. O. Ditlevsen and K.Sobczyk, Random fatigue crack growth with retardation, Engng Fracture Mech., 24, 861-878 (1986).
17. R. Arone, On retardation effects during fatigue crack growth under random overloads, to be published in Engng Fracture Mech.
18. R. Arone, Conservative estimation of crack growth under random overloads, to be published in Engng Fracture Mech.
19. B.V. Gnedenko, The theory of probability, Chelsea, New York 1968.

APPLICATION TO MARINE STRUCTURES OF ASYMPTOTIC VECTOR PROCESS METHODS

R. Cazzulo
Registro Italiano Navale
Via Corsica 12, 16128 Genova GE, Italy

1. INTRODUCTION

One of the major problems which has to be carefully considered when applying reliability methods to the design of marine structures, is the time varying effects induced by random process loads.

The response of marine structures to random process loads, such as the environmental loads induced by wave, wind and current, is important not only in terms of dynamic behavior but also, and perhaps mainly, of load combination.

It is relatively simple to take into account this problem when it is possible to include all time varying effects in only one load variable, its extreme value, defined for a suitable reference period [0,T], being substituted in the failure equation, thus transforming it in a time-independent form.

Similar conclusions may be obtained for random processes which appear to be physically independent, by applying the Turkstra rule /1/.

The problem discussed in this paper arises when more time varying loads act simultaneously, thus having to be considered as components of a vector random process.

This is often the case of marine structures. An example relevant to ships is the problem of the combination of the vertical and horizontal bending moments required in the reliability analysis of some ship components. Another example, relevant to offshore structures, is given by the wave forces on the joints of a jacket, which may be considered as components of a vector random process.

The evaluation of failure probability of structures subjected to a vector random process load, obtained by applying standard reliability

methods, is not straightforward.

The extreme distributions of each load component are no longer sufficient alone because, in general, the most probable failure does not occur when all components reach their extreme value at the same time /2/. In the case of a stationary gaussian vector random process, further information on the correlation between the vector process and its derivative are required.

At the moment, two possible solutions are known for stationary gaussian vector process loads. One, called here as the dummy variable technique, transforms the problem into a time-independent form, suitable for FORM or SORM procedures, by introducing a fictitious variable which includes all time varying effects.

The component failure probability may be successfully evaluated by defining the initial distribution of the time-independent variables and the extreme distribution of the dummy variable, obtained at each step of the iterative procedure as the outcrossing of a suitable stationary gaussian process /3/.

The other very interesting solution is obtained by applying recently developed theories which define an upper bound of the failure probability as the mean outcrossing rate from a safe domain of a stationary gaussian vector random process, evaluated by means of asymptotic techniques /4/, /5/, /6/.

In our view, a crucial point for potential applications of reliability methods to marine structures is the development of reliability based codes.

The problem is to identify a set of partial safety factors for a specified class of marine structures which can be considered invariant with respect to the life of these structures. These factors have to be applied to the notional deterministic values of the load components, or a suitable combination of them.

The present possibilities of evaluating partial safety factors of load components are significantly different with regard to the two above-mentioned techniques.

Using the dummy variable technique it is possible to evaluate correctly the probability of failure, the design values and partial safety factors of time-independent variables but it is not possible to separate the effects of each load component contained in the design value of the dummy variable.

On the other hand, the probability of failure evaluated by means of mean outcrossing techniques is based on initial distributions both of time-invariant variables and time varying ones.

The use of initial distributions reveals the possibility to define the design points of time-invariant as well as time varying load components, which cannot be defined by the dummy variable technique. Furthermore, these design points, being obtained by initial instantaneous distributions, do not depend on the life of the structures.

The point is whether these design values may be used for the proper definition of partial safety factors of load components and in particular whether the use of initial distributions instead of extreme ones considerably shifts the safety content from the capability to the load.

A first attempt to clarify this problem will be discussed in this paper by comparing the partial safety factors of time-independent variables obtained by initial and extreme distributions for the tripping collapse of a deck girder, already considered as a typical example of component reliability analysis of ship structures /7/.

2. DIRECT EVALUATION OF FAILURE PROBABILITY

The problem referred to here is the evaluation of the probability that a structural component of a marine system subjected to vector random process loads fails during its life.

Such a probability may be defined as the probability that the failure equation is less than 0 at least once during the reference interval [0,T]

$$P_f(T) = P\ \{g < 0 \quad \text{a.l.o.} \quad [0,T]\} \tag{2.1}$$

The failure equation may be defined as

$$g = g_0(\underline{X}) - g_1[\underline{X},\underline{Y}(t)] \tag{2.2}$$

where $\underline{X}$ is a vector of basic random variables and $\underline{Y}(t)$ is a vector random process which includes all time varying load components.

A first method for determining the component failure probability by FORM or SORM procedures is based on the definition of an additional random variable, with cumulative distribution

$$F_{\Xi}(\xi) = 1 - P\ \{[g_1[\underline{X},\underline{Y}(t)] > \xi \quad \text{a.l.o.} \quad [0,T]\} \tag{2.3}$$

The failure probability suitably defined for application of FORM or SORM procedures becomes

$$P_f(T) = P\ \{[g_0(\underline{X}) - \Xi\ ] < 0\} \tag{2.4}$$

The normal standard variables $\underline{U}$ are obtained from the basic physical ones $\underline{X}$ by the Rosenblatt transformation. In particular, for the additional dummy variable u_{n+1} the transformation is

$$u_{n+1} = \Phi^{-1}\ [\ H\ (\xi|\underline{x})\ ] \tag{2.5}$$

The conditional extreme distribution $H\ (\xi\ |\underline{x})$ is obtained by the equation (2.3), making the vector of basic variables $\underline{X}$ equal to the deterministic values $\underline{x}$, obtained at each step of the iterative procedure.

The evaluation of this conditional probability is obtained as the

mean outcrossing rate of a suitable stationary gaussian random vector from the region $g_1[\underline{X},\underline{Y}(t)]$ approximated by hyperplanes /8/, /9/.

An alternative point of view is given by the following definition of failure probability /5/

$$P_f(T) \leq P_f(0) + \nu_f \cdot T \tag{2.6}$$

which involves as upper bound the initial failure probability $P_f(0)$, the mean outcrossing of the vector process from the safe region ν_f and the reference interval [0,T].

Initial failure probability is often considered negligible with respect to the time-dependent one but it may be evaluated using standard FORM techniques.

Very interesting asymptotic techniques for the evaluation of the mean outcrossing rate of a gaussian vector process have recently been developed for convex surfaces bounded by hyperplanes and even for intersections of failure domains, necessary for the analysis of redundant systems /6/.

As an example, the mean outcrossing rate for a hyperplane at a distance β from the origin is /10/

$$\nu_f = \frac{1}{\sqrt{2\pi}} \varphi(\beta) \sqrt{\underline{\alpha}^T \dot{\underline{\underline{R}}} \underline{\alpha}} \tag{2.7}$$

This formula shows the dependance of the outcrossing from the safety index β, the vector of direction cosines $\underline{\alpha}$ at β-point and the covariance matrix between the process and its derivative $\dot{\underline{\underline{R}}}$. This result is quite general also for more complex failure surfaces.

The comparison of the failure probability obtained by the dummy variable and asymptotic techniques is still under review, although the two results are expected to be quite similar, at least for large β-s.

3. DEVELOPMENT OF A PROBABILISTIC BASED CODE

Our basic interest is the application of reliability methods to develop probability based codes for marine structures. This means adjusting a set of suitable partial safety factors for an appropriate class of structures on the basis of reliability calculations.

A target safety level is met if the design check is fulfilled by using, in the failure equation, the notional deterministic values $\overline{X}$ corrected by the partial safety factors γ

$$g\ (\gamma_i, \overline{X}_i) \geq 0 \tag{3.1}$$

For the sake of convenience, the partial safety factors are defined as the ratios between the design and the notional values of basic variables

$$\gamma_i = \frac{X^*_i - \overline{X}_i}{\overline{X}_i} \tag{3.2}$$

In the case of structures subjected to vector process loads, the development of a reliability based code is faced with a series of problems still partially unsolved.

One of the most important is the invariance of partial safety factors with respect to the life of the structure. Below, the results obtained by extreme distribution for different reference time-intervals [0,T] or by initial distribution are compared.

Figure 1 shows a simple case of a resistance random variable R and a single component random process L.

The safe region is bounded by the failure equation obtained by instantaneous (initial) distributions (small line) or by an extreme distribution of the load (broad line).

For a non-stationary load process, the bound obtained by initial distributions moves with time, whereas for a stationary process it

remains unchanged. The bound obtained by the extreme load distribution is different when the reference interval [0,T] changes.

Assuming that the design point, in both cases, is the point closest to the origin, the direction cosines at this point significantly change if obtained by initial or extreme distributions. Therefore, the resistance and load partial safety factors significantly move from the resistance to the load if initial distributions are used instead of extreme ones.

4. ILLUSTRATIVE EXAMPLE

This qualitative consideration is confirmed by the results of a numerical example of the tripping collapse of a deck longitudinal girder of a conventional tanker. This example was studied in detail during the work of the last ISSC Committee V.2 on Applied Design /7/.

The results were obtained by a procedure based on FORM techniques, which is able to evaluate the reliability, in terms of safety index and design values of basic variables, of a component of a linear marine system.

This procedure requires, as input, the response amplitude operators of time varying effects for the sea-states considered in the analysis. For each sea state, the stationary gaussian random process load components are fully described by the following covariance matrices

$$\underline{\underline{R}} = E\,[Y_i Y_j] = \int_o^\infty H_i(w)\, H^*_i\,(w)\, S(w)\, dw \qquad (4.1)$$

$$\underline{\underline{\dot{R}}} = E\,[Y_i \dot{Y}_j] = Re\,[\int_o^\infty iw\, H_i(w)\, H^*_j(w)\, S(w)\, dw\,] \qquad (4.2)$$

where $H_i(w)$ is the response amplitude operator and $S(w)$ is the wave spectrum.

Long-term results are obtained by evaluating the convolution integral over all the sea-states. For the sake of simplicity, in this example only a single sea state has been considered, with significative wave height 7.5 m and mean period 10 s.

The array of time-independent basic variables $\underline{X}$ has the 24 components shown in table 1. Vertical M_v and horizontal M_o bending moments are the two components of the stationary vector random process $\underline{Y}(t)$.

The failure equation for the tripping collapse of the deck girder is defined as

$$C - \frac{\chi_v M_v(t) + M_{sw}}{W_v} - \frac{\chi_o M_o(t)}{W_o} = 0 \qquad (4.3)$$

where C accounts for ultimate tripping capacity, W_v and W_o are the vertical and horizontal section modulus, M_{sw} is still water bending moment and χ_v and χ_o account for uncertainties in the vertical and horizontal wave bending moment.

Extreme distribution results have been obtained for several reference intervals [0,T], by applying the dummy variable method and ignoring initial failure probability with respect to the time-dependent one.

On the other hand, initial distribution results have been obtained by considering the vertical and horizontal bending moments as two additional basic variables and by applying the following Rosenblatt transformation

$$\begin{Bmatrix} u_v \\ u_o \end{Bmatrix} = (\underline{\underline{A}}\ \underline{\underline{B}}^{1/2})^{-1} \begin{Bmatrix} M_v \\ M_o \end{Bmatrix} \qquad (4.4)$$

where $\underline{\underline{A}}$ and $\underline{\underline{B}}$ are the eigenvector and eigenvalue matrices obtained as a solution to the following problem

$$\underline{\underline{A}}^T \underline{\underline{R}} \underline{\underline{A}} = \underline{\underline{B}} \; ; \; \underline{\underline{A}}^T = \underline{\underline{A}}^{-1} \tag{4.5}$$

The safety indices β obtained for reference intervals from 20 years to 1 hour and for the initial distributions are given in Figure 2. Obviously, the safety index decreases by increasing the time-interval and the initial distribution value is considerably larger than the value obtained by the extreme one.

What is interesting with regard to this discussion is the comparison of partial safety factors of basic variables, normalized with respect to the safety index

$$\gamma'_i = \frac{X^*_i - \bar{X}_i}{\bar{X}_i \, \beta} \tag{4.6}$$

The results in table 2 show that normalized partial safety factors which have noticeable values change significantly when obtained for a 20 year reference period by extreme distributions or initial ones.

The highest value refers to still water bending moment. This is a well known problem, because its high standard deviation is due to the high scatter in the ship' s loading condition documents.

Other variables, such as yield stress, the residual stress coefficient and the various model uncertainties, reflect the same difference in the partial safety factors obtained by the initial and the 20 year extreme distributions.

5. CONCLUSION

The study presented in this paper is at a very preliminary stage. However, even though results of the previous example are incomplete there are still doubts about the application of reliability techniques in the development of reliability based codes for structures subjected to vector process loads.

In particular, the partial safety factors, also of

time-independent variables, obtained by initial distributions seem to be inconsistent with respect to the ones obtained by extreme distributions.

Mean outcrossing rate techniques which seem so interesting for direct procedures, are based on initial distribution and so may lead to an inaccurate definition of the partial safety factors.

This conclusion has been reached by considering the design point as the point closest to the origin also for the initial distribution calculations.

This is not, in principle, required by mean outcrossing techniques and there are suggestions for choosing a different expansion point from which the vector process crosses the safe domain /10/, /11/. However, from the results of this paper, the choice of the point has to be closely connected to a consistent definition of partial safety factors.

The most suitable reliability procedure able to correctly take into account the time-invariant basic variables and the load components of a vector random process, which for long-term analysis are in general non-stationary and non-gaussian, is a philosophical problem still only partially solved with regard to the extensive use of reliability methods for the analysis of marine structures subjected to time varying effects.

REFERENCES

/1/ Turkstra C.J., "Theory of structural safety", S.M. Study no. 2, Solid Mechanics Division, University of Waterloo, 1970

/2/ Lind N.C., Krenk S., Madsen H.O., "Safety of Structures", Prentice Hall, 1985

/3/ Ferro G., Cervetto D., "Reliability of Marine Structures under Dynamic Loadings", International Workshop on Stochastic Methods in Structural Mechanics, Pavia, 1983

/4/ Breitung K., "Asymptotic Approximations for Multi-normal Domain and Surface Integrals", 4th Int. Conf. on Applications of Statistic and Probability in Soil and Structural Engineering, Firenze, 1983

/5/ Veneziano D., Grigoriu M., Cornell C. A., "Vector Process Models

for System Reliability", ASCE Journal of Engineering Mechanics, Vol. 103 No. EM3, 1977

/6/ Hohenbichler M., Rackwitz R., "Asymptotic Crossing Rate of Gaussian Vector Processes into Intersection of Failure Domains", Probabilistic Engineering Mechanics, Vol. 1 No. 3, 1986

/7/ Committee V.2, "Applied Design", 9th International Ship Structures Congress, Genova, 198885

/8/ Ferro G., Cervetto D., "Hull Girder Reliability", Ship Structure Symposium, Arlington, 1984

/9/ Ditlevsen O., "Gaussian Outcrossings from Safe Convex Polyhedrons", ASCE Journal of Engineering Mechanics, Vol. 109 No. 1, 1983

/10/ Ditlevsen O., "On the Choice of the Expansion Point in FORM or SORM", Structural Safety, Vol. 4 Pag. 243-245, 1987

/11/ Pearce H.T., Wen Y.K., "On linearization points for non-linear combinations of stochastic load process", Structural Safety, Vol. 2, 1985

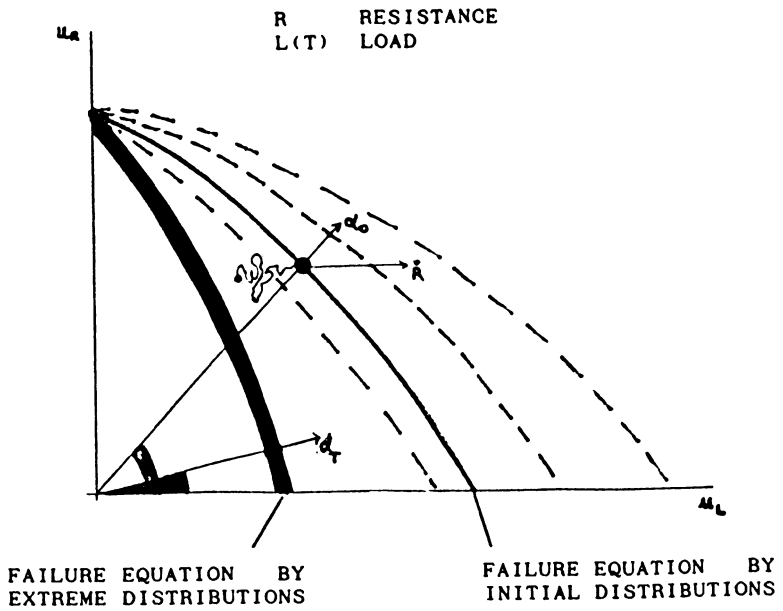

Figure 1 : Comparison of direction cosines at the design point (closest to the origin)

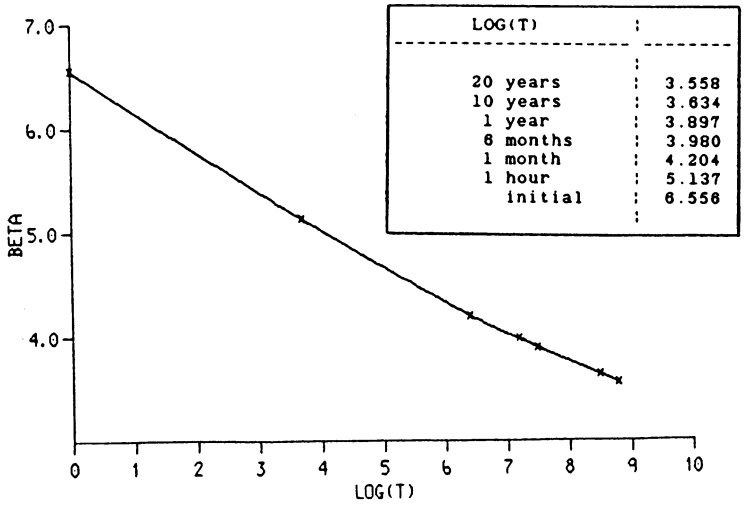

Figure 2 : Safety indices for different reference intervals and for initial distributions

CL.1/4 PLATE THICKNESS	= 0.0155
CL.2 PL. THICK. - CL.6 STIFF. FL. THICK.	= 0.0160
CL.3 PL. THICK. - CL.6 STIFF. WEB THICK.	= 0.0125
CL.1 STIFFNER WEB HEIGHT	= 0.2800
CL.2 STIFFNER WEB HEIGHT	= 0.4000
CL.3 STIFFNER WEB HEIGHT	= 0.3000
CL.6 STIFFNER WEB HEIGHT	= 1.6940
CL.7 STIFFNER WEB HEIGHT	= 2.5800
CL.1/7 STIFFNER WEB THICKNESS	= 0.0150
CL.2/3 STIFFNER WEB THICKNESS	= 0.0105
CL.2 STIFFNER FLANGE WIDTH	= 0.1200
CL.3 STIFFNER FLANGE WIDTH	= 0.1000
CL.6 STIFFNER FLANGE WIDTH	= 0.1800
CL.7 STIFFNER FLANGE WIDTH	= 0.2500
CL.2/7 STIFFNER FLANGE THICKNESS	= 0.0230
CL.3 STIFFNER FLANGE THICKNESS	= 0.0145
YIELD STRESS	= 280.000
YOUNG MODULUS	= 206000.0
POISSON COEFFICIENT	= 0.3000
RESIDUAL STRESSES COEFFICIENT	= 0.7500
STILL WATER BENDING MOMENT	= 137.000
MODEL UNCERTAINTIES ON STRENGTH	= 1.0000
MODEL UNCERTAINTIES ON VERTICAL MOMENT	= 0.9500
MODEL UNCERTAINTIES ON HORIZONTAL MOMENT	= 0.8500

Table 1 : Mean values of basic variables

NORMALIZED PARTIAL SAFETY FACTORS (XS-XM)/(XM*BETA)

BETA	20 YS 3.558	10 YS 3.634	1 Y 3.897	6 MS 3.980	1 M 4.204	1 H 5.137	INIT. 6.556
X							
1	-0.007	-0.007	-0.008	-0.008	-0.008	-0.008	-0.007
2	-0.002	-0.002	-0.002	-0.002	-0.001	-0.001	-0.001
3	-0.002	-0.002	-0.002	-0.002	-0.002	-0.002	-0.001
4	-0.001	-0.001	-0.001	-0.001	-0.001	-0.001	-0.001
5	-0.001	-0.001	-0.001	-0.001	-0.001	-0.001	-0.001
6	-0.001	-0.001	-0.001	-0.001	-0.001	-0.001	-0.001
7	-0.001	-0.001	-0.001	-0.001	-0.001	-0.001	-0.001
8	-0.001	-0.001	-0.001	-0.001	-0.001	-0.001	-0.001
9	-0.006	-0.006	-0.005	-0.005	-0.005	-0.004	-0.004
10	0.000	0.000	0.000	0.000	0.000	-0.002	-0.001
11	0.000	0.000	0.000	0.000	0.000	0.000	0.000
12	0.000	-0.001	-0.001	-0.001	0.000	-0.001	0.000
13	0.000	0.000	0.000	0.000	-0.001	-0.001	0.000
14	0.000	0.000	-0.001	0.000	0.000	-0.001	0.000
15	0.000	0.000	0.000	0.000	0.000	0.000	0.000
16	0.000	0.000	0.000	0.000	0.000	0.000	0.000
17	-0.033	-0.033	-0.033	-0.033	-0.033	-0.033	-0.029
18	-0.002	-0.002	-0.002	-0.002	-0.002	-0.002	-0.001
19	0.000	0.000	0.000	0.000	0.000	0.000	0.000
20	-0.043	-0.043	-0.042	-0.041	-0.039	-0.035	-0.028
21	0.976	0.979	0.987	0.991	0.997	0.989	0.856
22	-0.015	-0.015	-0.015	-0.015	-0.015	-0.014	-0.012
23	0.038	0.038	0.036	0.035	0.034	0.027	0.021
24	0.048	0.047	0.045	0.044	0.042	0.034	0.026

Table 2 : Normalized partial safety factors for different reference intervals and for initial distributions

RELIABILITY ANALYSIS OF DISCRETE DYNAMIC SYSTEMS UNDER NON-STATIONARY RANDOM EXCITATIONS

Tadeusz Chmielewski
Technical University of Opole, 45-951 Opole, Poland

INTRODUCTION

In this paper we shall describe an approach to the study the reliability of structures modeled as linear discrete dynamic systems which has been designed to withstand nonstationary random excitations. We shall discuss this problem upon consideration the following four steps:

1) The description of an input space F, an output space Y and a linear operator of the system should be estimated first. An equation of motion in a general sense takes form

$$L\,y(t) = f(t), \tag{1}$$

where $f(t) \in F$, $y(t) \in Y$ and L - the system operator. The space Y should be taken such that any state of the system could be considered.

Let us assume a complete knowledge of the dynamic properties and the initial state of a structure in a **deterministic sense, but the excitation** f(t) is random.

2) In the second step, the solution of the stochastic differential equation (1) should be found by the application of random vibration theory (see [10,18,31]).

3) In the third step one have to evaluate a quality space V which characterize the quality of the system. So, for any sample function y(t) may be found a sample function v(t). The dependence between y(t) and v(t) can be written in a form

$$v(t) = N\,y(t). \tag{2}$$

The operator N should be prescribed for any specific structure. In many cases for mechanical systems the quality space is a subspace of Y. In this step it is important to prescribe a tolarable domain D in the qua-

lity space V. It should be done on the base of technological and economical considerations for any **given** real structure. This domain is limited by the bound surface S.

4) The response of the structure under the random excitation will be random, too. Therefore, the answer to the question of reliability holds with a certain probability only. A formal definition of a reliability is as follows

$$P(t) = P\left[V(\tau) \in D; \quad 0 \leqslant \tau \leqslant t\right], \tag{3}$$

where P means a probability that characteristic process V(t) of the structural response remains within the prescribed tolerable domain D during interval (0,t).

Let F, U and V are Euclides spaces. On the Fig. 1 sample functions f(t), y(t) and v(t) are sketched upon assumption that F, U, V are three dimensional spaces.

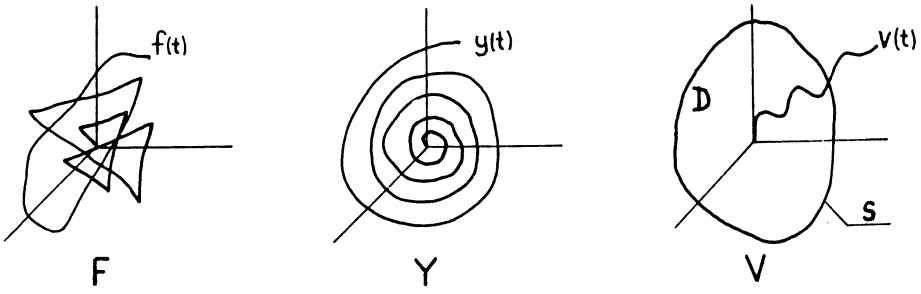

Fig. 1. Examples of sample functions f(t), y(t), v(t).

In the following chapters strong ground motion during earthquakes will be considered as an example of nonstationary random excitations. A linear structure will be modeled as a system with n degrees of freedom. Displacements, internal forces or the capacity of a cross section may be taken as parameters of the system quality.

STOCHASTIC MODEL OF SEISMIC GROUND MOTION

Earthquakes are typically random in nature. One cannot tell where, when and with what intensity next quake will happen. No two earthquake are alike. The mechanism of origin is not unique. The diffrent types of

earthquakes waves are often reflected and refracted on their way from the epicenter to the site. Therefore, the excitation process seem like an irregular motion.

The random nature of the quake requires a random model for the mathematical description of the acceleration process. This model must be influenced by the soil properties of the site and must include all past information. Various probabilistic models of strong ground motions during earthquakes have been proposed (see [2, 3, 5, 12, 28, 34]). These investigation ledto a commonly accepted model of uniformly modulated random process, representing the horizontal ground acceleration, as follows

$$\ddot{f}(t) = A(t)\ddot{\tilde{f}}(t), \tag{4}$$

where $A(t)$ is a deterministic envelope imposed on stationary process $\ddot{\tilde{f}}(t)$.

Some envelopes have been proposed in the literature (see [1, 4, 5, 29]) Examples of a few will be presented in next Chapter, but the Amin's and Ang's seems the most suitable (see [1]).

The stationary process $f(t)$ can be characterized by the Kanai-Tajimi spectrum (see [15, 33])

$$S_{\ddot{\tilde{f}}}(\omega) = \frac{\left[1 + 4\xi_g^2\left(\omega/\omega_g\right)^2\right] S_o}{\left[1 - \left(\omega/\omega_g\right)^2\right]^2 + 4\xi_g^2\left(\omega/\omega_g\right)^2}, \tag{5}$$

where ω_g and ξ_g are parameters reflecting local site conditions, whereas S_o are related to earthquake intensity.

DYNAMIC RESPONSE OF DISCRETE SYSTEMS

Note on the peak factor

The emphasis in this and next paragraphs is on the use of random vibrations theory to predict the response of structures to earthquake ground motion. Random vibrations analysis has its aim the prediction of the probability distribution of a dynamic response parameter of interest in terms of the dynamic properties of the structure and a statistical description of the earthquake. It holds a clear advantage over other procedures in that they yield information about the distribution of structural response, allowing direct assement of the probability of

exceeding intorelable response levels.

In this notes, the types of system treated probabilistically are linear multi-degree-of-freedom systems. The solution is stated in terms of the response $y_{T,p}$ in which the subscripts refer to an exceedance probability p and the strong-motion duration T. The response is expressed as follows

$$y_{T,p} = r_{T,p}\, \sigma_y(T) \ , \tag{6}$$

where $\sigma_y(T)$ = standard deviation of the linear system response at time T,

$r_{T,p}$ = peak factor which relates standard deviation to the response level not exceeded with probability p.

A general approach to estimating the peak factor $r_{T,p}$ for linear systems is described in next Chapter.

Problem statement

Consider a general multi-degree-of-freedom system represented by the familiar time invariant matrix equation of motion

$$[B]\{\ddot{Y}\} + [C]\{\dot{Y}\} + [K]\{Y\} = \{F(t)\} \ , \tag{7}$$

with the following initial conditions

$$\{Y(0)\} = \{Y^0\} \ , \quad \{\dot{Y}(0)\} = \{\dot{Y}^0\} \ , \tag{8}$$

where

$\{F(t)\} = \{F_1(t), F_2(t), \ldots, F_n(t)\}^T =$

$= -[B]\{1\}\ddot{f}_o(t)$ - the effective vector earthquake force,

$\{Y(t)\} = \{Y_1(t), Y_2(t), \ldots, Y_n(t)\}^T$ - displacement vector,

$\{\ \}^T$ - denotes transpositions of vector,

$[B]$, $[C]$, $[K]$ - mass, damping and stiffness matrices respectively.

The general solution of equation(7) can be written as

$$\{Y(t)\} = \{Y^I(t)\} + \int_0^t [h(\tau)]\{F(t-\tau)\}\, d\tau \tag{9}$$

The first homogeneous solution reflects the initial states. Whereas the effect of the externally applied forces is represented by the second particular solution in terms of the matrix of impulse response func-

tions $[h(\tau)]$.

The most general stochastic problem can be formulated as follows. Take a set of randomly chosen initial states and evolve them concurrently under the action of random forcing functions. The purpose of this analysis is to find out the solution of such a problem for statistical properties of the response vector; for consiseness advantage will be taken of matrix notation (see [9]). Denoting the operator of mathematical expectation by $\langle\ \rangle$, the mean displacement can be written as

$$\langle\{Y(t)\}\rangle = \langle\{F^I(t)\}\rangle + \int_0^t [h(\tau)]\langle\{F(t-\tau)\}\rangle\, d\tau \qquad (10)$$

Substracting equation (10) from equation (9), the fluctuating displacement can be expressed in following form

$$\{y(t)\} = \{y^I(t)\} + \int_0^t [h(\tau)]\ \{f(t-\tau)\}\, d\tau \qquad (11)$$

in which the fluctuations $\{y(t)\}$, $\{y^I(t)\}$ and $\{f(t)\}$ are defined by

$$\{y(t)\} = \{Y(t)\} - \langle\{Y(t)\}\rangle, \quad \{y^I(t)\} = \{Y^I(t)\} - \langle\{Y^I(t)\}\rangle$$

and $$\{f(t)\} = \{F(t)\} - \langle\{F(t)\}\rangle.$$

The influence of the fluctuation $\{y^I(t)\}$ is given in reference [10] and will not be considered here. The $\{y(t)\}$ moment of any order can be expressed in terms of the moment of $\{f(t)\}$. Since equation (11) is linear, the $\{y(t)\}$ - moment would involve the $\{f(t)\}$ moment of the same order. The matrix of variances of the response $[D_{\{y\}}(t)]$ may be expressed in terms of the covariance matrix $[K_f(t_1,t_2)] = \langle\{f(t_1)\}\{f^*(t_2)\}^T\rangle$ (asterisk denotes complex conjugate) in the following form

$$[D_{\{y\}}(t)] = \int_0^t\int_0^t [h(\tau_1)][K_f(t-\tau_1, t-\tau_2)][h(\tau_2)]^T\, d\tau_1 d\tau_2\ , \qquad (12)$$

where $[\ ]^T$ - denotes transposition of matrix.

The time domain equation (12) is valid for any arbitrary physical random processes and taking into account the stationary response $\{\tilde{y}(t)\}$ to stationary excitation $\{\tilde{f}(t)\}$ one can obtain its frequency-domain form, more convinient for practical computations (see [10,18])

$$[D_{\{\tilde{y}\}}] = [H(\omega)][S_{\tilde{f}}(\omega)][H(\omega)]^T\, d\omega\ , \qquad (13)$$

where $[H(\omega)]$ is the matrix of frequency response functions,

$[S_{\{\tilde{f}\}}(\omega)]$ is the matrix of the power spectral density functions of the stationary excitation vector $\{\tilde{f}(t)\}$

Input - output relations using evolutionary spectra.

The actual time integration of equation (12) is very tedious, although it involves only trivial computations. This complication may be circumvented by using the Fourier-Stieltes representation for nonstationary random processes, first introduced by Priestley [23,24]. Furthemore application of spectral description of random processes leads to relations having clear physical interpretations. Assume, that $\{f(t)\}$ can be written in form of the spectral representation

$$\{f(t)\} = \begin{Bmatrix} \int_{-\infty}^{\infty} A_1(t,\omega)\ e^{i\omega t}\ d\hat{f}_1(\omega) \\ \int_{-\infty}^{\infty} A_2(t,\omega)\ e^{i\omega t}\ d\hat{f}_2(\omega) \\ \\ \int_{-\infty}^{\infty} A_n(t,\omega)\ e^{i\omega t}\ d\hat{f}_n(\omega), \end{Bmatrix} \tag{14}$$

where $A_k(t,\omega)$, k=1,2, ... ,n are slowly varying deterministic functions of time t and frequency ω and symbols $\hat{f}_k(\omega)$, k=1,2, ... ,n, stand for orthogonal random processes in frequency domain with zero mean and the properties:

$$\langle d\hat{f}_k(\omega_1)\ d\hat{f}_k^*(\omega_2)\rangle = \begin{cases} \langle |df_k(\omega)|^2 \rangle = S_k(\omega)\, d\omega & \text{for } \omega_1=\omega_2=\omega \\ \\ 0 & \text{for } \omega_1 \neq \omega_2. \end{cases} \tag{15}$$

Orthogonality of increments of two different processes is also assumed, i.e.:

$$\langle d\hat{f}_j(\omega_1)\ d\hat{f}_k^*(\omega_2)\rangle = \begin{cases} \langle d\hat{f}_j(\omega)\, d\hat{f}_k^*(\omega)\rangle = S_{jk}(\omega)\, d\omega & \text{for } \omega_1=\omega_2=\omega \\ \\ 0 & \text{for } \omega_1 \neq \omega_2 \end{cases} \tag{16}$$

In equations (15) and (16) $S_j(\omega)$ and $S_{jk}(\omega)$ denote auto and cross power spectral density functions, in stationary sense, of vector random process $\{\tilde{f}(t)\}$ ($\{\tilde{f}(t)\} = \{f(t)\}$, when $A_k(t,\omega) = 1$ for k=1,2, ... , n).

The introduction of the vector orthogonal representation (14) into the second component of equation (11) gives

$$\{y(t)\} = \int_{-\infty}^{\infty} [M(t,\omega)]\, e^{i\omega t}\, \{d\hat{f}(\omega)\}\ , \tag{17}$$

where elements of matrix $[M(t,\omega)]$ are given by following formula

$$M_{jk}(t,\omega) = \int_{0}^{t} h_{jl}(\tau)\ A_k(t-\tau,\omega)\ e^{-i\omega\tau}\, d\tau\ , \tag{18}$$

$$j = 1,2,\ \ldots\ ,n$$
$$k = 1,2,\ \ldots\ ,n$$

and $h_{jk}(\tau)$ - elements of matrix of impulse response functions,

$$\{d\hat{f}(\omega)\} = \{d\hat{f}_1(\omega)\ ,\ d\hat{f}_2(\omega)\ ,\ \ldots\ ,\ d\hat{f}_n(\omega)\}^T\ . \tag{19}$$

Equation (17) can be used conveniently to find the joint cumulant functions of any order of the response. For example the covariance matrix can be derived as follows

$$K_{\{y\}}(t_1,t_2) = \{y(t_1)\}\ \{y^*(t_2)\}^T = \tag{20}$$

$$= \int_{-\infty}^{\infty}\int_{-\infty}^{\infty} [M(t_1,\omega_1)]\ e^{i(\omega_1 t_1 - \omega_2 t_2)} \langle \{d\hat{f}(\omega_1)\}\ \{d\hat{f}^*(\omega_2)\}^T \rangle [M^*(t_2,\omega_2)]^T$$

Taking into account the equation (15) and (16) one obtains

$$[K_{\{y\}}(t_1,t_2)] = \int_{-\infty}^{\infty} [M(t_1,\omega)]\,[S_{\{\tilde{f}\}}(\omega)]\,[M^*(t_2,\omega)]^T\, e^{i\omega(t_1-t_2)}\, d\omega. \tag{21}$$

For $t_1=t_2=t$ equation (21) reduces to the matrix of variances

$$[D_{\{y\}}(t)] = \int_{-\infty}^{\infty} [M(t,\omega)]\,[S_{\{\tilde{f}\}}(\omega)]\,[M^*(t,\omega)]^T\, d\omega. \tag{22}$$

The integrand in equation (22) represents the matrix of evolutionary power spectral density functions of the response (denoted by $[S_{\{y\}}(t,\omega)]$)

$$[S_{\{y\}}(t,\omega)] = [M(t,\omega)]\,[S_{\{\tilde{f}\}}(\omega)]\,[M^*(t,\omega)]^T. \tag{23}$$

It is interesting to note that when the excitation vector $\{f(t)\}$ is stationary, then $A_k(t,\omega) = 1$, $k=1,2,\ \ldots\ ,n$, and limits of integration in (18) are infinite. In this case $M(t,\omega) = H(\omega)$, hence equation (22) reduces to the known equation (13) for stationary processes.

Before closing it must be noted that practical estimation of the modulating functions $A_k(t,\omega)$ required in equation (18) is faced with dif-

ficulties unless the components of excitation vector $\{f(t)\}$ are uniformly modulated random processes (see [16,32,38]) i.e.:

$$A_k(t,\omega) = A_k(t) \qquad (24)$$

$$k = 1,2, \ldots ,n$$

$$f_k(t) = A_k(t)\ \tilde{f}_k(t), \qquad (25)$$

where $\tilde{f}_k(t) = \int_{-\infty}^{\infty} e^{i\omega t}\, d\hat{f}_k(\omega)$ are stationary random processes. Such the simplification may however be assumed in many engineering problems.

Two-degree-of-freedom system example

Consider a system with two degrees of freedom which is excited by motion of the foundation (Figure 2). The matrix equation of motion of the system is as follows

$$\begin{bmatrix} 2m & 0 \\ 0 & m \end{bmatrix} \begin{Bmatrix} \ddot{y}_1 \\ \ddot{y}_2 \end{Bmatrix} + \begin{bmatrix} c_1+c_2 & -c_2 \\ -c_2 & c_2 \end{bmatrix} \begin{Bmatrix} \dot{y}_1 \\ \dot{y}_2 \end{Bmatrix} + \begin{bmatrix} 3k & -k \\ -k & k \end{bmatrix} \begin{Bmatrix} y_1 \\ y_2 \end{Bmatrix} = \begin{Bmatrix} -2m\ddot{f}_o \\ -m\ddot{f}_o \end{Bmatrix}, \qquad (26)$$

where vector $\{y\}$ denotes the relative displacements of masses m_1 and m_2. Normal mode analysis gives natural frequencies of the system

$$\omega_1 = 2\pi \text{ rad/s}, \quad \omega_2 = 4\pi \text{ rad/s}, \quad \text{for } k/m = 8\pi^2 \text{ (rad/s)}^2.$$

Under the assumption that damping matrix is a linear combination of mass matrix and stiffness matrix, the matrix of impulse response functions may be calculated on the ground of solved eigenproblem, [10]. The calculations yield in this example

$$h(t) = \frac{1}{m\bar{\omega}_1} \begin{bmatrix} \frac{1}{6} & \frac{1}{3} \\ \frac{1}{3} & \frac{2}{3} \end{bmatrix} e^{-\xi_1\omega_1 t} \sin \bar{\omega}_1 t + \frac{1}{m\omega_2} \begin{bmatrix} \frac{1}{3} & \frac{1}{3} \\ \frac{1}{3} & \frac{1}{3} \end{bmatrix} e^{-\xi_2\omega_2 t} \sin \bar{\omega}_2 t, \qquad (27)$$

where: $\bar{\omega}_j = \omega_j \sqrt{1-\xi_j^2}$, $j = 1,2$

ξ_j - modal damping parameters, $\xi_1 = \xi_2 = 0{,}05$ in the present example.

It is assumed that the excitation process $\ddot{f}_o(t)$ is uniformly modulated random process

$$\ddot{f}_o(t) = A(t)\,\ddot{\tilde{f}}(t), \quad \langle \tilde{f}(t) \rangle = 0 \qquad (28)$$

Consider the stochastic response of the system (26) under assumption that power spectral density of the process $\tilde{\tilde{f}}(t)$ is described by the formula (5) with the parameters as

$$\omega_g = 15.6 \text{ rad/s}, \quad \xi_g = 0,6, \quad S_o = 4.65 \cdot 10^{-4} \text{ m}^2/\text{s}^3.$$

The envelopes A(t) may be assumed as follows:

$$A(t) = \begin{cases} 0 & \text{for } t < 0 \\ \left(\frac{t}{t_1}\right)^2 & \text{for } 0 \leqslant t < t_1 \\ 1 & \text{for } t_1 \leqslant t < t_2 \\ e^{-\beta(t-t_2)} & \text{for } t \geqslant t_2 \end{cases} \tag{29}$$

$$t_1 = 3s, \quad t_2 = 7s, \quad \beta = 0.2$$

$$A(t) = \begin{cases} 0 & \text{for } t < 0 \\ \beta_1 \left(e^{-\beta_2 t} - e^{-\beta_3 t}\right) & \text{for } t \geqslant 0 \end{cases} \tag{30}$$

$$\beta_1 = 2,95 \;, \quad \beta_2 = 0,25 \;, \quad \beta_3 = 0,65$$

$$A(t) = \begin{cases} 0 & \text{for } t < 0 \\ 1 & \text{for } t \geqslant 0 \end{cases} \tag{31}$$

$$A(t) = 1 \quad \text{for} \quad t \in (-\infty, \infty) \tag{32}$$

These envelopes are shown in Figure 3 .

The matrix of stationary power spectral density functions has in this example following form

$$S_{\{\tilde{\tilde{f}}\}}(\omega) = \begin{bmatrix} S_{\tilde{\tilde{f}}}(\omega) & S_{\tilde{\tilde{f}}}(\omega) \\ S_{\tilde{\tilde{f}}}(\omega) & S_{\tilde{\tilde{f}}}(\omega) \end{bmatrix}. \tag{33}$$

The elements of matrix $M(t,\omega)$ have been calculated using equation (18). Results for evolutionary power spectral density fuctions of dis-

placements y_1 and y_2 calculated using equation (23), are plotted in Figures 4a and 4b, respectively for the envelope (30) and $\xi_1=\xi_2=$ $=0.05$. For the bottom mass, as can be observed, the concentration of the spectral density about the natural frequencies is more distinct than for the upper one. Figure 5 presents the standard deviations of the displacement y_1 and y_2, obtained by applying equation (22).

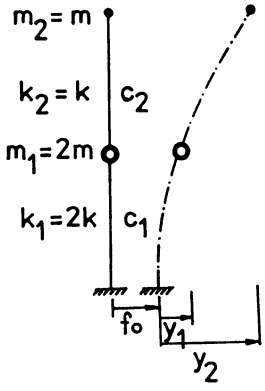

Fig. 2. A two degree of freedom system

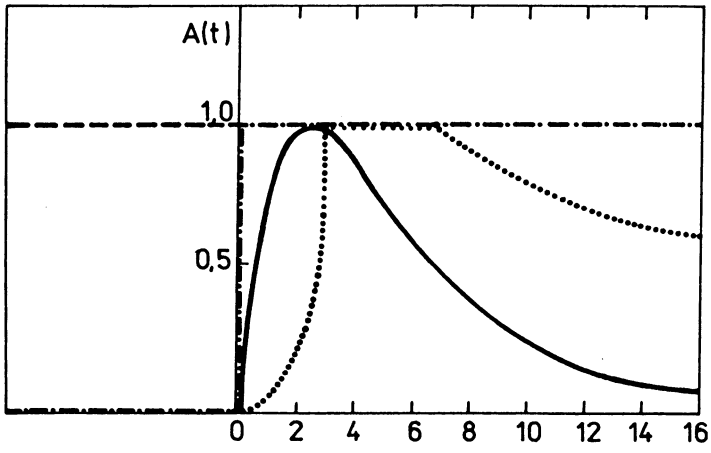

Fig. 3. Envelopes ..... eq. (29)
——— eq. (30)
—·—·— eq. (31)
— — — eq. (32)

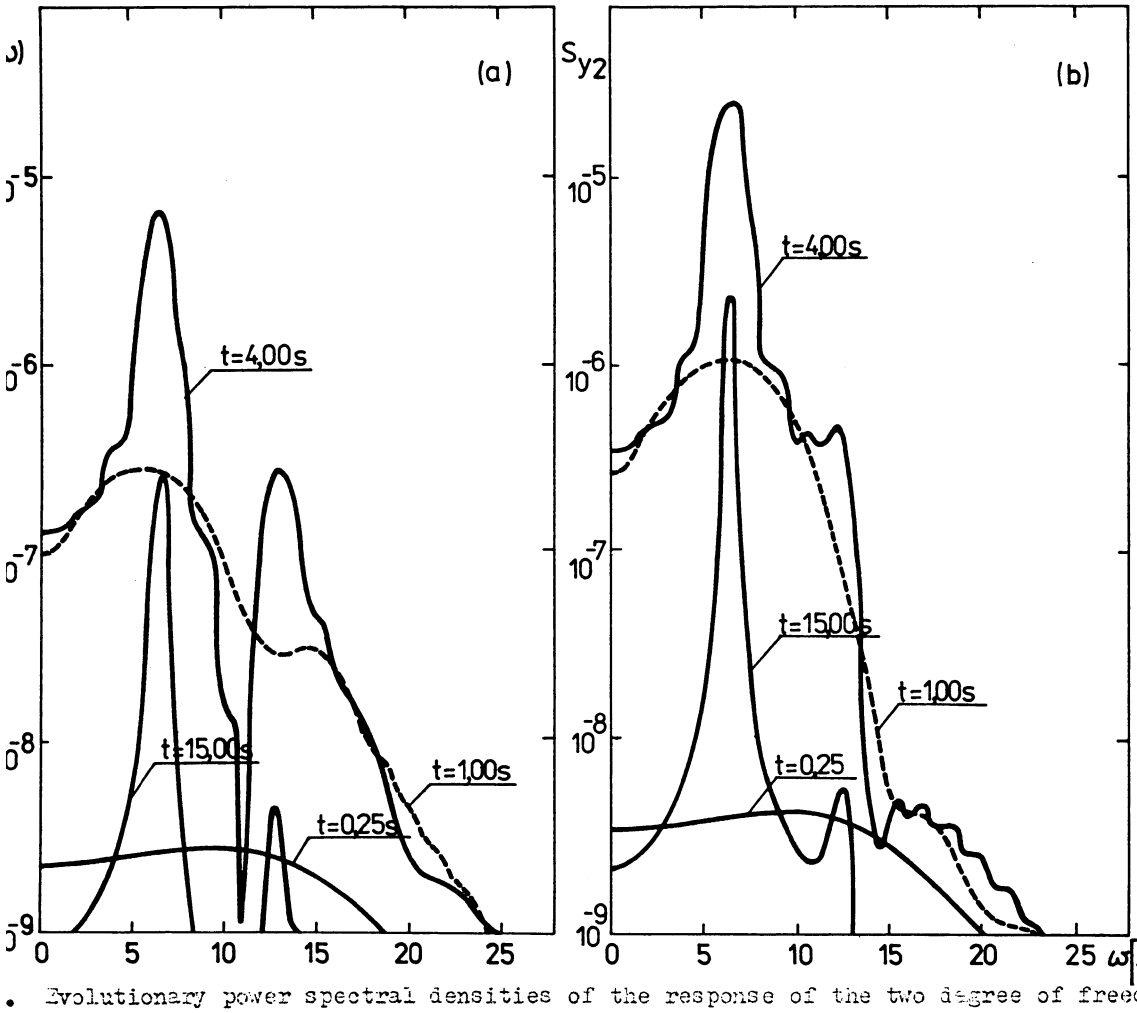

. Evolutionary power spectral densities of the response of the two degree of freedom syste

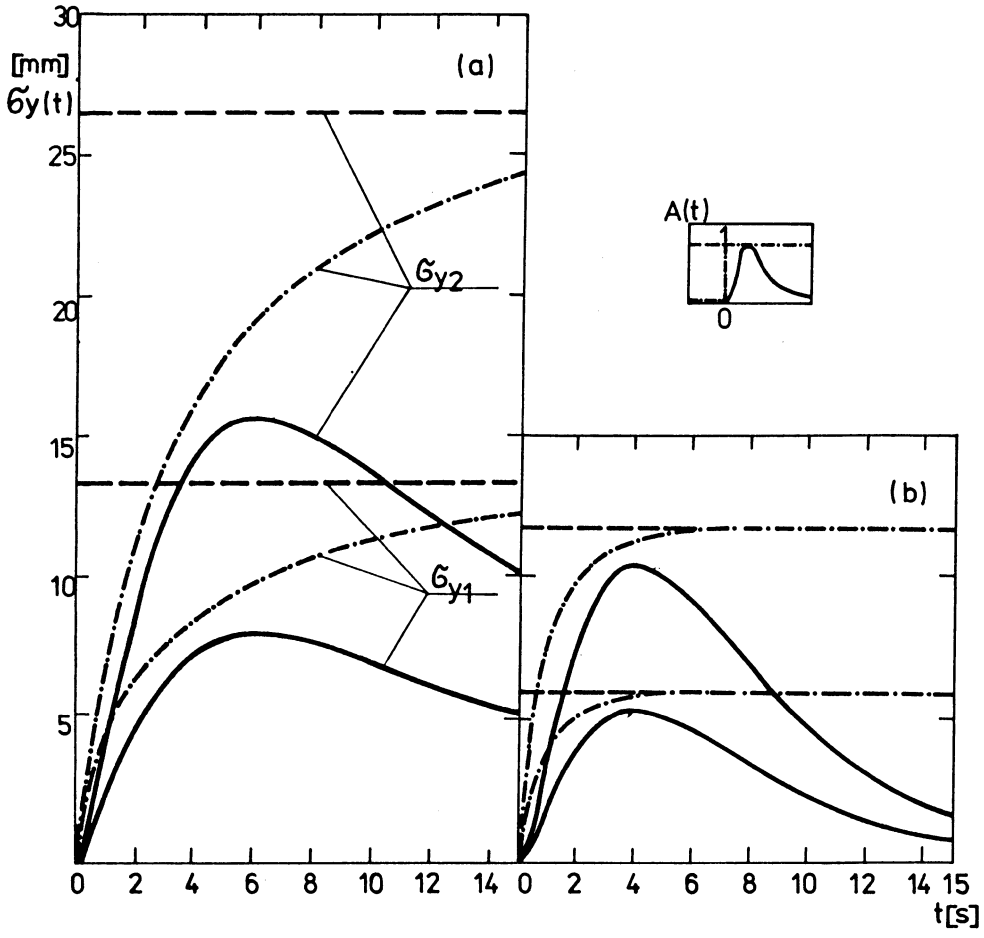

Fig. 5. Standard deviation of the response of the two degree of freedom system for envelopes (30), (32) and
(a) for $\xi = 0{,}01$
(b) for $\xi = 0{,}05$

ASEISMIC RELIABILITY AND FIRST - PASSAGE FAILURE

Classification of structures and earthquakes

Various types of structures have to withstand earthquakes. In regions where strong motion earthquakes are rare events, only special structures are designed under this load, e.g. power plant system, dams, broadcasting transmitters, etc. When the structure is a very complicated, it can be divided into the main structure, the so-called primary structure, and substructures, the so-called secondary structures.

To the structural designer, the only purpose in studying seismology is to enable him to predict the characteristics of the earthquake input for which his structures should be designed. In order to deal effectively with the combinations of extreme loading from earthquakes and low probability of its accurance, a strategy based on dual design criteria usually is adopted.

For example, with nuclear power plant systems two different types of "design earthquakes" are usually considered. First, an operatory basis earthquake (OBE) is considered. It is a moderate earthquake which reasonably may be expected during the life of the structure and must not endanger the operation of the power plant. Second, a safe shutdown earthquake (SSE) is considered. It is the most severe earthquake which possible could occur at the site and is applied as a test of the structural safety. It is not expected, that the whole plant including all main and auxiliary equipment will survive the quake without damage. But it must be demanded, that a shutdown of nuclear system is quaranteed without any danger for the surroundings.

Definition of reliability and first passage failure

The ultimate purpose in probabilistic structural analysis to earthquakes is to be able to judge the reliability of a structure which has been designed to withstand these excitations. Let $Y(t)$ be the nonstationary dynamic response (either a deflection, a strain, or a stress) at a critical point in given structure.

A structure will be called reliable, if a charasteristic value of the

structural response Y(t) remains with a certain probability within a prescribed tolerable domain D during the lifetime T_1 of the structure.

Here, reliability means the probability of success (one minus the probability of failure). We shall be concerned only with failures which are the result from dynamic response of stable high structures.

The probability that the structure response Y(t) passes out of the prescribed safety bounds of operation for the first time within a specified time interval, is called the first passage (or first-excursion) probability. It is called also first passage failure of the structure.

Modes of failure

Common to various methods of design of structures under static or dynamic load is the assumption, that a specific value of the maximum stress or certain deformation must not be exceeded within the structure. In the stochastic-process theory description this situation as far as failure is concerned is expressed as follows. We postulate that the structure will fail upon the occurrence of the following event:

1. Y(t) reaches, for the first time, either an upper bound level λ_1 or a lower bound level $-\lambda_2$, where λ_1 and λ_2 are large positive numbers (see Fig. 6). General, in some cases it can be that $\lambda_1=\lambda_2$ or $\lambda_2=0$.

Other failure modes under nonstationary random loadings is fatigue failure.

2. The structure is assumed to callapse under a specific stress level if a certain number of cycles has been reached. The reason for this mode of failure lies in mathematical deterioration.

3. Other modes of failure are: static or dynamic instability, failures due to corrosion, abrasion, etc. which are beyond the scope of this paper.

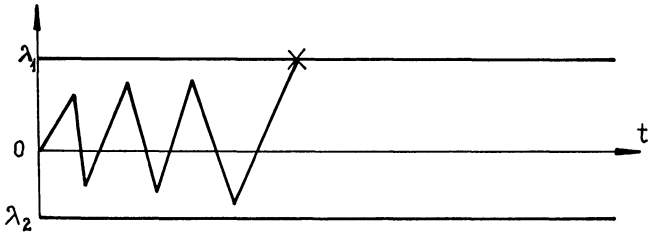

Fig. 6. The non-symetric double sided boundary for first passage problem.

Applying these considerstion to the aseismic reliability problem it can be concluded that:

(i) the question of (mainly low cycle) faituge is interesting in the case of design under OBE. In spite of a relatively small number of quake succesive deterioration of the masonry or concrete may cause failure. But because of lack of information the actual importance of this feature has not yet been clarified.

(ii) it is of primary interest to consider the structure under strong motion earthquakes. In this case the criteria 1. is that of practical importance and the definition of the reliable structure is justified.

It is further assumed that the structural resistance to the first passage failure is deterministic and it does not change with time, such that the prescribed safety bounds, called barrier levels or threshold levels, are constants.

Classification of first-passage problems

The first passage problem can be posed under various kinds of initial conditions (IC) and tolerable domain (safety region) D. General, we consider deterministic IC, for example zero initial conditions or random IC.

In application, two different types of domains D are usually met:

(1) the one-sided boundary problem -Fig. 7 ,

(2) The symmetric double-sided boundary problem (for a symmetric process with zero mean)-Fig.8.

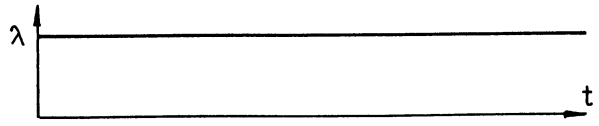

Fig. 7. The one-sided boundary problem.

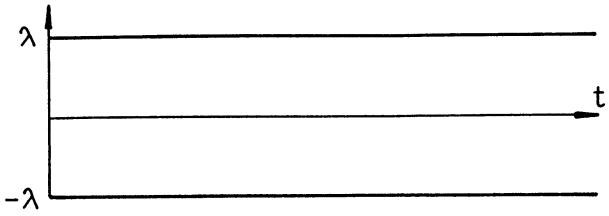

Fig. 8. The symmetric double-sided boundary problem.

First passage probability and prediction of peak factor

Generally speaking, the structural response $Y(\underset{\sim}{x},t)$ is a function of both space $\underset{\sim}{x}$ and time t. In order to estimate the reliability we have to find that specific point $\underset{\sim}{x}_o$ in space, that gives the worst result. The characteristic value of the structural response is defined by

$$Y(t) = \overline{Y}(x_o,t) = \max_{\underset{\sim}{x}} \overline{Y}(\underset{\sim}{x},t). \tag{34}$$

The second part of this relation holds only, if the barrier level of the safety domain D is independed of space. The problem how to find the critical point $\underset{\sim}{x}_o$ is not discussed herein, as it is well known from deterministic calculations.

First passage problem has for two decades been the subject of considerable research, and an exact solution does not exist, [18,25,26,27,35, 36,37]. Below, a relatively simple approximate procedure is presented to predict the maximum responses of multi degree linear system exposed to nonstationary earthquake acceleration process $\ddot{f}_o(t)$. A widely used assumption about the acceleration process $\ddot{f}_o(t)$ is that of a Gaussian probability distribution.

The purpose of this point is to evaluate the factor $r_{T,p}$ by which the response standard deviation $\sigma_y(t)$ must be multiplied to predict the level $y_{T,p}$ below which the absolute value of the response will remain, with probability p, during the time interval (0,T). The task is equivalent to finding the reliability function $R(\lambda,T)$ that the system response fails to make a "passage" across a specified response level λ during the time interval (0,T). In practise we calculate the first passage probability $U(\lambda,T)$ which with reliability function holds the relation

$$R(\lambda,T) + U(\lambda,T) = 1 \tag{35}$$

and for which only approximate solutions has been found. Among them the approach based on envelope crossings, including the clumping effect, seems the most favourable, because of its relative simplicity and numerical efficiency [see 35,36,40].

Most of the first-passage papers indicate exponential decay of the reliability (assuming that $T \to \infty$)

$$R = R(\lambda) = \exp\left[- \int_0^\infty f_\lambda(t)dt, \right] \tag{36}$$

where $f_\lambda(t)$ is the failure rate at time t, for barrier levels $\pm\lambda$. The first excursion probability is equal to

$$U(\lambda) = 1 - \exp\left[- \int_0^\infty f_\lambda(t)dt \right] \tag{37}$$

and for small probabilites (say <0.05) can be approximated by

$$U(\lambda) = \int_0^\infty f_\lambda(t)dt. \tag{38}$$

Taking into account that crossings of the response of lightly damped oscillators tend to occur in clumps one can approximate the failure rate in terms of the mean number of crossings at level λ with positive slope by the process itself $\nu_+(t,\lambda)$ and by its envelope $\nu_e(t,\lambda)$:

$$f_\lambda(t) = 2\nu_+(t,\lambda) \frac{1 - \exp\left[-\nu_e(t,\lambda)/2\nu_+(t,\lambda)\right]}{1 - \nu_+(t,\lambda)/\nu_+(t,0)} \quad . \tag{39}$$

The mean number of crossings λ by the process can be obtained after integrating the joint probability density function of the process y and its derivative $\dot{y}$

$$\nu_+(t,\lambda) = \int_0^\infty \dot{y} f_{y\dot{y}}(\lambda,\dot{y};t)d\dot{y} \quad . \tag{40}$$

Substituting two-dimensional standard Gaussian probability density into equation (40) and carrying out the integration leads to

$$\nu_+(t,\lambda) = \frac{\sigma_{\dot{y}}}{\sigma_y}\sqrt{\left(1 - \rho_{y\dot{y}}^2\right)}\exp\left(- \frac{\lambda^2}{2\sigma_y^2}\right)\left\{e^{-v^2} + \sqrt{\pi}\, v\left[1 + \operatorname{erf}(v)\right]\right\}\frac{1}{2\pi}, \tag{41}$$

where

$$v = \frac{\lambda \rho_{y\dot{y}}}{\sigma_y\sqrt{2(1 - \rho_{y\dot{y}}^2)}},$$

$$\sigma_y^2 = \sigma_y^2(t) = \langle y^2(t)\rangle, \quad \sigma_{\dot{y}}^2 = \sigma_{\dot{y}}^2\, t = \langle \dot{y}^2(t)\rangle, \tag{42}$$

$$\rho_{y\dot{y}} = \rho_{y\dot{y}}(t) = \langle y(t)\dot{y}(t)\rangle / \sigma_y(t)\sigma_{\dot{y}}(t) \quad .$$

A similar analysis can be done for the envelope crossing rate. Taking into account that the response modulating functions (equation (18)) slowly varies with time the envelope crossing rate can be approximated by

$$\nu_e(t,\lambda) \cong \frac{\sqrt{\gamma_2 - \gamma_1^2/\sigma_y^2}}{\sqrt{(2\pi)}}, \qquad (43)$$

where

$$\gamma_q = \gamma_q(t) = 2\int_0^\infty \left|\left[M(t,\omega)\right]\right|^2 \left[\omega + \dot{\delta}(t,\omega)\right]^q S_{\tilde{f}}(\omega)\,d\omega, \quad q = 1,2$$

are time-depended spectral moments, in which

$$\dot{\delta}(t,\omega) = \frac{\partial}{\partial t} \tan^{-1} \frac{\mathrm{Im}\left[M(t,\omega)\right]}{\mathrm{Re}\left[M(t,\omega)\right]} . \qquad (44)$$

Equation (37) can be solved numerically either for the first passage probability $U(\lambda)$ with assumed threshold level λ, or for the peak value of response λ_R. The peak factor may be defined as

$$r_R = \frac{\lambda_R}{\max \sigma(t)} \qquad (45)$$

where $\max \sigma(t)$ is the standard deviation of the response. In practical estimates of the typical peak response, median peak values $u_{0.5}$ and median peak factors $r_{0.5}$ can be applied.

The excellent numerical analysis of the reliability of the industrial concrete chimney 160m high is presented by Zembaty in the paper [40].

REFERENCES

1. Amin M. and Ang A., Nonstationary Stochastic Model of Earthquake Motions, Proc. ASCE, 94, EM2, 559, 1968.
2. Barstein M.P., Application of Probability Methods for Design, The Effect of Seismic Forces on Engineering Structures, Proc. 2nd WCEE, Tokyo, Japan, 1960.
3. Bogdanoff J.L. et al, Response of a Simple Structure to a Random Earthquake-type Disturbance, Bull. Seism. Soc. Am. Vol 51, 1961.
4. Bolotin V.V., Statistical Methods in Structural Mechanics, San Francisco, Holden-Day Inc., 1969.

5. Bolotin V.V., Statistical Theory of the Aseismic Design of Structures, Proc. 2nd WCEE, Tokyo, Japan, 1960.
6. Blume J., Structural Dynamics in Earthquake Resistant Design, Transactions ASCE 125, 1088, 1960.
7. Bycroft G.N., White Noise Representation of Earthquakes, Proc. Pap. 2434, J. Eng. Mech. Div. ASCE, vol. 86, no. EM2, April 1960.
8. Clough R.W. and Penzien J., Dynamics of Structures, McGraw Hill, 1975.
9. Chmielewski T. and Zembaty Z., The Dynamic Response of Discrete Systems to Nonstationary Random Excitations, Archives of Civil Engineering, vol. XXX, 1984 (in Polish).
10. Chmielewski T., Probabilistic Methods in Structural Dynamics, Technical University of Opole, 1982 (in Polish).
11. Cornell C.A., Stochastic Process Models in Structural Engineering, Technical Report No 34, Dept. of Civil Engineering, Stanford University, Stanford, Calif., USA.
12. Housner G.W., Characteristics of Strong Motion Earthquakes, Bull. Seism. Soc. Am. vol 37, no. 1, 1947.
13. Housner G.W., Properties of Strong Ground Motion Earthquakes, Bull. Seism. Soc. Am. vol 45, no. 3, July 1955.
14. Jenings P.C. et al, Simulated Earthquake Motions, Tech. Rep. Earth. Eng. Res. Lab., Cal. Tech. Pasadena, Cal. USA, April 1968.
15. Kanai K., An Empirical Formula for the Spectrum of Strong Earthquake Motions, Bull. Earthquake Res. Inst., University of Tokyo,39,85,1961.
16. Lee J., A New Formulation of the Linear Dynamic Response to Random Excitation, J. Sound and Vibration, vol. 35, no. 1, 1974.
17. Lin Y.K., Application of Nonstationary Shot Noise in the Study of System Response to a Class of Nonstationary Excitations, J. Appl. Mech., vol. 30, series E, no. 4, 1963.
18. Lin Y.K., Probabilistic Theory of Structural Dynamics, McGraw Hill, 1975.
19. Lennox W.D. and Fraser D.A., On the First Passage Distribution for the Envelope of a Nonstationary Narrow Band Stochastic Process, J. Applied Mech. 1974.
20. Liu S.C., Evolutionary Power Spectra Density of Strong Motion Earthquakes, Bull. Seism. Soc. Am. vol. 60, no. 3, 1970.

21. Newmark N.M. and Hall W.J., A Rational Approach to Seismic Design Standarts for Structures, Proc. 5th WCEE, Rome, Italy, 1973.

22. Newmark N.M. and Rosenblueth E., Fundamentals of Earthquake Engineering, Prentice-Hall, Inc., Englewood Cliffs, N. Y., 1971.

23. Priestley M.B., Evolutionary Spectra and Nonstationary Processes, J. Royal Statistical Society, vol. 27, 1965.

24. Priestley M.B., Power Spectral Analysis of Nonstationary Random Proceses, J. Sound and Vibration, vol. 6, 1976.

25. Rice S.O., Mathematical Analysis of Random Noise, Bell System Technical Journal, Part I: 23,282, 1944; Part II: 24,46,1945.

26. Roberts J.B., An Approach to the First Passage Problem in Random Vibration, J. Sound and Vibration, 8, 2,301, 1968.

27. Roberts J.B., Probability of First Passage Failure for Nonstationary Random Vibrations, J. Applied Mechanics, 42, 716, 1975.

28. Rosenblueth E. and Bustamante J., Distribution of Structural Response to Earthquakes. Proc. Pap. 3173, J. Eng. Mech. Div. ASCE, vol. 88 no. EM3, June 1962.

29. Shinozuka M. and Sato Y., Simulation of Nonstationary Random Processes, Proc. ASCE, 93, EM1, 11, 1967.

30. Shinozuka M., Random Processes with Evolutionary Power, J. Eng. Mech. Div., ASCE, vol. 96, EM1, August 1970.

31. Sobczyk K., Methods of Statistical Dynamics, PWN, Warsaw 1973 (in Polish).

32. Spanos P.Th.D. and Lutes L.D., Probability Response to Evolutionary Process, J. Eng. Mech. Div. ASCE, vol. 106, EM2, April 1980.

33. Tajimi H., A Statistical Method of Determining The Maximum Response of a Building Structure During an Earthquake, Proc. 2nd WCEE, 2,781, Science Council of Japan, 1960.

34. Thomson W.T., Spectral Aspect of Earthquakes, Bull. Seism. Soc. Am. vol. 49, 1959.

35. Vanmarcke E.H., On the Distribution of the First Passage Time for Normal Stationary Random Processes, J. Appl. Mech., 42, 215, 1975.

36. Yang J.N., Nonstationary Envelope Process and First Excursion Probability. Journal of Structural Mechanics, ASME, vol. 1, 1972.

37. Yang J.N., First Excursion Probability in Non-stationary Random Vibration, J. Sound and Vibration, vol. 27, 1973.

38. Yang J.N. and Lin Y.K., Tall Building Response to Earthquake Excitations, J. Eng. Mech. Div., ASCE, EM1, August 1980.

39. Zembaty Z., Nonstationary Random Vibration Analysis of the Seismic Response of Chimneys, Proc. 5th Int. Chimney Congress, Essen, October 1984.

40. Zembaty Z., On the Reliability of Tower Shaped Structures under Seismic Excitations, Earthquake Engineering and Structural Dynamics (to be published in 1987).

RELIABILITY OF PARTLY DAMAGED STRUCTURES

F. Vasco Costa
Consultant, Lisbon, Portugal

Summary

Reliability and optimization studies are usually based on the consideration of the probability of being reached a particular state of damage regarded as ultimate. In case of structural systems that pass through intermediate states of partial damage with a much higher probability of being reached than that of the ultimate state, the expectation of the expenses incurred when states of partial damage are reached are to be taken into consideration when alternative designs are to be compared.

Introduction

Engineers are expected to design economical jet reliable structures. But how reliable needs each particular structure to be designed ? This will mainly depend on the importance of the consequences of the eventual damage of the structure.

From a pure economical point of view, engineering structures are to be designed so as to minimize their "generalized cost", meaning by that the sum of their initial cost with the present value of all future expenses with their operation and maintenance plus the expectation of direct and indirect expenses in case of damage.

As the sudden collapse of very large structures, like high dams, long suspended bridges and offshore platforms built in deep water, are the events that attract the attention of all who are interested in structural realiability, there is a tendency to assume that for all structures exists a well defined frontier between safe and unsafe designs.

For a large variety of engineering structures such frontier does not exist. This is the case, for instance, with rubble-mound breakwaters, which even after being partly damaged can remain for long years in service.

The selection among alternative designs of engineering structures for which does not exist a clear frontier between safe and unsafe design is discussed in the following paragraphs.

Expectation of the Expenses Incurred in Case of Damage

The reliability of the members of a structure can increase or decrease while in use, depending on their type and function to be fulfilled. Hardening of concrete, plastic yielding at the hinges of steel members, and ajustments in the position of the bloks of an armour, can contribute to increase the reliability of the members; weathering, wearying, fatigue and damage accumulation can contribute to decrease the reliability of the members of a structure and, consequently, of the structure as a whole.

Some types of engineering structures behave as series or brittle systems; as soon as one member fails, the whole structure collapses. Some other types behave as parallel or ductile systems; the failure of one member does not necessarily imply the collapse of the structure. The failure of a member can even, in case of redundancy of members, give occasion to adjustments that will render the structure more stable. (Thoft-Christensen and Baker, 1982, Ferry and Castanheta, 1985, Baker and Turner, 1987, Vasco Costa, 1983)

The consequences of the failure of a structure can also vary between wide limits, from temporary restrictions in its utilization to the catastrophic destruction of property and lives.

By recourse to the concept of expectation all such circunstances can be taken into consideration in the design of engineering structures. As expectation is to be understood the probability of occurance of an event multiplied by the amount of all the direct and indirect expenses incurred if such event takes place. Not only the probability of the event to be considered and the amount of expenses incurred varies from member to member of a same structure, but as

well from structure to structure, depending on the function to be fulfilled by the member and by the structure.

Evaluation of the Generalized Cost of a Structure

In structural reliability analysis it is costumary to consider only one "failure state" or "limit state", which can be a cracking, a deformability, a serviceability or an ultimate state. As most structures can be maintained in service, certainly with some restrictions, even after being damaged to a small or large degree, let us see how to evaluate their reliability taking into consideration such circunstances.

We are all familiar with problems posed by restrictions caused by the partial damage of a structure: limitation of loads on certain floors of a building after a fire or earthquake; reduction of traffic velocity on a road which pavement is under repair; extra care during the berthing of ships to a damaged jetly; emergency measures after a flood.

If we really want to design economic jet reliable structures we have to quantify the probabilities of the different degrees of damage being reached and to identify and quantify also the diferent consequences that can result from the different degrees of damage to which a structure can be submitted.

Although most members of a structure and most types of structures present several modes of failure during their expected life, which are not necessarily independent of each other, it will be assumed in what follows, for the sake of clarity, that they can be dealt with as if they were just one mode of damage, which can go through increasing degrees of damage, some of them permiting the utilization, with light or severe restrictions, of the structure.

The probability of a certain member of a structure being damaged can be evaluated, in case of being known the distribution function F_R of its resistance and the distribution function F_S of the load effects, by the expression (Thoft-Christensen and Baker, 1982, pg 71)

$$P_f = P(R-S \leqslant 0) = \int_0^{+\infty} F_R(x)\, f_S(x)\, dx \qquad (1)$$

The probability of damage due to load effects with values in the internal x' x" can be evaluated by recourse to the same expresssion (see fig 1).

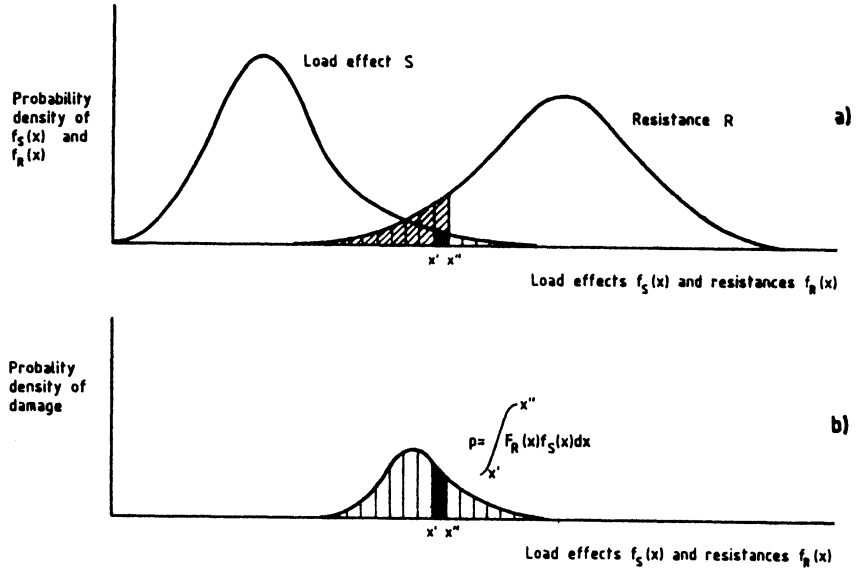

Fig. 1 - Probability of Damage for Load Effects in the Interval x' x"

The degrees of damaged suffered by a member of a structure, because dependent of the randomness of its resistance, are not necessarily proportional to the magnitude of action effects that cause the damage. Notwithstanding it can reasonably be assumed that the distribution function of the degree of damage will be quite similar to that of the probability of the action effects (see fig 2a).

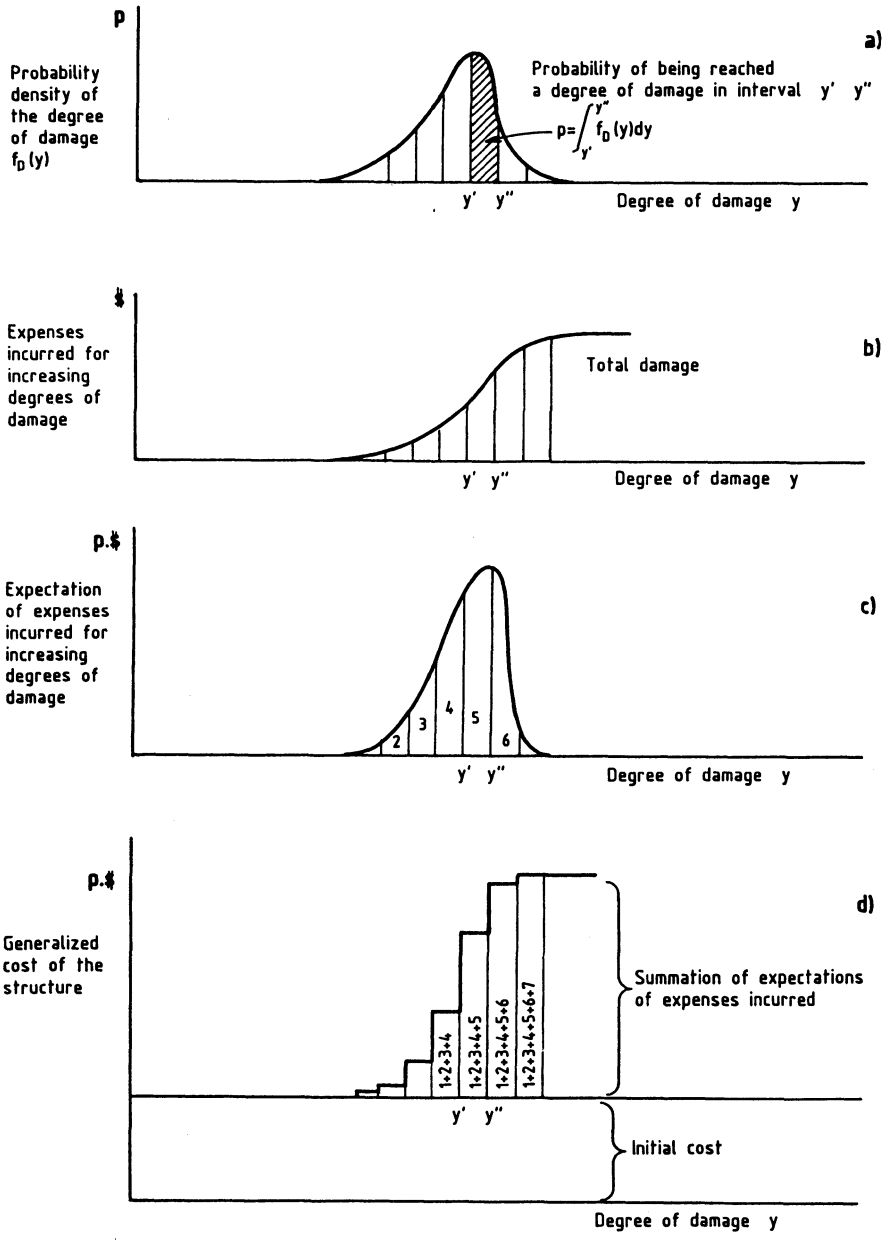

Fig 2 - Evaluation of The Generalized Cost of an Engineering Structure

Direct expenses, like those resulting from repairs, but also indirect expenses, like those resulting from restrictions in service and to indemnities to third parties, can be expected to increase with the degree of damage suffered by a structure. Not so with the probability of occurance of different degrees of damage, the same happening with the corresponding expectations. As is low the probability of being reached large degrees of damage, the expectation of the very large expenses being incurred in case of a high degree of damage, is also low (see fig 2c). The larger values of the expectation of expenses will correspond to intermediate degrees of damage with large probability of occurance, in spite of the fact that they do not imply very large expenses.

The circunstance that the expectation of expenses resulting from intermediate degrees of damage can be much larger than that resulting from higher degrees of damage, will imply a revision on the attitude of designers. Instead of caring for only a particular state — of deformability or of serviceability or an ultimate state — they better consider the successive degrees of damage through which can go a structure before is reached a collapse state.

From the considerations just presented it can be inferred that for reducing the generalized cost of some types of structures it will be more convenient to take measures to reduce the probability of occurance of relatively small damages and their consequences than to only care, as it has been the current practice, for a particular limit state of serviceability or an ultimate state.

How to Compare Alternative Designs Taking into Account Successive Degrees of Damage

The taking into consideration successive degrees of damage does not imply a much more complex analytic treatment than the consideration of only a limit state.

Let us denote:

C_o - initial cost of an alternative design to be considered;

d - number of degrees of damage to be considered for each mode of damage of such design;

m - number of its modes of damage;

n - number of periods of time the structure will be kept in service;

r - rate of interest being practiced;

$p^i_{11}, p^i_{12} \ldots p^i_{21} \ldots p^n_{dm}$ - probability of each degree of damage being reached in each mode of damage and during each period of time i;

$E^i_{11}, E^i_{12} \ldots E^i_{21} \ldots E^n_{dm}$ - direct and indirect expenses incurred for each degree and mode of damage and period of time i;

$M_1, M_2, \ldots M_n$ - maintenance and operation expenses during each period of the structure life,

$P_1, P_2, \ldots P_n$ - probability of survival of the structure, i.e., probability of its being maintained in service at the end of each period of time.

Assuming independence of occurance for the different degrees and modes of damage, the most economical design on the long run among alternative designs to be considered, will be the one that will minimize the sum

$$C_o + \quad \text{initial cost}$$

$$+ (M_1 + p^1_{dm} E^1_{dm}) (1+r)^{-1} P_1 \quad \text{present value of expenses incurred during the first period}$$

$$+ (M_2 + p^2_{dm} E^2_{dm}) (1+r)^{-2} P_1 P_2 \quad \text{present value of expenses incurred during second period}$$

$$+ \ldots\ldots\ldots\ldots$$

$$+ M_n + p^n_{dm} E^n_{dm} (1+r)^{-n} P_1 P_2 \ldots P_{n-1} \rightarrow \min \qquad (2)$$

The probability of the different degrees of damage being reached will possibly, due to ajustments on the position of some elements and the hardning of some materials, decrease with time, but more likely it

will increase with time, due to accumulated damages and to weathering. Expenses with the maintenance, operation and the direct and indirect consequences of the different degrees of distinct modes of damage, will likely increase during the life of the structure.

In case, for the sake of simplicity, such probabilities and expenses are assumed to be kept constant, and the probabilities of survival assumed to be equal to unity, the former expression can be given a much simpler form (Vasco Costa, 1968);

$$C_o + a_{\overline{n}|} \left(M + \sum p_{dm} E_{dm}\right) \longrightarrow \min \qquad (3)$$

where $a_{\overline{n}|}$ is the series present value factor,

$$a_{\overline{n}|} = (1+r)^{-1} + (1+r)^{-2} + \ldots + (1+r)^{-n} \qquad (4)$$

Expression (3) can be phrased as follows: among alternative designs is to be selected the one that will permit the minimization the initial cost added to the present value of future maintenance and operation expenses plus the expectation of all direct and indirect expenses incurred in case of intermediate and final degrees of damage considered being reached.

The higher the expectation of an intermediate degree of damage, the greater the interest in reducing its probability of ocurrance and the corresponding expenses incurred, if necessarily increasing the initial cost of the structure. On the other hand, the higher interest rates being practiced the greater the interest in reducing such initial cost, possible at the cost of larger maintenance and repair expenses and, even, of an increase in the probability of the structure being submitted more frequently to damage.

Final Considerations and Recommendations

The current practice of basing the evaluation of the reliability of structures on the consideration of only a particular limit state - of cracking, or of deformability, or of serviceability, or of collapse - is not adequate in the case of structures that pass through intermediate states or degrees of damage before the limit state considered is reached.

The evaluation of the overall reliability of such structures requires the consideration, for each degree of damage in each of the possible modes of damage, not only of the probability of being reached but as well of all the expenses incurred, not only with repairs but as well indemnities to third parties affected by restrictions on the utilization of the structure.

As the probabilities of being reached intermediate states of damage are always much larger than that of being reached a limit state of serviceability or of collapse (fig 2a), the expectation of expenses incurred when intermediate states or degrees of damaged are reached can much contribute to increase the generalized cost of the structure (fig 2c).

In order to reduce the expectation of expenses incurred when intermediate states of damage are reached, measures are to be taken to reduce not only the probability of their being reached but as well the consequent expenses incurred.

Careful control of the quality of the elements of a structure, good supervision during its erection, and periodic inspection and maintenance operations, will permit the reduction of the probability of intermediate degrees of damage being reached.

Measures taken to render possible prompt repairs and to reduce restrictions in the utilization of a structure, can contribute to minimize expenses incurred when are reached intermediate states of damage.

Acknowledgement

For most valuable comments to a draft of this communication thanks are due to Mário Castanheta, of the National Laboratory of Civil Engineering, Lisbon, Portugal.

References

Baker, M. J. & R. Turner, "Structural System Reliability Analysis Using Multi-Dimensional Limit State Criteria", 1st Working Conference

on Reliability and Optimization of Structural Systems, Aalborg, Denmark, 1987.

Corotis, Ross B., "Failure Cost Design of Random Structural Systems" Report, Department of Civil Engineering, The John Hopkins University, 1986.

Ferry Borges, J. and M. Castanheta, "Structural Safety", National Laboratory of Civil Engineering, Lisbon, Portugal, 3rd Ed. 1985.

Thoft-Christensen, P. and J.D. Sorensen, "Recent Advances in Optimal Design of Structures from a Reliability Point of View", Int. Journal of Quality & Publicity Management, Vol. 4, Nº 1, 1987.

Thoft-Christensen, P. and Machel J. Baker, "Structural Reliability Theory and Applications", Berlin, Springer-Verlag, 1986.

Vasco Costa, F., " Optimization of Structures", Eight Congress of the Int. Ass. for Bridge and Structural Engineering, New York, 1968.

Vasco Costa, F., " The Spreading of Damage in Breakwater Armours", The Dock & Harbour Authority, March, 1983.

CONTROLLED UNRELIABLE PROCESS WITH EXPLICIT OR IMPLICIT BREAKDOWNS AND MIXED EXECUTIVE TIMES

B. N. Dimitrov, N. V. Kolev, P. G. Petrov
Mathematical Institute, Bulgarian Academy of Sciences
1090 Sofia, P. O. Box 373

1. Introduction and model description.

This work continues the developments of the autors [5,10], concerning the minimization of the total executive time for unreliable processes until their correct finish by the help of suitable introduced controll schedule of tests, copies and check-points. It is supposed that there is an input flow of tasks (jobs, problems, service times) which must be executed for a given time X on a given apparatus (server, computer system etc.). The value X can be a mixture $X = p_1X_1+\ldots+p_rX_r$ of r different values $X_1,\ldots,X_r$, where p_i and X_i are known, but it is never previously clear which value of X_i will occur (we say the task is of type i, $i=1,\ldots,r$). Simultaneously during the executive time X some undesirable events (breakdowns, catastrophes) can arize in a random way and lead to execution interruption or to incorrect final results. To have a guaranteed correct final result one needs a control test to detect the appearance of incorrectness in the case of implicit breakdowns. The execution must be repeated from the origin until no breakdown is detected. In the case of explicit breakdowns the repetitions from the origin are necessary

This work is partially supported by the Committee of Science by the Bulgarian Conncil of Ministers, according to Contract No 43/87.

until no breakdown happens during the execution time. These repetitions make the total executive process duration $\tau(X)$ eventually greater than X.

Several autors like Chandy and others [3,4], IBM [6], Kovalenko and others [9], Brodezki [2], Hadjinov [8], Barosov [1], and the autors [5,10] notice that it will be is profitable to introduce a strategy for making intermediate copies (check-points) to remember the achieved correct executive statement. If a breakdown appears or is detected, the repetition starts (restsrts) from the last successfully copied statement. Every rule for determination of the copy epochs during the executive time of a separate task is said to be a control one. When this rule is given with the sequece $\{a_k\}$, where a_k is the interval of a pure executive time between the k th and the $(k-1)$ th control epochs, we say that $\{a_k\}$ is a control schedule.

The aim of the works mentioned above is to determine the optimal control rule under some assumptions about the elements of the executive process when some unreliability is supposed.

In our paper here we have the next suppositions:

a) there is a flow of breakdowns which forms a stationary Poisson process with intensity $\gamma > 0$;

b) during the execution time of a task only one type of breakdowns can occur, namely (i) - explicit breakdowns or (ii) - implicit breakdowns. The corresponding cases will be called, if necessary, as case i and case ii and their characteristics will be marked with the subscripts (i) or (ii) respectively;

c) the required pure execution time X (if the apparatus is absolutely reliable) has the form of a mixture $X=p_1X_1+\ldots+p_rX_r$, where X_j are known random variables as well as $p_j > 0$ and $p_1+\ldots+p_r=1$. We suppose that the distribution functions (d.f.) $A_j(x)=P(X_j<x)$ are given $j=1,2,\ldots,r$;

d) the k th next check-point during the execution of task is a random variable (r.v.) which consists of time $\theta_k^{(i)}$- the copy time duration for the case i , and $\delta_k^{(ii)}$ or $\delta_k^{(ii)}+\theta_k^{(ii)}$ for the

case *ii*. Here $\delta_k^{(ii)}$ is the time duration of a control test of implicit breakdowns; $\theta_k^{(ii)}$ is the copy duration which is used if no breakdown is detected; otherwise no copy is necessary before the successful repetition of the defective executive stage;

e) the sequences $\{\theta_k^{(i)}\}_{k=1}^{\infty}$, $\{\delta_k^{(ii)}\}_{k=1}^{\infty}$, $\{\theta_k^{(ii)}\}_{k=1}^{\infty}$ form renewal processes with d.f.s $\theta^{(i)}(x)$, $D^{(ii)}(x)$, $\theta^{(ii)}(x)$, and finite expected life-times θ^{i}, δ^{ii}, θ^{ii}; all the times for the elimination of defects after explicit or implicit breakdowns are equal to zero (instanteneous renevals);

f) the control shedule $\{a_k\}$ of check-points is valid during a separate executive times of a task and forms a deterministic process;

g) the optimal control problem is formulated as follows: Let $\tau_{(i)}(X,\{a_k\},\{\theta_k^{(i)}\})$ and $\tau_{(ii)}(X,\{a_k\},\{\delta_k^{(ii)}\},\{\theta_k^{(ii)}\})$ be the total executive time durations (with an unreliable apparatus) for a task requiring X executive time units (for absolutelly reliable apparatus), then the question is how to chose the control shedule $\{a_k^*\}$, such that the expected total executive time to be minimal, i.e.

$$E\tau_{(l)}(X,\{a_k^*\},\ldots) = \inf_{\{a_k\}} E\tau_{(l)}(X,\{a_k\},\ldots) \quad (l)=(i) \text{ or } (ii)$$

The sequence $\{a_k^*\}$ will be called optimal control schedule.

Furhter we shall use the capital Latin letters for the d.f.s of the considered r.v.s notations and the corresponding Greek letters for their Laplace-Stilties transforms (LST) notations. For example

$$\alpha_j(s) = Ee^{-sX_i} = \int_0^{\infty} e^{-sx} dA_j(x); \quad \theta(s) = \int_0^{\infty} e^{-sx} d\theta(x).$$

2. Some auxiliarry results

We shall need the next result,

Lemma 1. Under the above assumptions a)-g) hold:

- the LST of the total process duration whitout any control shedule is determinated by the expressions

$$\tau^{*}_{(i)}(s) = Ee^{-s\tau_{(i)}(X)} = \sum_{j=1}^{r} p_j \alpha_j(s+\gamma)\left\{1 - \frac{\gamma}{s+\gamma}\,[\,1-\alpha_j(s+\gamma)]\right\}^{-1};$$

$$\tau^{*}_{(ii)}(s) = Ee^{-s\tau_{(ii)}(X)} =$$

$$= \sum_{j=1}^{r} p_j\ \alpha_j(s+\gamma)\delta(s)\left\{1-[\alpha_j(s)-\alpha_j(s+\gamma)]\delta(s)\right\}^{-1}.$$

- the corresponding expected total process durations are

$$E\tau_{(i)}(X) = \gamma^{-1}\sum_{j=1}^{r} p_j\,[\ (\alpha_j(\gamma))^{-1} - 1];$$

$$E\tau_{(ii)}(X) = \sum_{j=1}^{r} p_j(EX_j+\delta)\,(\alpha_j(\gamma))^{-1}.$$

Proof. The proof is a simple consequence of Lemma 1 from [5], where this result is given for the partiqular case of $r=1$. Taking into account that now X is mixture of r.v.s $X_1,\ldots,X_r$, we get our assertion from the equation $\tau_l(X) = \sum_{j=1}^{r} I_{\{X=X_j\}}\tau_l(X_j)$, where $I_{\{X=X_j\}}$ is the indicator function of the random event $X=X_j$ (i.e. the task is of type j).

Lemma 2. If for all j the values X_j are known constants, i.e. if $P(X_j=x_j) = 1$ for given j and $0 < x_1 < \ldots < x_r$, then for any given control schedule $\{a_k\}$ holds

$$E\tau_{(i)}(X,\{a_k\},\{\theta_k\}) = \gamma^{-1}\sum_{j=1}^{r}\left\{ p_j\left[\, e^{\gamma(x_j-b_{n_j})} - 1\,\right] + \right.$$

$$\left. + \left[\, 1 - \sum_{q=1}^{j-1} p_q \,\right] \sum_{k=n_{j-1}+1}^{n_j} \left[\, (\theta(\gamma))^{-1} e^{\gamma a_k} - 1\,\right]\right\};$$

$$E\tau_{(ii)}(X,\{a_k\},\{\delta_k\},\{\theta_k\}) =$$

$$= \sum_{j=1}^{r}\left\{ p_j\,\left[\, n_j\theta + \delta + (x_j-b_{n_j})e^{\gamma(x_j-b_{n_j})}\,\right] + \right.$$

$$\left. + \left[\, 1 - \sum_{q=1}^{j-1} p_q \,\right] \sum_{k=n_{j-1}+1}^{n_j} (a_k+\delta)e^{\gamma a_k}\right\}.$$

Here the following notations $b_0=0$, $b_n=a_1+\ldots+a_n$, $n_0=0$,

$n_j = max(n: b_n < x_j)$, $\delta = E\delta_k$, $\theta = E\theta_k$, are used , as well as the convention $\sum_{k=1}^{0} p_k = 0$.

Proof. First of all we mention, that a schedule interval a_k and the next check-point duration form an interval of which the total executive duration until its sucessful finish is $\tau_{(l)}^{(k)} = \tau_{(l)}(a_k) + \theta_k$, $l=(i),(ii)$. There are exactly n_j such intervals in the pure executive time x_j (which realizes with probability p_j) and anincomplete interval of lenght $(x_j - b_{n_j})$ which finishes eventually whitout any copy, in difference of the first ones. In view of the particular form of resulrt b) of Lemma 1 for each one of the mentioned cases as well as the "lack of memory" property of the exponential distribution, according which the r.v.s $\left\{\tau_{(l)}^{(k)}\right\}_{k=1}^{\infty}$ are mutually independent and

$$\tau_{(l)}(x_j, \{a_k\}, \ldots) = \sum_{k=1}^{n_j} \tau_{(l)}^{(k)} + \tau_{(l)}(x_j - b_{n_j}),$$

we get the assertion of Lemma 2 after simply rearrangments of the corresponding results.

Corrolary 1. Under a given control shedule $\{a_k\}$ with $\sum_{k=1}^{\infty} a_k = \infty$ and a given mixture according to the above condition c) the expected executive times are determined by the expressions

$$E\tau_{(i)}(X, \{a_k\}, \{\theta_k\}) = \gamma^{-1} \sum_{j=1}^{r} p_j \left\{ \sum_{k=1}^{\infty} \left[(\theta(\gamma))^{-1} e^{\gamma a_k} - 1 \right] \left[1 - A_j(b_k) \right] + \right.$$

$$\left. + \sum_{k=0}^{\infty} \int_{b_k}^{b_{k+1}} \left[e^{\gamma(x-b_k)} - 1 \right] dA_j(x) \right\};$$

$$E\tau_{(ii)}(X, \{a_k\}, \{\delta_k\}, \{\theta_k\}) =$$

$$\sum_{j=1}^{r} p_j \sum_{k=1}^{\infty} \left\{ (a_k+\delta)\,[1-A_j(b_k)]e^{\gamma a_k} + \theta(k-1)\,[A_j(b_k)-A_j(b_{k-1})] \right\} +$$

$$+ \sum_{j=1}^{r} p_j \sum_{k=0}^{\infty} \int_{b_k}^{b_{k+1}} (x - b_k + \delta)\, e^{\gamma(x-b_k)}\, dA_j(x).$$

Here the notations of Lemma 2 are used.

Proof. These results follow from Lemma 2, Fubini's theorem and some simple transformations of the obtained relations. It is sufficient to remark that $n_j=k$ when $X_j \subseteq [b_k, b_{k+1}]$, and to use it in the expressions

$$E_j g(x) = \int_0^{\infty} g(x)\,dA_j(x) = \sum_{k=0}^{\infty} \int_{b_k}^{b_{k+1}} g(x)\,dA_j(x).$$

Definition. We say that a control shedule $\{a_k\}$ is an uniform one iff $a_k=a > 0$ for each $k=1,2,\ldots$

Corollary 2. If the separate required process durations X_j of a task are exponentially distributed with parameters $\lambda_j > 0$ and if the control schedule $\{a_k\}$ is an uniform one, then in the case $\gamma \neq \lambda_j$, $j=1,2,\ldots,r$ the expected total process durations are presented by the expressions

$$E\tau_{(i)}(X, \{a_k\}, \{\theta_k\}) = \gamma^{-1} \sum_{j=1}^{r} p_j \left(1-e^{-\lambda_j a}\right)^{-1} \left\{ \lambda_j (\gamma-\lambda_j)^{-1} \left[e^{a(\gamma-\lambda_j)} - 1 \right] + \right.$$

$$\left. + (\theta(\gamma))^{-1} e^{a(\gamma-\lambda_j)} - 1 \right\};$$

$$E\tau_{(ii)}(X, \{a_k\}, \{\theta_k\}, \{\delta_k\}) = \sum_{j=1}^{r} p_j \left\{ \lambda_j (\gamma-\lambda_j)^{-1} \left[(a+\delta) e^{a(\gamma-\lambda_j)} - \delta \right] + \right.$$

$$\left. + \lambda_j (\gamma-\lambda_j)^{-2} \left[1-e^{a(\gamma-\lambda_j)} \right] + (a+\delta) e^{a(\gamma-\lambda_j)} + \theta e^{-\lambda_j a} \right\} (1-e^{-\lambda_j a})^{-1};$$

if there is an index j for which $\lambda_j=\gamma$, then the j th expressions in the general form of the summands is exchanged by the forms

$$p_j\ [\ a\gamma\ +\ (\theta(\gamma))^{-1}\ -\ 1\ ]\,(1-e^{-\gamma a})^{-1} \qquad \text{for the case } i$$

and

$$p_j\ [\ \gamma a(\delta+\ldots\tfrac{a}{2}\ldots)+a+\delta+\theta e^{-\gamma a}]\,(1-e^{-\gamma a})^{-1} \qquad \text{for the case } ii$$

correspondingly.

Proof. Under the considered condition we have $A_j(x)= 1-e^{-\lambda_j x}$, $a_k=a$, and $b_k=ka$. By putting these values in the expressions of Corollary 1 and taking into account that $1-A_j(b_k)=e^{-k\lambda_j a}$,

$$A_j(b_{k+1})-A_j(b_k) = e^{-k\lambda_j a}(1-e^{-\lambda_j a}),\quad dA_j(x) = \lambda_j e^{-\lambda_j x}dx,$$

after not very complicated calculations, we confirm the truth of Corollary 2.

3. The optimal control schedules

Now we turn to the solution of the optimal control problem, formulated in part 1. As in [5] we shall establish the optimal properties of the uniform control schedules in both considered cases. We shall use the results of [5] to simplyfy some arguments here.

Theorem 1. Under the conditions of Lemma 2 the optimal control schedule $\{a_k\}$ is a partially uniform one: over the intervals $(x_k, x_{k+1}]$ all check-points $b_j^{(k)}$ are equidistant and form an arithmetical progression with first term $b_0^{(k)}=x_k$ and difference a_k^* of the form

$$a_k^* = (x_{k+1} - x_k)(n_k^* + 1)^{-1}.$$

Here the integers n_k^* are determined by the rule

$$n_k^* = max(n:\ x_{k+1}- x_k \le z_n),$$

where the numbers z_n form an increasing sequence $\{z_n\}$, defined for any fixed $n=1,2,\ldots$ as a root of the equations

$$[1+(\theta(\gamma))^{-1}(n+1)]e^{\gamma z(n+2)^{-1}}-[1+(\theta(\gamma))^{-1}n]e^{\gamma z(n+1)^{-1}}=1 \text{ for case } i$$

and

$$(z+n\delta)\left[e^{\gamma z n^{-1}} - e^{\gamma z (n+1)^{-1}}\right] - \delta e^{\gamma z (n+1)^{-1}} = \theta \quad \text{for case } ii.$$

Proof. We use the results and the notations of Lemma 2. The terms of any optimal control schedule $\{a_k^*\}$ are among the solutions of the system of equations

$$\frac{\partial}{\partial a_k} E\tau_{(l)}(X,\{a_k\},\ldots) = 0\ ,\ k=1,2,\ldots,\ (l)=(i),(ii) \qquad (1)$$

For simplicity we give the arguments only in the case $r=2$. It is easy to verify that in the case i of the explicit breakdowns the system (1) takes the form

$$e^{\gamma a_k} = \theta(\gamma)\left[p e^{\gamma(x_1-b_{n_1})} + (1-p)e^{\gamma(x_2-b_{n_2})}\right] \text{ for } k=1,2,\ldots n_1$$

$$e^{\gamma a_k} = e^{\gamma(x_2-b_{n_2})} \qquad \text{for } k=n_1+1,\ldots,n_2 \qquad (2)$$

Obviously all distants a_k satisfying system (2) are equal on the set $k=1,2,\ldots,n_1$ as well as on the set $n_1+1,\ldots,n_2$. Further we have to establish the extremum types of $E\tau_{(i)}(X,\{a_k\},\{\theta_k\})$ in the found points a_k^*. To this end we verify that the determinants

$$A_m = \mathrm{Det}\left[\frac{\partial^2}{\partial a_j \partial a_s} E\tau_{(i)}(X,\{a_k\},\{\theta_k\})\right]_{j,s=1}^{m}$$

are positive for any $m=1,2,\ldots,n_2$. According to Silvester criterion ([7],p.611), the quadratic form with coefficients

$a_{js} = \frac{\partial^2}{\partial a_j \partial a_s} E\tau_{(i)}(\ldots)$ is positive definite. It is sufficient to state [7] that the function $E\tau_{(i)}(\ldots)$ takes its minimal value at the points $\{a_k^*\}$. These points really form a partially uniform control schedule as mentioned in Theorem 1.

For $j=1,2,\ldots,n_1$ we have

$$\frac{\partial^2 E\tau_{(i)}}{\partial a_j^2} = \frac{\gamma}{\theta(\gamma)} e^{\gamma a_i + p\gamma e^{\gamma(x_1-b_{n_1})} + (1-p)\gamma e^{\gamma(x_2-b_{n_2})}} > 0; \quad (3)$$

for $j=n_1+1,\ldots,n_2$

$$\frac{\partial^2 E\tau_{(i)}}{\partial a_j^2} = \gamma(1-p)\left[e^{\gamma a_j} + e^{\gamma(x_2-b_{n_j})}\right] > 0 ; \qquad (4)$$

for $j=1,2,\ldots,n_1$, $s=n_1+1,\ldots,n_2$ and $j=n_1+1,\ldots,n_2$, $s=1,2,\ldots,n_1$ and $j\neq s$, $j,s=n_1+1,\ldots,n_2$ we have

$$\frac{\partial^2 E\tau_{(i)}}{\partial a_j \partial a_s} = (1-p)\gamma e^{\gamma(x_2-b_{n_2})} > 0 ; \qquad (5)$$

and for $j\neq s$, $j,s=1,2,\ldots,n_1$

$$\frac{\partial^2 E\tau_{(i)}}{\partial a_j \partial a_s} = p\gamma e^{\gamma(x_1-b_{n_1})} + \gamma(1-p)e^{\gamma(x_2-b_{n_2})} > 0 ; \qquad (6)$$

It is easy to see that the principal minors A_m of the matrix of the mixed derivatives are positive taking into account relations (3) - (6).

Keeping the same plan for the case *ii* we convince ourself, that system (1) is equivalent to the next one

$$[1+\gamma(a_k+\delta)]e^{\gamma a_k} = p[1+\gamma(x_1-b_{n_1}+\delta)]e^{\gamma(x_1-b_{n_1})} +$$

$$+ (1-p)[1+\gamma(x_2-b_{n_2}+\delta)]e^{\gamma(x_2-b_{n_2})} \quad \text{for } k=1,2,\ldots,n_1$$

$$[1+\gamma(a_k+\delta)]e^{\gamma a_k} = [1+\gamma(x_2-b_{n_2}+\delta)]e^{\gamma(x_2-b_{n_2})} \quad \text{for } k=n_1+1,\ldots,n_2.$$

As in the previous case we establish the statement about the partially uniform kind of the optimal control schedule $\{a_k^*\}$. Further we use again the Silvester criterion to verify that the matrix of mixed derivatives defines a positive definite quadratic form, and it is sufficient to assert that $E\tau_{(ii)}(\ldots)$ has a minimum for the found control schedule.

For the rest of the proof the result of Theorem 2 from [5] are used. Obviously, the control schedule $\{a_k^*\}$ is optimal whenever it is optimal over everyone of the segments $(x_k, x_{k+1}]$ during the task execution. In other words, after a possible task

duration x_k the control must be adjusted to the nearest one x_{k+1} in an optimal way. Here the results from [5] for the determination of the optimal control schedules with respect to the indicated variables are valid. It means that when the tresholds z_n of the control schedule changes are determined, then the optimal control schedule $\{a_k^*\}$ is determined by the rules circumscribed in Theorem 1. The theorem is proved.

Table 1

INTESIVITY γ=0.02

TEST AND COPY TIME FOR EXPLICIT BREAKDOWN = 1

TEST TIME FOR IMPLICIT BREAKDOWN = 0.7

COPY TIME FOR IMPLICIT BREAKDOWN = 0.3

	EXPLICIT			IMPLICIT		
RNOC	TRES	CAPD	UAPD	TRES	CAPD	UAPD
0	14.0	16.15	16.15	9.5	12.33	12.33
1	23.5	27.76	29.99	16.0	20.71	22.99
2	33.0	39.42	46.73	22.5	29.18	36.38
3	42.0	50.47	65.81	29.0	37.66	53.04
4	51.0	61.52	88.65	35.5	46.15	73.63
5	60.5	73.21	117.67	42.0	54.64	98.90
6	69.5	84.27	150.74	48.5	63.13	129.78
7	78.5	95.33	190.33	55.0	71.63	167.33
8	88.0	107.01	240.62	61.5	80.12	212.80
9	97.0	118.08	297.93	68.0	88.62	267.66
10	106.0	129.15	366.55	74.0	96.46	328.15
11	115.0	140.21	448.70	80.5	104.96	406.22
12	124.5	151.90	553.06	87.0	113.46	499.65
13	133.5	162.96	671.99	93.5	121.96	611.19
14	142.5	174.03	814.38	100.0	130.46	744.07
15	151.5	185.10	984.86	106.5	138.95	902.07

Note: RNOC is an abbreviation of Required Number Of Check-points; TRES of TREShold; CAPD of Controlled Average Process Duration; UAPD of Uncontrolled Average Process Duration.

A numerical example about the comparison of the tresholds of expected controlled and uncontrolled process durations in the cases of explicit and implicit breakdowns is shown in Table 1. Therein the breakdown intensity γ as well as the test and the copy expected time durations θ and δ are given constants.

Let us look now at the exponential case. As in corollary 2 we suppose that the separate required process durations X_j of a task are exponentially distributed with parameters $\lambda_j > 0$.

Under the given assumptions the following theorem is true:

Theorem 2. The optimal control schedule when the mixture X_j is an exponential one is an uniform control schedule. In addition the control is preferable:

- for case i, if there exists an index j, for which it is fulfilled

$$\lambda_j < \gamma[1-\theta(\gamma)]^{-1};$$

- for case ii - always.

Proof. One can prove the theorem using the results of Corollary 2 for the search of an optimal value a^* of the supposed uniform control schedule $\{a_k\}$. Such an approach is used in [5]. Here we prefere to prove the optimal properties of the uniform control schedule using the results of Corollary 1 in their particular form when $A_j(x) = 1-e^{-\lambda_j x}$, $\lambda_j > 0$. We shall use the same plan as in the proof of Theorem 1 . For simplicity it is sufficient to prove the theorem in the case r=1, as it is shown below.

For the case i we have (r=1)

$$E\tau_{(i)}(X,\{a_k\}) = \left[\frac{1}{\gamma\theta(\gamma)} + \frac{\lambda}{\gamma(\gamma-\lambda)}\right]\sum_{k=0}^{\infty} e^{-\gamma b_k}\, e^{(\gamma-\lambda)b_{k+1}} -$$

$$- \left[\frac{\lambda}{\gamma(\gamma-\lambda)} + \frac{1}{\lambda}\right]\sum_{k=0}^{\infty} e^{-\gamma b_k} .$$

If we denote by C_1 and C_2 the factors of the first and second summands correspondingly, we derive for $j=1,2,\ldots$ (remembering that $b_k=a_1+\ldots+a_k$)

$$\frac{\partial E\tau_{(i)}(X,\{a_k\})}{\partial b_j} = (\gamma-\lambda)C_1 e^{\gamma a_j} - \lambda C_1 e^{(\gamma-\lambda)a_{j+1}} + \gamma C_2 = 0 \quad (7)$$

Comparing two neighbouring equations of this system we get $a_j=a_{j+1}=a_{j+2}=\ldots=a$, i.e. the unique extremal control schedule is the uniform one. Furher, using the relation

$$(\gamma-\lambda)C_1 e^{\gamma a} + \gamma C_2 = \gamma C_1 e^{(\gamma-\lambda)a}$$

in the expressions $b_{js} = \frac{\partial^2 E\tau_{(i)}(X,\{a_k\})}{\partial b_j \partial b_s}$ and calculating the first two principal minors of the matrix $B = \left[b_{js} \right]_{j,s=1}^{\infty}$, we confirm that they are positive, iff $\lambda < \gamma[1-\theta(\gamma)]^{-1}$.
The matrix B is a threediagonal symetrical one. Let B_m is the principal minor of order m for the matrix B. It is easy to establish that the relations

$$B_m = b_{m,m} B_{m-1} + b_{m-1,m}^2 B_{m-2} \qquad m=3,4,\ldots \qquad (8)$$

are correct. To apply the Silvester criterion it is sufficient to prove that it is fulfilled

$$B_1 > 0,\ B_2 > 0,\ b_{mm} > 0 \quad \text{for any } m=2,3,.. \qquad (9)$$

In that case according to relations (8),(9) and the Silvester criterion the quadratic form determined by the matrix B is a positive definite one, i.e. the corresponding expected process time duration has a minimum for some uniform control schedule $\{a_k\}$.

For the case *ii* completely analogously we have

$$E\tau_{(ii)}(X,\{a_k\}) = \sum_{k=0}^{\infty} \left[\frac{\gamma}{\gamma-\lambda} a_{k+1} + \frac{\gamma\delta}{\gamma-\lambda} - \frac{\lambda}{(\gamma-\lambda)^2} \right] e^{\lambda a_{k+1}} e^{-\gamma b_{k+1}} +$$

$$+ \left[\theta - \frac{\lambda\delta}{\gamma-\lambda} + \frac{\gamma}{(\gamma-\lambda)^2} \right] \sum_{k=0}^{\infty} e^{-\lambda b_k}.$$

System (1) is equivalent to the following one

$$(D_1 + \gamma a_k)\, e^{\gamma a_k} = \left(\frac{\gamma^2}{\gamma-\lambda} a_{k+1} + D_2 \right) e^{(\gamma-\lambda)a_{k+1}} + D_3 \qquad (10)$$

where D_1, D_2, D_3 are given constsnts:

$$D_1 = 1+\gamma\delta, \quad D_2 = \frac{\gamma}{\gamma-\lambda} + \frac{\gamma^2\delta}{\gamma-\lambda} - \frac{\gamma\lambda}{(\gamma-\lambda)^2}, \quad D_3 = \gamma\left[\theta - \frac{\delta}{\gamma-\lambda} + \frac{\gamma}{(\gamma-\lambda)^2}\right].$$

It is sufficient to state that (a_k^*) are constants. Using (10) in the expressions for the mixed derivatives, the recurrent relations (8),(9) and the Silvester criterion we confirm the positive definitness (for all λ and γ) of the quadratic form with coefficients b_{js}. We omit here the trivial details.

In this way the optimality of the uniform control schedule is proved. Further one can use the same arguments as in Theorem 3 from [5] to determine the optimal value a^* of the corrsponding optimal uniform control schedule.

4. Some farther problems.

The found theoritical results need corresponding simplifications for presenting them in more convinient for the practical use form. In addition, some problems arrise in the case of Theorem 1, if one wants to determine an uniform control schedule, optimal for the executive time X, without changes in the points X_j. Cost functions more general than $E\tau(X)$ are also interesting being optimized as well as some problems under more general conditions.

REFERENCES

1. K.Barosov. An Optimal Control of the Service in a System with Evident and Latent Service Breackdown, *Math. and athematical Education*, Sofia (1987), 315-319.
2. G.L.Brodezki. Effectivness of Storing Intermediate Results in Systems with Refasuals Distroying the Information, Izv. Acad. Sci. USSR, *Technical Cibernetics* 6, (1978), 97-103. (In Russian).
3. K.M.Chandy, J.C.Browe, C.W.Dissly, W.R.Ohrig. Analytical Models for Roll-back and Recovery Strategies in Data Base Systems, *IEEE Trans. Software Eng.* 1, (1975), 100-110.
4. K.M.Candy. A Survey of Analytical Models of Roll-back and Recovery Strategies, *IEEE Trans. Computers* 8, (1975), 40-47.

5. B.N.Dimitrov and P.G.Petrov. Controlled Process with Explicit or Imlicit Breackdowns and Repeat Actions, In *"Fault Diagnostic and Reliability"*, Vol.1, Edit. Sp.Tzafestas at al., J.Reidal Publ.Comp., Dordrecht-Holland, (1987) (to appear).

6. DOS Supervisor and I/O Macros. No GC 24-5037-12. IBM System Reference Library.

7. V.Ilin, V.Sadovnitchi, B.Sendov. Mathematical Analysis, v.1, (1979), p.744. (in Russian).

8. V.Hadjinov. Determination of optimal time intervals betwen check-points when computations are performed onspecialized multiprocessors, *Electronic modelling* 7, No 2 (1985), 14-18 (in Russian).

9. I.A.Kovalenco and L.S.Stoykova. On the System Productiveness and the Solution Time by Random Refusals and Periodical Storing of Results, *Cybernetica* 5, Kiev (1974), 73-75. (In Russian).

10 P.Petrov and N.Kolev. On the Optimal Blocking Time by Serving with Unreliable Server with Implicit Breakdowns, *Serdica* 12 (1986), 245-249. (In Russian).

RELIABILITY COMPUTATIONS FOR RIGID PLASTIC FRAMES WITH GENERAL YIELD CONDITIONS

Ove Ditlevsen
Department of Structural Engineering
Technical University of Denmark
DK 2800 Lyngby, Denmark

ABSTRACT: The topic is reliability analysis of frame structures with rigid-ideal plastic constitutive behavior assigned to discretized hinge models. General yield conditions with internal force interaction are considered. Adoption of the associated flow rule assures the validity of the static theorem. On this basis a theorem about linear combinations of so-called linearly associated lower bound safety margins proves useful for setting up a strategy of fast identification of important collapse mechanisms. They are important in the sense of close upper bounding of the reliability against collapse.

Introduction

Many current reliability analysis models of ductile structural systems are claimed to be concerned with realistic modelling of the constitutive pre- and post-failure behavior of the potential failure elements of the system. However, these models are often of random vector type in their representation of loads and resistances. This implies that they are not mathematically fit for more than very simple random load path models. Generally they contain no load path information at all. Their user seems to rely on the help of a monster like a giant ten-armed octopus to keep the structure from failing during the phase of transfer of the load to the structure [3]. Moreover, the realism seems to be confined to the uniaxial modelling of the constitutive behavior. When modelling the post-failure multiaxial constitutive behavior of ductile elements it is not uncommon that recourse is had to the principles of the theory of ideal plasticity.

The difficulties of lack of consistency and clarity in so-called realistic modelling motivate a continued interest in improving the methods of reliability analysis for structural models with rigid-ideal plastic behavior. At least this behavior gives the considerable advantage that the safe set with respect to collapse is independent of the load history on the structure.

Finally it is worth-while to remember that in stochastic modelling there is no need for detailing the behavior of the individual outcomes of the random experiment beyond what can be captured by the probabilities of the events of practical relevance. More than that tends to overstep the threshold of objectivity [3,9].

Yield hinges and yield conditions

A plane or spatial frame structure is considered. It is assumed that all loads are given as concentrated forces attacking at a preselected set of nodal points of the frame structure. A finite set H of points of potential yield hinge formation is chosen among the nodal points such that a mechanism formation is possible.

The points of H may possess directional multiplicity in the following sense. Consider a nodal point with N joining beams numbered by 1, ..., N, and consider a subset $\{i_1,\ldots,i_m\}$ of m of these beams. For each i in this subset let a potential yield hinge be temporarily defined in the corresponding beam at a distance δ_i from the nodal point. Now let all δ_i approach zero. Then a point in H is obtained which is said to have directional multiplicity m. To each of the considered beam directions in the subset there is adjoined a yield condition

$$f_i(\bar{q}_i,\bar{Y}_i) = 0 \tag{1}$$

defined in terms of the internal forces $\bar{q}_i$ at the nodal point in the considered beam, and a vector $\bar{Y}_i$ of random yield strength variables.

The functions f_i are defined such that the sets

$$\{\bar{q}\,|\,f_i(\bar{q},\bar{Y}_i)>0\} \tag{2}$$

of no yielding are all convex and non-empty with probability one. Furthermore the associated flow rule (the normality condition) is postulated.

The m yield conditions of a potential yield hinge of directional multiplicity m may be joined into a single yield condition

$$f(\bar{q},\bar{Y}) = \min_i f_i(\bar{q}_i,\bar{Y}_i) = 0 \tag{3}$$

where $i \in \{i_1,\ldots,i_m\}$ and $\bar{q} = (\bar{q}_{i_1},\ldots,\bar{q}_{i_m})$ is a generalized internal force vector while $\bar{Y} = (\bar{Y}_{i_1},\ldots,\bar{Y}_{i_m})$. From the associated flow rule for each of the componental yield conditions it directly follows that the

associated flow rule is valid also for the joint yield condition. In case of simultaneous yielding in more than one beam the strain rate vector is situated at a singularity point of the joint yield condition.

Experiments with tubular joints of types as used in off-shore jacket frame structures show that interactions between the internal forces in the different joining beams may play a role in the initiation and the development of the failure of the joint [7]. A rigid plastic model for the joint failure as defined by Eq. 3 does not give an interaction effect of the mentioned type. However, Eq. 3 may be considered as a special case of the more general yield condition

$$f(\bar{q},\bar{y}) = 0 \tag{4}$$

where

$$\begin{aligned} &f((\bar{q}_{i_1},\bar{0},\ldots,\bar{0}),\bar{Y}) = f_{i_1}(\bar{q}_{i_1},\bar{Y}_{i_1}) \\ &\vdots \\ &f((\bar{0},\ldots,\bar{0},\bar{q}_{i_m}),\bar{Y}) = f_{i_m}(\bar{q}_{i_m},\bar{Y}_{i_m}) \end{aligned} \tag{5}$$

and where the associated flow rule is postulated.

Example 1: The yield condition format for large steel tubular joints may consistently with current practice [7] be chosen as

$$f(\bar{q},\bar{Y}) = \min_j\left[1-\sum_i\left(\frac{|q_{ij}|}{q_{uij}(\bar{Y})}\right)^{\nu_{ij}}\right] = 0 \tag{6}$$

where the minimum is taken over the set of the non-interactive parts of the yield condition and the summation is with respect to the internal forces q_{ij} contributing to the jth part. The denominator $q_{uij}(\bar{Y})$ is the ultimate absolute value of the internal force q_{ij} when it is acting alone. The ultimate internal force is a function of the random strength variables $\bar{Y}$ and the geometrical properties of the joint. These dependencies as well as the exponents ν_{ij} should be obtained by regression to experimental data. Generally they will be different in the different orthants of $\bar{q}$.

Linearly associated lower bound safety margins

In the following let r be the number of potential yield hinges with directional multiplicities m_1, m_2, ..., m_r respectively. Let

$f_i(\bar{Q}_i,\bar{Y}_i) = 0$ be the yield condition of hinge i. Then the structure is not in a state of collapse if and only if all the random functions

$$f_i(\bar{Q}_i,\bar{Y}_i) \quad , \quad i = 1, \ldots, r \tag{7}$$

take nonnegative values for some statically admissible set of values of the internal forces $\bar{Q}_1, \ldots, \bar{Q}_r$. The r random functions in Eq. 7 are called lower bound safety margins.

Consider the ith yield hinge and omit the index i whenever it is not needed. It is sufficient for the plastic analysis to make the convention that $\bar{Q}$ only contains as components those internal force components that not in all points of the yield surface are tangential to the yield surface. Thus the dimension of $\bar{Q}$ is at least 1 and at most 6 m.

Let $\bar{\alpha}$ be a vector of the same number of components as $\bar{Q}$. Assume that there is at least one point $\bar{P}$ on the yield surface at which the vector $\bar{\alpha}$ can act as a strain rate in accordance with the associated flow rule. Then the vector $\bar{\alpha}$ is called an admissible strain rate. If the yield surface is bounded in the active internal force components, any vector $\bar{\alpha}$ is an admissible strain rate. The scalar product

$$D(\bar{Y},\bar{\alpha}) = \langle\bar{P},\bar{\alpha}\rangle \tag{8}$$

is called the plastic dissipation corresponding to the admissible strain rate $\bar{\alpha}$, Fig. 1. For given $\bar{Y}$ the dissipation is uniquely defined by $\bar{\alpha}$ also if $\bar{P}$ is not unique. This follows from the convexity of the yield surface.

For each vector $\bar{\alpha}$ and internal force $\bar{Q}$ the difference

$$M(\bar{Q},\bar{Y},\bar{\alpha}) = D(\bar{Y},\bar{\alpha}) - \langle\bar{Q},\bar{\alpha}\rangle \tag{9}$$

is called a linearly associated lower bound safety margin to the lower bound safety margin $f(\bar{Q},\bar{Y})$.

Let $A(\bar{X})$ be the set of all admissible internal force vectors $(\bar{Q}_1,\ldots,\bar{Q}_r)$, that is, all internal force vectors which together with the external forces $\bar{X}$ constitute equilibrium. The following theorem proved in [6] is a generalization of a theorem proved in [2]:

THEOREM: Let $M_i(\bar{Q}_i,\bar{Y}_i,\bar{\alpha}_i)$, i = 1, ..., r, be linearly associated lower bound safety margins corresponding to the r different potential yield hinges. Then any linear combination

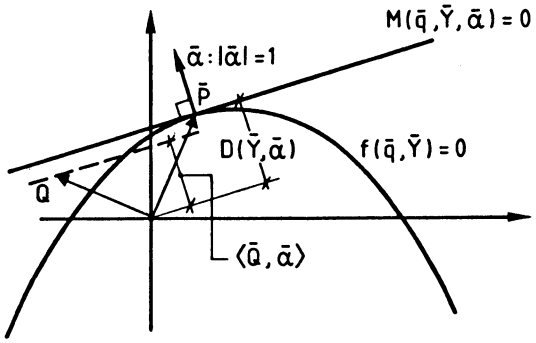

Fig. 1. Definition of dissipation and linearly associated safety margin corresponding to strain rate $\bar{\alpha}$.

$$\sum_{i=1}^{r} c_i \, M_i(\bar{Q}_i, \bar{Y}_i, \bar{\alpha}_i) \tag{10}$$

with nonnegative coefficients $c_1, \ldots, c_r$ is an upper bound safety margin if it is a constant within the set $A(\bar{X})$ of admissible internal forces.

Consider the special case where the yield condition in Eq. 7 is polyhedral in $\bar{Q}$. If $\bar{\alpha}$ is orthogonal to a face of the polyhedral yield surface, the equation of the hyperplane of the face directly defines the linearly associated safety margin. Otherwise the point $\bar{P}$ in Eq. 8 is a point at which two or more faces meet. Then $\bar{\alpha}$ can be written as a linear combination with nonnegative coefficients of normal vectors to the meeting faces. It follows from this that the linearly associated safety margin corresponding to $\bar{\alpha}$ is a linear combination of the linearly associated safety margins that correspond to the faces meeting at point $\bar{P}$ and with the same nonnegative coefficients as for $\bar{\alpha}$.

This property shows that each of the terms in Eq. 10 can be replaced by one or more terms. These are all linearly associated lower bound safety margins corresponding to some faces of the yield condition. These faces must meet each other at a single vertex of the yield surface. The actual vertex is that (or one of those) for which $\bar{\alpha}$ can

be a strain rate in accordance with the normality condition.

A potential yield hinge with a yield condition composed of noninteracting not necessarily polyhedral parts as in Eq. 3 can naturally be separated into as many spatially coinciding but noninteracting potential yield hinges. This directly defines a corresponding decomposition of the terms in Eq. 10.

Dominant linearly associated lower bound safety margins

It is possible to use the theorem as a basis for a general strategy of searching upper bound safety margins that contribute essentially to the reliability bounding from above. First step is to choose a statically determinate primary system for the n times redundant frame structure. The corresponding vector of internal force redundants is denoted by $\bar{z}$. As $\bar{z}$ varies over the n-dimensional space, the set of internal forces $(\bar{Q}_1,\ldots,\bar{Q}_r)$ varies over $A(\bar{X})$. Corresponding to each $\bar{z}$ there are $s \geq r$ local geometrical (Hasofer-Lind) reliability indices $\beta_1(\bar{z})$, ..., $\beta_s(\bar{z})$, at least one for each lower bound safety margin $f_i(\bar{Q}_i,\bar{Y}_i)$ (r = 6, s = 24 in Example 1; in very particular cases s can be infinite). There is at least one value of $\bar{z}$ for which some of the geometrical reliability indices are equal to a common value β characterized as being the largest value that can be taken by the smallest of the reliability indices $\beta_1(\bar{z})$, ..., $\beta_s(\bar{z})$. The problem of determining this common value β may be formulated as the optimization problem: Determine the maximal value of β under the constraints

$$\beta \leq \beta_i(\bar{z}) \quad , \quad i = 1, \ldots, s \tag{11}$$

for $\bar{z}$ varying over the n-dimensional space.

In the special case where $\beta_i(\bar{z})$ is linear in $\bar{z}$ for all i = 1, ..., s, this optimization problem is a linear programming problem which may be solved by a standard simplex procedure. Then there is a value of $\bar{z}$ giving the optimal solution so that at least a number of min{s,n+1} linearly associated lower bound safety margins have the common optimal reliability index. Moreover, the value of $\bar{z}$ can be determined so that the corresponding set of min{s,n+1} linearly associated safety margins has a coefficient matrix to $\bar{z}$ with the largest possible rank min{s,n}. A proof of these statements is given in [2].

The linearly associated lower bound safety margins of common optimal reliability index are called dominant.

Search for upper bound safety margins

Consider the case where $s \geq n + 1$ and assume that $n + 1$ dominant linearly associated lower bound safety margins have been determined so that the rank of the coefficient matrix to $\bar{z}$ is n. As mentioned in the larst section this is always possible if the geometrical reliability indices are linear in $\bar{z}$. Then there may be up to $n + 1$ regular (n,n) submatrices of the coefficient matrix. For each choice of such a regular (n,n) matrix there is a unique solution of $\bar{z}$ in terms of the corresponding safety margins. Let the corresponding set of hinge points be denoted by H_1. The search strategy is hereafter as follows. For each hinge point k in $H \setminus H_1$ the solution $\bar{z}$ is substituted in the equation for the general linearly associated safety margin $M_k(\bar{Q}_k, \bar{Y}_k, \bar{\alpha}_k)$, where $\bar{\alpha}_k$ is the variable strain rate vector. Since $\bar{Q}_k$ is linear in $\bar{z}$, this produces a linear combination like Eq. 10 with all or all but one lower bound safety margins being dominant. The $n + 1$ coefficients c_i are linear in $\bar{\alpha}_k$. Each coefficient is therefore nonnegative in a half-space of $\bar{\alpha}_k$. In case the intersection of all $n + 1$ half-spaces is not empty, it defines a simplex in the space of the $\bar{\alpha}_k$ vectors. Each point of this simplex can be represented as a convex linear combination (i.e. a combination with nonnegative coefficients that add to 1) of vectors in direction of the "edges" of the simplex. An edge is a half-part of a one-dimensional space defined by setting $\dim(\bar{\alpha}_k) - 1$ of the coefficients c_i to zero and requiring that the remaining coefficients are all nonnegative ($\dim(\bar{\alpha}_k)$ = dimension of $\bar{\alpha}_k$, $m_k \leq \dim(\bar{\alpha}_k) \leq 6m_k$). Let there be m edges. Of course, $m \leq n + 1$. (For plane structures the dimension of the $\bar{\alpha}_k$ space is usually either $2m_k$ or m_k. If $m_k = 1$, it is obvious that there can at most be 2 edges in the first case and 1 edge in the second case). The $\bar{\alpha}_k$ vectors in direction of the edges are of particular interest because any upper bound safety margin defined by the considered $n + 1$ lower bound safety margins may as indicated above be written as a convex linear combination of the m particular upper bound safety margins that correspond to suitably scaled $\bar{\alpha}_k$ vectors of the m edges. Let these upper bound safety margins be $S_1, \ldots, S_m$. Assume for the present that all the considered linearly associated lower bound safety margins are also linear with respect to the strength variables $\bar{Y}$, that is, the dissipation in each yield hinge is linear in the strength variables. Then the $\bar{\alpha}_k$ vectors of the edges may be scaled such that $\mathrm{Var}[S_i] = 1$ giving the reliability index $\beta_i = E[S_i]$ of S_i and the reliability index

$$\beta = \frac{\alpha_1\beta_1+\ldots+\alpha_m\beta_m}{\sqrt{\bar{\alpha}'\ \bar{\bar{P}}_{\bar{S}}\ \bar{\alpha}}} \tag{12}$$

of the linear combination $\alpha_1 S_1 + \ldots + \alpha_m S_m$. The coefficients $\alpha_1, \ldots, \alpha_m$ are all nonnegative and $\bar{\bar{P}}_{\bar{S}}$ is the correlation matrix of $\bar{S} = (S_1,\ldots,S_m)$. Since

$$\bar{\alpha}'\ \bar{\bar{P}}_{\bar{S}}\ \bar{\alpha} \leq (\alpha_1+\ldots+\alpha_m)^2 \tag{13}$$

it follows that

$$\beta \geq \frac{\alpha_1\beta_1+\ldots+\alpha_m\beta_m}{\alpha_1+\ldots+\alpha_m} \geq \min\{\beta_1,\ldots,\beta_m\} \tag{14}$$

Thus the most significant upper bound safety margins are among $S_1, \ldots, S_m$. It is therefore a reasonable strategy only to store these (or some of these) for later use in the calculation of an upper bound on the generalized reliability index. Of course, the strategy is applicable also when linearity with respect to Y is not present. Only it is not guaranteed that Eq. 14 holds.

If the number s of local geometrical reliability indices is at most equal to the degree of redundancy n, it is not possible to eliminate $\bar{z}$ by isolating a regular (n,n) matrix. In fact, if the coefficient matrix $\bar{\bar{K}}_{rn}$ to $\bar{z}$ in the set of s dominant linearly associated lower bound safety margins $M_1, \ldots, M_s$ has the maximal rank s, there is no linear combination

$$c_1M_1 + \ldots + c_sM_s = \bar{c}'\bar{\bar{K}}_{sn}\ \bar{z} + \text{terms independent of } \bar{z} \tag{15}$$

which is independent of $\bar{z}$. For the considered strategy to be applicable it is therefore required that if the number r of potential yield hinges is at most equal to the degree of redundancy n, then the corresponding yield surfaces must either consist of a sufficient number of non-interactive parts and/or of meeting polyhedral faces to make the number s larger than n. With this provision the aforementioned splitting properties of the terms in Eq. 10 can become active.

Example 2: The simple frame structure shown in Fig. 2 is made of beams with a yield condition as shown to the right-hand side. It is an idealization which corresponds to an ideal rigid-plastic material with coinciding yield stresses in tension and compression and a beam cross-section as shown. The discretized system is shown in Fig. 3 together with the system chosen as the statically determinate primary system.

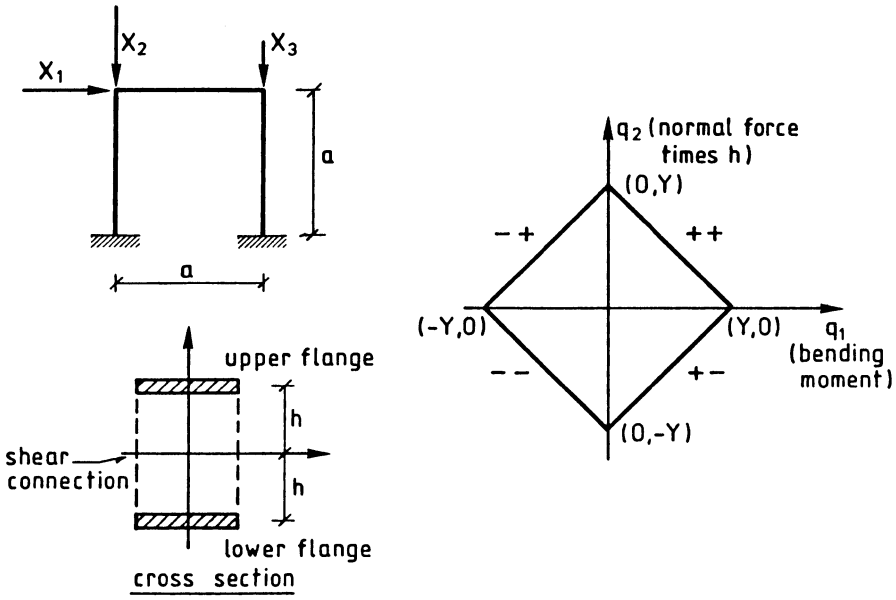

Fig. 2. Frame structure with beam cross section and corresponding yield condition

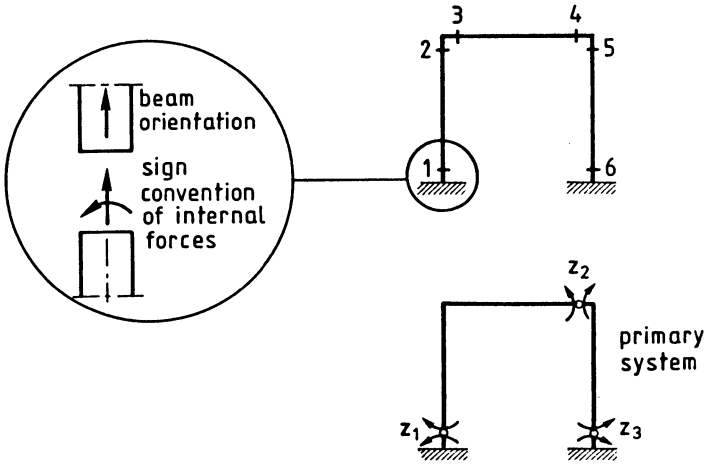

Fig. 3. The discretized system

The lower bound safety margin $f_i(\bar{Q}_i, Y_i)$ of the ith point of H = {1,2,3,4,5,6} can due to the polygonal yield condition with four sides be replaced by the four linear safety margins

$$\begin{aligned} M_i^{--} &= Y_i + Q_{1i} + Q_{2i} \\ M_i^{-+} &= Y_i + Q_{1i} - Q_{2i} \\ M_i^{+-} &= Y_i - Q_{1i} + Q_{2i} \\ M_i^{++} &= Y_i - Q_{1i} - Q_{2i} \end{aligned} \tag{16}$$

in which Q_{1i} and Q_{2i} are bending moment and normal force respectively both represented in the same physical unit as the yield stregth Y_i. The lower bound safety margin $f_i(\bar{Q}_i, Y_i)$ is nonnegative if and only if all the four linear safety margins of Eq. 16 are nonnegative. These four linear safety margins are linearly associated lower bound safety margins to $f_i(\bar{Q}_i, Y_i)$. There are an infitity of other linearly associated lower bound safety margins. These correspond to the vertices of the yield condition.

Let s_i represent the sign sequence corresponding to the sequence s_{1i}, s_{2i} of +1 or -1 (i.e. s_i = ++ for $s_{1i} = 1$, $s_{2i} = 1$, s_i = +- for $s_{1i} = 1$, $s_{2i} = -1$, s_i = -+ for $s_{1i} = -1$, $s_{2i} = 1$, and s_i = -- for $s_{1i} = -1$, $s_{2i} = -1$). Then the general linear lower bound safety margin in Eq. 16 may be written as

$$M_i^{s_i} = Y_i - [s_{1i}\ s_{2i}]\ (\bar{\bar{A}}_i \bar{X} + \bar{\bar{B}}_i \bar{z}) \tag{17}$$

in which the matrices $\bar{\bar{A}}_i$, $\bar{\bar{B}}_i$ are

$$\bar{\bar{A}}_1 = \begin{bmatrix} 0 & 0 & 0 \\ h & -h & 0 \end{bmatrix}, \quad a\bar{\bar{B}}_1 = \begin{bmatrix} a & 0 & 0 \\ h & 0 & -h \end{bmatrix} \tag{18}$$

$$\bar{\bar{A}}_2 = \begin{bmatrix} a & 0 & 0 \\ h & -h & 0 \end{bmatrix}, \quad a\bar{\bar{B}}_2 = \begin{bmatrix} a & a & -a \\ h & 0 & -h \end{bmatrix}$$

$$\bar{\bar{A}}_3 = \begin{bmatrix} a & 0 & 0 \\ 0 & 0 & 0 \end{bmatrix}, \quad a\bar{\bar{B}}_3 = \begin{bmatrix} a & a & -a \\ 0 & h & -h \end{bmatrix}$$

$$\bar{\bar{A}}_4 = \begin{bmatrix} 0 & 0 & 0 \\ 0 & 0 & 0 \end{bmatrix}, \quad a\bar{\bar{B}}_4 = \begin{bmatrix} 0 & a & 0 \\ 0 & h & -h \end{bmatrix}$$

$$\bar{\bar{A}}_5 = \begin{bmatrix} 0 & 0 & 0 \\ -h & 0 & -h \end{bmatrix}, \quad a\bar{\bar{B}}_5 = \begin{bmatrix} 0 & a & 0 \\ -h & 0 & h \end{bmatrix}$$

$$\bar{\bar{A}}_6 = \begin{bmatrix} 0 & 0 & 0 \\ -h & 0 & -h \end{bmatrix}, \quad a\bar{\bar{B}}_6 = \begin{bmatrix} 0 & 0 & a \\ -h & 0 & h \end{bmatrix}$$

as they follow from elementary statics. In order to be specific with numbers, the following example is chosen:

$$E[Y_i] = \mu_Y,\ E[X_1] = \gamma\mu_X,\ E[X_2] = E[X_3] = \mu_X, \tag{19}$$
$$D[Y_i] = \sigma_Y,\ D[X_1] = \gamma\sigma_X,\ D[X_2] = D[X_3] = \sigma_X,$$
$$i \neq j : \rho[Y_i,Y_j] = \rho,\ \text{all } i,j : \rho[Y_i,X_j] = 0,$$
$$\rho[X_2,X_3] = r,\ \rho[X_1,X_2] = \rho[X_1,X_3] = 0,$$
$$a/h = 50,\ a\mu_X/\mu_Y = 5,\ a\sigma_X/\sigma_Y = 2\sqrt{5},\ \gamma = 2/25$$

The reliability index $\beta_i^{s_i}$ (= ratio of mean to standard deviation) of each of the linear safety margins of Eq. 17 can then be calculated as a function of $\zeta_1 = z_1/\mu_Y$, $\zeta_2 = z_2/\mu_Y$, $\zeta_3 = z_3/\mu_Y$ except for proportionality with μ_Y/σ_Y. All variances of the linear safety margins turn out to be independent of the correlation coefficients ρ and r and thus also the reliability indices are independent of ρ and r.

The problem of maximizing β with respect to $\bar{\zeta} = (\zeta_1,\zeta_2,\zeta_3)$ under the 24 constraints $\beta \leq \beta_i^{s_i}$ (setting $\mu_Y/\sigma_Y = 1$) is first solved using any standard linear programming algorithm. The solution is $\beta = \beta_1^{--} = \beta_2^{+-} = \beta_5^{--} = \beta_6^{+-} = 0.785$ corresponding to $\zeta_1 = -0.1152$, $\zeta_2 = -0.1081$, $\zeta_3 = 0.1081$. The corresponding safety margins are the dominant lower bound safety margins. According to the static theorem of plasticity theory the set of optimal lower bound safety margins defines a lower bound on the reliability of the frame structure.

For $\mu_Y/\sigma_Y = 5$ the smallest lower bound safety margin reliability index is $5\beta = 3.93$ while the corresponding generalized reliability index based on all 24 linear lower bound safety margins is 3.56 for $\rho = r = 0$, 3.57 for $\rho = r = 0.5$, and 3.62 for $\rho = r = 0.8$ (formally assigning the joint Gaussian distribution to the set of basic variables [1]). However, considerable improvements may be obtained by non-linear programming optimization using first order reliability methods (FORM) on the parallel system obtained by introducing several different $\bar{z}$ vectors of redundants [8]. Alternatively, directional simulation may be an effective way to obtain essential improvements over the simple optimization used in this example [4]. Such directional simulation results are presented in Table 2.

The optimization results are interesting because of the theorem. In order to identify upper bound safety margins with small reliability indices it is a reasonable strategy to use lower bound safety margins with small reliability indices in the linear combinations. Therefore the dominant lower bound safety margins are of particular interest for

this purpose. The reliability index of the linear combination in Eq. 10 depends both on the coefficients in the combination and the correlations between the terms. Thus there is no guarantee that the linear combinations with nonnegative coefficients of the dominant lower bound safety margins among them contain the most important upper bound safety margin. In any case, the strategy of considering these particular linear combinations leads to upper bound safety margins and they are quite useful when judging possibilities of improvements of the construct of lower bounds on the reliability.

The dominant lower bound safety margins are

$$\begin{bmatrix} M_1^{--} \\ M_2^{+-} \\ M_5^{--} \\ M_6^{+-} \end{bmatrix} \sim \frac{1}{50} \begin{bmatrix} 51 & 0 & -1 \\ -49 & -50 & 49 \\ -1 & 50 & 1 \\ -1 & 0 & -49 \end{bmatrix} \begin{bmatrix} \zeta_1 \\ \zeta_2 \\ \zeta_3 \end{bmatrix} \tag{20}$$

where $\sim$ here means "equal to" except for terms which are independent of $\bar{\zeta}$ (i.e. terms that depend solely on the yield moments $Y_1, \ldots, Y_6$ and the external forces X_1, X_2, X_3). All four 3-dimensional submatrices of the coefficient matrix in Eq. 20 are regular. Thus there are four possible solutions

$$\bar{\zeta} \sim \frac{1}{50} \begin{bmatrix} 50 & 1 & 1 \\ 0 & -1 & 49 \\ 50 & 51 & 51 \end{bmatrix} \begin{bmatrix} M_1^{--} \\ M_2^{+-} \\ M_5^{--} \end{bmatrix}; \quad \bar{\zeta} \sim \frac{1}{50} \begin{bmatrix} 49 & 0 & -1 \\ -49 & -50 & -49 \\ -1 & 0 & -51 \end{bmatrix} \begin{bmatrix} M_1^{--} \\ M_2^{+-} \\ M_6^{+-} \end{bmatrix}$$

$$\bar{\zeta} \sim \frac{1}{50} \begin{bmatrix} 49 & 0 & -1 \\ 1 & 50 & 1 \\ -1 & 0 & -51 \end{bmatrix} \begin{bmatrix} M_1^{--} \\ M_5^{--} \\ M_6^{+-} \end{bmatrix}; \quad \bar{\zeta} \sim \frac{1}{50} \begin{bmatrix} -49 & -49 & -50 \\ -1 & 49 & 0 \\ 1 & 1 & -50 \end{bmatrix} \begin{bmatrix} M_2^{+-} \\ M_5^{--} \\ M_6^{+-} \end{bmatrix} \tag{21}$$

when each one of the equations in Eq. 20 is excluded in turn.

These linear combinations of dominant lower bound safety margins are next substituted for $\bar{\zeta}$ in $M_i(\bar{Q}_i, Y_i, \bar{\alpha}) + [\alpha_1 \ \alpha_2] \bar{\bar{B}}_i \bar{\zeta}$ for those i that are not contributing to $\bar{\zeta}$. In this way linear combinations independent of $\bar{\zeta}$ are obtained. Consider the first $\bar{\zeta}$ of Eq. 21 and i = 3. Then

$$[\alpha_1\ \alpha_2]\ \bar{\bar{B}}_3\ \bar{\zeta} \sim -\ [\alpha_1\ \alpha_2]\ \frac{1}{2500}\begin{bmatrix} 0 & 2550 & 50 \\ 50 & 52 & 2 \end{bmatrix}\begin{bmatrix} \bar{M}_1^{--} \\ M_2^{+-} \\ M_5^{--} \end{bmatrix} \tag{22}$$

which gives nonnegative coefficients to M_1^{--}, M_2^{-+}, and M_5^{--} for $\bar{\alpha}$ chosen within the simplex defined by the inequalities

$$\alpha_2 \leq 0,\ 2550\alpha_1 + 52\alpha_2 \leq 0,\ 50\alpha_1 + 2\alpha_2 \leq 0 \tag{23}$$

The edges of the simplex are $\{\alpha_1 \leq 0, \alpha_2 = 0\}$ and $\{\alpha_1 \geq 0, 2550\alpha_1 + 52\alpha_2 = 0\}$. The first edge corresponds to a strain rate vector proportional to

$$(-50,0) = 25(-1,-1) + 25(-1,1) \tag{24}$$

which, in turn, corresponds to the linearly associated safety margin

$$M_3(\bar{Q}_3, Y_3, (-50,0)) = 25\ M_3^{--} + 25M_3^{-+} \tag{25}$$

The resulting edge-linear combination with nonnegative coefficients is

$$25M_3^{--} + 25M_3^{-+} + 51M_2^{+-} + M_5^{--} \tag{26}$$

The second edge corresponds to a strain rate vector proportional to

$$(52,-2550) = 1249(-1,-1) + 1301(1,-1) \tag{27}$$

giving the edge-linear combination

$$1249M_3^{--} + 1301M_3^{+-} + 51M_1^{--} + M_5^{--} \tag{28}$$

This type of calculations made for the twelve combinations of the four $\bar{\zeta}$ from Eq. 21 and the three indices i relevant for each $\bar{\zeta}$ give 14 different of $\bar{\zeta}$ independent linear combinations with nonnegative coefficients. The coefficients to M_1^{--}, M_1^{-+}, M_1^{+-}, M_1^{++}, ..., M_6^{--}, M_6^{-+}, M_6^{+-}, M_6^{++} are given in this order as the rows in Table 1. The rows are ordered according to increasing reliability index of the corresponding upper bound safety margin in the case $\rho = r = 0$. The reliability indices are given in Table 2 in the columns marked by $\diamond$ (the columns marked by O concern Example 3). Experience shows that the upper bound safety margins identified by this approach can be sufficient for calculating a satisfying close upper bound on the generalized reliability index of

1	0	0	0	0	0	0	0	0	0	0	0	0	0	0	0	0	0	0	0	0	25	0	26	0
0	0	0	0	25	0	26	0	0	0	0	0	0	0	0	0	1	0	0	0	0	0	0	0	0
1	0	0	0	0	0	0	0	0	0	0	0	0	0	0	0	25	0	25	0	0	0	1	0
25	0	25	0	0	0	1	0	0	0	0	0	0	0	0	0	1	0	0	0	0	0	0	0
51	0	0	0	0	0	0	0	1249	0	1301	0	0	0	0	0	1	0	0	0	0	0	0	0
1	0	0	0	0	0	0	0	0	0	0	0	1275	0	1225		0	0	0	0	0	0	51	0
49	0	0	0	0	0	51	0	0	0	0	0	1226	0	1224	0	0	0	0	0	0	0	0	0
0	0	0	0	0	0	0	0	0	1276	0	1274	0	0	0	0	49	0	0	0	0	0	51	0
0	25	0	24	0	0	0	0	0	0	0	0	0	0	0	0	0	0	0	0	0	0	1	0
0	0	0	0	0	0	1	0	0	0	0	0	0	0	0	0	0	25	0	24	0	0	0	0
1	0	0	0	0	25	0	25	0	0	0	0	0	0	0	0	0	0	0	0	0	0	1	0
0	0	0	0	0	0	1	0	0	0	0	0	0	0	0	0	1	0	0	0	0	25	0	25
1	0	0	0	0	0	0	0	0	0	0	0	0	0	51	1	51	0	0	0	0	0	0	0
0	0	0	0	0	0	51	0	25	25	0	0	0	0	0	0	1	0	0	0	0	0	0	0

TABLE 1: Coefficients to lower bound safety margins M_1^{--}, M_1^{-+}, M_1^{+-}, M_1^{++}, ..., M_6^{++} row by row defining 14 upper bound safety margins

the structural system. Some results are summarized in Table 2. For comparison the table includes the results of uniform directional simulation of a confidence interval estimate of the generalized reliability index of the discretized frame structure system. Otherwise the identified upper bound margins can be used for defining an importance directional simulation procedure for fast estimation of the generalized reliability index [4,5].

		ρ = r = 0		ρ = r = 0.5		ρ = r = 0.8	
yield condition		◇	o	◇	o	◇	o
β_i	1	4.53	4.57	4.49	4.51	4.46	4.47
	2	4.57	4.61	4.52	4.55	4.50	4.51
	3	4.62	4.70	4.53	4.57	4.48	4.50
	4	4.66	4.74	4.57	4.61	4.52	4.54
	5	5.05	5.09	5.00	5.02	4.97	4.98
	6	5.09	5.13	5.04	5.06	5.01	5.02
	7	5.14	5.22	5.04	5.08	4.98	5.00
	8	5.17	5.25	5.08	5.11	5.02	5.03
	9	5.53	5.57	5.47	5.49	5.44	5.45
	10	5.57	5.61	5.51	5.53	5.48	5.49
	11	5.62	5.70	5.51	5.54	5.44	5.45
	12	5.66	5.74	5.55	5.58	5.48	5.49
	13	6.74	6.86	5.47	5.57	4.99	5.07
	14	6.76	6.73	5.49	5.52	5.00	5.04
optimal lower bound of β_G		[3.560, 3.560]		[3.563, 3.568]		[3.596, 3.635]	
upper bound of β_G using 4 first combinations		[4.290, 4.290]	[4.349, 4.349]	[4.224, 4.225]	[4.257, 4.258]	[4.207, 4.228]	[4.225, 4.247]
upper bound of β_G using all 14 identified combinations		[4.281, 4.281]	[4.339, 4.339]	[4.214, 4.216]	[4.247, 4.249]	[4.198, 4.228]	[4.216, 4.246]
lower bound of β_G obtained by uniform directional simulation *)		[4.26, 4.28]	[4.25, 4.45]	[4.17, 4.20]		[4.12, 4.15]	
average		4.269	4.33	4.189		4.137	
sample size		40000	1000	40000		40000	

*) The interval corresponds to the estimated mean ±k times the estimated standard deviation of the simulated probabilities. k = 0.675 (∿ 50% probability interval)

Table 2: Single upper bound margin reliability indices β_i and bounds of the generalized reliability index β_G (the bounds are bounded within intervals) for the frame structure system in Examples 2 (◇) and 3 (o). σ_Y/μ_Y = 0.2. All variables are jointly Gaussian.

Substitute yield conditions

Assume that an upper bound safety margin corresponding to a given set A of yield conditions is obtained from Eq. 10. If the corresponding strain rates are admissible for another set B of yield conditions, then the linear combination obtained from Eq. 10 with unchanged coefficients $c_1, \ldots, c_r$ and strain rates $\bar{\alpha}_1, \ldots, \bar{\alpha}_r$ but with dissipations calculated from the set B will be an upper bound safety margin corresponding to the set B. This is a direct consequence of the theorem and the fact that the dissipations are independent of the internal forces. Therefore, if the yield conditions of the set A give simpler computations than those for set B, it can be advantageous to use set A instead of set B given that set A is a reasonable approximation to set B. In particular, set A may be chosen so that the geometrical reliability indices become linear in the redundants. A sufficient condition for this is that the yield conditions of set A are polyhedral in $(\bar{Q}_i, \bar{Y}_i)$, $i = 1, \ldots, r$. Then the optimization problem is reduced to a linear programming problem. Also the polyhedral approximation can be chosen so that the number of geometrical reliability indices exceeds n avoiding the problem of Eq. 15. Moreover, on account of the static theorem (the lower bound theorem) it is so that if the given yield conditions of set B are replaced by yield conditions which all are inscribed in/circumscribing the yield conditions of set B, then the reliability evaluation is affected to the conservative/unconservative side.

Example 3. The same frame structure as in Example 2 is considered except that the yield condition in Fig. 2 is changed to the circle

$$y^2 - q_1^2 - q_2^2 = 0 \tag{29}$$

in all the potential yield hinges. Noting that the yield condition in Fig. 2 is inscribed in this circle, it can be concluded that the reliability against collapse is increased relative to the reliability of the structure in Fig. 2.

Each set of the 14 strain rate vectors $\bar{\alpha}_1, \ldots, \bar{\alpha}_6$ obtained in Example 1 define some linearly associated lower bound safety margins corresponding to the circular yield conditions at those hinge points at which the strain rate vector is not the zero vector. The linear combination of these linearly associated lower bound safety margins as defined by the corresponding coefficients $c_1, \ldots, c_{24}$ is an upper bound safety margin for the structure of this example (both $\bar{\alpha}_1, \ldots,$

$\bar{\alpha}_6$ and c_1, ..., c_{24} can be read row by row from Table 1). Each upper bound safety margin is simply obtained by removing the yield strength term Y_i from M_i^s in Eq. 17 and instead adding the linear combination

$$\sqrt{2}\left(\sqrt{c_1^2+\ldots+c_4^2}\ Y_1+\ldots+\sqrt{c_{21}^2+\ldots+c_{24}^2}\ Y_6\right) \tag{30}$$

of Y_1, ..., Y_6 to the linear combination $c_1M_1^{--} + \ldots + c_{24}M_6^{++}$.

The upper bound reliability index results obtained by this construction are shown in the columns of Table 2 marked with o. As compared to Example 1 only a modest increase of the upper bound is observed.

It turns out that the nonlinear optimization problem of Eq. 11 as defined for the 6 geometrical reliability indices corresponding to the circular yield conditions leads to a larger upper bound of the reliability index [6]. However, this observation allows no general conclusions about methodological superiority.

References

1. Ditlevsen, O.: "Generalized Second Moment Reliability Index". J. Struct. Mech., Vol. 7, No. 4, 1979, pp. 435-451.

2. Ditlevsen, O. and Bjerager, P.: "Reliability of Highly Redundant Plastic Structures". J. Eng. Mech., ASCE, Vol. 110, No. 5, 1984, pp. 671-693.

3. Ditlevsen, O.: "The Structural System Reliability Problem". Qualitative Considerations. Proc. of ICASP5: Reliability and Risk Analysis in Civil Engineering 1, N.C. Lind (ed.), Institute for Risk Research, University of Waterloo, Waterloo, Ontario, Canada, 1987, pp. 1-11.

4. Ditlevsen, O. and Bjerager, P.: "Plastic Reliability Analysis by Directional Simulation". DCAMM Report No. 353, 1987, Technical University of Denmark, DK 2800 Lyngby, Denmark.

5. Ditlevsen, O., Hasofer, A.M., Bjerager, P., and Olesen, R.: "Directional Simulation in Gaussian Processes". DCAMM Report No. , Technical University of Denmark, DK 2800 Lyngby, Denmark, 1987.

6. Ditlevsen, O.: "General Probabilistic Statics of Discretized Ideal Plastic Frames". DCAMM Report No. 1987, Technical University of Denmark, DK 2800 Lyngby, Denmark.

7. Krenk, S.: "Yield Criteria for Tubular Joints". Survey worked out for A.S. Veritas Research. 1985.

8. Madsen, H.O. and Skjong, R.: "Lower Bound Reliability Evaluation for Plastic Truss and Frame Structures". A.S. Veritas Research Report No. 84-2043, Høvik, Norway, 1984.

9. Matheron, G.: Estimer et choisir, Les Cahiers du Centre de Morphologie, Mathématique de Fontainebleau, Facicule 7, France, 1978. Translated 1987 into English: Estimating and Choosing, by A.M. Hasofer, to be published by Springer Verlag.

PARALLEL SYSTEMS OF SERIES SUBSYSTEMS

Thore Egeland
Institute of Mathematics, University of Oslo, N-0316 Oslo 3, Norway

Lars Tvedt
A.S. Veritas Research, P. O. Box 300, N-1322 Hovik, Norway

1. INTRODUCTION

Throughout this paper we consider the structure at a fixed point in time and the structure is assumed to depend only on the state of its components. Moreover, only two states are considered: functioning and nonfunctioning of the components and the system. Any system can be represented as a Series System of Parallel Subsystems (SSPS) or as Parallel System of Series System (PSSS). High reliability SSPS are handled by PROBAN, a program developed at *Det Norske Veritas* and *The Technical University of Munich*. A SSPS may be reformulated as PSSS, this may however be very large. The scope of this paper is therefore to develop methods for computing or bounding the reliability of parallel systems of series subsystems. In a number of applications it is desired to deal with such systems. One example is the computation of the reliability of the tether system of a Tension Leg Platform. Other examples of PSSS in Structural System Reliability are provided in Madsen and Skjong (1984) and Madsen et al (1986). Barlow and Proschan (1975) provides examples from other fields.

Section 2 reviews some of the basic concepts in addition to formulating the problem in detail. Section 3 presents the general method and a useful combinatorial formula is derived. Some important special cases are dealt with in Section 4. The general setup does not depend on any particular distribution of the components. In Section 4, however, the components are assumed to be multinormally distributed.

2. BASIC CONCEPTS

The general system consists of M components. Series number i contains N_i components. In some cases the representation of the system can be determined directly by inspection. The *minimal cuts* and *minimal paths* are useful when identifying the system representation. A *path vector* is a set of components which, if they all function, assures that the system functions. A *minimal* path vector is a path vector which cannot be reduced without ceasing to be a path vector. Parallel Systems of Series Systems are defined uniquely by their minimal path vectors. Equivalently, the minimal cut vectors determine the system. The minimal path vectors are the series in Figure 2.1. The figure also shows a typical minimal cut vector $\mathbf{k} = (k(1),\ldots,k(M))$.

The reliability problems we have in mind can be formulated in terms of random variables $U_1,\cdots,U_d$ and the state functions defined by

$$g_{ij}(u)\begin{cases} <0 & \textit{failure set} \\ =0 & \textit{state surface} \quad i=1,\ldots,M \;\; j=1,\ldots,N_i \\ >0 & \textit{safe set} \end{cases} \tag{2.1}$$

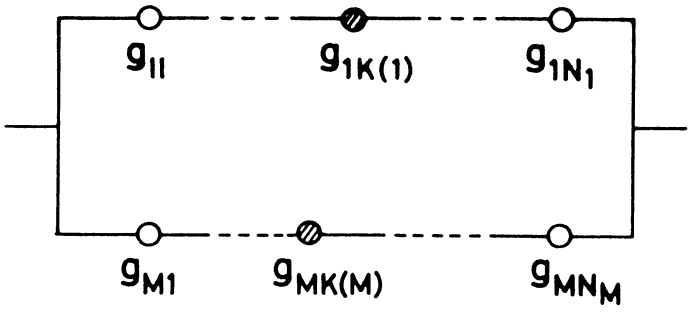

Figure 2.1 Parallel System of Series Systems.

For ease of notation we put $X_{ij} = g_{ij}(U)$ recalling that the particular distribution of $g_{ij}(U)$ is of no significance as far as the general method is concerned. The announced precise formulation of the problem is to compute

$$P(\textit{system failure}) = P\Big(\bigcap_{i=1}^{M}\bigcup_{j=1}^{N_i}\{X_{ij} \leqslant 0\}\Big) \tag{2.2}$$

for large systems. There are $\prod_{i=1}^{M} N_i$ minimal cut vectors. In general, the number of minimal cut vectors determines the numerical complexity of the problem. The last Section includes a system with $M = 6$ series and $N = 20$ components in each series implying that there is a total of $20^6 = 64 \cdot 10^6$ minimal cut vectors.

We close this section noting that the problem in question may be formulated entirely without reference to reliability problems: namely as that of computing (2.2)

3. THE METHOD

The basic idea is to expand the system failure set into a disjoint union. This allows the probability of system failure to be written as a sum which is easier to handle than (2.2).

To each minimal cut vector $\mathbf{k}$ we associate the corresponding disjoint cut set

$$\{cut_{\mathbf{k}}\} = \{X_{11} > 0,\ldots, X_{1k(1)-1} > 0, X_{1k(1)} \leqslant 0, X_{21} > 0, \cdots, X_{Mk(M)} \leqslant 0\} \tag{3.1}$$

Since

$$\textit{system failure set} = \bigcup_{\mathbf{k}} \{cut_{\mathbf{k}}\}$$

is a disjoint union

$$P(\textit{system failure set}) = \sum_{\mathbf{k}} P(cut_{\mathbf{k}}) \tag{3.2}$$

The number of safe sets in $\{cut_k\}$ is $n(k) = k(1)-1+\ldots+k(M)-1 = s$, say. The number of disjoint cut sets with s safe sets is denoted by $c(s)$, for instance $c(0) = 1$, $c(1) = M$ and

$$c(2) = \left\lfloor \frac{M+1}{2} \right\rfloor .$$

In this section we derive a formula for $c(s)$ in terms of s, M and N_i. The usefulness of this formula is especially apparent for systems with exchangeable components; i.e. when all subsets of $X = \{X_{ij}\}$ of equal cardinality have the same distribution. Then different disjoint cut sets contribute with the same probability content provided they contain the same number of safe sets. Writing $\{cut_k\} = \{cut(s)\}$ in this case, it follows that

$$P(\text{system failure}) = \sum_{s=0}^{L-M} c(s)\, P(cut(s)) \tag{3.3}$$

where $L = \sum N_i$. In the general case, denote by $\{cutmax(s)\}$ and $\{cutmin(s)\}$, respectively, the largest and smallest disjoint cut sets with s safe sets. Then

$$\sum_{s=0}^{L-M} c(s)\, P(cutmin(s)) \leqslant P(\text{system failure}) \leqslant \sum_{s=0}^{L-M} c(s)\, P(cutmax(s)) \tag{3.4}$$

The quality of the inequalities depends on

$$\sum_{s=0}^{K-M} c(s)\,[P(cutmax(s)) - P(cutmin(s))] \tag{3.5}$$

and the number of terms needed to achieve good approximations. Of course, more sophisticated bounds are possible at the cost of including more than merely the probability contents of the smallest and largest disjoint cut sets.

To derive a formula for $c(s)$ it is convenient to consider systems with identical independent components. Letting

$$p = P(X_{ij} \leqslant 0)\ ,\ i = 1,\ldots,M \text{ and } j = 1,\ldots,N_i$$

we may write

$$P(\text{system failure}) = \sum_{l=0}^{L-M} C(l)\, p^M (1-p)^l . \tag{3.6}$$

On the other hand

$$P(\text{system failure}) = p^M \Big[\prod_{i=1}^{M} (1+(1-p)+\ldots+(1-p)^{N_i-1})\Big] \tag{3.7}$$

since system failure is equivalent to the failure of all series systems. Hence, by comparing the expressions (3.6) and (3.7), it is seen that $c(l)$ is obtained as the coefficient of $x^l = (1-p)^l$ in the polynomial:

$$\prod_{i=1}^{M} (1+x+\ldots+x^{N_i-1}) \tag{3.8}$$

A routine generating the coefficients has been written solving the problem of counting the the number of disjoint cut sets.

Some comments on the special case $N_1 = \cdots = N_M = N$ are due: By (3.8) and the formula for the sum of a geometric series we get

$$\sum_{l=0}^{M(N-1)} C(l)\, x^l = \Big[\frac{1-x^N}{1-x}\Big]^M \tag{3.9}$$

The Taylor series expansion of the right side of (3.9) around $x = 0$ provides the closed formula ($l = 0,\ldots,M(N-1)$)

$$C(l) = \frac{1}{l!} \frac{\partial^l}{\partial x^l} \Big[\frac{1-x^N}{1-x}\Big]^M_{x=0} \tag{3.10}$$

When $l < N$ the nature of the problem implies that $C(l)$ is independent of N. l times differentiation produces

$$C(l) = \left\lfloor \begin{matrix} M+l-1 \\ l \end{matrix} \right\rfloor \tag{3.11}$$

The last formula also follows from a combinatorial argument: $\left\lfloor \begin{matrix} M+l-1 \\ l \end{matrix} \right\rfloor$ is the number of ways of choosing l objects from a collection of M when each object may chosen several times, corresponding to the fact that there may be several safe sets from each series.

Example 3.1

It suffices to consider a very small system to illuminate the concepts above. There are $M=3$ series and $N=3$ components in each series of the structure. Assume the components X_{ij} are identically normally distributed with *safety index*

$$\beta = \frac{E(X_{ij})}{SD(X_{ij})} = 2.0$$

and equicorrelated with common correlation coefficient $\rho = 0.9$. Then

$$P(\textit{system failure}) = P(\bigcap_{i=1}^{M} \bigcup_{j=1}^{N_i} \{X_{ij} \leqslant 0\})$$

$$= P(\bigcap_{i=1}^{3} \bigcup_{j=1}^{3} \{Z \leqslant -\beta\}) = 0.895 \cdot 10^{-2} + \cdots + 0.791 \cdot 10^{-4} = 0.223 \cdot 10^{-1} \tag{3.12}$$

where Z is a standard normal variable. Further numerical details are provided in Table 3.1 below.

Table 3.1 Disjoint cut method

#SAFE	$c(\cdot)$	$c(\cdot)\,P(cut\,(s))$
0	1	$0.895\ 10^{-2}$
1	3	$0.535\ 10^{-2}$
2	6	$0.406\ 10^{-2}$
3	7	$0.223\ 10^{-2}$
4	6	$0.114\ 10^{-2}$
5	3	$0.355\ 10^{-3}$
6	1	$0.791\ 10^{-4}$

Consider next the system above with the β-s generated uniformly on [1.5,2.5].

Table 3.2 Bounding disjoint cuts

#SAFE	$P(cutmin\,(s))$	$P(cutmax\,(s))$	$c(s)\,P(cutmin\,(s))$	$c(s)\,P(cutmax\,(s))$
0	$0.266\ 10^{-1}$	$0.266\ 10^{-1}$	$0.266\ 10^{-1}$	$0.266\ 10^{-1}$
1	$0.377\ 10^{-3}$	$0.151\ 10^{-2}$	$0.113\ 10^{-2}$	$0.454\ 10^{-2}$
2	$0.296\ 10^{-4}$	$0.716\ 10^{-3}$	$0.178\ 10^{-3}$	$0.429\ 10^{-2}$
3	$0.151\ 10^{-5}$	$0.459\ 10^{-4}$	$0.105\ 10^{-4}$	$0.321\ 10^{-3}$

Ignoring disjoint cut sets of dimension higher than 3 and using the bounding formula (3.4) it follows that

$$0.277 \cdot 10^{-1} \leqslant P(\textit{system failure}) \leqslant 0.357 \cdot 10^{-1} \tag{3.13}$$

whereas the exact answer is $P(\textit{system failure}) = 0.318 \cdot 10^{-1}$. In this case $\{cutmax\,(s)\}$ and $\{cutmin\,(s)\}$ were found by computing the probability contents of all disjoint cuts and sorting.

The above example is only meant to illustrate the method. In fact, the above example is handled more efficiently by the methods in the next section.

4. THE NORMAL CASE

Throughout this section it is assumed that the components are normally distributed. This is the case if $U_1, \ldots, U_d$ are normal - possibly after a transformation - and the limit state functions $g_{ij}(\mathbf{u})$ are linear. Moreover, introducing the standard normal variables $(i = 1,\ldots,M \quad j = 1,\ldots,N_i)$

$$Z_{ij} = \frac{X_{ij} - E(X_{ij})}{SD(X_{ij})} \tag{4.1}$$

and the safety indices

$$\beta_{ij} = \frac{E(X_{ij})}{SD(X_{ij})} \tag{4.2}$$

the problem is to compute

$$P(\textit{system failure}) = P(\bigcap_{i=1}^{M} \bigcup_{j=1}^{N_i} Z_{ij} \leqslant -\beta_{ij}) \tag{4.3}$$

Restricted correlation structure

For general correlations structure no simple expression for (4.3) is obtainable. However, assuming that

$$\rho(Z_{ij}, Z_{kl}) = \rho_{ij}\,\rho_{kl} < 1.0 \qquad (ij) \neq (kl) \tag{4.4}$$

we derive a closed formula for the failure probability involving essentially only one integration. The model in Madsen et al (1986) corresponds to the case $N_i = 1$, $i = 1,\ldots,M$. Letting V, and V_{ij} , $i = 1,\ldots,M$, $j = 1,\ldots,N_i$ be independent and standard normally distributed , we may write

$$Z_{ij} = \rho_{ij} V + (1-\rho_{ij}^2)^{1/2} V_{ij} \tag{4.5}$$

Conditioning on V and denoting by Φ and ϕ respectively the distribution function and density of the standard normal variable, it follows that

$$P(\textit{system failure}) = \int_{-\infty}^{\infty} \prod_{i=1}^{M} P(\bigcup_{j=1}^{N_i} \{\rho_{ij} v + (1-\rho_{ij}^2)^{1/2} V_{ij} \leqslant -\beta_{ij}\}) \, \phi(v)\, dv \tag{4.6}$$

since the components are independent given V. The probability in the integrand may be rewritten

$$1 - P(\bigcap_{j=1}^{N_i} V_{ij} \geqslant \frac{-\beta_{ij} - \rho_{ij} v}{(1-\rho_{ij}^2)^{1/2}}) = [1 - \prod_{j=1}^{N_i} \Phi(\frac{\beta_{ij} + \rho_{ij} v}{(1-\rho_{ij}^2)^{1/2}})]$$

leading to the closed formula

$$P(\textit{system failure}) = \int_{-\infty}^{\infty} \prod_{i=1}^{M} [1 - \prod_{j=1}^{N_i} \Phi(\frac{\beta_{ij} + \rho_{ij} v}{(1-\rho_{ij}^2)^{1/2}})] \, \phi(v)\, dv \tag{4.7}$$

Remark that no computational problems arises for large systems in this case.

Example 4.1

This example expands on Example 4.4 in Madsen et al (1986) where a bar loaded by a time varying axial load $S(t)$ is considered. The resistance of the bar is a deterministic constant r. The variables $S_1,\ldots,S_N$ have the second moment representation

$$E(S_i) = \mu_s \tag{4.8}$$

$$var(S_i) = \sigma_s^2 \tag{4.9}$$

and

$$cov(S_i, S_j) = \rho\sigma_s^2 \tag{4.10}$$

The probability of the bar failing is

$$P(\bigcup_{i=1}^{N}(r-S_i) \leqslant 0) = P(\bigcup_{i=1}^{N}\frac{S_i-\mu_s}{\sigma_s}) \geqslant \beta_{HL}) = P(\bigcup_{i=1}^{N} Z_{ij} \leqslant -\beta_{HL}) \tag{4.11}$$

where

$$\beta_{HL} = \frac{r-\mu_s}{\sigma_s}$$

is the Hasofer-Lind reliability index. Our generalization amounts to consider M bars in parallel implying that system failure coincides with the failure of all bars. The loads of bar b ($b=1,...,M$) are S_{bi} ($i=1,...,N$) and they have the same marginal distributions and correlations as above, c.f. Figure 4.1, (There is no load redistribution).

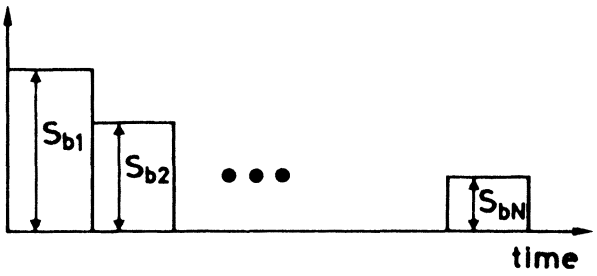

Figure 4.1 Bar loaded by time varying axial force.

From 4.11 and 4.7 it follows that

$$p_f = P(\textit{system failure}) = P(\bigcap_{i=1}^{M}\bigcup_{j=1}^{N}(r-S_i) \leqslant 0) = P(\bigcap_{i=1}^{M}\bigcup_{j=1}^{N} Z_{ij} \leqslant -\beta_{HL}) \tag{4.12}$$

$$= \int_{-\infty}^{\infty}[1-\Phi^N(\frac{\beta_{HL}+\rho^{1/2}v}{(1-\rho)^{1/2}})]^M \phi(v)\,dv$$

The *generalized reliability index* is

$$\beta_G = \Phi^{-1}(1-p_f) \tag{4.13}$$

Figure 4.2 shows how β_G varies as a function of ρ, N and M. The picture is somewhat more complicated than for series systems where β_G increases monotonically in ρ.

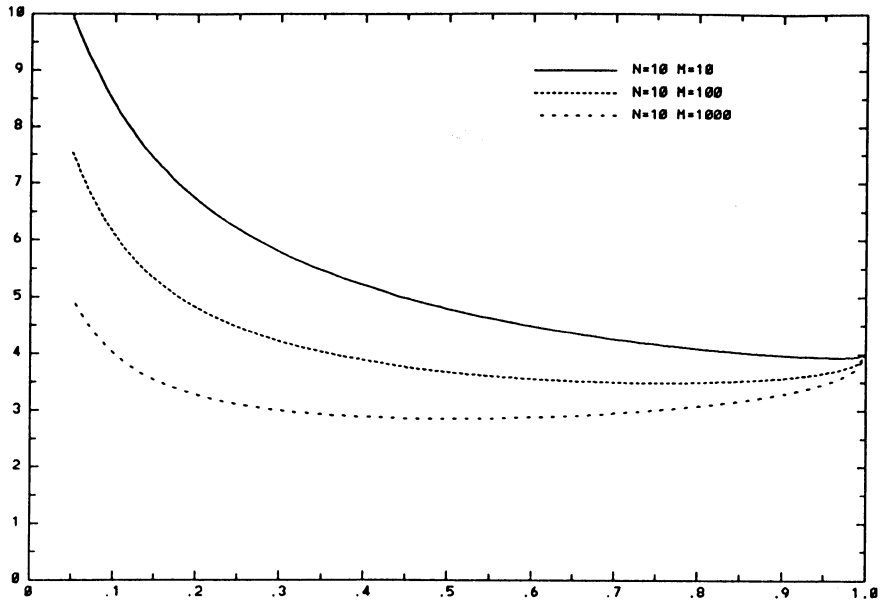

Figure 4.2 The generalized reliability index β_G as function of ρ for several values of M and N.

General correlation structure

When there are no restrictions on the correlation structure we can in principle compute all disjoint cuts by applying the *Hohenbichler* integral (1982). This is not feasible within reasonable computer time for large systems and we are left with the previously described bounding techniques. Let X_k be the components of the disjoint cut set indexed by k. Moreover, assume X_k is normally distributed with positive definite correlation matrix Σ_k and $E(X) = 0$. In order to use the upper bound

$$P(\textit{system failure}) \leqslant \sum_{s=0}^{L-M} c(s)\, P(\textit{cutmax}(s)) \tag{4.14}$$

we need to determine

$$P(\textit{cutmax}(s)) = \max_{k:n(k)=s} P(X_k \leqslant x_k) = \max_{k:n(k)=s} P(X_k \geqslant -x_k) \tag{4.15}$$

To make these probabilities comparable we transform to independent standard variables Y_k defined by

$$Y_k = \Sigma_k^{-1/2} X_k \tag{4.16}$$

The largest disjoint cut set is selected as the one which minimizes

$$\beta_k^2 = y_k^t y_k \tag{4.17}$$

subject to

$$\Sigma_k^{1/2} y_k \geq -x_k$$

the idea being the same as the one which underlies the general reliability index. We tried the procedure using PROBAN finding that the ordering of the β's reflects the ordering of the probabilities. However, the constrained minimization problem have to be coded specifically for the problem at hand for the procedure to be useful; the minimization problem in PROBAN aims at far more general problems than we consider.

In the following example we investigate the numerical quality of the previously outlined bounding technique closer.

Example 4.2

The system consists of $M = 6$ series and $N = 20$ components in each series. We generated the β_{ij} $-s$ uniformly on [2,5]. The correlation structure is given by

$$\rho(X_{ij}, X_{kl}) = 0.9^{|k-l|+1} \quad (ij) \neq (kl) \tag{4.18}$$

and the components are marginally standard normal. Each series is sorted by increasing β's. All disjoint cuts of dimension less than 11 were computed using the Hohenbichler integral. The probabilities were sorted and the upper bound was based on the 3 largest disjoint cut sets. To be more specific, let the 3 largest disjoint cuts of dimension s in descending order be *cut(1,s) cut(2,s) cut(3,s)*. Then the upper bound is

$$cut\,(1,0) + \sum_{s=1}^{114} \{\, cut(1,s) + cut(2,s) + (c(s)-2)\, cut(3,s) \,\} \tag{4.19}$$

In Table 4.1 the cumulative upper bounds are denoted 'UPPER'; the analogous lower bounds are called 'LOWER'. The correct numbers are entered under 'RIGHT'.

From Table 4.1 it is seen that the bounds based on 7 safe sets are $0.006 \leq P(system\ \ failure) \leq 0.035$. The corresponding bounds derived using only the smallest and largest disjoint cut sets are $0.005 \leq P(system\ \ failure) \leq 0.121$.

Table 4.1 Bounding disjoint cuts

#SAFE	$c(\cdot)$	LOWER	RIGHT	UPPER
0	1	0.00339	0.00339	0.00339
1	6	0.00571	0.00715	0.00828
2	21	0.00590	0.00779	0.00943
3	56	0.00596	0.00832	0.01137
4	126	0.00598	0.00877	0.01450
5	252	0.00590	0.00913	0.01901
6	462	0.00600	0.00943	0.02858
7	792	0.00600	0.00964	0.03537
8	1287	0.00600	0.00976	0.04484
9	2002	0.00600	0.00984	0.05070
10	3003	0.00601	0.00988	0.05792

5. SUMMARY AND CONCLUSIONS

In the paper the problem of estimating the reliability of parallel system of series systems has been addressed. The general method is based on the disjoint cut set expansion of the system failure set along with a formula for counting the number of disjoint cut sets. For the multinormal case with a special correlation structure it is demonstrated that the probability of system failure involves essentially only one integration. Several examples are provided.

6. REFERENCES

Barlow, R. E. and F. Proschan *Statistical Theory of Reliability and Life Testing*, Holt, Rinehart and Winston, New York, 1975.

Hohenbichler, M. *An Approximation to the Multivariate Normal Distribution*, in Proceedings, EUROMECH 155 Reliability Theory of Structural Engineering Systems, DIALOG 6-82, Danish Engineering Academy, Lyngby, Denmark, 1982, pp. 79-100.

Madsen, H. O., S. Krenk and N. C. Lind *Methods of Structural Safety*, Prentice Hall, N.J., 1986.

Madsen, H.O and R. Skjong *Lower Bound Evaluation for Plastic Truss and Frame Structures*, Veritas Report no 84-2043, Det Norske Veritas, Oslo, Norway, 1984.

RANGE-MEAN-PAIR EXCEEDANCES IN STATIONARY GAUSSIAN PROCESSES

D. G. Ford
Aeronautical Research Laboratories, Melbourne.

1. INTRODUCTION

One of the most important stress (or stress intensity) parameters in fatigue is the range-(mean)-pair or rainflow count[1,2]. The distribution of rainflow amplitudes has recently been discussed by Rychlik and Lindgren[3,4,5]. However counting is more easily discussed in terms of range-pair exceedances[6], rather than occurrences, paralleling the usefulness of load exceedance counters[7] for less accurate fatigue estimates. In this paper we discuss the first passage time for an *exceedance* of a range-pair with fixed amplitude and mid-value.

For many practical cases it is also true that the stress response of a structure may be regarded as a stationary random process which is the output of white or coloured noise filtered by a linear system[8,9]. General load histories may often be regarded as eras of different stationary processes joined in sequence. This includes the important cases of differing sea states and atmospheric turbulence[10] in which the process variance follows a folded Normal density.

There are several equivalent ways[6] of establishing the passage of a range-pair exceedance, all based on the successive first crossings of the two defining levels u and v. In the discussion below we define an exceedance by two first upcrossings of u and v in succession. Although such an occurrence is sufficient for counting, the time taken must begin from the last upcrossing, of the first level, which establishes the previous count. We closely follow Reference [11], Cramér and Leadbetter, which will often be denoted CL. However the overall approach is also similar to that of Rice and Beer[13] and we derive a similar approximation to avoid parent densities of arbitrary order. The Sections 2.3,2.4,3.1,3.2 and 3.3 are introductory.

We conclude with brief discussions of the exact density, asymptotic results and the application to linear systems.

2. GENERAL MODEL

An exceedance of the type described is shown in Figure 1. Here $X(t)$ is a stationary Normal process of unit variance,mean zero and a given covariance (and autocorrelation) function $r(t)$ for which $\dot{r}(0) = 0$ to ensure that the realizations are differentiable almost everywhere [12]. It also has a finite second spectral moment λ to ensure the existence of $\dot{r}(t)$ and continuity of $\dot{X}(t)$ [12]. λ is also the variance of the derivative process $\dot{X}(t)$ as one may see by regarding the Fourier transform as a moment generating function.

2.1 Curve Crossing Approach

Under the described conditions $X(t)$ is regular [11] and separable. The expected number of recurrent events (crossings here) in an interval $(t,t+dt)$ can be written

$$E(dU) = \omega(t)dt + o(dt) \tag{2.1}$$

where $\omega(t)$ is an intensity of occurrence. From the viewpoint of an ensemble (2.1) is also a Binomial probability for the interval dt. We may therefore follow the approach of Cramér and Leadbetter(CL)[8] and consider $X(t)$ as the limit of finite dimensional processes defined by $r(t)$ at the times $2^{-n}k$. As in CL this approach may be adapted to crossings of curves and for our purposes these are chosen to be $ABCD$ and $DEFG$ of Figure 1.

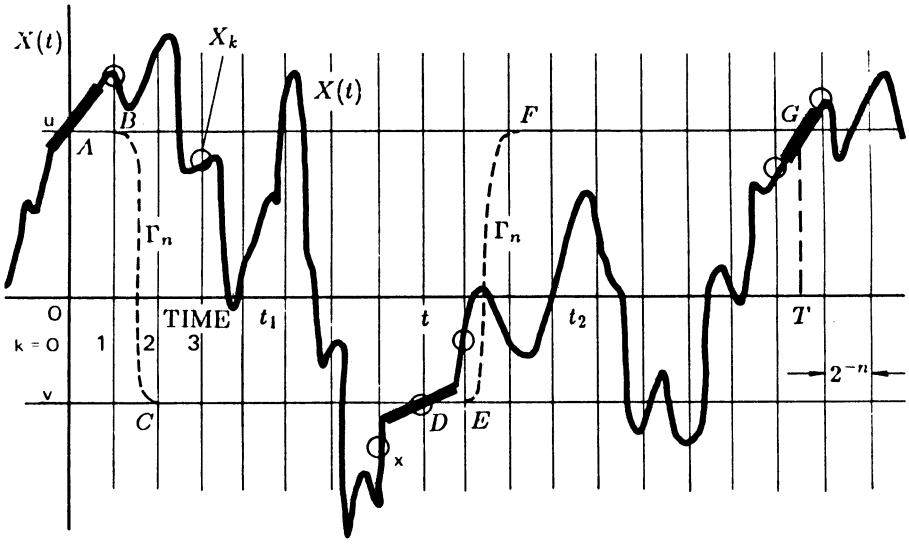

FIGURE 1 RANGE-PAIR EXCEEDANCE OF (u,v) OVER TIME T

As required by the analysis the dashed sections Γ_n place the curves in $C[0,T]$ and the transition BC is always in the first interval after D. The limiting process $n \to \infty$ is done for fixed t,T and then t is removed by convolution after averaging over extraneous random slopes.

In CL the finite dimensional densities approximate the regular crossing densities $\omega(t)$ at T regardless of previous occurrences; for range-pair times only first crossings can be considered. We first validate the extension of the curve crossing analysis to limiting curves $\in C^2$ and then consider the first crossing as part of a pure birth process.

2.2 Validity of Combined Limits

At this stage we must ensure that the effect of crossing a "moving" curve Γ_n as $n \to \infty$ can be neglected. Before proceeding we let the polygonal function $X_n(t) \in C[0,T]$ approximate $X(t)$ as $n \to \infty$ using the successive curves Γ_n, Γ_{n+1} etc. We now use $\omega_n(t)$ for the crossing intensity of $X_n(t)$.

If the limit exists

$$\int_0^T (\omega(t) - \omega_n(t))dt \leq T\|\omega(t) - \omega_n(t)\|$$

using the maximum norm on [0 T] which exists for a regular process if some isolated points are excluded.

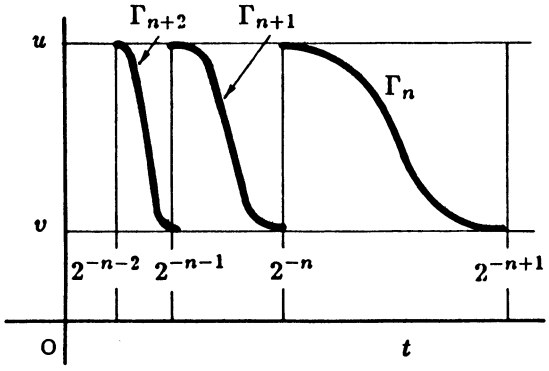

FIGURE 2. SEQUENCE OF TRANSITION CURVES TO BE CROSSED.

Now one may write

$$T\|\omega(t) - \omega_n(t)\| = (3 * 2^{-n+1} + (T - 3 * 2^{-n+1}))\,\|\omega(t) - \omega_n(t)\|, \qquad (2.2)$$

abstracting two time intervals of size $[2^{-n-1}, 2^{-n+1}]$ containing successive transitions Γ_n,Γ_{n+1} between the two levels.

In equation (2.2) Γ_n is associated with ω_n. If Γ_n had been used for all ω_k,$k < n$, then (2.2), arrived at by a finite number of steps, would still be obtained. Now consider ω'_{n+1} which still uses Γ_n. In this way a sequence ω'_{n+1} can be countably defined for all n.

We now need to show that $\omega'_n \to \omega$, assuming uniform continuity of $\omega(t)$. Firstly, if M is some constant,

$$|\omega(t_1) - \omega(t_2)| < M|t_1 - t_2|$$

for all Γ_n.

Then

$$\begin{aligned} |\omega(t) - \omega'_n(t)| &= |\omega(t) - \omega_n(t) + \omega_n(t) - \omega'_n(t)| \\ &< \|\omega(t) - \omega_n(t)\| + 3M2^{-n-1} \end{aligned} \qquad (2.3)$$

and corresponding to (2.2)

$$\int_0^T (\omega(t) - \omega_n'(t))dt \;\le\; T\|\omega(t) - \omega_n'(t)\|$$

$$\le\; 3 * 2^{-n-1}(\|\omega(t) - \omega_n(t)\| + 3M2^{-n-1} + (T - 3 * 2^{-n-1})\|\omega(t) - \omega_n(t)\|$$

$$\to\; 0$$

The terms without T correspond to the upper limit so that a fortiori:

$$\omega_n'(t) \to \omega(t)$$

and one may safely use moving curves Γ_n in the CL procedure.

2.3 First Crossings

The crossing density $\omega(t)$ for any stationary or non-stationary process defines the probability[12]

$$\omega(t)dt + o(dt) \tag{2.4}$$

that just one crossing occurs during $(t\,,\, t + dt)$. With respect to the time origin this is an n-th crossing for $n = 1, \infty$ which can be regarded as a pure birth process. If $F_i(t)$ is the distribution of i-th crossing times then

$$\begin{aligned} F_i(t + dt) &= F_i(t) + f_i(t)dt + o(dt) \\ &= F_{i-1}(t)\omega(t)dt + F_i(t)(1 - \omega(t)dt) \end{aligned}$$

or

$$F_i'(t) + \omega(t)F_i(t) \;=\; \omega(t)F_{i-1}(t)$$

with the recursive solution

$$F_i(t) = \int_0^t \omega(t')F_{i-1}(t')\exp\Big(-\int_{t'}^t \omega(t)dt\Big)dt'. \tag{2.5}$$

For $F_0(t)$, the probability for no crossings, the birth equation is

$$F_0(t) + F_0'(t)dt = F_0(t)(1 - \omega(t)dt), \qquad F_0(0) = 1, \tag{2.6}$$

with the waiting time type of solution

$$F_0(t) = \exp\Big(-\int_0^t \omega(t')dt'\Big). \tag{2.7}$$

which may be called an exclusion factor.

With (2.5) and (2.6) this leads to a first crossing density in the form of a reliability density

$$f_1(t) = \omega(t) \exp\Big(-\int_0^t \omega(t')dt'\Big). \tag{2.8}$$

When ω is constant one is led to the well known relations between waiting times and occurrences for the Poisson process. These formulae are analogous to those of Rice and Beer[10] where they are a probability for the absence of intermediate extrema. Like them they are conditioned on events at particular times, as described below, and exact results would be conditioned by *all* the necessary events $\in (0, T)$. The discussion in [10] applies here with minor changes and a similar accuracy is expected. However further dissection of the events is also required as described below.

In (2.4) the probability $\omega(t)dt$ may refer to a union of mutually exclusive sub-events which gives it the nature

$$\omega(t) \;=\; \sum_i \omega(t|A_i)\, P_r(A_i) \;=\; \sum_i \omega(t \cap A_i).$$

If any of these components is taken separately the analysis in Section 2.4 may be repeated to return a formula like (2.8) for $f_1(t \cap A_i)$, a crossing combined with the side condition A_i. *This we do not want*; the factor (2.7) in (2.8) would merely exclude *Crossings* $\cap$ A_i before the time t; we would like to exclude *all* prior crossings.

The argument from (2.4) to (2.8) is also applicable if each i-th crossing is also associated with its own side condition; this of course will reduce F_i to $P_r(A_i)\, F_i(t|A_i)$ and suitable crossings will be less frequent.

Our only interest here is in first crossings and (2.8) may be extended to

$$P_r(\textit{First crossing} \cap A_i) = P_r(\textit{Any crossing} \cap A_i)\, P_r(\text{All } \textit{prior crossings excluded})$$

or symbolically

$$f_1(t \cap A_i) \;=\; \omega(t \cap A_i) \exp\Big(-\int_0^t \omega(t')dt'\Big). \tag{2.8A}$$

This may be proved as above; the side condition on F_0 is the whole event space $\mathcal{U}$ or, colloquially, it is anything and there is no restriction so that (2.7) is retained as above. The next recursion, now with A_i leads to (2.8A).

2.4 Distribution of Total Time

In (2.8) and (2.8A) the density embraces any allowable vector of crossing slopes but these are correlated with the ordinate densities everywhere so that they must be treated separately. In particular, convolution cannot proceed before the crossing densities are summed over slopes for a particular set of times $0, t$ and T; conditioned convolutions cannot be combined into one that is not conditioned.

In (2.8) let $\omega = \omega_t$ describe second upward crossings (D in Figure 1) and put ω_T for the density of the third crossings (at G say) necessary to establish the range-pair time. It is convenient to compute ω_T with respect to the same time origin so that with the same side conditions

$$f_1(T - t \cap A_i) = \omega_T(T \cap A_i) \exp\Big(-\int_t^T \omega(t')dt'\Big).$$

Now consider the particular rainflow exceedance at T for which t is the second crossing time. The double crossing density with side conditions may be written as $\omega(t\,T \cap A_i|0)$. To contribute to a range-pair count two exclusion factors like (2.7) are also needed. However these must exclude more than merely A_i-types of prior crossings.

For the first phase (2.7) is replaced by

$$\exp\Big(-\int_0^t \omega(t'|0\,t\,T)dt'\Big) \tag{2.9}$$

for level v at t' whilst at level u there is a second factor

$$\exp\Big(-\int_t^T \omega(t'|0\,t\,T)dt'\Big) \tag{2.9A}$$

where

$$\omega(t'|0\,t\,T) \;=\; \sum_j \omega(t'|0\,t\,T\,A_j)P_r(A_j).$$

In (2.9) the levels crossed are of course $\{u\,v\,v\,u\}$ and $\{u\,v\,u\,u\}$ respectively.

Let us now write $f_1(t, T \cap A_i|0)$ for the reduced probability density of the particular rainflow count suggested by the notation, with the side condition A_i. Without loss of generality these are disjoint and

$$f_1(t\,T|0) \;=\; \sum_i f_1(t\,T \cap A_i|0)$$

and the extension of A_i to a continuous random variable is obvious. We therefore change from A_i to $\mathbf{Z} \sim F(\mathbf{z})$.

Our desired density of time to the first range-pair exceedance is

$$f_1(T) = \int_0^T f_1(t\,T|0)dt$$

corresponding to a convolution of two independent intervals (0,t) and (t,T). Our intervals however depend on $\mathbf{Z}$ and if this dependence is exposed then

$$\begin{aligned} f_1(T) &= \int_0^T dt \int f_1(t\,T|0\,\mathbf{z})dF(\mathbf{z}) \\ &= \int_0^T \int \omega(t\,T|0\,\mathbf{z})dF(\mathbf{z})\ \exp\Big(-\int_0^T \omega(t')dt'\Big)dt. \end{aligned} \tag{2.10}$$

Here

$$\omega(t') = \omega(t'|0\,t\,T\,\mathbf{Z})$$

but the crossing level is v or u according to whether $0 < t' < t$ or $t < t' < T$. It is convenient to still call the form (2.10) a convolution and this we do.

2.5 Slope Conditions

By definition (2.10) is conditioned on $X(0) = u, X(t) = v$ and $X(T) = u$. To ensure crossings it will also be necessary to consider the joint density of X_i and $Z_i = \dot{X}_i$ so that (2.10) strictly applies to the limiting case $f_1(T|u\,v\,u\,Z_0\,Z_1\,Z_2)$. The first three conditions , on levels reached, are of course intrinsic to the problem but the slopes $\mathbf{Z} = \{Z_0\,Z_1\,Z_2\}$ are extraneous, forming the side conditions introduced above. If desired variable thresholds $u(t)$ and $v(t)$ could be used but this has not been done.

The convolution integral with respect to t in (2.10) means that $f_{\mathbf{Z}}(\mathbf{z})$ depends on t because of variation in the separation times t and $T - t$. Thus $\omega(t\,T|0)$ must be averaged over positive components of $\mathbf{Z}$ before convolution as in (2.10).

With these explicit conditions (2.10) must be specialised to

$$f_1(T|\mathbf{Z} > \mathbf{0}) = \int_0^T dt \int_0^\infty dF(\mathbf{z})\omega(t\,T|0\,\mathbf{z}) \exp\Big(-\int_0^t \omega_1(t)dt\Big)\ \exp\Big(-\int_t^T \omega_2(t)dt\Big). \tag{2.11}$$

In words, this is the density function of the time taken for a triple crossing on the condition of positive slopes at $0, t$ and T. The similarly conditioned intermediate crossing probabilities ω_1 and ω_2 are derived from the unconditional multiple crossing/slope densities $\omega(0\,t\,T\,\mathbf{z})$, $\omega(0\,t'\,t\,T\,z_i\,\mathbf{z})$, derived below, which lead to most of the necessary manipulation.

From conditional probability

$$\omega_i \equiv \omega(t'|0\,t\,T\,\mathbf{z}) = \frac{\omega(0\,t'\,t\,T\,\mathbf{z})}{\omega(0\,t\,T\,\mathbf{z})} \tag{2.12}$$

and for
$i = 1$ Crossing level v with $0 < t' < t$
$i = 2$ " " u with $t < t' < T$.

The actual form of these crossing densities will be found in Section 4 after further discussion of $f_{X\,Z}(x\,z)$.

3. DENSITIES AND CONDITIONAL DISTRIBUTIONS

Consider details of $f_X(x_i)$, using the covariances from the finite-dimensional densities. Suppose the times $0, t, T$ correspond, with subdivisions of 2^{-n}, to the zero-th, k-th and K-th interval. Where convenient the notation will be abbreviated by writing some functions in their limiting form , taking advantage of proofs in CL.

3.1 Conditional Normal Densities

We will be concerned often with conditional Normal distributions and therefore collect the relevant standard results here.

Let $\mathbf{Y} = \{\mathbf{X}_0\,\mathbf{X}\}$ be Normally distributed with the density

$$\begin{aligned} f_{\mathbf{Y}}(\mathbf{y}) &= \phi_{\mathbf{Y}}(\mathbf{y} - \mu_{\mathbf{Y}}) \\ &= |A|^{1/2}(2\pi)^{-n/2}\exp(-\frac{1}{2}(\mathbf{y} - \mu_{\mathbf{Y}})^t A(\mathbf{y} - \mu_{\mathbf{Y}})) \end{aligned} \tag{3.1}$$

where $A^{-1} \equiv \Sigma$ is the covariance matrix and the means $\mu_{\mathbf{Y}} = \{\mu_0\,\mu\}$.

In general if A, D are regular one may write

$$\begin{bmatrix} A & C \\ B & D \end{bmatrix}\begin{bmatrix} E & F \\ G & J \end{bmatrix} = \begin{bmatrix} I & \\ & I \end{bmatrix} \tag{3.2}$$

The four equations here implied have the solution

$$\begin{aligned} E &= (A - CD^{-1}B)^{-1} & J &= (D - BA^{-1}C)^{-1} \\ G &= -D^{-1}BE = -JBA^{-1} & F &= -A^{-1}CJ = -ECD^{-1} \end{aligned} \tag{3.3}$$

where the last equalities come from a commuted version of (3.2).

Apply this to the symmetric covariance matrix $\Sigma_T = \begin{bmatrix} \Sigma_u & \Sigma_{uz} \\ \Sigma_{zu} & \Sigma_z \end{bmatrix}$

to obtain

$$\Sigma_T^{-1} = \begin{bmatrix} E & -\Sigma_u^{-1}\Sigma_{uz}J \\ -J\Sigma_{zu}\Sigma_u^{-1} & J \end{bmatrix} \qquad \begin{aligned} E &= (\Sigma_u - \Sigma_{uz}\Sigma_z^{-1}\Sigma_{zu})^{-1} \\ J &= (\Sigma_z - \Sigma_{zu}\Sigma_u^{-1}\Sigma_{uz})^{-1} \end{aligned} \tag{3.4}$$

which establishes some notation for later use.

3.2 Density Exponent

If $\mathbf{X}_0$ is given the quadratic form in the exponent may be written

$$[(\mathbf{x}_0 - \mu_0)^t \ (\mathbf{x} - \mu)^t] \begin{bmatrix} E & F \\ F^t & J \end{bmatrix} \begin{bmatrix} \mathbf{x}_0 - \mu_0 \\ \mathbf{x} - \mu \end{bmatrix} \tag{3.5}$$

$$= (\mathbf{x} - \mathbf{M})^t J (\mathbf{x} - \mathbf{M}) + (\mathbf{x}_0 - \mu_0)^t \Sigma_u^{-1} (\mathbf{x}_0 - \mu_0) \tag{3.6}$$

$$\text{where} \quad \mathbf{M} = \Sigma_{zu} \Sigma_u^{-1} (\mathbf{x}_0 - \mu_0) + \mu. \tag{3.6A}$$

To prove this the form of $\mathbf{M}$ is obtained by equating those parts of (3.5) and (3.6) which are linear in $\mathbf{x}$ or $\mathbf{x}^t$. It must then be shown that $\mathbf{M}^t J \mathbf{M}$ from (3.6A) accounts for all the constants in (3.6).

Putting $\mathbf{z}_0 = \mathbf{x}_0 - \mu_0$ and $\mathbf{z} = \mathbf{x} - \mu$, (3.5) becomes

$$[\mathbf{z}_0^t \, \mathbf{z}^t] \Sigma_T^{-1} \begin{bmatrix} \mathbf{z}_0 \\ \mathbf{z} \end{bmatrix} = \mathbf{z}^t J \mathbf{z} + \mathbf{z}_0^t F \mathbf{z} + \mathbf{z}^t F^t \mathbf{z}_0 + \mathbf{z}_0^t E \mathbf{z}_0$$

$$= \mathbf{z}^t J \mathbf{z} + \mathbf{z} J J^{-1} F^t \mathbf{z}_0 + \mathbf{z}_0^t F J^{-1} J \mathbf{z} + \mathbf{z}_0^t E \mathbf{z}_0$$

$$= (\mathbf{z} + J^{-1} F^t \mathbf{z}_0)^t J (\mathbf{z} + J^{-1} F^t \mathbf{z}_0) + \mathbf{z}_0^t (E - F J^{-1} F^t) \mathbf{z}_0$$

$$= (\mathbf{z} - \Sigma_{zu} \Sigma_u^{-1} \mathbf{z}_0)^t J (\mathbf{z} - \Sigma_{zu} \Sigma_u^{-1} \mathbf{z}_0) + \mathbf{z}_0^t \Sigma_u^{-1} \mathbf{z}_0 \tag{3.7}$$

from (3.4); this is the desired result.

The partitioning (3.7) corresponds to the identity

$$f_{\mathbf{Z}\,\mathbf{X}_0}(\mathbf{z}\,\mathbf{x}_0) = f_{\mathbf{Z}|\mathbf{X}_0}(\mathbf{z}|\mathbf{x}_0) f_{\mathbf{X}_0}(\mathbf{x}_0)$$

and when the densities are Gaussian normalisation demands that

$$|\Sigma_T| = |\Sigma_u| / |J|. \tag{3.8}$$

The results (3.6), (3.7) and (3.8) apply for any partitions, in particular when either X_0 or the conditioned variate Z is scalar.

For single variates $\phi(ax)$ shall indicate the unit Normal density function, used with an explicit normalising factor if $a \neq 1$.

3.3 Slopes and Crossings

Put r_k for the covariance of X with the lag $2^{-n}k$. Then for the quantities of interest, associated with subdivision intervals 2^{-n},

$$R = E\{\mathbf{X} - \mu\}[\mathbf{X} - \mu]^t$$

$$= \begin{bmatrix} 1 & r_1 & r_k & r_{k+1} & r_K & r_{K+1} \\ r_1 & 1 & r_{k-1} & r_k & r_{K-1} & r_K \\ r_k & r_{k-1} & 1 & r_1 & r_{K-k} & r_{K-k+1} \\ r_{k+1} & r_k & r_1 & 1 & r_{K-k-1} & r_{K-k} \\ r_K & r_{K-1} & r_{K-k} & r_{K-k-1} & 1 & r_1 \\ r_{K+1} & r_K & r_{K-k+1} & r_{K-k} & r_1 & 1 \end{bmatrix}$$

using stationarity. The means μ are given by Γ_n above at the times $2^{-n}, 2^{-n}k$ etc.

We are now interested in local slopes (Fig.3) approximated by

$$Z_k = 2^n(X_{k+1} - X_k) = [-2^n\, 2^n]\begin{bmatrix} X_k \\ X_{k+1} \end{bmatrix}.$$

This forms a part of

$$\begin{bmatrix} X_k \\ Z_k \end{bmatrix} = S\begin{bmatrix} X_k \\ X_{k+1} \end{bmatrix} \quad \text{where} \quad S = \begin{bmatrix} 1 & 0 \\ -2^n & 2^n \end{bmatrix}$$

When triplicated this mapping leads to the transformed variates

$$\mathbf{Z} = \begin{bmatrix} S & \cdot & \cdot \\ \cdot & S & \cdot \\ \cdot & \cdot & S \end{bmatrix}(\mathbf{X} - \mu)$$
$$= A(\mathbf{X} - \mu),$$

say, with the covariance matrix ARA^t. This has the typical submatrix

$$S\begin{bmatrix} r_{K-k} & r_{K-k+1} \\ r_{K-k-1} & r_{K-k} \end{bmatrix}S^t = \begin{bmatrix} r_{K-k} & 2^n\delta r_{K-k+1/2} \\ r_{K-k-1} & r_{K-k} \end{bmatrix}$$

$$= \begin{bmatrix} r_{K-k} & 2^n\delta r_{K-k+1/2} \\ -2^n\delta r_{K-k-1/2} & 2^{2n}\delta^2 r_{K-k} \end{bmatrix}$$

where δ refers to the appropriate central difference of r.

Along the diagonal submatrices

$$r_{K-k} = 1 \quad \text{and} \quad 2^n\delta r_{K-k+1/2} \;\to\; -\dot{r}(0)$$

as $n \to \infty$. This is zero here and the last element $\to \lambda = -\ddot{r}(0)$ if we remember the symmetry of $r(t)$.

Off-diagonal elements converge similarly to the appropriate derivatives so that in a notation which emphasises actual times

$$ARA^t \to \begin{bmatrix} 1 & \cdot & r(t) & \dot{r}(t) & r(T) & \dot{r}(T) \\ \cdot & \lambda & -\dot{r}(t) & -\ddot{r}(t) & -\dot{r}(T) & -\ddot{r}(T) \\ r(t) & -\dot{r}(t) & 1 & \cdot & r(T-t) & \dot{r}(T-t) \\ \dot{r}(t) & -\ddot{r}(t) & \cdot & \lambda & -\dot{r}(T-t) & -\ddot{r}(T-t) \\ r(T) & -\dot{r}(T) & r(T-t) & -\dot{r}(T-t) & 1 & \cdot \\ \dot{r}(T) & -\ddot{r}(T) & \dot{r}(T-t) & -\ddot{r}(T-t) & \cdot & \lambda \end{bmatrix} \tag{3.9}$$

similar to the covariance matrix used by Rice and Beer[13]. In the corresponding CL calculation the diagonal submatrices are related to p_{nk} on page 286 which is stationary. Here however there are time varying coupling matrices containing $r(t), \dot{r}(t), \ddot{r}(T)$ etc. which determine the conditional densities of p_{nk}. However the CL arguments of dominated convergence are not affected by this or by our premature passage to the limit which has been anticipated in order to simplify notation.

3.4 Joint Density of Thresholds and Slopes

In CL the expected total crossing rate $\omega(t)$ is determined for downslopes at time t and the final result is an average over these slopes for a process density *conditioned* upon $X(t)$.

To reach (2.11) with a given exclusion factor we are given three upslopes to average over in a density with three crossing levels. We first rearrange the variate $\mathbf{Z}$ as $\{X_0\, X_t\, X_T\, Z_0\, Z_t\, Z_T\}$ with mean values $\{u\, v\, u\, 0\, 0\, 0\}$ for crossing levels Γ_n.

The corresponding covariances are

$$\Sigma_T = \begin{bmatrix} 1 & r(t) & r(T) & \cdot & \dot{r}(t) & \dot{r}(T) \\ r(t) & 1 & r(T-t) & -\dot{r}(t) & \cdot & \dot{r}(T-t) \\ r(T) & r(T-t) & 1 & -\dot{r}(T) & -\dot{r}(T-t) & \cdot \\ \cdot & -\dot{r}(t) & -\dot{r}(T) & \lambda & -\ddot{r}(t) & -\ddot{r}(T) \\ \dot{r}(t) & \cdot & -\dot{r}(T-t) & -\ddot{r}(t) & \lambda & -\ddot{r}(T-t) \\ \dot{r}(T) & \dot{r}(T-t) & \cdot & -\ddot{r}(T) & -\ddot{r}(T-t) & \lambda \end{bmatrix} \tag{3.10}$$

$$= \begin{bmatrix} \Sigma_u & \Sigma_{uz} \\ \Sigma_{zu} & \Sigma_z \end{bmatrix}$$

say, with inverse, conditioned matrices and means from (3.4) to (3.6A).

4. CROSSING DENSITIES

The machinery above will now be used to find the conditional densities (2.12) in Section 2.5. These require unconditional triple and quadruple slope/crossing densities $\omega(0\,t\,T\,\mathbf{z}), \omega(0\,t'\,t\,T\,z_1\,\mathbf{z})$ and $\omega(0\,t\,t'\,T\,z_2\,\mathbf{z})$.

The derivation of first crossings under slope conditions has already been discussed in Sections 2.4 and 2.5 where it transpired that densities of triple and quadruple conditioned crossings were needed. Single crossings were first discussed by S.O. Rice[13] though we follow CL[8] to obtain $\omega, \omega(0\,t\,T\,\mathbf{z})$ etc. as limits of the corresponding discrete processes $\omega_n, \omega_n(0\,t\,T\,\mathbf{z})$ over time steps 2^{-n}.

4.1 Defining Events

The conditions and events which define a range-pair period are:

A Upcrossing of u at $t = 0$. This a prior condition whose probability must not be counted since it has already confirmed the previous range-pair exceedance.

B First upcrossing of v at time $t|$A ie. first after A

C " " of u " " $T\,|$ B.

To discuss "first" upcrossings or "first after..." one must consider the general density of crossings, first or otherwise. Furthermore we must begin with the unconditional crossing densities.

As we have seen the definition of range-pair periods in terms of first crossings involves simultaneous slope and crossing conditions for one old followed by two new crossings in succession. Each set of the events A, B and C above must be conditional upon common slopes. The resultant rainflow count is similarly conditioned and the density must be averaged over the three slopes before convolution as in (2.12).

Condition A may be divided into mutually exclusive subsets which represent different ranges of upcrossing slopes. Within each such condition the upcrossing slopes for B and C also form a mutually exclusive family.

In CL the condition A is absent but the event B is similarly divided. There the crossing density is integrated over B-slopes to obtain the integrand of their (13.2.1). Our approach will be similar but $A \cap B \cap C$ leads to an averaging over slopes for A, B and C as well as slopes for excluded intermediate crossings.

As in CL the regularity of the basic process means that for a single crossing density

$$\begin{aligned}\omega(t|A)dt &= E(Crossings)\\ &= \sum_i iP_r(i\ crossings|A)\\ &= P_r(B \subset dt|A) + o(dt)\end{aligned}$$

with some abuse of notation. For the two crossings needed the range-pair count rate satisfies

$$\begin{aligned}\omega(t\,T|A)dt\,dT &= E(Simultaneous\ crossings(sc's)) \\ &= \sum_i iP_r(i\ \text{sc's} \subset dt\,dT|t\,T\,A) \\ &= P_r(B \cap C \subset dt\,dT|A) + o(dt\,dT).\end{aligned}$$

We now consider a single upwards crossing, concentrating on the events which define it. Since the result is the limit of that for a discrete process consider a stage n when the time interval is 2^{-n}. To save notation, densities will be written in their final form but convergence proofs can be developed.

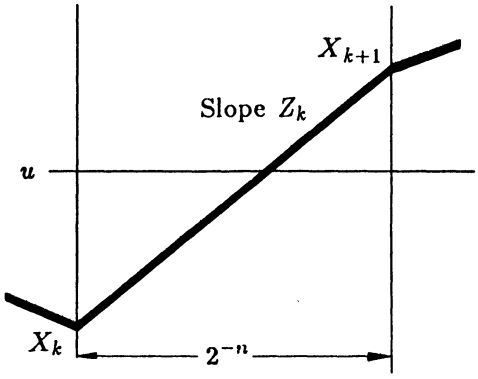

FIGURE 3 UPWARDS CROSSING OF n-th APPROXIMATE PROCESS

A single upwards crossing is shown in Figure 3 for the n-th discrete member of a sequence tending to the separable continuous process with derivatives. In terms of events from Figure 3,

$$\begin{aligned}Upwards\ crossing &= \{X_2 > u\ ,\ X_1 < u\} \\ &= \{2^n(X_2 - X_1) > 2^n(u - X_1)\ ,\ X_1 < u\} \\ &= \{Z_1 + O(2^{-n+1}) > 2^n(u - X_1)\ ,\ X_1 < u\} \qquad ,Z_1 = X'(2^{-n}), \\ &= \{2^{-n}Z_1 + o(2^{-n+1}) > (u - X_1)\ ,\ X_1 < u\} \\ &= \{u - 2^{-n}Z + o(2^{-n+1}) < X < u\}, \qquad (4.1)\end{aligned}$$

dropping the subscripts. With suitable Z values or slopes any $X < u$ can be associated with an upwards crossing and all positive slopes are allowable.

Integrating over the region (4.1)

$$2^{-n}\omega_n(2^{-n}) + o(2^{-n}) = \int_0^\infty dz \int_{u-2^{-n}z}^{u} f_{XZ}(x\,z)dx \qquad (4.2)$$

which corresponds to (13.2.4) from CL for downcrossings; essentially by the same derivation.

For a given slope Z (4.2) obviously reduces to

$$2^{-n}\omega_n(2^{-n} \cap z) = f_Z(z) \int_{u-2^{-n}z}^{u} f_{X|Z}(x|z)dx \tag{4.3}$$

or, interpreting $2^{-n}z$ as zdt,

$$\omega_n(2^{-n} \cap z)dt = z f_Z(z) f_{X|Z}(u|z)dt$$

or in the limit

$$\omega(0\, z) = z f_{X\, Z}(u\, z). \tag{4.4}$$

Integration or direct argument from (4.2) leads to

$$\omega(0) = \int_0^\infty z f_{X\, Z}(u\, z)dz, \tag{4.5}$$

half the standard CL result (their (10.3.1)) because only upcrossings have been counted here.

For multiple crossings there are results analogous to (4.4) and (4.5); crossing levels are substituted into appropriate joint densities $f_{\mathbf{X}\,\mathbf{Z}}(\mathbf{x}\,\mathbf{z})$; the conditional joint crossing densities are proportional to $Z_0, Z_t, Z_0 \cdot Z_t$ etc. so that the unconditional crossing densities are partial expectations of the products between allowable slopes.

It is now possible to evaluate (2.11) and (2.12). For the latter it is most convenient to find $\omega_i \cap z_i$ and integrate; as (4.5) follows from (4.4). The double density $\omega(t\, T\, \mathbf{z}|0)$ in (2.11) comes from the multiple-crossing analogue of (4.4) and

$$\phi_{\mathbf{X}\,\mathbf{Z}}(\mathbf{x}\,\mathbf{z}) = \frac{1}{(2\pi)^3}|\Sigma_T|^{-1/2} \exp\{-\frac{1}{2}[\mathbf{x}^t\, \mathbf{z}^t]\Sigma_T{}^{-1} \begin{bmatrix} \mathbf{x} \\ \mathbf{z} \end{bmatrix}\}$$

as

$$\omega(t\, T\, \mathbf{z}|0) = z_0\, z_t\, z_T \phi_{\mathbf{X}\,\mathbf{Z}}(\mathbf{u}\,\mathbf{z})/\phi(u) \tag{4.6}$$

where $\mathbf{u} = \{u\, v\, u\}$, $\mathrm{E}[\mathbf{X}\,\mathbf{Z}] = \mathbf{0}$ and Z_0, Z_t and $Z_T > 0$. For quadruple densities $\{\mathbf{X}\,\mathbf{Z}\}$ becomes $\{X_i\, Z_i\, \mathbf{X}\,\mathbf{Z}\}$ and Σ_T is appropriately bordered.

In (2.12) then from (4.4),(4.5) and (4.6) with its extension

$$\omega_2 = \int_0^\infty z_2 \frac{\phi_{X\, Z\, \mathbf{X}\,\mathbf{Z}}(u\, z_2\, \mathbf{u}\,\mathbf{z})}{\phi_{\mathbf{X}\,\mathbf{Z}}(\mathbf{u}\,\mathbf{z})}$$

$$= \int_0^\infty z_2 f_{Z|X\,\mathbf{X}\,\mathbf{Z}}(z_2|u\,\mathbf{u}\,\mathbf{z})dz_2$$

$$= \frac{1}{\sqrt{2\pi}} \int_0^\infty z_2 \frac{|\Sigma_2|^{1/2}}{|\Sigma_T|^{1/2}} \exp\Big\{ -\frac{1}{2}[u\, z_2\, \mathbf{u}^t \mathbf{z}^t] \Sigma_2^{-1} \begin{bmatrix} u \\ z_2 \\ \mathbf{u} \\ \mathbf{z} \end{bmatrix} + \frac{1}{2}[\mathbf{u}^t \mathbf{z}^t] \Sigma_T^{-1} \begin{bmatrix} \mathbf{u} \\ \mathbf{z} \end{bmatrix} \Big\} \quad (4.7)$$

with a similar expansion of ω_1.

4.2 Density of First Passage Time

In general if $Z \sim N(\mu, \sigma^2)$ or $\sigma f_Z(z) = \phi((z-\mu)/\sigma)$ then

$$\int_0^\infty z\, f_Z(z) dz = \mu(1 - \Phi(-\mu/\sigma)) + \sigma\phi(\mu/\sigma) \quad (4.8)$$

where Φ refers to the unit Normal distribution. In our case $f_Z(z)$ is the conditional density $f_{Z|X\,\mathbf{X}\,\mathbf{Z}}(z_i|v_i\,\mathbf{u}\,\mathbf{z})$ from (4.7) with the variance

$$\sigma_i^{\,2} = \lambda - [0\ \dot{\mathbf{r}}_i^t\ \ddot{\mathbf{r}}_i^t] \begin{bmatrix} 1 & \mathbf{r}_i^{\,t} & \dot{\mathbf{r}}_i^t \\ \mathbf{r}_i & \Sigma_u & \Sigma_{uz} \\ \dot{\mathbf{r}}_i & \Sigma_{zu} & \Sigma_z \end{bmatrix}^{-1} \begin{bmatrix} 0 \\ \dot{\mathbf{r}}_i^t \\ \ddot{\mathbf{r}}_i \end{bmatrix} \quad (4.9)$$

in the notation of (3.10) and the mean value

$$\mu_i = [0\ \dot{\mathbf{r}}_i^t\ \ddot{\mathbf{r}}_i^t][\ ditto\ ]^{-1} \begin{bmatrix} v_i \\ \mathbf{u} \\ \mathbf{z} \end{bmatrix} \quad (4.10)$$

In these equations $v_1 = v\ (t' < t)$, $v_2 = u$, $(t < t' < T)$ and

$$\mathbf{r}_i = \{r(t')\ r(t-t')\ r(T-t')\}$$

for t' corresponding to ω_1 or ω_2. Substitution into (2.11) and (2.12) then produces the overall first passage density

$$\begin{aligned} f_1(T) = \int_0^T \frac{\phi_{\mathbf{X}}(\mathbf{u})}{\phi(u)} dt \int_0^\infty z_t z_T \phi_{\mathbf{Z}|\mathbf{X}}(\mathbf{z} - \mu_{\mathbf{Z}|\mathbf{u}}) \\ \times \quad \exp\Big\{ -\int_0^t \phi_{X(t_1)|\mathbf{X}\,\mathbf{Z}}(v - \mu_{X(t_1)|\mathbf{u}\,\mathbf{z}}) [\mu_1(1 - \Phi(-\frac{\mu_1}{\sigma_1})) + \sigma_1 \phi(-\frac{\mu_1}{\sigma_1})]_{t_1} dt_1 \\ - \int_t^T \phi_{X(t_2)|\mathbf{X}\,\mathbf{Z}}(u - \mu_{X(t_2)|\mathbf{u}\,\mathbf{z}}) [\mu_2(1 - \Phi(-\frac{\mu_2}{\sigma_2})) + \sigma_2 \phi(-\frac{\mu_2}{\sigma_2})]_{t_2} dt_2 \Big\} d\mathbf{z}. \end{aligned} \quad (4.11)$$

where $\mu_{\mathbf{Z}|\mathbf{u}} = \Sigma_{zu}\Sigma_u^{-1}\mathbf{u}$, with variances J^{-1} from (3.4),

$$\mu_{X(t_i)|\mathbf{u}\,\mathbf{z}} = [\mathbf{u}^t\, \mathbf{z}^t] \begin{bmatrix} \Sigma_u & \Sigma_{uz} \\ \Sigma_{zu} & \Sigma_z \end{bmatrix}^{-1} \begin{bmatrix} \mathbf{r}_i \\ \dot{\mathbf{r}}_i \end{bmatrix}$$

and the variances are

$$1 - [\mathbf{r}_i^t \dot{\mathbf{r}}_i^t]\,[\ ditto\ ]^{-1} \begin{bmatrix} \mathbf{r}_i \\ \dot{\mathbf{r}}_i \end{bmatrix}$$

In (4.11) the conditional densities may also be written in the fractional forms such as $\phi_{\mathbf{Z}|\mathbf{X}} = \phi_{\mathbf{ZX}}/\phi_{\mathbf{X}}$ as in part of (4.7). Because the elements of all the covariance matrices are arbitrary functions of time through $r(t)$ further integration of (4.11) is generally impossible. However the exact theoretical form of (4.11) is somewhat simpler, at least in appearance. For this the Rice type [16] of inclusion-exclusion series is used instead of the approximate exclusion factor exp .... This will now be derived from the discrete-time cases; necessarily for ω_1 and ω_2 together. Suppose the time interval 2^{-n} corresponds to $K = 2^n T - 2$ variates altogether and k up to the time t. Then two non-crossings are

$$\bigcap_{j=1}^{K} (\mathcal{U} - \omega_j 2^{-n}) = \mathcal{U} + \bigcup_{M=1}^{K} \bigcap_{j=1}^{M} (-1)^M (\omega_j 2^{-n}), \tag{4.12}$$

using $\omega_j 2^{-n}$ to represent an upwards crossing of the j-th interval. Consider the event of m out of M crossings occurring before t. Each M-th order union of mutually exclusive events contains K^M ordered terms , of which $K^M - K!/M!$ are repetitions captured by unions of lower order. From the hypergeometric distribution the number of these terms which contribute for the partition $(m, M-m)$ is

$$K^M \binom{k}{m} \binom{K-k}{M-m} \Big/ \binom{K}{M} \to \binom{M}{m} k^m (K-k)^{M-m}$$

as $K \to \infty$ while $k/K = t/T + O(1/K)$. This corresponds to $\binom{M}{m}$ of the same unions of mutually exclusive events. The corresponding probabilities converge to

$$\binom{M}{m} \int_0^t dt_1 \ldots \int_0^t dt_m \int_t^T dt_{m+2} \ldots \int_t^T dt_M\ \omega(\mathbf{t}_m\, t\, \mathbf{t}_{M-m}\, T\, \mathbf{z}_M | X(0) = u, z_0 \geq 0)$$

where the defining crossings at t, T and conditions at the origin have now been included.

As one may also discover by direct expansion on the left of (4.12) such terms belong to the complete series

$$\frac{\omega(0\, t\, T\, \mathbf{z})}{\omega(0\, z_0)} + \sum_{M=1}^{\infty} \Big(-\int_0^t dt_i - \int_t^T dt_j \Big)^M \omega(\mathbf{t}_m\, t\, \mathbf{t}_{M-m}\, T\, \mathbf{z}_M | X(0) = u, z_0 \geq 0) \tag{4.13}$$

where $\mathbf{t}_m = \{t_1 \ldots t_i \ldots t_m\}$, $\mathbf{z}_M = \{z_1 \ldots z_M\}$ and $\mathbf{t}_{M-m} = \{t_{m+2} \ldots t_j \ldots t_M\}$.

This corresponds to the approximate expression (4.11) apart from averaging over positive slopes (z_0 and $\mathbf{z}_M$ here) and the convolution. When this is done it is obvious that individual terms contain orthant Normal probabilities of all orders from densities conditioned at the times $\{0\, \mathbf{t}_m\, t\, \mathbf{t}_{M-m}\, T\}$. It should be noted that truncation of this series corresponds to neglecting the exclusion of more than $M-2$ intermediate multiple crossings which is serious when $T = O(M-2)\mu_T$ or more. Thus for large T's the asymptotic formula (4.14) below could be more accurate.

4.3 Asymptotic Density and Narrow-Band Noise

If T is sufficiently large then t is also almost certainly large and (4.11) simplifies remarkably. For a slightly closer approximation we will introduce a time R over which the correlation is almost perfect so that no occurrence is possible for $T < 2R$. If this is done then (4.11) becomes

$$f_1(T) \sim \int_R^{T-R} \frac{\lambda}{2\pi}\phi(u)\phi(v)\exp\Big(-\sqrt{\frac{\lambda}{2\pi}}\Big\{\int_R^t \phi(v)dt' + \int_t^{T-R}\phi(u)dt'\Big\}\Big)dt$$

$$= \sqrt{\frac{\lambda}{2\pi}}\,\frac{\phi(u)\phi(v)}{\phi(v)-\phi(u)}\Big(\exp-\sqrt{\frac{\lambda}{2\pi}}(T-2R)\phi(u) - \exp-\sqrt{\frac{\lambda}{2\pi}}(T-2R)\phi(v)\Big) \tag{4.14}$$

This is actually an approximate density for the whole range $T > 2R$ with a first moment $(1/\phi(u) + 1/\phi(v) + 2R)$. It should be noted that λ and R are not independent and that, if the concept is valid, $2R = R_0(\lambda, u, v) + R_t(\lambda, u, v)$, say.

Suppose that the non-zero spectrum is uniform but confined to the frequency bands $\pm\Omega \pm \Delta$. Then

$$r(t) \;=\; \cos\Delta t \sin\Omega t/\Omega t \tag{4.15}$$

If Δ/Ω is small enough then in (4.11) and (4.13) the rapid fluctuations of (4.15) are damped by integration over time. In addition if $t > 2\pi/(\Omega \pm \Delta)$ then (4.15) is small and all the components of (4.11) and (4.13) approach their asymptotic form with $R = O(2\pi/\Omega)$. In effect the dithering at rate Ω makes (4.14) applicable for much shorter time intervals.

The clumping of outcrossings with narrow band noise discussed by some authors corresponds here to first passages $T \approx 2\pi/\Omega$ so that one must then expect $f_1(2\pi/\Omega)$ to be large. This is outside the range of (4.14).

5. ONE DEGREE OF FREEDOM SYSTEM

We finally consider exceedances from a process which is the response of a simple linear system to white noise [8]. The extension to several degrees of freedom [8,9] is similar and not difficult in concept but the details become messy without producing further insight. Let $X(t)$ be the stationary solution of

$$\ddot{X} + 2\varsigma\nu\dot{X} + \nu^2 X = dW(t) \tag{5.1}$$

The Fourier transform of this presents us with the transfer function

$$H(s) = [\nu^2 - s^2 - 2i\varsigma]^{-1} \tag{5.2}$$

and when this acts upon white noise the resultant spectrum

$$HH^* = [(\nu^2 - s^2) + 4\varsigma^2\nu^2 s^2]^{-1} \tag{5.3}$$

which has poles when

$$(s/\nu)^2 = 1 - 2\varsigma^2 \pm 2i\varsigma\sqrt{1-\varsigma^2}$$
$$= (\alpha \pm i\beta)^2 \quad \text{say.}$$

At each pole $|s| = \nu$ so that $\alpha^2 + \beta^2 = 1$ and we define the phase difference $\varphi = \arctan \beta/\alpha$. The inverse of (5.3) reduces to the covariance

$$R(t) = \frac{\exp(-\beta\nu t)}{4\alpha\beta\nu^4}\cos(\alpha\nu t - \varphi).$$

The magnification factor can be cancelled by suitably scaling the white noise input leading to

$$r(t) = \alpha^{-1}\exp(-\beta\nu t)\cos(\alpha\nu t - \varphi). \tag{5.4}$$

If we define $\gamma = \alpha + i\beta$ then this has the complex form

$$r(t) = \frac{1}{2\alpha}(\gamma e^{-i\nu\gamma^* t} + \gamma^* e^{i\nu\gamma t}). \tag{5.4A}$$

The derivatives are

$$\dot{r}(t) = -(\nu/\alpha)e^{-\beta\nu t}\sin\alpha\nu t \tag{5.5}$$

$$= \frac{\nu}{2i\alpha}(e^{-i\nu\gamma^* t} - e^{i\nu\gamma t}). \tag{5.5A}$$

and

$$\ddot{r}(t) = (\nu^2/\alpha)e^{-\beta\nu t}\cos(\alpha\nu t + \varphi) \tag{5.6}$$

$$= -\frac{\nu^2}{2\alpha}(\gamma^* e^{-i\nu\gamma^* t} + \gamma e^{i\nu\gamma t}). \tag{5.6A}$$

The derivations here take advantage of the facts that $\sin\varphi = \beta$ and $\cos\varphi = \alpha$. It will also be noted that $\lambda = \beta\nu^2/\alpha = \nu^2\tan\varphi$. For linear systems of higher order in canonical form the autocorrelation matrices are summations of terms like (5.40,(5.5) and (5.6).

5.1 Correlation Structure and Computation

The density (4.11) may be used for any stationary Gaussian probabilities and the correlations above can be substituted, preferably by a computer program. The computation requires inversions like those in (4.6),(4.7) or (4.9) but some insight into their structure can be gained for systems like (5.1) and possibly for linear dynamic systems. Since we are interested now in several times for a stationary process it is useful to emphasise time differences by the notational change $\{0\ t\ T\} \rightarrow \{T_0\, T_1\, T_2\}$. The 3×3 submatrices Σ_u and Σ_z are similar and easily inverted. Thus from (5.4A)

$$\alpha^{-1}\det[e^{-\beta\nu|T_j - T_i|}\cos(\alpha\nu|T_j - T_i| - \phi)]\Sigma_{\mathbf{u}}^{-1}$$
$$= \frac{1}{2}e^{-\beta\nu|T_j - T_i|}\{\cos(\alpha\nu|T_j - T_i|) + \cos(\alpha\nu T_{ij} - 2\phi)\}$$
$$- \alpha\cos(\alpha\nu|T_j - T_i| - \phi) \tag{5.7}$$

where $T_{ij} = 2T_k - T_i - T_j$ if i, j and k are all different or $T_{ii} = 2|T_j - T_k|$. Similarly for the slope covariances (5.6A) leads to

$$(\nu^2/\alpha)\det[e^{-\beta\nu|T_j-T_i|}\cos(\alpha\nu|T_j - T_i| + \phi)]\Sigma_z^{-1}$$
$$= \frac{1}{2}e^{-\beta\nu|T_j-T_i|}\{\cos(\alpha\nu|T_j - T_i|) + \cos(\alpha\nu T_{ij} + 2\phi)\}$$
$$- \alpha\cos(\alpha\nu|T_j - T_i| + \phi). \tag{5.8}$$

The complex forms of these are not shown here but with (5.5A) they lead to the conditional slope density $\phi_{\mathbf{Z}|\mathbf{X}}(\mathbf{z}|\mathbf{u})$. After $\phi_{\mathbf{X}}(\mathbf{u})/\phi(u)$ the essential computation in (4.11) is

$$\mathrm{E}(z_0 z_1 z_2 \cdot (Exclusion\ factors|z_i > 0, \mathbf{u}). \tag{5.9}$$

From mixed derivatives of a generating function $\mathrm{E}(\exp(\mathbf{s}^t\mathbf{z})|z_i > 0)$ it can be shown that $\mathrm{E}(z_0 z_1 z_2)|z_i > 0)$ involves several Normal orthant probabilities up to the trivariate case as well as the corresponding densities. Therefore it cannot be expected that (5.10), the inner integral of (4.11), would be any simpler. If one presumes upon a family relationship to gamma densities then the the asymptotic form (4.14) might be improved by collocation at one time.

6. DISCUSSION

From the preceding arguments it can be seen that formulae similar to (4.11) or (4.13) describe the density of range-pair passage times for any sort of load input; the differences arise from the different probability models used for evaluation. Corresponding formulae for other types of range-pair or for other definitions of the same type can also be written by analogy(see [13]).Prima facie it seems that each definition[6], even of the same type of count, will lead to a different density function.

For long times the asymptotic form (4.14) is suggested. This tends toward the standard Poisson model in virtue of reduced correlations. Narrow band noise extends the range of this simple asymptotic density.

The results of Rychlik and Lindren[3,4,5] should relate to those here as

$$f_{U\,V}(u, v) = E_{T|X(0)\,X(T)}\left(\frac{\partial^2 f_1(T|u\,v)}{\partial u \partial v}\right)$$

where the range is $U - V$ and only upwards counts are considered, over long histories.

As mentioned in Section 2.5, all the results except (4.14) hold for variable thresholds but the notational burden has been refused. However this may have applications in earthquake engineering and similarly modulated cases.

The waiting-time or exclusion factors used here are actually approximations since the densities used are conditioned only on $X(t)$ and $\dot{X}(t)$ at the crossing times instead of the intermediate history. This has been discussed by J.R. Rice and Beer[13] for their problem and S.O. Rice[16] has previously treated another similar case. From the experimental comparisons by Rice and Beer the effect of

the approximation is expected to be small. The frequency of extremes has been discussed in the earlier work of Sjöström[17] and originally by S.O. Rice[16].

The response to linear systems can be represented as a linear summation of terms such as (5.4) to (5.6) and the various submatrices of the covariance are very similar. Sherman has counted range-pairs from simulated data[18]. This includes results from single degree of freedom systems and it is planned to compare the means of the present densities with these.

REFERENCES

[1] Endo, T.,Kobayashi, K., Mitunaga, K. and Sugimua, N.
Numerical comparison of the cycle count methods for fatigue damage evaluation and plastic-strain damping energy of metals under random loading. 1975 Joint JSME-ASME Applied Mechanics Western Conference. 75-AM JSME A-17

[2] Fraser, R.C.
A one-pass method for counting range-mean-pair cycles for fatigue analysis. Aeronautical Research Laboratories(Melbourne), Structures Note 454, June 1979.

[3] Rychlik, I.
A new definition of the rainflow cycle counting method. International Journal of Fatigue,**9** 2, February 1987, pp 119-121.

[4] Rychlik, I.
Rain flow cycle distribution for a stationary Gaussian load process. Statistical Research Report 1986:4, University of Lund,Sweden,1986, pp 1-36.

[5] Lindgren, G. and Rychlik, I.
Rain flow cycle distributions for fatigue life prediction under Gaussian load processes. Statistical Research Report, University of Lund,Sweden,1986, pp 1-17. To appear in Fatigue of Engineering Materials and Structures.

[6] Ford, D.G. and Patterson, A.K.
A range-pair counter for monitoring fatigue. Aeronautical Research Laboratories(Melbourne), Technical Memorandum SM 195, January 1971.

[7] Sewell, R.
An investigation of flight loads counting methods and effects on estimated fatigue life. NAE Report 1412-ST 431 (Canada), October 1975.

[8] Crandall, Stephen H. editor
Random Vibrations. MIT Press 1958.

[9] Lin, Y.K.
Probabilistic Theory of Structural Dynamics. McGraw Hill 1967.

[10] Garrison, J.N.
An assessment of atmospheric turbulence data for aeronautical applications. Royal Aeronautical Society Society, London. Conference on Atmospheric Turbulence, 18-21 May 1971.

[11] Cramér, Harald and Leadbetter, M.R.
Stationary and Related Stochastic Processes. Wiley, 1967.

[12] ibid. Chapter 9.
[13] Rice, J.R. and Beer, F.P.
On the distribution of rises and falls in a continuous random process.
Journal of Basic Engineering(Trans. ASME D **87** 2) June, 1965, pp 398-404.
[14] Dobrushin, R.L.
Properties of sample functions of a stationary Gaussian process.
Teoriya Veroyatnostei i ee Primeneniya **5**,1960. pp 132-134.
[15] Cox, D.R. and Lewis, P.A.W.
*The Statistical Analysis of Series of Events.*Methuen and John Wiley, 1966.
[16] Rice, S.O.
Mathematical Analysis of Random Noise. Bell System Technical Journal,
23 3 July 1944, pp 282-332 and **24** 1 January 1945, pp 46-156.
[17] Sjöström, Sverker
On Random Load Analysis. Kungl. Tekniska Högskolans Handlingar,
Stockholm. Report KTH 181(Math. & Physics 19), 1961.
[18] Sherman, D.J.
Gust Measurements and the N_0 Problem.*Aircraft Structural Fatigue.* Proceedings of a symposium held in Melbourne, 19-20 October, 1976
ARL/STRUC-Report 363 or MAT-Report 104.

A SAMPLING DISTRIBUTION FOR SYSTEM RELIABILITY ASSESSMENT

Gongkang Fu & Fred Moses
Department of Civil Engineering
Case Western Reserve University
Cleveland, Ohio 44106, USA

ABSTRACT

This paper introduces a sampling distribution (WGNSD) for Importance Sampling method, which can be used in structural system reliability assessment. Four numerical examples of various cases presented verify success of the approach. It is clarified that independent sampling distribution produces poor estimates for correlated structural system.

1 INTRODUCTION

A structural system consists of a number of random variables $\underline{X}$ such as loads and component resistances. Its system reliability analysis can be formulated by considering M significant failure modes

$$g_m = g_m(\underline{X}) \qquad (m=1,2,\ldots,M) \qquad (1)$$

and the probability measure of system failure occurrence

$$P_{f(sys)} = \text{Prob}[\text{ any } g_m(\underline{X})\leq 0\ ] \qquad (m=1,2,\ldots,M)$$
$$= \int_{\underline{x}} G(\underline{x})\ f(\underline{x})\ d\underline{x} \qquad (2)$$

where $f(\underline{x})$ is the joint probability density distribution of $\underline{X}$, $G(\underline{x})$ is an indicator function

$$G(\underline{x}) = \begin{cases} 1 & \text{any } g_m(\underline{x})\leq 0 \\ 0 & \text{all } g_m(\underline{x})>0 \end{cases} \qquad (m=1,2,\ldots,M) \qquad (3)$$

In general it is extremely difficult to find the joint probability density distribution of g_m's, which is necessary to carry out the probability integration in (2). The multifold integration involved would be terribly time-consuming even if the joint distribution would be available since the failure region $G(\underline{x})=1$ would be intractable. Two alternatives available are bounding techniques and Monte Carlo simulation.

The research on bound searching has shown that as a narrower bound is desired, more information on mode occurrence unions must be accessible. Examples are comparisons among bounds of first order [Cornell 1967], second order [Ditlevsen 1979] and third order [Ramachandran 1985]. It by no means excludes the possibility of exhaustively taking advantage of the required information without "wasting", for instance, a proper "ordering" of failure modes. Unfortunately, the joint distributions of failure event pairs or trios are not always available, and sometimes not even their correlation coefficients.

Monte Carlo simulation is another alternative to estimate system failure probability. Developments of high speed digital computers have made this method much more attractive than ever. However, it is still far from perfect despite advantages of simplicity and automatic inclusion of correlations. The major concern is its efficiency. This paper is to focus on improvement of its accuracy and efficiency by using Importance Sampling. A sampling distribution (WGNSD) is introduced for general system reliability assessments.

2 IMPORTANCE SAMPLING METHOD

Importance Sampling is a variance reduction technique well known in statistical simulation. Recently its application to structural reliability attracted researchers in this area [Harbitz 1983, Melchers 1984]. Its basic idea is to completely disturb the original distribution function $f(\underline{x})$ and sample from another distribution function which gives much more realizations of system failure, and then "correct" the result by a proper weighting. Eq.(2) is then rewritten as follows :

$$P_{f(sys)} = \int_{\underline{x}} [G(\underline{x}) \frac{f(\underline{x})}{p(\underline{x})}] \; p(\underline{x}) \; d\underline{x} \tag{4}$$

where $p(\underline{x})$ is the sampling distribition function to generate random samples $\underline{x}$ from. The Importance Sampling estimator $\tilde{P}_{f(sys)}$ of $P_{f(sys)}$ is to be obtained by the following scheme :

$$\tilde{P}_{f(sys)} = \frac{1}{N} \sum_{k=1}^{N} \frac{G(\underline{x}_k) \; f(\underline{x}_k)}{p(\underline{x}_k)} \tag{5}$$

where $\underline{x}_k$ are samples from $p(\underline{x})$ instead of $f(\underline{x})$ and N is sample size. This gives an unbiased estimator of $P_{f(sys)}$:

$$E[\tilde{P}_{f(sys)}] = P_{f(sys)} \tag{6}$$

Its variance turns out to be

$$Var[\tilde{P}_{f(sys)}] = \frac{1}{N} \left(E[\frac{G(\underline{x}) \; f(\underline{x})}{p(\underline{x})}]^2 - P_{f(sys)}^2 \right) \tag{7}$$

Eq.(7) gives the most attractive feature of Importance Sampling, as the term in the parenthesis can vanish without any requirement on N. It states that the variance can, in theory, be reduced to zero without increase of sample size N. Obviously, the variance reduction depends on the choice of the sampling distribution $p(\underline{x})$. It is noticed that $p(\underline{x})$ has to be chosen such that more important contributions to $P_{f(sys)}$ can be included.

3 WEIGHTED GENERAL NORMAL SAMPLING DISTRIBUTION (WGNSD)

Importance Sampling is very promising but care must be exercised to determine the sampling distribution $p(\underline{x})$. The theory does promise the possibility of zero variance, but not guarantee it at all. As a matter of fact, a careless choice of the sampling distribution may lead to a variance increase instead of reduction! Unfortunately, this has never been mentioned by structural reliability researchers interested in Importance Sampling. The examples in this paper will impress, hopefully, the reader how an improper sampling distribution may lead to poor estimates.

An ideal choice of sampling distribution for Importance Sampling is to yield zero variance of the estimator $\hat{P}_{f(sys)}$ [Kahn 1956]:

$$p(\underline{x}) = \frac{G(\underline{x})\, f(\underline{x})}{P_{f(sys)}} \tag{8}$$

One can verify it by simply substituting (8) into (7). It is, however, disappointing to notice that the optimal sampling distribution dependes on the exact solution $P_{f(sys)}$ to be estimated. Nevertheless, eq.(8) offers important information for an ideal optimal sampling distribution (see Fig.1 for an example of 2-dimensional problem): a) Indicator function $G(\underline{x})$ serves to truncate the original distribution $f(\underline{x})$ and to require all samples be from the "tail" part of $f(\underline{x})$ as well as in the failure region $G(\underline{x})=1$. b) The optimal sampling distribution is proportional to the "tail" part of the original one. c) The truncated original distribution is factored by $1/P_{f(sys)}$ to be qualified as a probability distribution function.

Considering these important features and taking advantage of reliability information of individual modes: reliability indices β_m and corresponding design points $\underline{x}_m^*$ (m=1,2,...,M), a general sampling distribution is introduced in eq.(9). It is named as Weighted General Normal Sampling Distribution (WGNSD).

$$p(\underline{x}) = \sum_{m=1}^{M} w_m\, p_m(\underline{x}) \tag{9}$$

where $p_m(\underline{x})$ is joint normal distribution of the basic random variable vector $\underline{X}$ with the same covariance matrix as $f(\underline{x})$ and design point $\underline{x}_m^*$ of the m-th mode as its mean

vector; w_m is a weight for $p_m(\underline{x})$. The weights are required to satisfy the proportional conditions

$$\frac{f(\underline{x}_l^*)}{f(\underline{x}_m^*)} = \frac{p(\underline{x}_l^*)}{p(\underline{x}_m^*)} = \frac{\sum_{j=1}^{M} w_j \, p_j(\underline{x}_l^*)}{\sum_{k=1}^{M} w_k \, p_k(\underline{x}_m^*)} \qquad (m=2,3,\ldots,M) \tag{10}$$

and the qualification condition

$$\begin{cases} \sum_{m=1}^{M} w_m = 1 \\ w_m \geq 0 \end{cases} \qquad (m=1,2,\ldots,M) \tag{11}$$

One may take advantage of WGNSD as follows:

1) Easy understanding and controlling in samplings by normal distributions $p_m(\underline{x})$. This chioce is also based on the fact that the type of sampling distribution does not make much difference as long as the important information around design points $\underline{x}_m^*$ are included.

2) Closeness to the "tail" part of the original distribution $f(\underline{x})$. The proportional conditions (10) are to make the peak value ratios of WGNSD match the original ones of $f(\underline{x})$ by adjusting weights w_m. These peak values occur at the design points, based on which reliability indices of modes β_m are measured. The employment of the same covariance as $f(\underline{x})$ is to avoid large deviation of the sampling distribution $p(\underline{x})$ from the original one $f(\underline{x})$, especially when some of basic random variables are, or close to, fully correlated.

3) Use of important information obtained in mode reliability analysis. WGNSD consists of M sub-distributions $p_m(\underline{x})$ which are centered at the corresponding design points $\underline{x}_m^*$ of mode m. These points can be obtained by quite successful approximation methods such as first order second moment or maximizations of the original distribution $f(\underline{x})$ subject to the corresponing failure mode equations. The latter reveal importance of these points as maxima, from whose neighbourhoods most of contributions to $P_{f(sys)}$ and approximately 50% of samples realizing failure are expected if the failure surfaces are not nonlinear of high order.

4) Feasibility of separate sampling and weighted sample sizes for individual modes. Substituting (9) into (4), one has the sampling scheme of WGNSD:

$$\tilde{P}_{f(sys)} = \sum_{m=1}^{M} \frac{w_m}{N_m} \sum_{k_m=1}^{N_m} \frac{G(\underline{x}_{k_m}) \, f(\underline{x}_{k_m})}{\sum_{j=1}^{M} w_j \, p_j(\underline{x}_{k_m})} \tag{12}$$

in which sampling of WGNSD is grouped corresponding to failure modes. N_m is the size for the m-th mode sampling, $\underline{x}_{k_m}$ is the k-th realization of the basic random variable vector from the m-th general normal distribution $p_m(\underline{x})$. Contributions of individual modes to $P_{f(sys)}$ are not expected to be equal in general obviously. Another weighting on the sample sizes N_m is reasonable and economic in computation . The weighting is suggested to be proportional to the ratio of corresponding density distribution values:

$$N_m \tilde{=} \frac{f(\underline{x}_m^*)}{f(\underline{x}_1^*)} N_1 \qquad (m=1,2,\ldots,M) \qquad (13)$$

The approximate equality is due to that N_m has to be an integer in practice.

Eq.(11) must be satisfied for $p(\underline{x})$ being a probability density distribution. It should be noticed that determination of weights w_m subject to (10) and (11) may fail because of the closeness of design points. In this case, a single general normal sampling distribution should be used to "cover" these nearby design points or, equivalently, modes.

WGNSD construction is inspired by Melchers' [1984] sampling distribution, which is a special case of WGNSD in (9):

$$p(\underline{x}) = \frac{1}{M} \sum_{m=1}^{M} h_m(\underline{x}) \qquad (14)$$

where w_m has been set equal to 1/M for every mode, $h_m(\underline{x})$ is similar to $p_m(\underline{x})$ defined in eq.(9) except that its covariance matrix is diagonal. The covariance matrix keeps the original diagonal terms of $f(\underline{x})$'s as $p_m(\underline{x})$ in (9), and sets the off-diagonal terms zero. It obviously ignores the correlation information of the original joint distribution. It will be seen in examples later that this implies significant loss of important information about $P_{f(sys)}$ to be estimated.

In summary for this section, the WGNSD is constructed to possess some of the important features of the optimum. Numerical examples in the next section will show that WGNSD works quite successfully for various types of problems in structural system reliability analysis.

Eq.(8) also inspires an iteration strategy of estimation. However, the authors' experience showed that this idea failed here due to 1) estimated approximation of the criterion and search direction for iteration and 2) lack of start point. The variance of estimator $\tilde{P}_{f(sys)}$ can be used as a search objective and criterion for iteration termination, however, it has to be estimated and its doubtful accuracy affects directly the determination of new sampling distribution for the next iteration. The extremely small value of failure probability to be estimated increases the degree of difficulty in the particular problem. WGNSD can be used as the first trial of optimal sampling distribution search, as far as the start point is

concerned, but the following examples will display accurate enough results of WGNSD to make further iterative searches unnecessary.

4 NUMERICAL EXAMPLES BY WGNSD

Examples in this section are to show how WGNSD works in estimation of structural system reliability for different cases such as unequal β_m's of modes, correlated failure modes, correlated basic random variables and discontinuous failure mode equations due to brittle behavior of material. The same sampling distribution has been employed for system reliability assessments of bridge structures [Fu & Moses 1987, 1986].

* Example 1: Independent Modes with Unequal β_m's

Consider a system with two failure modes:

$$g_1 = R - S$$
$$g_2 = 42 - R - S \qquad (15)$$

where R and S are resistance and load effect random variables, respectively. They are assumed to be independent of each other and normally distributed: $R \sim N(20,2)$ and $S \sim N(9,2.7)$. The two modes concerned are mutually independent. This kind of problem may be encountered in practice when the resistance may act as a load from another view. An example can be the gravity of a structure, being a resistance to overturning moment of horizontal loads as well as a load to the foundation.

$\tilde{P}_{f(sys)}$ vs. number of samples used is plotted in Fig.2, and details of the individual modes. The weighted sample sizes suggested in (13) is employed. The values in the parentheses near the marked estimates of Fig.2 are relative errors of the estimates. Using only 1,000 samples, for example, WGNSD has given quite satisfactory result with relative error of 12.5%.

Fig.3 is a comparison of weighted and non-weighted sample sizes in application of WGNSD for the same problem. A range of total sample size practically affordable from 1,000 to 2,000 is plotted in Fig.3. About 1 second of CPU time is used to obtain each estimate on the VAX 780 computer system. Most of cases of Fig.3 show that weighted sample sizes give better estimates than non-weighted ones, i.e. more accurate values are obtained by using the same total number of samples, while the cost for the weighting in sample sizes is almost zero.

* Example 2: Correlated Modes with Unequal β_m's

In this example, mode 2 of Example 1 is replaced by

$$g_2 = 20 - S \qquad (16)$$

so that g_1 and g_2 are now correlated. Basic random variable R and S are the same as in Example 1. A comparison of the sampling scheme WGNSD with Melchers (14) is made in Fig.4 over a range of total sample size N_t. The former shows better accuracy, obviously.

* Example 3: Multiple Correlated Variables and Modes

Consider a structure system of M components in series. The components are assumed equally correlated with a common correlation coefficient ρ. They are identical and normally distributed random variables under a deterministic load S (Fig.5). R and σ are their common mean and standard deviation, respectively. Every component is designed equally reliable. This system has M similar failure modes:

$$g_m = R_m - S \qquad (m=1,2,\ldots,M) \tag{17}$$

These failure modes are correlated whenever the components are correlated. The design point R_m is found

$$\underline{R}^*_m = (R^*_{m,1}, R^*_{m,2}, \ldots, R^*_{m,M})^T \tag{18a}$$

$$R^*_{m,i} = \begin{cases} \rho S + R(1-\rho) & i \neq m \\ S & i=m \end{cases} \qquad (i=1,2,\ldots,M) \tag{18b}$$

by maximizing the original joint distribution of $\underline{R}$

$$f(\underline{r}) = \frac{1}{(2\pi)^{M/2}\,|\sum\rho|^{1/2}\,\sigma^M} \mathrm{Exp}\left[-\frac{1}{2\sigma^2}\left\{\underline{r}-\bar{R}\underline{1}\right\}\sum\nolimits_{\rho}^{-1}\left\{\underline{r}-\bar{R}\underline{1}\right\}^T\right] \tag{19}$$

in which T denotes transpose of a vector hereafter, $|\sum\rho|$ and $\sum_{\rho}^{-1}$ are determinant and inverse of correlation coefficient matrix:

$$|\sum\rho| = (1-\rho)^{M-1}[(M-1)\rho + 1] \tag{20}$$

$$\sum\nolimits_{\rho} = \frac{(M-2)\rho+1}{(1-\rho)[(M-1)\rho+1]} \begin{bmatrix} 1 & & & & & -\frac{\rho}{(M-2)\rho+1} \\ & 1 & & & & \\ & & 1 & & & \\ & & & \ddots & & \\ & & & & 1 & \\ -\frac{\rho}{(M-2)\rho+1} & & & & & 1 \end{bmatrix} \tag{21}$$

The WGNSD is constructed based on the design points of (18),

$$p(\underline{x}) = p(\underline{r}) = \frac{1}{M}\sum_{m=1}^{M} P_m(\underline{r}) \tag{22a}$$

$$P_m(\underline{r}) = \frac{1}{(2\pi)^{M/2}\,|\sum\nolimits_{\rho}|^{1/2}\,\sigma^M} \mathrm{Exp}\left[-\frac{1}{2\sigma^2}\left\{\underline{r}-\underline{R}^*_m\right\}\sum\nolimits_{\rho}^{-1}\left\{\underline{r}-\underline{R}^*_m\right\}^T\right] \tag{22b}$$

The weights have been set equal to 1/M as the ratios of the peak values are equal and

unity, as all modes are obviously equally important to $P_{f(sys)}$.

This problem has been solved by Grigoriu and Turkstra [1979] using numerical integration. Their results are considered as exact and plotted in solid curves in Fig.5 for M=2,4,6,8,10. Discrete points marked are from WGNSD with weighted sample sizes for comparisons. Total sample size of 1,000 is used.

It is observed that the WGNSD suggested give estimates of good agrrement with the exact values, and estimate points deviate more from the exact values when M increases. This is due to that less samples for individual modes are used with a constant total sample size (1,000) for larger M. Overall speaking, for total 108 estimates of M=2,3,...,9,10 and =0,.1,.2,...,.9,.95,1 only 5 of them have relative errors over 10% and the maximum one is 16.15% by using 1,000 samples. For the most costly case M=10, the 1,000 evaluations take about 4 seconds CPU time of the VAX 780 computer. It is quite satisfactory from a practical view.

* Example 4: Correlated and Discontinuous Failure modes

A two bar parallel structural system is considered (Fig.6). The components R_1 and R_2 are assumed to be of brittle failure and jointly normally distributed with a correlation coefficient ρ. They are designed to have common coefficient of variance 20% and mean value proportional to a deterministic load S by design factor 2.2:

$$\bar{R}_1 = \bar{R}_2 = 2.2*(S/2) = 1.1*S \tag{23}$$

The discontinuous failure mode equations g_1 and g_2 are shown in Fig.6. The design point $\underline{R}_1^*$ corresponding to mode 1

$$\underline{R}_1^* = (R_1^*, R_2^*)^T \tag{24a}$$

is formed by

$$R_1^* = S/2$$

$$R_2 = \begin{cases} S(1.1-0.6\ ) & 1/6 \le \rho \le 1 \\ S & 0 \le \rho \le 1/6 \end{cases} \tag{24b}$$

$\underline{R}_2^*$ for mode 2 can be found readily by symmetry of the two modes. The WGNSD is constructed as (22) except setting M=2 and $\underline{R}_m^*$ (m=1,2) as defined by (24). Estimated $P_{f(sys)}$ vs. correlation coefficient by using 2,000 samples are plotted in Fig.6. The exact solution of solid curve is obtained by using the table of bivariate normal distribution integration [National Bureau of Standards 1959]. The circled estimates are from WGNSD estimation, and the triangled ones from Melchers scheme (14), which disregards the correlation between R_1 and R_2 in sampling. It is not surprising that the latter yields large deviations from the exact solutions when two components are close to fully correlated, owing to extreme large deviation of the sampling distribution (14) from the original one (19) when ρ is closed to 1. This observation disqualifies (14) as a successful sampling distribution for cases of highly correlated variables.

5 SUMMARY AND ACKNOWLEDGEMENTS

A new sampling distribution (WGNSD) for application of Importance Sampling in structural system reliability assessment is developed. It improves Monte Carlo simulation both in efficiency and accuracy. It has been clarified that independent sampling distributions are not proper for correlated structural systems. Numerical examples show success of the introduced method in various cases. The support for this research from the National Science Foundation of U.S.A. is appreciated.

REFERENCES

1 Cornell,C.A. "Bounds on the Reliability of Structural System" J. Stru. Div. ASCE Vol.93 St1 1967 pp.171-200
2 Ditlevsen,O. "Narrow Reliability Bounds for Structural System" J. Stru. Mech. Vol.7 1979 pp.435-451
3 Fu,G. & Moses,F. "Lifetime System Reliability Models with Apllication to Highway Bridges" (to appear) Proc. ICASP5 Vancouver, Canada May 1987
4 Fu,G. & Moses,F. "Application of Lifetime System Reliability" Preprint No.52-1 ASCE Structures Congress'86 New Orleans, LA Sep.1986
5 Grigoria,M. & Turkstra,C. "Safety of Structural Systems with Corrlated Resistances" Appl. Math. Modelling Vol.3 1979 pp.130-136
6 Hammersley,J.M. & Handscomb,D.C. Monte Carlo Methods London: Methuen & Co Ltd. 1964
7 Harbitz,A. "Efficient and Accurate Probability of Failure Calculation by Use of the Importance Sampling Technique" Proc. ICASP4 (Ed.) Augusti,G. et al Italy June 1983 pp.825-836
8 Kahn,H. "Use of Different Monte Carlo Sampling Techniques" Symposium on Monte Carlo Methods (Ed.) Meyer,H.A. John Wiley & Sons, Inc. New York 1956 pp.146-190
9 Kleijnen,J.P.C. Statistical Techniques in Simulation Part I Marcel Dekker, Inc. 1974
10 Melchers,R.E. "Efficient Monte-Carlo Probability Integration" Report No.7/1984 Monash University 1984
11 National Bureau of Standards Tables of the Bivariate Normal Distribution Function and Related Functions Applied Math. Series 50 June 1959
12 Pugh,E.L. "A Grdient Technique of Adaptive Monte Carlo" SIAM Review Vol.8 No.3 July 1966 pp.346-355
13 Ramachandran,K. "New Reliability Bounds for Series Systems" Structural Safety and Reliability ICOSSAR'85 (Ed.) Konishi,I. et al Kobe, Japan May 1985
14 Thoft-Christensen,P. & Baker,M.J. Structural Reliability Theory and Its Applications Springer-Verlay New York 1982

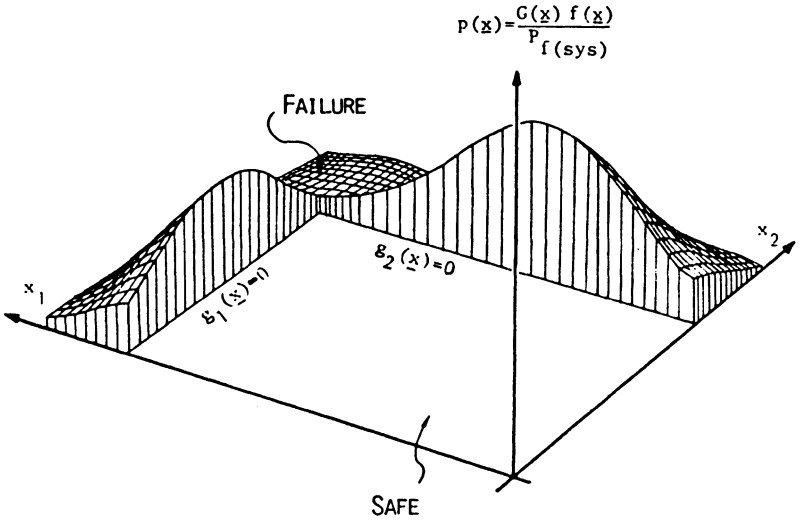

Fig.1 Ideal Optimal Sampling Distribution

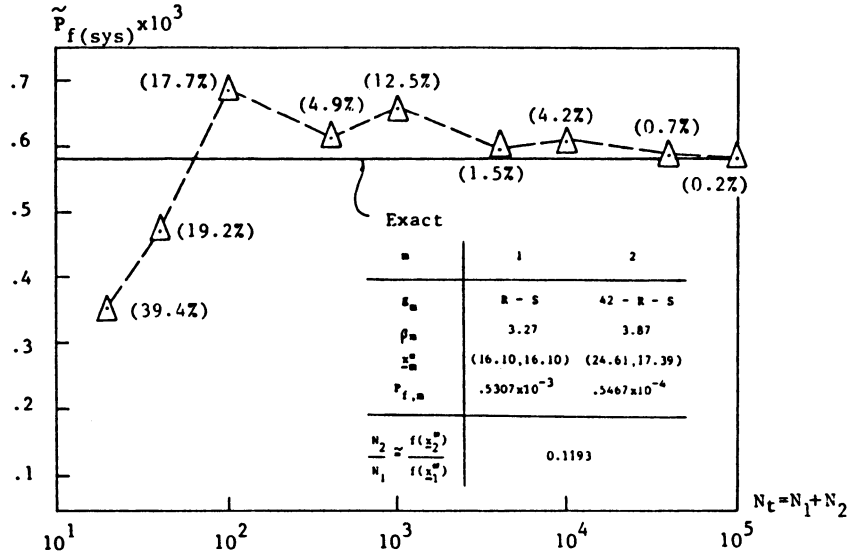

Fig.2 WGNSD Estimates and Their Relative Errors (Example 1)

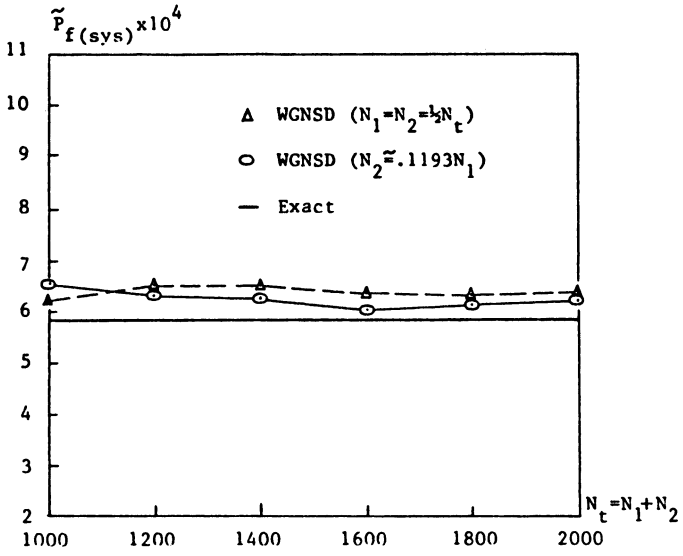

Fig.3 WGNSD Estimates
with Weighted and Non-weighted Sample Sizes (Example 1)

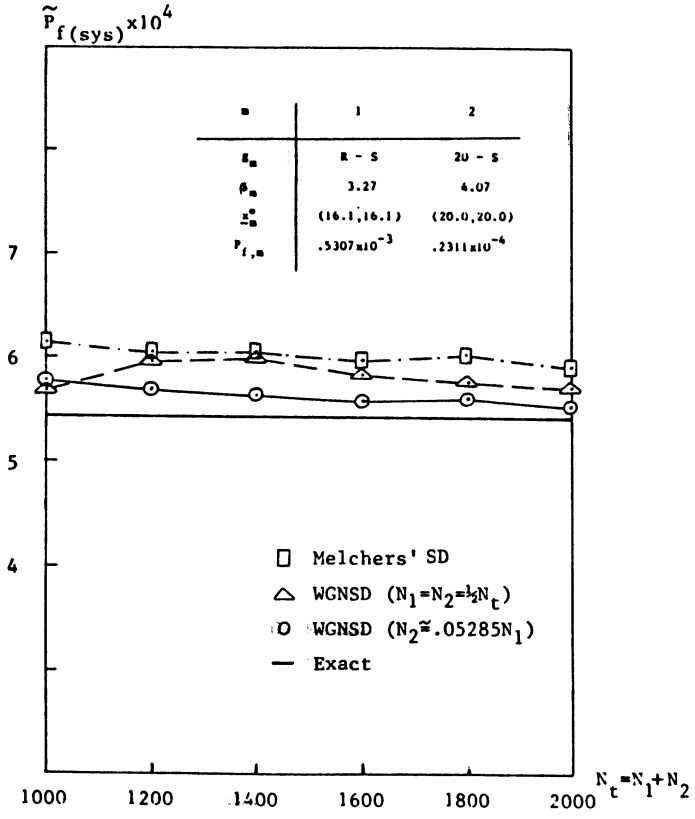

Fig.4 Estimates by WGNSD and Melchers' SD
(Example 2)

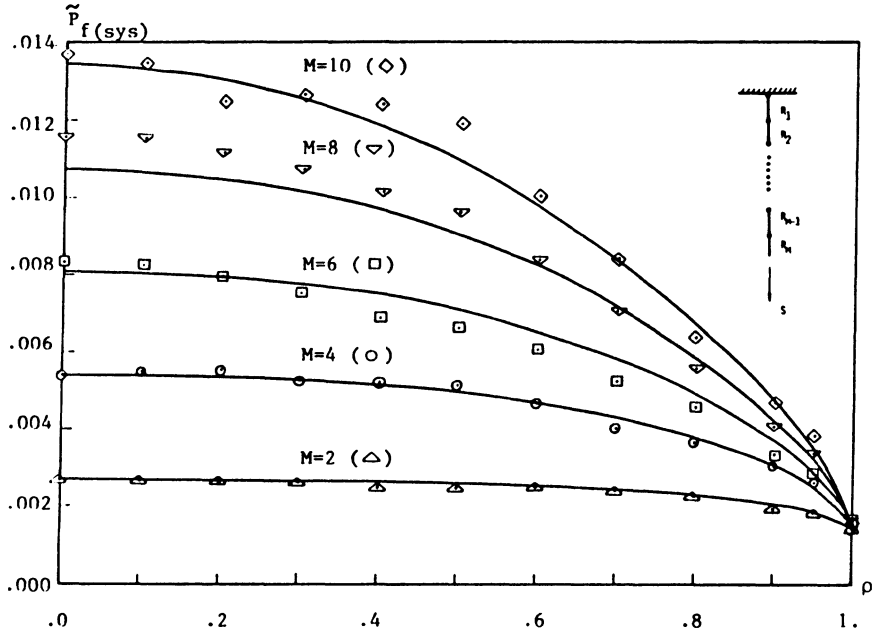

Fig.5 Comparisons of WGNSD Estimates and Exact Values (Example 3)

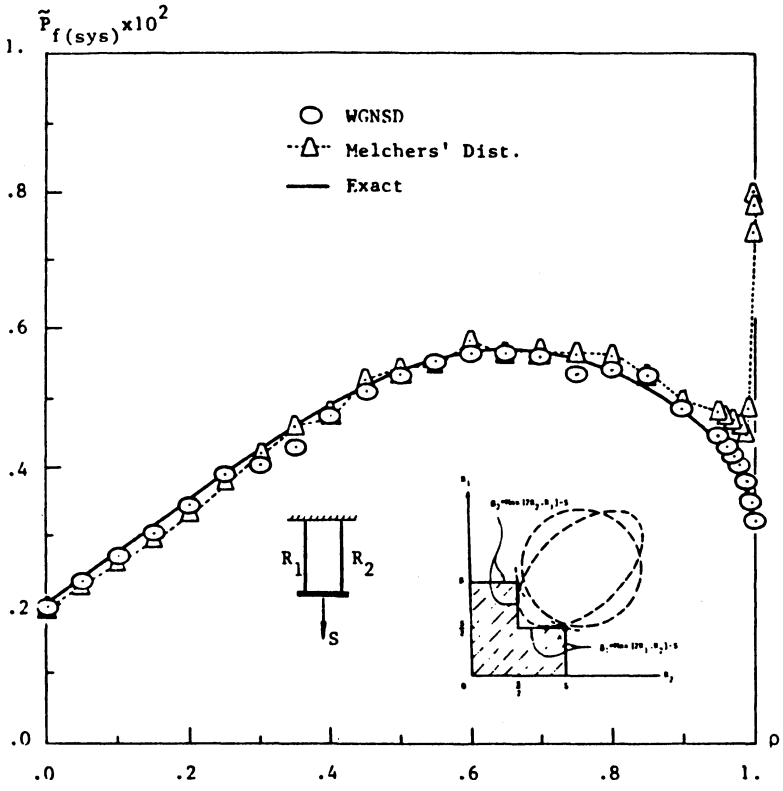

Fig.6 Estimates by WGNSD and Melchers' SD (Example 4)

COMPARISON OF NUMERICAL SCHEMES FOR THE MULTINORMAL INTEGRAL

S. Gollwitzer* & R. Rackwitz**
* Bogenstr. 9, D-8000 München 80
** Technische Universität München
Arcisstr. 21, D-8000 München 2

1. Introduction

The numerical determination of the multinormal integral is required in many problems of statistics and, recently, turned out to be a key problem in structural and operational system reliability [1,2]. For example, the analysis of multi-component systems with multiple failure modes (series - or weakest-link systems) requires the evaluation of the probability of a union of failure events. If equivalent hyperplanes [3] in the so-called standard normal space [4] which represent the modal and/or componental failure sets of the system can be produced, e.g. by FORM/SORM methods, the union probability can be computed as a multinormal integral. As another example the quantification of the redundancy in a system in a probabilistic sense requires the evaluation of intersection probabilities [5,6]. Again, this problem can be reduced to the computation of a multinormal integral if the boundaries of the failure sets can be linearised appropriately. Even if asymptotic second-order approximations of the failure surfaces are used, the evaluation of multinormal integrals is part of the solution to general intersection probabilities [2,7].

Unfortunately, no general analytical solution exists for this integral in higher dimensions. There exist some reduction formulae and series expansions but their numerical effort increases exponentially with the dimension of the integral and the numerical accuracy is only moderate as discussed in [8] and [9]. The same holds for direct numerical integration [10,11] or crude Monte Carlo simulation methods.

Numerically feasible approximations for the general case have, recently, been proposed in [1,9,12] and [13]. They are based on classical FORM/SORM techniques [1,2], on the equivalent hyperplane concept [9,12] and on concepts of asympotic analysis [13] as put forward in [2,7,14]. Two importance sampling schemes for the

evaluation of the multinormal integral are also available one of which is applied here to the evaluation of the multinormal integral for the first time [15,16,17].

In this paper a review of the more recent methods is presented supplementing the discussions given in [8] and [9]. Primary emphasis is given to the validation of the quality of the various approximations, their numerical effort and the identification of their appropriate area of application.

2. Review of some recent approximation methods

2.1 Formulation and classification of the computational tasks

Let $\underline{c} = (c_1,\ldots,c_n) \in \mathbb{R}^n$ and let $\underline{X} = (X_1,\ldots,X_n)$ be a standard normal random vector with correlation matrix $\underline{\underline{R}}$, i.e. with $E[X_i] = 0$, $E[X_i^2] = 1$ and $E[X_i X_j] = \rho_{ij}$ $(1 \leq i,j \leq n)$. The n-dimensional normal distribution is defined as:

$$\Phi_n(\underline{c};\underline{\underline{R}}) = P[\underline{X} \leq \underline{c}] = P[\bigcap_{i=1}^{n} (X_i \leq c_i)] \tag{1}$$

For the considerations in the sequel it is of advantage to make a distinction between two cases. The first case is the case of a "small intersection", i.e. there is at least for one i, $c_i < 0$, in eq. (1) or, equivalently, $\underline{0} \notin D$ with

$$D = \bigcap_{i=1}^{n} \langle D \rangle = \langle \bigcap_{i=1}^{n} (X_i - c_i \leq 0) \rangle \tag{2a}$$

and $\underline{0}$ the coordinate origin. "Large intersections", i.e. all $c_i \geq 0$ or $\underline{0} \in \langle D \rangle$, represent the second case, where none of the individual events contain the origin. Then, one can write:

$$P[\bar{D}] = 1 - P[D] = 1 - P[\cup(X_i > c_i)] = P[\cap(X_i \leq c_i)] \tag{2b}$$

2.2 Approximations based on the equivalent plane concept

The basic ideas to use the equivalent plane concept are as follows

[9,12]. The vector $\underline{X}$ can be represented in terms of an independent standard normal vector $\underline{U}$ by

$$X_i = \sum_{j=1}^{i} a_{ij} U_j \qquad (1 \leq i \leq n) \tag{3}$$

with $a_{11} = 1$ and the other coefficients determined such that the left-hand and the right-hand side of eq. (3) have the same correlation matrices [1]. The multinormal integral can then be rewritten as

$$\begin{aligned} P[\underline{X} \leq \underline{c}] &= P[X_1 \leq c_1]\ P[\bigcap_{i=2}^{n} (X_i \leq c_i | X_1 \leq c_1] \\ &= \Phi(c_1)\ P[\bigcap_{i=2}^{n} (a_{i1} \bar{X}_1 + \sum_{j=2}^{i} a_{ij} U_j - c_i \leq 0)] \\ &= \Phi(c_1)\ P[\bigcap_{i=2}^{n} (g_i(\underline{U}) \leq 0)) \end{aligned} \tag{4}$$

where the variable $\bar{X}_1$ is again standard normal but truncated at c_1 and independent of the other U's. $\bar{X}_1$ can be represented by its Rosenblatt-transformation [9,12]:

$$\bar{X}_1 = \Phi^{-1}[\Phi(c_1)\ \Phi(U_1)] \tag{5}$$

Hence, the g-functions in eq. (4) are:

$$\begin{aligned} g_i(\underline{U}) &= a_{i1}\ \Phi^{-1}[\Phi(c_1)\ \Phi(U_1)] + \sum_{j=2}^{i} a_{ij} U_j - c_i \\ &= a_{i1}\ \Phi^{-1}[\Phi(c_1)\ \Phi(U_1)] + (1 - a_{i1}^2)^{1/2} Y - c_i \end{aligned} \tag{6}$$

For later convenience, the second term of eq. (6) is replaced by an equivalent term in one standard normal variable Y. Linearisation of eqs. (6) at their respective β-points yields another intersection domain which can easily be put into the form eq. (4). Repeated application of this procedure yields a crude first-order estimate of the multinormal integral [1]. It will be denoted by estimate "A0" in the following. It is not further discussed because significant and straigthforward improvements can be achieved by applying the above-mentioned equivalent plane concept.

For this purpose, denote the conditional failure events in eq. (6) as:

$$D_i = (g_i(\underline{U}) \leq 0) = (a_{i1}\bar{X}_1 + a_{i2}\, Y_i) \qquad (2 \leq i \leq n) \tag{7}$$

Replacing D_i by a "similar" event B_i such as the "equivalent half-space" proposed in [3] leads to:

$$B_i = (b_{i1}\bar{X}_1 + b_{i2}\, Y_i < e_i) \tag{8}$$

with

$$\alpha_{ij} = -\frac{\partial}{\partial \epsilon_j} P[(\bar{X}_1 + \epsilon_1,\ Y_1 + \epsilon_2) \in F_i]_{|\underline{\epsilon} = \underline{0}} =$$

$$= -P[D_i]\, E[Z_{ij}|D_i] \text{ where } Z_{ij} = \begin{cases} \bar{X}_1 \text{ for } j = 1 \\ Y_i \text{ for } j = 2 \end{cases}$$

$$b_{ij} = (\alpha_{i1}^2 + \alpha_{i2}^2)^{-1/2}\, \alpha_{ij}$$

$$e_i = \Phi^{-1}(P[D_i])$$

$E[.|.]$ is the conditional expectation which has the same probability as D_i and the same relative sensitivity with respect to small variations in the variables X_1 and Y_i. One obtains the approximation

$$P[\bigcap_{i=2}^{n} D_i] \approx P[\bigcap_{i=2}^{n} B_i] = \Phi_{n-1}(\underline{e};\underline{T}) \tag{9}$$

with

$$\underline{e} = (e_2, \ldots, e_n)$$

and

$$\underline{T} = (t_{ij}) = b_{i1}\, b_{j1} + b_{i2}\, b_{j2}(\rho_{ij} - a_{i1}\, a_{j1})/(a_{i2}\, a_{j2}) \qquad (2 \leq i,j \leq n)$$

and, finally:

$$\Phi_n(\underline{c};\underline{R}) \approx \Phi(c_1)\ \Phi_{n-1}(\underline{e};\underline{T}) \qquad (10)$$

Recursive application of the last equation again expresses Φ_n as a product of univariate normal probabilities. Both the e_i and the α_{ij} of eq. (8) can be computed by FORM/SORM methods. In this case $\underline{\alpha}_i$ is the gradient at the β-point of $g_i(\underline{U}) = 0$ and $e_i = -\beta_i$. The $\underline{\alpha}_i$ and the e_i may be improved further at the expense of some more numerical effort involving one dimensional integrations (for details see [12]). In particular, the e_i can be obtained from binormal probabilities. In the sequel these approximations to Φ_n are referred to as "A1" (FORM/SORM) and "A2" (including improvements by numerical integrations).

2.3 Approximation based on asymptotic analysis

This approximation is studied in some detail in [13] following ideas put forward in [7]. The general formula for an asymptotic approximation for the probability content of an intersection is [2]:

$$P[\bigcap_{i=1}^{m} D_i] \sim \Phi_k(\underline{c};\underline{R})\ (\det(\underline{I} - \underline{H}))^{-1/2} = \Phi_k(\underline{c};\underline{R})\ C \qquad (11)$$

Herein, Φ_k is the k-dimensional standard normal integral, $\underline{c} = \underline{A}^T\underline{u}^*$, $\underline{R} = \underline{A}^T\underline{A}$, $C = (\det(\underline{I} - \underline{H}))^{-1/2}$ a second-order correction term with $\underline{I}$ the identity matrix and $\underline{H}$ the Hessian matrix collecting the second-order derivatives of the domain boundaries. $\underline{u}^*$ is a point defined by:

$$\underline{u}^* = \min\{\|\underline{u}\|\} \text{ for } \{\underline{u} : \bigcap_{j=1}^{m} g_j(\underline{u}) \leq 0\} \qquad (12)$$

k ($1 \leq k \leq m$) is the size of the index set J for "active" constraints, i.e. for which $g_j(\underline{u}^*) = 0$. $\underline{A}$ collects as columns the linearly independent, normalized gradients ($\|\underline{\alpha}_j\| = \|\text{grad } g_j(\underline{u}^*)\| = 1$) of the active constraints. As seen eq. (11) involves a multinormal integral. Taking D in eq. (11) as in eq. (2a) suggests to apply formula (11) to itself.

The procedure for the evaluation of Φ_n starts as above (see eqs. (3) to (6)). Next, an approximation for the second factor in eq. (4) is according to eq. (11)

$$P(\bigcap_{i=2}^{n} (g_i(\underline{U}) \leq 0)) \sim P(\bigcap_{i \in J_2} (\underline{\alpha}_i^T(\underline{u} - \underline{u}^*) \leq 0))\ C_2$$

where, $J_2 \subseteq (2,\ldots,n)$ is the subset of $k \leq n-1$ active constraints at $\underline{u}^*$ and C_2 the second-order correction factor as in eq. (11). Therefore, eq. (4) can be rewritten as

$$P(\underline{X} \leq \underline{c}) = \Phi(c_1)\ C_2\ P(\bigcap_{i \in J_2} (\underline{\alpha}_i^T(\underline{u} - \underline{u}^*) \leq 0)) \qquad (13)$$

which shows the main difference as compared to method "A" apart from the fact that now the joint β-point is used as an approximation point. For the last factor one, in turn, proceeds as described in eq. (4) with new X_i in eq. (3) given by $X_i = \underline{\alpha}_i^T \underline{U}$ being standard normal with correlations $\rho_{ij} = \underline{\alpha}_i^T \underline{\alpha}_j$ and the new c_i defined by $c_i = \underline{\alpha}_i^T \underline{u}^*$. Repeated at most (n-1)-fold application of this scheme finally yields the result. Further technical details can be found in [13].

In the sequel this approximation is referred to as "B". It should be noted that for large intersections this method coincides with method "A1" if SORM-approximations to the e_i's are used.

2.4 Directional importance sampling for large intersections

An approximation to Φ_n by directional simulation which is restricted to the case of large intersections has been proposed by Ditlevsen [15] who extended an idea of Deak [16]. The restriction is caused by the assumption of a convex safe set in that method. Eq. (2b) may be rewritten as

$$1 - P[\bar{D}] = P[D] = \int_{\substack{\text{unit}\\ \text{sphere}}} 1 - \kappa_n^2[r(\underline{\alpha})^2]\ \lambda\ d\underline{\alpha} \qquad (14)$$

where $\lambda(.)$ is the uniform probability measure and $d\underline{\alpha}$ the area element on the unit sphere in the n-dimensional standard normal space. $\kappa_n^2[.]$ is the Chi-sqare distribution function of n degrees of freedom. $r(\underline{\alpha})$ is the distance from the origin to the boundary of D in the direction of the unit vector $\underline{\alpha}$. The integral in eq. (14) can be estimated from

$$P[D] = \frac{1}{N} \sum_{l=1}^{N} (1 - \kappa_n^2[r(\underline{\alpha})^2]) \tag{15}$$

which essentially is the proposal in [16]. Alternatively, it can be expressed as

$$P[D] = E\left[\frac{1-\kappa_n^2(r(\underline{\alpha}))^2}{f(\underline{\alpha})}\right] \approx \frac{1}{N} \sum_{l=1}^{N} \frac{1-\kappa_n^2(r(\underline{\alpha}_l))^2}{f(\underline{\alpha}_l)} \tag{16}$$

where $f(\underline{\alpha})$ is a suitable sampling density function [15]. Using eq. (3) the boundary of D is:

$$\partial D : \langle \underline{a}_i \underline{U} = c_i \rangle = \bigcup_{(i)} \langle \underline{g}_i(\underline{U}) = 0 \rangle \quad (1 \leq i \leq n) \tag{17}$$

For eqs. (2) and (14) the following inequality holds:

$$P[D] \leq \sum_{i=1}^{n} P_i \quad \text{where } P_i = \Phi(-c_i) \tag{18}$$

This suggests a mixed sampling density:

$$f_n(\underline{\alpha}) = \frac{\sum_{(i)} P_i \, f_i(\underline{a}_i;\underline{\alpha}_i)}{\sum_{(i)} P_i} \tag{19}$$

The sampling density for the i-th part of ∂D is (see [15])

$$f_i(\underline{a}_i;\underline{\alpha}_i) = \frac{1-\kappa_n^2(\gamma_i^2)}{1-\Phi(c_i)} = \frac{1-\kappa_n^2(\gamma_i^2)}{P_i} \tag{20}$$

with γ_i the distance of the i-th part of the boundary to the origin in the sample direction $\underline{\alpha}_i$. In case of the multinormal integral this distance is easily computed:

$$\gamma_i = \frac{c_i}{(\underline{\alpha}_i^T \underline{\alpha}_i)}$$

$r(\underline{\alpha})$ in eqs. (15) and (16) simply is:

$$\Gamma = \min_{(i)} (\max (0, \gamma_i)) \tag{21}$$

The n sample directions $\underline{\alpha}_i$ are obtained from

$$\underline{\alpha}_i(\underline{y}, v) = \frac{\underline{y} + (v_i - \underline{a}_i^T \underline{y})\underline{a}_i}{\| \underline{y} + (v_i - \underline{a}_i^T \underline{y})\underline{a}_i \|}; \quad y_k = \Phi^{-1}(w_k) \qquad (1 \leq k \leq n) \tag{22}$$

where $\underline{y}$ is a sample of standard normal vector of dimension n obtained from pseudo-random numbers w_k ($w_k \in (0,1)$) and v_i is a standard normal variable truncted at c_i, i.e.

$$v_i = - \Phi^{-1}[\Phi(- c_i)(1 - w_{n+1})]$$

Finally, the right-hand side of eq. (16) can be written as:

$$P[D] \approx \sum_{i=1}^{n} P_i \left\{ \frac{1}{N} \sum_{l=1}^{N} \frac{1-\kappa_n^2 [\Gamma(\gamma_i)]}{\sum_{(i)} 1-\kappa_n^2 [\gamma_i(\underline{y}_l, v_l)]} \right\}$$

$$= \sum_{i=1}^{n} \Phi(- c_i) \left\{ \frac{1}{N} \sum_{l=1}^{N} \varphi_l \right\} \tag{23}$$

φ_l is set to 0 if $\Gamma(\underline{y}_l v_l)$ is equal to 0. This approximation is referred to as method "C" in the sequel.

2.5 An importance sampling scheme for small intersections

It is not obvious though probably possible to derive an importance sampling scheme for small intersections on the lines of section 2.4. However, based on a proposal by Melchers [17], it is possible to derive another importance sampling scheme for small intersections which, in principle, could also be generalized to large intersections. The general formula is:

$$P[D] = \int 1_D(\underline{u}) \varphi(\underline{u}) d\underline{u} = E\left[1_D(\underline{u}) \frac{\varphi(\underline{u}+\underline{u}^*)}{\varphi(\underline{u})} \right]$$

$$\sim \frac{1}{N} \sum_{k=1}^{N} \left[1_D(\underline{u}_k + \underline{u}^*) \frac{\varphi(\underline{u}_k+\underline{u}^*)}{\varphi(\underline{u}_k)} \right] \qquad (24)$$

$1_D(\underline{u})$ is an indicator function:

$$1_D(\underline{u}) = 0 \quad \text{for } \underline{u} \notin D$$

$$1_D(\underline{u}) = 1 \quad \text{for } \underline{u} \in D$$

D is defined as in eq. (2a). The $\underline{u}_k$ are sampled standard normal vectors. The sampling density is the n-dimensional standard normal density with mean $\underline{u}^*$ which is the joint β-point for the small intersection according to eq. (12) with the $g_i(\underline{U})$ defined in eq. (3). For the multinormal integral it is easy to obtain $\underline{u}^*$ analytically in making use of eq. (3):

$$\underline{u}^* = (u_i^*) = \begin{cases} u_1^* = c_1 \\ u_i^* = c_i - \sum_{j=1}^{i-1} a_{ij} u_j^* \quad (2 \leq i \leq n) \end{cases} \qquad (25)$$

Also, the indicator function $1_D(\underline{u})$ is easily evaluated. In noting that $\Phi(-\beta_c) \geq P[D]$ a numerically more convenient expression of eq. (24) is:

$$P[D] = \Phi(-\beta_c) \cdot \frac{1}{N} \sum_{\ell=1}^{N} \psi_\ell \quad \text{with}$$

$$\beta_c = \|\underline{u}_c^*\| \quad \text{and}$$

$$\psi_\ell = \exp\left[-\frac{1}{2} \sum_{i=1}^{n} (u_i^{*2} + 2u_i^* u_{i,\ell}) - \ln \Phi(-\beta_c)\right]$$

Just simple evaluations of the g-functions are needed to obtain $1_D(\underline{u})$. This approximation to Φ_n is referred to as method "D".

3. Examples

3.1. The symmetrical case

In all examples below the results are given in terms of the equi-

valent safety index $\beta = -\Phi^{-1}$ (P[D]). If in eq. (1) all $\rho_{ij} = \rho$ and all $c_i = c$ $(1 \leq i,j \leq n)$, Φ_n has an exact solution [18] involving one-dimensional integration. It is used here as a reference.

In table 1a the results of the various methods can be compared for $0 \leq \rho < 1$, $n = 10$ and $c = -4$, 0 and +2. For $c = -4$, only method "D" is applicable. For $c = 0$ both simulation methods are inadequate. For the case $c = +2$, only method "C" is possible. The intervals in tables 1a and 1b represent the 95% confidence intervals for method "C" or "D" with N = 1000 sample points. This equicorrelated case with identical c_i's is considered the most unfavourable for methods "A1", "A2" and "B". They, nevertheless, reproduce almost the exact results for the extremes $\rho = [-1/(n-1)] + \epsilon$, $\rho = 0$ and $\rho = 1 - \epsilon$ with ϵ a machine dependent small number. From table 1a the error with these methods is largest for medium values of ρ, $\rho = 0.6$, say. Therefore, in figure 1 and in table 1b the dimension n is varied from 1 to 50 for $\rho = 0.6$ and $c = -4$, 0, 2 demonstrating the behaviour of these methods for larger n. Method "A1" produces relatively good results. Method "A2" sometimes is more accurate but at the expense of about 10 times the computational effort of method "A1". Method "B" clearly is superior to methods "A" in the "small" intersection case. That it gives better results than method "A1" also in the case of "large" intersections is due to a numerically more consistent computer program. Method "B" usually requires about the same computation time as method "A1". All in all, the methods "A" and "B" are suprisingly accurate over the full range of values of n, c and ρ. For not too large n, $n < 20$ say, the computation time of methods "A" and "B" are significantly smaller than for any simulation procedure. For very large n, $n >> 20$, say, the importance sampling schemes become more attractive. But one has to bear in mind that method "C" can only be applied to "large" intersections whereas method "D" is efficient only for "small" intersections. Furthermore, method "D" fails for correlation matrices approaching singularity (see also section 3.3).

3.2. A degenerate case [9,12]

Let U_1 and U_2 be two independent standard normal variables and λ a

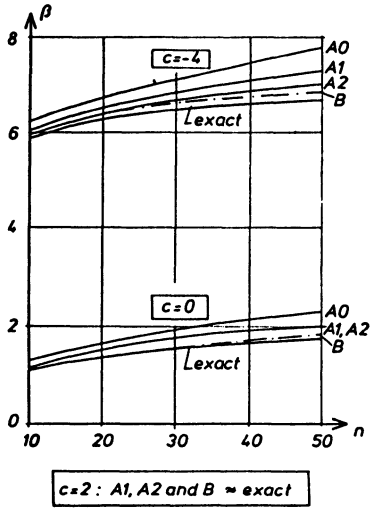

Figure 1: Accuracy of computation methods for equicorrelated variables (ρ = 0.6) for various arguments c

Table 1a

c = -4 , n = 10

ρ	"A1"	"A2"	"B"	"C"	"D"	exact
0.0	14.15	14.15	14.15	-	13.00 - ∞	14.15
0.2	8.97	8.95	8.94	-	8.90 - ∞	8.93
0.4	7.14	7.10	7.08	-	6.91 - 7.40	7.05
0.6	6.04	5.97	5.97	-	5.85 - 5.95	5.92
0.8	5.19	5.10	5.10	-	5.04 - 5.10	5.06
0.99	4.20	4.18	4.17	-	4.14 - 4.18	4.17

c = 0 , n = 10

ρ	"A1"	"A2"	"B"	"C"	"D"	exact
0.0	3.10	3.10	3.10	-	-	3.10
0.2	2.18	2.10	2.08	-	-	2.09
0.4	1.65	1.57	1.55	-	-	1.55
0.6	1.22	1.16	1.14	-	-	1.13
0.8	0.80	0.76	0.74	-	-	0.73
0.99	0.17	0.16	0.15	-	-	0.15

c = +2 , n = 10

ρ	"A1"	"A2"	"B"	"C"	"D"	exact
0.0	-0.82	-0.82	-0.82	-0.73 - -0.83	-	-0.82
0.2	-0.90	-0.92	-0.90	-0.85 - -0.94	-	-0.92
0.4	-1.01	-1.04	-1.02	-1.01 - -1.13	-	-1.05
0.6	-1.17	-1.20	-1.19	-1.09 - -1.22	-	-1.20
0.8	-1.40	-1.41	-1.42	-1.34 - -1.48	-	-1.41
0.99	-1.86	-1.85	-1.86	-1.80 - -1.95	-	-1.85

Table 1b

c = -4 , ρ = 0.6						
n	"A1"	"A2"	"B"	"C"	"D"	exact
10	6.04	5.97	5.97	-	5.85 - 5.95	5.92
20	6.55	6.42	6.41	-	6.25 - 6.34	6.28
30	6.84	6.68	6.63	-	6.42 - 6.51	6.46
40	7.05	6.87	6.79	-	6.52 - 6.63	6.58
50	7.25	7.00	6.92	-	6.60 - 6.73	6.67
c = 0 , ρ = 0.6						
n	"A1"	"A2"	"B"	"C"	"D"	exact
10	1.22	1.16	1.14	-	-	1.13
20	1.54	1.48	1.42	-	-	1.40
30	1.73	1.68	1.59	-	-	1.55
40	1.86	1.82	1.71	-	-	1.65
50	2.00	1.90	1.80	-	-	1.73
c = +2 , ρ = 0.6						
n	"A1"	"A2"	"B"	"C"	"D"	exact
10	-1.17	-1.20	-1.19	-1.15 - -1.27	-	-1.20
20	-0.95	-0.97	-0.97	-0.91 - -1.04	-	-0.98
30	-0.83	-0.83	-0.85	-0.84 - -0.98	-	-0.86
40	-0.74	-0.73	-0.77	-0.68 - -0.82	-	-0.78
50	-0.67	-0.65	-0.71	-0.66 - -0.79	-	-0.70

real number. The X_i's are defined by

$$X_i = U_1 \cos(\lambda_i) + U_2 \sin(\lambda_i) \qquad (1 \leq i \leq n)$$

$$\lambda_i = \lambda \frac{(i-1)}{(n-1)}$$

yielding the correlation matrix:

$$\underline{\underline{R}} = \langle \rho_{ij} \rangle = \cos(|\lambda_i - \lambda_j|)$$

The probability $P[D] = \Phi_n(c,\underline{\underline{R}}) = P[\cap(X_i \leq c)]$ can be shown to be the probability content of a plane polygon in the space of (U_1,U_2) as demonstrated in figure 2. In the case $\lambda = \pi/2$ (figure 2a) all correlations are non-negative and $\rho_{n_1} = 0$.

For $c > 0$, the exact result is

$$P[D] = \Phi_n(\underline{c},\underline{\underline{R}}) = \Phi(c) + (n-1)\, P(\Delta) - 0.25$$

Δ is the shaded triangle in figure 2a. Some results are given in table 2a for the case $c = 2$. For $n \to \infty$, one has

$$P[F] \sim \Phi(c) + \frac{\varkappa_2^2(c^2)}{4} - 0.25$$

From table 2a one concludes that methods "A" and "B" are very accurate. Method "C" is less satisfying.

For $c \leq 0$, only the variables X_1 and X_n contribute (see figure 2a). The exact result is:

$$P[D] = \Phi_n(\underline{c},\underline{\underline{R}}) = P(X_1 \leq c \cap X_n \leq c) = \Phi^2(c)$$

Methods "A" and "B" reproduce the exact results for arbitrary n in this case.

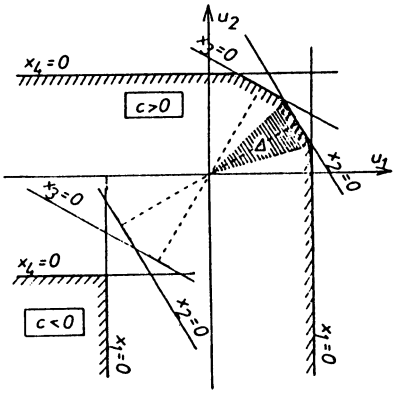

n = 4 $\gamma = \pi/2$

FIGURE 2a

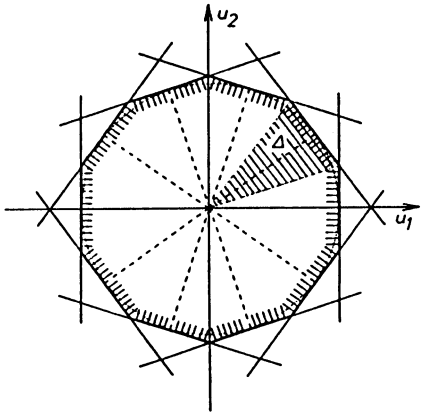

n = 10 $\gamma = 2\pi(n-1)/n$

FIGURE 2b

Figure 2: Degenerate cases for numerical schemes (from [9])

Figure 2b and table 2b deal with the case $\lambda = 2\pi(n-1)/n$ and $c > 0$, of course. The exact result is

$$P[D] = \Phi_n(\underline{c},\underline{\underline{R}}) = n\, P(\Delta)$$

Table 2a

$\lambda = \pi/2$, $c = 2$

n	"A1"	"A2"	"B"	"C"	"D"	exact
3	-1.61	-1.62	-1.61	-1.56 - -1.64	-	-1.62
5	-1.59	-1.61	-1.58	-1.50 - -1.61	-	-1.59
10	-1.57	-1.61	-1.58	-1.52 - -1.66	-	-1.58
20	-1.57	-1.61	-1.58	-1.44 - -1.60	-	-1.58

Remark : The asymptote for $n \to \infty$ is $\beta = -1.577$

Table 2b

$\lambda = 2\pi\ (n-1)/n$, $c = 0.01$

n	"A1"	"A2"	"B"	"C"	"D"	exact
3	2.34	2.57	3.63	3.48 - 5.08	-	3.67
5	18.64	6.81	3.81	3.0 - 5.5	-	3.85
10	?	?	?	?	-	3.88
20	?	?	?	?	-	3.89

Remark : The asymptote for $n \to \infty$ is $\beta = 3.890$

$\lambda = 2\pi\ (n-1)/n$, $c = 0.1$

n	"A1"	"A2"	"B"	"C"	"D"	exact
3	2.00	2.19	2.23	2.27 - 2.58	-	2.40
5	2.82	2.75	2.53	2.38 - 2.88	-	2.53
10	3.00	2.90	2.63	2.30 - 3.05	-	2.56
20	3.01	2.91	2.49	2.35 - 3.07	-	2.57

Remark : The asymptote for $n \to \infty$ is $\beta = 2.577$

$\lambda = 2\pi\ (n-1)/n$, $c = 0.5$

n	"A1"	"A2"	"B"	"C"	"D"	exact
3	0.81	0.92	0.89	0.82 - 0.92	-	0.90
5	1.15	1.14	1.19	1.02 - 1.16	-	1.11
10	1.24	1.19	1.21	1.09 - 1.26	-	1.17
20	1.25	1.20	1.22	1.10 - 1.28	-	1.18

Remark : The asymptote for $n \to \infty$ is $\beta = 1.188$

Δ is the shaded triangle in figure 2b. For $n \to \infty$, one obtains

$$P[D] \sim \chi^2_2(c^2)$$

For $c = 0$, there is $\beta = +\infty$. An example of the correlation matrix for $n = 10$ is given below (table 3). The entries speak for themselves.

Table 3

$n = 10$, case : b

1.0									
.809	1.0								
.309	.809	1.0							
-.309	.309	.809	1.0						
-.809	-.309	.309	.809	1.0					
-1.000	-.809	-.309	.309	.809	1.0				
-.809	-1.000	-.809	-.309	.309	.809	1.0			
-.309	-.809	-1.000	-.809	-.309	.309	.809	1.0		
.309	-.309	-.809	-1.000	-.809	-.309	.309	.809	1.0	
.809	.309	-.309	-.809	-1.000	-.809	-.309	.309	.809	1.0

Table 2b indicates that both methods "A" and "B" fail for very small c. Method "D" is not applicable. Method "C" is particularly suitable (see figure 2b and table 2b).

It is seen that in these examples the methods "A" and "B" only produce acceptable results if the c_i's are sufficiently large. The use of an importance sampling scheme as in method "C" is advantageous although that method also fails when c is very small.

3.3. Negative correlations, the singular case

Consider now $P[D] = \Phi_n(\underline{c},\underline{\underline{R}})$ with $n = 5$, $c_i = c = -3$ and $\rho_{ij} = \rho$ with $-1/n-1 = -0.25 < \rho \leq 0$. For $\rho = -1/(n-1)$, $\underline{\underline{R}}$ becomes singular and $\beta = -\Phi^{-1}(P[D]) = +\infty$. Because there is no easily accessible exact result, reference values for β are produced by method "D" despite the fact that the efficiency of method "D" is poor in this case. For example, for $\rho \leq -0.20$, roughly 100 000 sample points were necessary to obtain a coefficient of variation less than 100% for the correction factor to $\Phi(-\beta_c)$ in eq. (25). The corresponding results are collected in table 4 showing that method "B" is superior to all other methods. This is readily explained by its asymptotic nature.

Table 4

n = 5, c = -3						
ρ	"A1"	"A2"	"B"	"C"	"D"	exact
-0.10	9.71	9.71	9.71	-	9.64 - 9.76	-
-0.15	11.62	11.61	11.62	-	≅ 11.6	-
-0.20	15.81	15.75	15.92	-	≅ 15.9	-
-0.22	19.8	19.7	20.2	-	≅ 20.8	-
-0.24	30.8	30.3	34.2	-	≅ 35	-
-.249	54.0	50.9	106.4	-	?	-

4. Conclusions

Apparently, there is no method which is superior to others over the whole range of arguments in the multinormal integral both with respect to numerical accuracy and with respect to the numerical effort.

Method "A1" behaves suprisingly well despite its somewhat dubious theoretical background for the "small" intersection case. It is to be preferred to the simple FORM-method "A0" because it requires only very little additional numerical effort but is considerably more accurate. The improvements employed in method "A2" usually do not deserve the large additional effort.

Because method "B" is theoretically identical to method "A1" for "large" intersections but has a sound theoretical background for "small" intersections and requires about the same computation time, it is prefereable to method "A1".

However, these methods can fail for almost rotationally-symmetric, domains containing the origin where the directional sampling method "C" is a natural alternative. This method as implemented herein is only suitable for the "large" intersection case, however. The numerical effort of methods "A" and "B" roughly increase as n^2 whereas the simulation methods have only an increase proportional to n. Therefore, simulation methods generally become more efficient for very high dimensions and should, in fact, be preferred for $n >> 50$. The importance sampling scheme "D", which still carries the potential for further improvement, might be advantageous for very high dimensional, non-degenerate "small" intersection problems. It is worth mentioning

that if simulation methods are used the quality of the random number generator is of crucial importance.

In summary, method "B" is recommended for general applications except for very high-dimensional cases where importance sampling schemes appear to be more powerful. Such schemes which can also handle almost degenerate cases, however, still need to be developed. Both methods "C" and "D" as used in the above comparisons are not yet satisfying. Method "B" as opposed to simulation methods has the additional advantage of providing consistent derivatives of the multi-normal integral with respect to its arguments and which are needed in certain reliability problems. For these reasons, method "B" has been implemented in the general-purpose probabilistic analysis program package PROBAN [19].

References

[1] Hohenbichler, M., Rackwitz, R., First-Order Concepts in System Reliability, Structural Safety, 1, 3, 1983, pp. 117-188
[2] Hohenbichler, M., Gollwitzer, S., Kruse, W., Rackwitz, R., New Light on First- and Second-Order Reliability Methods, accepted for publication in Structural Safety, 1987
[3] Gollwitzer, S., Rackwitz, R., Equivalent Components in First-order System Reliability, Reliability Engineering, 5, 1983, pp. 99-115
[4] Hohenbichler,M., Rackwitz,R., Non-normal Dependent Vectors in Structural Safety, Journ. Eng. Mech. Div., ASCE, 107, 6, 1981, pp. 1227-1249
[5] Hohenbichler, M., Rackwitz, R., Reliability of Parallel Systems under Imposed Uniform Strain, Journ. Eng. Mech. Div., ASCE, 109, 3, 1983, pp.896-907
[6] Gollwitzer, S., Rackwitz, R., First-order System Reliability of Structural Systems, Proc. ICOSSAR'85, Kobe, 1985, Vol. I, pp. 171-180
[7] Hohenbichler, M., An Asymptotic Formula for the Probability of Intersections, in: Berichte zur Zuverlaessigkeitstheorie der Bauwerke, SFB 96, H. 69, Technische Universitaet Muenchen, 1984, pp. 21-48
[8] Johnson, N.L., Kotz, S., Distributions in Statistics: Continuous Multivariate Distributions, John Wiley & Sons, New York, 1976
[9] Hohenbichler, M., Rackwitz, R., A Bound and an Approximation to the Multivariate Normal Distribution Function, Math. Japonica, 30, 5, 1985, pp. 821 - 828
[10] Milton, D.C., Computer Evaluation of the Multivariate Normal Integral, Technometrics, 14, 4, 1972, pp. 881-889
[11] Bohrer, R.E., Schervish, M.J.: An error-bounded algorithm for normal probabilities of rectangular regions, Technometrics, 23, 1981, pp. 297-300
[12] Hohenbichler, M., An Approximation to the Multivariate Normal Distribution, Proc. Euromech 155 (DIALOG), Danish Engineering Academy, Lyngby, Denmark, 1982, pp. 79-110

[13] Gollwitzer, S., Rackwitz, R., An Efficient Numerical Solution to the Multinormal Integral, Berichte zur Zuverlaessigkeitstheorie der Bauwerke, Technische Universitaet Muenchen, H. 80, 1986
[14] Breitung, K., Asymptotic Approximations for Multinormal Integrals, Journ. Eng. Mech. Div., ASCE, 110, 3, 1984, pp. 357-366
[15] Ditlevsen,O., Directional Simulation in Gaussian Processes, private communication, Aug. 1986
[16] Melchers, R., Efficient Monte Carlo Probability Integration, Res. Rep. No. 7-1984, Monash University, Monash, 1984
[17] Deak, I., Three digit accurate multiple normal probabilities. Numer. Math., 35, 1980, pp. 369-380
[18] Dunnett, C.W., Sobel, M., Approximations to the Probability and Percentage Points of a Multivariate Analogue of Student's t-Distribution, Biometrika, 42, 1955, pp. 258-260
[19] PROBAN - Probabilistic Analysis Program, Users Manual, A.S. Norske Veritas, Veritas Research / Technische Universitaet Muenchen, 1987

RELIABILITY OF FIBER BUNDLES UNDER RANDOM TIME-DEPENDENT LOADS

Mircea Grigoriu
Department of Structural Engineering
Cornell University
Ithaca, NY 14853

INTRODUCTION

Fiber bundles are parallel systems with brittle components (fibers). A fiber bundle with n fibers can resist a load in one of the damage states m = n, n-1, ...,1 characterized by m unfailed fibers and n-m failed fibers. It is generally assumed that the applied load is equally shared among unfailed fibers and components have independent, identically distributed failure times (1,3,4). Fiber bundles and Daniels systems have common features. However, the strength of the fibers of the Daniels systems is usually time invariant so that the weakest fiber in any damage state fails instantaneously or survives indefinitely.

The failure time has been studied extensively for fiber bundles subject to constant and time-dependent deterministic loads (3). The case of elementary random load processes began to be investigated only recently (1,4). The objectives of this paper are to extend some of the results in Ref. 1 to more general load processes and include in the analysis dynamic effects that may cause significant differences between characteristics of load and load effect.

FAILURE TIME OF INDIVIDUAL FIBERS

Consider a fiber subject to a deterministic time-dependent load $l(\tau) \geq 0$. According to an extended version of Zhurkov's model, the failure time T_1 of the fiber exceeds t with probability (1,3,4)

$$P(T_1 > t) = \exp\left(-\int_0^t \mu\,(l(\tau))d\tau\right) \qquad (1)$$

in which $\mu \geq 0$ is the breakdown rule. A common form of μ is the power law breakdown rule

$$\mu(x) = kx^{\rho} \qquad (k,\rho \geq 0) \tag{2}$$

From Eqs. 1 and 2,

$$P(T_1 \geq t) = \exp(-kl^{\rho}t) \tag{3}$$

when $l(\tau) = l$ is a constant. In this case, T_1 follows an exponential distribution with mean $ET_1 = 1/(kl^{\rho})$. If the load is not always positive the breakdown rule in Eq.2 can be modified, e.g., to $\mu(x) = k|x|^{\rho}$.

The Zhurkov model is based on experimental data on static fatigue of polymers and composites. These data show a linear relationship between the applied load and the logarithm of the failure time. The extension of this model in Eq. 1 is similar to Miner's rule in the sense that contributions to damage of various load cycles are additive and independent of each other.

FAILURE TIME OF FIBER BUNDLES

Consider a bundle with n fibers characterized by independent failure times following the distribution in Eqs. 1 and 2. The bundle is subjected to a load process $nX(\tau) \geq 0$ so that the load per fiber in state m is $\frac{n}{m} X(\tau)$ since the load is equally shared by the unfailed fibers and there are m unfailed fibers in state m. Let Y_m be the residence period in state m. The probability distribution of this variable, conditional on $Y_n = y_n,\ldots,Y_{m+1} = y_{m+1}$, is (1,3,4)

$$P(Y_m > y \mid Y_n = y_n,\ldots,Y_{m+1} = y_{m+1}) = \exp\left(-mk \int_{y_{(m)}}^{y_{(m)}+y} [\tfrac{n}{m} X(\tau)]^{\rho} d\tau\right) \tag{4}$$

in which $y_{(m)} = y_n+\ldots+y_{m+1}$. Note that the residence time in state m is independent of the damage accumulated in previous system states. The failure time of the bundle is

$$T_n = \sum_{m=1}^{n} Y_m \qquad (5)$$

Probabilistic descriptions of T_n and the reliability of the bundle in time t, $P_S(t) = P(T_n > t)$, can be obtained in principle from Eqs. 4 and 5. However, such an analysis may be impractical. Following sections illustrate several simple methods for estimating T_n and $P_S(t)$.

CONSTANT LOAD PROCESS

Let X(r) be a constant load of deterministic magnitude x. From Eq.4,

$$P(Y_m > y) = \exp(-km^{1-\rho_n}\rho_x\rho_y) \qquad (6)$$

so that the mean and the variance of T_n are

$$ET_n = \frac{1}{kx^{\rho}} \sum_{m=1}^{n} \left(\frac{m}{n}\right)^{\rho-1} \frac{1}{n} \qquad (7)$$

and

$$E(T_n - ET_n)^2 = \frac{1}{k^2x^{2\rho_n}} \sum_{m=1}^{n} \left(\frac{m}{n}\right)^{2(\rho-1)} \frac{1}{n} \qquad (8)$$

These moments of T_n can be approximated by $1/(k\rho x^{\rho})$ and $1/(k^2(2\rho-1)\, x^{2\rho_n})$ for large values of n. It can also be shown that T_n approaches a Gaussian variable as $n \to \infty$ (3,4). However, the convergence to this asymptotic distribution is rather slow.

Results are also available in closed-form for the distribution and the characteristic function of T_n (3,4). Therefore, the reliability in time t can be determined simply.

TIME VARIANT LOAD PROCESS

Assume that X(t) is a deterministic function of time x(t) and consider the change of varibles

$$s = H(t) = k \int_0^t x(\tau)^{\rho} \, d\tau \qquad (9)$$

It can be shown by direct calculations that the images Z_m of the residence periods Y_m in space s are independent and follow the exponential distribution $P(Z_m > z) = \exp(-m^{1-\rho_n} \rho z)$, (1,3,4). From Eq. 6, Z_m corresponds to a bundle with n fibers with k = 1 and subject to a constant load of intensity nx = n. Let

$$S_n = \sum_{m=1}^{n} Z_m \qquad (10)$$

The probability characterictics of this variable are given in the previous section.

From Eq. 9,

$$S_n = H(T_n) \qquad (11)$$

Since H(t) is a monotonically increasing function it has an inverse and (4)

$$T_n = H^{-1}(S_n) \qquad (12)$$

This equation can be used to estimate T_n from probability descriptors of S_n. Other methods for characterizing T_n are considered in Ref.1.

INDEPENDENT LOAD PROCESS

Let $X(\tau)$ be a load process taking constant independent identically distributed values x_i with probability p_i over periods of constant duration Δ. Therefore, $ds/dt = kx_i^{\rho}$ with probability p_i in Δ. The failure time can be obtained from

$$T_n = \int_0^{S_n} Y(s) \, ds \qquad (13)$$

in which $Y(s) = a_i = 1/(kx_i^{\rho})$ with probability

$q_i = (p_i/a_i) / (\sum_{j=1}^{q} p_j/a_j)$. These probabilities can be interpreted as the fraction of time Y(s) is equal to a_i.

Probabilistic descriptors can be obtained for T_n from Eq. 13. For example, the mean of T_n is (1)

$$ET_n = E(ET_n|S_n) = \frac{ES_n}{k\ EX^{\rho}} \tag{14}$$

in which $EX^{\rho} = \sum_i x_i\ p_i$. It takes the form

$$ET_n = \frac{ES_n}{k} E\frac{1}{X^{\rho}} \tag{15}$$

or

$$ET_n = \frac{ES_n}{k(EX)^{\rho}} \tag{16}$$

when the load process becomes a random variable with the distribution the marginal distribution of $X(\tau)$ or a constant of value $EX(\tau)$. The mean value of T_n in Eq. 14 is always smaller than the one in Eq. 16 by Hölder's inequality. This result is expected because the two failure times correspond to fatigue under fluctuating and constant loads. On the other hand, ET_n in Eq. 15 is usually larger than the corresponding value in Eq. 16 suggesting longer lifetimes under random constant loads (3). However, the reliability of bundles subject to these loads are typically in a reverse order to their average failure times for values of practical interest (1).

LINEAR DYNAMIC SYSTEMS WITH BRITTLE COMPONENTS

Consider a single story frame with n nominally identical columns subject to a load $Q(t) = Q \sin\omega t$ applied horizontally at the beam level. It is assumed that (i) structural mass is concentrated at beam level; (ii) beams are continuous, infinitely stiff, and unbreakable; (iii) failure can occur only in columns and is characterized by independent failure times with distribution in Eq. 1 where $\mu(x) = k|x|^{\rho}$; (iv) columns behave linearly and have the same

deterministic stiffness K and damping C; and (v) failed columns loose both stiffness and damping but continue to carry gravity loads.

The equation of motion of the frame in state m is

$$M\,\ddot{V}_m(\tau) + (mC)\,\dot{V}_m(\tau) + (m\,K)\,V_m(\tau) = Q \sin \omega\tau \qquad (17)$$

in which M = the structural mass, $V_m(\tau)$ = the story displacement at τ, and $\tau = 0$ defines the initiation of state m. An alternative form of the equation of motion is

$$\ddot{X}_m(\tau) + 2\varsigma_m\,\omega_{o,m}\,\dot{X}_m(\tau) + \omega_{o,m}^2\,X_m(\tau) = q \sin \omega\tau \qquad (18)$$

with the notations $X_m(\tau) = V_m(\tau)/h$, h = the frame height, $\omega_{o,m}^2 = mK/M$, $2\varsigma_m\omega_{o,m} = mC/M$, and $q = Q/(Mh)$. Note that both the natural frequency $\omega_{o,m} = \omega_{o,n}\sqrt{m/n}$ and the damping ratio $\varsigma_m = \varsigma_n\sqrt{m/n}$ decrease as damage progresses. The damping model can be unsatisfactory in some applications, e.g., damping usually increases in structures damaged by earthquake due to additional friction that may develop in failed components. Effects of the uncertainty in the damping model on system reliability are not evaluated in this study. These effects can be significant because initially overdamped systems may become underdamped in later damage states for the model in Eq. 18 and vice versa for a model that assumes an increase of damping with damage.

The solution $X_m(\tau)$ in Eq. 18 can be obtained in closed form and depends on the initial values $X_{m,o} = X_m(o)$ and $\dot{X}_{m,o} = \dot{X}_m(o)$ of the response in state m. These values are equal to $X_{m+1}(Y_{m+1})$ and $\dot{X}_{m+1}(Y_{m+1})$. The residence in state m has the conditional distribution

$$P(Y_m > y \mid Y_n = y_n, \ldots, Y_{m+1} = y_{m+1}) = \exp\{-\,km \int_{y_{(m)}}^{y_{(m)}+y} |X_m(\tau)|^{\rho} d\tau\} \qquad (19)$$

Table 1 gives estimates of the mean and the coefficient of variation for the failure time of the weakest column and the frame. The estimates are based on simulation and Eqs. 18 and 19.

Two preliminary conclusions follow from Table 1. First, redundant frames subject to lateral dynamic loads can be much safer than their

components. This result suggests that current reliability analyses for seismic design based on component performance may be unsatisfactory. Second, the usual consideration in, e.g., earthquake engineering that stiffness degradation is favorable needs further studies. Such favorable effects may be insignificant when the system starts at resonance, as shown by results in Table 1 for $\omega = \omega_{0,n} = 1$.

Reliability and other performance measures of the frame can also be determined by a method in Ref. 2 for estimating the reliability of Daniels systms with degrading strength and subject to time dependent loads. According to this method and the Rosenblatt transformation, the residence periods Y_m in Eq. 19 can be mapped into the standard Gaussian space $(U_1,\ldots,U_n)$ by

$$\begin{aligned} P(Y_n > w_n) &= \exp(-nkI_n) = \Phi(-U_n) \\ &\vdots \\ P(Y_m > w_m | Y_n = y_n,\ldots,Y_{m+1} = y_{m+1}) &= \exp(-mkI_m) = \Phi(-U_m) \quad (20) \\ &\vdots \\ P(Y_1 > w_1 | Y_n = y_n,\ldots,Y_2 = y_2) &= \exp(-kI_1) = \Phi(-U_1) \end{aligned}$$

in which Φ = the distribution of the standard Gaussian variable and $I_m = \int_{y_{(m)}}^{y_{(m)}+w_m} |X_m(\tau)|^\rho d\tau$ is a function of w_m for given values of $(Y_n,\ldots,Y_{m+1})$. The reliability $P_S(t)$ of frame in t is the probability of the event $\sum_{m=1}^{n} Y_m > t$. From Eq. 20, this event is equivalent to $\sum_{m=1}^{n} I_m^{-1}[-\frac{1}{km}\log(\Phi(-U_m))] > t$ and the probability of this condition can be determined approximately by methods for the analysis of time invariant reliability problems (2). The inverse I_m^{-1} of function I_m has to be determined numerically.

CONCLUSIONS

Methods have been examined for estimating the reliability and the failure time of parallel systems with brittle components refered to as fiber bundles. It has been assumed that the fibers fail at independent identically distributed times following Zhurkov's model.

The paper has developed new estimates for the reliability of fiber bundles subject to random load processes and incorporated in the analysis effects of the dynamic response of these systems. These effects have been illustrated by a study of a one story portal frame with brittle columns having independent identically distributed failure times excited by a sinusoidal load.

REFERENCES

1. Grigoriu, M., "Failure Time of Fiber Bundles Under Random Loads", Report 87-3, Department of Structural Engineering, Cornell University, April, 1987.
2. Guers, F., Dolinski, K., and Rackwitz, R., "Outcrossing Formulation for Redundant Structural Systems under Fatigue", 1st Working Conference on Reliability and Optimization of Structural Systems, Aalborg, Denmark, May 6-8, 1987
3. Phoenix, S.L., "The Asymptotic Distribution for the Time to Failure of a Fiber Bundle", Advances in Applied Probability, Vol. 11, 1979, pp. 153-187
4. Taylor, H.M., "The Time to Failure of Fiber Bundles Subjected to Random Loads", Advances in Applied Probability, Vol. 11, 1979, pp. 527-541

Table 1: Failure Times for a Portal Frame with n = 8 Columns

Estimated Values (30 samples)	Failure Times	
	Weakest Columns	Frame
$q = 1.0$; $\omega = \omega_{o,n}/2 = 0.5$		
Mean	3.21	16.10
C.o.v.	0.22	0.27
$q = 1.0$; $\omega = \omega_{o,n} = 1$		
Mean	2.85	6.75
C.o.v.	0.27	0.29

Structural Parameters : $\varsigma_n = 0.05$; $\omega_{o,n} = 1.0$
Failure Model Parameters : $k = 0.1$; $\rho = 1.0$

A PRACTICAL APPLICATION OF STRUCTURAL SYSTEM RELIABILITY ANALYSIS

Y. Guenard & G. Lebas
Elf Aquitaine - CSTCS - 64018 Pau - France

INTRODUCTION

This study was originated by a decision to drill new wells from an existing offshore platform with a drilling system different from the one the structure was originally designed for.

A drilling system is usually supported by a substructure (see figure 1), itself connected to the platform. The new drilling system was going to induce heavier loads in the substructure, and it was therefore decided to study the safety of the new installation.

Samples were taken from beams of the substructure. CHARPY V tests performed on those samples showed very low impact strengths, and the problem of the substructure safety against brittle fracture arised. In particular, the following questions were raised : are brittle failures likely to occur, and what are the consequences of such failures on the integrity of the substructure ? Is it necessary to replace the substructure ?

In order to answer those questions, it was decided to perform a probabilistic study taking into account the various sources of uncertainty (loads and resistances) and the redundancy of the structure. The study was performed in three steps :

- statistical analysis of CHARPY test data,
- definition of a brittle failure criterion,
- system reliability analysis of the substructure.

This paper presents the three steps with particular emphasis on the last one.

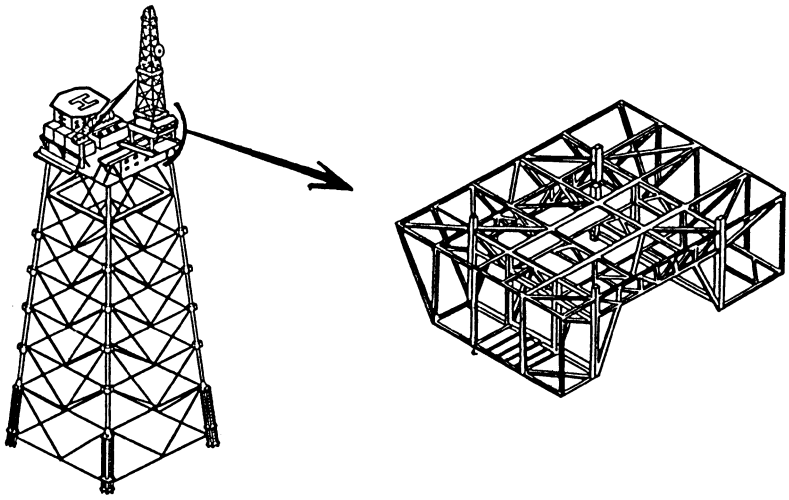

Figure 1 : drilling system substructure

STATISTICAL ANALYSIS OF CHARPY TEST DATA

On each sample taken from a beam, three CHARPY tests were performed, and this for two different temperatures (-5°C and +15°C). The results expressed by the impact energy Kcv showed a very large scatter, as can be seen on figure 2. There was not only scatter in the results from one beam to another, but also from one test to the other, within a single beam sample.

As a first step, a variance analysis was carried out in order to assess the significance of the temperature as well as of the beam type on the scatter. Temperature was found to be a significant parameter but not the beam type. As a consequence, all the results corresponding to a given temperature could be considered as coming from a homogeneous population and mixed in a single histogram. One of the two histograms is shown on figure 2. Both of them showed a bimodal shape which could easily be fitted by mixed WEIBULL laws. Hence, the cumulative distribution function F kcv (x) of the results could be expressed as follows :

$$Fkcv(x) = p \times F1kcv(x) + (1-p) \times F2kcv(x) \qquad (1)$$

with

$$Fikcv(x) = 1 - \exp\left(-(x/ti)^{bi}\right)$$

where ti is a scale parameter, bi a shape parameter, and p the proportion of data in the first population.

In each case, the two populations seemed to correspond to a brittle and to a ductile population. As expected, we observe a translation of the populations as the temperature changes.

In addition to the CHARPY test values Kcv's, yield stress measurements were obtained. They showed a much smaller scatter (coefficient of variation of about 10%) and were well fitted by a Lognormal distribution.

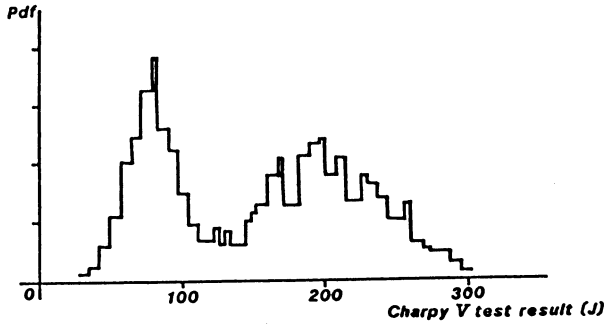

Figure 2 - Histogram of the CHARPY test results

DEFINITION OF A BRITTLE FAILURE CRITERION

Principal assumptions

Different welds of the substructure were inspected in order to detect any existing defect but none was found. However, in order to define a brittle failure criterion, we conservatively assumed that a preexisting crack was present at each connection.

Based on the conclusions of two papers, (10) and (11), devoted to crack detection in offshore structures, two additional assumptions were made :

- all the defects are located at the weld toe,
- all are semi-elliptical surface cracks.

Regarding the statistical distribution of the defect dimensions (crack depth and length), the one given in (2) was chosen. It results from a statistical analysis of defects measured in nuclear pressure vessels, i.e. in structure of better quality than offshore structures as far as welding is concerned. Nevertheless the most probable crack dimension (length and depth) agree well with those given in (10) and in (11).

According to fracture mechanics theory, brittle failure occurs if the stress intensity factor K is larger than the fracture toughness K_{IC}. Therefore, we had to characterize the distributions of these two parameters.

Stress intensity factors

Different formulas have been proposed in the literature to compute the stress intensity factors in semi-elliptical surface cracks. Most of them take the following form :

$$K = S \times \sqrt{\pi\, a/Q(a,h)} \times F(a,b,h,) \qquad (2)$$

Where S, a, b and h are respectively the tensile stress, the crack length, the crack depth, and the sample thickness (here the beam flange thickness) as shown on figure 3. In each case we decided to use the formula giving the largest stress intensity factor. These formulas can be found in (1), (5), (7), (8), (12).

Fracture toughness

The results of a CHARPY V test, Kcv, is not the fracture toughness KIc. However, these parameters are correlated. Using the data given by G.LECLERC (6), we performed a linear regression by the least square method between the two parameters Xi = log(KCv) and Yi = log(KIc). The following relationship was obtained :

$$KIc = 10\ Kcv^{.64} \times R \qquad (3)$$

where R accounts for the model uncertainty. We looked for the distribution of the residual values Ri, Ri being calculated for each point (Xi, Yi) from Eq (3). The histogram was well fitted by a normal distribution with a mean equal to 1.01 and a variance equal to 0.021.

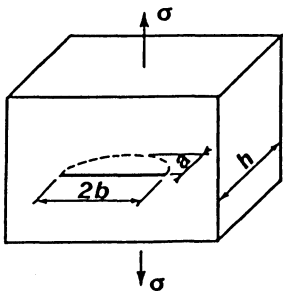

Stress intensity factor

$$K = \sigma\sqrt{\pi \frac{a}{Q}}\ F$$

Figure 3 - Dimensional characteristics of a semi-elliptical crack

Brittle strength distribution

Using the expression of K given by equation 2, and the expression of Klc given by equation 3, the brittle failure equation ($K > K_{IC}$) may also be written as follows :

$$S > Sbrit \qquad (4)$$

where Sbrit is defined by :

$$Sbrit = \frac{10\ Kcv^{.64} \times R}{\sqrt{\pi a\ /\ Q(a,b)}\ F(a,b,h)} \qquad (5)$$

The distributions of Kcv and R were obtained from the statistical analysis described above. The distributions of a and b were taken in the literature (see above). For each temperature and for different values of the thickness h, the distribution of Sbrit was obtained by MONTE-CARLO simulations.

As expected, this distributions showed two modes, corresponding to the two populations of the CHARPY V test results. Each population was fitted by a WEIBULL law and the resulting distribution could be written as :

$$F(Sbrit;h) = p \times F1(Sbrit;h) = (1-p) \times F2(Sbrit;h) \qquad (6)$$

Note that when h increases, all the parameters of the distribution tend to constant values. Also, the smaller the thickness, the more detrimental the distribution of Sbrit. These results could be expected.

Probability of failure

The probability of failure Pf is the probability of having a stress greater or equal to the brittle strength

$$Pf = P(S>Sbrit) = \int_0^{+\infty} Fb(x)\ f(x)\ dx \qquad (7)$$

where f(x) is the probability density function (pdf) of S and Fb(x) the cumulative distribution function of Sbrit. Noting Fb1(x) and Fb2(x) the pdf of the two populations, this expression becomes :

$$Pf = p \times \int_0^{+\infty} Fb1(x)\ f(x)dx + (1-p) \times \int_0^{+\infty} Fb2(x)\ f(x)dx \qquad (8)$$

In a first approximation, and especially for the low temperature (-5°C), the second term can be neglected. In other words the probability of failure is almost the probability of being in the first population AND of having a stress greater than the brittle strength. This approximation was used thoughout the subsequent analysis.

STRUCTURAL SYSTEM RELIABILITY ANALYSIS

Methodology

Because a complete description of the methodology can be found elsewhere (e.g. reference (4)), only some general ideas are given here.

A structural system such as the substructure studied here is made of many members which can fail individually in various modes. The finite element model of the structure is shown on figure 4. There are more than 1000 degrees of freedom. The usual failure modes accounted for in the codes are overall buckling of a member or plastification of a section. In this particular study, the brittle failure mode described earlier, is also considered.

Each failure mode is described by an equation $g(X)=0$ such that failure occurs if $g(X) \leqslant 0$, where X is a vector of parameters such as internal forces and moments, material properties, and geometrical characteristics. In a probabilistic analysis, some of the parameters are treated as random variables and each failure mode has a probability of occurrence. Estimating individual probabilities of failure is the first step of a structural system reliability analysis.

Once a member has failed, the structure stiffness is modified and the load initially carried by the failed member has to be more or less redistributed among other members. The load redistribution may trigger another member failure which itself leads to other failures until the structure cannot satisfactorily support the loads applied to it. Identifying the most critical failure sequences and estimating their probabilities of occurrence is the second and main step of a structural system reliability analysis.

In the two steps of the analysis, the so-called Advanced First Order Reliability Methods were used. These methods allow us to estimate individual probabilities of failure as well as probabilities of intersections or unions of failure events. A description of these methods can be found in many references, and in particular in (13) and (4).

The probability of a sequence occurring is always smaller than the probability of occurrence of the initial failure of that sequence. How much smaller ? This is a critical issue because the answer is directly linked to the amount of safety reserve available beyond initial failure, i.e. the **effective redundancy** of the structure. One of the most interesting outcome of a system analysis is that it provides a mean of assessing that effective redundancy. For a better understanding of the results given below, it must be noted that the effective redundancy of a structural system depends on three main factors :

- mechanical redundancy,
- post-failure behavior of the members,
- statistical dependence of the individual failures.

Mechanical redundancy, measured by the degree of hyperstaticity of a structure, is what structural engineers usually mean by redundancy. Having some mechanical redundancy is a necessary condition in order to have effective redundancy, but it is not sufficient. Post-failure behavior (ductile, brittle or semi-brittle) of a member is an important factor because it governs the amount of load that has to be redistributed among the intact members. Statistical dependence is another important factor which comes from various sources. One of them is a common random source of loading such as the wind. In short, if the wind effect is likely to be high in one member, it is likely to be high in an other member. Hence the two individual failures are not independent. It turns out that statistical dependence is detrimental to effective redundancy.

Finally, it must be noted that the absolute values of the probabilities of failure are rather meaningless for various reasons that will not be discussed here. It is only when compared to each others that they can be best exploited. This is what is done when the effective redundancy of a structure is assessed. It can also be of interest to compare individual probabilities of failure or failure sequences probabilities.

In structural reliability analysis, probabilities of failure are often replaced by **safety indices**. The safety index, often called β, is a decreasing function of the probability of failure and hence, the two are interchangable. However, there are two advantages in using safety indices : their values are usually between one and ten, and it is less tempting to give them an absolute meaning.

Failure modes definitions and general assumptions

Three failure modes were accounted for in this analysis : overall buckling of a member, plastification of a section, and brittle fracture of a connection. The corresponding equations and the parameters involved are briefly presented.

Buckling : Fcr - Fx = 0
with brittle post-failure behavior.

Plastification : $1 - Fx/Np - Mz/Mp = 0$
with ductile post-failure behavior

Brittle fracture : $Sbrit - SCF(Fx/A + Mz/(I/v)) = 0$

Fx and Mz are the internal axial force and the bending moment about the strong axis at one of the two extremities. Both are function of random load variables and are hence random variables themselves. The random load variables are the following :

- Total dead load resultant (the same for all load combinations) assumed to have a lognormal distribution with a coefficient of variation of 10%,

- Total live load resultant (depends on the load combination) assumed to have a lognormal distribution with a coefficient of variation of 10%,

- Wind load resultant (depends on the load combination) assumed to have a lognormal distribution with a coefficient of variation of 30%. This load corresponds to the 100 year extreme 1 minute sustained wind speed and includes model uncertainty.

The assumptions regarding the above distribution types and coefficients of variation are based on reference (3) and on in-house data. The other parameters are defined as follows :

- Fcr is the compressive strength (buckling about the weak axis with effective length factor equal to 1) assumed to follow a lognormal distribution. SVEIN FJELD (3) suggests a coefficient of variation of 17%, but other references give lower values. Hence an average value of 15% is chosen.

- Np and Mp are respectively the plastic axial strength and the plastic moment (strong axis bending). Both are proportional to the yield strength which was found to follow a lognormal distribution with a coefficient of variation of 10% according to the test results analysis (see above).

- A and (I/v) are respectively the section area and elastic section modulus assumed to be deterministic parameters.

- SCF is the stress concentration factor at the tension flange connection. Its value is conservatively assumed constant and equal to 1.7, which is an upperbound for the type of connections encountered (see reference (9)).

- Sbrit is the brittle fracture strength defined above, where it was found to follow a bimodal probability distribution. The uncertainty associated to Sbrit is rather high (coefficient of variation larger than 50%).

As can be noted, only strong axis bending is considered in the failure equations. This can be considered as a good assumption for the type of loading applied to the structure.

Results and comments

The results consist mainly in a listing of the critical failure sequences and the associated safety indices. They can be easily presented on failure trees with the following conventions :

- each branch represents a beam (or beam connection) failure in one of the three possible failure modes (Bu=buckling, Br=brittle, P=plastification),

- each node represents a damaged state of the structure, resulting from the occurrence of the failure sequence defined by the branches leading to that node,

- the numbers indicated on the branches are the beam numbers (defined on figure 4),

- the numbers indicated at the nodes are the safety indices corresponding to the probability of the structure being in the damaged state associated to that node.

Two load combinations were considered. They correspond to different lay-outs of the drilling system. In each case, the worst wind direction was considered. Hence two failure trees were obtained, and one of them is shown on figure 5. Only the most likely failures are shown on this figure. The comments that follow apply to the two failure trees.

The first comment that must be made about these results is that brittle failure modes are predominant. This is mainly due to the large uncertainty associated to the random variable Sbrit but also to the conservative assumptions made about this failure mode.

The second comment is about the redundancy of the structure. Eventhough brittle failure modes predominate (e.g. no residual strength to help after failure), the structure shows a large amount of redundancy. This can be inferred from the significant increase in safety index that shows up between every two consecutive failures. In terms of probabilities, this means that the probability of an additional failure occurring, given that one has already occurred is rather small (typically a few percents). In this case, the origin of the redundancy is twofold : mechanical redundancy and independence of the failure modes. The (almost complete) independence of the failure modes stems here from the large uncertainty associated to the Sbrit variables, reasonably assumed themselves independent. Comparatively the common source of uncertainty (loading variables) that induces a dependency of the failure modes is rather small. Hence, globally, the failure modes are almost independent from each other.

The failure tree shown on figure 5 is quite small for such a large structure. This is so because the loading is disymmetric and therefore only a few members are heavily loaded and likely to fail. This failure tree however is sufficient to show the effective redundancy of the structure. This is fortunate because only a few structural analyses (expensive part of the reliability analysis with a large structure) were required. Actually none of the sequences shown on the failure tree corresponds to the failure of the structure. Hence the effective redundancy of the structure is even larger than indicated by the results.

Finally, something must be said about members 171 and 177. They are not primary members as far as the integrity of the structure is concerned (their only role is to support small pieces of equipment). This is why no branch stems from the nodes corresponding to their failure, eventhough they are the most likely initial ones.

Figure 4 - Finite element model of the substructure

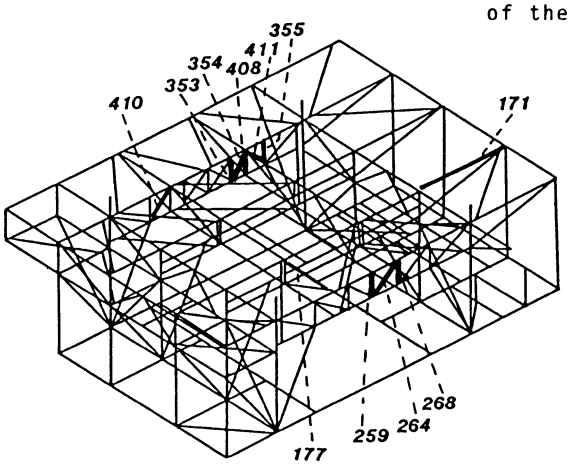

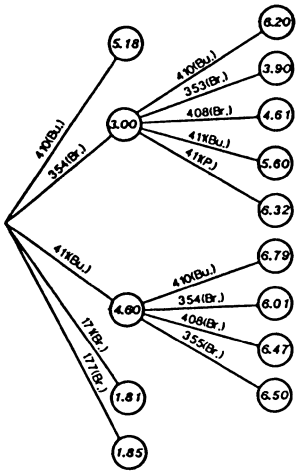

Figure 5 - Failure tree corresponding to one load combination

Bu. : Buckling
P. : Plastification
Br. : Brittle fracture

CONCLUSION

The conclusions of the study were that eventhough brittle failures are more likely than other failures, the structure is so redundant that a catastrophic sequence of brittle failures is very unlikely.

We recommended not to replace the structure but to inspect regularly the most critical areas identified by the analysis.

More generally, it has been shown that structural system reliability analysis can now be applied to practical situations. It must be noted that the most costly steps of the analysis were not the probability estimations but the structural analyses used as inputs to these estimations.

Fortunately, only a few structural analyses had to be carried out to conclude that the structure was redundant and safe. This will probably often be the case in practical situations where disymmetry in the structure as well as in the load will result in only a few most likely failure sequences.

Of course, the methods used are not perfect and inprovements are still required but it is believed that they have now reached a stage such that they can be used as rational decision tools.

REFERENCES

(1) **Anderson, Holms R. and Orange T.**
Stress intensity magnification for deep surface cracks in sheets and plates
NASA TN D.6054, 1970

(2) **Dufresne J.**
Probabilistic application of fracture mechanics
ICF5 Vol.2, 1981 - pp 517-531

(3) **Fjeld S.**
Reliability of offshore structures
OTC paper 3027, 1977

(4) **Guénard Y.**
Application of structural system reliability analysis to offshore structures
PhD thesis, Stanford University, 1984

(5) **Irwin G.**
Journal of applied mechanics
Vol.29, n°4, 1962, pp 651-654

(6) **Leclercq G., Marandet B. and Sanz G.**
Evolution de la tenacité des matériaux à partir de paramètres issus d'essais mécaniques simples
Rapport IRSID REP 123, mai 1975

(7) **Newman J. and Raju I.**
Analysis of surface cracks in finite plates under tension of bending loads
NASA TP, 1978

(8) **Paris P. and Sih G.**
ASTM STP 381, 1965, pp 30-83

(9) **Peterson R.E.**
Stress concentration factors
John Wiley & Sons, 1974

(10) **Rodrigues, Wong and Rogerson**
Weld defect distribution in offshore platforms and their relevance to reliability studies, quality control and in-service inspection
OTC paper 3693

(11) **Rogerson and Wong**
Weld defect distributions in offshore structures and their influence on structural reliability
OTC paper 4237

(12) **Tada H, Paris P. and Irwin G.**
The stress analysis of cracks handbook
DEL research corporation, 1973

(13) **Hohenbichler M., Rackwitz R.**
First order concepts in system reliability, structural safety
Vol.1, 1983, pp 177-188

OUTCROSSING FORMULATION FOR REDUNDANT STRUCTURAL SYSTEMS UNDER FATIGUE

F. Guers*, K. Dolinski** & R. Rackwitz*
* Technical University Munich, Munich, FRG
** Institute of Fundamental Technological Researches, Warsaw, Poland

1. Introduction

In many cases the resistance properties of structural systems as well as the loads acting on the structure depend on time. If the loads can be modelled by stationary processes and the resistances are time-invariant the determination of the time-dependent reliability essentially is a problem of load combination for which a number of solution procedures exists. The only method capable to handle nonstationary loading with some rigour appears to be the outcrossing approach [1] and the same appears to be true for cases where resistances deteriorate with time, e.g. due to load-induced fatigue, corrosion or aging. This is demonstrated in [2] and elsewhere for structural components. If, however, such deterioration occurs in a redundant structural system a reliability analysis meets serious complications. Structural failure, then, is most likely the result of a sequence of single or multiple componental failures at different random times each of which changing the stress regime in the structure. Furthermore, the load trajectory determines the specific failure sequences. Failure phenomena of this type will especially be found in certain types of railway bridges, aircraft structures and in maritime structures such as ships or offshore platforms. The quantification of the time-dependent reliability of those structures is not only the basis for a proper design of such structures but, probably more important, allows the selection of suitable inspection strategies and rational decisions about time and necessity of repairs.

The only studies known to the authors which have addressed this problem so far are due to Martindale/Wirsching [3], Stahl/Geyer [4], Knapp/Stahl [5] and the last author [6]. The first mentioned

references assume the distribution of times between componental failures as known but depending on the system states. Reliabilities are determined by Monte-Carlo-methods. In the last mentioned reference a first, not yet satisfactory attempt has been made to formulate the problem in the context of modern reliability methods.

In this study the widely analytical outcrossing approach proposed in [2,7] for the determination of time-variant structural reliability under stationary and ergodic loading and non-deteriorating structural resistances is summarised and generalised to fatigue-induced deterioration of structural components (see also [8]). Formulations are sought such that reliability calculations can be performed with modern first- and second-order reliability methods. This might enable the analysis of larger systems with many uncertain variables. The formulations are demonstrated at a simple example.

2. Reliability of deteriorating structural components

Assume a statically reacting, linear-elastic and redundant structural system subject to loads modelled by a stationary (and ergodic) Gaussian vector process $\underline{L}(\tau)$. Further, suppose that failure can occur only in a finite number of preselected control points (hot spots) which will be denoted by elements or components of the structure. For these components it is always possible to derive the load effect process which, here, is assumed to be a scalar process, i.e. $S_j(\tau) = \sum_i a_{ji} L_i(\tau)$, and whose mean and covariance function are easily determined from the properties of $\underline{L}(\tau)$. Component failure occurs whenever $S_j(\tau)$ exceeds some resistance (residual strength) $R_j(\tau)$ for the first time. Componental failure or componental state changes are understood as discontinuous changes (decreases) in stiffness at that time causing a more or less abrupt redistribution of internal forces in the system. Here, only perfectly brittle elemental failures will be considered. In practical applications one might wish to model the rupture phenomenon more realistically, e.g. by retaining at least some fraction of the original stiffness after failure. The considerations to come also hold in this case with minor modifications.

The resistances $R_j(\tau)$ depend on a time-invariant vector of uncertain parameters such as initial strength $R_j(o)$ and parameters

determining the details of strength degradation. They are collected in the uncertain vector $\underline{Q}$ with given distribution function $F_{\underline{Q}}(\underline{q})$. Let, for the moment, $\underline{Q}$ be kept fixed at $\underline{Q} = \underline{q}$.

In order to determine the componental failure probability one needs to know the distribution of the time to first failure which, unfortunately, can only be given exactly under very special conditions for the processes $S_j(\tau)$ and functions $R_j(\tau)$. However, a general, asymptotic formula for the failure probability is [9]

$$P_{f,j} = P\,(T_j \leq t) = F_{T_j}(t) \sim 1 - \exp[-\int_0^t \nu_j(\tau)\, d\tau] \qquad (1)$$

provided that the process $R_j(\tau) - S_j(\tau)$ fulfills certain mixing conditions. Herein, $\nu_j(\tau)$ is the upcrossing rate defined by:

$$\nu_j(\tau) = \lim_{\Delta \to o} \frac{P(\{S_j(\tau) \leq R_j(\tau)\} \cap \{S_j(\tau + \Delta) > R_j(\tau + \Delta)\})}{\Delta} \qquad (2)$$

Eq. (1) is valid provided that $\nu_j(\tau)$ exists. For example, $\nu_j(\tau)$ exists for Gaussian processes with continuously differentiable sample paths and sufficiently smooth deterioration functions.

In the case of fatigue, the residual strength, strictly spoken,is a non-stationary process which depends on the load-effect process. Furthermore, the actual load amplitude determines the loadinduced decrement of residual strength. For high cycle fatigue, however, one can assume that, asymptotically (large τ), the process $R_j(\tau)$ not only becomes uncorrelated with the process $S_j(\tau)$ but also has vanishing load-induced variability [2,10]. Therefore, it can be assumed that the $R_j(\tau)$ are sufficiently smooth functions with existing derivative. Then, with $R_j(\tau)$ being approximately a deterministic function with possibly uncertain parameters the following formula for $\nu_j(\tau)$ can be derived [1] (reference to τ now being ommitted)

$$\nu_1 = \omega_o \varphi(r)\, \Phi(\dot{r}/\omega_o) \qquad (3)$$

where $(r = (R - m_s)/\sigma_s$, $\dot{r}$ the time derivative of r, ω_o^2 the variance of the derivative of the normalized load effect process $s = (S - m_s)/\sigma_s$

and $\Psi(x) = \Phi(x) - x\,\phi(-x)$.

The residual strength function, typically, has the form

$$r(\tau) = K_1\,(1 - K_2\,\nu_o\,\tau\,E[\Delta S^A])^B \qquad (4)$$

where the constants can have concrete physical meaning. Assume, for example, the crack propagation law due to Paris/Erdogan [1,2]

$$\frac{da}{dn} = C\,(\Delta S\,\sqrt{\pi a})^m \qquad (5)$$

with a the crack length, ΔS the effective stress-range and C and m two material parameters. The crack becomes unstable for $K = \sqrt{\pi a}\,S \geq K_c$ with K_c the fracture toughness. Then, it can be shown that for $m > 2$, $K_1 = K_c\,(\pi a_o)^{-1/2}$, $K_2 = C\,\pi^{m/2} a_o^{m/2-1}\,(m-2)/4$, $A = m$, $B = (m-2)^{-1}$. a_o is the initial crack length. ν_o is the rate of positive zero crossings of $s(\tau)$. For a sufficiently narrow-band process $s(\tau)$, it is finally $E[\Delta S^A] = (2\sqrt{2})^A\,\sigma_S^A\,\Gamma(1 + A/2)$ according to Palmgren/Miner's rule [1].

The integral in eq. (1) of the outcrossing rate eq. (3) with threshold function eq. (4) can be approximated fairly well for sufficiently large thresholds $r(\tau)$ by using the method of Laplace [2]. Following [2] where the application of this method to fatigue reliability problems is investigated in some detail, one obtains

$$I(t) = \int_o^t \nu(\tau)\,d\tau \approx \frac{h(t)}{f'(t)}\,\exp[f(t)][1 - \exp[-tf'(t)]] \qquad (6)$$

with

$$h(t) = \frac{\omega_o}{\sqrt{2\pi}}\,\Psi\left(\frac{\dot r(t)}{\omega_o}\right) \qquad (7)$$

$$f(t) = -\frac{1}{2}\,r^2(t) \qquad (8)$$

$$f'(t) = -\,r(t)\,\dot r(t) \qquad (9)$$

Eq. (6) can further be improved on those lines if necessary (see [2,10]).

The total failure probability with the paramters $\underline{Q} = \underline{q}$ now being random is:

$$P_{f,j}(t) \sim 1 - \int_{\mathbb{R}} \exp[-I_j(t|\underline{q})] \, dF_{\underline{Q}} \tag{10}$$

A serious obstacle in applications is the multidimensional integration required in eq. (10). It is possible to reformulate the problem such that first- and second-order reliability methods become applicable (FORM/SORM) [12]. Introducing an auxiliary standard normal variate [2]

$$P(T_j(\underline{q}) \leq t) = 1 - \exp[-I_j(t|\underline{q})] = P(U_{T_j} \leq u) = \Phi(u), \tag{11}$$

we find by solving for $T_j(\underline{q})$

$$T_j(\underline{q}) = I_j^{-1}[-\ln \Phi(-U_{T_j})|\underline{q}] \tag{12}$$

the Rosenblatt-transformation [13] for the random first-passage time. The required formulation for FORM/SORM is:

$$P_{f,j}(t|\underline{q}) = P(T_j(\underline{q}) - t \leq o) \tag{13}$$

The total failure probability can be given as

$$P_{f,j}(t) = P(T_j(\underline{T}(\underline{U}_{\underline{Q}})) - t \leq o) \tag{14}$$

with $\underline{Q} = \underline{T}(\underline{U}_{\underline{Q}})$ the Rosenblatt-transformation of $\underline{Q}$. Then, for small failure probabilities an accurate probability estimate is [12]

$$P_{f,j}(t) \sim \Phi(-\beta) \prod_{i=1}^{n_j} (1 - \kappa_i \theta)^{-1/2} \tag{15}$$

where

$$\beta = \|\underline{u}^*\| = \min \{\|\underline{u}^*\|\} \text{ for } \{\underline{u}: g(\underline{u}) \leq o\} \tag{16}$$

and the κ_i's are the main curvatures in $\underline{u}^*$, $\theta = \varphi(-\beta) / \Phi(-\beta)$ and $g(\underline{u}) \leq 0$ the event at the rigth-hand side of eq. (14). The inversion of the integral $I_j(t)$ in eq. (12) is best made by Newton's algorithm:

$$T_j(\underline{q})^{(k+1)} = T_j(\underline{q})^{(k)} - \frac{I_j(T_j(\underline{q})^{(k)}) + \ln \Phi(-U_{T_j})}{\nu_j(T_j(\underline{q})_j^{(k)})} \tag{17}$$

Formula (3) has been found to be rather conservative for not too large values of r(t) especially for narrow band processes such as wave loading processes. The consideration of crossings of the envelope process E(τ) of S(τ) may yield better results. In this case, eq. (3) has to be modified into [1]:

$$\nu_2 = \omega_E \, f_{Ray}(r) \, \Phi(\dot{r}/\omega_E) \tag{18}$$

with $\omega_E^2 = \omega_o^2 \, (1 - (\lambda_1(\lambda_o\lambda_2)^{-1/2})^2)$ and $f_{Ray}(r) = r \exp[-r^2/2]$ the Rayleigh-density. An even better result is obtained by using the interpolation between eq. (3) and eq. (18) proposed in [14]

$$\nu_3 = \nu_1 \, [1 - \exp[- \nu_2/\nu_1]] \tag{19}$$

The conditions for the validity of the approximation eq. (5) are still fulfilled but eq. (7) is replaced by:

$$h(t) = \frac{\omega_o}{\sqrt{2\pi}} \Phi(\dot{r}(t)/\omega_o) \, [1 - \exp[- \nu_2/\nu_1]] \tag{20}$$

with

$$\nu_2/\nu_1 = \frac{\omega_E \Phi(\dot{r}(t)/\omega_E)}{\omega_o \Phi(\dot{r}(t)/\omega_o)} \, r(t) \tag{21}$$

Formula (18) should be used in practical applications, not only because it gives more accurate results for a larger range of thresholds and bandwidth parameters $\delta = \lambda_1(\lambda_o\lambda_2)^{-1/2}$ with λ_i the i-th spectral moment of S(τ), but is also more consistent with the basic assumptions underlying eq. (4).

There are several further refinements to eqs. (11) which, however, have been found relatively insignificant in numerical applications.

3. System reliability

Consider now system failure which in redundant structures requires several components to fail simultaneously or in a sequence. In general, many different sets of componental failures exist which imply system failure. For the moment,we concentrate on a certain set of componential failures or a failure path k consisting of N = N(k) components. Further analysis now must distinguish between various cases. Although the structure is assumed to behave statically (no accelerated mass forces) under normal loading, dynamic effects usually need to be considered for the internal load redistribution process.

Assume that during a "local extreme" of the loading process there is a brittle componental failure. The load effect in another component

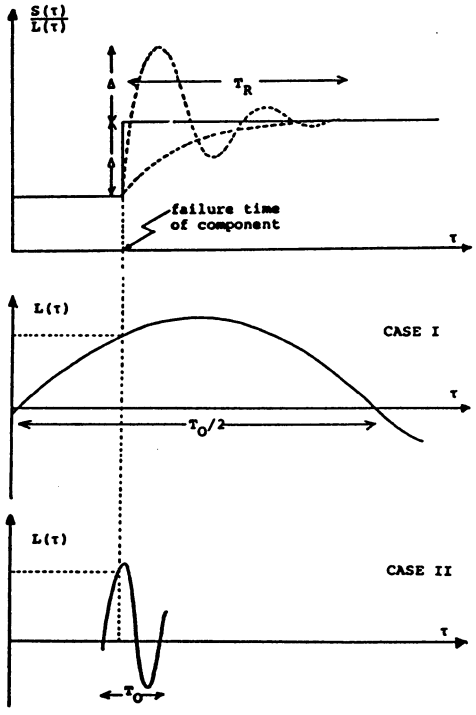

Figure 1: Immediate and delayed load-effect redistribution with and without dynamic effects

will perform a damped oscillation around the statically redistributed load-effect function. Two extreme cases can be visualized. If there is small damping and a relatively large frequency of the oscillations as

compared to some characteristic frequency of the load, the additional dynamic load-effect after brittle failure of some component can be at most twice the difference between the static loadeffects before and after failure. The other extreme is where load-effect redistribution is of a rather damped nature. The redis-tribution follows nearly a negative exponential function. No dynamic overshooting occurs. Unfortunately, the details of dynamic effects in rupture phenomena have found very little attention in the literature and it is, in general, hard to say which of the two limiting cases is closer to reality. The authors are inclined to presume that the latter case is more representative in many cases. A numerical study of the two extreme cases of dynamic effects during load redistribution in a later example may highligth their significance. Except for this example we shall assume that no dynamic effects are present.

Furthermore, we consider, in simplifying the subject, two extreme cases of the load redistribution regimes defined by the two limits of the ratio T_R of (almost perfect) load-effect redistribution and the predominant period T_o of the load process. The case where redistribut-ion of forces takes a time much shorter than T_o, i.e. $T_R << T_o$, is denoted by case I. For case II, on the other hand, the time required to redistribute the forces is much larger than T_o (See figure 1). During a "local" extreme of the load multiple failures can occur in either case. It is even possible that all components in a failure path fail in a single "load wave" causing system collapse. An example of the corresponding failure tree is given in figure 2. In case I with "immediate" load redistribution during one local extreme of the load-ing process, there can be even progressive collapse during the process of redistribution while that is unlikely in case II. Therefore, case I is more critical than case II.

Componental individual or multiple failures occur along the failure path at different failure times. The time to system collapse simply is the sum of the times between those partial failures. For non-deter-iorating structures, we have [7]:

$$P_{f,k}(t) = P\left(\sum_{i=1}^{N(k)} T_i(\underline{q}) - t \leq 0\right) \qquad (22)$$

Herein, t is some prespecified service time of the structure or, alternatively, the time to the next inspection.

For deteriorating structures the problem is somewhat more complex. The second failure time now depends on the first failure time since the latter determines the two damage accumulation regimes to be considered when computing the second failure time. And the third, forth, ... failure times analogously depend on all previous failure times, respectively. Hence, a possible formulation is [8,10]:

$$P_{f,k}(t) = P\left(\sum_{i=1}^{N(k)} T_i(\underline{q}) \,|\, T_1(\underline{q}),\ldots,T_{i-1}(\underline{q})\right) - t \leq 0) \qquad (23)$$

A crucial assumption when proceeding further is that the various failure times can be assumed to be conditionally independent. More precisely, the failure times are conditionally independent and exponentially distributed according to eq. (1). This requires that the failure events even at the end of a failure path are still rare events and, hence, the Poissonian character of the crossing events can be maintained also for the more developed degradation states of the system. That assumption also implies that after each single or multiple failure the load effect process has a "restart" from the intersection of the safe domains of all still unfailed components. Finally, it is assumed that the times between failures in a multiple failure event can be neglected as compared to the times between those events, i.e. $\theta_1 << T_1$. Then, in generalising the approach for component failure as in eqs. (10) to (16) the following transformation appears natural:

$$1 - \exp\left[-\int_0^{T_1} \nu_1(\tau|\underline{q})\, d\tau\right] = \Phi(U_{T_1})$$

$$1 - \exp\left[-\int_0^{T_i} \nu_1(\tau|\underline{q},U_{T_1},\ldots,U_{T_{i-1}})\, d\tau\right] = \Phi(U_{T_i})$$

$$1 - \exp\left[-\int_0^{T_{N(k)}} \nu_{N(k)}(\tau|\underline{q},U_{T_1},\ldots,U_{T_{N(k)-1}})\, d\tau\right] = \Phi(U_{T_{N(k)}}) \qquad (24)$$

Thus, estimates of conditional path failure probabilities can be obtained by eqs. (15) and (16) together with eq. (23), too.

These probabilities are not only conditioned on the specific parameter vector $\underline{Q} = \underline{q}$. They are further conditioned on the particular sequence of failure events in a path to failure and on the event that that particular path is the path to system collapse. One also has to

specify at a certain system state whether the next failure will be a single or multiple failure. The situation may be described for a system with only two components with time-invariant levels $r_1 \leq r_2$ (see figure 2).

Failure of these components under the assumption that there is delayed redistribution can occur in two ways. Either the load exceeds level r_1 but not r_2 so that the system fails in two time steps or a crossing of level r_1 is immediately followed by a crossing of r_2 which implies system collapse as before. As mentioned the short time θ_1 between those crossings is neglected. Now, the mean number of crossings

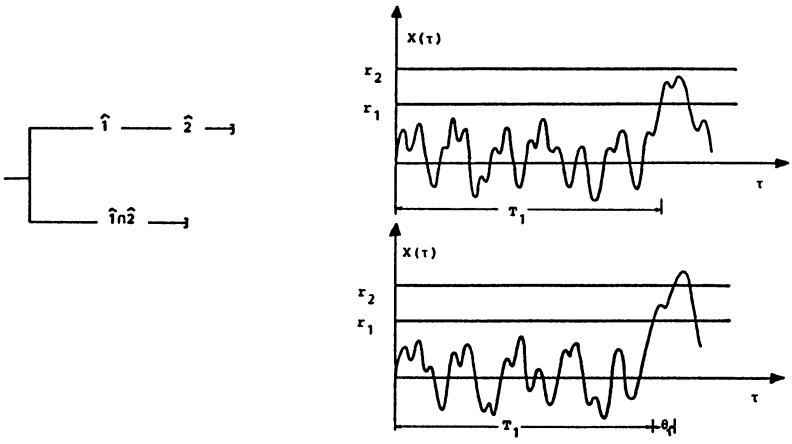

Figure 2: Single and double crossings in failure tree for two-component system

of r_1 but not of r_2 in [0,t] is $(\nu_1 - \nu_2)t$ whereas the mean number of unconditional crossings of r_2 is $\nu_2 t$. Appropriately renormalised, these quantities may be interpreted as probabilities of having a single or the other type of crossings. The probability of occurence of failure by double crossings in the interval [0,t] then is the probability that r_1 and r_2 are crossed subsequently times the probability that the first passage time T_1 remains smaller than t. As indicated before, these probabilities must be normalised, i.e. divided by the probability that r_1 is crossed. This can be written as

$$\frac{\nu_2}{\nu_1} P(T_1 \leq t)$$

with $P(T_1 \leq t) = 1 - \exp[-\nu_1 t]$. Analogously, for failure in two time steps it is

$$\frac{\nu_1 - \nu_2}{\nu_1} \frac{\nu_2 - 0}{\nu_2} P(T_1 + T_2 \leq t) = \frac{\nu_1 - \nu_2}{\nu_2} P(T_1 + T_2 \leq t)$$

where T_2 has distribution function $F_{T_2}(t) = 1 - \exp[-\nu_2 t]$ (see [7] for a rigorous derivation of this result). The terms ν_2/ν_1 and $(\nu_1 - \nu_2)/\nu_1$ may, in fact, be interpreted as the probabilities of developing system failures in either of the branches of the corresponding failure tree. Generalisation to more than two levels, to immediate load effect redistribution and to time-variant thresholds is conceptually straigthforward.

In order to calculate the total branch probabilities one finally has to remove the condition on $\underline{Q} = \underline{q}$ which, in general, also implies the consideration of a specific ordering of the thresholds. Note, that all events discussed so far depend on those parameter values.

Therefore, consider now a general system with K possible failure paths to system collapse. The number of time steps in the k-th path is L_k. In order to completely define the failure sequence in that path, an ordering of the reduced resistances must be performed for each of the time steps and the elements must be grouped into components failing at the end of each time step. For convenience of notation, only the case of time-variant resistances is written out explicitely. The probability of occurrence of the k-th failure sequence during [0,t] can be given as:

$$P(F_k) = \int_{\underline{Q}=\underline{q}} P_k(t|\underline{Q}=\underline{q})\, P\Big(\underbrace{\bigcap_{l=1}^{L_k}}_{\text{for each time step}} \underbrace{\bigcap_{i=1}^{I_k^l}}_{\text{for all present elements}} r^l_{n_{kl}(i)} \leq r^l_{n_{kl}(i+1)}\Big)\, dF_{\underline{Q}}(\underline{q}) \qquad (25)$$

The second probability corresponds to the specific ordering. In numerical calculations the variables r are represented by their Rosenblatt-transformations. The first probability is:

$$P_k(t|\underline{Q}=\underline{q}) = P^k \; P\Big(\sum_{l=1}^{L_k} T_l^k(r^l_{n_{kl}(1)}| \; . \;) \leq t\Big) \qquad (26)$$

where the second term corresponds to eq. (23) with new notation. The first probability is the probability to be on path k. In these equations, the following notations are used:

* $\underline{I}_k^l$ denotes the numbers of the control points in the k-th path surviving at the beginning and along the l-th time step.
* $n_{kl}(i)$ is an integer function which assigns in ascending order the numbers of the reduced thresholds during the l-th time step.
* $P^k = \prod_{l=1}^{L_k} P_k^l$ is the weighting probability of being on the k-th failure path where

$$P_k^l = \frac{\nu^l_{n_{kl}(i_{kl})} - \nu^l_{n_{kl}(i_{kl}+1)}}{\nu^l_{n_{kl}(1)}}$$

* P_k^l is the weighting probability for the l-th time step which ends at the upcrossing of i_{kl} thresholds corresponding to the elements $n_{kl}(1)$ to $n_{kl}(i_{kl})$ without upcrossing the $n_{kl}(i_{kl}+1)$-th level. Again, the corresponding events are expressed in the standard space by auxiliary standard normal variables making use of $P_k^l = \Phi(U_k^l)$ (see [10], for details).
* $T_l^k(r^l_{n_{kl}(1)})$ is the time to the first upcrossing of the lowest relevant level for the l-th time step, which is also the length of this time step.

A similar formulation can be given for deteriorating resistances. From eq. (25) it can be seen that the computational task now also involves the computation of the probability of intersections which can conveniently be carried out by the methods desribed in [12].

Finally, if the parameter $\underline{Q} = \underline{q}$ is uncertain and there are K possible paths to system failure the overall failure probability is the probability of the union of the path failure events

$$P_f(t) = P\Big(\bigcup_{k=1}^{K} F_k\Big) \qquad (27)$$

This probability can be bounded by (see,for example, [12]:

$$P_f(t) \begin{cases} \leq P(F_1) + \sum_{\nu=2}^{K} (P(F_\nu) - \max_{\mu<\nu} (P(F_\nu \cap F_\mu))) \\ \geq P(F_1) + \sum_{\nu=2}^{K} (\max(0, P(F_\nu) - \sum_{\mu<\nu} P(F_\nu \cap F_\mu))) \end{cases} \quad (28)$$

In general, many paths to system failure exist. In practical computations it will, therefore, be necessary to limit the analysis to only a few failure paths which prefereably are the dominant (most likely) ones. They can be found by appropriate search algorithms. Suitable algorithms have been proposed by several authors [15,16] for time-invariant structural system reliability analyses. The one proposed in [15] which has been adapted to time-variant reliability in [10] may also be used here. The algorithm can be described as follows. Let there be a set of M = (1, 2, ...,) failure events a finite number of subsets of which lead to system failure. For the intact structure all componental failure probabilities are computed. Each component is the starting point of a failure tree. The component with largest failure probability, then, is transferred into a failed state which implies an updating of the stiffness matrix of the system. In order to find the next most likely state changes in the system the joint probabilities of the first state change event and the remaining failure events are computed. If one or more of these joint probabilities are larger than the previously calculated probabilities the corresponding component(s) is (are) transferred into a failure state. A second updating of the stiffness matrix is performed and the process continues with now exactly three failure events involved. If, however, smaller probabilities have been calculated previously, the degradation process continues at those components after having restored the system properties back to the degradation state of interest. Eventually, a sequence failure event will be found. Its failure probability is the probability of all events in that sequence. One still has to check whether there are probabilities for some incomplete failure sequences which are larger than the sequence probability just found. If so, the degradation process in these sequences must also be continued until sequence failure or until all probabilities of in-complete sequences become smaller than the smallest sequence probab-ility observed so far. This terminates the algorithm. A lower bound for the system failure probability then is the probability of the union of all complete failure sequences. The lower bound in eq. (28) applies. An

upper bound is the probability of the union of all complete and incomplete failure sequences for which the upper bound in eq. (28) should be used. This technique to produce strict probability bounds by a combination of an optimal search for dominant complete and the investigation of further incomplete failure paths and eq. (28) facilitates the analysis of larger systems very much.

4. Numerical example

Following [17] we shall investigate in more detail one of the mechanically simplest redundant systems shown in figure 3. This so-called Daniels-system (after Daniels who first studied its time-invariant reliability in [18]) has n physical components whose stochastic properties all have identical distribution function. If a component fails its load is distributed equally among the remaining components. These assumptions enable not only a number of simplifications in the formulation but also circumvent the problem of considering a large number of failure paths by introducing order statistics for the elemental resistances which is possible even for relatively complex stochastic dependence structures of the components. We shall especially use certain results presented in [19] for the time-invariant case.

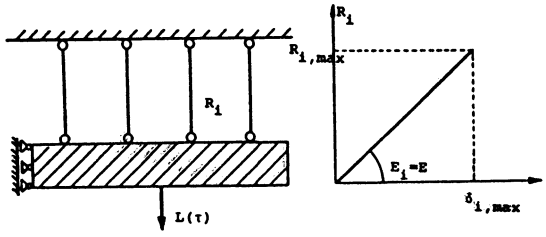

Figure 3: 4-component Daniels-system

We adapt the following fatigue deterioration model which is somewhat simpler than the one associated with eq. (5) (See, for example, [20]). It is assumed that the decrement of residual strength is pro-portional to some function of the stress range ΔS and inversely pro-portional to some power of the actual strength, i.e. the governing

differential equation is:

$$\frac{dR_j(\tau)}{d\tau} = - h(\Delta S_j)/(m\ R_j(\tau))^{m-1} \qquad (29)$$

Using the usual S-N-curve information in the form $KNS^b = 1$ together with Palmgren-Miner's damage accumulation hypothesis for a narrow-band Gaussian load effect process leads to [2]:

$$R_j(\tau) = R_j(o)\ (1 - K\ \frac{(2\sqrt{2})^b}{R_j^m(o)}\ \sigma_{S_j}^b\ \Gamma(1 + b/2)\ \nu_o\ \tau)^{1/m} \qquad (30)$$

This is a monotonically decreasing function for any positive m. Assume further that the only uncertain variable is the initial strength R(0) which is normally distributed with mean E[R(0)] and standard deviation D[R(0)]. Alternatively, the paramters K, b, and m can be introduced as random variables, but must not depend on j in order to render the used formulation possible. By some additional considerations, this idealisation could be removed. In applications, there are good reasons to assume a non-negligible inter-element correlation. Therefore, for initial strength values which are positively and equally correlated one has the following representation (Rosenblatt-transformation) for the various $R_j(o)$'s:

$$R_j(0) = E[R(0)] + D[R(0)]\ (U_o\ \sqrt{\rho} + U_j\ \sqrt{1-\rho}),\ j = 1, \ldots, n \qquad (31)$$

In order to establish the sequence of element failures, we need the order statistics of $(\hat{R}_1(\tau), \hat{R}_2(\tau), \ldots, \hat{R}_n(\tau))$. Since the parameters in the second factor in eq. (30) are assumed constant, the order statistics $\hat{R}_1(\tau) \leq \hat{R}_2(\tau) \leq \ldots \leq \hat{R}_n(\tau)$ can be derived from the order statistics of the $R_j(0)$'s. In [19] it is shown that the order statistics of a vector of independent standard normal variables have the Rosenblatt-transformation:

$$\hat{U}_1 = \Phi^{-1}\ [1 - \Phi(-U_1)^{1/n}]$$

$$\hat{U}_j = \Phi^{-1}\ [1 - \prod_{k=1}^{j} \Phi(-U_k)^{1/(n-k+1)}] \qquad (32)$$

Therefore,

$$\hat{R}_j(0) = E[R(0)] + D[R(0)]\ (U_o \sqrt{\rho} + \hat{U}_j \sqrt{1-\rho}) \qquad (33)$$

with $\hat{U}_j$'s as given in eq. (32). Eq. (33) inserted in the corresponding eq. (30) yields the required order statistics $\hat{R}_j(\tau)$.

The numerical calculations are performed with the following set of data:

$S(\tau) \sim N\ (0.5,\ 0.1)$,
$R_j(o) \sim N\ (0.9,\ 0.2)$,
$n = 4,\ \rho = 0.3,\ \nu_o = 1,\ t = 10^6$

Furthermore, for simplicity formula (3) is used throughout instead of the presumeably better formula (18).

At first, the case of time-invariant elemental resistance is investigated by setting $m \to \infty$. It will be used to quantify the effect of dynamic load redistribution after failure of a redundant component. Case I, that is immediate load redistribution without dynamic overshooting is calculated as follows. The extreme value distribution of the load is:

$$F_{\max_{[0,t]} S}(x) = \exp\ [-\nu(x)\ t] \qquad (34)$$

which easily is transformed by:

$$S_{max} = \frac{1}{t}\ \nu^{-1}\ (\ln \Phi(U_S)) \qquad (35)$$

The system failure probability must be determined from [17,19]:

$$P_f(t) = P(\bigcap_{j=1}^{n}\ \{(n - j + 1)\ \hat{R}_j\ (o) - S_{max} \leq O\}) = P(\bigcap_{j=1}^{n}\ \hat{F}_j) \qquad (36)$$

The numerical calculations by using the schemes developed in [12] yield the following results in terms of the equivalent or generalized safety index $\beta = -\Phi^{-1}[P(.)]$. The individual failure event and intersection safety indices are:

$\beta(\hat{F}_1) = 2.79;\ \beta(\hat{F}_1) = 2.79;$

$\beta(\hat{F}_2) = 3.36;\ \beta(\hat{F}_1 \cap \hat{F}_2) = 3.48;$

$\beta(\hat{F}_3) = 2.93;\ \beta(\hat{F}_1 \cap \hat{F}_2 \cap \hat{F}_3) = 3.66;$

$\beta(\hat{F}_4) = 0.33;\ \beta(\hat{F}_1 \cap \hat{F}_2 \cap \hat{F}_3 \cap \hat{F}_4\ ) = 3.66;$

It is obvious from the individual safety indices and from the increments in the system indices that the second component "dominates" the system. If this fails there is only a slight increase in reliability. And given that the third component fails, there is a probability of almost 0,5 that the forth component will also fail.

The case of (maximum) dynamic overshooting is also easily formulated. Let j-1 components already be broken. An upper bound to the additional dynamic load for component j to break is $\hat{R}_{j-1}$. Therefore, eq. (36) is modified to:

$$P_f(t) = P(\bigcap_{j=1}^{n} \langle (n-j+1)\,\hat{R}_j(o) - \hat{R}_{j-1}(o) - S_{max} \leq 0 \rangle) = P(\bigcap_{j=1}^{n} \hat{F}_j) \quad (37)$$

The numerical results for that case are:

$\beta(\hat{F}_1) = 2.79;\ \beta(\hat{F}_1) = 2.79;$

$\beta(\hat{F}_2) = 2.43;\ \beta(\hat{F}_1 \cap \hat{F}_2) = 3.31;$

$\beta(\hat{F}_3) = 0.03;\ \beta(\hat{F}_1 \cap \hat{F}_2 \cap \hat{F}_3) = 3.31;$

$\beta(\hat{F}_4) = -3.22;\ \beta(\hat{F}_1 \cap \hat{F}_2 \cap \hat{F}_3 \cap \hat{F}_4\ ) = 3.31;$

As expected, the order statistics safety indices now decrease rapidly. The effect of redundancy is moderate after failure of the weakest component. The system safety index is smaller than in the case without dynamic effects. Having in mind that the Daniels-system is one of the most favourable ones with respect to redistribution with or without dynamic effects one concludes that dynamic effects, in

general, require special attention in applications. They are neglected in the following.

Note that the foregoing formulation followed the classical extreme value approach, i.e. did not explicitely use the time step approach proposed in section 3. A recalculation by the time step approach includung multiple failures with immediate load-effect redistribution actually reproduces the same system safety index which verifies the assumptions made and the theory developed.

Instead, the case of delayed load-effect redistribution is studied in more dedail by explicitly considering the possibilities of multiple failures in subsequent time steps. The basic formulation is given in eq. (22). Various failure paths as shown in figure 4 must be taken into account. Two safety indices are given for each node in the

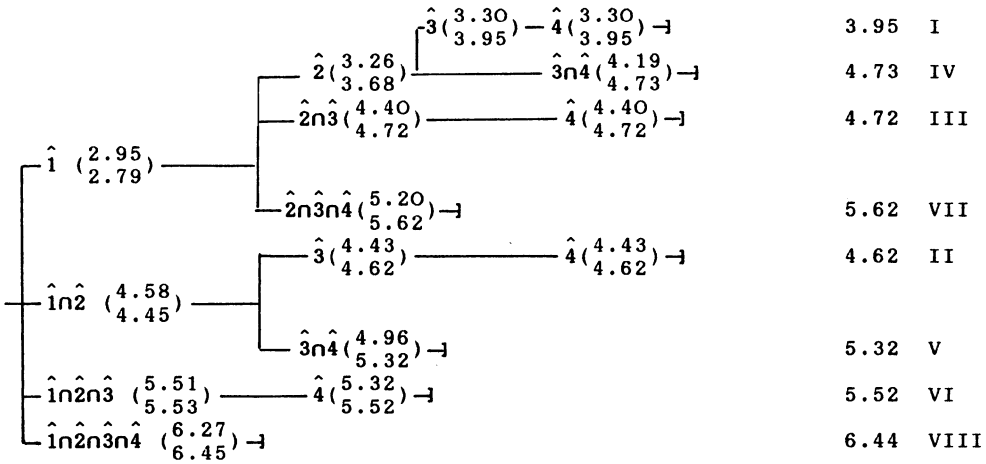

Figure 4: Time step appraoch for Daniels-system - delayed redistribution, time-invariant resistances

failure tree. The upper value corresponds to the first-order reliability method, i.e. to $\Phi(-\beta)$. The lower value corresponds to eq. (15), i.e. the (asymptotic) second-order reliability method which can be shown to be very accurate in this case. It is seen that the second-order corrections are significant in this example.

The system safety indices along a failure path increase as it should be. But from figure 4 it is evident that after individual or

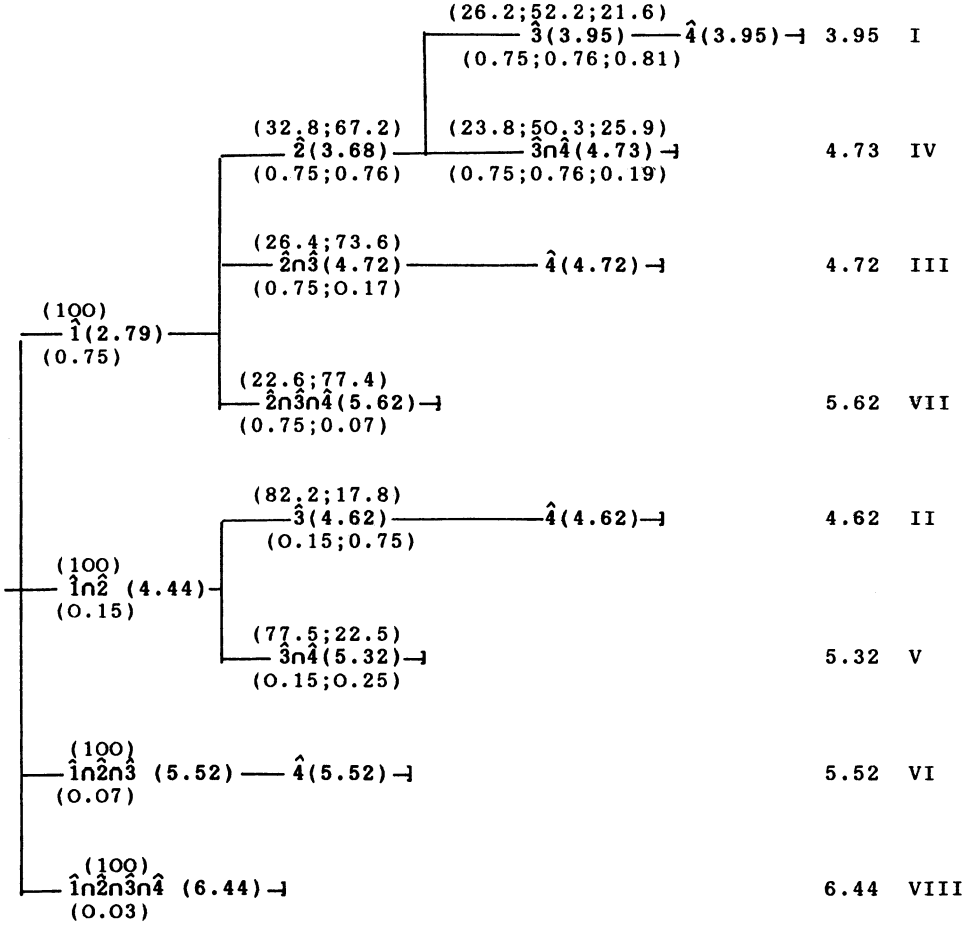

Figure 5: Time step appraoch for Daniels-system - delayed redistribution, time-invariant resistances

multiple failure of the two weakest elements in a failure path little extra reliability is gained when the last two elements are also included in the analysis. This corresponds to the findings for case I.Furthermore, although the dominant failure path has no multiple failures, failure paths with two or more multiple failures cannot be

discarded a priori as insignificant. In fact, the second most likely failure sequence starts with a double crossing (the ordering of failure paths according to increasing safety indices is indicated in the last column in figure 4 by roman numbers).

An interesting piece of information about system behavior is also the (most likely) fraction of time spent in each system state of the

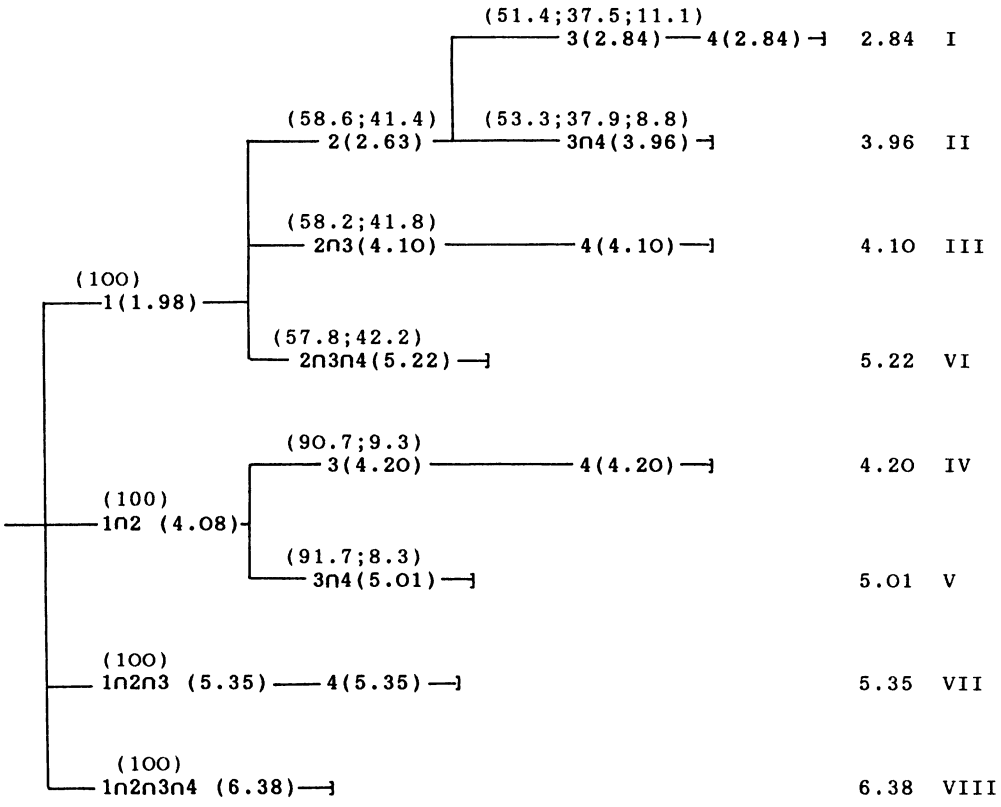

Figure 6: Time step appraoch for Daniels-system - delayed redistribution, time-variant resistances

total "most likely" time to a degradation state in a specific failure path indicated in figure 5 just above the node system safety index. For example, for the first failure sequence we see that it takes 26.2 % of the sequence life to failure of the first component, another 52.2

% to the second component failure and 21.6 % to the third component failure which is immediately followed by failure of the last component. In the second-critical fifth failure sequence 82.2 % of the sequence life is spent without any failure but sequence failure occurs shortly after joint failure of the first two components. The values below the safety indices are the branch probabilities P_k^1 described below eq. (26). For each node in the failure tree these proabilities add up to one, of course. The system safety index according to eq. (28) is $3.95 \geq \beta \geq 3.93$.

Comparison of the system-β's corresponding to case I ($\beta = 3.66$) and case II ($3.95 \geq \beta \geq 3.93$) finally verifies that case II has higher reliability as it should be; although the difference is not very large in this example.

A similar figure 6 has been produced for components subject to fatigue, i.e. by applying eq. (23) with eq. (30) with the following parameters and distribution functions (LN (.) = log-normal distribution):

$b = 3;$

$m \sim LN\ (E[m] = 4,\ V[m] = 0.2)$

$K\ (2^{3/2})^b\ \sigma_{S_j}^b\ \Gamma(1 + b/2) \sim LN\ (E[.] = 10^{-3}, V[.] = 0.2)$

These parameters are common to all system components. The other parameters are kept as in the case with non-deteriorating resistances. Therefore, the ordering of the residual strength levels introduced by ordering the R(0)'s remains the same throughout the life time of the structure. Only case II is evaluated numerically. The safety indices now are substantially smaller. The system safety index is bounded as $2.84 \geq \beta \geq 2.83$. In addition, the ordering of the failure sequences according to their system safety index is different from that in figure 4. As expected, the sequences spend more time of their total life-time in the earlier degradation states as indicated by the fractions of time just above the node safety indices and which may be compared with those in figure 5.

5. Summary and Conclusions

The reliability of degrading structural systems under stationary Gaussian loading with and without strength deterioration of the components due to fatigue is investigated. The fatigue deterioration model is based on fracture mechanics concepts. A formulation is chosen which allows to follow up structural degradation in time. The possibility of multiple componental failure is taken into account. Two extreme load effect redistribution regimes after componental failure, i.e. immediate and delayed redistribution, are investigated. Dynamic effects during redistribution have been considered by a limiting case, i.e. that the additional dynamic load effect in an unfailed element can be at most as large as the difference between the static load-effects before and after load redistribution. A rigorous treatment of dynamic effects appears to be rather complicated and is under study at present.

The numerical results for system collapse according to the above time-variant formulation based on time steps have been checked with the appropriate extreme-value formulations. Excellent agreement was found supporting the various theoretical (asymptotic) arguments in the derivations.

In contrast to extreme-value formulations the time-step formulation provides not only the time-lenghts between componental failures in different failure paths which may or may not be identified as the dominant ones. The time-step formulation is also capable to handle the various internal load redistribution regimes including dynamic effects.

In another paper under preparation, it will be shown how to incorporate inspection results as a means for updating the probability estimates via Bayes theorem [21]. It appears that the proposed methodology is a promising tool for correctly treating reliability problems connected with inspection and maintenance of structures.

References

[1] Madsen, H.O., Krenk, S., Lind N.C., Methods of Structural Safety, Prentice Hall, Englewood Cliffs, 1968

[2] Guers, F., Rackwitz, R., On the Calculation of Upcrossing Rates for Narrow-Band Gaussian Processes Related to Structural Fatigue, Berichte zur Zuverlässigkeitstheorie der Bauwerke, Technische Universität Muenchen, Heft 79, 1986

[3] Martindale, S.G., Wirsching, P.H., Reliability-Based Progressive Fatigue Collapse, Journ. Struct. Eng., ASCE, Vol. 109, 8, 1983

[4] Stahl, B., Geyer, F., Fatigue Reliability of Parallel Member Systems, Journ. Struct. Eng., ASCE, Vol. 110, 10, 1984,

[5] Knapp, E., Stahl, B., Offshore Plattform Fatigue Cracking Probability, Journ. Struct. Eng., ASCE, Vol. 111, 8, 1985,

[6] Rackwitz, R., Reliability of Structural Systems Subject to Fatigue, Proc. Conf. on Struct. Anal. and Design of Nuclear Power Plants, October 1984, Porto Alegre, Brasil, 1984, pp. 117-131

[7] Guers, F., Dolinski, K., Rackwitz, R., Progressive Failure of Brittle, Redundant Structural Systems in Time, submitted for publication in Structural Safety, 1987

[8] Guers, F., Rackwitz,R., Time-Variant Reliability of Structural Systems Subject to Fatigue, Proc. ICASP-5, Vol.1, Vancouver, 1987,

[9] Cramer, H., Leadbetter, M.R., Stationary and Related Stochastic Processes. Wiley, New York, 1967

[10]Guers, F., Zur Zuverlässigkeit redundanter Tragsysteme bei Ermüdungsbeanspruchung durch zeitinvariante Gauß'sche Lasten, Dissertation submitted to the Technical University Munich, 1986

[11]Copson, E.I., Asymptotic Expansions, Cambridge University Press, Cambridge,1968

[12]Hohenbichler, M., Gollwitzer, S., Kruse, W., Rackwitz, R., New Light on First- and Second-Order Reliability Methods, Accepted for publication in Structural Safety, 1987

[13]Hohenbichler, M., Rackwitz, R., Non-Normal Dependent Vectors in Structural Safety, J. Eng. Mech. Div., ASCE, Vol. 107, 6, 1981,

[14]Vanmarcke, E.H., On the Distribution of the First-passage Time for Normal Stationary Random Processes, J. Appl. Mech., Vol. 42, 1975,

[15]Guenard, Y.F., Application of System Reliability Analysis to Offshore Structures, J.A. Blume Engineering Center, Rep. No. 71, Stanford University, 1984

[16]Gollwitzer, S., Zuverlässigkeit redundanter Tragsysteme bei geometrischer und stofflicher Nichtlinearität, Diss., Technical University Munich, 1986

[17]Guers, F., Rackwitz, R., Outcrossing Formulation for Deteriorating Structural Systems, presented at ASCE-Structures Congress, New Orleans, September, 1986

[18]Daniels, H.E., The Statistical Theory of the Strength of Bundles of Threads, I, Proc. Roy. Statist. Soc., A, 183, 1945, pp. 405-435

[19]Hohenbichler, M., Rackwitz, R., Reliability of Parallel Systems under Imposed Uniform Strain, Journ. Eng. Mech. Div., ASCE, 1983, Vol.109, 3, pp.896-907

[20]Yang, J.N., Lin M.D., Residual Strength Degradation Model and Theory of Periodic Proof Tests for Graphite/Epoxy Laminates, Journ. Composite Materials, 11, pp. 176-203.

[21]Madsen, H.O., Model Updating in Reliability Theory, Proc. ICASP-5, Vol. 1, Vancouver, 1987, pp. 564-577

OPTIMAL BRIDGE DESIGN BY GEOMETRIC PROGRAMMING

N. C. Das Gupta H. Paul C. H. Yu
Department of Civil Engineering
National University of Singapore

ABSTRACT

This paper presents an application of generalized geometric programming to the optimal design of a prestressed concrete pedestrian bridge deck. The actual cost of construction consisting of prestressing, formwork and concreting is minimized. Constraints are formulated as stipulated by the British Code of Practice CP 110, related to bending and shear stresses and minimum concrete cover. A sample optimal design is included in the paper. The method presented can be applied to other engineering design problems by appropriately modifying the problem formulation.

1. INTRODUCTION

In structural engineering, the general layout of any structural system is usually governed by its functional requirements. The system is then analysed for specified loads and the various elements of the system are designed to satisfy certain performance criteria. The design also aims at finding the least cost of the system. The methodology adopted to achieve the specific goal of least cost subject to satisfying the performance criteria is structural optimization.

One of the optimization techniques which has been used in some structural design problem is geometric programming (GP). The basic theory and formal proofs for this optimization technique can be found in (1), (2) and (3). A GP problem is associated with objective functions and constraints, which can be expressed in the form of signomials. Most structural design equation as stipulated by the engineering codes of practice are expressed in the form of signomials. Hence, the computational algorithms to solve GP problems are well suited to such structural optimization problems.

Several researchers [4, 5, 6] have used the GP model for optimal design of structural systems. This paper presents the formulation of a GP model for the optimal design of prestressed concrete hollow pedestrian bridge decks. Fig. 1 shows sectional views of such a bridge deck. The design problem presented in this paper is formulated on the geometry, imposed loads, stresses and deflection criteria

permitted by the relevant British Code of Practice.

2. OBJECTIVE FUNCTION

The objective function of the GP model incorporates the cost of concrete, formwork and prestressing steel. The total variable costs are obtained as follows:

Y_o = Cost of concrete + Cost of prestressing + Cost of formwork

$$C_c A_c L + \frac{F}{0.7 f_{pu}} \cdot \ell_t \rho_{st} C_p + C_f \cdot A_f \qquad (1)$$

C_c, C_p, C_f are unit costs of concrete ($/m^3), prestressing steel ($/kg) and formwork ($/m^2) respectively. It may be noted that C_p includes the cost of material and prestressing operation. L and L_t are the span length (m) and the length of prestressing tendon (m) respectively; A_c and A_f cross-sectional area of concrete (m^2) and surface area of formwork (m^2) respectively; ρ_{st} the density of prestressing steel (kg/m^3); F the prestressing force at transfer (N); f_{pu} the steel characteristic strength (N/mm^2); the coefficient 0.7 is the ratio of minimum steel stress to the characteristic strength of prestressing steel.

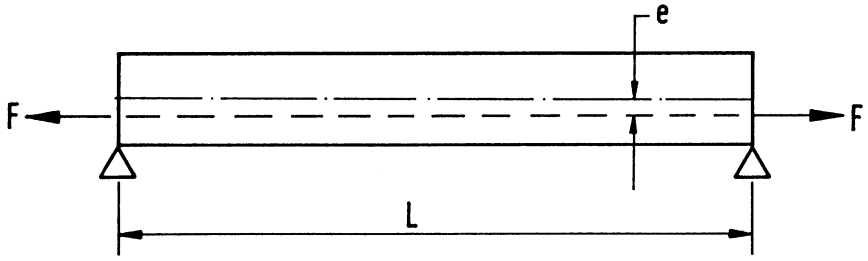

(a) Simply Supprted Span

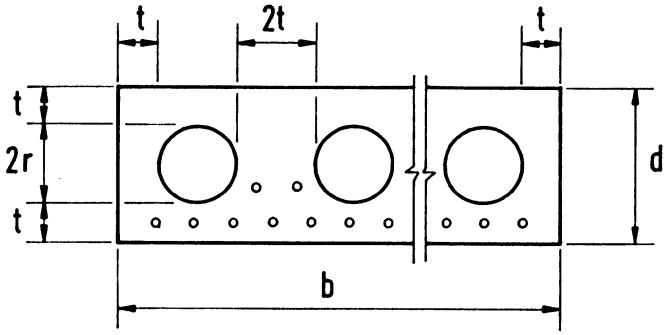

(b) Cross-sectional view

Fig. 1 Bridge Deck

3. CONSTRAINTS

The constraints of the GP model are obtained from the following considerations: allowable bending stresses of concrete at transfer of prestressing and at serviceability limit state, allowable shear stresses of concrete, adequacy of concrete section, maximum available eccentricity of prestressing force and geometrical restrictions. The formulation of the constraints is carried out in accordance with the BS Code of Practice CP 110 [7] for prestressed concrete design. The ultimate moment and deflection at service are not included as constraints in the formulation as these are expected to be non-governing. This is to reduce the complexity of the problem but these conditions are later verified manually.

3.1 Bending Stress Requirements

The bending stresses in concrete at transfer of prestressing and at serviceability limit state must not exceed the allowable stresses as specified in section 4.3 of the CP 110. The allowable tensile and compressive stresses at transfer are denoted by f_{tt} and f_{ct} respectively and those at service conditions by f_{ts} and f_{cs} respectively. The critical sections for this constraint are at midspan and at end-supports. The bending stress constraints are as follows:

$$e \leq k + (1/F)\,(M_{min} - f_{tt}Z)$$

$$e \leq -k + (1/F)\,(M_{min} + f_{ct}Z)$$

$$e \geq k + \left[\frac{1}{\eta F}\right](M_{max} - f_{cs}Z)$$

$$e \geq -k + \left[\frac{1}{\eta F}\right](M_{max} + f_{ts}Z) \qquad (2)$$

where e is the eccentricity of prestressing tendons with respect to the centroidal axis of the concrete section; M_{min} and M_{max} the minimum and maximum bending moments (kNm) at transfer and service conditions respectively; k and Z the distance (m) from the centroid of concrete section to the limit of central kern and section modulus (m^3) of the deck section respectively; η the ratio of the final prestressing force to the initial prestressing force; F the prestressing force at transfer and η the long term loss factor.

3.2 Section Adequacy

To ensure the minimum concrete section to satisfy the bending stresses, the following constraints are required in general for each of the critical sections

$$Z \geq (M_{max} - \eta M_{min})/(f_{cs} - nf_{tt})$$

$$Z \geq (M_{max} - \eta M_{min})/(nf_{ct} - f_{ts}) \qquad (3)$$

3.3 Maximum Eccentricities

The maximum eccentricity of the prestressing tendons allowed for any section is half the section depth reduced by the minimum concrete cover required, c(mm), ie.,

$$e_{max} \leq [\ d/2 - c\ ] \qquad (4)$$

where d is the section depth (mm).

3.4 Shear Criteria

As specified in CP 110 [7], shear is checked for ultimate limit state for both cracked and uncracked sections in flexure. The most critical section considered for such shear check is 0.5 m from the end support. The shear constraints are expressed as follows:

For uncracked sections,
the ultimate shear resistance of concrete alone is

$$V_{co} = 0.67\ (b - 2jr)d\ \sqrt{(f_t^2 + 0.8\ f_{cp} f_t)} \geq V \qquad (5)$$

where j is the number of hollow cores, b the overall width (mm) of the deck, r the core diameter (mm),

$$f_t = 0.25\ \sqrt{f_{cu}},$$

$$f_{cp} = \eta\ F/A \qquad (6)$$

f_{cu} the characteristic concrete cube strength (N/mm^2), A the effective cross-sectional area (mm^2) and V the shear force (kN) due to ultimate load.

For cracked sections,

the ultimate shear resistance of concrete alone is

$$V_{cr} = (1 - 0.55\ f_{pe}/f_{pu})\ \nu_c(b - 2jr)(d - c) + M_o V/M > V \qquad (7)$$

where $M_o = 0.8\ f_{pt}\ I/e$

$$f_{pt} = \eta\ F/A + \eta\ Fe^2/I \qquad (8)$$

and f_{pe} is the effective prestress (N/mm^2) ν_c the ultimate allowable shear stress (N/mm^2), V and M the shear force (kN) and bending moment (kNm) respectively at the section considered due to ultimate load, I the second moment of area (mm^4).

4. AN EXAMPLE

In order to illustrate the application of the method, an example of a simply supported prestressed concrete pedestrian bridge deck with three hollow cores is presented in this section.

4.1 The Design Problem

A prestressed concrete bridge deck as shown in Fig. 1 is to be designed for a live load of 5 kN/m^2, where L = 22 m and b = 2.3 m. The design specifications are given in Table 1.

Table 1 Design Specifications

Design Code	: CP 110
Concrete Strength	: f_{cu} = 40 N/mm^2, f_{ci} = 28 N/mm^2, (transfer at 7 days)
	f_{ct} = 14.0 N/mm^2, f_{tt} = −1.0 N/mm^2
	f_{cs} = 13.2 N/mm^2, f_{ts} = 0
Prestressing steel strength	: f_{pu} = 1750 N/mm^2
Concrete cover	: 50 mm (min.)
Imposed load	: 5 kN/m^2
η	: 0.8

The assumed costs of various items are

$C_c = \$300/m^3$

$C_f = \$\ 25/m^2$

$C_p = \$\ \ 2/kg$

The objective function and constraints are obtained substituting the values based on design specifications and cost factors and are summarized below. The number of hollow cores considered for the formulation of the model is three. It is also noted that the shear for the cracked state is checked manually to reduce the difficulty of the problem.

Minimize

$$Y_o = 16280d + 3.26F + 10367r - 62204r^2$$

Subject to

Bending constraint at mid-span section

$$0.00261eFd^{-2} + 12.29r^4d^{-3} + 35.70r^2d^{-2} + 0.01r^4A^{-1}d^{-3}F - 8.71d^{-1}-FA^{-1} \leq 1$$

$$0.00030eFd^{-1} + 4.10r^2d^{-1} + 19.76r^4d^{-2} + 0.00012dFA^{-1} - 1.61d - 0.00141r^4FA^{-1}\ d^{-2} \leq 1,$$

$$0.38\ d^2A^{-1}e^{-1} + 4174F^{-1}de^{-1} + 870F^{-1}e^{-1} + 77754F^{-1}r^4d^{-1}e^{-1} - 4.71r^4d^{-1}A^{-1}e^{-1} - 17106F^{-1}r^2e^{-1} - 6325F^{-1}d^2e^{-1} \leq 1,$$

$$4.71r^4d^{-1}A^{-1}e^{-1} + 4174F^{-1}de^{-1} + 870F^{-1}e^{-1} - 0.38d^2A^{-1}e^{-1} - 17106F^{-1}r^2e^{-1} \leq 1,$$

Bending constraint at end sections

$$2.3deZ^{-1} - 9.43r^2eZ^{-1} \leq 1,$$

$$0.00007FA^{-1} + 0.00007FeZ^{-1} \leq 1,$$

Section adequacy constraint

$$0.16d^{-1} + 0.13d^{-2} + 12.29r^4d^{-3} - 0.64r^2d^{-2} \leq 1,$$

Maximum eccentricity constraint

$$2ed^{-1} + 0.1d^{-1} \leq 1,$$

Shear constraint

$$0.53\, x^{-0.5} + 0.13d^{-1}x^{-0.5} + 2.61r - 0.64r^{2}d^{-2} \leq 1,$$

$$2.30x^{-1} + 0.00097FA^{-1}x^{-1} \leq 1.$$

4.2 Solution of the Design Problem and Discussion

There are several algorithms which can be used for solution of the design problem described in section 4.1. The primal-based GGP, as developed by Dembo [8] and dual-based SIGNOPT, as developed by Templeman [9] are two such algorithms. This GP model has 7 independent variables and 22 degrees of difficulty. The optimization by GGP has been performed on the formulation given in section 4.1 and also on other cross-sections with two, four and five hollow cores and a solid cross-section. The results of such optimization, as given in Table 2, show the comparative evaluation of the variables with the increasing number of hollow cores. The most economic cross-section is with the one with two hollow cores.

Table 2 Optimum design variables for simply supported bridge deck (Width = 2.3 m ; span = 22.0 m)

Variables	No. of hollow cores				
	0	2	3	4	5
d (m)	1.035	1.000	0.787	0.823	0.869
F (kN)	16664	6882	7369	10161	12131
e (m)	0.172	0.234	0.189	0.172	0.165
r (m)	0	0.400	0.283	0.187	0.130
A (m^2)	2.380	1.295	1.053	1.452	1.733
Obj. Function ($)	82690	39600	39870	53220	62570
CPU time (sec)	1.52	1.70	1.70	1.70	1.70

The same pedestrian bridge with solid cross-section has also been optimized using SIGNOPT and the values of d, F, e and objective function obtained are 0.948 m,

15192 kN, 0.158 m and $75,462 respectively. The CPU time consumed for the problem is 2.8 sec. All the values are about 8-10% less than the corresponding values obtained for the same problem by GGP optimization.

4.2 An Example of a Two-Span Pedestrian Bridge

The GP-optimization model has been applied to another design problems. Fig. 2a and 2b show the elevation of two span simply supported bridge and two span continuous bridge respectively. The sectional view of both the bridges is same and is given in Fig. 2c. The objective function and constraints are formulated in the similar manner as given in Section 4.1. The cost of transportation and erection are not considered in the model formulation as in the previous example.

For the solution of this design problem, the primal based GGP algorithm is used. The results of this optimization model are given in Table 3. The construction of two span continuous bridge results in 20% saving over the two span simply supported construction. The simple span design has 8 variables and 43 degrees of difficulty while that for continuous span 7 variables and 38 degrees of difficulty.

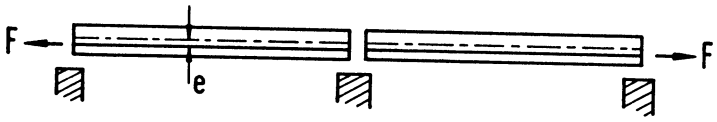

Fig. 2a Two Span Bridge with Simple Spans

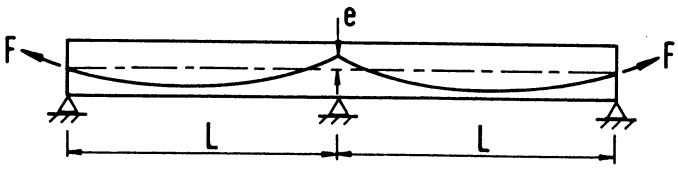

Fig. 2b Two Span Continuous Bridge

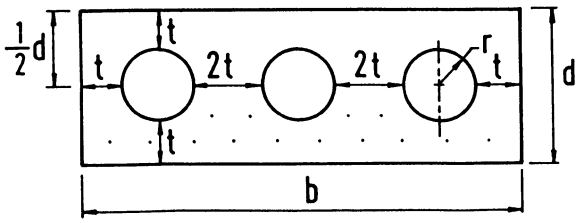

Fig. 2c Sectional View of Both the Bridge

Table 3 Optimum Design Variables for Two Span Continuous and Simply Supported Bridge (No. of hollow cores = 3)

Variables	Continuous	Simply Supported
d(m)	0.767	0.787
F(kN)	5208	7369
e(m) at midspan	0.333	0.189
r(m)	0.283	0.283
Obj. Fn ($)	63,879	79,734

5. CONCLUSIONS

This article illustrates how GP can be used in practical design problems of a structural system. The optimal designs of simply supported and continuous bridges were determined and the results were compared.

Both the algorithms, GGP and SIGNOPT, are found to be reliable for the class of problems they can solve.

For the number of independent variables and degree of difficulty encountered in these problems, the amount of CPU time required on an IBM 3033 computer or an equivalent, is considered reasonable. Wherever possible, the degree of difficulty and CPU time required can be reduced by leaving out constraints that are loose and manual checking can be performed after the optimum solution is obtained.

In general practice, the use of GP model is expected to result in saving in the overall cost of the system over the conventional design model of trial and error. Savings in design time and cost could be significant if the model can be used for the design of a large number of similar structures with varying specifications as the optimization problem is impossible to be solved manually.

ACKNOWLEDGEMENT

The authors acknowledge with thanks the assistance of Mr Thiew Ming Tuck, a senior Civil Engineering, in this study.

REFERENCES

1. G.S. Beveridge and R.S. Schecter, "Optimization : Theory and Practice", McGraw-Hill, N.Y. (1970).

2. D.J. Wilde adn C.S. Beightler, "Foundation of Optimization", Prentice-Hall, Englewood Cliffs, N.J. (1967).

3. D.T. Phillips, A. Ravindran and J. Solberg, "Operations Research Principles and Practice", pp. 552-561, Wiley, N.Y.

4. A.B. Templeman, "Geometric Programming with Examples of the Optimum Design of Floor and Roof Systems", International Symposium on Computer Aided Structural Design, University of Warwick, July (1972).

5. S. Ramamurthy, "Structural Optimization using Geometric Programming", pp. 63-96, Ph.D. thesis, Cornell University, (1977).

6. N.C. Das Gupta, H. Paul and C.H. Yu, "An Application of Geometric Programming to Structural Design", Computers and Structures, Vol. 22, No. 6, pp. 965-971, 1986.
7. British Standard Institution, "Code of Practice for the Structural Use of Concrete, CP 110", February 1976.

8. R.S. Dembo, "GGP - A Computer Programme for the Solution of Generalized Geometric Programming Problems", User's Manual, Department of Chemical Engineering, Haifa, 1972.

9. A.B. Templeman, A.J. Wilson and S K Winterbottom", SIGNOPT - A Computer Code for the Solution of Signomial Programming Problems", Department of Civil Engineering, University of Liverpool, 1972.

AN APPLICATION OF FUZZY LINEAR AND NONLINEAR PROGRAMMING TO STRUCTURAL OPTIMIZATION

Ken Koyama, Yuji Kamiya
Dept. of Civil Engineering
Shinshu University, Nagano, Japan

1. Introduction.

General structural optimization in civil engineering has been done that only one objective function is to be maximized or minimized under constraints of crisp condition(1). But many civil engineering structures have high public utilities or serviceabilities like highway or railway bridges, tunnel, airport, marine structure, etc. Then they are required multi level objectives, generally. Furthermore these objectives may have competitive or conflicting needs, utilities or serviceabilities, among themselves. Therefore, to satisfy the needs, the planning or design of types, locations or sizes of these structures should be required the multi objective decision making sense, essentially(2). In this sense, the multi objective optimization approach may be useful for the decision making of the problem.

In this paper the multi objectives are taken that they have vague meaning, semantically(3,4,5). For example, "as minimum as possible" or "if possible" means fuzzy or vague condition. The general crisp constraints and multi objectives are translated into fuzzy or vague constraints. Then the general structural optimization problems are changed to fuzzy optimization ones.

Fuzzy optimization problems are solved by using linear or nonlinear programming techniques. Two types of problems are taken into consideration in this paper. One is non-fuzzy decision under fuzzy constraints and another is fuzzy decision under the same conditions. Allowable stress design of simple beam model and plastic design of portal frame are calculated for example of fuzzy optimization problem of structure in civil engineering.

2. Membership Function and Formulation of Fuzzy Optimization.

It is shown that the general optimization problems take the form

$$\text{minimize or maximize} \quad z = c^T x \tag{1}$$

$$\text{subject to} \quad A^T x \geqq b \tag{2}$$

in which z denotes the objective function; and x is the design variables to be optimized;A,b,c are constants.

The general optimization problm is translated into fuzzy optimization problem,if z or A,b,c or x has vagueness or fuzziness,$\underset{\sim}{z}$,$\underset{\sim}{A}$,$\underset{\sim}{b}$,$\underset{\sim}{c}$ or $\underset{\sim}{x}$,respectively.In this case ,Eq.1 and 2 are modified as

$$\text{aim} \quad z=\underset{\sim}{c}^{T}x \lesssim z_{o}^{*} \tag{3}$$

$$\text{subject to} \quad \underset{\sim}{A}^{T}x \lesssim \underset{\sim}{b} \tag{4}$$

in which $\lesssim$ denotes semantical meaning of vaguness or fuzziness which constraints have; and z_{o}^{*} is an aim or goal which may be specified or taken apriori by human judgement.

It is assumed that the fuzzy set of constraints and goals or objectives are expressed by $\underset{\sim}{\Omega}$ and $\underset{\sim}{\Phi}$,and their membership functions are $\mu_{\underset{\sim}{\Omega}}(x)$ and $\mu_{\underset{\sim}{\Phi}}(x)$,respectively.Then the grade of x which belong to the fuzzy decision set $\underset{\sim}{D}$ is defined by

$$\mu_{\underset{\sim}{D}}(x)=\min \{ \mu_{\underset{\sim}{\Omega}}(x), \mu_{\underset{\sim}{\Phi}}(x) \} \tag{5}$$

The problem to obtain the solution x^{*} which satisfies the following equation

$$\max \ \mu_{\underset{\sim}{D}}(x)= \mu_{\underset{\sim}{D}}(x^{*}) \tag{6}$$

is fomulated into fuzzy programming problem. It is shown in Fig.1, schematically.

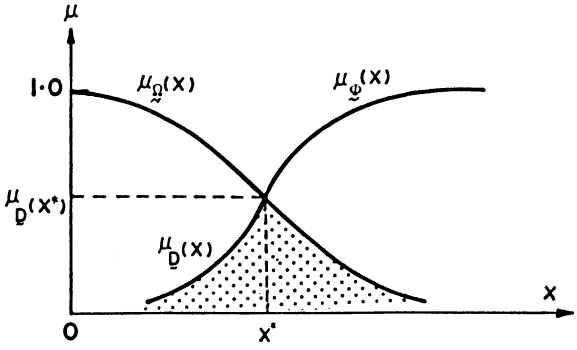

Fig.1 Fuzzy set $\underset{\sim}{\Omega}$, $\underset{\sim}{\Phi}$ and decision $\underset{\sim}{D}$

The membership function used in this paper is shown in Fig.2. In Fig.2,the membership function of A has so called the mean value m and the spread d,and the expression is

$$\mu_{\tilde{A}_i}(a_i)=\begin{cases} 1.0-|a_i-m_i|/d_i & ; \ m_i-d_i \leqq a_i \leqq m_i+d_i \\ 0 & ; \text{except above} \end{cases} \tag{7}$$

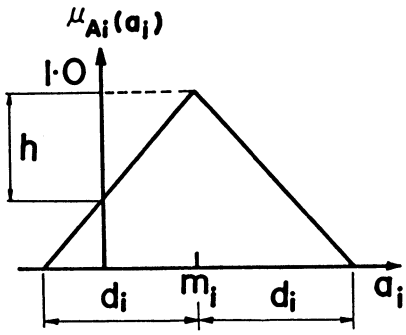

Fig.2 Membership Function

Using this membership function,two type of fuzzy programming problems are solved.

3.Non-fuzzy Decision Problem and Fuzzy Decision Problem

3.1 Formulation of non-fuzzy decision problem

Assume first that the constant A ,b and c are not crisp(i.e. fuzzy) but x is crisp variables,here.

In Eq.3 and 4,the aim or objective and the constraints are expressed by the same formulae as

$$\tilde{Y}=\tilde{A}^T x \gtrsim 0 \tag{8}$$

in which

$$\tilde{Y}_i=\tilde{b}_i x_0+\tilde{A}_{i1}x_1+\tilde{A}_{i2}x_2+\cdots\cdots+\tilde{A}_{in}x_n \gtrsim 0, (i=1,\cdots\cdots,k) \tag{9}$$

In Eq.9 $\gtrsim$ means that Y_i is nearly positive,$\tilde{A}_{i0}=\tilde{b}_i$ and $x_0=1$.

Fuzzy parameter $\tilde{A}$ is defined using m and d by

$$\tilde{A}=(m,d) \tag{10}$$

and the membership function of $\tilde{Y}$ which is linear combinations of $\tilde{A}$ and x is given(4,5) as

$$\mu_{\tilde{Y}}(y)=\begin{cases} 1.0-|y-x^T m|/(d^T x) & ; x=0 \\ 1.0 & ; x=0, y=0 \\ 0 & ; x=0, y=0 \end{cases} \tag{11}$$

Follwing definition is used to keep fuzzy set $\underset{\sim}{Y}_i$ nearly positive(4,5).

$$\underset{\sim}{Y}_i \gtrsim 0 \Leftrightarrow \mu_{\underset{\sim}{Y}i}(0) \leqq 1-h,\ x^T m_i \geqq 0 \tag{12}$$

According to Eq.12,Eq 9 is replaced by Eq.13,using Eq.11.

$$\mu_{\underset{\sim}{Y}i}(0)=1-(m_i^T x)/(d_i^T x) \leqq 1-h,\quad m_i^T x \geqq 0,(i=1,\ldots,k) \tag{13}$$

Finally,Eq.13 is reduced to

$$(m_i-hd_i)^T x \geqq 0,\ (i=1,\ldots,k) \tag{14}$$

If h becomes larger,then the degree of $\underset{\sim}{Y}_i \gtrsim 0$ becomes greater.For example,if h=0.5 then the area belong to positive part becomes 87.5 percent to the whole area of the membership function.Therefore,the problem is to find the solution h^* and x^* that maximize h(see Fig.2),subject to Eq.14.It is called fuzzy nonlinear programminig problem as non-fuzzy decision,here. Because the solution x of the problem is determined by crisp(non-fuzzy) value.

3.2 Formulation of fuzzy decision problem

In this section,the parameter A and c are taken to be crisp variables,but b is vague variable.Therefore ,how fuzzy the solution can be determined under fuzzy condition b is concerned about here.That is,the solution x is obtained by fuzzy set.

In this case Eq.9 is replaced by

$$\underset{\sim}{Y}_i=\underset{\sim}{X}_{i0}+m_{i1}\underset{\sim}{X}_1+m_{i2}\underset{\sim}{X}_2+\ldots.+m_{in}\underset{\sim}{X}_n \gtrsim 0,(i=1,\ldots.,k) \tag{15}$$

in which $\underset{\sim}{X}_{i0}=\underset{\sim}{b}_i x_0$, $\{\underset{\sim}{X}_{i0},\underset{\sim}{X}_1,\ldots.,\underset{\sim}{X}_n\}^T=\{\bar{x}_i,d_i\}^T$

It is assumed that the fuzzy set $\underset{\sim}{X}i$ has so called mean value $\bar{x}_i$ and spread d_i.

Using the definition of Eq.11, Eq.15 is reduced to like as Eq.14.

$$\bar{x}_i^T m_i-h|m_i|^T d_i \geqq 0,\ (i=1,\ldots,k) \tag{16}$$

in which $m_i=(1,m_{i1},\ldots.,m_{in})^T$.

Finally,subject to Eq.16, the fuzzy solution is obtained that

$$\text{objective}\quad z=\sum_i w_i d_i \longrightarrow \max. \tag{17}$$

in which w_i denotes the weight to evaluate which $\underset{\sim}{X}_i$ sholud be determined as fuzzy or vague as posible.

To obtain $\underset{\sim}{X}_i=(\bar{x}_i,d_i)$ which makes z maximum is called fuzzy linear programming problem as fuzzy decision,here.

4.Applications

4.1 A simple example of non-fuzzy decision

A simple example of non-fuzzy decision is studied(4)to get the solution of the fuzzy optimization problem,using Eq.14.
The constraints are

$$\begin{aligned} &\tilde{6}x_1+\tilde{5}x_2\lesssim\tilde{30};\ \tilde{Y}_1=-\tilde{30}+\tilde{6}x_1+\tilde{5}x_2\gtrsim 0\\ &\tilde{2}x_1+\tilde{9}x_2\lesssim\tilde{45};\ \tilde{Y}_2=\tilde{45}-\tilde{2}x_1-\tilde{9}x_2\gtrsim 0\\ &\tilde{11}x_1-\tilde{5}x_2\lesssim\tilde{44};\ \tilde{Y}_3=\tilde{44}-\tilde{11}x_1+\tilde{5}x_2\gtrsim 0\\ &-\tilde{2}x_1+\tilde{3}x_2\lesssim\tilde{12};\ \tilde{Y}_4=\tilde{12}+\tilde{2}x_1-\tilde{3}x_2\gtrsim 0 \end{aligned} \tag{18}$$

and the fuzzy parameter A are assumed as

$A_1=\{m_1=(-30,6,5),d_1=(6,2,1)\}$, $A_2=\{m_2=(45,-2,9),d_2=(8,2,3)\}$
$A_3=\{m_3=(44,-11,5),d_1=(4,2,1)\}$, $A_4=\{m_4=(12,2,-3),d_4=(4,1,2)\}$
Then,Eq.18 is expressed by the form of Eq.14 as

$$\begin{aligned} &\text{subject to;}\\ &-30-6h+(6-2h)x_1+(5-h)x_2\geqq 0 \quad (a)\\ &45-8h-(2+2h)x_1-(9+3h)x_2\geqq 0 \quad (b)\\ &44-4h-(11+2h)x_1+(5-h)x_2\geqq 0 \quad (c)\\ &12-4h+(2-h)x_1-(3+2h)x_2\geqq 0 \quad (d)\\ &\text{objective}\quad h\longrightarrow \max. \end{aligned} \tag{19}$$

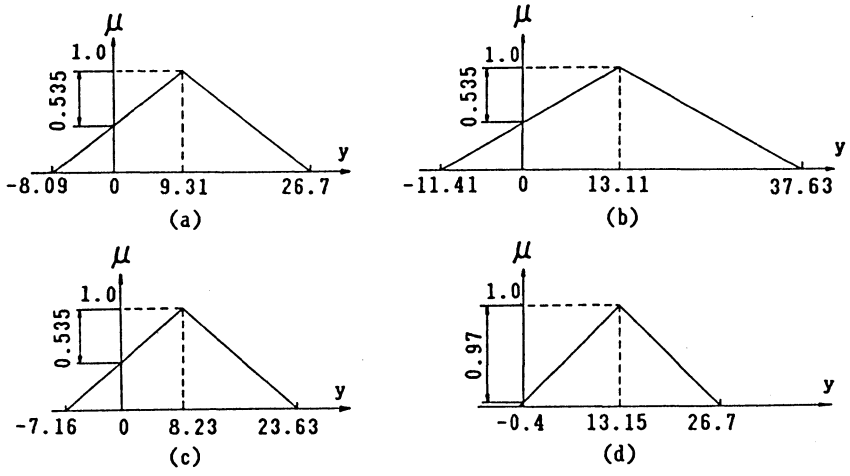

Fig.3 The membership function of $\tilde{Y}$

Eq.19 is a non-linear programming problem.Tanaka et.al(4) obtained the solution $x=(x_1,x_2)=(4.50,2.62)$, assuming $h=0.5$. But,accurate solution is obtained as $x=(4.416,2.562)$ by using non-LP technic.In this paper SLP is used to solve non-LP problem.The degree of satisfuction that each constraints should be as nearly positive as possible is shown by their membership functions,in Fig.3. It is also shown that (a),(b) and (c) in Eq.19 are critical constraints in this example.

4.2 Working stress design of simple beam

The minimum weight design of simple beam is employed(6). In this example,the span length and the height of the beam and load condition are shown in Fig.4.The working stress of this beam is assumed as 127.4Mpa(1300kg/cm²). To find the width of the beam x_1 and x_2 which makes the weight of the beam minimum is example of fuzzy decision under fuzzy constraints. The crisp constraints on size is given as

$$x_2 \geqq (3/4)x_1 \tag{20}$$

$$x_1+x_2 \geqq 14 \tag{21}$$

The stress limit constraints are added to Eq.20 and 21,then finally

$$\text{objective;}\quad z=x_1+2x_2 \longrightarrow \text{mini.} \tag{22}$$

$$\begin{aligned} \text{subject to;}\quad & x_1 \geqq 7.21 && \text{(a)} \\ & x_2 \geqq 4.81 && \text{(b)} \\ & 3x_1-4x_2 \leqq 0 && \text{(c)} \\ & x_1+x_2 \geqq 14.0 && \text{(d)} \end{aligned} \tag{23}$$

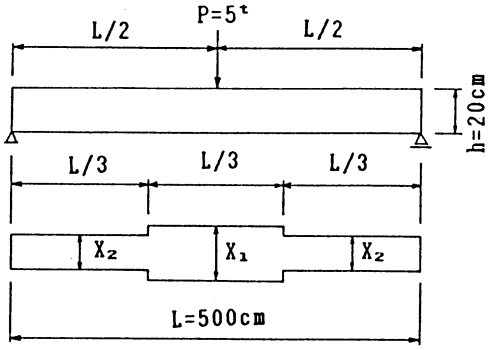

Fig.4 Simple Beam Model

The solution of this problem under the crisp constraints is obtained as $x=(x_1,x_2)=(8.0,6.0)$,$z=20.0$(6).If the value of z is allowed to increase from 20.0 to 24.0,26.0,28.0.It should be given by designer's

judgement which depends on the safety or utility or economical conditions.

Acording to these z,let the aim objectives z_0 are assumed to be about 24.0,26.0,28.0,respectively.Then,the problem is transrated into fuzzy optimization one and is shown as

fuzzy constraints;

$$\begin{aligned} x_1 &\lesssim x_{10} \quad (a)\\ x_2 &\lesssim x_{20} \quad (b)\\ 3x_1-4x_2 &\gtrsim x_{30} \quad (c)\\ x_1+x_2 &\lesssim x_{40} \quad (d)\\ x_1+2x_2 &\gtrsim x_{50} \quad (e)\\ x_1 &\gtrsim x_{60} \quad (f)\\ x_2 &\gtrsim x_{70} \quad (g) \end{aligned} \tag{24}$$

in wich Eq.24(e),(f),(g) are added to Eq.23,and they are the aim objective and upper limit of $x=(x_1,x_2)$,respectively.

If $x_{10}=(x_{10},d_{10})=(7.21,0.721)$, $x_{20}=(x_{20},d_{20})=(4.81,0.481)$, $x_{30}=(x_{30},d_{30})=(0.0,0.1)$,$x_{40}=(x_{40},d_{40})=(14.0,1.4)$,$x_{50}=(x_{50},d_{50})=(24.0,2.4)$,$x_{60}=(x_{60},d_{60})=(15.0,1.5)$,$x_{70}=(x_{70},d_{70})=(12.0,1.2)$ is given,where the spread d_{i0} is assumed to be $0.1x_{i0}$,then,

objective; $z=d_1+d_2 \longrightarrow \max.$

subject to;

$$\begin{aligned} x_1 - hd_1 &\geqq 7.21q_1\\ x_2 - hd_2 &\geqq 4.81q_1\\ 3x_1-4x_2+3hd_1+4hd_2 &\geqq -0.1h\\ x_1+x_2-hd_1-hd_2 &\geqq b_0q_1\\ x_1+2x_2+hd_1+2hd_2 &\leqq z_iq_2 \quad (i=1,2,3)\\ x_1+hd_1 &\leqq 15q_2\\ x_2+hd_2 &\leqq 12q_2 \end{aligned} \tag{25}$$

in which $q_1=1.0+0.1h$;$q_2=1.0-0.1h$;$b_0=14.0$ and $z_i=24.0,26.0,28.0$

The degree of satisfaction of fuzzy constraints is depends on the design level h.In this example h is assumed to be 0.5 and 0.6.The solutions of this example are shown in Table 1(a) and (b) for h=0.5 and 0.6,respectively.

Table.1 fuzzy decision of simple beam example(unit=cm)

	(a)				(b)			
	h=0.5				h =0.6			
i	x_1	x_2	d_1	d_2	x_1	x_2	d_1	d_2
1	8.483	6.845	1.255	0.0	8.535	6.774	0.788	0.0
2	8.530	7.367	1.919	0.476	8.551	7.256	0.925	0.686
3	8.530	7.842	1.919	1.426	8.551	7.726	0.925	1.469

To be expected,design should have large spread if z_0 is allowed to have large weight. But the mean values are not so different among the designs.

4.3 Optimum plastic design of portal frame

Optimum plastic design based on fuzzy decision problem is solved by the same way as 4.2. The portal frame employed here is shown in Fig.5. The crisp objective and constraints are given by(6)

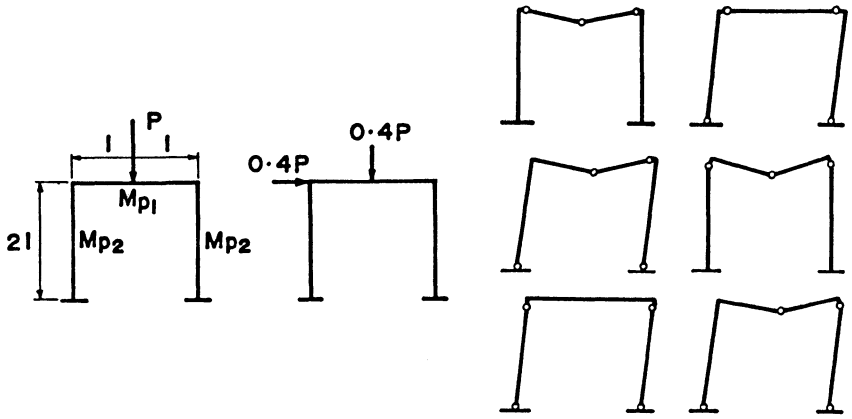

Fig.5 Load Conditions and Failure Mechanisms of Frame

$$\text{objective;}\quad G=2Mp_1 l+4Mp_2 l \longrightarrow \text{mini.}$$

$$\begin{aligned}
\text{subject to;}\quad & 4Mp_1 \geqq Pl \\
& 2Mp_1+2Mp_2 \geqq Pl \\
& 4Mp_2 \geqq 0.4Pl \\
& 2Mp_1+2Mp_2 \geqq 0.8Pl \\
& 4Mp_1+2Mp_2 \geqq 1.2Pl \\
& 2Mp_1+2Mp_2 \geqq 0.4Pl \\
& 4Mp_2 \geqq 0.8Pl \\
& 2Mp_1+4Mp_2 \geqq 1.2Pl
\end{aligned} \tag{26}$$

The solution is obtained by Mp $=(Mp_1,Mp_2)=$ $(0.3Pl,0.2Pl)$ and $G=1.4Pl^2$(6) under crisp condition. From this result,if the aim objective is settled to be $G_0=1.6Pl^2$,and furthermore,the upper limits for Mp_1, Mp_2 which comes from engineering considerations is added to Eq.26, and also if the fuzziness of Mp and Pl is expressed by the fuzzy parameter

$$(M_{10},Mp_1,Mp_2)=\{(m_{10},d_{10}),(mp_1,d_1),(mp_2,d_2)\} \tag{27}$$

in which $(m_{i0}, d_{i0}) = (\mu_{p1}, 0.1\mu_{p1})$.

Then, the constraints and objective are

$$\text{objective;}\quad z = d_1 + d_2 \longrightarrow \max.$$

$$\begin{aligned}
\text{subject to;}\quad & 4mp_1 - 4hd_1 \geqq q \\
& 2mp_1 + 2mp_2 - 2hd_1 - 2hd_2 \geqq q \\
& 4mp_1 + 2mp_2 - 4hd_1 - 2hd_2 \geqq 1.2q \\
& 4mp_2 - 4hd_2 \geqq 0.8q \\
& 2mp_1 + 4mp_2 - 2hd_1 - 4hd_2 \geqq 1.2q \\
& 2mp_1 + 4mp_2 + 2hd_1 + 4hd_2 \leqq 1.6(1.0 - 0.1h)\mu_{p1} \\
& mp_1 + hd_1 \leqq 0.5 - 0.1h \\
& mp_2 + hd_2 \leqq 0.5 - 0.1h
\end{aligned} \tag{28}$$

in which $q = \mu_{p1} + 0.1h\mu_{p1}$.

Three constraints are, though, excluded from Eq.26 by the engineering judgement. To obtain the solution, linear programming problem is solved by setting h=0.6, then we can get $(mp_1, d_1, mp_2, d_2) = (0.323, 0.008, 0.212, 0.0)\mu_{p1}$.

In this example, d_2 which represents the fuzziness of plastic moment Mp2, becomes 0. It shows that Mp_2 must have crisp value if design level h is required relatively high(h=0.6 means that the degree of fuzzy constraints to be positive is 92 percent satisfactory).

5. Conclusions

Non-fuzzy decision problem under fuzzy constraints and fuzzy decision problem under same enviroment are studied through examples. In fuzzy decision problem, the judgement of the desgin level, which is expressed by its membership functions, is required based on h. Design variables are determined by the mean and its spread which represents fuzziness.

In non-fuzzy decision problem, non linear programing technique is needed to get the solution.

Concludingly, more complex problem of structures can not be available, now. Because if both the constant A and variable x are fuzzy, then the membership function of their linear combination $\tilde{A}\tilde{X}$ is not defined yet, in this paper. It makes the application of this problem to more complicated structural optimization problems difficult.

And also the choice of membership function depends on greatly the kind of problems and subjectives of designers.

References

1. For example, L.A.Schmit,Jr. et.al,"Structural Synthesis 1959-1969 A Decade of Progress,"Matrix Methods of Structural Analysis and Design, August 25-30,1969, Tokyo, Japan.
2. For example, Kiyotaka SHIMIZU," Multi objectives and Competitive Theory," Kyoritsu Publishing Co.Inc.,in Tokyo,1982(in Japanese).
3. L.A.Zadeh,"The Concept of a Linguistic Variable and its Application to Approximate Reasoning-I," Information Science,Vol.8,PP.199-249,1975.
4. H,TANAKA and K,ASAI,"A Formulation of Linear Programming Problems by Fuzzy Function," Systems and Control,Vol.25, No.6,pp.351-357,1981(in Japanese).
5. H,TANAKA,et.al.,"Evaluation of Information in Fuzzy Linear Programming Problem," Systems and Control,Vol.28, No.10, pp.583-589,1984(in Japanese).
6. Takashi,CHOU,"Optimum Design of Structures," Asakura Publishing Co.Inc.,in Tokyo,1971(in Japanese),

ON THE CALIBRATION OF ARMA PROCESSES FOR SIMULATION

S. Krenk & J. Clausen
Department of Structural Engineering
Technical University of Denmark
DK-2800 Lyngby, Denmark

ABSTRACT

Auto-Regressive Moving-Average processes have found increased application in recent years in connection with simulation of stochastic loads on structures. Computational efficiency and limitations on available time for simulation in connection with tests require the number of coefficients in the ARMA process to be small, thereby stressing the need for efficient calibration. The most convenient calibration scheme makes use of the covariance function through the Yule-Walker equations. However, for narrow band, non-rational spectral densities, such as the Pierson-Moskowitz and the JONSWAP spectra for wave elevation, difficulties may be encountered. Some analytical remedies have been proposed in the literature specifically for the Pierson-Moskowitz spectrum. In this paper the difficulty is attributed to the use of a calibration time interval of insufficient length in connection with the non-rational form of the spectrum. The problem is solved by extending the calibration interval in connection with a least squares fit. Calculations suggest that structural resonance contributions to the spectrum are most efficiently incorporated via a separately calibrated filter.

INTRODUCTION

Within the field of structural engineering simulation of stochastic load processes such as wind, waves and earthquakes has traditionally been based on some version or other of the Fourier transform. The process is then represented by a finite number of sine functions, and the stochastic aspect is reduced to the selection of amplitudes and phases. These processes are discrete in the frequency domain and continuous in time. All frequency components contribute at any given time, and the amount of computation in each time step therefore grows rapidly with the required spectral resolution. This

is partly compensated for by use of the Fast Fourier Transform algorithm, but then the full time history must be calculated simultaneously. In recent years sequential simulation algorithms have been introduced in the form of Moving-Average, Auto-Regressive and the combined Auto-Regressive Moving-Average process. These processes are discrete in time and continuous in the frequency domain. The general form is

$$X_n + \sum_{k=1}^{N} a_k X_{n-k} = \sum_{k=0}^{M} b_k \xi_{n-k} \qquad (1)$$

Here $..X_{n-2}, X_{n-1}, X_n..$ is the process to be simulated, and $..\xi_{n-2}, \xi_{n-1}, \xi_n..$ is a sequence of independent random pulses, most often taken to be normal variables. The sequential simulation method corresponds to passing a white noise process through a discrete filter, and available methods of analysis for digital filters can be used to describe the properties of the simulated sequence, see e.g. Oppenheim & Schafer (1975). In the analysis of offshore structures the spatial load distribution must also be considered. The dispersive nature of the waves favours the frequency domain, but sequential methods can be used in connection with time convolution as shown by Samii & Vandiver (1984).

The moving-average (MA) process corresponds to $N=0$, whereby X_n is a linear combination of M values of the white noise process ξ_j. The auto-regressive (AR) process corresponds to $M=0$, whereby X_n is generated from a linear combination of N previous values plus a single independent random variable. These two types of processes have widely different correlation properties. While the MA process has a finite correlation length determined by the length of the filter, the AR process is correlated over any finite time separation. Auto-regressive processes are used in spectral estimation by the maximum entropy method - see e.g. Holm & Hovem (1979) - and they have also been proposed for load simulation, Spanos (1983) and Lin & Hartt (1984). However, typical wave load spectra are nearly zero over an interval of low frequencies, and it is difficult to obtain a uniformly good fit with an AR process of low order. The limitations of the individual MA and the AR processes are to a great extent removed by the combination into an ARMA process. Furthermore the ARMA process is particularly suited for analysis of random vibration of linear systems, as it can be shown that an ARMA process

with $N=M+1=2n$ is an exact representation of the discretely sampled response of an n degree of freedom linear structure to white noise input, see e.g. Gersch & Liu (1976). In spite of the versatility of the ARMA process problems have been encountered in connection with typical offshore wave load spectra based on the Pierson-Moskowitz format, Spanos (1983) and Spanos & Mignolet (1986). A partial, but not fully satisfactory, solution was found by replacing the exponential function in the Pierson-Moskowitz spectrum with its 9-term Taylor expansion. Cleary this type of approach suffers from the limitation that a simple analytical form of the spectral density must be known and expanded explicitly into a rational function. In the following the procedure for calibrating an ARMA process to fit a given spectrum is outlined. The importance of the time interval used in the calibration procedure is identified, and the success of overdetermination via a least squares fit is demonstrated. Calculations indicate that structural response contributions to the spectrum are most efficiently incorporated via a separately calibrated filter.

SPECTRUM AND Z-TRANSFORM

It is customary to characterize the spectral properties of time series such as (1) by the z-transform, defined as

$$\tilde{X}(z) = \sum_{-\infty}^{\infty} X_n z^{-n} \qquad (2)$$

z is a complex variable, and the value on the unit circle is closely related to the sampling period T and the frequency f,

$$z = e^{i\theta} \quad , \quad \theta = T\omega = 2\pi T f \qquad (3)$$

For a discretely sampled process $X_n=X(nT)$ the symmetric frequency interval is bounded by the Nyquist frequency $f_N=\frac{1}{2T}$.

The transfer function of a system is the ratio between output and some standardized input. In terms of the z-transform the transfer

function of (1) is

$$\tilde{H}(z) = \frac{\sum_{k=0}^{M} b_k z^{-k}}{1 + \sum_{k=1}^{N} a_k z^{-k}} \qquad (4)$$

For white noise input of unit variance the spectral density of the output is

$$S_{ARMA}(\omega) = \frac{T}{2\pi} |\tilde{H}(z)|^2 \qquad (5)$$

The normalizing factor 2π is needed to account for the use of angular frequency, while the sampling period normalizes the white noise to unit intensity per unit time. It is seen that the AR and MA processes correspond to special forms of the transfer function (4) in which the numerator and denominator are unity, respectively. Each of these special forms impose limitations on the spectra that can be represented accurately.

The transfer function (4) is very useful for establishing the qualitative spectral properties of ARMA processes. It also leads to an explicit expression for the coefficients a_k for the output of a linear second order system with n degrees of freedom, with uncoupled modes. The impulse response function of such a system is of the form

$$h(t) = \sum_{j=1}^{n} \left\{ A_j e^{i\Omega_j t} + A_j^* e^{-i\Omega_j^* t} \right\} \qquad (6)$$

where an asterisk indicates the complex conjugate and

$$\Omega_j = \omega_j e^{i\theta_j} \quad , \quad \zeta_j = \sin(\theta_j) \qquad (7)$$

is the complex, damped eigenfrequency of mode j with damping ratio ζ_j . A_j are constants depending on the participation of the modes. By matching the discrete output of a process of the form (1) with that from the continuous system at times T, 2T, ..etc. the transfer function is seen to be of the form

$$\tilde{H}(z) = T \sum_{n=0}^{\infty} h(nT)\, z^{-n}$$

$$= T \sum_{j=1}^{n} \left\{ \frac{A_j}{1 - e^{i\Omega_j T} z^{-1}} + \frac{A_j^*}{1 - e^{-i\Omega_j^* T} z^{-1}} \right\} \qquad (8)$$

Matching this expression with the denominator of (4) gives the following polynomial relation

$$z^{2n} + \sum_{k=1}^{2n} a_k z^{2n-1} = \prod_{j=1}^{n} (z - e^{i\Omega_j T})(z - e^{-i\Omega_j^* T})$$

$$= \prod_{j=1}^{n} \left\{ z^2 - 2 e^{-\zeta_j \omega_j T} \cos(\sqrt{1-\zeta_j^2}\, \omega_j T)\, z + e^{-2\zeta_j \omega_j T} \right\} \qquad (9)$$

This relation uniquely determines the coefficients a_k, and these coefficients are independient of the participation factors A_j. Strictly speaking the discrete system should not be matched to the impulse response function $h(nT)$ itself but rather to an average value over the sampling interval in order not to violate the stationarity of the continuous process. However, the averaged impulse response function is also of the form (6) and independence of the coefficients A_j makes the relation (9) exact in its present form.

The coefficients b_k can now be determined in two ways; either by use of the suitably averaged impulse response function in (6) or by constructing a set of equations directly from the original equation (1). The first procedure is straightforward but tedious. The second procedure has some bearing on the following, and is therefore briefly indicated.

Multiplication of (1) with X_{n-j} and ξ_{n-l} gives the following equations for the covariances

$$\sum_{k=0}^{N} a_k R_{k-j} = \sum_{k=0}^{M} b_k C_{k-j} \qquad (10)$$

$$\sum_{k=0}^{N} a_k C_{l-k} = b_l \sigma_\xi^2 \qquad (11)$$

where σ_ξ^2 is the variance of the random pulses, and the following notation has been used for the covariances

$$R_j = E(X(n) X(n+j)) \tag{12}$$

$$C_j = E(\xi(n) X(n+j)) \tag{13}$$

The variable X_n is independent of any future pulses ξ_{n+j}, and therefore $C_{-j}=0$ for $j=1,2,\ldots$. If the coefficients a_k are known, the equations (11) can be solved recursively for C_l in terms of the coefficients b_j.

$$C_l = \sigma_\xi^2 b_l - \sum_{j=1}^{l} a_j C_{l-j} \quad , \quad l = 0,1,\ldots,M \tag{14}$$

Substitution of C_l from (14) into (10) gives a set of quadratic equations in the coefficients b_l. To calibrate a high-order ARMA process in this way would be rather complicated due to the nonlinear form of the latter part of the procedure, but for a second order equation corresponding to a single degree of freedom the method is quite feasible, Gersch & Liu (1976).

EXTENDED YULE-WALKER EQUATIONS

In the case of a general spectrum the coefficients a_k are not known. Nonetheless the equations (10) and (11) remain valid and can be used to determine the coefficients a_k and b_k efficiently. The key problem is that generally the cross covariances C_j are unknown. As suggested by Gersch & Liu (1976) the cross covariances can be determined approximately by rearranging the original ARMA process into the form of an equivalent AR process.

$$X_n + \sum_{k=1}^{\hat{N}} \hat{a}_k X_{n-k} = \hat{b}_0 \xi_n \tag{15}$$

In principle the number of terms $\hat{N}$ is now infinite, but in practice good approximations may be obtained with systems of a size well

within practical computation capability. The folowing examples indicate a magnitude of about 40 to 50 to be suitable. Multiplication of (15) with X_{n-j} gives the so-called Yule-Walker equations

$$\sum_{k=1}^{\hat{N}} \hat{a}_k R_{j-k} = - R_j \quad , \quad j = 1,2,3,... \tag{16}$$

These equations are of Toeplitz type and can be effectively solved recursively by the Levinson algorithm, see e.g. Press et al. (1986). The equations do not depend on any common factor in the covariances R_j . The intensity of the AR process is determined from the expectation of the square of the equation (15). When the equations (16) are used to reduce the double sum, the resulting expression for the coefficient $\hat{b}_0$ is

$$\sigma_\xi^2 \hat{b}_0 = R_0 + \sum_{k=1}^{\hat{N}} \hat{a}_k R_k \tag{17}$$

Due to the large size of $\hat{N}$ and a tendency of the equations (15) to develop instablities, the AR process (14) is generally not suitable for simulation. A drastic improvement with respect to filter order and stability is obtained by rearranging the process into the ARMA format. This can be done either in the time domain by use of the equations for the covariances as proposed by Gersch & Liu (1976) or in the frequency domain by matching the power series expansions of the transfer functions as proposed by Spanos & Mignolet (1986). The following concentrates on the time domain procedure and illustrates some simple precautions that are necessary, when this method is used on wave load spectra.

The AR process (15) is a rearrangement of the original ARMA process (1), and the cross covariances C_l for both processes can therefore be evaluated from the coefficients $\hat{a}_k$, accepting the approximation inherent in the truncated form of (15). Multiplication of (15) with ξ_{n-l} gives a set of equations of the form (11) with the recursive solution

$$C_0 = \sigma_\xi^2 \hat{b}_0 \tag{18}$$

$$C_l = - \sum_{j=1}^{l} \hat{a}_j C_{l-j} \quad , \quad l = 1,2,3,... \tag{19}$$

When the cross covariances C_l have been determined, the equations (10) and (11) for the coefficients a_k and b_k of the ARMA process can be rewritten in the form

$$\sum_{k=1}^{N} a_k R_{k-j} - \sum_{k=0}^{M} b_k C_{k-j} = - R_j \tag{20}$$

$$\sum_{k=1}^{N} a_k C_{l-k} - b_l \sigma_\xi^2 = - C_l \tag{21}$$

These equations are in the form of a set of extended Yule-Walker equations for the vector $(a_1,a_2,...,a_N,b_0,b_1,...,b_M)$, and thus the problem of determining these coefficients is solved in principle. However, the choice of the specific equations to be used still require some attention. In the papers by Gersch & Liu (1976) and Spanos & Mignolet (1986) and in the vector process case considered by Samaras et al. (1985) the equations were selected with smallest possible index, i.e. $j=0,1,...,N-1$ and $l=0,1,...M$, or with minor variations with respect to the first equation index and the parameter b_o . As demonstrated in the next section this choice is not satisfactory for narrow band spectra of non-rational form.

OVERDETERMINATION AND LEAST SQUARES

In the calibration of an ARMA process to fit a given spectrum it is often of interest to obtain the shortest possible filter to minimize computation time and storage requirements of the algorithm. This, on the other hand, leads to a small number of equations in the system (20)-(21). For narrow band processes these equations may furthermore concentrate on fitting the coefficients to the covariance functions within a fraction of a single period leading to a rather poor fit to the spectral density function. A simple solution to this problem lies in overdetermination in connection with the use of a

least squares fit. The influence of the parameters N , $\hat{N}$ and the degree of overdetermination is discussed in connection with the wave spectrum of Pierson & Moskowitz (1964) in the parametric form proposed by ISSC (1964). In terms of the standard deviation σ_x and the mean zero-crossing period T_z the spectral density is

$$S_{PM}(\omega) = \frac{4}{\pi} \sigma_x^2 \left[\frac{2\pi}{T_z}\right]^4 \omega^{-5} \exp\left\{ - \frac{1}{\pi} \left[\frac{2\pi}{T_z}\right]^4 \omega^{-4} \right\} \qquad (22)$$

The covariance function corresponding to (22) is obtained numerically by application of the FFT algorithm.

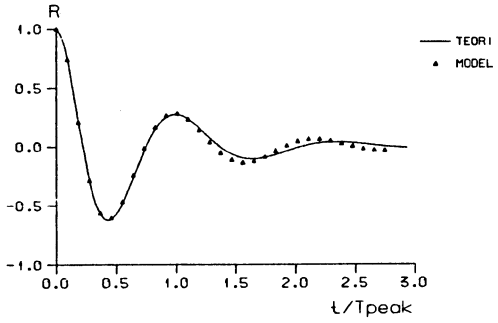

Fig.1. PM covariance fit of ARMA(4,4), $\hat{N}$ =40.

The calibration problem is illustrated in Fig. 1, showing the covariance function $R(t)$ of the Pierson-Moskowitz spectrum and the values R_j from an ARMA(4,4) process, i.e. an ARMA process with $N=M=4$. The calibration has been done in the traditional way by use of the equations (20) and (21) with indices $j=1,..,4$ and $l=1,..,4$. The time scale is normalized with respect to the time T_p corresponding to the peak frequency of the spectrum, and for illustration purposes the sampling period is $T=0.1T_p$. In practice the sampling period would not be less than around $T\simeq 0.05T_p$ in order to obtain the peaks with sufficient accuracy. It is seen that the equations (20) and (21) are limited to the first half period due to the short length of the filter. After the first period a substantial drift of the estimated values R_j is observed.

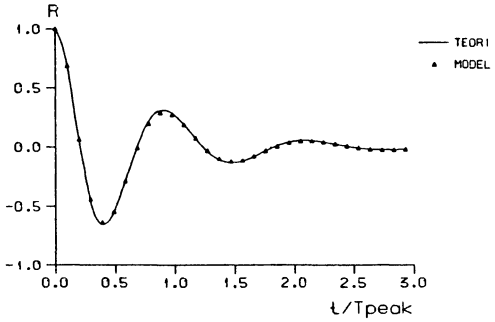

Fig.2. PM covariance fit of ARMA(6,6), $\hat{N}$ =50. Overdetermination factor 3.

The parameter $\hat{N}$ has been chosen rather large, leaving two possible causes for the problem in Fig. 1, the undesirable concentration of the calibration points in the first half period and the possibility of a too low order of the ARMA filter. In order to obtain a fully satisfactory fit an ARMA(6,6) filter was found to be necessary, and the calibration was made by solving a three times overdetermined system of equations (20)-(21) by least squares. In this way the process is calibrated uniformly over nearly two full

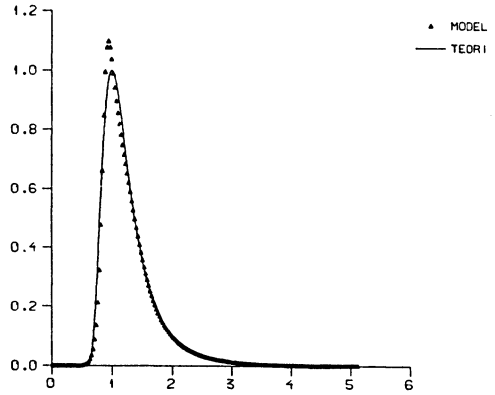

Fig.3. PM spectrum fit of ARMA(6,6), $\hat{N}$=50. No overdetermination.

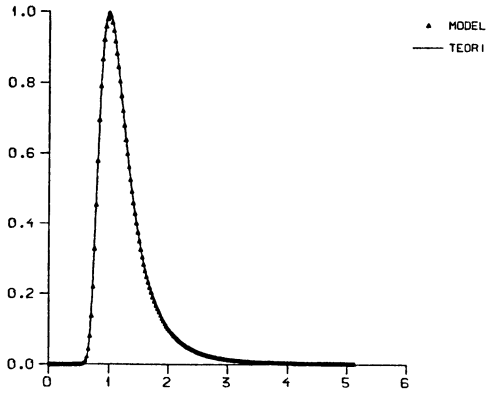

Fig.4. PM spectrum fit of ARMA(6,6), $\hat{N}$=50. Overdetermination factor 3.

periods. The result is shown in Fig. 2. Increasing the filter order or the degree of overdetermination did not result in any improveent in the fit.

While the covariance functions shown in Figs. 1 and 2 illustrate the calibration procedure, the quality of the resulting ARMA process is perhaps better evaluated in terms of the spectral density. Figures 3 and 4 show the effect of overdetermination on the spectrum for the ARMA(6,6) filter. It is seen that overdetermination leads to a nearly perfect fit in the full frequency interval by properly adjusting the spectrum around the peak. This is precisely the effect illustrated in Figs. 1 and 2. The quality of the ARMA(6,6) filter shown in Fig 4 is fully comparable with the ARMA(7,7) reprsentation obtained by Spanos and Mignolet (1986) from a rational approximation of the Pierson-Moskowitz spectrum. For 20 samples per peak period it was found that the degree of overdetermination should be approximately doubled to give the same kind of accuracy, and thus it appears that the calibration time interval should not be less than around two periods for the present non-rational spectrum. This is a logical consequence of the tendency of the approximation to drift from the covariance function, if too few peaks are included in the calibrating equations, thereby explaining the potential problems with use of covariance calibration of low order filters without overdetermination. Figure 5 shows part of a simulated time history corresponding to the ARMA(6,6) filter from Fig. 4.

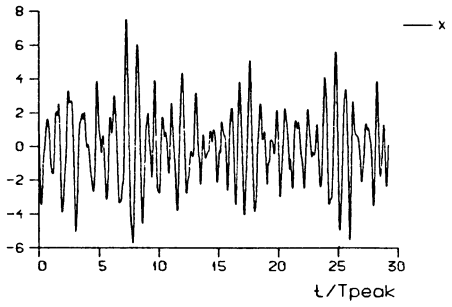

Fig.5. Time history for the ARMA(6,6) process in Fig. 4.

In order to achieve the full accuracy of an ARMA process of given order by the present method the order $\hat{N}$ of the approximating AR process must be sufficiently large. A parametric study indicated that for the Pierson-Moskowitz spectrum a value of $\hat{N}=30$ was clearly insufficient, leading to errors near the peak of the spectrum. The values $\hat{N}=40$ and $\hat{N}=50$ gave nearly identical, and fully satisfactory, results. For a rational spectrum corresponding to a harmonic oscillator a value of $\hat{N}=20$ was found to be fully satisfactory. An example of a minimal representation of a simple harmonic oscillator with damping ratio $\zeta=0.1$ by an ARMA(2,2) process is shown in Fig. 6.

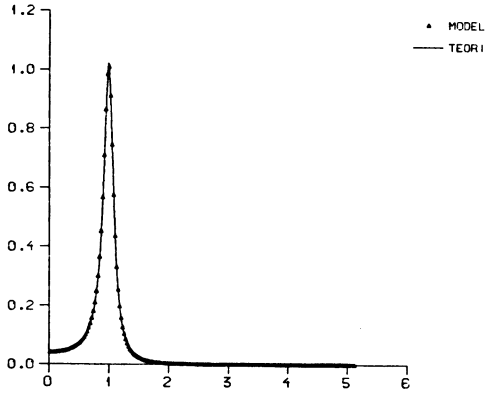

Fig.6. Harmonic oscillator and ARMA(2,2), damping $\zeta=0.1$.

In the simulation of stress histories for offshore structures it is not sufficient to consider unimodal spectra. Structural resonance may give an additional amplification of the spectrum corresponding to the harmonic oscillator, see e.g. Wirsching & Light (1980).

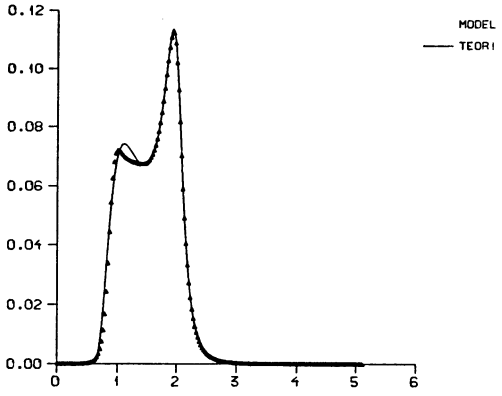

Fig.7. Pierson-Moskowitz spectrum with resonance.
ARMA(6,6), $\hat{N}$=50. Overdetermination factor 5.

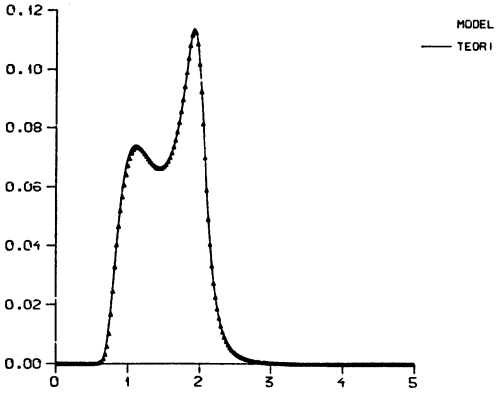

Fig.8. Pierson-Moskowitz spectrum with resonance.
ARMA(10,10), $\hat{N}$=50. Overdetermination factor 5.

$$S_{res}(\omega) = \frac{\omega_0^4}{(\omega^2 - \omega_0^2)^2 + 4\,\zeta^2\,\omega_0^2\,\omega^2} \qquad (23)$$

The representation of this spectrum by an ARMA(2,2) process was illustrated in Fig. 6. The special form of this spectrum leads to the minimum order of the filter, $N=M=2$. The parameters a_k and b_k can be determined analytically from the eigenfrequency ω_0 and the damping ratio ζ , but as indicated in Fig. 6 direct application of the equations (20) and (21) gives excellent results. A process with the combined spectrum

$$S(\omega) = S_{PM}(\omega)\, S_{res}(\omega) \qquad (24)$$

can be calibrated directly or by convolution of the ARMA coefficients for each of the two factors. Figures 7 and 8 show results from direct calibration in the case of $\omega_0=2.0\omega_p$ and $\zeta=0.1$. Figure 7 illustrates the effect of a too low order of the ARMA filter, showing up in the form of a poor fit around the peak of the Pierson-Moskowitz spectrum, while the resonant part is well represented. In Fig. 8 the filter order is more than sufficient, but even so the fit is not quite as good as in the calibration of the individual spectra with ARMA(6,6) and ARMA(2,2) processes. This suggests the advantage of calibrating the individual factors of the spectrum (24), and then either using a two-stage simulation algorithm or combining the coefficients by convolution.

CONCLUSIONS

The use of Auto-Regressive Moving-Average processes for simulation of structural load and response has been discussed, and potential problems in connection with covariance calibration of ARMA processes to non-rational, narrow band spectra has been linked to the length of the calibration time interval compared with the mean period of the process. Calculations indicate the need for at least two periods to be included in the calibration procedure. Appropriate extension of the calibration time interval by overdetermination and least squares solution of the equations lead to excellent results, e.g. an ARMA(6,6) representation of the Pierson-Moskowitz spectrum.

ACKNOWLEDGMENTS

This paper was written as part of a project on fatigue of offshore structures supported by the Danish Technical Research Council and the National Agency of Technology.

REFERENCES

Gersch, W. and Liu, R. S-Z., "Time series methods for synthesis of random vibration systems", Journal of Applied Mechanics, Vol. 43, pp. 159-165, 1976.

Holm, S. and Hovem, J. M., "Estimation of scalar ocean wave spectra by the maximum entropy method", IEEE Journal on Oceanic Engineering, Vol. OE-4, pp. 76-83, 1979.

International Ship Structures Congress, "Report of Committee 1", Proceedings of the Second International Ship Structures Congress, Delft, Netherlands, July 20-24, 1964.

Lin, N. K. and Hartt, W. H., "Time series simulations of wide-band spectra for fatigue tests of offshore structures", Journal of Energy Resources Technology, Vol. 106, pp. 466-472, 1984.

Oppenheim, A. V. and Schafer, R. W., Digital Signal Processing, Prentice-Hall, Englewood Cliffs, N. J., 1975.

Pierson, W. J and Moskowitz, L., "A proposed spectral form for fully developed wind seas based on the similarity theory of S. A. Kitaigorodski", Journal of Geophysical Research, Vol. 69, pp. 5181-5190, 1964.

Press, W. H., Flannery, B. P., Teukolsky, S. A. and Vetterling, W. T., Numerical Recipes, Cambridge University Press, Cambridge, 1986.

Samaras, E., Shinozuka, M. and Tsurui, A., "ARMA representation of random processes", Journal of Engineering Mechanics, Vol. 111, pp. 449-461, 1985.

Samii, K. and Vandiver, J. K., "A numerically efficient technique for the simulation of random wave forces on offshore structures", Proceedings of the 16th Offshore Technology Conference, Houston, Texas, OTC 4811, pp. 301-308, 1984.

Spanos, P-T. D., "ARMA algorithms for ocean wave modeling", Journal of Energy Resources Technology, Vol. 105, pp. 300-309, 1983.

Spanos, P. D. and Mignolet, M. P., "Z-transform modeling of P-M wave spectrum", Journal of Engineering Mechanics, Vol. 112, pp. 745-759, 1986.

Wirsching, P. W. and Light, M. C., "Fatigue under wide band random stresses", Journal of the Structural Division, ASCE, Vol. 106, pp. 1593-1607, 1980.

LEVEL FOUR OPTIMIZATION FOR STRUCTURAL GLASS DESIGN

Niels C. Lind
Institute for Risk Research
University of Waterloo, Waterloo, ON, N2L 3G1, Canada

ABSTRACT

A design standard for structural glass in the limit state design format is calibrated to a target level of reliability against windstorm damage. The selection of reliability level presents special problems because the structural response is geometrically nonlinear and because the strength is highly dependent on time, size, and loading history. Selection of safety level so as to achieve a social and economic optimum is described. The optimum reliability index is determined as a function of known quantities and of the social and economic costs of failure. Optimal ranges of applicability over cost for a family of importance factors are also determined.

INTRODUCTION

This paper describes the selection of the resistance factor and the importance factors for use in the limit states design of glass in buildings against wind loading. The selection is based on consideration of optimal investment level to minimize the total cost.

Glass plate is gaining importance as a structural building element and as cladding of large buildings. There is a need to develop the structural design of glass plate elements into consensus standards conforming in philosophy to other codes and standards for structural design (CSA 1981) that prescribe limit states design formats based on structural reliability theory.

Glass is different from all other common building materials. Window glass apparently loses about half the original strength or more after

20 years, depending on exposure and atmosphere (Ablassi,1981). The rectangular glass plate is one of the simplest structural forms, but the glass plate deflects in the order of ten times the thickness before failure, so that membrane stresses provide an important part of the load carrying capacity. The response is thus modelled as time-dependent, size-dependent and geometrically nonlinear.

Safety margins for other materials may be based on experience; there is little experience with glass as a structural material. The appropriate safety level must be determined from first principles of risk and cost of safety, quite separately from the question of how such a safety level may be achieved. This paper describes considerations necessary to implement this philosophy in a practical design standard for structural glass. A more detailed account is given in a later paper (Lind 1987). The actual calibration of the standard so as to produce the safety level that is selected in this paper is quite another matter, to be described separately (Davenport and Lind, 1987).

CODE OPTIMIZATION

The process to develop a reliability-based structural design standard has two phases: formatting and calibration of the format (Madsen, Krenk and Lind (1986). The writing of the provisions of the standard, in which all reliability-related parameters are identified as variables, is called formatting. Calibration is the subsequent selection of appropriate values for these variables so as to approach the reliability objective (Ravindra and Lind 1983; Madsen et al. 1986).

The format is given in the National Building Code of Canada (NBCC 1985), which also specifies the wind loading and the wind load factor, $\alpha_Q = 1.5$ in the limit states design equation

$$[1] \quad \phi R_S = \gamma \alpha_Q Q$$

where Q is the specified wind load in NBCC (1985); α_Q is the wind load factor; γ is an importance factor that is applied to the loads and takes into account the consequences of failure; R_s is the calculated nominal required resistance based on the specified material properties and design formula; and ϕ is a resistance factor applied to account for variability of material properties and uncertainty in the prediction of resistance.

DESIGN OBJECTIVE

A level 4 safety criterion aims for a reliability that is optimal in the socio-economic sense of a balanced allocation of resources invested to reduce risk. Design standards and design procedures are also characterized by level. The level follows from the safety criteria they employ. Level 2 is in practice the highest that can be specified at the present state of the art, because full distribution details are not available to a professionally acceptable extent for some of the variables, e.g. human error in design or workmanship. Level 1 is the highest level now attainable for glass design.

Rational calibration of a standard involves the selection of a target reliability for each limit state, and this must be done on a level that is higher than the format of the standard. Standards are intended to serve the common interest of society in respect of safety; all calibration is ultimately aimed to approach level 4 as far as practical. The economic considerations given in the following lay a basis for level 4 balancing of incremental total social and monetary expected costs against incremental initial cost. They are formulated in level 2 terms, however, i.e. expressed in terms of a generalized reliability index.

THE HAZARDS

The hazards to structural glass and window glass are human factors

and natural factors, singly or in combination. Human factors (e.g. wilful damage, errors during design, manufacture, workmanship, control or use) are perhaps the most common hazards. Many provisions of a glass design standard aim to reduce the risk of these human hazards, but those provisions are outside the scope of this paper.

The natural hazards to structural glass are mainly windstorms and severe thermal gradients. Bird collision damage is also common. Windstorms have two primary effects: dynamic wind pressure and windborne missiles. The latter are important, but it is uneconomical to design glass against large missiles. It is better to rely on the minimum thickness required for safe handling and for wind pressure incidentally to provide some safety against windborne missiles up to a certain size. Similarly, to design against tornado wind pressures is uneconomical.

The design of the standard involves the determination of the reliability-sensitive constant ϕ in Eq. 1. This constant is effective only in the control of the reliability against breakage due to the dynamic effects of wind pressure. Wind pressure is not the major cause of breakage of installed glass,but the need to control this type of breakage largely controls the material expenditure in glazing and curtain walls, and thus it is the most important factor to be optimized in design. It is not the absolute breakage rates, but the marginal costs of preventing breakage that matter.

THE MATERIAL

A detailed account of the mechanical behaviour of glass is unnecessary for the present purpose, but it is important to note that the strength of glass, unlike other building materials, decreases rapidly with time. Abiassi (1981) studied the influence of weathering, aging (and normal wear and tear) on glass taken from three buildings in Texas and found that the strength was much reduced. In the case of

tension on the unweathered side the mean strength was reduced to 39 per cent of the original value. With tension on the weathered side - the case more commonly critical in design - the mean strength was reduced by a factor of 0.45. The relative dispersion of the strength, expressed by the coefficient of variation was not reduced with time in Abiassi's study.

The strength also decreases with size. The strength of a glass plate of thickness h under pressure is approximately proportional to $h^{1.5}$ instead of h^2 (Lind 1986).

SELECTION OF DESIGN LIFE

The design life of glass in a building is dictated by the design life of the building as a whole. It makes no sense to aim for replacement of the glass during the useful life of the building. On the other hand it doesn't make sense that the glass should outlast the rest of the building. The design life is therefore taken as equal to that of the building, which is assumed to be 50 years in the ordinary case.

ECONOMICS OF DESIGN

To determine the optimal value of the resistance factor ϕ, imagine that this parameter is varied to generate a family of design standards that are identical in all respects except for ϕ. A small decrease in the resistance factor ϕ in Eq. 1 will cause an increase in the required resistance R_s and hence increase the required thickness. This will mostly leave the selected thicknesses unaffected, because thickness is generally rounded off upwards to the next standard thickness. However, for a few lights it will lead to a size larger, and will thus decrease the probability of failure, thereby decreasing the expected cost of failure EC_F but increasing the initial cost of the glass, C_I. The decrease in EC_F is subject to diminishing returns, and when the optimum failure probability is reached, the present value of the decrement in

EC_F is cancelled by the increment in C_I.

Fig. 1 gives a synopsis of this economic process. (1) Let the resistance factor Ψ receive an infinitesimal decrement $q\Psi$. (2) This causes a similar relative increment qR_S in the required resistance R_S.

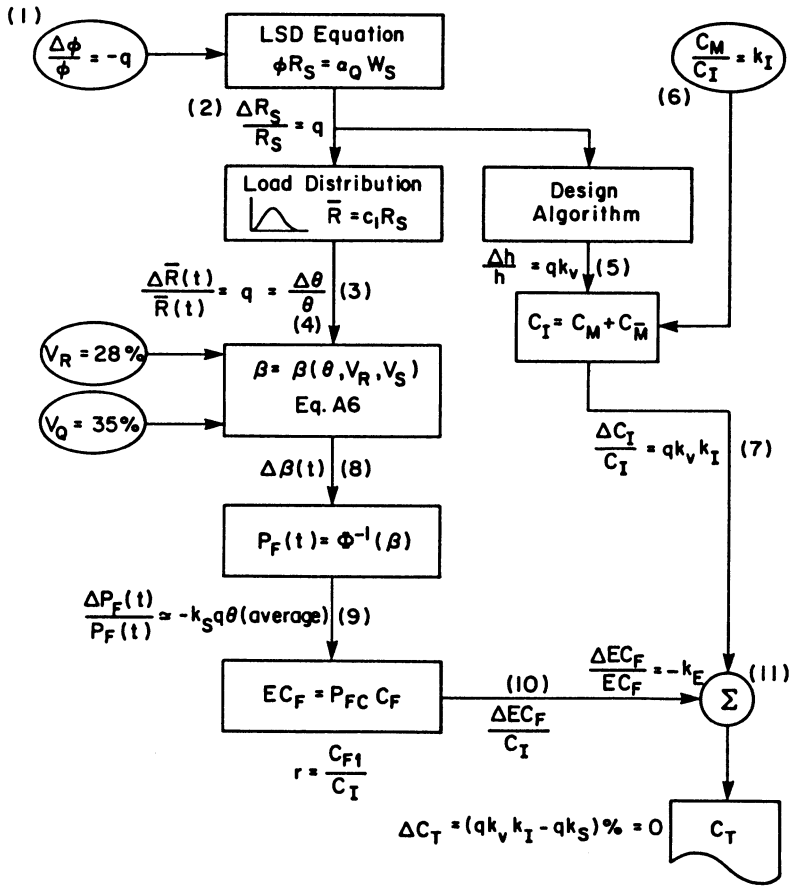

Fig. 1 Influence of resistance factor Ψ on total cost C_T.

(3) This, in turn, causes an increase $q\bar{R}$ in the mean resistance, and (4) an increase $q\theta = q\bar{R}/\bar{Q}$ in the central safety factor θ as a result. (5) Because of the size effect, the increment qR_s gives a relative increment of only qk_v in the required thickness, where k_v is a constant that depends on the design formula, determined below. This translates directly into a relative increase of approximately qk_v in the supplied thickness, as an average for a large number of lights, see Fig. 2. Material cost C_M constitutes a fraction, s, of the cost C_I of installed glass. (7) This implies an increased initial cost of sqk_vC_I.

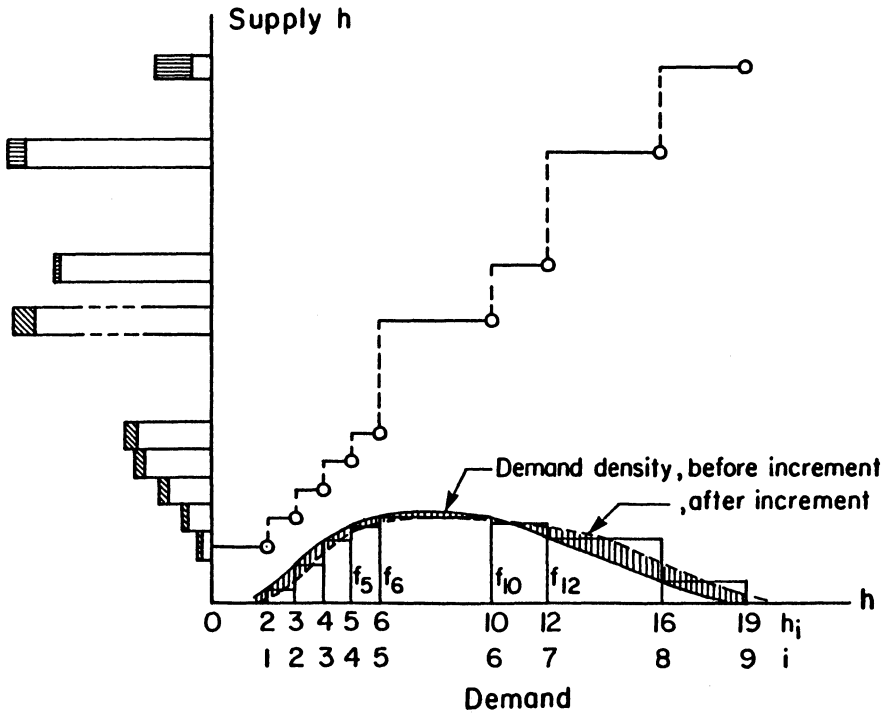

Fig. 2 Influence of a change in required thickness on the distribution of h and on thickness supplied.

Reference is now made to Fig. 3 to calculate the expected cost of failure. The figure shows an event tree covering the 50 year design life, based on a one-year accounting cycle. The outcome each year i is either survival to the next year, i+1, or failure F_i, indicated by a rising or descending branch, respectively. The conditional probability of survival of year i+1, given survival to the beginning of year i, is denoted by R_i and of failure F_i. By following a path from the origin to any node, one calculates the probability of of the corresponding outcome as the product of such conditional probabilities for the branches of the path from the origin to the node. The present expected value of the cost of failure is the product of its present value and its probability. Let I denote the true annual rate of interest net of inflation; then the backward capitalization factor for one year is $K = (1 + I)^{-1}$. Fig. 3 shows that the expected cost of failure is

$$[2] \quad EC_F = C_1P_1 + KC_2R_1P_2 + K^2C_3R_1R_2P_3 + \ldots$$

where C_i (i=1,...,50) is the cost of failure (i.e. cost of breakage due to wind pressure) occurring in year i; P_i is the probability of failure due to wind pressure during year i; R_i is the rate of survival of year i of the glass for <u>all hazards</u> including wind, given survival of year

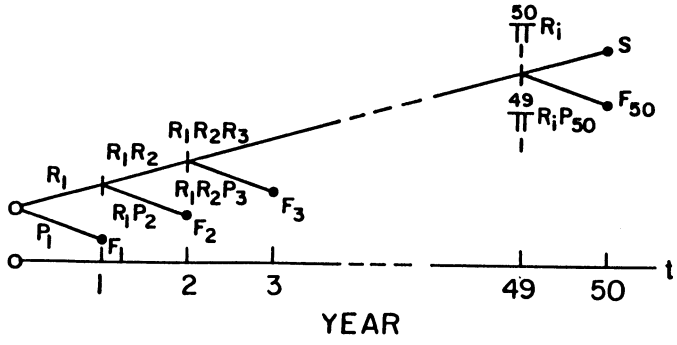

Fig. 3 Lifetime failure event tree with time scale.

i-1. C_i should take account of depreciation. However, the influence of this factor is negligible; glass failure during the 50th year is just about as serious as during the first year, and C_i is therefore replaced with the constant value C_F.

Note that R_i+P_i is less than unity because R_i includes all hazards; however, R_i is sufficiently close to 1 that it may be included in the factor K without noticeable error. Finally, introducing the equivalent lifetime failure probability, defined as

$$[3] \quad P_{FC} = \sum_{1}^{50} K^{i-1} P_i$$

makes it possible to rewrite Eq. 2 as

$$[4] \quad EC_F = P_{FC} C_F$$

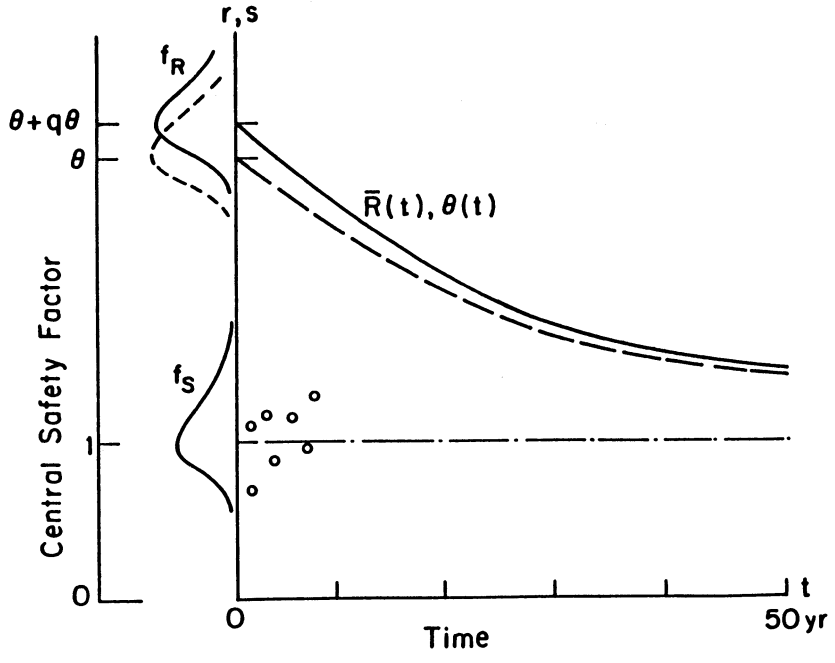

Fig. 4 Influence of a change in ϕ on lifetime failure probability.

The individual term in Eq. 3 is called the discounted breakage rate. Eqs. 3 and 4 show that the equivalent lifetime failure probability and the present value of the expected cost of failure are both linear combinations of the failure probabilities P_i. The change in the safety factor θ translates into a change in the present value of the expected cost of failure. The steps are labeled (8),(9),and (10) in Fig. 1.

(11) The optimality condition $\delta(EC_F + C_I) = 0$ gives the failure rate that is in balance against the cost of providing a lower rate (see Fig. 1). Fig. 4 shows the influence of a change in the safety factor on the expected cost of failure . The loading is taken as the maximum wind pressure during a storm, of which there are approximately 100 each year. The resistance deteriorates with time and is represented by the central safety factor $\theta(t) = R(t)/S$. The influence of an infinitesimal increase in θ is a proportional increase in $\theta(t)$. This, in turn, causes a proportional reduction $k_g q\theta$ in the probability of failure in each load application which varies from 6.95 $q\theta$ to 4.75 $q\theta$ when $\beta(t)$ varies from 3.16 to 1.90. Thus, although the probability of failure may vary by a factor of 100 or more over a lifetime, the relative influence of a change in the resistance factor ψ on the probability of failure in all the load applications is fairly constant. The value 5.85 $q\theta$ may be used as representative.

It is convenient to introduce the failure cost ratio

[5] $\quad r = C_F/C_I$

Substituting into Eq. 4 gives the optimum lifetime discounted failure probability.

In the future Canadian and U.S. standards design will likely be governed by the "failure prediction method". Repeated computer design has shown that the required volume v of glass designed according to this method varies with the strength factor ψ

approximately as $\psi^{-.991}$. Hence,

[6] $\delta v/v = -k_v \, \delta\psi/\psi$

with $k_v = 0.991$. The initial cost C_I, similarly, depends on the volume of glass, giving

[7] $\delta C_I/C_I = k_I \, \delta v/v$.

Depending on the type of construction k_I may be as low as 0.1 or as high as 0.5; $k_I = 0.25$ is a reasonable point estimate. Finally,

[8] $\delta EC_F/EC_F = -k_E \, \delta\theta/\theta = k_E \, \delta\psi/\psi$

in which k_E lies between 4.75 and 6.95.

By Eqs. 4,6,7 and 8 the total cost is minimum when the equivalent lifetime failure probability P_{FC} takes the value

[9] $P_{FC}^{o} = (k_v k_I/k_E)/r$

Because of the uncertainty in k_I the value of β at optimum could be anywhere in the range from 2.78 to 3.27. Inserting the values $k_v = 0.99$, $k_I = 0.25$ and $k_E = 5.85$, and selecting $P_{FC} = 0.00135$ corresponding to $\beta = 3.0$ gives the result that P_{FC} is optimum when the failure cost ratio r equals approximately 30 (31.0 to be exact).

For most applications of glass in buildings, the failure cost ratio $r = C_F/C_I$ lies between roughly 10 and 100. Taking the value 30 as representative gives the discounted lifetime reliability index $\beta^{o}_{DL} = 3.0$. Thus, for "normal" consequences of failure β^{o}_{DL} can be chosen as 3.0.

IMPORTANCE FACTORS

In practice it is convenient to use a constant value of the resistance factor ϕ for all ordinary cases of glass in buildings. This means that the failure cost ratio $r = C_F/C_I$ must be sufficiently close to the value 30. If the actual r is less than 30 but the same value of ϕ is used, the reliability will be greater than optimum and vice versa. The importance factor γ in Eq. 1 is intended to reflect the consequences of failure in design by allowing a higher (resp. lower) value of the resistance factor, denoted by ϕ/γ, in cases when failure is of more (less) serious consequence. For a given value of the importance factor γ it is possible to determine the range of r over which this factor should be used. Moreover, it is possible to determine an appropriate value of the importance factor for structures with serious failure consequences as well as the range of r for which this factor is applicable.

Fig. 5a illustrates the situation. The required resistance is plotted along the abscissa according to an equidistant scale. Assume that γ^o is optimum for a given application, but that γ_s is specified instead. If $\gamma^o<\gamma_s$(the situation illustrated in Fig. 6a) then the light is overdesigned. Lind and Davenport (1972) have shown that there is a loss in the substitution that plots as shown by the full curve in Fig. 5a. Overdesign is associated with higher values of γ or lower values of ϕ. The loss is significantly greater in the case of overdesign, consisting mainly of material waste, than underdesign with an exponential increase in expected loss of failure. It has been shown (Lind, 1977) that the curve becomes practically parabolic when mapped into a logarithmic scale (Fig. 5b). Moreover, the parameter of the parabola is invariant (its value in absolute terms is unimportant for the argument in the following). Thus, if there are three standardized values of γ used in the standard, optimal at points 1,2 and 3 in Fig. 5c, the expected loss curve will be as shown if each is used over the

intervals indicated.

Suppose now that it has been decided to use three fixed values of the importance factor, viz. γ_1, 1.00, and γ_2. Suppose, furthermore, that the values of γ_1 and γ_2 are to be determined such that the maximum expected loss in discretization is minimized over a given interval $(\gamma_{min}, \gamma_{max})$. Then - see Fig. 5d and refer to Lind (1977) for details - this interval must be divided into six equal ratios, which gives

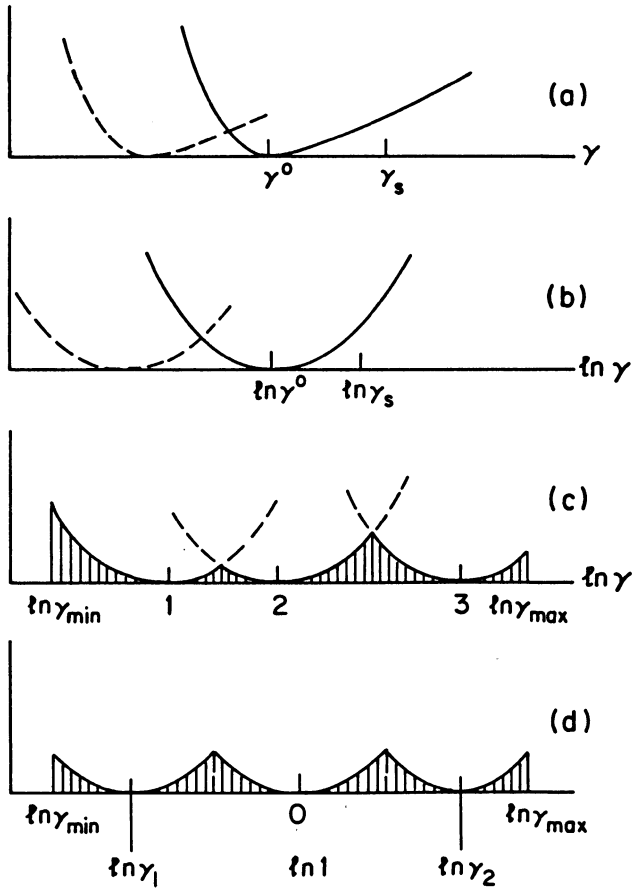

Fig. 5 Optimization of a catalog of importance factors.

[10] $\gamma_1/1.00 = 1.00/\gamma_2 = (\gamma_{min}/\gamma_{max})^{1/3}$

A reasonable value is $\gamma_1 = 0.80$ (used in NBCC(1985)); this gives $\gamma_2 = 1.25$, $\gamma_{min} = 0.72$ and $\gamma_{max} = 1.40$. It can be shown that γ_1 corresponds to $\beta_1 = 2.5$ and failure cost ratio $r_1 = 7$, while γ_2 corresponds to $\beta_2 = 3.5$ and $r_2 = 170$ approximately.

CALIBRATION

The results of this paper permit the code parameters ψ and γ to be determined for glass, given all other parameters in Eq. 1. The resistance factor follows directly from β_{DL} and the statistics of the basic random variables, see Madsen et al.(1986).

Importance factors $\gamma_1 = 0.8$ and $\gamma_2 = 1.25$ are an optimal pair appropriate, respectively, when the ratio r of the cost of failure to the initial cost lies in the interval [4,15] and [70,420].

CONCLUSIONS

The structural design of glass in buildings should ensure that the reliability of the glass over a specified design lifetime, assumed here to be dictated by the overall design life of the building (50 years) should be uniform, controlled, and predictable.

The reliability of glass in buildings, expressed in terms of a reliability index, has an optimal value that depends only on the failure cost ratio r and the dispersion of the basic random variables. The failure cost ratio is somewhat difficult to determine, but its influence on the optimal reliability index is not large. The optimal target value of the reliability index was determined to equal 3.0 for ordinary applications of structural glass in buildings.

Applications that call for values of the safety margins higher or lower than ordinary buildings occur frequently (e.g. agricultural and hospital buildings, respectively). An importance factor may be used to

take care of such situations. There will be a waste associated with importance factors that are too low as well as too high. Importance factors 0.8 and 1.25 minimize the absolute maximum value of this waste for situations of low (r = 4 to 15) and high (r= 70 to 420) consequences of failure,respectively.

ACKNOWLEDGMENTS

The work reported here is part of a study of the strength and safety of structures financially supported by the Natural Sciences and Engineering Research Council of Canada.

REFERENCES

Abiassi, J. J.(1981) "The Strength of Weathered Glass", Texas Tech. University.

CSA (Canadian Standards Association) (1981), "Guidelines for the Development of Limit States Design", CSA Special Publication S408-1981, Rexdale, ON. 34 pp.

Davenport, A. and Lind, N. C. (1987) "Calibration of a Limit States Design Standard for Glass in Buildings", IRR Paper, University of Waterloo, Institute for Risk Research (to be published).

Lind, N. C. (1977) "Rationalization of Section Properties Tables", Journal of the Structural Division, ASCE, Vol. 103, No. ST3, March 1977, pp.649-662.

Lind, N. C. (1986). "Approximate Strength Analysis for Glass Plates", Journal of Structural Engineering, ASCE, Vol. 112, No. 7, July, pp. 1704-1720.

Lind, N. C. (1987). "Calibration Basis for Structural Glass Design", Canadian Journal of Civil Engineering, (to appear).

Lind, N. C. and Davenport, A. (1972) "Towards Practical Application of Structural Reliability Theory", Proc. American Concrete Institute Symposium on Probabilistic Methods (Denver, Colorado, March 1971), Probabilistic Design of Reinforced Concrete Buildings, ACI Publ. SP-31, pp.63-110, ACI, Detroit, MI.

Madsen, H.O., Krenk, S. and Lind, N.C.(1986) Methods of Struc tural Safety, Prentice-Hall, Inc., Englewood Cliffs, N.J.

NBCC (1985) National Building Code of Canada , National Research Council, Ottawa, ON, Canada. xviii + 454 pp.; Supplement xi + 278 pp.

Ravindra, M. K. and Lind, N. C.(1982), "Trends in Safety Factor Optimization", Beams and Beam Columns, R. Narayanan (Ed.), Applied Science Publishers, London.

CONTRIBUTION TO THE IDENTIFICATION OF DOMINANT FAILURE MODES IN STRUCTURAL SYSTEMS

Yoshisada Murotsu & Satoshi Matsuzaki
Department of Aeronautical Engineering
University of Osaka Prefecture
Sakai, Osaka 591, Japan

Abstract

This paper is concerned with the extension and application of a multiplication factor method to the identification of dominant failure modes in structural systems. First, the multiplication factor method proposed for a simple limit state function consisting of two basic variables, i.e., a resistance and a load, is extended to estimate the failure probabilities of the general cases where the resistance and the load effect are expressed as linear combinations of basic random variables. Second, the proposed method is compared through numerical examples with the advanced first-order second-moment method, and its effectiveness is verified. Third, the multiplication factor method is implemented to the automatic selection of dominant failure modes in structural systems by using the branch-and-bound method. Finally, the validity of the proposed procedure is demonstrated by identifying the dominant failure modes which include the non-normal basic variables.

Key Words: Reliability Engineering, Non-normal Basic Variables, Multiplication Factor Method, Reliability Assessment, Dominant Failure Modes, Branch-and-bound Method

1. Introduction

Many studies have been done on the identification of dominant failure modes in structural systems which have linear safety margins with normal basic random variables [1-16]. In reality, the safety margins are non-linear, e.g., when interaction effect of bending moment and shearing force on yielding condition is considered

[9,10,14]. Resistances and loads which are taken as basic variables follow in many cases non-normal distributions. Nevertheless, there are few studies reported for the structures where non-linear safety margins and non-normal basic variables are included [8-10].

This paper proposes an approach to identify dominant failure modes in structural systems which have linear safety margins with non-normal basic random variables. To incorporate the non-normality of the basic variables, a transformation employed in an advanced first-order second-moment (AFOSM) method and an approximation of the basic variable at an appropriate fractile point are applied. The accuracies and computation times are compared between the proposed method and typical AFOSM algorithms. Finally, the proposed approximation method is implemented in the branch-and-bound method to identify the dominant failure modes of the structural systems. Further, numerical examples are provided to discuss the validity of the proposed method.

2. Linear Limit State Function with Non-normal Basic Variables

A linear limit state function is assumed to be expressed as follows

$$Z = g(\mathbf{X}) = \sum_{i=1}^{n+m} a_i X_i \tag{1}$$

where $X=(X_1, X_2, \cdots, X_{n+m})$ is a basic variable vector.
The basic variables X_i $(i=1,2,\cdots,n+m)$ are assumed to be independent and the following standard normalization is performed:

$$\begin{cases} \Phi(U_i) = \Phi((X_i - \mu_{X_i})/\sigma_{X_i}) = F_i(X_i) \\ (1/\sigma_{X_i}) \cdot \phi((X_i - \mu_{X_i})/\sigma_{X_i}) = f_i(X_i) \end{cases} \tag{2}$$

where $F_i(x_i)=\int_{-\infty}^{x_i} f_i(t)dt$ is the probability distribution function of X_i. The normalization parameters μ_{X_i}, σ_{X_i} are given by

$$\begin{cases} \mu_{X_i} = X_i - \sigma_{X_i} \Phi^{-1}[F_i(X_i)] \\ \sigma_{X_i} = \phi\{\Phi^{-1}[F_i(X_i)]\} / f_i(X_i) \end{cases} \tag{3}$$

Then, the limit state function is transformed into

$$Z = h(\mathbf{U}) = \sum_{i=1}^{n+m} a_i \sigma_{X_i}(X_i) U_i + \sum_{i=1}^{n+m} a_i \mu_{X_i}(X_i) \tag{4}$$

Eq.(4) becomes a non-linear function of the normalized random variables. Consequently, the β-point is to be searched. Many methods have been proposed for searching the design point. Typical methods are Rackwitz-Fiessler algorithm and the method using an optimization method. The methods give us the accurate β-values. However, they need many iterations to find the design point and thus they are time-consuming. This is not a desirable aspect when they are used to select the dominant failure modes because in that case very many safety margins are generated and failure probabilities are evaluated.

Considering this, an approximation method called " multiplication factor method " [MFM, 14] was proposed which assumes the design point based on heuristics. The basic idea and its extension are given in the following section.

3. Multiplication Factor Method

Consider a simple limit state function

$$Z = R - S \tag{5}$$

In the multiplication factor method [14], the design point is assumed to be at an appropriate fractile points of the resistance and load, i.e., $r^*=\mu_R-\delta_R\sigma_R$ and $s^*=\mu_S+\delta_S\sigma_S$, where δ_R and δ_S are taken for example to be 3.0, and $\mu_{(\cdot)}$ and $\sigma_{(\cdot)}$ are the mean and standard deviation of $(\cdot)$. Then, the non-normal basic variables R and S are normalized at the assumed β-point.

This concept is extended to a general case, where the resistance and load actions are expressed as linear combinations of non-normal basic variables:

$$Z = \sum_{i=1}^{n} a_i X_i + \sum_{j=n+1}^{n+m} a_j X_j \tag{6}$$

In Eq.(6), the terms with positive coefficients are aggregated in the the first term, i.e., $a_i>0$ $(i=1,2,\cdots,n)$ and those with negative coefficients in the second term, i.e., $a_i<0$ $(i=n+1,\cdots,n+m)$. This means that the first term corresponds to the resistance and the second term to the load. Consequently, they are expressed as

$$R = \sum_{i=1}^{n} a_i X_i, \qquad S = -\sum_{j=n+1}^{n+m} a_j X_j \tag{7}$$

The means and variances of R and S are calculated as

$$\begin{cases} \mu_R = \sum_{i=1}^{n} a_i \mu_i , & \mu_S = -\sum_{j=n+1}^{n+m} a_j \mu_j \\ \sigma_R^2 = \sum_{i=1}^{n} a_i^2 \sigma_i^2 , & \sigma_S^2 = \sum_{j=n+1}^{n+m} a_j^2 \sigma_j^2 \end{cases} \tag{8}$$

where μ_k and σ_k are the mean and standard deviation of X_k.
The design points r^* and s^* of the aggregated resistance and load actions are assumed to be given in the same way as in the simple case, i.e.,

$$r^* = \mu_R - \delta_R \cdot \sigma_R , \quad s^* = \mu_S + \delta_S \cdot \sigma_S \tag{9}$$

Eq.(9) is satisfied if the design points x_i^* (i=1,2,$\cdots$,n) and x_j^* (j=n+1, $\cdots$,n+m) of the componental resistances and loads are taken to be

$$\begin{cases} x_i^* = \mu_i - \alpha_R \cdot \sigma_i & (i=1,2,\cdots,n) \\ x_j^* = \mu_j + \alpha_R \cdot \sigma_j & (j=n+1,\cdots,n+m) \end{cases} \tag{10}$$

where

$$\begin{cases} \alpha_R = \delta_R \cdot \sigma_R \ / \ (\sum_{i=1}^{n} a_i \sigma_i) \\ \alpha_S = \delta_S \cdot \sigma_S \ / \ (-\sum_{j=n+1}^{m} a_j \sigma_j) \end{cases} \tag{11}$$

Then, the non-normal basic variables are normalized at the assumed design points, i.e., Eq.(10). The resulting β-value is given by

$$\beta = \frac{\sum_{i=1}^{n} a_i \mu_{X_i} + \sum_{j=n+1}^{n+m} a_j \mu_{X_j}}{\sqrt{\sum_{i=1}^{n+m} a_i^2 \sigma_{X_i}^2}} \tag{12}$$

where

$$\begin{cases} \mu_{X_k} = x_k^* - \sigma_{X_k} \Phi^{-1} [F_k(x_k^*)] \\ \sigma_{X_k} = \phi \{ \Phi^{-1} [F_k(x_k^*)] \} \ / \ f_k(x_k^*) \end{cases} \quad (k=i,j)$$

The failure probability is evaluated by

$$P_f = \Phi(-\beta) \tag{13}$$

4. Comparison between MFM and AFOSM

The accuracies and computation times are compared among the MFM and two AFOSM algorithms, i.e., multiplier method [17] and Rackwitz-Fiessler method [18]. The failure modes and their limit state functions are given in Fig. 1 and Table 1. The numbers in the rows (a), (b) and (c) correspond to the results of the three limit state functions. The columns indicate those corresponding to the different combinations of distribution for the resistances and loads. The first number in the bracket of IPD shows the type of distribution for the resistances, and the second shows that for the loads. The numbers indicate 1: normal distribution, 2: log-normal distribution, 3: Weibull distribution, and 4: Gumbel distribution. It is observed that the two AFOSM methods give almost the same values and the results of the multiplication factor method are fairly accurate. The computation times are one or two order of magnitude smaller in case of the MFM.

5. Identification of Dominant Failure Modes

The multiplication factor method extended in the previous section is applied to identify dominant failure modes of structural systems when basic variables are non-normally distributed. The safety margins are generated, considering only the effect of bending moment on plasticity condition of the sections [3,14]. The branch-and-bound method combined with the heuristic method is applied to select the dominant failure paths, where the one-dimensional branching is adopted [6,14].

5.1 One-bay two-storied frame structure

Consider a frame structure shown in Fig. 2. The numerical data are listed in Table 2. The coefficients of variation for the resistances and loads are 0.05 and 0.30, respectively. The types of distribution are log-normal for the resistances and Gumbel for the loads. The selected failure modes and their failure probabilities are

given in Table 3. The numbers of the selected failure paths are shown in the brackets. The total computation time is 185.8 sec by using ACOS 850 at the Computer Center, University of Osaka Prefecture. The failure probabilities evaluated by the AFOSM using the multiplier method and their computation times are listed in the table.

It is noticed that although the numerical values of the failure probabilities are slightly different between the MFM and the AFOSM, the relative order of the failure probabilities are almost the same. This is a desirable aspect of the MFM to be used for selecting the dominant failure modes because in that case only the ordering of the failure modes is important and the accurate values of the failure probabilities may be evaluated afterwards by using the more advanced method. It is also noted that the computation time is very short when the MFM is used.

5.2 Asymmetric two-bay two-storied structure

Consider a structural system shown in Fig. 3. The numerical data are listed in Table 4. The types of distribution are Weibull for the resistances and Gumbel for the loads. The selected dominant failure modes and their failure probabilities are given in Table 5, where the failure probabilities evaluated by the AFOSM and their computation times are also given. The similar conclusion is drawn in this example as stated in the previous example.

6. Conclusions

(1) The multiplication factor method (MFM) has been extended to evaluate the failure probabilities when the limit state functions are expressed as linear combinations of non-normal basic variables.

(2) The MFM has been compared through numerical examples with the two AFOSM algorithms, i.e., Rackwitz-Fiessler algorithm and that by using a multiplier method. It is concluded that the MFM is fairly good in its accuracies and computationally efficient. Another important aspect of the MFM is that the

relative order of the failure probabilities of the different failure modes does not change although the magnitudes are sometimes different from those of the AFOSM.

(3) The MFM has been successfully applied to identify the dominant failure modes of the structural systems when the basic variables are non-normally distributed.

References

[1] Murotsu, Y., Okada, H,. Niwa, K. and Miwa, S : A New Method for Evaluating Lower and Upper Bounds of Failure Probability in Redundant Truss Structures. Bull. Univ. Osaka Pref., Ser. A, 28, 1 (1979), pp. 79-91.

[2] Murotsu, Y., Okada, H., Niwa, K. and Miwa, S : Reliability Analysis of Truss Structures by Using Matrix Method. Trans. of the ASME, J. Mechanical Design, 102, 4(1980), pp. 749-756.

[3] Murotsu, Y., Okada, H., Yonezawa, M and Taguchi, K : Reliability Assessment of Redundant Structures. Structural Safety and Reliability (ed. Moan, T. and Shinozuka, M.), Elsevier (1981), pp. 315-329.

[4] Thoft-Christensen, P. and Sorensen, J. D. : Calculation of Failure Probabilities of Ductile Structures by the β-unzipping Method. Institute of Building Technology and Structural Engineering, Aalborg, Report 8208, 1982.

[5] Murotsu, Y. : Reliability Analysis of Frame Structure through Automatic Generation of Failure Modes. Reliability Theory and Its Application in Structural and Soil Mechanics (ed. Thoft-Christensen, P.), Martinus Nijihoff, 1982, pp. 525-540.

[6] Murotsu, Y., Okada, H., Yonezawa, M. and Kishi, M. : Identification of Stochastically Dominant Failure Modes in Frame Structure. Proc. 4th Int. Conf. Appl. Stat. and Prob. in Soil and Struc. Eng., Universita di Firenze (Italy). Pitagora Editrice, 1983, pp. 1325-1338.

[7] Moses,F and Rashedi, M. R. : The Application of System Reliability to Structural Safety. Proc. 4th Int. Conf. on Appl. of Statistics and Probability in Soil and Structural Mechanics, Universita di Firenze (Italy). Pitagora Editrice, Blogna, 1983, pp. 573-584.

[8] Grimmelt, M. J., Schueller, G. I. and Murotsu, Y. : On the

Evaluation of Collapse Probabilities. Chen, W. F. and Lewis, A. D. M. (ed.), Recent Advances in Engineering Mechanics and Their Impact On Civil Engineering Practice, Proc. 4th ASCE-EMD Specialty Conf., Purdue University, 1983, pp. 859-862.

[9] Crohas, H., Tai, A., Hachemi, V. and Barnoin, B. : Reliability of Offshore Structures under Extreme Environmental Loading. OTC Conference Paper 4826, 1984.

[10] Baadshaug, O. and Bach-Gansmo, O. : System Reliability Analysis of Jacket Structure. Structural Safety and Reliability (eds. Konishi, I., et al.), Vol.II, IASSAR, 1985, PP.613-617.

[11] Ditlevsen, O. and Bjerager, P. : Reliability of Highly Redundant Plastic Structures. J. Engrg. Mech., ASCE, Vol. 10, EM-5 (1984), pp. 671-693.

[12] Melchers, R. E. and Tang, T. K. : Dominant Failure Modes in Stochastic Structural Systems. Structural Safety, 2, 1984, pp. 127-143.

[13] Bennett, R. M. : Reliability Analysis of Frame Structures with Brittle Components. Structural Safety, 2, 1985, pp. 281-290.

[14] Thoft-Christensen, P., and Murotsu, Y. : Application of Structural Systems Reliability Theory, Springer Verlag, Berlin (West) ,1986.

[15] Murotsu, Y. : Development in Structural Systems Reliability Theory. Nuclear Engineering and Design, 94, 1986, pp. 101-114.

[16] Murotsu, Y., Matsuzaki, S. and Okada, H. : Automatic Generation of Stochastically Dominant Failure Modes for Large-scale Structures. JSME International Journal, Vol. 30, No. 260, 1987, pp. 234-241.

[17] Murotsu, Y., Yonezawa, M., Okada, H., Matsuzaki, S. and Matsumoto, T. : A Study on First-Order Second-Moment Methods in Structural Reliability. Bulletin of University of Osaka Prefecture, Series A, Vol. 33, No. 1, 1984, pp. 23-26.

[18] Rackwitz, R. and Fiessler, B. : An Algorithm for Calculation of Structural Reliability under Combined Loading. Berichte zur Sicherheitstheorie der Bauwerke, Lab. f. Konstr. Ingb., Techn. Univ. Munchen, Munchen, 1977.

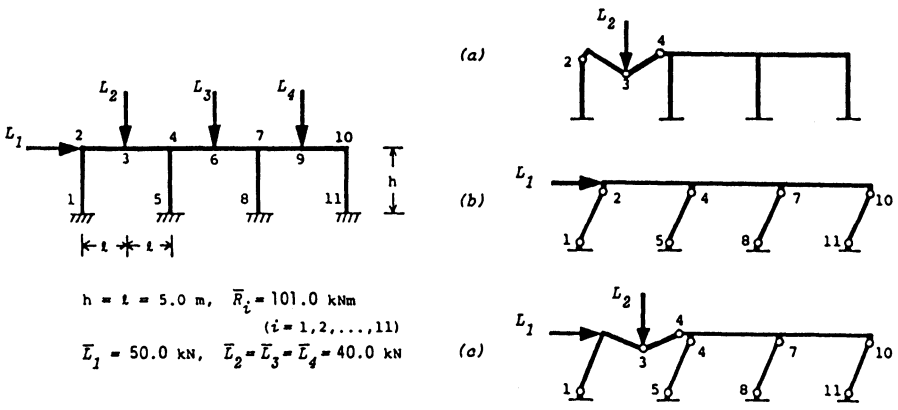

Fig. 1 Failure modes and numerical data

Table 1 Comparison between MFM and AFOSM

	Failure probability P_f				
	IPD[1,1]	*method*	IPD[3,1]	IPD[1,4]	IPD[3,4]
(a)#	0.1916×10^{-2} (0.781×10^{-3}) *FOSM method*	*AFOSM method (Multiplier method)*	0.1951×10^{-2} (0.168×10^{1})*	0.9371×10^{-2} (0.110×10^{1})	0.8462×10^{-2} (0.317×10^{1})
		AFOSM method (R-F method)	0.1951×10^{-2} (0.118×10^{1})	0.9371×10^{-2} (0.980×10^{0})	0.8462×10^{-2} (0.588×10^{0})
		Multiplication factor method	0.1765×10^{-2} (0.305×10^{-1})	0.9371×10^{-2} (0.916×10^{-2})	0.7279×10^{-2} (0.376×10^{-1})
(b)	0.5236×10^{-10} (0.640×10^{-3}) *FOSM method*	*AFOSM method (Multiplier method)*	0.7664×10^{-10} (0.154×10^{1})	0.5189×10^{-4} (0.817×10^{0})	0.4280×10^{-4} (0.361×10^{1})
		AFOSM method (R-F method)	0.7664×10^{-10} (0.199×10^{1})	0.5190×10^{-4} (0.177×10^{1})	0.4280×10^{-4} (0.874×10^{0})
		Multiplication factor method	0.7297×10^{-10} (0.455×10^{-1})	0.9819×10^{-5} (0.909×10^{-2})	0.6527×10^{-5} (0.523×10^{-1})
(c)	0.2568×10^{-6} (0.687×10^{-3}) *FOSM method*	*AFOSM method (Multiplier method)*	0.2883×10^{-6} (0.148×10^{1})	0.9657×10^{-4} (0.324×10^{1})	0.7737×10^{-4} (0.110×10^{2})
		AFOSM method (R-F method)	0.2883×10^{-6} (0.264×10^{1})	0.9658×10^{-4} (0.985×10^{1})	0.7737×10^{-4} (0.352×10^{1})
		Multiplication factor method	0.2542×10^{-6} (0.453×10^{-1})	0.4142×10^{-4} (0.992×10^{-2})	0.2800×10^{-4} (0.530×10^{-1})

Limit state function : Z , CV_{R_i}/CV_{L_j} = 0.15/0.30

(a) Beam mechanism : $Z = R_2 + 2R_3 + R_4 - 2L_2$

(b) Side sway mechanism : $Z = R_1 + R_2 + R_4 + R_5 + R_7 + R_8 + R_{10} + R_{11} - hL_1$

(c) Combined mechanism : $Z = R_1 + 2R_3 + 2R_4 + R_5 + R_7 + R_8 + R_{10} + R_{11} - hL_1 - 2L_2$

* The figure in parenthesis designates computation time (sec).

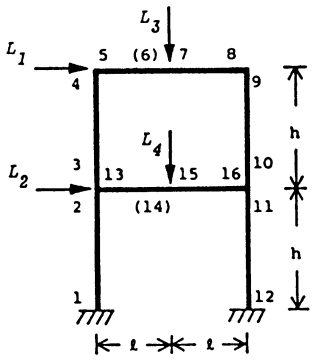

Fig. 2 One-bay two-storied frame

Table 2 Numerical data of one-bay two-storied frame

Element end number	*Cross sectional area* $A_{pi} = A_i$ m^2	*Moment of inertia* I_i m^4	*Mean value of reference strength* $\bar{R}_i$ kNm
1, 2 3, 4 9, 10 11, 12	3.60×10^{-3}	2.58×10^{-5}	76.1
5, 6 7, 8 13, 14 15, 16	4.40×10^{-3}	3.70×10^{-5}	99.8

Young's modulus E = 210 GPa
Mean value of yield stress $\bar{\sigma}_{yi}$ = 276 MPa
Correlation coeff. $\rho_{L_iL_j} = 0.0$ $\rho_{R_kR_l} = 0.0$

Table 3 Selected failure modes and their failure probabilities (one-bay two-storied frame)

$\gamma = 1.0$, $\varepsilon^{\#} = 0.0$, $CV_{R_i}/CV_{L_j} = 0.05/0.30$, IPD[2,4]

Failure mode No.	*Failure probability* P_{fq} ## *Multiplication factor method*	P_f *AFOSM method* **(*Off-line time* (sec))
1@ (1,4,9,12,13,16)	0.1182×10^{-1} [27]*	0.1489×10^{-1} (0.88)**
2 (1,5,9,12,13,16)	0.7499×10^{-2} [13]	0.9819×10^{-2} (1.00)
3 (1,4,8,12,13,16)	0.7499×10^{-2} [22]	0.9819×10^{-2} (1.00)
4 (1,2,11,12)	0.5901×10^{-2} [63]	0.7500×10^{-2} (1.62)
5 (1,4,9,12,15,16)	0.5542×10^{-2} [36]	0.7513×10^{-2} (2.14)
6 (1,7,9,12,13,16)	0.5511×10^{-2} [47]	0.7492×10^{-2} (2.11)
7 (1,5,8,12,13,16)	0.4634×10^{-2} [14]	0.6467×10^{-2} (1.17)
8 (1,2,3,4,9,12,16)	0.4146×10^{-2} [9]	0.5906×10^{-2} (1.23)
9 (1,4,9,10,11,12,13)	0.4146×10^{-2} [4]	0.5906×10^{-2} (1.24)
10 (1,5,9,12,15,16)	0.3451×10^{-2} [22]	0.4977×10^{-2} (2.45)
11 (1,4,8,12,15,16)	0.3451×10^{-2} [16]	0.4977×10^{-2} (2.45)
12 (1,7,9,12,15,16)	0.2696×10^{-2} [49]	0.3822×10^{-2} (2.64)
13 (1,2,3,4,8,12,16)	0.2482×10^{-2} [2]	0.3886×10^{-2} (1.21)
14 (1,4,8,10,11,12,13)	0.2482×10^{-2} [9]	0.3886×10^{-2} (1.20)
15 (1,5,9,10,11,12,13)	0.2482×10^{-2} [4]	0.3886×10^{-2} (1.20)
16 (1,7,8,12,13,16)	0.2098×10^{-2} [13]	0.3292×10^{-2} (2.28)
17 (1,5,8,12,15,16)	0.2098×10^{-2} [16]	0.3292×10^{-2} (2.28)
18 (1,2,3,7,9,12,16)	0.1861×10^{-2} [15]	0.3000×10^{-2} (2.59)
19 (1,7,9,10,11,12,13)	0.1861×10^{-2} [19]	0.3000×10^{-2} (2.58)
20 (4,7,9)	0.1612×10^{-2} [68]	0.1891×10^{-2} (0.78)
21 (1,5,8,10,11,12,13)	0.1447×10^{-2} [9]	0.2556×10^{-2} (1.23)
Computation time (sec) ACOS 850	185.8$	T_{AFOSM} (35.3)

\# Criterion of structural failure is based on singularity of reduced total structure stiffness matrix.

* The figure in brackets designates the number of selected failure modes.

$ The element end which has safety factor greater than 5.0 is discarded.

$$ Branching operation is based on one-dimensional branching.

$P_{fq} = P[z_{r_{pq}}^{(pq)} \leq 0]$

@ Failure mode ; The failure of the element end is governed simply by the bending moment.

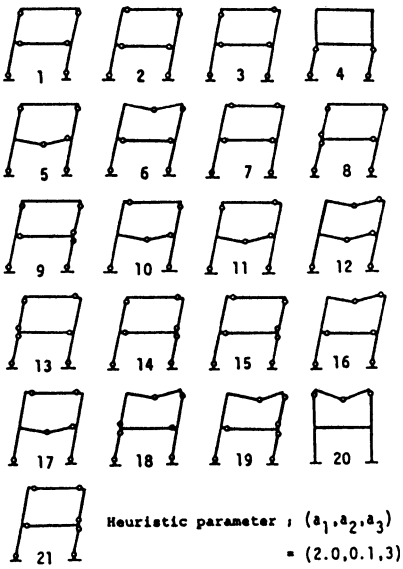

Heuristic parameter ; $(a_1, a_2, a_3) = (2.0, 0.1, 3)$

Heuristic operation.

$$I_p = (i_{p_1} \mid P[z_{i_p}^{(p)} \leq 0] \leq a_1 \cdot P[z_{r_{p-1}}^{(p-1)} \leq 0])$$

$$I_p = (i_{p_2} \mid a_{i_p r_1}^{(p)} \geq a_2)$$

The number of branchings from one failure stage is limited to a_3.

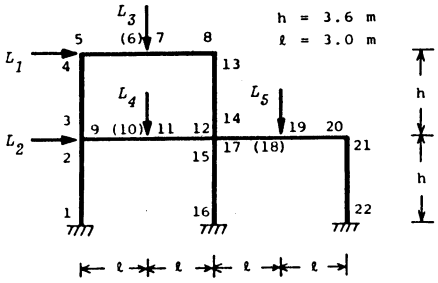

$\bar{L}_1$ = 31.0 kN $\quad \bar{L}_4$ = 140.0 kN

$\bar{L}_2$ = 62.0 kN $\quad \bar{L}_5$ = 112.0 kN

$\bar{L}_3$ = 89.0 kN

Fig. 3 Asymmetric two-bay two-storied frame

Table 4 Numerical data of asymmetric two-bay two-storied frame

Element end number	*Cross sectional area* $A_{pi} = A_i$ m^2	*Moment of inertia* I_i m^4	*Mean value of reference strength* $\bar{R}_i$ kNm
1, 2 3, 4 13, 14 15, 16 21, 22	4.60×10^{-3}	3.36×10^{-5}	95.0
5, 6 7, 8	4.80×10^{-3}	6.96×10^{-5}	122.0
9, 10 11, 12	6.80×10^{-3}	13.82×10^{-5}	204.0
17, 18 19, 20	5.40×10^{-3}	8.54×10^{-5}	163.0

Young's modulus E = 210 GPa

Mean value of yield stress $\bar{\sigma}_{yi}$ = 276 MPa

Correlation coeff. $\rho_{L_iL_j}$ = 0.0 $\quad \rho_{R_kR_l}$ = 0.0

Table 5 Selected failure modes and their failure probabilities (asymmetric two-bay two-storied frame)

γ = 1.0, $\varepsilon^{\#}$ = 0.0, CV_{R_i}/CV_{L_j} = 0.05/0.30, IPD[3,4]

Failure mode No.	*MF method* *Failure probability* P_{fq}		*AFOSM method* *Failure probability* P_f	*(Off-line time (sec))* **
1@ (4,7,13)	0.2935×10^{-1}	[15]*	0.3682×10^{-1}	(4.51)**
2 (5,7,13)	0.1990×10^{-1}	[13]	0.2403×10^{-1}	(4.90)
3 (4,7,8)	0.1990×10^{-1}	[1]	0.2403×10^{-1}	(4.90)
4 (17,19,21)	0.1891×10^{-1}	[19]	0.2291×10^{-1}	(4.98)
5 (5,7,8)	0.1318×10^{-1}	[1]	0.1564×10^{-1}	(5.07)
6 (2,3,11,12)	0.9304×10^{-2}	-	0.1103×10^{-1}	(4.71)
7 (17,19,20)	0.8061×10^{-2}	[25]	0.9687×10^{-2}	(5.18)
8 (9,11,12)	0.7975×10^{-2}	[260]	0.9589×10^{-2}	(4.62)
9 (3,7,13,14)	0.6874×10^{-2}	[4]	0.1084×10^{-1}	(7.50)
10 (2,7,11,12,13,14)	0.4376×10^{-2}	[91]	0.7288×10^{-2}	(14.1)
11 (1,3,11,12,15,16, 21,22)	0.4132×10^{-2}	[51]	0.7409×10^{-2}	(12.2)
12 (1,2,15,16,21,22)	0.4066×10^{-2}	[76]	0.6293×10^{-2}	(9.71)
13 (1,7,11,12,13,14, 15,16,21,22)	0.3445×10^{-2}	[13]	0.5490×10^{-2}	(17.6)
Computation time (sec) ACOS 850		734.7$	Σ_{AFOSM}	(100.0)

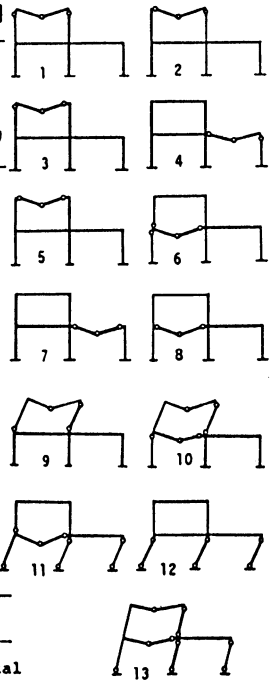

\# Criterion of structural failure is based on singularity of reduced total structure stiffness matrix.

* The figure in brackets designates the number of selected failure modes.

$ The element end which has safety factor greater than 5.0 is discarded.

$$ Branching operation is based on one-dimensional branching.

@ Failure mode ; The failure of the element end is governed simply by the bending moment.

RELIABILITY ESTIMATES BY QUADRATIC APPROXIMATION OF THE LIMIT STATE SURFACE

Arvid Naess
Department of Civil Engineering
The Norwegian Institute of Technology
N-7034 Trondheim

The limit state surface in normalized Gaussian space is approximated at the design point by a quadratic surface. For an approximation of this type, the calculation of the reliability amounts to determining the probability distribution of a quadratic form in Gaussian variables. Simple, closed-form expressions for the probability distributions of a specific type of quadratic forms in Gaussian variables is used to obtain reliability estimates for two classes of quadratic approximations to the limit state surface.

INTRODUCTION.

In this paper the problem of structural reliability is formulated in terms of a set of random parameters that are assumed to determine the state of a given structural facility. It is assumed that the parameter space can be divided into two disjoint sets separated by a surface. For the parameter values in one of these sets, the structure is assumed to be in an intact, unfailed condition. This set is called the safe set or the set of safe states. Similarly, the parameter values in the other set corresponds to a condition of failure or damage, and the set is consequently called the failure set or the set of failed states. The surface separating the safe set and the failure set is called the limit state surface or the failure surface. The reliability of the structure is understood here to mean the probability that the state of the structure is safe, i.e. the vector of random parameters describing the system has a value belonging to the safe set.

The difficulty of calculating the reliability in a particular case, depends very much on the geometry of the limit state surface. A practical calculation of the reliability often depends on replacing the original limit state surface with one of simpler geometry. This simplification is usually carried out after the problem has been transferred to a normalized Gaussian space, by a suitable transformation of the initial random parameters. In this paper we shall study reliability estimates obtained by replacing the given limit state surface by an approximate quadratic surface.

THE RELIABILITY PROBLEM.

It is assumed here that the problem of structural reliability can be formulated in terms of a safety margin or safety function of a set of random influencing parameters. Specifically, let $X_1, \ldots, X_n$ denote the set of influencing parameters. It is then assumed that a safety function g can be found so that $g(\underset{\sim}{X}) = g(X_1, \ldots, X_n)$ expresses the state of the structural system under study. When $g(\underset{\sim}{X}) > 0$, the system is in a safe state, while the system fails for $g(\underset{\sim}{X}) < 0$. The states satisfying $g(\underset{\sim}{x}) = 0$ are called limit states, and the set of points in R^n (n-dimensional Euclidean space) where $g(\underset{\sim}{x}) = 0$ is called the limit state surface or the failure surface.

Let D_s denote the set of safe states. The reliability of the structure, P_s, is then identified with the probability that the vector of influencing parameters, $\underset{\sim}{X}$, belongs to the safe set D_s. Then

$$P_s = \text{Prob}\{\underset{\sim}{X} \in D_s\} = \text{Prob}\{g(\underset{\sim}{X}) > 0\} \qquad (1)$$

The probability of failure, P_f, is defined by $P_f = 1 - P_s$. If $f_{\underset{\sim}{X}}$ denotes the joint probability density function (jpdf) of the random vector $\underset{\sim}{X}$, P_s can be expressed as

$$P_s = \int_{D_s} f_{\underset{\sim}{X}}(x_1, \ldots, x_n)\, dx_1 \ldots dx_n \qquad (2)$$

For the subsequent developments it is convenient to consider the random vector $\underset{\sim}{X}$ to belong to a normalized Gaussian space i.e. the components $X_1, \ldots, X_n$ are independent N(0,1)-variables. This can be achieved by suitably transforming the initial random vector, see e.g. reference [1]. In the following it is assumed that this transformation has been carried out, so that $\underset{\sim}{X}$ denotes a vector in normalized Gaussian space.

A direct calculation of the reliability P_s by using equation (2) now amounts to integrating a multidimensional Gaussian density over the safe set D_s. The boundary of D_s, which equals the limit state surface, is therefore usually approximated by simple surface geometries to facilitate the estimation of the integral in equation (2). Since we are in a normalized Gaussian space, it is clear that the the point on the limit state surface with the shortest distance to the origin is of of particular interest. Let $\underset{\sim}{x}^*$ denote this point. $\underset{\sim}{x}^*$ will be referred to as the design point. The length $\|\underset{\sim}{x}^*\|$, which equals the distance from the origin to the design point, is called the Hasofer - Lind reliability index, denoted here by β, i.e. $\beta = \|\underset{\sim}{x}^*\|$.

QUADRATIC APPROXIMATION OF THE LIMIT STATE SURFACE.

Assuming that the limit state surface $g(\underset{\sim}{x}) = 0$ is sufficiently smooth in the vicinity of the design point $\underset{\sim}{x}^*$, a Taylor expansion of $g(\underset{\sim}{x})$ gives

$$g(\underset{\sim}{x}) = g(\underset{\sim}{x}^*) + \underset{\sim}{g}_x^T (\underset{\sim}{x}-\underset{\sim}{x}^*) + \frac{1}{2} (\underset{\sim}{x}-\underset{\sim}{x}^*)^T G_x (\underset{\sim}{x}-\underset{\sim}{x}^*) + .. \qquad (3)$$

where $\underset{\sim}{g}_x^T$ denotes the vector $(\frac{\partial}{\partial x_i} g(\underset{\sim}{x}^*))_{i=1}^n$ and G_x denotes the matrix

$(\frac{\partial}{\partial x_i \partial x_j} g(\underset{\sim}{x}^*))_{i,j=1}^n$. The notation $\underset{\sim}{x}$ indicates a column vector, $\underset{\sim}{x}^T$ its transposed.

The simplest approximation to the limit state surface is obtained by retaining the first two terms on the rhs of equation (3). This gives a hyperplane through the design point, and the resulting approximation is usually referred to as a first order reliability method (FORM). The FORM estimate of the reliability is clearly $\Phi(\beta)$, where Φ denotes the cdf of an N(0,1)-variable (only one design point is assumed).

In second order reliability methods (SORM), also the third term on the rhs of equation (3) is included. This complicates considerably the evaluation of the corresponding reliability, which is equivalent to establishing the probability distribution of a general non-homogeneous quadratic form in Gaussian variables. Since this is not available, the integral in equation (3) must be evaluated numerically for a general quadratic safe domain D_s. Several numerical methods have been developed for this purpose. The one developed by Rice [2] is mentioned in particular. A procedure described by Deak [3] for estimating the probability content in regions of Gaussian space, has been further developed and applied to reliability problems by several authors, see for example references [4,5].

In this paper we shall investigate two particular quadratic approximations to the limit state surface at the design point $\underset{\sim}{x}^*$. To get a convenient representation of these approximations, the original coordinate system (X) is rotated into a new system (Y) so that the design point has the coordinates $(\beta, 0, \ldots, 0)$. The first approximation, called hyperparabolic, is then given by [6]

$$y_1 - \beta + \hat{\underset{\sim}{y}}^T A \hat{\underset{\sim}{y}} = 0 \quad . \qquad (4)$$

The second approximation is called hyperellipsoidal, and is given by [6]

$$\lambda_1 (y_1-\delta_1)^2 + \hat{\underset{\sim}{y}}^T B \hat{\underset{\sim}{y}} = 1 \quad (\lambda_1 > 0) \qquad (5)$$

Here A and B are symmetric matrices of order n-1 and $\hat{\underset{\sim}{y}} = (y_2, \ldots, y_n)^T$. By another orthogonal transformation (rotation) leaving the y_1-axis fixed, a new coordinate system (Z) with coordinates $z_1 = y_1, z_2, \ldots, z_n$ can be obtained so that equations (4) and (5) take the form

$$z_1 - \beta + \sum_{j=2}^{n} \lambda_j z_j^2 = 0 \tag{6}$$

and

$$\lambda_1(z_1-\delta_1)^2 + \sum_{j=2}^{n} \lambda_j z_j^2 = 1 \tag{7}$$

In equation (6) (respectively equation (7)) the λ_j's are the eigenvalues of A (respectively B). For the approximation of equation (7), it is found that $\beta = \delta_1 - 1/\sqrt{\lambda_1}$ when $\beta < \delta_1$, while $\beta = \delta_1 + 1/\sqrt{\lambda_1}$ when $\beta > \delta_1$. Having assumed that the design point has coordinates $(\beta, 0, \ldots, 0)$, which lies on the positive part of the z_1-axis, it is seen that if the original limit state surface is replaced by the quadratic surface given by equation (7) and if $\beta > \delta_1$, then $\delta_1 < 0$.

Let $\underset{\sim}{Z} = (Z_1, \ldots, Z_n)^T$ denote a vector in normalized Gaussian space, and introduce the random variable U by

$$U = Z_1 + \sum_{j=2}^{n} \lambda_j Z_j^2 \quad . \tag{8}$$

The SORM estimate of the reliability corresponding to the hyperparabolic approximation of the limit state surface at the design point is then given by $P_s = \text{Prob}\{U < \beta\} = F_U(\beta)$. F_U denotes the cdf of the random variable U.

Similarly, a random variable V is introduced by

$$V = \lambda_1(Z_1 - \delta_1)^2 + \sum_{j=2}^{n} \lambda_j Z_j^2 \quad . \tag{9}$$

It then follows that the SORM estimate of the reliability associated with the hyperellipsoidal approximation of the limit state surface is obtained as $P_s = \text{Prob}\{V > 1\} = 1 - F_V(1)$ if $\delta_1 > \beta$, and $P_s = \text{Prob}\{V < 1\} = F_V(1)$ if $\delta_1 < \beta (\delta_1 < 0)$. F_V denotes the cdf of V. In the first case ($\delta_1 > \beta$), the interior of the ellipsoid corresponds to the failure set, while in the second case ($\delta_1 < 0$), the interior corresponds to the safe set.

To calculate the reliability associated with the two classes of quadratic approximations to the limit state surface that have been discussed above, it is

necessary to determine the cdf F_U and F_V. In the general case, these functions are not available as closed-form expressions. However, a very neat asymptotic formula for estimating the reliability of quadratic safe sets has been given by Breitung [7]. In the case of a single design point, it takes the form

$$P_f \sim \Phi(-\beta) \prod_{j=2}^{n} (1-\beta\,\kappa_j)^{-1/2}, \quad (\beta \to \infty) \quad . \tag{10}$$

Here κ_j, j=2, ..., n, are the main curvatures of the limit state surface at $\underset{\sim}{x}^*$. In the hyperparabolic case, $\kappa_j = 2\lambda_j$. In the hyperellipsoidal case, $\kappa_j = \lambda_j/\sqrt{\lambda_1}$. Despite its simplicity, the Breitung formula seems to be reasonably accurate except for small β and when one of the factors $\beta\,\kappa_j (< 1.0)$ is close to 1.0.

An alternative approach, which cannot compete with equation (10) in simplicity, but which has the advantage of providing exact solutions in a wide range of cases, has been described in reference [8]. There a class of special-case, closed-form expressions for the cdf of quadratic forms in normalized Gaussian variables is exploited to establish upper and lower bounds on the general F_U and F_V.

The upper and lower bounds coalesce in the case when the eigenvalues λ_j, j=2, ..., n, are pairwise equal. Specifically, assume that n = 2N + 1 and $\nu_j = \lambda_{2j} = \lambda_{2j+1}$, j=1, ..., N. Provided that none of the ν_j are equal, which can be arranged in most practical situations by a slight change in numerical values if necessary, it can be shown that [8]

$$P_f = 1 - F_U(\beta) = \Phi(-\beta) + \sum_{j=1}^{N} \operatorname{sign}(\nu_j)\, k_j \exp\!\left(-\frac{1}{2\nu_j}\left(\beta - \frac{1}{4\nu_j}\right)\right) \Phi\!\left[\operatorname{sign}(\nu_j)\left(\beta - \frac{1}{2\nu_j}\right)\right] \tag{11}$$

Here $\operatorname{sign}(\nu_j) = +1$ if $\nu_j > 0$, $= -1$ if $\nu_j < 0$ and

$$k_j = \prod_{\substack{i=1 \\ i \neq j}}^{N} \left(1 - \frac{\nu_i}{\nu_j}\right)^{-1} \tag{12}$$

In the general case equation (11) can be used to establish upper and lower bounds on the reliability. Assume that $\lambda_2 \geq \lambda_3 \geq \ldots \geq \lambda_n$ and n = 2N + 1. The case n=2N is discussed in reference [8]. Let $\nu_j = \lambda_{2j+1}$ and $\mu_j = \lambda_{2j}$, j = 1,...,N, and introduce the random variables $U_1 = \sum_{j=1}^{N} \nu_j R_j^2$ and $U_2 = \sum_{j=1}^{N} \mu_j R_j^2$, where $R_j^2 = z_{2j}^2 + z_{2j+1}^2$ is a χ^2-variable with 2 degrees of freedom. Then $U_1 \leq U \leq U_2$, and $F_{U_1}(\beta) \geq F_U(\beta) \geq F_{U_2}(\beta)$, where $F_{U_1}(\beta)$ and $F_{U_2}(\beta)$ are obtained by using equation (11).

The hyperellipsoidal failure surface is more complicated to deal with than the hyperparabolic case. For the sake of simplicity, we shall here limit the discussion to two particular cases. The general case is analysed in reference [8]. Firstly, assume $\delta_1 > 0$, which implies $\delta_1 > \beta$, and $\lambda_j < 0$ for each $j=2,..,n$. In the situation at hand here the quadratic surface given by equation (7) has two disconnected components, and only the component containing the design point is retained. In the instance of pairwise equal eigenvalues $v_j=\lambda_{2j}=\lambda_{2j+1}$, $j = 1,...,N$, it can be shown that [8]

$$P_f = F_V(1) = \Phi(-\beta) + \sum_{j=1}^{N} \frac{k_j}{\sqrt{a_j \lambda_1}} \exp\left\{\frac{1}{2|v_j|}\left(1 - \frac{\delta_1^2}{a_j}\right)\right\} \Phi\left(-\sqrt{a_j} + \frac{\delta_1}{\sqrt{a_j \lambda_1}}\right) \qquad (13)$$

In addition to the notation previously introduced,

$$a_j = \frac{1}{|v_j|} + \frac{1}{\lambda_1} \qquad (14)$$

For the second case, assume $\delta_1 = 0$, i.e. $\beta = 1/\sqrt{\lambda_1}$, $\lambda_1 > \lambda_j > 0$, $j = 2,...,n$. For pairwise equal eigenvalues $v_j = \lambda_{2j} = \lambda_{2j+1}$, $j = 1,...,N$, it can be shown that [8] (note that there are two design points, at $\pm 1/\sqrt{\lambda_1}$)

$$P_f = 1 - F_V(1) = 2\Phi(-\beta) + \sum_{j=1}^{N} \frac{k_j}{\sqrt{2\lambda_1}} \exp\left\{-\frac{1}{2v_j}\right\} \gamma^*\left(\frac{1}{2} ; -\frac{1}{2} a_j\right) \qquad (15)$$

$\gamma^*(a ; x) = x^{-a} \Gamma(a)^{-1} \gamma(a ; x)$ where $\gamma(a ; x)$ is the incomplete gamma function and $\Gamma(a) = \gamma(a ; \infty)$ is the gamma function [9]. Values of $\gamma^*(1/2 ; -x)$ have been tabulated in reference [8].

In the case when the eigenvalues are not pairwise equal, a lower bound V_1 and an upper bound V_2 to V are established in a manner entirely analogous to the hyperparabolic case. The corresponding $F_{V_1}(1)$ and $F_{V_2}(1)$, satisfying $F_{V_1}(1) \geq F_V(1) \geq F_{V_2}(1)$, can then be calculated by using equation (13).

INTERPOLATION PROCEDURES.

In this section a short discussion is given on interpolation methods for estimating the reliability of quadratic safety regions by using the upper and lower bounds. The discussion here is based on the results of reference [10]. Two classes of interpolation procedures were investigated. The methods of the first class perform the interpolation on the parameter level, while the methods of the second class do the interpolation on the distribution function level.

Specifically, in the methods of the first class the random variable $W = \sum_{j=2}^{n} \lambda_j Z_j^2$ is approximated by $\hat{W} = \sum_{j=1}^{N} \theta_j R_j^2$ where $\theta_j = \theta_j(v_j, \mu_j) = \theta_j(\lambda_{2j}, \lambda_{2j+1})$. In the second class a parameter q is sought so that $\hat{F}_I(1) = (1 - q) F_{I_1}(1) + q F_{I_2}(1)$ gives a good approximation to $F_I(1)$, I = U,V.

General rules for an optimum choice of parameters in each particular case are difficult to establish. Of the methods belonging to the first class that were tested initially, the following was chosen: Assume $\lambda_1 \geq \ldots\ldots \geq \lambda_n > 0$, and let

$$\sigma_j(\alpha) = \frac{1}{2}\left(\frac{\lambda_{2j+1}}{\lambda_{2j}}\right)^{\alpha} ; \; j = 1,\ldots,N, \; 0 \leq \alpha < \infty. \tag{16}$$

It is seen that $0 < \sigma_j(\alpha) \leq 1/2$. The parameters $\theta_j = \theta_j(\lambda_{2j}, \lambda_{2j+1})$ are now introduced as follows

$$\theta_j = \theta_j(\alpha) = (1 - \sigma_j(\alpha))\lambda_{2j} + \sigma_j(\alpha)\lambda_{2j+1} \tag{17}$$

The modification needed in case of negative λ_j is quite obvious. From the examples tested in reference [10], it seems that $\alpha = 0.5$ is quite close to an overall optimum choice.

Concerning methods of the second class, two procedures were investigated. One was the "obvious" arithmetic mean, i.e. q = 0.5. The other method was quite involved, but in general it did not improve on the simple arithmetic mean. We shall therefore not elaborate any further on that method here. It is discussed in detail in reference [10].

NUMERICAL EXAMPLES.

In the subsequent examples, it is convenient to give the failure probability P_f instead of P_s. For this purpose, the following notation is introduced

$$G_X(x) = 1 - F_X(x), \tag{18}$$

where X denotes any random variable.

Example 1: Consider the following hyperparabolic failure surface $z_1 + 0.14\, z_2^2 + 0.07\, z_3^2 = 3.5$. Then $\beta = 3.5$ and $U = Z_1 + 0.14\, Z_2^2 + 0.07\, Z_3^2$. The appropriate bounding approximations are $U_1 = Z_1 + 0.07\, R_1^2$ ($R_1^2 = Z_2^2 + Z_3^2$) and $U_2 = Z_1 + 0.14\, R_1^2$. The bounding failure probabilities are calculated from

equation (11) and it is found that $G_{U_1}(\beta) = 4.61 \cdot 10^{-4}$ and $G_{U_2}(\beta) = 12.68 \cdot 10^{-4}$. The corresponding FORM estimate is $\Phi(-\beta) = 2.33 \cdot 10^{-4}$. A numerical integration has been carried out to determine $G_U(\beta)$, giving $G_U(\beta) = 8.0 \cdot 10^{-4}$. Let $G_{\hat{U}}(\beta)$ denote the failure probability obtained by the interpolation method of the first type with $\alpha = 0.5$. Similarly, let $\hat{G}_U(\beta)$ denote the arithmetic mean of $G_{U_1}(\beta)$ and $G_{U_2}(\beta)$. It is found that $G_{\hat{U}}(\beta) = 8.60 \cdot 10^{-4}$ and $\hat{G}_U(\beta) = 8.65 \cdot 10^{-4}$. Using the Breitung formula (equation (10)), it is found that $G_{U_1}(\beta) \sim 4.57 \cdot 10^{-4}$, $G_U(\beta) \sim 23.07 \cdot 10^{-4}$ and $G_{U_2}(\beta) \sim 116.5 \cdot 10^{-4}$. It is seen that the Breitung formula gives a very accurate estimate of $G_{U_1}(\beta)$, which is a case with $\beta\kappa_j$ significantly less than 1.0. This does not hold in the other two cases, and the accuracy decreases notably.

Example 2: Assume for this example that $V = 16^{-1}[(Z_1 - 8)^2 - 0.9Z_2^2 - 0.6Z_3^2]$, implying $\beta = 4.0$. The lower bound $V_1 = 16^{-1}[(Z_1 - 8)^2 - 0.9R_1^2]$, the upper bound $V_2 = 16^{-1}[(Z_1 - 8)^2 - 0.6R_1^2]$. Using equation (13), the bounding failure probabilities are calculated: $F_{V_1}(1) = 12.44 \cdot 10^{-5}$ and $F_{V_2}(1) = 7.20 \cdot 10^{-5}$. The corresponding FORM estimate is $\Phi(-\beta) = 3.17 \cdot 10^{-5}$. Using a notation similar to that in Example 1, it is found that $F_{\hat{V}}(1) = 9.89 \cdot 10^{-5}$ and $\hat{F}_V(1) = 9.82 \cdot 10^{-5}$. Equation (10) gives $F_{V_1}(1) \sim 31.7 \cdot 10^{-5}$, $F_V(1) \sim 15.9 \cdot 10^{-5}$ and $F_{V_2}(1) \sim 7.93 \cdot 10^{-5}$. The accuracy of equation (10) is again satisfactory when the $\beta\kappa_j$ is significantly less than 1.

Example 3: In this example assume that $V = 16^{-1}[Z_1^2 + 0.8Z_2^2 + 0.4Z_3^2]$, implying $\beta = 4.0$. The lower bound $V_1 = 16^{-1}[Z_1^2 + 0.4R_1^2]$, the upper bound $V_2 = 16^{-1}[Z_1^2 + 0.8\,R_1^2]$. The corresponding failure probabilities are calculated from equation (15). It is found that $G_{V_1}(1) = 1.10 \cdot 10^{-4}$ and $G_{V_2}(1) = 4.06 \cdot 10^{-4}$. The FORM estimate is $2\Phi(-\beta) = 0.63 \cdot 10^{-4}$. By numerical integration the failure probability is calculated to be $G_V(1) = 2.3 \cdot 10^{-4}$. Using the interpolation methods, we find $G_{\hat{V}}(1) = 2.12 \cdot 10^{-4}$ and $\hat{G}_V(1) = 2.58 \cdot 10^{-4}$. Equation (10) gives $G_{V_1}(1) \sim 1.05 \cdot 10^{-4}$, $G_V(1) \sim 1.82 \cdot 10^{-4}$ and $G_{V_2}(1) \sim 3.15 \cdot 10^{-4}$.

CONCLUDING REMARKS.

It is assumed that the limit state surface in normalized Gaussian space can be approximated by a quadratic surface at the design point. For an approximation of this type, the calculation of the reliability amounts to determining the probability distribution of a quadratic form in Gaussian variables. In the general case, this is not available in closed form in terms of tabulated functions. In this paper we have studied two types of quadratic limit state

surfaces, the hyperparabolic and the hyperellipsoidal. It is shown that exact expressions for the reliability of a wide range of such limit state surfaces can be given. On the basis of these special case solutions, upper and lower bounds on the reliability in the general hyperparabolic or hyperellipsoidal case can be established.

The existence of upper and lower reliability bounds is exploited as a basis for seeking interpolation methods for estimating the reliability. It is shown by examples that simple interpolation methods give accurate estimates of the reliability. An asymptotic formula for the reliability of quadratic safe sets has also been tested on the examples presented, and it is shown to give good estimates except in cases where parameters are close to critical values.

REFERENCES

1. Madsen, H.O., Krenk, S. and Lind, N.C. (1986). Methods of Structural Safety. Prentice-Hall, Inc., Englewood-Cliffs, NJ.

2. Rice, S.O. (1980). " Distribution of Quadratic Forms in Normal Random Variables - Evaluation by Numerical Integration". SIAM Journal Sci. Stat. Comput., 1 (4), 438-448.

3. Deak, I. (1980). "Three Digit Accurate Multiple Normal Probabilities". Numerische Mathematik, 35, 396-380.

4. Bjerager, P. (1986). "Probability Integration by Directional Simulation". Symposium on the Application of Probabilistic Methods in the Design of Structrues, June 16.-17., 1986. Chalmer's University of Technology, Gothenburg, Sweden.

5. Ditlevsen, O., Olesen, R. and Mohr, G. (1987). "Solution of a Class of Load Combination Problems by Directional Simulation". Structural Safety, 1987 (4), 95-109.

6. Fiessler, B., Neumann, H.-J. and Rackwitz, R. (1979). "Quadratic Limit States in Structural Reliability". Journal of the Engineering Mechanics Division, ASCE, 105 (EM4), 661-676.

7. Breitung, K. (1984). "Asymptotic Approximations for Multinormal Integrals". Journal of the Engineering Mechanics Division, ASCE, 110 (3), pp. 357-366.

8. Naess, A. (1987). "Bounding Approximations to some Quadratic Limit States". Journal of Engineering Mechanics, ASCE. To appear.

9. Abramowitz, M. and Stegun, I. (1965). Handbook of Mathematical Functions. Dover Publications Inc., New York.

10. Naess, A. (1987). Interpolation Methods for Estimating the Reliability of Quadratic Safe Domains. Report R-5-87. Division of Port and Ocean Engineering, The Norwegian Institute of Technology, Trondheim, Norway.

FAILURE MODE ENUMERATION FOR SYSTEM RELIABILITY ASSESSMENT BY OPTIMIZATION ALGORITHMS

Avinash M. Nafday & Ross B. Corotis
Department of Civil Engineering
The Johns Hopkins University
Baltimore, MD 21218, USA

INTRODUCTION

System reliability evaluation of frames for ultimate collapse by the kinematic approach requires the enumeration of the failure modes, calculation of the probability of failure for each mode and then computation of the overall reliability by suitable aggregation [16]. Practical experience shows that even relatively simple frames have a very large number of failure modes. Identification, enumeration and description of all these modes is a difficult combinatorial problem.

Failure modes can be generated by exhaustive enumeration, repeated elastic analysis and optimization. Exhaustive enumeration is not practical for most realistic structures. Discrete elastic frame models lead to a system of simultaneous linear equations in terms of the variables of the problem. If the system has a solution (i.e., a failure mode), it is unique. For generating the other modes, when the variables are randomly varying, the structural problem has to be solved repeatedly for different realizations of the variables. A large number of methods based on repeated elastic analysis have been proposed [see 17 for details]. These methods are computationally expensive and often depend on complex heuristic rules or trial and error procedures. Thus, theoretically at least, one cannot guarantee a successful termination in a finite time interval on a digital computer.

It is necessary here to distinguish between the terms 'method,' 'procedure,' and 'algorithm.' A 'method' finds the solution to a problem, irrespective of whether it can be solved by a computer or not. A 'procedure' has to be describable by a finite number of steps, be unique, take finite interval to perform each step and be closed, i.e., use information only from the previous steps. An 'algorithm' can be defined as a procedure that terminates in a finite number of steps on a digital computer. Since the failure modes will most likely be solved by using a computer, an algorithm is necessary for implementation of any procedure. Different algorithmic procedures can then be rationally compared by evaluating their time and space complexity.

At present, only the optimization procedures appear to have algorithmic possibilities that the other approaches lack. For example, partial satisfaction of structural constraints for redundant frames will generate a subspace in R^n and the final solution can be obtained by a suitable optimality criterion. The optimal solution of the model will give the same result (i.e., failure mode) as the solution of simultaneous linear equations in the traditional methods. The power of the extremum methods, however, is that all the suboptimal solutions can also be easily obtained from the model, and these suboptimal solutions correspond to various random realizations of the variables, i.e., any suboptimal solution can become optimal for a particular realization of random variables. Thus, potentially, all the solutions (i.e., failure modes) of the structural problem for all possible combinations of random variables can be obtained directly by using powerful algorithmic procedures developed in the mathematical and computer science literature. The aim here, therefore, is to consider the algorithmic procedures based on optimization strategies for generating failure modes of building frames failing in the mechanism mode.

REVIEW OF PREVIOUS APPROACHES

Linear and nonlinear programming models (LP and NLP, respectively) have previously been proposed for failure mode enumeration of rigid plastic frames [9,24]. Two alternative NLP formulations were given by Ma [9], leading to constrained and unconstrained optimization problems. The failure modes were 'assumed' to correspond to the local minima of the nonlinear objective function. Although this observation seems to be correct, the hypothesis has yet to be proven rigorously. The direct search method used for the solution missed several of the modes and generated the modes in an arbitrary order depending upon the chosen starting points. Thus, the proposed NLP formulation cannot be useful without an efficient algorithmic procedure for the generation and ranking of modes.

A static LP-based model was formulated by Rashedi and Moses [24]. Approaches depending on sensitivity analysis and simulation were specified for the generation of the modes. Trial and error-based complex heuristic strategies and rules were proposed for this in terms of certain empirically defined parameters. However, the modes by these procedures are generated in an arbitrary order. Often, the same mode may be generated in various trials, and a large number of modes may be missed altogether.

These previous optimization-based strategies for failure mode generation lack suitable and systematic algorithmic procedures for the solution of the models as formulated. Recently, some effort has been made to develop algorithmic procedures

based on LP, NLP, and multiobjective linear programming (MOLP) models [17,21,18,19], and some of these results will be described here.

EXTREMUM MODELS FOR RIGID PLASTIC FRAMES

Proportional Loading -- It is well known that many problems of plastic analysis of structures can be solved by extremum approaches [10]. For example, the problem of limit analysis of frames, in which plastic behavior is activated by a single stress resultant (such as flexure), may be formulated as an LP model for the case of proportionally applied loads. Structural models formulated from static and kinematic considerations have been shown to be a primal-dual pair in LP format [5,6,12]. Such LP models have been derived in the literature in many different forms, and a model based on the approach given in [2] is adopted here for subsequent development.

In this model, a plane frame with proportionally applied loads has been considered. Plastic hinges are assumed to form at a set of discrete locations (j=1, ..., J), and the plastic moment capacity at the j^{th} section is denoted by M_{p_j}. Then, the primal-dual LP pair is given by [2]:

KINEMATIC LP

$$\lambda = \text{Min } \lambda^{+} = \text{Min } [\Sigma_{j=1}^{J} M_{p_j} (\theta_j^{+} + \theta_j^{-})]$$

s.t.

$$\theta_j^{+} - \theta_j^{-} = \sum_{k=1}^{M} t_k \theta_{kj} \qquad j=1,\ldots,J$$

$$\sum_{k=1}^{M} t_k e_k = 1$$

$$\theta_j^{+}, \theta_j^{-} \geq 0$$

STATIC LP

$$\lambda = \text{Max } \lambda^{-}$$

s.t.

$$\sum_{j=1}^{J} \theta_{kj} M_j = \lambda^{-} e_k \qquad k=1,\ldots,M$$

$$-M_{p_j}^{-} \leq M_j \leq +M_{p_j}^{+} \qquad j=1,\ldots,J$$

in which the variables are

M_j = moment at section j, $M_j = M_j^{+} - M_j^{-}$

θ_j = rotation at section j, $\theta_j = \theta_j^{+} - \theta_j^{-}$

t_k = a coefficient indicating the contribution of the k^{th} elementary mode to collapse

λ^+, λ^- = collapse load factors for the kinematic and static LP's, respectively

and the parameters are

θ_{kj} = hinge rotation of elementary mechanism k at joint j

e_k = external work associated with elementary mechanism k

M= number of equations of equilibrium/number of elementary mechanisms

M_{p_j} = member capacity at section j ($M_{p_j}^+$ and $M_{p_j}^-$ are capacities related to the two directions of rotation)

A study of the geometric structure of the primal and dual models shows that the failure modes are given by the extreme points of the associated primal (kinematic) polytope (see Appendix for illustration) and the facets of the dual (static) polytope. Duality transformations of LP actually map extreme points of one model to the hyperplanes of the other and vice versa. Thus, the kinematic approach seems to be the natural one to follow for the generation of failure modes. One great advantage of the kinematic approach is the availability of an extensive mathematical literature and algorithms for extreme point enumeration of polytopes [11]. Failure modes can, of course, be generated from the dual variables of the static LP (available from the reduced cost rows). However, the lack of algorithmic possibilities makes the approach difficult to implement, as demonstrated in [24].

Multiparameter Loading -- Proportional loading indicates a system of concentrated loads, each of which is proportional to a parameter, λ. However, the actual loading on the structures may not satisfy the restriction of proportional loading. It is necessary, in such cases, to consider the independent variation of load factor parameters for the various loads acting on the frame. A static MOLP model has recently been formulated for the plastic collapse analysis of frames due to multiparameter loading [18,19] as:

$$\text{Max } \underline{\lambda}^- = \text{Max } \{\lambda_1,\ldots,\lambda_Q\}^T$$

$$\text{s.t.} \quad \sum_{j=1}^{J} C_{kj} M_j - \sum_{q=1}^{Q} D_{kq} \lambda_q = 0$$

$$k=1,\ldots,M$$

$$-M_{p_j}^{-} \leq M_j \leq +M_{p_j}^{+}$$

$$j=1,\ldots,J$$

where $(q=1,\ldots,Q)$ denotes Q independent load parameters and C_{kj} and D_{kq} are constant coefficients.

Unlike scalar optimization problems, the vector optimal solutions are not completely ordered. Therefore, one of the main distinguishing factors in the vector optimal problems is the absence of a unique "optimal" solution. The notion of an optimal solution is replaced by the concept of a noninferior solution (also referred to as a Pareto-optimal, efficient or non-dominated solution). Two types of noninferiority, viz., strong and weak noninferiority are defined [18]. It has been shown that weak noninferiority is relevant for the limit analysis [18] problem, whereas design optimization problems are likely to seek strong noninferior solutions.

The concept of noninferior solutions is well established [22], but only fairly recently have algorithms been developed for generating noninferior solutions. Chankong and Haimes [1] give a state of art review, and Stadler [25] has described applications in Mechanics. The special structure of MOLP problems has made it possible to develop powerful theoretical and algorithmic results for direct generation of exact noninferior sets. Several simplex-based algorithms have been proposed [see 19 for details] for this purpose.

The geometrical structure of the MOLP static model shows that it has two different associated polytopes instead of just one, as in LP models. These polyhedral regions are defined by the feasible regions of the MOLP model in objective (load) space and decision (basic variable) space, respectively. The two polyhedral feasible regions have frontiers made up of only polyhedral facets. It has been shown [19] that maximal facets of these polyhedra correspond to the failure modes of the structure and union of all maximal facets gives the global limit surface for the frame.

Based on the foregoing, the static MOLP model seems to be naturally suited for generating the global limit hypersurface of frames. This, in turn, is useful for the evaluation of system reliability by the random variable approach [16]. The direct procedure for failure mode generation, i.e., the kinematic MOLP model, has yet not been formulated. Thus, for multiparameter loading, if one wants the failure modes, they must be generated indirectly, i.e., from the reduced cost rows of the static MOLP model.

ALGORITHMS FOR FAILURE MODE GENERATION

Polytopes (and polyhedra) have been thoroughly studied by mathematicians [e.g., 8]. In recent years, many algorithms have been proposed for generating their extreme points and facets. A survey of these methods, contrasting the main features and computational results for representative methods, is given by Matheiss and Rubin [11].

Proportional Loading -- In the context of the kinematic LP model, one is interested in enumerating the extreme points of the polytope. Algorithms for enumerating all extreme points of a polytope are divided into two classes: pivoting methods and non-pivoting methods. Some of the methods rank the vertices in the process of enumeration, but most generate the vertices in an arbitrary order. Since ordering of extreme points is very important for reliability analysis, only ranking algorithms are relevant. Three such algorithms have been proposed [3,13,14,15,23]. Among these three, the extreme point ranking algorithm of Murty was selected to generate the failure modes in ascending order of their collapse loads [17]. This algorithm has also been applied for the fixed charge bidding problem [13], the travelling salesman problem [14], and near optimality analysis [20].

The algorithm ranks the extreme points of $\underline{A}\ \underline{x} = \underline{b}$ in nondecreasing order of the value of $z(\underline{x})$. The method is based on a theorem which states that if $\underline{x}^1$, $\underline{x}^2$, ...,$\underline{x}^\gamma$ are the 'γ' best extreme points, $\underline{x}^{\gamma+1}$ will be an adjacent extreme point of one of the first 'γ' points. The new point is distinct from the first γ and minimizes $z(\underline{x})$ among all eligible points.

The algorithm starts with a basic feasible solution corresponding to the optimal extreme point as the only extreme point in the enumerated list. It finds all the adjacent extreme points by bringing, one by one, the nonbasic variables into the basis to form a candidate list. The top ranked point in the candidate list is added to the list of enumerated extreme points and excluded from the candidate list. The candidate list is then revised by adding in appropriate order all the adjacent extreme points of the point just selected. The procedure is repeated until either a prespecified number of extreme points, π, is found or all the extreme points in ranked sequence whose objective value is less than a prespecified value α are obtained. A consequence of Murty's theorem is that if at each stage the candidate list contains more than π extreme points, only the best π entries are kept in the candidate list, discarding the rest. Similarly, for the case of a prespecified objective value, at each stage all the adjacent extreme points with an objective value greater than α can be discarded. If the polytope is degenerate, then all the basic feasible solutions corresponding to a given extreme point have

to be incorporated in the solution process.

The size of the LP increases rapidly for larger structures. However, LP algorithms work efficiently in practice for even very large sized problems with thousands of variables and hundreds of constraints. Thus, the proposed LP-based procedure is likely to be a useful alternative for generating the failure modes of realistic structural frames. Detailed computational experience is not available so far, and this will be an important area for further research. Fortunately, structural reliability problems do not require generation of all of the thousands of possible modes that a structure might have. Identifying around 50 modes in ranked order should give a reasonably accurate estimate of system reliability.

Murty's algorithm considers only linear significance criteria, and this implies an assumption of perfect correlation among member plastic moment capacities in the polytope extreme point (PEP) model of [17]. Although the order of mode generation is not very sensitive [24] to correlation betwen component strengths (for coefficient of correlation < 0.3), the method needs to be extended to account for the actual correlation between members. Algorithms for extreme point enumeration of the polytope for independent and correlated member strengths are currently under investigation [21]. Once the important modes are identified by this procedure, it is possible to use the associated load values to determine the orientation of an incremental load vector for each mode. A general nonlinear structural frame analysis can then be performed for each proportional load orientation thus defined. This will lead to refined modal loads based on the more comprehensive structural analysis.

Multiparametric Loading -- The algorithms for MOLP problems are based on a systematic search for the noninferior extreme points of the associated polytopes. Since not every extreme point is noninferior, it is necessary to determine the potential noninferiority of adjacent extreme points by an examination of the reduced cost matrices. Most of the adjacent extreme points are either eliminated in this process or are classified as noninferior. For the few remaining extreme points not directly falling in one of these categories, a small linear subproblem test is formulated, the solution of which indicates their category. The subproblem uses the reduced cost information of the current basis to search for a set of positive weights to check the dominance of the new basis.

As the noninferior extreme point set has been shown to be connected, a systematic procedure for storing and keeping track of the bases can be devised. Various multiobjective simplex algorithms primarily differ in the ways they generate and store these noninferior extreme points. In the static MOLP model, the simplex tableaux corresponding to different noninferior extreme points will have

information about the failure modes in the reduced cost rows. Thus, the solution of the MOLP model automatically generates all the failure modes as shown in [18,19]. Ranking the failure modes will, of course, require additional information regarding probabilistic behavior of the random variables. The kinematic MOLP model has not been formulated in the literature so far, but it is likely to provide a direct method for failure mode enumeration under multiparameter loading.

COMPLEXITY OF ALGORITHMS

Traditionally, a common approach for the comparison of alternative methods for the solution of a given problem is based on empirical tests on sample problems. For example, Grimmelt and Schüeller [7] recently compared different methods for determining the collapse failure probabilities of redundant structures by testing these on certain arbitrary problems. However, recent research in algorithm theory has provided theoretical criteria for the study of computation problems in terms of their time and space complexity. Dyer [4] has applied some of these ideas and results to the extreme point enumeration problem. From his results, it becomes clear that the problem of failure mode enumeration is NP-hard, and there is no polynomial time algorithm for its solution. There has been no such study regarding the complexity of MOLP algorithms, but these are certainly harder than ordinary LP-problems.

CONCLUSIONS

The problem of failure mode generation of frames is a complex problem. Optimization-based strategies seem to be the best procedures for algorithmic developments in this regard. However, significant computational resources will be required to solve even the most efficient algorithm because there are no known polynomial time algorithms to solve such problems.

REFERENCES

1. Chankong, V., Haimes, Y.Y., Thadathil, J., and Zionts, S., "Multiple Criteria Optimization: A State of Art Review," Proceedings, Decision Making with Multiple Objectives, Y.Y. Haimes and V. Chankong (Eds.), Cleveland, 1984, Springer-Verlag, New York, 1985.
2. Cohn, M.Z., Ghosh, S.K., and Parimi, S.R., "Unified Approach to the Theory of Plastic Structures," Journal of the Engineering Mechanics Division, ASCE, Vol. 98, No. EM5, Oct., 1972, pp. 1133-1158.
3. Dahl, G., and Storøy, S., "Enumeration of Vertices in Linear Programming Problem," Report No. 45, October, 1973, University of Bergen.

4. Dyer, M.E., "The Complexity of Vertex Enumeration Methods," Mathematics of Operations Research, Vol. 8, No. 3, Aug. 1983, pp. 381-402.
5. Gavarini, C., "Fundamental Plastic Analysis Theorems and Duality in Linear Programming," Ingegneria Civile, No. 18, 1966.
6. Gavarini, C., "Plastic Analysis of Structures and Duality in Linear Programming," Meccanica, Vol. 1, 1966, pp. 95-97.
7. Grimmelt, M., and Schüeller, G.I., "Benchmark Study on Methods to Determine Collapse Failure Probabilities of Redundant Structures," Structural Safety, Vol. 1, 1982/83, pp. 93-106.
8. Grümbaum, B., "Convex Polytopes," John Wiley and Sons, New York, 1967.
9. Ma, H.F., "Reliability Analysis of Ductile Structural Systems," thesis presented to the University of Illinois, at Urbana, Illinois, in 1981, in partial fulfillment of the requirements for the degree of Doctor of Philosophy.
10. Maier, G., and Munro, J., "Mathematical Programming Applications to Engineering Plastic Analysis," Applied Mechanics Review, Vol. 36, No. 12, Dec., 1982, pp. 1631-1643.
11. Matheiss, T.H., and Rubin, D.S., "A Survey and Comparison of Methods for Finding All Vertices of Convex Polyhedral Sets," Mathematics of Operations Research, Vol. 5, No. 2, May, 1980, pp. 167-185.
12. Munro, J., and Smith, D.L., "Linear Programming Duality in Plastic Analysis and Synthesis," International Symposium on Computer-aided Structural Design, Conventry, 1972, Vol. 1, Peter Peregrinus, Stevenage, 1972, pp. A1.22-A1.54.
13. Murty, K.G., "Solving the Fixed Charge Problem by Ranking the Extreme Points," Operations Research, Vol. 16, 1969, pp. 682-687.
14. Murty, K.G., "An Algorithm for Ranking All Assignments in Increasing Order of Costs," Operations Research, Vol. 16, 1969, pp. 682-687.
15. Murty, K.G., "Linear Programming," John Wiley and Sons, New York, 1983.
16. Nafday, A.M., Corotis, R.B., and Cohon, J.L., "System Reliability of Rigid Plastic Frames," Reliability and Risk Analysis in Civil Engineering I (ed. N.C. Lind), ICASP-5, University of Waterloo, Canada, 1987.
17. Nafday, A.M., Corotis, R.B., and Cohon, J.L., "Failure Mode Identification for Structural Frames, Journal of Structural Engineering, ASCE, Vol. 113, No. 7, July, 1987.
18. Nafday, A.M., Corotis, R.B., and Cohon, J.L., "Multiparametric Limit Analysis of Frames: Part I-Model," Journal of Engineering Mechanics, ASCE, accepted.
19. Nafday, A.M., Cohon, J.L., and Corotis, R.B., "Multiparametric Limit Analysis of Frames: Part II-Computations,: Journal of Engineering Mechanics, accepted.
20. Nafday, A.M., Corotis, R.B., and Cohon, J.L., "Near Optimality Analysis for Linear Models," Journal of Computers in Civil Engineering, ASCE, accepted.
21. Nafday, A.M., Corotis, R.B., and Cohon, J.L., "Dominant Failure Modes for Structural Frames," under preparation for the Journal of Structural Safety.
22. Pareto, V., "Cours d'Economie Politique Rouge," Lausanne, 1896.
23. Pollatschek, M., and Avi-Itzhak, B., "Sorting Extremum Point Solutions of a Linear Program," presented at the Third Annual Israel Conference on Operations Research, Israel, 1969.
24. Rashedi, M.R., and Moses, F., "Studies on Reliability of Structural Systems," Report No. R83-3, Case Western Reserve University, Cleveland, 1983.
25. Stadler, W., "Multicriteria Optimization in Mechanics: A Survey," Applied Mechanics Review, Vol. 37, No. 3, March, 1984.

APPENDIX

Polytopes are n-dimensional analogs of 2-D polygons. As the structural problems mostly lead to irregular and degenerate polytopes in higher dimensional (>3) spaces, it is difficult to visualize the details of the problem. Therefore, a hypothetical example is shown here to illustrate the proposed approach. A regular polytope (Fig. 1) in a 3-D space is assumed to represent the feasible region of a kinematic LP model for a certain hypothetical structural problem.

A 2-D (hyper)plane is shown to just touch the extreme point A of the polytope, which denotes the optimal solution, i.e., the structure will fail in mode A. It is conceivable that a variation in the slope of the hyperplane (by changing parameters in the equation of hyperplane) may lead it to touch another extreme point B. Then, the structure will fail due to failure mode B. For a certain slope of the hyperplane, there is the possibility of it touching the edge AB, leading to simultaneous failure in modes A and B. Similarly, if the hyperplane coincides with the plane ABCD, there will be an occurrence of four simultaneous modes at failure (denoted by A,B,C and D). Thus, the failure mode in which the structure will actually fail is determined by the coefficients in the equation describing the hyperplane, i.e., its slope.

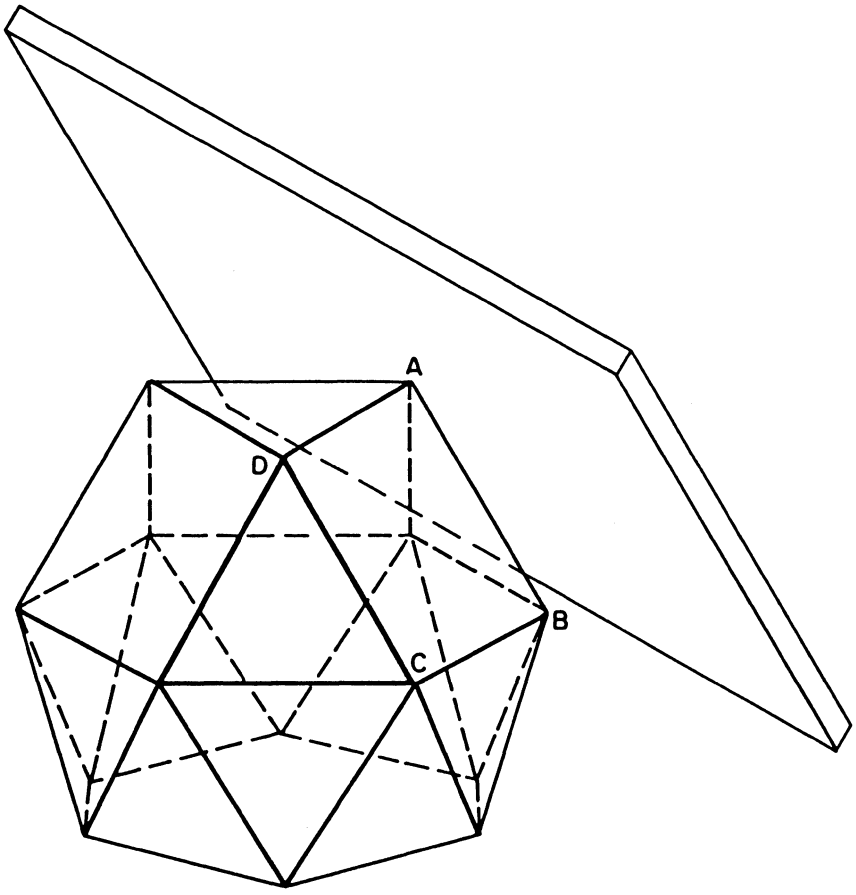

Fig. 1. Illustration for failure mode enumeration of a hypothetical structural problem.

RELIABILITY ANALYSIS OF HYSTERETIC MULTI-STOREY FRAMES UNDER RANDOM EXCITATION

S. R. K. Nielsen, K. J. Mørk, P. Thoft-Christensen
University of Aalborg
Sohngaardsholmsvej 57, DK-9000 Aalborg, Denmark

ABSTRACT

An analytical method for determining the response of a hysteretic structural system under random excitation including safety measures is presented. The formulation of the integrated dynamic system made up of the structural system, the safety measures and the loading process is expressed by the use of the Itô stochastic differential equations. By introducing an approximate non-Gaussian probability distribution with adjustable parameters for the response and using the statistical moment equation, obtained from using the Itô-formula to calibrate the parameters, the resulting probability distribution is used to provide approximate response statistics.

KEYWORDS

Stochastic differential equation. Hysteretic structures. Non-Gaussian closure. Cumulative plastic deformation.

1. INTRODUCTION

Reliability of hysteretic structures may be studied based on stochastic differential equations, [1-4]. In these formulations extra internal degrees-of-freedom are introduced, for which extra differential equations are formulated. These equations are virtual constitutive equations on incremental form.

If the external excitations are modelled as filtered Gaussian white noise processes, the resulting equations may be formulated as a system of Itô-differential equations, [5-7]. Because the associated Fokker-Planck-Kolmogorov or backwards-Kolmogorov equations can hardly be solved either analytically or numerically, one has concentrated on determining the time-dependent moments of the solution process.

The differential equations for the moments of the solution process can be obtained in various ways, [6, 7]. The most natural way is to apply the Itô-formula to products of increasing order of the involved stochastic variables and perform the expectation. Alternatively one can start from the Fokker-Planck-Kolmogorov-equation in combination with the divergence theorem. This will result in an infinite hierarchy of moment equations.

In applications these systems of differential equations must be truncated at a certain order. The main problem in doing this is that the moment equations generally involve expectations of all state variables, which can only be calculated if the full joint distribution of all state variables is known. Hence, the joint distributions must be estimated from the joint moments calculated from the retained moment equations. This process is referred to as closure techniques in the literature, [6, 7].

If only the first and second order moments are retained, the resulting equations are easily shown to be identical to those obtained by the equivalent linearization method, [10-12], when this is based on a minimization of the expected value of the mean square error term between the right hand sides of the non-linear system differential equations and their equivalent linear representation.

In the so-called Gaussian closure technique the above-mentioned expectations are calculated, assuming a joint normal distribution for all state variables with expected values and covariances as calculated from the process, [9]. When only first and second order moments are considered, the covariance equations can be further reduced by application of the Price theorem, [10, 12]. In this case the Gaussian closure technique is consistent, because the equivalent linear system equations imply normal response processes.

The response processes of strongly non-linear processes may differ significantly from normality and hence Gaussian closure schemes may lead to erroneous results. In these cases non-Gaussian schemes, based on Gram-Charlier series, have been suggested, [7, 13]. The parameter in these series can only be estimated if the moment hierarchy is closed at higher than 2nd order, i.e. differential equations of the joint moments of the state vector beyond the mean value function and the covariance function have to be formulated.

In general, the method of non-Gaussian closure consists of constructing a non-Gaussian probability distribution with adjustable parameters for the response and using statistical moment equations to obtain differential or algebraic equations for the unknown parameters. With calibrated parameters, the resulting probability distribution is then used to obtain approximate response statistics.

The aim of the present study is to form the basis of a non-Gaussian closure method for the integrated dynamic system made up of structural state variables, the loading process and various safety measures, which are defined as random functions, which are non-decreasing with time at least with probability one.

In the structural analysis geometrical linearity is assumed. The material behaviour is assumed to be linear elastic, ideal plastic. Constitutive equations are formulated for both beam elements with distributed plastic deformations within the elements as for yield hinge models, where the plastic deformations are restricted to the member end sections.

Stochastic differential equations are formulated for the loading process and for the safety measure. As illustration a seismic excitation is considered, modelled as a Gaussian white noise filtered through a Kanai-Tajimifilter. The maximum value of the numerical value of the rotations of the beam element end sections encountered during the excitation time is selected as safety measure.

The Itô differential equations for the vector process of all state variables in the integrated dynamic system are then formulated. Corresponding to a closure of the hierarchy of statistical moments at the second order level, the differential equations of the mean and covariance function of the vector process are indicated. The appropriate approximations, necessary to reduce the calculation of the expectations in the said differential equations to beam element level are indicated, only involving stochastic variables associated with a certain beam element.

In case of yield hinge models an approximate probability density functions for all state variables associated with a certain beam element is indicated, which has a degree-of-freedom to represent a discrete probability mass corresponding to yielding at the member end sections. For other beam models the probability mass will be continuously distributed. However, the probability density function will have dominant peaks close to the yield bending moment. The said probability density function for the yield hinge model is then also applied in this case.

The relevance of the assumed probability density is demonstrated by extensive simulation studies for a 2-storey yield hinge frame.

2. COMPATIBILITY RELATIONS

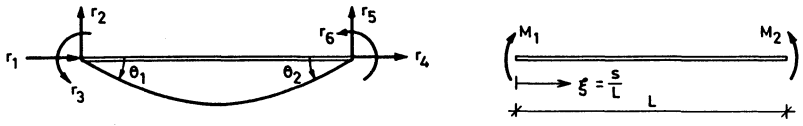

Figure 1: Definition of nodal and internal degrees of freedom.

The member end moments $\underline{M}_e^T = (M_1, M_2)$ of a beam element is introduced as internal degrees of freedom in the element. The end rotations from the element chord are termed $\underline{\theta}_e^T = (\theta_1, \theta_2)$. Assuming geometrical linearity corresponding to small deflections, $\underline{\theta}_e$ are related to the nodal point deformations $\underline{r}_e^T = (r_1, \ldots, r_6)$ through the

compatibility equations.

$$\underline{\theta}_e = \underline{a}_e \; \underline{r}_e \tag{1}$$

$$\underline{a}_e = \begin{bmatrix} 0 & -\frac{1}{L} & -1 & 0 & \frac{1}{L} & 0 \\ 0 & \frac{1}{L} & 0 & 0 & -\frac{1}{L} & 1 \end{bmatrix}_e \tag{2}$$

3. ANALYSIS OF BEAM ELEMENTS

Constitutive equations will be derived for beam models with distributed plasticity as well for a yield hinge model with plastic deformations concentrated at the end sections.

3.1 Distributed plasticity models.

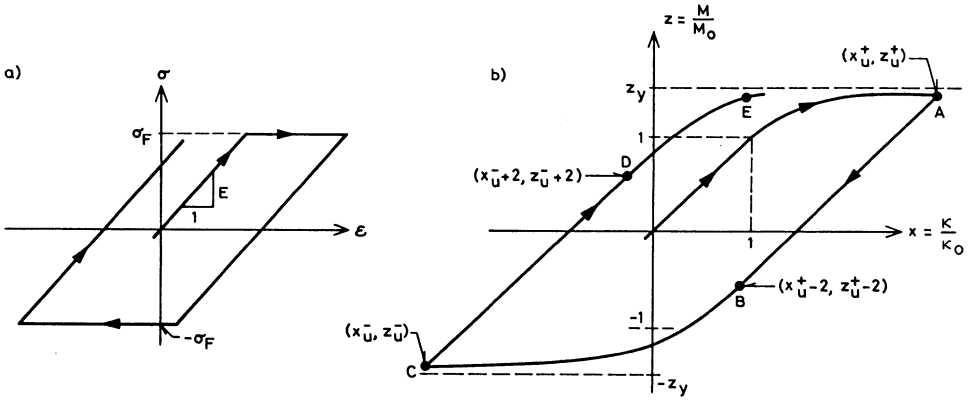

Figure 2: Constitutive equations. a) Stress-strain curve for linear elastic-ideal plastic material. b) Non-dimensional moment-curvature curve for symmetric section of linear elastic-ideal plastic material.

The following assumptions are applied

1) Bernoullis hypothesis that plane sections remain plane during deformation
2) The beam material is linear elastic-ideal plastic
3) Normal forces have negligible influence on the load-bearing capacity
4) External loads are applied at system nodes, i.e. all elements are free of external loadings
5) All sections are symmetrical

The last-mentioned assumption, which is not crucial, has been included to facilitate the calculations.

In figure 2b M_o and κ_o represent the moment and curvature on the skeleton curve, corresponding to the elastic limit deformation. From the above assumptions the following can be derived

$$M_o = EI_o\kappa_o \tag{3}$$

where E is the modulus of elasticity and I_o is the bending moment of inertia.

(x_u^+, z_u^+) and (x_u^-, z_u^-) represent the non-dimensional curvature κ/κ_o and moment M/M_o at unloading from positive and negative moments respectively.

Finally, $z_y = M_y/M_o$ represent the non-dimensional bending moment capacity of the section.

The constitutive equations on differential form may be written

$$\dot{M} = EI(\{M\}_o^t, \xi)\dot{\kappa} \Rightarrow$$

$$\dot{z} = i(\{z\}_o^t, \xi)\dot{x} \quad , \quad i = \frac{I}{I_o} \in]o, 1] \tag{4}$$

where (3) is applied. $\{M\}_o^t$ and $\{z\}_o^t$ are sets of all previous M- and z-values during the interval [o, t], specifying the history dependence of I and i. I is the moment of inertia of all elastic fibres in the section. Hence $i(\{z\}_o^t, \xi) = 1$ corresponds to totally elastic deformations, whereas $i(\{z\}_o^t, \xi) = 0^+$ indicates plastic deformations of all fibres in the section. $\xi = \frac{s}{L}$ is a non-dimensional coordinate, measured along the beam axis, see figure 1.

It turns out that $i(\{z\}_o^t, \xi)$ on the loading branch ABC in figure 2b only depends on the latest values of the non-dimensional moment at unloading z_u^+ and the present value of z. Similarly $i(\{z\}_o^t, \xi)$ on branches CDE only depends on z_u^- and the present value of z.

For a rectangular beam section the following result on differential form may be derived

$$\dot{z} = \begin{cases} \dot{x} & , \text{ branch AB} \\ \left(\frac{2z+3}{2z_u^+ - 1}\right)^{3/2}\dot{x} & , \text{ branch BC} \\ \dot{x} & , \text{ branch CD} \\ \left(\frac{2z-3}{2z_u^- + 1}\right)^{3/2}\dot{x} & , \text{ branch DE} \end{cases} \tag{5}$$

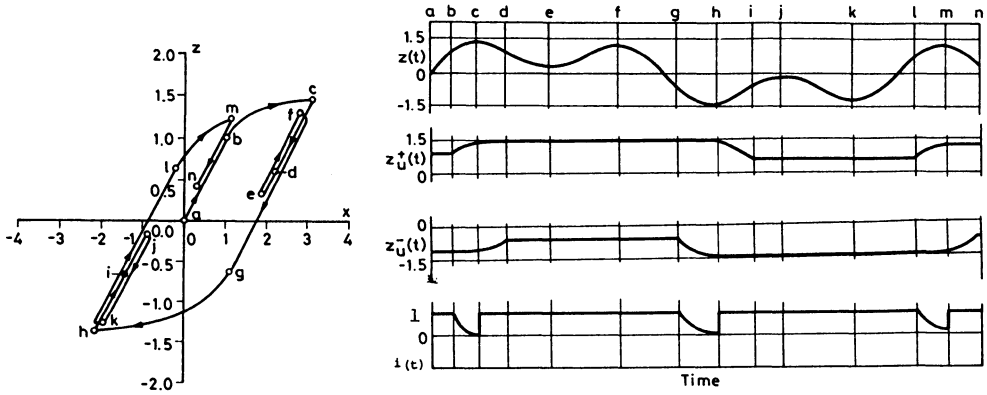

Figure 3. Realization of processes $z(t)$, $z_u^+(t)$, $z_u^-(t)$, $i(t)$.

The non-dimensional moments at most recent unloading z_u^+ and z_u^- are determined from the following differential equations.

$$\begin{aligned}\dot{z}_u^+ &= [2H(z-z_u^+)-1]\max\{H(z-z_u^+), H(z_u^+-z_u^--2)\}\dot{z}H(\dot{z})\\ \dot{z}_u^- &= [2H(z_u^--z)-1]\max\{H(z_u^--z), H(z_u^+-z_u^--2)\}\dot{z}H(-\dot{z})\end{aligned} \tag{6}$$

with initial conditions $z_u^+(0) = 1$, $z_u^-(0) = -1$. $H(\cdot)$ is given by

$$H(x) = \begin{cases} 1 & , x \geq 0 \\ 0 & , x < 0 \end{cases} \tag{7}$$

Realizations of $z(t)$, $z_u^+(t)$ and $z_u^-(t)$ are shown in figure 3. It is seen that z_u^+ remains constant at the most recent unloading value of $z(t)$ at point c independently of succeeding elastic re- and unloadings until unloading from the plastic branch g-h at point h. Similarly $z_u^-(t)$ remains constant at the most recent unloading value of $z(t)$ at point d until the succeeding unloading from the plastic branch l-m at point m independently of preceeding elastic loading loops.

The plastic branches g-h and l-m are defined by $z_u^- - z = 0 \wedge z_u^+ - z_u^- - 2 > 0$ and $z - z_u^+ = 0 \wedge z_u^+ - z_u^- - 2 > 0$, respectively. All elastic branches are defined by $z_u^+ - z_u^- - 2 < 0$. $i(\{z\}_o^t, \xi) = i(z, z_u^+, z_u^-, \xi)$ for a rectangular section may then be written

$$\begin{aligned}&i(z, z_u^+, z_u^-, \xi) =\\ &1+H(z_u^+ - z_u^- - 2)\,[H(z_u^- - z)\,((\frac{2z+3}{2z_u^+-1})^{\frac{3}{2}} - 1) + H(z-z_u^+)\,((\frac{2z-3}{2z_u^-+1})^{\frac{3}{2}} - 1)]\end{aligned} \tag{8}$$

where $H(\cdot)$ is defined by (7). The corresponding sample curve of i has also been shown in figure 3.

In principle extra state variables (z_u^+, z_u^-) must be introduced at all cross-sections of the beam. Introducing $\dot{z} = \frac{1}{M_o}((1-\xi)\dot{M}_1+\xi\dot{M}_2)$ into (6), the differential equations at a given section, specified by ξ, is obtained. In a discretized model only a finite number of sections is considered, between which (z_u^+, z_u^-) is linearly interpolated. The discrete numbers of state variables thus obtained for the said member are assembled in element state vectors $\underline{z}_{u,e}^+$, $\underline{z}_{u,e}^-$

$\dot{\kappa}$ in (4) is related to the rate of the end section moments $\dot{\underline{M}}_e^T = (\dot{M}_1, \dot{M}_2)$ through

$$\dot{\kappa} = \frac{1}{EI_o} \frac{(1-\xi)\dot{M}_1+\xi\dot{M}_2}{i(z, z_u^+, z_u^-, \xi)} \tag{9}$$

The rate of the end section rotations $\dot{\underline{\theta}}_e^T = (\dot{\theta}_1, \dot{\theta}_2)$ can now be calculated from κ, e.g. from the conjugate beam theory. The following relationship between $\dot{\underline{\theta}}_e$ and $\dot{\underline{M}}_e$ for a certain member is obtained.

$$\dot{\underline{M}}_e = \underline{k}_e(\underline{M}_e, \underline{z}_{u,e}^+, \underline{z}_{u,e}^-)\dot{\underline{\theta}}_e \tag{10}$$

$$\underline{k}_e^{-1} = \frac{L}{EI_o}\begin{bmatrix} d_{11} & d_{12} \\ d_{12} & d_{22} \end{bmatrix}_e \tag{11}$$

$$d_{11}(\underline{M}_e, \underline{z}_{u,e}^+, \underline{z}_{u,e}^-) = \int_o^1 \frac{(1-\xi)^2}{i(\underline{M}_e, \underline{z}_{u,e}^+, \underline{z}_{u,e}^-, \xi)} d\xi \tag{11a}$$

$$d_{12}(\underline{M}_e, \underline{z}_{u,e}^+, \underline{z}_{u,e}^-) = \int_o^1 \frac{\xi(1-\xi)}{i(\underline{M}_e, \underline{z}_{u,e}^+, \underline{z}_{u,e}^-, \xi)} d\xi \tag{11b}$$

$$d_{22}(\underline{M}_e, \underline{z}_{u,e}^+, \underline{z}_{u,e}^-) = \int_o^1 \frac{\xi^2}{i(\underline{M}_e, \underline{z}_{u,e}^+, \underline{z}_{u,e}^-, \xi)} d\xi \tag{11c}$$

$\underline{k}_e^{-1}$ represents the inverse of the stiffness matrix $\underline{k}_e$.

From (1) and (11) the following stiffness relationship is obtained

$$\dot{\underline{M}}_e = \underline{k}_e(\underline{M}_e, \underline{z}_{u,e}^+, \underline{z}_{u,e}^-)\underline{a}_e\dot{\underline{r}}_e \tag{12}$$

Inserting (10) in (6), the following differential equations are obtained for $\underline{z}_{u,e}^+$ and $\underline{z}_{u,e}^-$

$$\begin{aligned} \dot{\underline{z}}_{u,e}^+ &= \underline{f}_e^+(\dot{\underline{\theta}}_e, \underline{M}_e, \underline{z}_{u,e}^+, \underline{z}_{u,e}^-) \\ \dot{\underline{z}}_{u,e}^- &= \underline{f}_e^-(\dot{\underline{\theta}}_e, \underline{M}_e, \underline{z}_{u,e}^+, \underline{z}_{u,e}^-) \end{aligned} \tag{13}$$

Corresponding to (12), $\dot{\underline{\theta}}_e$ can be eliminated in (13), and $\dot{\underline{r}}_e$ introduced as state variables by means of (1).

Instead of the moment-curvature relationship (5) empirical Ramberg-Osgood functions can be used, resulting in equations similar to (6) and (8).

3.2 Yield hinge model.

As a special example of the class of constitutive equations presented in the previous chapter a yield hinge model with bilinear hysteretic characteristics is considered. In this model, plastic deformations only take place at the end sections, whereas the beam remains elastic between these points.

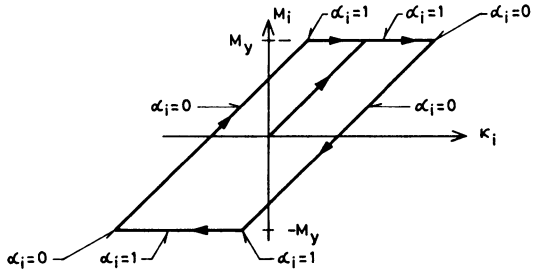

Figure 4: Yield hinge model. Moment-curvature relationship.

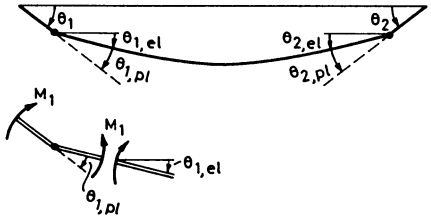

Figure 5: Definition of elastic and plastic end rotations.

In this case it is necessary to introduce the rate of plastic end rotations $\dot{\underline{\theta}}_{e,pl}^{T} = (\dot{\theta}_{1,pl}, \dot{\theta}_{2,pl})$, instead of the present values of $\underline{z}_{u,e}^{+}$ and $\underline{z}_{u,e}^{-}$, to control the loading and unloading sequences. The local stiffness matrix (11) then becomes

$$\underline{k}_e(\underline{M}_e, \dot{\underline{\theta}}_{e,pl}) = [(1-\alpha_1)(1-\alpha_2)\underline{k}_o + \alpha_1(1-\alpha_2)\underline{k}_1 + \alpha_2(1-\alpha_1)\underline{k}_2] \tag{14}$$

$$\underline{k}_o = 2\frac{EI_o}{L}\begin{bmatrix} 2 & -1 \\ -1 & 2 \end{bmatrix} \tag{14a}$$

$$\underline{k}_1 = 3\frac{EI_o}{L}\begin{bmatrix} 0 & 0 \\ 0 & 1 \end{bmatrix} \tag{14b}$$

$$\underline{k}_2 = 3\frac{EI_o}{L}\begin{bmatrix} 1 & 0 \\ 0 & 0 \end{bmatrix} \tag{14c}$$

$$\alpha_i(\underline{M}_e, \dot{\underline{\theta}}_{e,pl}) = H(-M_y+M_i)[1-H(-\dot{\theta}_{i,pl})] + H(-M_y-M_i)[1-H(\dot{\theta}_{i,pl})], i = 1, 2 \tag{15}$$

$\alpha_i = 1$, when yield hinge i is open and loaded, see figure 4. In this condition $\dot{\theta}_{i,pl} \neq 0$.
$\alpha_i = 0$, when yield hinge i is closed or is at the point of being unloaded into the elastic range, see figure 4.

The plastic end rotation $\underline{\theta}_{e,pl}$ is determined from the following relation, cf. figure 5.

$$\underline{\theta}_e = \underline{\theta}_{e,el} + \underline{\theta}_{e,pl} \tag{16}$$

where $\underline{\theta}^T_{e,el} = (\theta_{1,el}, \theta_{2,el})$ is the elastic part of the end rotations. These are related to the end section moments $\underline{M}_e$ through the stiffness relationship.

$$\underline{M}_e = \underline{k}_o \, \underline{\theta}_{e,el} \tag{17}$$

where $\underline{k}_o$ is given by (14a).
From (10), (17) follows

$$\dot{\underline{M}}_e = \underline{k}_e \, \dot{\underline{\theta}}_e = \underline{k}_o \, \dot{\underline{\theta}}_{e,el} \Rightarrow$$

$$\dot{\underline{\theta}}_{e,el} = \underline{k}_o^{-1} \, \underline{k}_e \, \dot{\underline{\theta}}_e \tag{18}$$

From (14), (16), (18) then follows

$$\dot{\underline{\theta}}_{e,pl} = \underline{g}_e (\underline{M}_e, \dot{\underline{\theta}}_{e,pl}) \, \dot{\underline{\theta}}_e \tag{19}$$

$$\underline{g}_e (\underline{M}_e, \dot{\underline{\theta}}_{e,pl}) = \left[\begin{array}{c|c} \alpha_1 & -\frac{1}{2}\alpha_1(1-\alpha_2) \\ \hline -\frac{1}{2}\alpha_2(1-\alpha_1) & \alpha_2 \end{array}\right] \tag{20}$$

For given $\underline{M}_e$, $\dot{\underline{\theta}}_e$, (19) can be solved for $\dot{\underline{\theta}}_{e,pl}$, i.e.

$$\dot{\underline{\theta}}_{e,pl} = \underline{h}_e (\underline{M}_e, \dot{\underline{\theta}}_e) \tag{21}$$

Inserting (21) in (14), the constitutive relation can be written

$$\dot{\underline{M}}_e = \underline{k}_e (\underline{M}_e, \dot{\underline{\theta}}_e) \, \dot{\underline{\theta}}_e \tag{22}$$

The rate of the end section rotations $\dot{\underline{\theta}}_e$ can be eliminated from (22), and $\dot{\underline{r}}_e$ can be introduced as state variables by means of the compatibility equation (1).

4. SYSTEM ANALYSIS

System equations are derived, expressing the equations of momentum and moment of momentum for all free nodes, due to elastic restoring forces, restoring forces from member end moments and external loadings. The resulting equation may be written

$$\underline{m} \, \ddot{\underline{r}} + \underline{k}_o \, \underline{r} + \underline{a}^T \, \underline{M} = \underline{f}(t) \tag{23}$$

(23) is easily derived from the principle of virtual displacements.

$\underline{r}$ is a vector of all translational and rotational nodal degrees of freedom.

$\underline{M}$ is a vector of all member end moments, which have been introduced as internal degrees of freedom.

$\underline{f}$ is a vector of external loadings conjugated to $\underline{r}$.

$\underline{m}$ is the mass matrix. In the present formulation it is assumed that rotational inertia is included, e.g. through a consistent mass matrix. $\underline{m}$ is assumed to be positive definite.

$\underline{k}_o$ is a stiffness matrix, specifying the elastic restoring forces from nodal degrees of freedom not conjugated to $\underline{M}$. Further storey drift from P-δ effects may be included in $\underline{k}_o$. Notice that $\underline{k}_o$ here signifies a global stiffness matrix and must not be mismistaken for the element stiffness matrix (14a).

$\underline{a}^T\underline{M}$ represents the restoring forces from the member end moments. $\underline{a}$ is the compatibility matrix of eq (1) in global coordinates, assembled in rows according to the components of $\underline{M}$. Hence, $\underline{a}$ relates the internal degrees of freedom $\underline{\theta}$ to the global degrees of freedom $\underline{r}$. Note that restoring forces from $\underline{M}$ occur in both rotational and translational degrees of freedom.

Further, the constitutive equations (12), (13) for each beam element are accessible, one for each component in $\underline{M}$. These are assembled in the following equations.

$$\dot{\underline{M}} = \underline{k}(\underline{M}, \underline{z}_u^+, \underline{z}_u^-)\,\underline{a}\,\dot{\underline{r}} \tag{24}$$

$$\left.\begin{aligned} \dot{\underline{z}}_u^+ &= \underline{f}^+(\dot{\underline{r}}, \underline{M}, \underline{z}_u^+, \underline{z}_u^-) \\ \dot{\underline{z}}_u^- &= \underline{f}^-(\dot{\underline{r}}, \underline{M}, \underline{z}_u^+, \underline{z}_u^-) \end{aligned}\right\} \tag{25}$$

$\underline{k}$ is an assembly of local stiffness matrices given by (12) and (22). Further $\underline{z}_u^+$ and $\underline{z}_u^-$ are assemblies of corresponding element quantities $\underline{z}_{u,e}^+$ and $\underline{z}_{u,e}^-$.
In order to maintain dynamic equilibrium at each time stage during the process, $\underline{M}$ should be eliminated from (23) by (24). Hence,

$$\underline{m}\,\ddot{\underline{r}} + [\underline{k}_o + \underline{a}^T\,\underline{k}(\underline{M}, \underline{z}_u^+, \underline{z}_u^-)\,\underline{a}]\,\dot{\underline{r}} = \dot{\underline{f}}(t) \tag{26}$$

The system equations are then given by (24), (25), (26).

In order to increase the numerical stability of the system equations high frequency modes can be removed by the use of a Guyan reduction [18] or a normal mode transformation. Both transformations considered are related to loss of information compared to the original equations. In the Guyan transformation this is due to disregarding of the inertial forces related to the introduced slave-degrees-of-freedom. In the normal mode transformation this is due to the truncation of the eigenmode expansion describing the response process.

5. LOADING PROCESS

The external loading $\underline{f}(t)$ in (26) is modelled as a filtered white noise process.

Consider the case of seismic excitation with a Kanai-Tajimifilter with the parameters ζ_g and ω_g, [15]. If $\underline{r}$ specifies the deformation of the frame relative to the earth surface, $\underline{f}(t)$ is given by

$$\underline{m}^{-1}\underline{f} = \underline{U}[2\zeta_g\omega_g\dot{r}_o+\omega_g^2 r_o] \tag{27}$$

$\underline{m}^{-1}$ is the inverse of the mass matrix, r_o is the earth surface motion relative to bed rock level, and $\underline{U}$ is a vector specifying the deflection in all global degrees of freedom for a unit horizontal earth surface motion.

The bed rock acceleration is modelled as an amplitude modulated Gaussian white noise process $\beta(t)W(t)$. $\beta(t)$ is a deterministic intensity function and $W(t)$ is a unit intensity Gaussian white noise process, i.e.

$$E[W(t)] = 0 \tag{28}$$

$$E[W(t_1)W(t_2)] = \delta(t_1-t_2) \tag{29}$$

The bed rock acceleration process is related to the earth surface motion through the stochastic differential equation

$$\ddot{r}_o + 2\zeta_g\omega_g\dot{r}_o+\omega_g^2 r_o = -\beta(t)W(t) \tag{30}$$

The filter parameters ζ_g and ω_g may be modelled as deterministic functions of time in case of time-varying spectral contents of the earth surface motion process.

From (27) and (30) the following differential equation for the loading process can be derived

$$\underline{m}^{-1}\dot{\underline{f}} = \underline{U}[-2\zeta_g\omega_g^3 r_o+\omega_g^2(1-4\zeta_g^2)\dot{r}_o-2\zeta_g\omega_g\beta(t)W(t)] \tag{31}$$

If the auto-spectral density of the earth surface motion has multiple spectral peaks a more involved filter should be applied. If the frequency response function of the filter can be written as a rational function, the filter is equivalent to an ordinary differential equation similar to (30) and (31).

In other applications such as offshore engineering and wind loading $\underline{f}(t)$ should be modelled as a filtered Gaussian white noise vector process $\{\underline{W}(t)\}$. The loading process is then obtained as the solution of a coupled system of ordinary stochastic differential equations.

6. SAFETY MEASURES

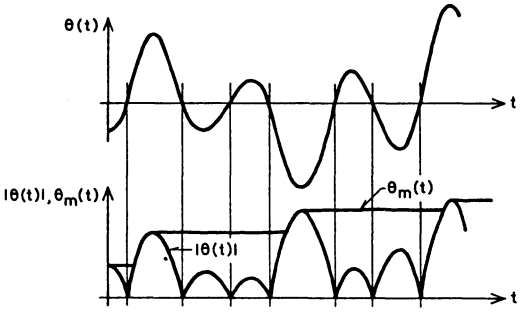

Figure 6: Sample curves of $\theta(t)$, $|\theta(t)|$, $\theta_m(t)$

Failure of a beam element is defined to take place, when the ultimate strain in the end sections exceeds an allowable level. In yield hinge models the rotational capacity of a section is normally related to the ultimate strain. Failure then takes place, when $|\theta|$ in a beam element exceeds a critical level α for the first time. Hence, the reliability can be controlled by introducing an extra state variable θ_m defined by

$$\theta_m(t) = \sup_{\tau \in [0,t]} |\theta(\tau)| \tag{32}$$

Sample curves of $\theta(t)$, $|\theta(t)|$ and $\theta_m(t)$ are shown in figure 6. All sample curves of $\theta_m(t)$ are non-decreasing functions with time.

The sample curves of θ_m are differential with probability 1 except at a set of t-values with Lebesgue measure 0. Under these restrictions $\theta_m(t)$ fulfils the following differential equation, cf figure 6 .

$$\dot{\theta}_m(t) = \frac{d}{dt}|\theta(t)|H[|\theta|(1-H[-\frac{d}{dt}|\theta|]) - \theta_m(t)]$$

$$= \text{sign}(\theta)\dot{\theta}\, H[|\theta|(1-H[-\text{sign}(\theta)\dot{\theta}]) - \theta_m(t)] \tag{33}$$

where H is defined by (7).

θ and $\dot{\theta}$ can be expressed by already introduced state variables $\underline{r}$ and $\dot{\underline{r}}$, using the compatibility equation (1). All equations (33) can then be assembled in the following vector differential equation

$$\dot{\underline{\theta}}_m = \underline{g}(\underline{r}, \dot{\underline{r}}, \underline{\theta}_m) \tag{34}$$

7. DYNAMIC SYSTEM ANALYSIS

(26) and (30) are written as equivalent coupled first order differential equations. In combination with (24), (25), (27), (34) the integrated dynamic system made up of the structural system, the safety measures and the loading process can be written as the following Itô-differential equations

$$d\underline{Z} = \underline{A}\,\underline{Z}\,dt + \underline{c}(\underline{Z})dt + \underline{b}\,dB,\ \underline{Z}(t_o) = \underline{Z}_o,\ t>t_o \tag{35}$$

$$\underline{Z}=\begin{bmatrix} \underline{r} \\ \dot{\underline{r}} \\ \ddot{\underline{r}} \\ \underline{r}_o \\ \dot{\underline{r}}_o \\ \underline{M} \\ \underline{z}_u^+ \\ \underline{z}_u^- \\ \underline{\theta}_m \end{bmatrix} \underline{A}=\left[\begin{array}{c|c|c|c|c|c|c|c|c} 0 & \underline{I} & 0 & 0 & 0 & 0 & 0 & 0 & 0 \\ \hline 0 & 0 & \underline{I} & 0 & 0 & 0 & 0 & 0 & 0 \\ \hline 0 & -\underline{m}^{-1}(\underline{k}_o+\underline{a}^T\underline{k}\,\underline{a}) & 0 & r_1\underline{U} & r_2\underline{U} & 0 & 0 & 0 & 0 \\ \hline 0 & 0 & 0 & 0 & 1 & 0 & 0 & 0 & 0 \\ \hline 0 & 0 & 0 & r_3 & r_4 & 0 & 0 & 0 & 0 \\ \hline 0 & \underline{k}\,\underline{a} & 0 & 0 & 0 & 0 & 0 & 0 & 0 \\ \hline 0 & 0 & 0 & 0 & 0 & 0 & 0 & 0 & 0 \\ \hline 0 & 0 & 0 & 0 & 0 & 0 & 0 & 0 & 0 \\ \hline 0 & 0 & 0 & 0 & 0 & 0 & 0 & 0 & 0 \end{array}\right] \underline{c}(\underline{Z})=\begin{bmatrix} \underline{0} \\ \underline{0} \\ \underline{0} \\ 0 \\ 0 \\ \underline{0} \\ \underline{f}^+(\underline{Z}) \\ \underline{f}^-(\underline{Z}) \\ \underline{g}(\underline{Z}) \end{bmatrix} \underline{b}=\begin{bmatrix} \underline{0} \\ \underline{0} \\ b_1\underline{U} \\ 0 \\ b_2 \\ \underline{0} \\ \underline{0} \\ \underline{0} \\ \underline{0} \end{bmatrix} \tag{35a}$$

$$r_1 = 2\zeta_g\omega_g^3,\ r_2 = \omega_g^2(1-4\zeta_g^2),\ r_3 = -\omega_g^2,\ r_4 = -2\zeta_g\omega_g \tag{35b}$$

$$b_1 = -2\zeta_g\omega_g\beta(t),\ b_2 = -\beta(t) \tag{35c}$$

$\{B(t)\}$ is a Brownian motion process. Because the vector $\underline{b}$ is independent of the state vector $\underline{Z}$, the solutions of (35) will be identical with probability 1, whether (35) is interpreted as an Itô or as a Stratonovich differential equation, [5, 6].

In the specification of the matrix $\underline{A}$ vector and matrix designations have mostly been omitted for simplicity. $\underline{I}$ signifies the identy matrix.

The idea behind the partioning of the state variables as indicated by (35a) is to separate linear and non-linear differential equations. In this context it should be noted that $\underline{k} = \underline{k}(\underline{M}, \underline{z}_u, \underline{z}_u)$ is variable, so $\underline{A}$ is actually a stochastic matrix. However, it will be assumed that $\underline{k}$ during short instants of time after $t = t_o$ can be replaced by its expectation $E[\underline{k}]$ at $t = t_o$, where t_o is the time of most recent updating. During the solution process $E[\underline{k}]$ is then currently updated. Note that replacing $\underline{k}$ will $E[\underline{k}]$ means that the impacts of the variance of $\underline{k}$ on the variance of $\underline{r}$, $\dot{\underline{r}}$, $\ddot{\underline{r}}$, $\underline{M}$ is ignored. Hence, it is to be expected that the variance of these quantities will be under-estimated.

The differential equations for the moments of the vector process can be obtained in various ways. The most natural way is to apply the Itô-formula [6, 7] to the combined

stochastic variable $q(\underline{Z}) = z_1^{k1} z_e^{k2} \ldots z_n^{kn}$, and perform the expectation. Alternatively, one can start from the Fokker-Planck-Kolmogorov equation associated with (35). In combination with natural boundary conditions and applying the divergence theorem, the differential equations for the moments are obtained. For the mean value function $\mu_i(t) = E[Z_i(t)]$ and the covariance function $C_{ij}(t) = E[(Z_i - \mu_i(t))(Z_j - \mu_j(t))]$ the following differential equations valid for $t > t_o$ are obtained, [6, 7]:

$$\frac{d\mu_i}{dt} = A_{ij}\,\mu_j + E[c_i(Z_k)] \,, \quad \mu_i(t_o) = E[Z_i(t_o)] \tag{36}$$

$$\frac{dC_{ij}}{dt} = A_{ik}C_{kj} + A_{jk}C_{ki}$$

$$+E[c_i(Z_k)(Z_j - \mu_j)] + E[c_j(Z_k)(Z_i - \mu_i)] + b_i(t)b_j(t) \,, \; C_{ij}(t_o) = C_{o,ij} \tag{37}$$

In the above equations the summation convention has been applied. A_{ij}, c_i, b_i, signify components of $\underline{A}$, $\underline{c}$, $\underline{b}$ in (35) respectively.

(36), (37) represent $n(n+3)/2$ different differential equations to be solved numerically, n being the dimension of $\underline{Z}$. During the solution process A_{ij} is updated sequentially as explained above.

When the hierarchy of moments is truncated at second order level as with (36), (37), the main problem is that only the first and second order moments are determined, whereas the expectations on the right hand sides of the equations require that the full distribution of $\underline{Z}$ is known. Hence, the joint frequency function $f_{\underline{Z}}$ of $\underline{Z}(t)$ has to be estimated solely from the second order moments. In the next chapter it is demonstrated, how this may be properly done with due considerations to the physics of the problem.

8. MODELLING OF JOINT PROBABILITY DENSITY FUNCTION OF SYSTEM STATE VARIABLES

For a certain element in the structure the following state variables have been defined $\underline{Z}_e = (\underline{\theta}_e, \dot{\underline{\theta}}_e, \underline{M}_e, \underline{\theta}_{me}, \underline{z}^+_{u,e}, \underline{z}^-_{u,e})$ where $\underline{\theta}_{me} = (\theta_{m1}, \theta_{m2})$, $\theta_{mi}(t)$ being the numerical maximum value of θ_i encountered in $[o, t]$. It will now be demonstrated that (36), (37) can be applied approximately if only the joint probability density of $\underline{Z}_e$ is known.

As mentioned, the stochastic matrix $\underline{k}$ in (34) is replaced by its expectation $E[\underline{k}]$, which is updated sequentially during the solution process. $\underline{k}$ is merely an assembly of the element stiffness matrices $\underline{k}_e$ given by (11) or (22). $E[\underline{k}_e]$ can be calculated from the joint probability density function of $\underline{M}_e$, $\underline{z}^+_{u,e}$, $\underline{z}^-_{u,e}$ or $\underline{M}_e$, $\dot{\underline{\theta}}_e$.

The non-zero components of the vector $\underline{c}(\underline{Z})$ are made up of the vectors $\underline{f}^+(\underline{Z})$, $\underline{f}^-(\underline{Z})$, $\underline{g}(\underline{Z})$. These quantities are assemblies of the corresponding quantities at element le-

vel $\underline{f}_e^+(\dot{\underline{\theta}}_e, \underline{M}_e, \underline{z}^+_{u,e}, \underline{z}^-_{u,e})$, $\underline{f}_e^-(\dot{\underline{\theta}}_e, \underline{M}_e, \underline{z}^+_{u,e}, \underline{z}^-_{u,e})$, $\underline{g}_e(\underline{\theta}_e, \dot{\underline{\theta}}_e, \underline{\theta}_{me})$. Hence, $\underline{c}(\underline{Z})$ only depends on $\underline{Z}$ through the local element stochastic variables, i.e. $\underline{c}(\underline{Z}) = \underline{c}(\underline{Z}_e)$ and the expectation $E[\underline{c}(\underline{Z})] = E[\underline{c}(\underline{Z}_e)]$ in (36) can be evaluated at element level.

For the expectations in (37) the following approximation is applied

$$E[c_i(\underline{Z})(Z_j-\mu_j)] \simeq E[\frac{\partial c_i(\underline{Z})}{\partial z_k}]C_{kj} \tag{38}$$

(38) holds exactly, when $\underline{Z}$ is jointly normally distributed, [12], or when $\underline{c}(Z)$ is a linear vector function of $\underline{Z}$. (38) is the crucial assumption in the equivalent linearization method. As shown above, $c_i(\underline{Z})$ only depends on $\underline{Z}$ through the local element stochastic variables $\underline{Z}_e$, i.e. $c_i(\underline{Z}) = c_i(\underline{Z}_e)$. For the partial derivative in (38) then follows $\frac{\partial c_i(\underline{Z}_e)}{\partial z_k} = 0$, if $Z_k \notin \underline{Z}_e$. The non-zero components of $E[\frac{\partial c_i(\underline{Z})}{\partial z_k}]$ can consequently be calculated at element level.

Because of the indicated approximations, the application of (36), (38) is straightforward, if the joint probability density function $f_{\underline{Z}_e}(\underline{z}_e)$ is known for all beam elements. These are assumed on the form

$$f_{\underline{Z}_e}(\underline{z}_e) = f_{\underline{X}_e \underline{M}_e \underline{\theta}_{me}}(\underline{x}, \underline{m}, \underline{t}_m) \prod_{i=1}^{I} [\delta(z^+_{u,i}-E[z^+_{u,i}])\delta(z^-_{u,i}-E[z^-_{u,i}])] \tag{39}$$

where $\underline{X}_e = (\theta_1, \theta_2, \dot{\theta}_1, \dot{\theta}_2)$.

I signifies the number of sections within the considered beam element, at which the unloading and loading sequences from the plastic ranges as specified by the non-dimensional moments $z^+_{u,i}$, $z^-_{u,i}$ are determined. As indicated by (39) these quantities are assumed to vary with zero variance at their expected values, $E[z^+_{u,i}]$, $E[z^-_{u,i}]$. Physically this means that all loading branches ABC in figure 2b at a given time and place on the beam are all geometrically identical. Similarly, the loading branches CDE will be geometrically identical. The elastic-plastic transition points B and D will, however, vary deterministically with time and place on the beam.

θ_{mi} turns out to be approximately Gamma distributed

$$f_{\theta_{mi}}(x) = \begin{cases} 0 & , x < 0 \\ \frac{1}{\beta_i^{\alpha_i}\Gamma(\alpha_i)} x^{\alpha_i-1} e^{-\frac{x}{\beta_i}} & , x \geq 0 \end{cases} \quad i = 1, 2 \tag{40}$$

The parameters α_i and β_i are related to the mean μ_{mi} and variance σ^2_{mi} of $\theta_{mi}(t)$ as follows

$$\alpha_i(t) = \frac{\mu^2_{mi}(t)}{\sigma^2_{mi}(t)} \tag{41}$$

$$\beta_i(t) = \frac{\sigma^2_{mi}(t)}{\mu_{mi}(t)} \tag{42}$$

In case of yield hinge models, the states $M_i = M_y$ and $M_i = -M_y$, corresponding to plastic deformations, are associated with a finite probability, cf [17]. Formally this means that the joint probability density function $f_{\underline{X}_e \underline{M}_e}$ of $(\underline{X}_e, \underline{M}_e)$ takes infinite values at the hyperplanes $M_1 = \pm M_y$ or $M_2 = \pm M_y$. $f_{\underline{X}_e \underline{M}_e}$ is then assumed on the following form, which is a generalization of a suggestion due to Minai & Suzuki [3].

$$
\begin{aligned}
f_{\underline{X}_e \underline{M}_e}(\underline{x}, \underline{m}) &= \varphi_6(\underline{x}, m_1, m_2) \\
&+ \delta(M_y - m_1) \int_{M_y}^{\infty} \varphi_6(\underline{x}, u_1, m_2)\, du_1 + \delta(M_y + m_1) \int_{-\infty}^{-M_y} \varphi_6(\underline{x}, u_1, m_2)\, du_1 \\
&+ \delta(M_y - m_2) \int_{M_y}^{\infty} \varphi_6(\underline{x}, m_1, u_2)\, du_2 + \delta(M_y + m_2) \int_{-\infty}^{-M_y} \varphi_6(\underline{x}, m_1, u_2)\, du_2 \\
&+ \delta(M_y - m_1)\delta(M_y - m_2) \int_{M_y}^{\infty}\int_{M_y}^{\infty} \varphi_6(\underline{x}, u_1, u_2)\, du_2 du_1 + \delta(M_y + m_1)\delta(M_y - m_2) \int_{-\infty}^{-M_y}\int_{M_y}^{\infty} \varphi_6(\underline{x}, u_1, u_2)\, du_2 du_1 \\
&+ \delta(M_y - m_1)\delta(M_y + m_2) \int_{M_y}^{\infty}\int_{-\infty}^{-M_y} \varphi_6(\underline{x}, u_1, u_2)\, du_2 du_1 + \delta(M_y + m_1)\delta(M_y + m_2) \int_{-\infty}^{-M_y}\int_{-\infty}^{-M_y} \varphi_6(\underline{x}, u_1, u_2)\, du_2 du_1
\end{aligned}
\tag{43}
$$

(43) is valid for $(M_1, M_2) \in [-M_y, M_y] \times [-M_y, M_y]$. $f_{\underline{X}_e \underline{M}_e}(\underline{x}, \underline{m}) = 0$ for $(m_1, m_2) \notin [-M_y, M_y] \times [-M_y, M_y]$.

$\varphi_6(\underline{x}, m_1, m_2)$ is the frequency function of a 6-dimensional normal stochastic variable with mean μ_i^o and covariance matrix C_{ij}^o. In general $\mu_i^o \neq \mu_i$ and $C_{ij}^o \neq C_{ij}$, where μ_i, C_{ij} are the mean and covariance of $(\underline{X}_e, \underline{M}_e)$ as calculated from (36), (37). However, the relationship between these quantities is easily calculated from (43).

In case of a moment-curvature relationship as shown in figure 2 the total probability mass will be continuously distributed in $]-M_y, M_y[\times]-M_y, M_y[$. However, $f_{\underline{X}_e \underline{M}_e}(\underline{x}_e, m_1, m_2)$ will have dominant peaks for $m_1 \to \pm M_y$ or $m_2 \to \pm M_y$. (43) is then approximately used also in this case.

In order to calculate $E[g(\theta, \dot{\theta}, \theta_m)]$ and $E[(Z - \mu_z)\, g(\theta, \dot{\theta}, \theta_m)]$, where $g(\theta, \dot{\theta}, \theta_m)$ is the right hand side of (33) and $Z \in \{\theta, \dot{\theta}, \theta_m\}$, the joint probability density $f_{\theta_m \theta \dot{\theta}}$ of $(\theta_m, \theta, \dot{\theta})$ should be estimated.

As seen from (33), $g(\theta, \dot{\theta}, \theta_m) = 0$ except at the semiplanes $\theta - \theta_m = 0 \wedge \dot{\theta} > 0$ or $\theta + \theta_m = 0 \wedge \dot{\theta} < 0$, where $g(\theta, \dot{\theta}, \theta_m) = \frac{d}{dt}|\theta|$. The events $\{\theta - \theta_m = 0 \wedge \dot{\theta} > 0\}$ and $\{\theta + \theta_m = 0 \wedge \dot{\theta} < 0\}$ are however related to a finite probability. Formally this means that $f_{\theta_m \theta \dot{\theta}}$ takes infinite values at the said semiplanes.

Instead of θ_m consider the auxiliary state variable

$$S = |\theta|(1 - H[-\text{sign}(\theta)\dot{\theta}]) - \theta_m \tag{44}$$

The event $\{\theta - \theta_m = 0 \wedge \dot{\theta} > 0\} \cup \{\theta + \theta_m = 0 \wedge \dot{\theta} < 0\}$ is then tantamount to the event $\{S = 0\}$. The joint probability density of $(S, \theta, \dot{\theta})$ is then assumed on the form

$$f_{S\theta\dot{\theta}}(s, t, \dot{t}) = \varphi_3(s, t, \dot{t}) + \delta(s) \int_0^\infty \varphi_3(u, t, \dot{t})\,du, \quad s \leq 0 \tag{45}$$

The mean values and covariances of $(S, \theta, \dot{\theta})$ are calculated from the corresponding mean values and covariances of $(\theta_m, \theta, \dot{\theta})$ by means of (44). The adjustable parameters of the 3-dimensional normal probability density function φ_3 are then easily calibrated. The joint distribution of $(\theta_m, \theta, \dot{\theta})$ can now be expressed in terms of $f_{S\theta\dot{\theta}}$ as follows.

$$F_{\theta_m\theta\dot{\theta}}(t_m, t, \dot{t}) = P(|\theta|(1-H[-\text{sign}(\theta)\dot{\theta}]) - S \leq t_m \wedge \theta \leq t \wedge \dot{\theta} \leq \dot{t})$$

$$= \int_{-\infty}^{\min(0,t)} \int_{0}^{\max(0,t)} \int_{-t_m}^{0^+} f_{S\theta\dot{\theta}}(s, \tau, \dot{\tau})\,ds\,d\tau\,d\dot{\tau} + \int_{0}^{\max(0,\dot{t})} \int_{-t_m}^{\min(0,t)} \int_{-t_m}^{0^+} f_{S\theta\dot{\theta}}(s,\tau,\tau)\,ds\,d\tau\,d\tau$$

$$+ \int_{-\infty}^{\min(0,\dot{t})} \int_{-t_m}^{\min(0,t)} \int_{-\tau-t_m}^{0^+} f_{S\theta\dot{\theta}}(s, \tau, \dot{\tau})\,ds\,d\tau\,d\dot{\tau} + \int_{0}^{\max(0,\dot{t})} \int_{0}^{\max(0,t)} \int_{\tau-t_m}^{0^+} f_{S\theta\dot{\theta}}(s,\tau,\dot{\tau})\,ds\,d\tau d\dot{\tau}$$

$$-t_m \leq t \leq t_m,\ 0 \leq t_m < \infty,\ -\infty < \dot{t} < \infty \tag{46}$$

$$f_{\theta_m\theta\dot{\theta}}(t_m, t, \dot{t}) = f_{S\theta\dot{\theta}}(|t|(1-H[-\text{sign}(t)\dot{t}]-t_m, t, \dot{t}), \begin{matrix} -t_m \leq t \leq t_m \\ 0 \leq t_m < \infty \\ -\infty < \dot{t} < \infty \end{matrix} \tag{47}$$

9. RELIABILITY ANALYSIS

The reliability of the structural system can now be calculated based on the assumed probability density function (40).

Failure of the system in the interval $[o, t]$ has taken place, if at least one of the safety measures $\theta_{mi}(\tau)$ exceeds an allowable limit α_i for $\tau \in [o, t]$. Because the safety measures are non-decreasing function with time, the probability of failure in the time interval $[o, t]$ is then given by

$$P_f(t) = 1 - P\Big(\bigcap_{i=1}^{M} \sup_{\tau\in[o,t]} \theta_{mi}(\tau) \leq \alpha_i\Big) = 1 - P\Big(\bigcap_{i=1}^{M} \theta_{mi}(t) \leq \alpha_i\Big) \tag{48}$$

M signifies the number of control points. The system reliability (48) can only be calculated if the joint probability density of the considered safety measures θ_m is known, which has not been considered in the present study. The failure in a certain control point i can, however, be obtained as

$$P_{fi}(t) = 1-P(\theta_{mi}(t)\leq\alpha_i) = \int_{\alpha_i}^{\infty} f_{\theta_{mi}}(x;t)dx, i=1,\cdot\cdot,M \qquad (49)$$

$f_{\theta_{mi}}(x;t)$ is given by (40).

10. NUMERICAL EXAMPLE

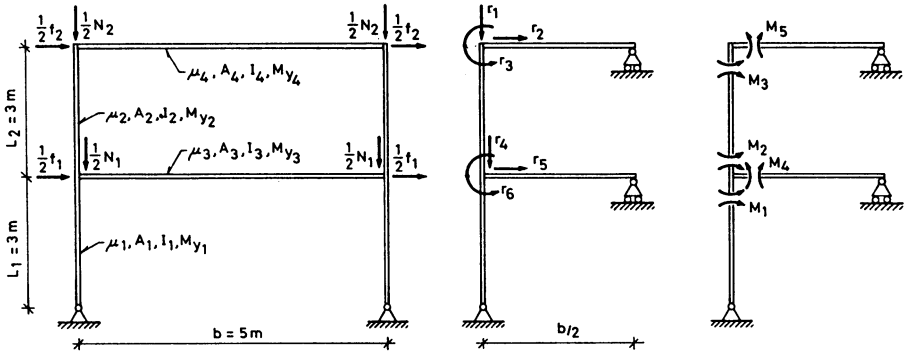

Figure 7: 2 storey-single bag frame. Designation of global degrees-of-freedom and end section moments.

Application of the theory will be demonstrated by the simply supported 2 storey-single bay frame shown on figure 7.

μ_i, A_i, I_i, M_{y_i} specifies the mass per unit length, cross-sectional area, inertial bending moment of inertia and bending moment capacity of element i. All elements have the same elasticity modulos. Further the frame is modelled as a yield hinge model.

The frame is loaded with horizontal forces f_1, f_2 and storey loads N_1, N_2, which are applied symmetrical at the system nodes as shown on figure 7. Deformations of the frame will then be antimetric and the symmetry can be utilized to reduce the problem.

The system then has 2 rotational degrees of freedom and 4 translational degrees of freedom. The distributed element masses are taken into consideration through a consistent mass matrix $\underline{m}$. Further the P-δ effect due to the storey loads N_1, N_2 are approximately considered.

The following data are applied

Beam	μ_i (kg/m)	A_i ($10^{-3} m^2$)	I_i ($10^{-5} m^4$)	M_o (10^3 Nm)	M_y (10^3 Nm)
1	46.0	5.86	2.63	78.7	82.8
2	46.0	5.86	2.63	78.7	82.8
3	2000	∞	3.89	77.8	85.0
4	1000	∞	1.945	46.6	51.1

$E = 2.1 \cdot 10^{11}$ N/m^2

$N_1 = (\mu_1 L_1 + \mu_3 L_2 + \mu_3 b)g$, $g = 9.81$ m/s^2

$N_2 = (\mu_2 L_2 + \mu_4 b)g$

$\omega_g = 15.6$ s^{-1}, $\zeta_g = 0.6$

The autospectral density S_o of the bedrock-excitation process is $2\pi S_o = 0.15$ m^2/s^2

To evaluate the results from the proposed non-Gaussian closure method, totally 10,000 simulations with the initial conditions $\underline{Z}_o = \underline{0}$ are performed. Generations of realisations of the broad banded zero mean Gaussian process is performed by the method of Penzien [16]. The integrated dynamical system is solved by a 4th order Runge-Kutta sceme from 0 to 20 T_o, where $T_o = 0.98$ s is the fundamental period of undamped linear eigenvibrations.

In figure 8 the simulated probability density functions for the end section moments M_1 and M_3 respectively are compared with the assumed distribution given by (43) for $N = 20$ periods. At the section at M_1 heavily yielding has taken place, whereas the section at M_3 has deformed primarily elastically.

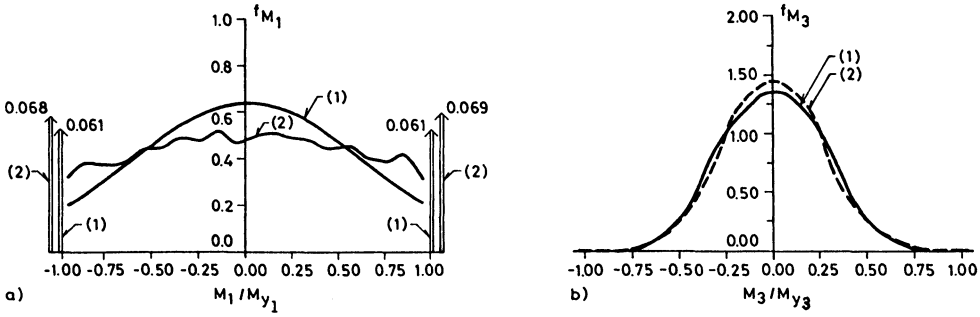

Figure 8. Density functions for the end section moments M_1 and M_3 respectively.

(1) Theoretical probability density with parameters calibrated from simulated mean value and covariance.

(2) Simulation.

From figure 8 it may be concluded that the proposed marginal distribution of the end section is applicable with or without yielding present.

In figure 9 the distribution of the state variable θ_m for various number of periods is shown for end section 1 and 3 respectively (cf. fig. 7) in comparison with the respective proposed distribution given by (40).

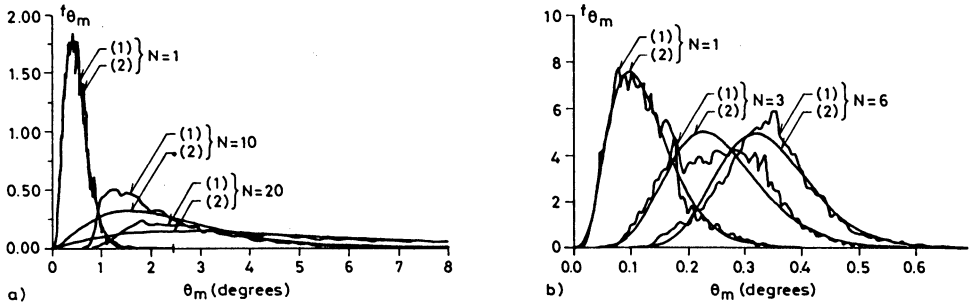

Figure 9. Density functions for the state variable θ_m

a) End section 1
b) End section 3

1) Simulation
2) Theoretical probability density. Parameters α and β estimated from simulated mean and covariance.

It should be emphasized that the scatter on the simulated curves is due to scarcity of sample data and not a physical condition.

It may be concluded that the assumption that $\theta_{m_i}(t)$ is Gamma distributed seems promising for a small ratio of yielding present.

11. CONCLUSIONS

Based on physical arguing a non-Gaussian closure method for hysteretic multi-storey frame is suggested in which the adjustable parameters can be determined solely from the moment equations at second order. Further the proposal will be asymptotically correct in the absence of plastic deformation, and can hence be considered representative at least in case of moderate plastic deformations.

The relevance of the model has been demonstrated by extensive simulation for a 2 storey yield hinge frame. From these simulation studies it further follows that the proposed safety measures to a great extent follow a Gamma distribution.

Results from the application of the present model will be addressed later on. At present work is done on modelling the joint probability density of the safety measures,

making a true system reliability calculation possible. Further improved marginal probability density functions for the safety margins are searched for in terms of truncated Laurent series, which necessitates the formulation of extra moment equations in order to determine the extra parameters in these series.

12. REFERENCES

[1] Wen, Y.K.: Method for Random Vibration of Hysteretic Systems.J . Eng. Mech. Div., ASCE, Vol. 102, No. EM2, April, 1975, pp. 249-26

[2] Baber, T.T., and Wen, Y.K.: Stochastic Response of Multi-storey Yielding Frames. Earthquake Engineering and Structural Dynamics, Vol. 10, pp. 403-416. 1982.

[3] Minai, R, and Suzuki, Y.: Seismic Reliability Analysis of Building Structures. Proc. ROC-Japan Joint Seminar on Multiple Hazards Migration, National Taiwan University, Taipei, Taiwan, ROC, March, 1985, pp. 193-208.

[4] Suzuki, Y., and Minai, R.: Seismic Reliability Analysis of Hysteretic Structures Based on Stochastic Differential Equations, Proc. 4th International Conf. on Structural Safety and Reliability, Vol. II, pp.177-186, 1985.

[5] Gihman, I.I., and Skohorod, A.V.: Stochastic Differential Equations. Ergebnisse der Mathematik und Ihrer Grenzgebiete. Vol. 72, Springer Verlag, 1972.

[6] Sobczyk, K.: Stochastic Differential Equations for Applications. Report No. 177, Dept. Struct. Engng., Technical University of Denmark, Lyngby, Denmark.

[7] Soong, T.T.: Random Differential Equations in Science and Engineering. Academic Press, 1973.

[8] Arnold, L.: Stochastic Differential Equations: Theory and Applications. J. Wiley and Sons, 1974.

[9] Iyengar, R.N., and Dash, P.K.: Study of Random Vibration of Non-Linear Systems by the Gaussian Closure Technique. J. Appl. Mech., 45, pp. 393-399, 1978.

[10] Spanos, P.-D.: Stochastic Linearization in Structural Dynamics. Applied Mechanics Reviews, Vol. 34, No. 1, January, 1981, pp. 1-8.

[11] Wen, Y.K.: Equivalent Linearization for Hysteretic Systems Under Random Excitation. J. Appl. Mech., Vol. 47, March, 1980, pp. 150-154.

[12] Atalik, T.S., and Utku, S.: Stochastic Linearization of Multi-Degree-of-Freedom Non-linear Systems. Earthquake Engineering and Structural Dynamics, Vol. 4, pp. 411-420, 1976.

[13] Crandall, S.H.: Non-Gaussian Closure for Random Vibration of Non-linear Oscillators. Int. J. Non-linear Mechanics, 15, pp. 303-313, 1980.

[14] Kaldjean, M.J.: Moment-Curvature of Beams as Ramberg-Osgood Functions. J. Struct. Div., ASCE, Vol. 93, No. ST5, October, 1967, pp. 53-65.

[15] Tajimi, H.: A Statistical Method of Determining of the Maximum Response of a Building Structure During an Earthquake. Proc. Second World Conference on Earthquake Engineering, Tokyo, July, 1960, Vol. II, pp. 781-797.

[16] Mørk, K.J., Thoft-Christensen, P., and Nielsen, S.R.K.: Simulation Studies of Joint Response Statistics for a One-Degree of Freedom Elasto-Plastic Structure. Structural Reliability Theory Series, Paper 27, University of Aalborg, 1987.

[17] Thoft-Christensen, P., Nielsen, S.R.K., and Mørk, K.J.: Simulation Studies of Joint Response Statistics for a Two-Storey Hysteretic Frame Structure. Structural Reliability Theory Series, Paper 28, University of Aalborg, 1987.

[18] Guyan, R.J.: Reduction of Stiffness and Mass Matrices. AIAA Journal, Vol. 3, p. 380, 1965.

SYSTEM RELIABILITY MODELS FOR BRIDGE STRUCTURES

Andrzej S. Nowak & Niels C. Lind
Department of Civil Engineering
University of Michigan, Ann Arbor, MI, USA 48109

1. INTRODUCTION

An important problem in the developed part of the world concerns the state of repair of society's technology infrastructure, of which highway bridges are an important part. According to a recent survey by the U.S. Federal Highway Administration more than 200,000 bridges in the U.S.A are considered deficient because they do not satisfy the requirements of current design specifications. On the other hand, bridge tests often reveal that the actual strengths exceed the calculated values considerably. This points to a need for a different approach to the evaluation of existing structures.

In traditional bridge analysis the calculations are performed for individual members, using conservative values of load. This does not adequately reflect the ductility and load sharing of the structure. Accurate analysis is extremely difficult because of random variations in geometry and mechanical properties of materials. The objective of the paper is to describe system reliability models for the analysis of highway bridges. The models serve in the development of design provisions, particularly in the selection of load and resistance factors.

Ultimate and serviceability limit states are considered. The ultimate limit states include the bending moment capacity and shear capacity. The acceptability criteria for ultimate limit states are based on the magnitude of load and resistance. The serviceability limit states include cracking, vibrations and deflections. Fatigue is also treated formally as a serviceability limit state. In serviceability limit states the frequency of occurrence plays an important role in the criteria for acceptability.

Load models are based on the available data, truck surveys, weigh-in-motion

studies and overweight citations of Police. Bridge structures are considered as systems. The resistance of component elements is developed for composite steel girders, prestressed concrete girders and for timber stringers. The system reliability is evaluated using computer programs specially developed for the purpose. The models are demonstrated by means of practical examples.

The composite steel girder bridge is modelled as a grid of elements composed of sections with nonlinear moment curvature relationships. For a fixed truck configuration, the ultimate load is calculated by gradually increasing the initial wheel weights until the deformations exceed pre-established limits.

Moment-curvature relationships have been developed for various types and sizes of prestressed concrete girders. Live load spectra are calculated for various girders. The results may serve as a basis for the analysis of the serviceability limit states.

Three types of timber decks are considered: sawn stringers, non-prestressed laminated decks and prestressed laminated decks. The reliability is calculated using simulation.

Considerable differences between the reliability of single members and the reliability of systems was observed. The study indicates that the actual safety reserve must be evaluated by analysis of the structural system rather than single members (the traditional approach). Further work is required to develop more efficient numerical procedures.

2. LOAD MODELS

The major load components for highway bridges are dead load, live load with impact, environmental loads (wind, earthquake), and special loads (braking forces, collision). The magnitudes of the load effects depend on the structural type, span length, type of traffic and other characteristics. For example, for long and short spans (up to 100 m.), the major loads are live load and dead load. The truck position on the bridge and multiple presence (side-by-side or in one lane) are also

important. For short spans (less than 30 m) it is particularly important to know how the truck weights are distributed on the structure. In case of very short spans (less than 6 m), the live load is dominated by axle weights. In this study three load components are considered: Dead load, live load and impact load.

The dead load, D, is the gravity load of the structural and nonstructural elements permanently connected to the bridge. The mean-to-nominal ratio and coefficient of variation are different for various dead load components. In particular, they are 1.03 and 4 per cent respectively for factory-made members, 1.05 and 8 per cent for cast-in-place concrete and 1.0 and 25 per cent for asphalt respectively. Because the dispersion of D is small in comparison with the dispersion of L, it may be assumed that D is normally distributed.

The live load, L, covers a range of forces produced by vehicles moving on the bridge. The model uses existing Canadian and U.S. data, together with data on some 1600 Police citations of overweight trucks in the state of Michigan. Maximum moments, M_L, were calculated due to these trucks for various spans. The ratio M_L/M_A was also calculated, where M_A is the moment due to the AASHTO truck.

The 50 year maximum live load was developed by extrapolation. For several spans the basic parameters are given in Table 1. For comparison the means and coefficients of variation are also given for two models using other data bases: Ontario truck survey (Nowak and Zhou 1985) and weigh-in-motion (Ghosn and Moses 1984). The latter includes impact. The means in Table 1 are expressed in terms of the AASHTO specified moment.

A vehicle's position on the bridge is important to determine the load distribution to girders. The transverse location is modelled on the basis of observation (Nowak and Grouni 1986; Tantawi 1986).

Impact is traditionally expressed as a fraction of live load. Recent tests have indicated that the mean impact factor is about 0.05. The coefficient of variation is larger for steel bridges than for prestressed concrete, and larger for smaller spans; an average value is V = 0.45.

The dynamic effect is an integral part of the live load model. The major factors that affect the dynamic load on a bridge include: surface condition (bumps, potholes), natural frequency of the bridge (span length, stiffness, mass) and dynamics of the vehicle (suspension, shock absorbers). It is very difficult to model the individual contributions of these three factors. Some dynamic bridge tests were carried out in conjunction with the development of the OHBDC (Nowak and Zhou, 1985). The resulting distribution parameters are listed in Table 2.

Table 1. - 50 Year Live Load in terms of AASHTO moment.

Model	Statistics	Span (m) 18	24	30	36
Ontario truck survey	mean	1.69	1.77	1.92	2.05
	COV	0.11	0.11	0.11	0.11
Weigh-in-motion	mean	2.2	2.45	2.55	2.65
	COV	0.18	0.12	0.12	0.07
Used in this study	mean	1.85	1.95	2.15	2.21
	COV	0.1	0.1	0.09	0.1

Table 2. - Dynamic Load Factors.

Type of structure	Mean Value		Standard Deviation	
	Range	Assumed Value	Range	Assumed Value
Steel	0.08-0.20	0.14	0.05-0.20	0.10
Prestressed concrete:				
AASHTO type girders	0.05-0.10	0.09	0.03-0.07	0.05
Box girders and slabs	0.10-0.15	0.14	0.08-0.40	0.30
Others frames, trusses, ... etc.	0.10-0.25	0.17	0.12-0.30	0.26

3. MECHANICS OF BRIDGE RESISTANCE

The grid model and direct stiffness method are combined together with the incremental load procedure to predict the post-elastic behavior of three types of highway bridges. The steps are:

1. Modelling the bridge deck as a set of grid elements and computing their properties (using the specially developed computer program).
2. Defining and assembling the general form of the element stiffness

matrix that can be updated at each level of loading.

3. Distributing the wheel loads to grid nodes and forming the load vector.

In evaluating the ultimate strength capacity of the grid system the following assumptions are made: (1) The members lie all in the same plane; (2) all loads are perpendicular to this plane; (3) the deformations are small; and (4) the joints between elements are rigid. The overall stiffness matrix of the structure is composed of different element stiffness matrices. The stiffness matrix for a member with a plastic hinge is formed as for a nonprismatic beam element. Numerical integration is used to form the flexibility matrix of such an element.

Special consideration is given to load partitioning. When the position of a load does not coincide with a grid node, it is distributed linearly in the longitudinal direction without taking into account the moments that are associated with this distribution. The load is distributed nonlinearly in the transverse direction, i.e. the moments associated with the apportioning are accounted for. This idealization is reasonably accurate if the bridge is divided in the longitudinal direction into panels of length not more than 1.5 times the spacing of longitudinal elements (Tantawi 1986).

The elasto-plastic analysis is performed using a stepwise repeated load incremental procedure. Initially the bridge is analyzed elastically. For each load increment, member stiffness matrices are updated to account for the newly formed plastic hinges. The procedure is as repeated until unacceptable permanent deformation has occurred (taken as one per cent of the span length).

4. STOCHASTIC RESISTANCE MODEL

The resistance of a bridge member, R, is a random variable. It is convenient to consider R as the product of three random variables

$$R = R(M,F,P) = R_n \; M \; F \; P \qquad (1)$$

where R_n is the nominal (design) value of the resistance, M is a factor representing material properties (including strength, modulus of elasticity, cracking stress and chemical composition), F is a factor representing fabrication effects (geometry,

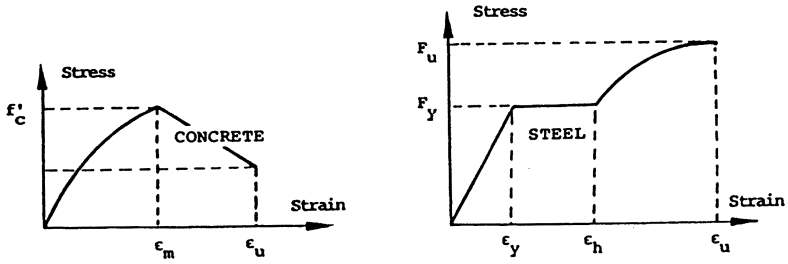

FIGURE 1. STRESS-STRAIN RELATIONSHIP

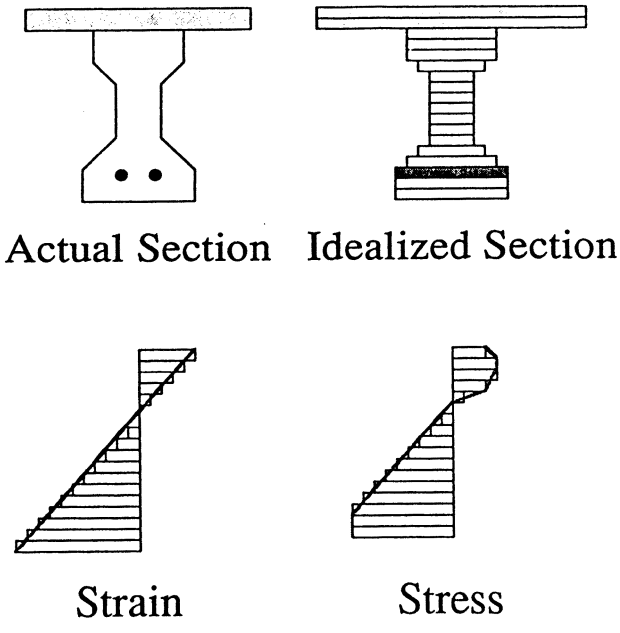

FIGURE 2 IDEALIZATION OF GIRDER SECTION

dimensions and workmanship and P is an analysis factor (including uncertainties due to approximate analysis, idealized stress and strain models and support conditions).

Some information about the variation of parameters M, F and P is available for the basic structural materials, members and connections. However, bridge members are often made of several materials (composite sections) and require special analysis.

Typical stress-strain curves for concrete, reinforcing steel and structural steel are shown in Fig. 1. The cross section of a girder was divided into several rectangular horizontal strips of small depth, as shown in Fig. 2. The load-deformation relationship for the section was developed by incremental loading, using the stress-strain curves of the basic materials together with the Bernoulli hypothesis. The resulting parameters are given in Table 3 for selected span lengths for composite steel girders, for reinforced concrete girders and for prestressed concrete girders. The method of Rosenblueth (1975, 1981) was used in the stochastic analysis.

The major parameters determining the behavior of timber members are the modulus of rupture and the modulus of elasticity. Extensive test data indicate large variation in both. The coefficient of variation of the modulus of rupture exceeds 30% and therefore it dominates the reliability analysis.

The resistance of a bridge depends on the resistance of the members (girders) and the connections, as well as on the redundancy. Redundancy is here taken in the general sense as the ability of the structure to continue to function safely in an almost normal manner despite failure of one of the main load carrying elements. To evaluate the redundancy of a structure, the failure modes of the main load carrying members must be examined to determine the possible secondary (redundant) load paths. These load paths must then be evaluated to determine that there are no weak links that could prevent the development of their full capacity. There are at least two load paths in a redundant structure, namely the primary path and a secondary path. However, the secondary path is not as stiff as the primary path. There must be some indication that the bridge is in distress. If not, the bridge may continue to be used without repair until the secondary path also fails.

Redundancy must be clearly separated in concept from the natural interaction of

bridge members that is often underevaluated in the design process. In the past, the use of the load distribution factor has generally resulted in an underevaluation. Newer methods of analysis permit more accurate evaluation. Tests have shown that the interaction of non-structural elements such as wearing surface, curbs, parapets etc. may be significant in serviceability conditions.

5. PRACTICAL EXAMPLES

Three cases were considered: No correlation, partial correlation, and perfect correlation between the strengths of the girders. The reliability indices were calculated for the whole bridge in each case. For comparison, the reliability was also evaluated for a single girder or beam. The study considered a reinforced concrete T-beam bridge. The bridge was built in New Zealand in 1937 and tested to failure in 1977 after being in service for 40 years (Buckle et al. 1985). Also considered were four composite steel girder bridges with spans of 40 ft to 100 ft (12 m to 30 m). These bridges were designed following the allowable stress design procedure outlined in the AASHTO Specifications (1983). The procedure was finally demonstrated on a timber deck bridge structure. Stringers were made of Douglas Fir, Select Structural grade, with a span of 16.5 ft. (4.75m). The distribution of the minimum ratio of modulus of rupture-to-actual stress was derived using simulation. The results are summarized in Table 3.

6. CONCLUSIONS

Highway bridges of small and intermediate span are relatively simple structural systems, but they require a systems reliability analysis for accurate assessment of the structural adequacy.

Load models require refinement in the range of high values. Police records of overweight citations may be useful in addition to weigh-in motion and survey data.

A grid analysis procedure has been found useful for the nonlinear analysis of girder bridges including the shear forces and torsional effects. The procedure apparently provides accurate results and requires considerably less computer time than conventional finite element methods.

In addition to straightforward simulation, Rosenblueth's point estimates may be used to determine the influence of random variables on the structural system response. This considerably reduces the number of required computer runs.

Correlation between the strength of the main girders, which is a factor that is very difficult to ascertain, does not appear to have much effect on the system reliability.

TABLE 3 RESISTANCE PARAMETERS

Span ft(m)	FM	V_{FM}	P	V_P	R/R_n	V_R
COMPOSITE STEEL GIRDERS						
40 (12)	1.03	0.089	0.99	0.08	1.02	0.12
60 (18)	1.02	0.0902	0.99	0.08	1.01	0.12
80 (24)	1.02	0.0866	0.99	0.08	1.01	0.12
100 (30)	1.02	0.0864	0.99	0.08	1.01	0.12
REINFORCED CONCRETE GIRDERS						
40 (12)	1.24	0.095	1.00	0.046	1.24	0.11
60 (18)	1.20	0.105	1.00	0.046	1.20	0.11
80 (24)	1.23	0.106	1.00	0.046	1.23	0.12
PRESTRESSED CONCRETE GIRDERS						
40 (12)	1.05	0.037	1.00	0.046	1.05	0.06
60 (18)	1.04	0.036	1.00	0.046	1.04	0.06
80 (24)	1.05	0.037	1.00	0.046	1.05	0.06
100 (30)	1.05	0.040	1.00	0.046	1.05	0.06

* FM represents two parameters M and F.

Table 4. Results of Reliability Analysis with Correlation

Bridge Type	Reliability Index, β			
	Element, β_e	System, β_s		
		ρ = 1.0	ρ = 0.5	ρ = 0.0
Reinforced Concrete	4.8	7.1	7.5	7.9
Composite Steel	3.8	6.0	6.3	6.9
Prestressed Concrete	3.4	5.0	5.1	5.3
Sawn Stringers	2.5			4.2*
Laminated Deck	---			3.0*
Prestressed Deck	---			7.5*

* Calculated for actual correlation coefficient

REFERENCES

Buckle, I.G., Dickson, A.R. and Phillips, M.H., "Ultimate Strength of Three Reinforced Concrete Highway Bridges," Canadian Journal of Civil Engineering, Vol. 12, 1985, pp. 63-72.

Ghosn, M. and Moses, F., "Bridge Deck Analysis," John Wiley and Sons, London, 1975.

Nowak, A.S. and Grouni, H. N., "Serviceability Criteria in Prestressed Concrete Bridges," ACI Journal, Vol. 83, No. 10, Jan.-Feb. 1986, pp. 44-49.

Nowak, A. S. and Lind, N. C., "Practical Bridge Code Calibration", ASCE, Journal of the Structural Division, Vol. 105, No. ST 12, Dec. 1979, pp. 2497-2510.

Nowak, A. S., and Zhou, J., "Reliability Models for Bridge Analysis," Report No. UMCE 85-3, Department of Civil Engineering, University of Michigan, March, 1985.

Ontario Highway Bridge Design Code, Ministry of Transportation and Communications, 2nd Edition, Downsview, Ontario, 1983.

Rosenblueth, E., "Point Estimates for Probability Moments", Proceedings of the National Academy of Sciences, U.S.A., Vol. 72, No. 10, Octoaber 1975, pp. 3812-3814.

Rosenblueth, E., "Two-point Estimate in Probabilities", Journal of Applied Mathematical Modelling, May, 1981.

Standard Specifications for Highway Bridges, American Association of State Highway and Transportation Officials, AASHTO, Washington, D.C., 1977.

Tantawi, H. M., "Ultimate Strength of Highway Girder Bridges", Ph.D. Thesis, University of Michigan, Ann Arbor, MI, 1986.

MODELLING OF THE STRAIN SOFTENING IN THE BETA-UNZIPPING METHOD

Wieslaw Paczkowski
Technical University of Szczecin
Al. Piastow 50, PL-70-311 Szczecin

1. INTRODUCTION

The strain softening is a phenomenon where the increasing generalized strain is accompanied by the decreasing generalized stress.
Both experimental and theoretical results indicate that compressed steel members of space trusses display considerable loss of load - - carrying capacity in the process of increasing axial deformations. In the most commonly used range of the slenderness ratio such loss can reach the value of 75% of the maximum force carried by the member, while the total axial deformation does not exceed 0.5% of the initial strut length. The phenomenon can be considered as strain softening.
A similar phenomenon appears in the plastic hinges of concrete frames, however, with less considerable quantities concerning bending moment and corresponding curvature.
Most of the existing reliability algorithms take into account the strain softening in a simplified way by means of an elastic-brittle model with a constant residual force. The paper deals with the strain softening elements modelled by C^0 continuous P-d relations, where P is an axial force carried by the element and d is the axial deformation. The beta-unzipping method has been applied for the reliability analysis of trusses made of elements displaying strain softening behaviour.
The beta-unzipping method, first suggested by Thoft-Christensen [1], developed by Thoft-Christensen and Sørensen [2], and fully described in Thoft-Christensen and Murotsu [3], provides an efficient tool for the estimation of the reliability index of complex strut structures. Usually such structures possess a high degree of redundancy and therefore, their reliability model cannot be established explicitly. An approximate approach based on presentation of the structure as a set of parallel systems connected in series makes it possible to calculate the reliability index. The reliability index can be calculated at different levels. From the practical point of view 0, 1, 2 and mechanism levels can be of interest. The definition of a failure state of each possible failure element is a basic information necessary for performing calculations. The actual version of the beta-unzipping method

considers three models of member behaviour: perfectly brittle, per - fectly ductile and elastic-residual. Ductile and elastic-residual elements lose their stiffness after reaching the failure state, but retain their ability to carry full or partial constant force independently of progressing displacement. Perfectly brittle elements are removed from the structure after reaching the failure state. The considered models are presented in figure 1.
It has been experimentally observed that in the process of increasing external load some members of space trusses lose their ability to carry the load while diflections remain in the range acceptable for small - from the theoretical point of view - displacements. The main purpose of the paper is to present how a general member behaviour including strain softening may be taken in accout in the reliability analysis of structures. The beta-unzipping method has been used to perform the analysis, thus some details of the solution are discussed.

2. STRAIN SOFTENING BEHAVIOUR OF COMPRESSED BARS

Some spectacular collapses of spatial strut structures contributed substantially to a view that the full information concerning post - - buckling behaviour of compressed bars should be available [4]. The information is necessary to perform the limit state analysis of the structure as well as the reliability analysis. A short review of the post-buckling behaviour of compressed bars presented below is limited to a static, single process of loading or unloading.
Different theoretical approaches were adopted to analyse the post - - buckling behaviour of compressed bars. The most sophisticated approach which makes it possible to take into account such phenomena as initial stresses, local imperfections and non-linear material behaviour is to use the finite element method /FEM/. However, because of its complexity,it did not gain wide popularity. Usually the whole structure is analysed and thus the full FEM analysis of each singular member

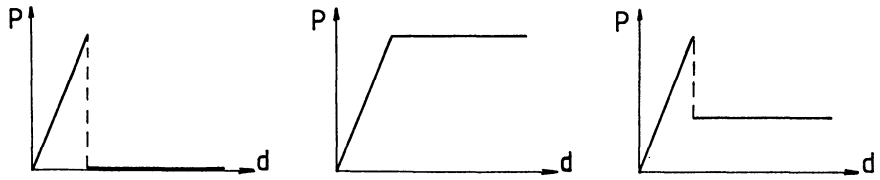

Figure 1. Models of member behaviour.

becomes unacceptable.
In the most typical cases the post-buckling behaviour can be considered as an in-plane phenomenon. This allows for reduction of the compressed bar usually to a one or two-degrees-of-freedom system with a developing plastic hinge. Equilibrium conditions and geometrical compatibility of such a system are sufficient to find the relation between the axial load and axial shortening /P-d curve/.
Usually the influence of initial imperfections can be taken into account reducing all of them to the influence of an equivalent initial curvature.
Much effort has been made to establish the P-d relations. Some recently published theoretical models which have found further applications in more advanced problems /cyclic loading/ are briefly described below. Such models were assumed to fit the purpose of the paper, which gave a full description of the element behaviour in the process of loading and unloading appearing at any stage. Only pin-ended bars are considered.
Higginbotham and Hanson [5] formulate and examine two analytical solutions employing the plastic hinge concept. Geometry of a bar with a developing plastic hinge under compression and tension is shown in figures 2a and 2b respectively. In the first solution exact expres - sions for the length of the bar S and its projection X are calculated from the elliptic integrals of the first and second kind using an exact expression for the curvature between the member ends and its mid length. This model gives a force-deformation pattern which corresponds to the displacement controlled behaviour of the bar.
The same pattern can be obtained using another analytical solution where linear variation of the bending moment between the member ends and mid length is assumed. This leads to the formulation where the force for the assumed displacements of the bar ends is calculated as a root of a sixth degree polynomial. Deviation less than 5% for these two solutions in comparison with test results is reported.
Papadrakakis and Chrysos [6] applied to their model the influence of

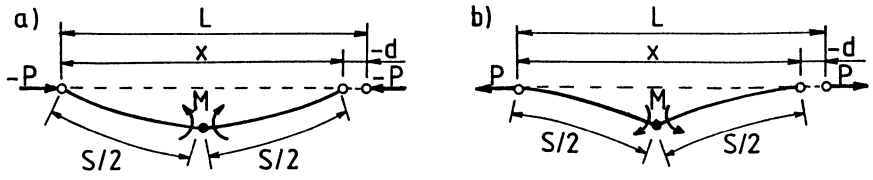

Figure 2. Plastic hinge under compression and tension.

initial imperfections in the form of initial out-of-straightness following a model developed by Nonaka [7] for perfect bars. As the relation P-d is sought, the components of d are as follows:

$$d = d_e + d_g + d_p + d_t \qquad / 2.1 /$$

where

d_e is the displacement between the ends due to uniform elastic axial deformation existing in all loading phases,

d_g is the change of displacement caused by lateral deflection,

d_p is the plastic axial deformation,

d_t is the plastic elongation in the straight configuration distributed along the bar axis.

The initial imperfect shape is assumed in the form of a sine curve. In the elastic phase the additional deflection shape also becomes a sine curve. Because of initial curvature the critical value of axial load is defined as a force for which a plastic hinge either in tension or compression is produced. The critical force depends on the magnitude of the initial imperfection and on the type of the cross-section. The post-buckling shape of the bar is described by the small displacement equation applied to each half part with boundary conditions modified by the developing plastic hinge. To find the angle of plastic rotation and corresponding plastic displacement the yield curves between axial force P and bending moment M is presented - for the sake of simplicity - in the piecewise linear form which allows easy calculation of the derivative dM/dP. This simplification makes it possible to obtain an expression for the displacement d in a closed form. The phase of plastic recovery is calculated from the same equation with properly modified boundary conditions.

W. F. Chen and D. J. Han present in [8] some fundamental relations concerning compressed tubular elements. [8] is related to previous works by W. F. Chen et al. To trace the post-buckling behaviour of the element the assumed deflection method was developed. The method is a simplified approach based on the additional assumption of the deflected shape of the column. It is assumed that an initially assigned deflection function does not change during the loading process but simply changes its magnitude. The load-shortening relation P-d can be obtained in a numerical way taking into account shortening due to the axial strains and due to the geometrical change of the lateral shape of the column.

All presented approaches claim good agreement with test results and are confirmed in other works. Some fundamental results based on these

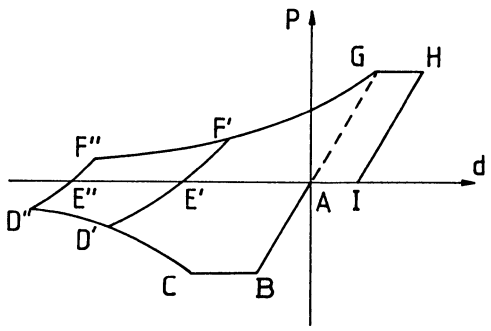

Figure 3. One cycle behaviour of an axially loaded bar.

theoretical models are shown below.
The most characteristic parts of a one cycle behaviour of a compressed element can be seen from a diagram shown in figure 3 [5]. This diagram was obtained using the plastic hinge concept in the displacement controlled mode.
The following phases can be distinguished:

A - B pre-buckling shortening. This phase can be linear or slightly non-linear if initial curvature is taken into account.

B - C post-buckling elastic shortening. The critical load is reached at point B. Point C marks the beginning of plastic deformation, thus up to that point the behaviour is elastic and therefore reversible.

C - D the plastic hinge formation, elasto-plastic behaviour. The shape of a compressed bar corresponds to that shown in figure 2a. The reverse of displacements can appear at any point D /D', .../.

D - F elastic unloading caused by the reverse of displacements. At point E /E', E'', .../ there is a change of the sign of the internal force P and a change of the bar shape from that shown in figure 2a to that shown in figure 2b.

F - G plastic rotation in the plastic hinge due to progressing increment of the member end displacements.

G - H perfectly plastic displacement of a tensile bar.

H - I elastic unloading of a tensile bar with residual plastic deformation.

Two main factors contribute to the force-deformation pattern of compressed bars: slenderness λ and initial imperfections. The influence of initial imperfections can be taken into account by means of an equivalent initial curvature. Figure 4 shows three basic patterns of

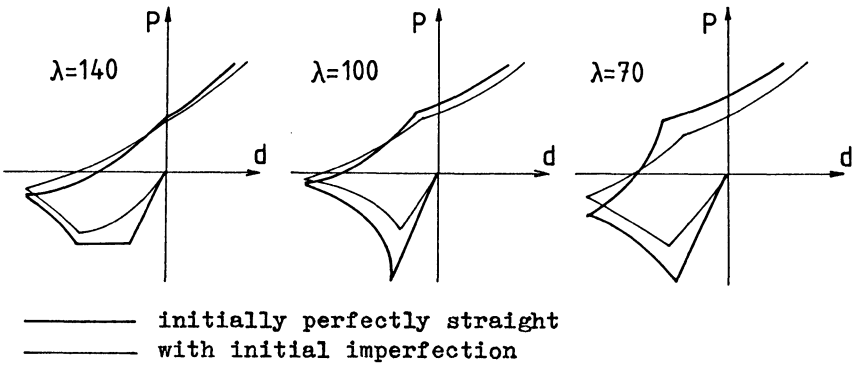

Figure 4. Influence of initial imperfection.

behaviour influenced by the slenderness and initial imperfections [6]. These curves can be considered to be typical and they reflect all features of curves obtained in other ways.

To compare a typical behaviour of struts of the same linear-elastic stiffness but of different slenderness all the curves can be presented in one set of coordinates: ε axial strain, σ axial stress as shown in figure 5 [9].

A very limited amount of data is available for the estimation of random parameters of the P-d curves. In general, the P-d relation is a stochastic process, but from the point of view of efficiency of calculation a proper simplification should be adopted.

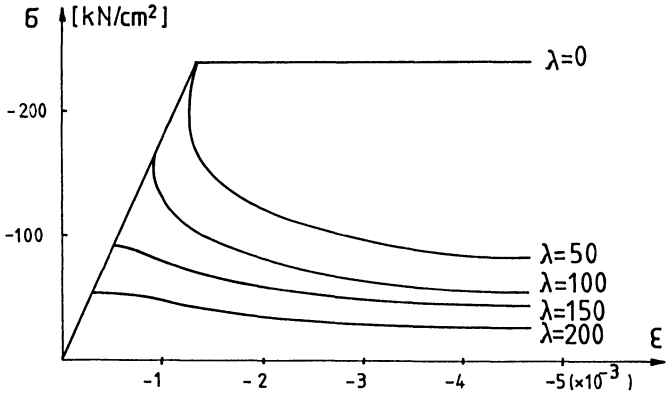

Figure 5. Influence of slenderness.

3. DISCRETE MODEL OF ELEMENT AND STRUCTURE BEHAVIOUR

Linearization plays an important role in the process of reliability estimation of complex systems. Thus an introduction of linear relations at possibly early stage of calculations may lead to significant simplification of the whole analysis. It is proposed to apply a piecewise linear presentation of the P-d relation. Such a model has already been used e. g. in [9, 10]. A number of stretches approximating the relation depends on the sensitivity of the structure and the burden of numerical calculations. Figure 6 presents an example of a piecewise linear relation for a medium slender strut.

The following notions are introduced:

a phase - it is each strech of the P-d relation characterized by a beginning d_{i-1} and an end d_i as well as by corresponding axial forces P_{i-1} and P_i. All of them can be random. To maintain linear probabilistic relations there is assumed constant axial stiffness k_i for each phase /i=1, 2,.../, which reduces the total number of independent random variables. Axial stiffness k_i can be positive, negative or equal to zero.

a configuration - it is a set of actual phases of all elements. Whenever any element changes its phase then there is a change of configuration. At each configuration the structure behaves in a linear way determined by the actual global stiffness matrix and the corresponding set of fictitious loads.

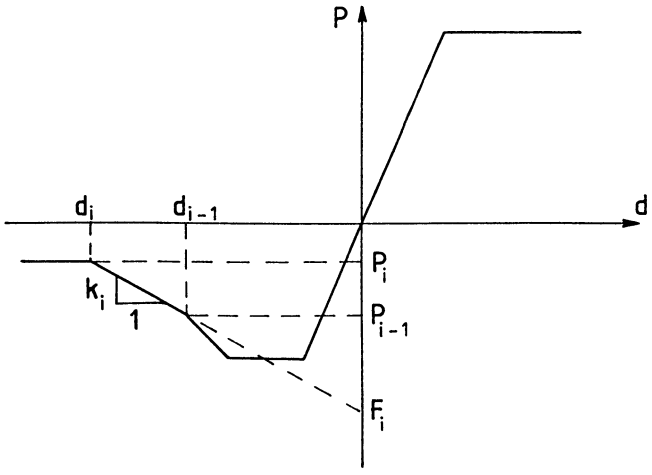

Figure 6. Piecewise linear model.

a generalized failure element - each phase is considered as a failure element. To distinguish it from a real physical failure element a word "generalized" is introduced. A generalized failure element is indicated by j^i where j is a physical element number and i is a phase number.

Classical approach to the limit state analysis in the plasticity theory is displacement independent. Existence of strain softening requires displacement dependent analysis. A short description of a step-by-step approach applying an idea of fictitious loads will be given. The approach corresponds to the dual load method [10] based on the initial stress method [11] and the residual force method [12]. Fictitious loads are used to modify structural behaviour according to actual properties of elements in the collapse process. The description is given for a one parameter load process for a deterministic structure. Proper modifications necessary for the reliability analysis will be presented in the next section.

The state of equilibrium at the end of any i-th configuration is given in the form:

$$\underline{K}_i \, \underline{u}_i = a_i \, \underline{r} + \underline{f}_i \qquad / 3.1 /$$

where:

$\underline{K}_i$ - stiffness matrix at the i-th configuration,
$\underline{u}_i$ - vector of displacements at the end of the i-th configuration,
a_i - load parameter at the end of the i-th configuration,
$\underline{r}$ - basic load vector,
$\underline{f}_i$ - vector of fictitious loads at the i-th configuration.

An inductive formulation of the problem is presented. For i=1 all elements are working in the linearly elastic phase. Vector of displacements at the beginning of the configuration is $\underline{u}_o = \underline{0}$ and vector of fictitious loads is $\underline{f}_1 = \underline{0}$. Thus

$$\underline{K}_1 \, \underline{u}_1 = a_1 \, \underline{r} \qquad / 3.2 /$$

The load factor a_1 can be found from:

$$a_1 = \min_k g_k^1 \qquad / 3.3 /$$

where g_k^1 is a relative length of the first phase of k-th element. Vector $\underline{u}_1$ can be found from /3.2/.

Assuming that full solution is known for i = n then the following formulae can be derived from the continuity condition for i = n+1 configuration:

$$\underline{f}_{n+1} = \underline{f}_n + \underline{K}_z \, \underline{u}_n \qquad / 3.4 /$$

$$\underline{K}_{n+1} = \underline{K}_n + \underline{K}_z \qquad / 3.5 /$$

where $\underline{K}_z$ is a change of the global stiffness matrix resulting from the change of element axial stiffness. The load factor is calculated according to /3.3/ for a positively definite stiffness matrix and according to /3.6/ for a negative stiffness matrix:

$$a_{n+1} = \max_k g_k^{n+1} \qquad / 3.6 /$$

Vector of displacements for i=n+1 can be found from /3.1/.
A mechanism is detected when

$$\det \underline{K}_i = 0 \qquad / 3.7 /$$

however first some other possibilities must be rejected: pseudo-mechanism, temporary mechanism, hidden unloading.

4. DISPLACEMENT DEPENDENT RELIABILITY ANALYSIS

A one parameter load process described in the previous section is used in the limit state analysis being a basis for the physical interpretation of the reliability analysis. In general there is assumed a constant level of the load vector /fixed value of the load factor/, however the load vector is random itself. This requires some modification in the formulation of the problem in the reliability analysis. A vector of fictitious loads is presented as a sum of vectors corresponding to the actual phases of each particular element. According to figure 6 a contribution of the j-th element working in the i-th phase to the global vector of fictitious loads can be calculated from:

$$\underline{f}_i^j = / P_i - k_i \, d_i / \, \underline{c}^j \qquad / 4.1 /$$

where $\underline{c}^j$ is a global vector of directional cosines and all other quantities are shown in figure 6. P_i and d_i may be random. Correlation between P_i and d_i depends on the choice of basic variables. Usually P_i or d_i or both of them are expressed by means of some other basic random variables corresponding to the previous phases.
Assuming that a unique relation between the phase number and the configuration number exists, the global formulation of the statical probabilistic analysis can be expressed in the following simplified form for the i-th configuration:

$$\underline{K}_i \, \tilde{\underline{u}} = \tilde{\underline{r}} + \sum_j \tilde{\underline{f}}_i^j \qquad / 4.2 /$$

where a curl ~ indicates random quantities and $\underline{f}_i^j$ is a vector of the fictitious load from the j-th element in the i-th configuration. At any configuration there are sought parameters of the random displacement vector for the given load vector and corresponding vectors of fictitious loads. A detailed description of the full beta-unzipping reliability analysis can be found in [3].

A great advantage of a piecewise linear model of element behaviour is that at any configuration all safety margins for all generalized failure elements are linear. Let us consider the situation shown in figure 6. Expression for the safety margin depends on data used for the description of the P-d relation. For the simplest case shown in figure 6 this will be:

$$\tilde{M}_{k_i | k_{i-1}, k_{i-2}, \ldots} = \tilde{d}_i + \underline{a}_j^T \tilde{\underline{r}} + \sum_l \underline{b}_{lj}^T \tilde{\underline{f}}_j^l \qquad / 4.3 /$$

where:

$\underline{a}_j$ - a vector of the influence coefficients for external load at the j-th configuration,

$\underline{b}_{lj}$ - a vector of the influence coefficients for the l-th fictitious load in the j-th configuration.

All necessary correlations must be derived from the data available.

5. STRATEGY OF THE ANALYSIS

Existance of the strain softening leads to the unstable states of the structure. It is relatively easy to satisfy full compatibility of displacements in the incremental deterministic analysis. However, the reliability analysis performed for the nonincremental load requires special strategy which will ensure logical consistency of structural behaviour. In general no unique criterion exists for the direction of element displacements in the progressing process of failure, thus the following rules are applied.

At any configuration each actual potential generalized failure element is considered. If the actual axial stiffness is nonnegative /$k_i \geq 0$/, then a fictitious load is applied and both positive and negative safety margins are calculated. R stands for resistance variables and S cumulates load influence:

$$M_i^+ = R_i^+ - S_i \qquad / 5.1 /$$

$$\bar{M}_i = \bar{R}_i + S_i \qquad / 5.2 /$$

Assuming that all basic variables are collected in a vector $\tilde{\underline{x}}$, the safety margin can be calculated as:

$$\tilde{M}_1 = \underline{d}^T \tilde{\underline{x}} \qquad / 5.3 /$$

where $\underline{d}$ is a vector of the coefficients of influence.
Let all basic variables be normally distributed, then they can be transformed to the standardized set of uncorrelated variables

$$\tilde{\underline{z}} = \underline{D}\,\tilde{\underline{x}} + \underline{b} \qquad / 5.4 /$$

where $\underline{D}$ is a linear operator and $\underline{b}$ a vector. The safety margin /5.3/ expressed by means of $\tilde{\underline{z}}$ has a form:

$$\tilde{M}_1 = \underline{d}^T \underline{D}^{-1} / \tilde{\underline{z}} - \underline{b} / = \underline{a}^T \tilde{\underline{z}} + a_o \qquad / 5.5 /$$

After normalization the reliability index β can be found

$$\tilde{M} = \frac{1}{|\underline{a}|} / \underline{a}^T \tilde{\underline{z}} + a_o / = \underline{q}^T \tilde{\underline{z}} + \beta \qquad / 5.6 /$$

and used to calculate the design point:

$$\underline{x} = \underline{D}^{-1} / \beta\, \underline{q} - \underline{b} / \qquad / 5.7 /$$

Design points and corresponding element displacements are calculated for both positive and negative safety margins. There are four possible situations:

a/ axial element displacement at the design point is positive for both safety margines, thus the reliability index corresponding to the positive safety margin is chosen for the process of unzipping,

b/ axial element displacement is negative for both safety margins - - the reliability index corresponding to the negative safety margin is chosen,

c/ axial element displacements at the design points agree in signs with the safety margins - both reliability indices are considered and the smaller one is chosen,

d/ the signs of axial element displacements at the design points are in contradiction with the assumed signs of safety margins - the failure of such an element is not considered.

The further process of unzipping follows the standard way of the method.

For generalized failure elements with negative axial stiffness the approach depends on the determinant of the actual global stiffness

matrix. If the determinant is positive then the calculations follow the scheme presented above for nonnegative axial stiffness. If both the axial stiffness and the determinant are negative then it is assumed that the given element terminates the configuration and no other failure elements are considered.
To maintain the consistency of all failure elements with the actual state of the structure the signs of axial deformations of all elements are checked for the actual design points. If the inconsistency is detected then the given branch of the failure tree is rejected.
A special modification of the safety margin is required when the determinant of the global stiffness matrix is negative. Let two negative resistance variables belong to the same physical element and let be $R_2 < R_1 < 0$. Then, if det $\underline{K}_1 > 0$ the safety margin is

$$\tilde{M}_1 = -\tilde{R}_1 + \underline{a}_1^T \tilde{\underline{r}} \qquad / 5.8 /$$

while for det $\underline{K}_2 < 0$ the safety margin becomes

$$\tilde{M}_2 = \tilde{R}_2 - \tilde{R}_1 + \underline{a}_2^T \tilde{\underline{r}} \qquad / 5.9 /$$

6. APPLICATION OF THE APPROACH

Different numerical experiments were performed to study the applicability of the proposed approach to the structures with strain softening elements. Normal distribution for all random variables was assumed.

Example 1.

A simple fan truss subjected to the compressive load consists of three elements as shown in figure 7. Elements 1 and 3 are characterized by a linearly elastic - perfectly plastic model and element no. 2 is a

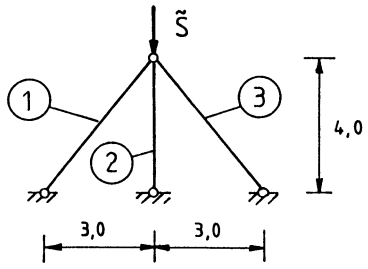

Figure 7. Fan truss under compression.

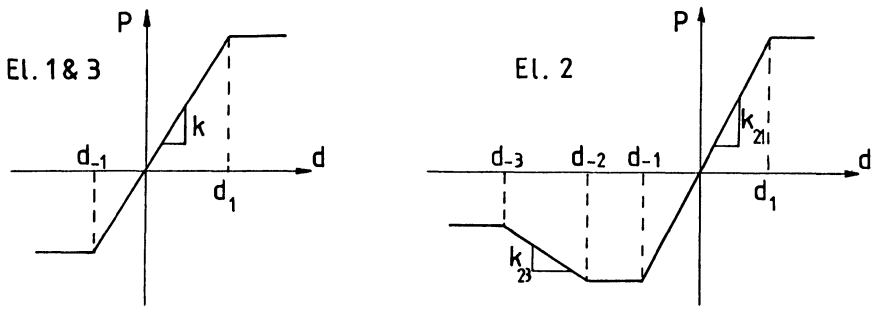

Figure 8. Element data.

strain softening element as shown in figure 8.
The following data is assumed:
external load: S N / 100; 10 /
element no. 1: k = 1000
d_1 ~ N / 0.1; 0.005 /, d_{-1} ~ N / -0.05; 0.004 /
element no. 2: k_{21} = 1000 , k_{23} = -400

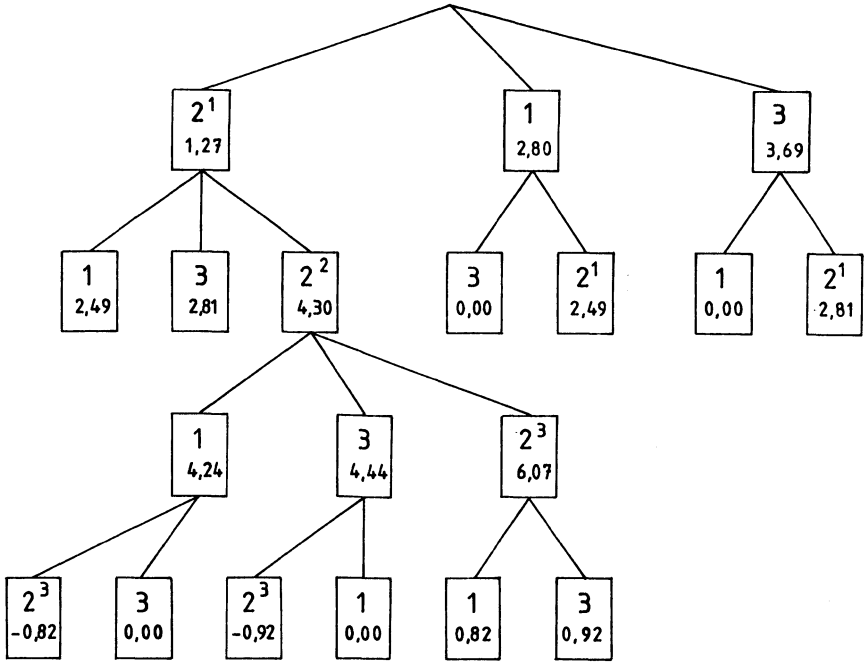

Figure 9. Failure tree at mechanism level.

$d_1 \sim N / 0.1; 0.005 /$, $d_{-1} \sim N /-0.05; 0.002 /$
$d_{-2} \sim N / -0.125; 0.019 /$, $d_{-3} \sim N / -0.175; 0.019 /$

element no. 3: $k = 1000$
$d_1 \sim N / 0.1; 0.005 /$, $d_{-1} \sim N / -0.05; 0.002 /$

The correlation matrix for element no. 2 / d_1, d_{-1}, d_{-2} ,d_{-3}/has a form

$$\begin{matrix} 1.00 & 0.00 & 0.00 & 0.00 \\ & 1.00 & -0.42 & -0.16 \\ & \text{symm.} & 1.00 & 0.89 \\ & & & 1.00 \end{matrix}$$

All other variables are uncorrelated.

A full failure tree obtained using the beta-unzipping method is presented in figure 9. Each box contains a generalized failure element number and the corresponding reliability index. All branches were terminated when a mechanism was detected. The global system reliability index is $\beta = 2.44$. The failure tree presented in figure 9 was obtained for calculations without checking the design point. Introduction of the design point checking led to the rejection of those branches which were initiated by the reliability index equal to zero, which corresponded to an inconsistent mechanism. However, rejection of some branches did not change the global reliability index.

Example 2.

A simple regular space truss loaded with two concentrated forces shown in figure 10 was analysed. The analysis was performed for different P-d curves as shown in figure 11. All these curves had the same parameters of distribution for all corresponding characteristic points.

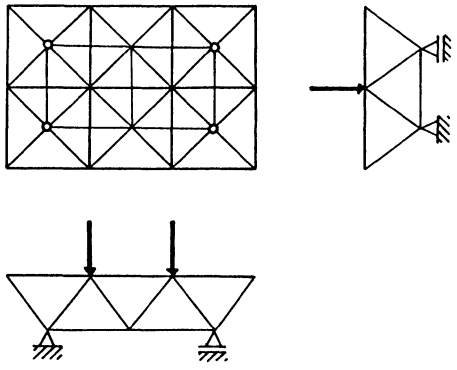

Figure 10. Regular space truss.

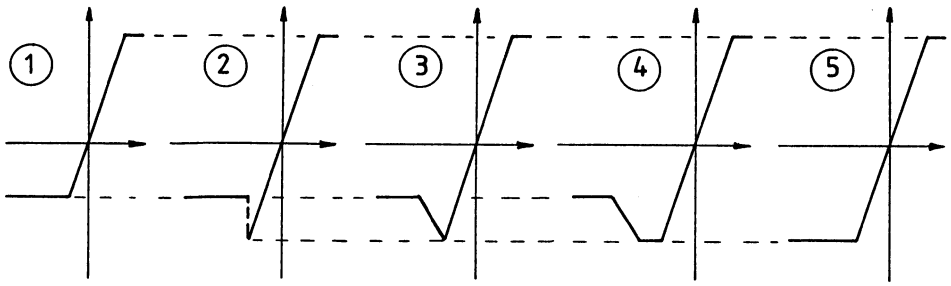

Figure 11. Different types of P-d curves.

The purpose of the analysis was to find the global reliability indices assuming that for each analysed case the structure was built up of elements characterized by only one P-d relation. The order in which the curves are presented in figure 11 from type 1 up to type 5 corresponds to the predicted order of reliability indices from the lowest to the highest.
The following reliability indices were obtained after the proper modification of the safety margins in the unstable range of the structure

$$\beta_1 = 0.58$$
$$\beta_2 = 2.22$$
$$\beta_3 = 2.22$$
$$\beta_4 = 2.61$$
$$\beta_5 = 2.59$$

When classical formulation of the safety margins was used for $\det \underline{K} < 0$ there was obtained $\beta_3 = 3.42$. Some inconsistency observed in the presented results may be due to approximation applied in the whole process of reliability estimation.

7. CONCLUSIONS

The paper presents an attempt of taking into account the influence of strain softening which appears in truss members under compression. The beta-unzipping method has been used to perform the reliability analysis. A piecewise linear model of the strut P-d characteristic was applied. The beta-unzipping method has proved to be fully able to accomodate all requirements caused by a new element model. Special attention was payed to satisfy the consistency and compatibility conditions. It was possible to obtain results concerning the reliability

of the whole structure, however it seems to be justified to look for closer relation between the results and physical interpretation of the phenomenon, especially in the unstable range.

8. ACKNOWLEDGEMENTS

The author wishes to express his gratitude to Professor P. Thoft-Christensen and to Dr. J. D. Sørensen for considerable help he obtained in preparation of this paper.

REFERENCES

1. Thoft-Christensen, P.: The Beta-Unzipping Method. Institute of Building Technology and Structural Engineering. University of Aalborg, Report 8207, 1982.
2. Thoft-Christensen, P., Sørensen, J. D.: Calculation of Failure Probabilities of Ductile Structures by the Beta-Unzipping Method. Institute of Building Technology and Structural Engineering, University of Aalborg, Report 8208, 1982.
3. Thoft-Christensen, P., Murotsu, Y.: Application of Structural Systems Reliability Theory. Springer-Verlag, 1986.
4. Smith, E. A.,Epstein, H. I.: Hartford Coliseum Roof Collapse: Structural Collapse Sequence and Lessons Lerned. Civil Engineering, ASCE, April 1980, pp. 59-62.
5. Higginbotham, A. B., Hanson, R. D.: Axial Hysteretic Behavior of Steel Members. J. Struct. Div., ASCE, Vol. 102, No. ST7, July 1976, pp. 1365-1381.
6. Papadrakakis, M.,Chrysos, L.: Inelastic Cyclic Analysis of Imperfect Columns. J. Struct. Eng., ASCE, Vol. 111, No. 6, June 1985, pp. 1219-1234.
7. Nonaka, T.: Approximation of Yield Condition for the Hysteretic Behavior of a Bar under Repeated Axial Loading. Int. J. of Solids and Structures, Vol. 13, 1977, pp. 637-643.
8. Chen, W. F., Han, D. J.: Tubular Members in Offshore Structures. Pitman Publishing Inc., Marshfield, MA, 1985.
9. Papadrakakis, M.: Inelastic Post-Buckling Analysis of Trusses. J. Struct. Eng., ASCE, Vol. 109, No. 9, Sept., 1983,pp. 2129-2147.
10. Schmidt, L. C., Gregg, B. M.: A Method for Space Truss Analysis in the Post-Buckling Range. Int. J. Num. Meth. Eng., Vol. 15, 1980, pp. 237-247.
11. Zienkiewicz, O. C., Valliappan, S., King, I. P.: Elasto-Plastic Solutions of Engineering Problems; Initial Stress Finite Element Approach. Int. J. Num. Meth. Eng., Vol. 1, 1969, pp. 75-100.
12. Nayak, G. C., Zienkiewicz, O. C.: Elasto-Plastic Stress Analysis; A Generalization for Various Constitutive Relations Including Strain Softening. Int. J. Num. Meth. Eng., Vol. 5, 1972, pp. 113-135.

PROBABILISTIC FRACTURE MECHANICS APPLIED TO THE RELIABILITY ASSESSMENT OF PIPES IN A PWR

Th. Schmidt, U. Schomburg
University of the Federal Armed Forces
P. O. Box 70 08 22, D-2000 Hamburg 70

Abstract

A probabilistic fracture mechanics approach for the reliability assessment of pre-cracked pipes in a PWR subjected to cyclic fatigue is described. The principal model assumptions are given and three different numerical evaluation techniques briefly discussed. Finally the capabilities of the approach are illustrated by determining the relative merits of different inspection measures and schemes with respect to a safety increase of nuclear components.

1. Introduction

Nuclear Power Plants are highly complex systems. The assessment of their reliability with respect to different failure categories is a difficult and comprehensive task /1, 2/. However, with respect to catastrophic failures, e.g. core melt, the reliability of rather few subsystems plays a dominating role. In a pressurized water reactor (PWR) such a subsystem is the primary coolant circuit, which mainly consists of the reactor pressure vessel, the steam generators, the main coolant pumps, the main coolant pipes and the pressurizer with the surgeline.

In this paper the attention is focussed to the even smaller subsystems of the main coolant pipe and the surgeline.

A quantitative reliability assessment for these pipes can obviously not be obtained from the rules of any regulatory codes, since these prescribe only certain quality standards to be obeyed. In addition, it is not possible to infer this reliability from available statistical data of operational performance. All adequate operational experience covers only some hundred years, which is nothing compared to the supposed failure probabilities. Furthermore, even this small population is rather heterogeneous, so that no specific features of a certain pipe under consideration are taken into account. The same is true for the regulatory code. In addition, the effect of changes in regulation rules, operating or design

parameters can be jugded qualitatively only, if at all. This awkwardness can be overcome - at least on a model basis - by the application of probabilistic fracture mechanics methods (PFMM).
The PFMM approach is not applied to the pipe as a whole, but to each single failure element (or component) of the pipe, where the pipe is modelled simply as a series of failure elements. These failure elements are the welds of the pipe.

This approach is justified by the knowledge that the overwhelming majority of failures for adequate designed welded steel components is caused by the imperfect integrity of the welds /3, 4/. These initial imperfections may lead to failure due to extreme overloads like for example earthquakes, but much more contributing to the failure probability is low and perhaps high cycle fatigue (vibrations) in the presence of a corrosive medium. This failure mechanism can be described deterministically by means of fracture mechanics. The constituting variables of the fracture mechanics description as well as the initial situation (imperfection rate, size, location etc.) are of stochastic nature or may be assumed to be so to incorporate data uncertainty. This is taken into account by modelling them as random variables.

2. Probabilistic Fracture Mechanics Model of a Pipe Weld

Since the model is described in detail elsewhere /5/, it shall be summarized here only by giving the major assumptions.

(i) The considered pipe weld is a circumferential weld.
(ii) Failure occurs due to the propagation of crack-like flaws introduced during fabrication. Failure has to be distinguished into leak and break failure.
(iii) No crack initiation and crack interaction takes place.
(iv) Crack propagation is caused by the main load transients, i.e. cyclic fatigue. The crack growth may be stable or unstable and is a function of the present crack size.
(v) The initial crack distribution can be obtained form the results of ultrasonic testing.
(vi) For the crack growth calculations all flaws are transformed in a conservative manner into semi-elliptical surface cracks at the inner side of the weld, i.e. exposed to the corrosive coolant (cf. figures 1 and 2).
(vii) During stable fatigue crack growth the crack remains a semi-elliptical surface crack. Crack growth can take place simultaneously in depth and length directions.

(viii) Initial crack depth and length-to-depth-ratio as well as all other initial random variables are distributed independently.

(ix) The probability of detecting cracks at ultrasonic inspections is a function of the present crack size. Subsequent inspection results are independent.

(x) Cracks found by non-destructive examinations or leakage tests are repaired immediately.

The model characterized by assumptions (i) to (x) can in principle be completely deterministic (e.g. dirac distributions for every random variable) or completely stochastic. Usually it is constituted by a mixture of random and deterministic variables. Typically at least the following variables are taken to be random

- crack occurrence rate
- crack size distribution, given a crack is present
- functional parameters in the stable and unstable crack propagation relations
- crack detection rate by ultrasonic inspections.

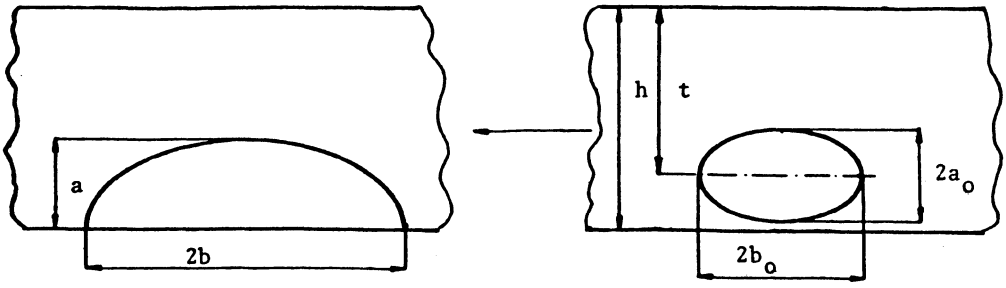

figure 1 - Transformation of an elliptical embedded crack into a semi-elliptical surface crack. The depth and depth-to-length ratio remain constant ($a = 2a_o$ and $a_o/b_o = a/b$). The location depth is denoted by t.

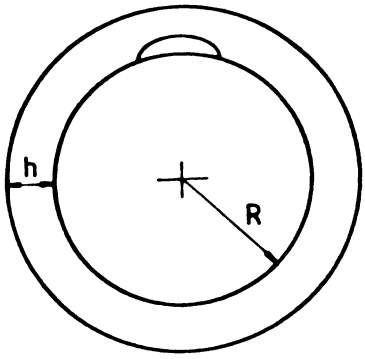

figure 2 - location of transformed crack and pipe geometry parameters

3. Evaluation of Failure Probabilities

In this section we will start with some general remarks on calculating failure probabilities based on the model given before. Then three possible numerical approaches are briefly discussed.

3.1. General features of the model

Since we assumed no crack interaction to take place, the failure probability of a component containing N cracks is given by

$$Q^{(N)} = 1 - (1 - Q_C)^N \qquad (3.1)$$

where Q_C is the failure probability of the component conditioned on the presence of exactly one crack in the component. If the frequency of cracks in a component is Poisson distributed, as it is often reasonably assumed, the unconditioned failure probability of the component is given by

$$Q = 1 - \exp(-M\, Q_C) \qquad (3.2)$$

where M is the expected number of cracks in the component according to the Poisson distribution.

Thus, in this case we need only to determine the conditional failure probability Q_C and we will therefore restrict our attention in the remainder to the problem of estimating Q_C.

In eqns. (3.1) and (3.2) we tacitly assumed Q_C to be defined for some time period T. This period T is usually the projected operating time, i.e. length of design life. Since T may be a design variable we shall write more precisely $Q_C(T)$ instead of Q_C. It is further important to notice that like most often in reliability considerations not only Q(T) but Q(t) for any t between 0 and T is of interest. These informations are of great relevance for example to inspection strategies. Thus we like to determine Q(t) as a function of t over (0,T). In practive Q(t) is a non-decreasing function, at least from some time t_e on.

How is Q(t) related to the set of model variables? Let X(t) denote the vector of model variables a time t, g(X) a safety margin or failure function, i.e. g is a realvalued function with $g(X) \leqslant 0$ denoting failure, while $g(X) > 0$ means no failure, then Q(t) is the expectation of the set function $1_{(g(X) \leqslant 0)}$

$$Q(t) = E\,(1_{g(X(t) \leqslant 0)}) \tag{3.3}$$

If C denotes the vector of all deterministic model variables (assumed to be time-independent) an Y denotes the vector of all random model variables and given that Y is absolute continuous for every t regarded, i.e. has a density function $f_t(y)$, eqn. (3.3) becomes the well known form

$$Q(t) = \int_{g(c,y(t)) \leqslant 0} f_t(y)\, dy \tag{3.4}$$

Fortunately only some of the random variables alter the distribution in time, e.g. typically the crack depth and length-to-depth ratio distribution, while the other distributions remain unchanged. Let $u = (u_1,\ldots,u_k)$ and $v = (v_1,\ldots,v_m)$ denote the time-independent and time-dependent random vectors respectively and f(.) their corresponding densities, then (3.4) becomes of the form

$$Q(t) = \int_{g(c,u,v(t)) \leqslant 0} f(u_1)\ldots f(u_k) f_t(v_1,\ldots,v_m)\, du_1\ldots du_k\, d(v_1,\ldots,v_m) \tag{3.5}$$

Sometimes it is explicitly possible and then often more appropriate to take into account the time-dependency of some variables not by altering their distribution but instead letting the g-function change equivalently in time, which leads to

$$Q(t) = \int_{g_t(c,u,v) \leq 0} f(u_1)\ldots f(u_k)\, f(v_1)\ldots f(v_m)\, du_1\ldots du_k\, dv_1\ldots dv_m \qquad (3.6)$$

instead of (3.5). This formulation is preferable especially when the distribution of V changes to a mixed type distribution, i.e. points or lower-dimensional subspaces of $\mathbb{R}^k$ are having a non-zero probability mass. The integral of (3.5) has to be written then in a more general form.

In the following sections we will restrict ourselves to the case that only the crack size variables and optionally parameters of the crack propagation rules are time-dependent.

3.2. Monte Carlo Simulation

Since Q(t) is the solution of a higher dimensional integral over a complicated integration region and furthermore the integration region or the integrand are time-dependent, the Monte Carlo approach to solve eqns. (3.4), (3.5) or (3.6) is a most natural choice. To allow a better illustration of the numerical evaluation we rewrite (3.6) in the form

$$Q(t) = \int_S P_f(t/(a,r))\, f(a)\, f(r)\, dr\, da \qquad (3.7)$$

where $P_f(t/(a,r))$ is the failure probability up to time t of a crack with given initial depth a and depth-to-length ratio r and S is the space of all possible initial crack sizes.

The integration is solved by providing estimators of $P_f(t/(a,r))$ for a usually large sample of (a,r)-values and some previously chosen evaluation times t_0, $t_1,\ldots,t_e$ with a Monte Carlo simulation. The simulation is carried out for every (a,r)-value by sampling an event sequence (transients, inspections, leakage tests etc.) with corresponding event occurence times and realizations of the random variables associated to these events. Then the crack size variables are up-dated according to this event sequence and event times and it is noticed whether the crack has failed (exceeded some critical size) or not until some time t_i, given that it has not been detected by previous inspections. Denoting the failure or non-failure of an initial crack (a,r) at time t by an one-zero-variable I(t/(a,r)) and the probability of non-detection of the crack until time t by

$$P_{ND}(t/(a,r)) = \prod_{T_j<t} P_{ND}(T_j/(a,r)) \tag{3.8}$$

where T_j denotes the j-th inspections time in the event sequence, it is evident that

$$P_f(t/(a,r)) = I(t/(a,r)) \cdot P_{ND}(t/(a,r)) \tag{3.9}$$

is an estimation of $P_f(t/(a,r))$. When no inspections are modelled this procedure is a direct simulation of binomial sampling.

Details of such a Monte Carlo simulation for the pipes under consideration are given e.g. in /5, 6/ and shall not be elaborated here. It is important to remark that the sampling of (a,r) should in general not be performed according to their original distribution with regard to the expected small probabilities. Necessary to obtain efficient simulation procedures and results of sufficient accuracy is the employment of variance reduction techniques like importance sampling or stratified sampling. Both methods have been successfully applied to the problem formulated here /7/.

3.3. Markovian Crack Propagation Evaluation

According to the aforementioned assumptions the crack growth and crack detection rate associated with a load transient or inspection respectively is depending on the actual crack size but not on the crack sizes of earlier transients or inspections. This property is already used in the simulation procedure (cf. section 3.2) and it obviously forces the crack propagation process to be markovian.

In the context of markov process theory our problem can be formulated as follows: Given the state space S of all possible crack sizes with initial probability mass function P_0 and the event space E of all load transients, inspections and repair measures with all their random and deterministic properties, which each defines a transition probability function P_e, what are the values of $P_t(\text{leak})$ and P_t (break), where the failure states leak and break are adequately defined subsets of S and P_t is the probability mass function belonging to time t?

For a pipe of wall thickness h and inner radius R we have S being the subset (0,h) x(0,1) where $a/r < \pi R$ is satisfied (cf. figures 1 an 2). The probability mass function P_t can be easily derived by a recursion formula from P_0 and the set $\{P_e : e \in E\}$, when the event sequence is fixed and the corresponding load and

inspection quality variables are individual constants for every event so that we restrict our considerations to this case here:

$$P_{t_0} = P_0 \qquad t_0 = 0 \tag{3.10}$$
$$P_t = P_{t_{j-1}} \otimes P_{e_i} \qquad t_j \leqslant t < t_{i+1}$$

where t_i is the time of the i-th event e_i and the meaning of the operation $\otimes$ is given by

$$P_t \otimes P_e(A) = \int_S P_e(A/(a,r))\, dP_t(a,r) \tag{3.11}$$

If P_t, $P_{t_{i-1}}$ and P_{e_i} have the probability densities f_i, f_{i-1} and f_e respectively, (3.9) is equivalent to the more famous relation

$$f_i(u,v) = \int_S f_e((u,v)/(a,r))\, f_{i-1}(a,r)\, d(a,r) \tag{3.12}$$

Unfortunately eqn. (3.12) has usually no analytical solution so that numerical integration schemes must be employed, which provide pointwise estimations of f_i. But f_i has to be known completely to obtain f_{i+1} so that a fitting procedure has to be carried out or, alternatively a recursive numerical integration scheme based on always the same points has to be used. Furthermore the probability mass functions do not continue to possess densities so that several cases have to be distinguished. All these difficulties can be overcome by discretizing the state space S into several parts and approximating f_i by a sum of weighted uniform densities or dirac distributions. Then P_0 becomes a probability vector, each P_e a transition probability matrix and the recursive formula (3.10) means simply a series of matrix multiplications. However, the matrix elements of each P_e have to be obtained usually still by numerical integration, but only once for all. The markov process is thus approximated by a homogeneous markov chain.

3.4. FORM / SORM

The so called first or second order reliability methods have not been dealt with by the authors for the problem under consideration, but shall not be unmentioned due to their increasing importance and potential. The first idea of these concepts was appearingly formulated by Cornell /8/ and it has been further elaborated

namely by Ditlevsen and Rackwitz (for historical remarks see e.g. Ditlevsen /9/). Its basic idea can be illustrated for our problem by regarding eqn. (3.5). The integration is solved by linearizing the failure function g at the so called design-point and replacing the original distributions by normal distributions of the same expectation, variance and covariance and identical density value in the design point. Then the such derived integration problem can be solved by analytical approximation formulas. The design-point will be found by an iteration procedure at least when some regularity conditions are met /10/. In SORM g is approximated by a second order Taylor expansion.

FORM/SORM can be applied at every time t, if the distributions are known at this time. Since their dependence on time may be very complicated, e.g. they may be a product of a markov process as outlined in section 3.3, this is no trivial condition. However, if it is possible to approximate them as a function of time or to express g as a function of time and the initial random variables (eqn. 3.6) the FORM/SORM-approach is very versatile. Recent works seem to indicate the capability of the method to solve some of those time dynamic problems /11, 12/.

3.5. Common Considerations

All three methods have their respective merits. FORM/SORM requires some amount of previous work to gather information to be able to formulate the problem in appropriate manner, but if possible the method is very exploitable, since it does not only provide an approximative result of the sought failure probabilities but also approximative sensitivity measures (cf. e.g. Bjerager /13/). However, no boundaries for the approximation errors are given, but comparisons with Monte Carlo results show usually good agreement. An advantage is certainly the ability to deal with correlated random variables.

The markov chain approach can handle correlated initial random variables of the state space components only. The concept ist rather simple and easy to implement, if the event history is not too complicated. It is computational very efficient, if the discretization is adequate. Furthermore a lot of information gathered can be used again for the solution of additional but related problems. So far no estimates of the approximation errors are provided, but they may be obtainable in principle. However, crosschecking of the results with Monte Carlo estimations showed usually acceptable accuracy. Often the approximation can be carried out such that upper bounds of the failure probability are provided.

The Monte Carlo simulation is probably the conceptual simplest one, although perhaps computationally not efficient even if variance reduction techniques are employed. This is particularly true, when correlated variables shall be dealt with (if at all practicable). On the other hand since statistical error estimations are provided, the approach will retain its significance at least as a check or calibration method for the other techniques.

4. Application to Piping Reliability

This section is meant to illustrate the application of a probabilistic fracture mechanics model as outlined before in some numerical examples rather than to give a thorough reliability assessment of a piping system, which for example is done in /5, 6/. We therefore concentrate on the specific aspect of inspection measures. The most important inspection measures are

- ultrasonic testing (UT)
- hydrostatic proof test (PT)
- leakage test (LT)

Ultrasonic testing of the welds is performed manually or automatically before the plant starts operating (pre-service) and periodically during operation (in-service). According to german regulations the in-service ultrasonic testing (ISUT) is repeated every four or eight years /14/. As assumed in section 2 the probability of non-detection is a function of the crack size. For the following calculations a simple generalization of the function found by Marshall /15/ is used:

$$PND(a) = (1-e)\exp(-0.1134\,a) + e \qquad (4.1)$$

where a is the crack depth in mm and e is a free parameter, that is a measure of the quality of the inspection affecting mainly the chance to detect very deep cracks, which are the most critical (cf. figure 3). Here e = 0.005 was chosen. The influence of the choice of e combined with different inspection frequencies and times when only UT is applied was investigated in another paper /16/.

Contrary to UT the hydrostatic proof test and the leakage test are destructive examinations. In both cases the pipe is pressurized at a temperature which is high enough to avoid brittle fracture, but low compared to the operating temperature so that it is commonly noted as cold pressurization. The pressure is about 1.3 times the design pressure of the pipe for the PT and the maximum normal operating pressure for the LT. The pressurization might cause existing cracks to grow stably or unstably through the wall resulting in a leak or break. But such failures are

not critical with respect to the operating conditions and should therefore not account to the failure probability. These leaks and breaks are thus treated equivalently to cracks being detected by UT. Consequently this does mean a beneficial effect of these tests. On the other hand the pressurization is a load, which causes uncritical cracks not to fail but to grow further and be therefore perhaps more likely to fail in the critical phase of an operating transient. Thus PT and LT also have an antagonistic effect. This is especially true for the LT, since it is performed before every regular heat-up/cool-down cycle of the plant, i.e. in average 200 times in 40 years projected plant operating time. The PT is carried out once as a pre-service measure and may be repeated according to the KTA-Regeln /14/ every eight years. There has been discussion in Germany about the question whether the beneficial or harmful effects especially of the LT are prevailing, since for example no LT is performed in U.S. PWR's. The answer to this question with respect to the failure probability of the main coolant pipe is given by the following results.

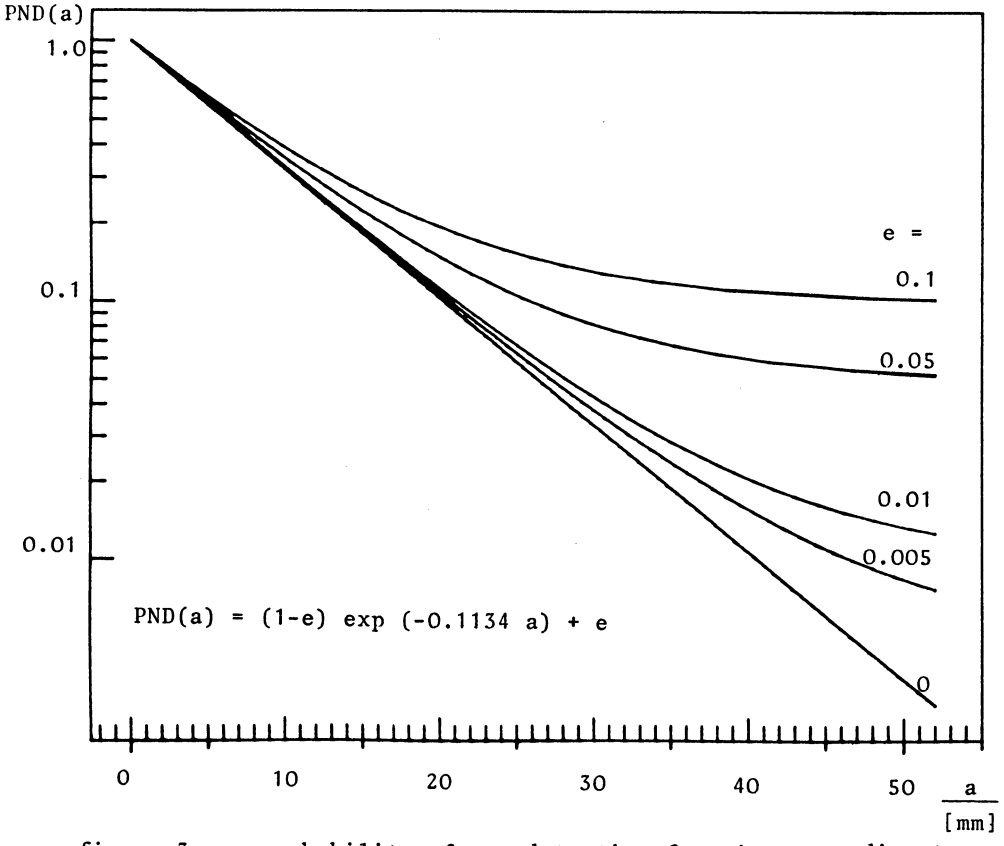

figure 3 - probability of non-detection function according to /15/ for different e-values

The calculations are based on the pipe data presented in /5/. The stable crack growth relation was a randomized ASME-curve for low alloy feritic steel in corrosive environment /17/, while unstable crack growth was due to exceedance of the critical net-section flow stress. 200 heat-up/cool-down cycles equally spaced in time were performed in the simulation. All material and other data except inspection parameters were identical in the cases considered.

In figure 4 the leak probabilities Q(t) are shown for five different situations:

C1: no inspections are performed
C2: pre-service UT and PT are performed
C3: pre-service UT and PT are performed and the UT is repeated every eight years .
C4: pre-service UT and PT as well as periodical ISUT after every four years are performed
C5: like C4, but additionally a leakage test before every heat-up/cool-down cycle is carried out

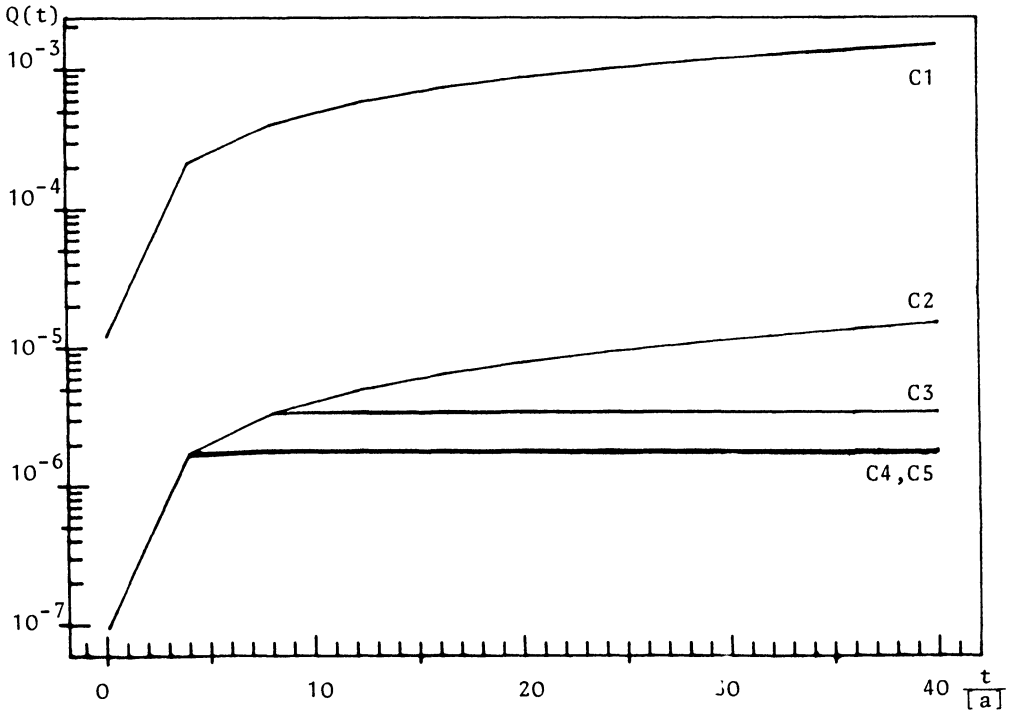

figure 4

Since the curves C4 and C5 nearly coincide even numerous leakage tests appearingly have no influence on the leak probabilities, when they are combined with repeated ultrasonic testing, which is the realistic case. If no inspections or only leakage test are performed, virtually the same is true (not shown in figure 4). UT on the other hand has a tremendous beneficial influence on the leak probability, especially when performed early during life-time. This is due to a substantial change of the initial crack size distribution, which probably is the most sensitive variable (cf. e.g. /18/). Repeated ISUT seems to force to nearly vanish the contribution of crack growth to the leak probability at some time. However, to conclude that a concentration of ISUT only in the first years provides the highest reliability is not justified, since then the independence assumption of subsequent UT is certainly not valid.

In figure 5 the break probabilities are shown for the same situations as in figure 4. The results are very similar. The benefits of inspections are even more pronounced and in contrary to figure 4 the leakage tests have a positive influence now.

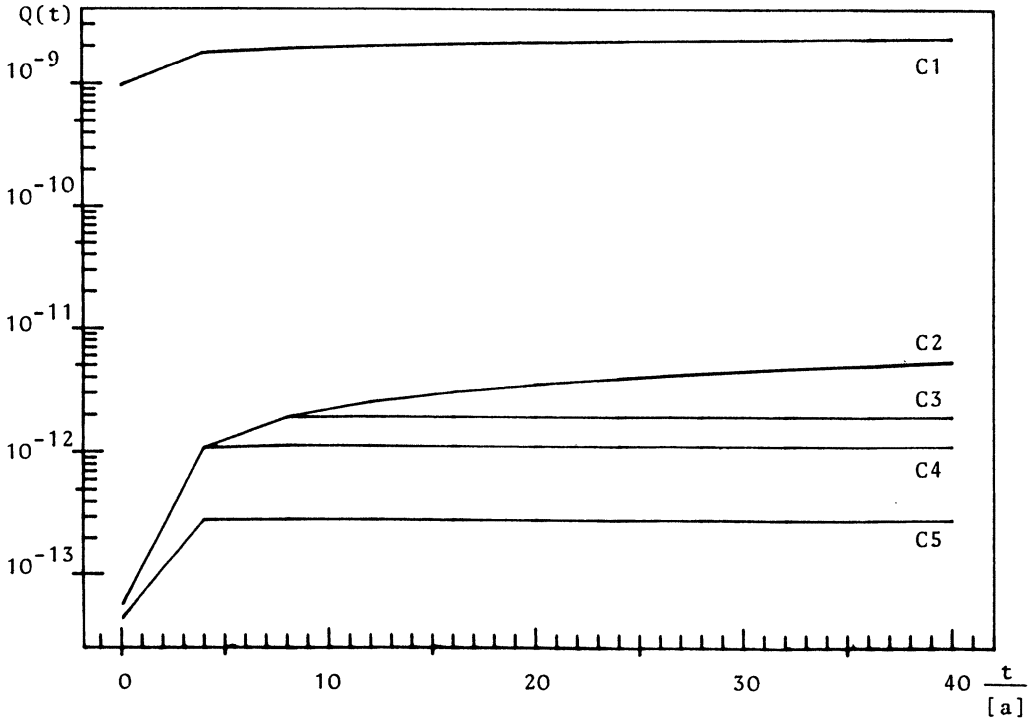

figure 5

In figures 6 and 7 the efficiency of the different inspection measures with respect to the break probabilities as a function of time are further investigated. Besides the case C1 as a reference curve the following situations are modelled:

C6: only pre-service PT is performed
C7: pre-service PT and UT are performed
C8: pre-service PT and UT plus 200 LT's are performed
C9: like C8, but with four additional in-service PT's, carried out every eight years

C10: pre-service UT and nine ISUT's are performed
C11: like C10, but with additional pre-service and four in-service PT's plus 200 LT's performed

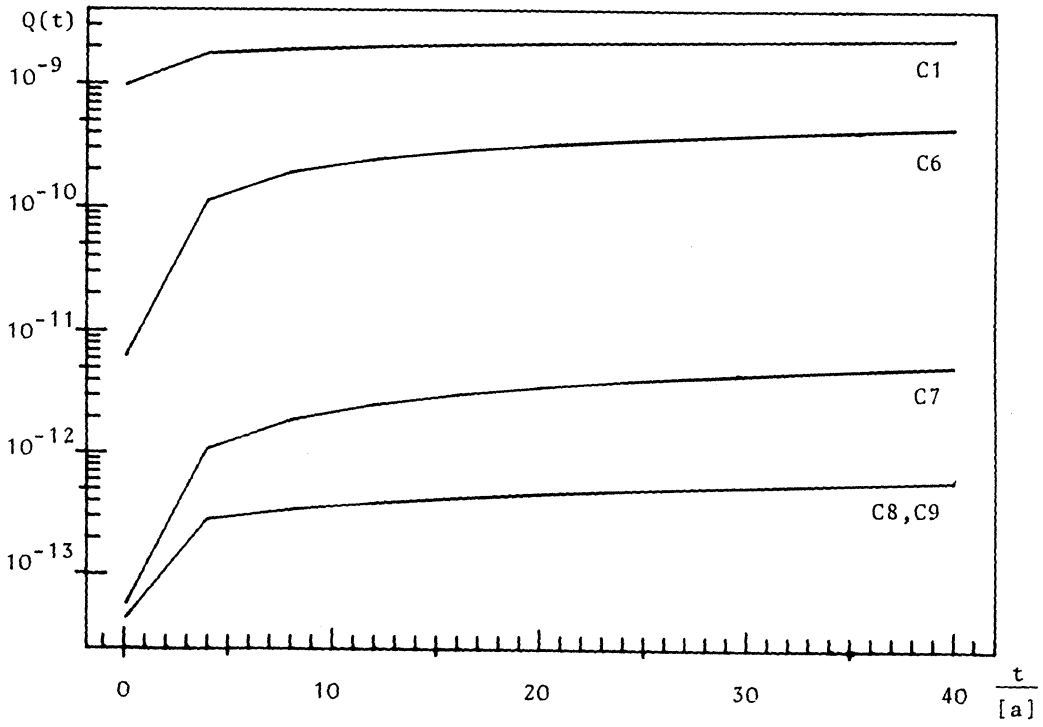

figure 6

It can be seen that a pre-service PT has some positive influence, which is markedly enhanced by simultaneous pre-service UT. The performance of leakage tests decreases the break probability further, while additional proof tests seem to be of no significance. On the other hand it is obvious that UT alone cannot provide the same benefits as together with pre-service PT and regular leakage tests.

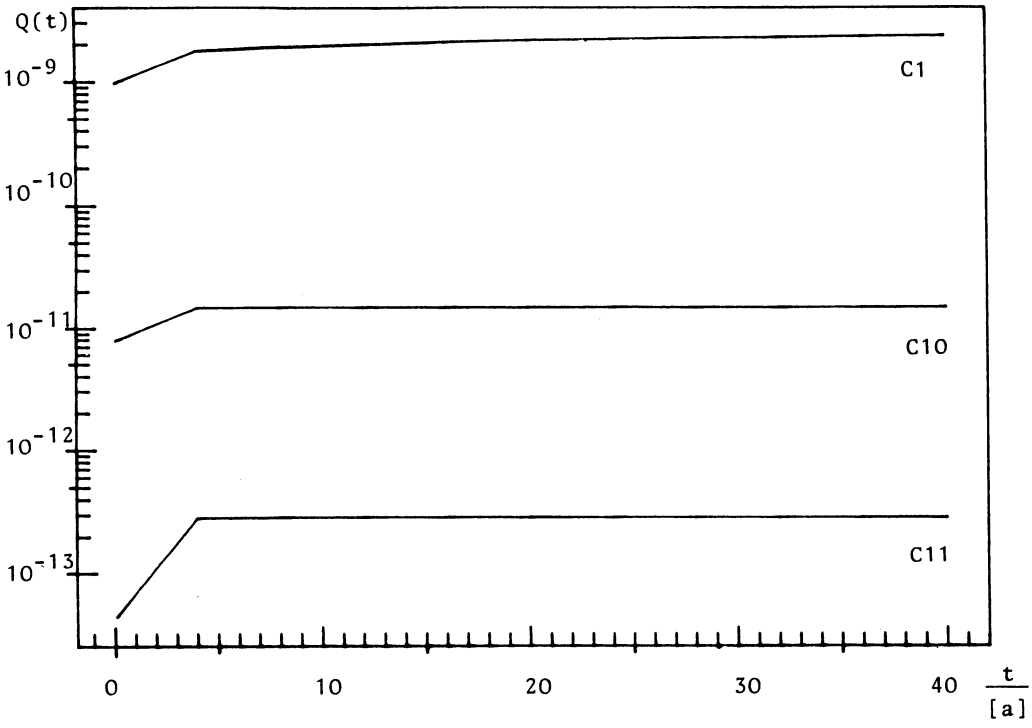

figure 7

Thus it can be concluded that the performance of leakage tests is a reasonable measure to reduce further the failure probability, in particular in combination with ultrasonic testing.

5. Conclusions

Probabilistic fracture mechanics has been shown able to provide reliability estimations of a pipe component containing initial cracks. Although due to data uncertainty and model restrictions no absolute values or strict confidence limits can be determined, careful modelling may provide upper bounds of the failure pro-

bability and futhermore important insight in the effects, efficiency and limits of changes in design, operating and inspection variables is obtained. For the pipes of a PWR the great relevance of the three most important inspection methods practiced so far in order to increase the reliability of nuclear subsystems has been demonstrated.

6. References

/1/ "Reactor Safety Study", An Assessment of Accidents in U.S. Commercial Nuclear Power Plants, Wash-1400, Nureg 75/014

/2/ "Deutsche Risikostudie Kernkraftwerke", Eine Untersuchung zu dem durch Störfälle in Kernkraftwerken verursachten Risiko, Verlag TÜV-Rheinland, Köln 1980 (2. Auflage)

/3/ "Characteristics of Pipe System Failures in Light Water Reactors", EPRI, NP-438, August 1977

/4/ S. H. Bush: "Pressurized Water Reactors", Batelle Memorial I Laboratories, Richland, Washington, USA; IAES-IWG-RRPC, 15-SM-269, 1983

/5/ Hegemann, Krieger, Loevenich, Paul, Schmidt, Schomburg: "Auslösende Ereignisse und Ereignisabläufe für Kühlmittelverluststörfälle", Bericht zum Forschungsvorhaben RS 0591 des BMFT, Essen 1985

/6/ D. O. Harris, E. Y. Lim, D. D. Dedhia, "Probabilistic Fracture Mechanics Analysis", Volume 5 of "Probability of Pipe Fracture in the Primary Coolant Loop of a PWR Plant", Lawrence Livermore National Laboratory, NUREG/CR-2189, August 1981

/7/ A. Brückner-Foit, Th. Schmidt, J. Theodoropoulos: "A Comparison of the PRAISE Code and the PARIS Code for the Evaluation of the Failure Probability of Components Containing Cracks", to be published

/8/ C. A. Cornell: "A Probability-based Structural Code", ACI J. 66 (12), 1969, p. 974-985

/9/ D. Ditlevsen, "Uncertainty Modelling", McGraw Hill, New York, 1981

/10/ D. Ditlevsen, "Principles of normal tail approximation", Proc. ASCE, J. Eng. Mech. Div.107, 1981, p. 1191-1208

/11/ H. O. Madsen, R. Skjong, A. G. Tallin, F. Kirkemo, "Probabilistic Fatigue Crack Growth Analysis of Offshore Structures with Reliability Updating through Inspection", to appear in the proceedings of Marine Structures Reliability Symposium, Virginia, October 1987

/12/ H. Riesch-Oppermann, A. Brückner, "Approximative Determination of Failure Probabilities in Probabilistic Fracture Mechanics", appears in the proceedings of the 9th Int. Conf. on Structural Mechanics in Reactor Technology, Lausanne, August 1987

/13/ P. Bjerager, "Sensitivity Measures in Systems Reliability", lecture at the 1st Working Conf. on Reliability and Optimization of Structural Systems, Aalborg, May 1987

/14/ KTA 3201: "Komponenten des Primärkreises von Leichtwasserreaktoren", Teil 4: Wiederkehrende Prüfungen und Betriebsüberwachung, Herausgeber: Geschäftsstelle des Kerntechnischen Ausschusses (KTA) bei der Gesellschaft für Reaktorsicherheit (GRS), Köln 1982

/15/ "An Assement of the Integrity of PWR Pressure Vessels", Report by a Study Group under the Chairmanship of Dr. W. Marshall, UKAEA, October 1976

/16/ Th. Schmidt, U. Schomburg, "Markovian Probabilistic Fracture Mechanics Analysis Applied to Estimating Failure Probabilistics of a PWR Primary Coolant Pipe", appears in the proceedings of the 9th Int. Conf. on Structural Mechanics in Reactor Technology, Lausanne, August 1987

/17/ ASME Boiler and Pressure Vessel Code, Section XI, App. A, 1980

/18/ U. Schomburg, Th. Schmidt, "Probability of Fracture in the Main Coolant Pipe of a Pressurized Water Reactor", in Probabilistic Methods in the Mechanics of Solids and Structures, IUTAM Symposium Stockholm 1984, Editors: S. Eggwertz/N. C. Lind, Springer 1985

THEORETIC INFORMATION APPROACH TO IDENTIFICATION AND SIGNAL PROCESSING

Kazimierz Sobczyk
Institute of Fundamental Technological Research
Polish Academy of Sciences
Swietokrzyska 21, PL-00-049 Warsaw

1. Introduction

In his pionieering work on the theory of communication systems Shannon showed that the concepts of entropy and mutual information are extremely useful and effective for evaluating the performance of communication systems. The fact that these concepts are so effective in communication theory is, very likely, responsible for the fact that the information theory is often considered as synonymous with communication theory. This may also be a reason that relatively few conclusive results have been obtained in other fields with use of the information theoretic approach.

A correct point of view, as it has been underlined by Kullback [1] is that the information theory is a branch of mathematical probability theory and mathematical statistics. As such, its concepts and methods are applicable to analysis of various physical and engineering systems. Theoretic-information reasoning is well known in physics, especially in thermodynamics where the relationship between the amount of information on physical system and its thermodynamical entropy is well established (cf. [2]).

Information theory is especially relevant to data processing and statistical inference. As a matter of fact, an information in a technically defined sense was first introduced in statistics (R.A.Fisher - 1925) in his work on theory of estimation. His concept of a measure of the amount of information supplied by data about unknown parameter is well known to statisticians. Generally speaking, the aparatus of the information theory is applicable to any probabilistic system of observations since whenever we make statistical observations (or design and conduct statistical experiments) we seek information. The basic questions which arise in this context are:
how much information can we infer from a particular set of observations or experiments about the sampled phenomenon (population) ?

More particular problem concerns estimation of an unobserved quantity X through observations on another quantity Y; these quantities can be random variables, stochastic processes, random fields etc.
Another question is concerned with optimal design of experiment: how should an experiment be designed to obtain maximum information about the sampled random phenomenon ?

The objective of this paper is to show how the information-theoretic approach can be adopted to such problems as: identification of empirical systems, random signal processing and to optimal design of experiments in stochastic dynamics of engineering systems.

2. Entropy and mutual information

An inherent feature of any random phenomenon is that a result of its observation can not be predicted a priori (before observation). This uncertainty (or indeterminancy) can often be evaluated qualitatively by comparison of different random quantities. A convenient quantitative measure of uncertainty of real random phenomena is a certain function of probabilities which is called entropy.

Let $(\Gamma, \mathcal{F}, P)$ be a basic probability space and let $\underline{X}(\gamma)$ be a random variable in R_n; $\gamma \in \Gamma$.
Entropy of a continuous random variable $\underline{X}(\gamma)$ with probability density $f(\underline{x})$ is defined as

$$H(\underline{X}) = -\int_{R_n} f(\underline{x}) \log f(\underline{x})\, d\underline{x} = \langle -\log f(\underline{X}) \rangle \tag{2.1}$$

where $\langle \cdot \rangle$ denotes the average value.
Let $X(\gamma)$ and $Y(\gamma)$ be two scalar random variables with the joint probability density $f(x,y)$. The average conditional entropy of $X(\gamma)$ with respect to $Y(\gamma)$ is defined as

$$\overline{H}_Y(X) = -\int_{-\infty}^{\infty}\int_{-\infty}^{\infty} f(x,y) \log f(x|y)\, dx\, dy \tag{2.2}$$

It can be easily shown that

$$\begin{aligned} H(X,Y) &= H(X) + \overline{H}_X(Y) \\ &= H(Y) + \overline{H}_Y(X), \end{aligned} \tag{2.3}$$

$$H(X,Y) \leqslant H(X) + H(Y) \tag{2.4}$$

where equality holds if and only if the random variables are independent. The entropy of n-dimensional Gaussian vector $\underline{X}(\gamma)$ is given by the formula

$$H(\underline{X}) = \log \sqrt{(2\pi e)^n |\underline{K}|} \tag{2.5}$$

Often we have to do with situations where random variable $\underline{X}(\gamma)$ is unobservable, but the variable $Y(\gamma)$ associated with $X(\gamma)$ can be observed. The information about $X(\gamma)$ provided by the observation of $Y(\gamma)$ affects (decreases) the uncertainty (entropy) of $X(\gamma)$. This suggests the following definition.

The Shannon information $I(X,Y)$ about $X(\gamma)$ provided by the observation of $Y(\gamma)$ is

$$I(X,Y) = H(X) - \overline{H}_Y(X) = H(X) + H(Y) - H(X,Y) \tag{2.6}$$

For continuous random variables

$$I(X,Y) = \int_{-\infty}^{\infty}\int_{-\infty}^{\infty} f(x,y) \log \frac{f(x,y)}{f_1(x) f_2(y)}\, dx\, dy \tag{2.7}$$

where $f_1(x)$ and $f_2(y)$ are the marginal distributions. It is known that

a) $I(X,Y) \geq 0$, equality holds if and only if $X(\gamma)$ and $Y(\gamma)$ are independent

b) $I(X,Y) = I(Y,X)$,

c) $I(X,Y) \quad I(X, g(Y))$, where $g(y)$ is any mapping defined on R ; equality holds if and only if the mapping $g(y)$ is one-to-one.

Several generalizations of the Shannon measure of information have been suggested in statistics (cf. [3]). There is an interesting relationship between the Shannon information measure $I(X,Y)$ and the Kullback-Leibler measure of divergence. Let us assume that $f_1(x)$ is unknown true probability distribution (of a random variable $X(\gamma)$ and $f_2(x)$ is a certain hypothetical approximation of $f_1(x)$.

The Kullback-Leibler divergence of $f_2(x)$ from $f_1(x)$ is defined as

$$\mathcal{J}\left[\begin{matrix} f_1 \\ f_2 \end{matrix}\right] = \int_{-\infty}^{\infty} f_1(x) \log \frac{f_1(x)}{f_2(x)}\, dx \tag{2.8}$$

In order to relate the Kullback-Leibler measure (2.8) to the Shannon information (2.7) it is useful to consider the problem of identification of an unobservable variable $X(\gamma)$ on the basis of observation of another variable $Y(\gamma)$ which is statistically related to $X(\gamma)$.

The Shannon measure of information about the true value of $X(\gamma)$ when $Y(\gamma)$ is observed is given by (2.7). Assuming in (2.8) $f_1(x) = f(x,y)$ and $f_2(x) = f(x)f(y)$ we have

$$\mathcal{J}\left[\begin{matrix} f_1 \\ f_2 \end{matrix}\right] = \mathcal{J}\left[\begin{matrix} f(x,y) \\ f(x)f(y) \end{matrix}\right] = I(X,Y) = \int_{-\infty}^{\infty}\int_{-\infty}^{\infty} f(x,y) \log \frac{f(x,y)}{f(x)f(y)}\, dx\, dy \tag{2.9}$$

It is clear from (2.7) and (2.9) that the Shannon amount of information about $X(\gamma)$ provided by observation of $Y(\gamma)$ can be regarded to

be equal to the Kullback divergence between $f_1(x)$ $f_2(y)$ and the joint distribution $f(x,y)$.

Another quantity related to $I(X,Y)$ and J is the inaccuracy measure introduced by Kerridge [4] and defined as

$$A\left[\begin{matrix} f_1 \\ f_2 \end{matrix}\right] = -\int_{-\infty}^{\infty} f_1(x) \log f_2(x)\, dx \tag{2.10}$$

By virtue of (2.1),(2.8) and (2.10) one obtains the following relationship

$$\begin{aligned} A\left[\begin{matrix} f_1(x) \\ f_2(x) \end{matrix}\right] &= -\int_{-\infty}^{\infty} f_1(x) \log f_1(x)\, dx + \int_{-\infty}^{\infty} f_1(x) \log \frac{f_1(x)}{f_2(x)}\, dx \\ &= H\left[f_1(x)\right] + J\left[\begin{matrix} f_1 \\ f_2 \end{matrix}\right]. \end{aligned} \tag{2.11}$$

where $H\left[f_1(x)\right]$ denotes the entropy of the distribution $f_1(x)$.
The inaccuracy (2.10) is non-negative and and additive quantity. If $f_1(x)$ represents true probability distribution of a random variable $X(\delta)$ and $f_2(x)$ is an approximation of $f_1(x)$ based on some inaccurate knowledge of $X(\delta)$, then - as it follows from (2.11) - the inaccuracy measure $A\left[\begin{matrix} f_1 \\ f_2 \end{matrix}\right]$ can be regarded as a measure of total uncertainty of $X(\delta)$ which occurs due to its inherent randomness (entropy of $f_1(x)$) and because of inaccuracy of our knowledge of the true distribution.

3. System identification

3.1. Informational quality criterion

The concept of system identification is not univocal in the literature. Often "identification" is identified with "modelling". In both cases one wish to find a model of a considered real system which would be the best in the sense of assumed quality criterion. A quality of a model is characterized by functional $Q(Y,Y_M)$ defined on the output of the real system Y and on the model output Y_M; the quality criterion selects from all admissible models such a model for which functional $Q(Y,Y_M)$ takes extremal value. The identification criterion expresses how close should be the model to the true real system and it is a key issue in identification. Most often the root mean square error(between Y and Y_M) is taken as quality criterion (cf. [5] , [6]).

It seems that more general optimality criteria would be useful, especially if one deals with complicated systems. The informational criterion appears to be very promising. It can be formulated as:
a model M_o should be selected from the class $\{M\}$ of the admissible models in such a way that the model output Y_M contains maximum information (in the Shannon sense) about the real system output Y, that is:

$$Q(Y, Y_M) = I(Y, Y_M) = \left\langle \log \frac{f(y, y_M)}{f_1(y) f_2(y_M)} \right\rangle$$
$$= \left\langle \log \frac{f(y|y_M)}{f_1(y)} \right\rangle = max \tag{3.1}$$

Since the model output Y_M depends on the model input X_M that is in the simplest case $Y_M = g(X_M)$ then due to basic properties of the mutual information

$$I(Y, Y_M) = I(Y, g(X_M)) \geqslant I(Y, X_M) \tag{3.2}$$

If there are the reasons for assuming that the joint distribution of the system response and the model response is Gaussian then

$$I(Y, Y_M) = \frac{1}{2} \log [1 - \varrho^2(Y, Y_M)] \tag{3.3}$$

where $\varrho(Y, Y_M)$ is the correlation coefficient of Y and Y_M .

3.2. Model entropy

Since the entropy characterizes an information content (prior experiment) it can be used for judging of the model quality. In this context it is instructive to know what is the relationship between the entropies of the model output Y_M and the model input X_M .
In the simplest situation of a linear model

$$\underline{Y}_M = \underline{A}\, \underline{X}_M \tag{3.4}$$

where $\underline{Y}_M$ and $\underline{X}_M$ are random vectors and $\underline{A}$ is a matrix we have

$$H(Y_M) = H(X_M) + \log \det \underline{A} \tag{3.5}$$

Let us consider now the following differential equation model of a dynamical system with random initial conditions

$$\frac{dY_i^M}{dt} = F_i \left[Y_1^M(t), \dots, Y_n^M(t) \right], \quad Y_i^M(t_0) = \overset{\circ}{Y}_i^M(t), \quad i = 1, \dots, n \tag{3.6}$$

Assume that functions F_i and probability density $f(y_1, \dots, y_n)$ have partial derivatives with respect to $y_1, \dots, y_n$ and t and that the products fF_i are equal to zero if any of variables $y_1, \dots, y_n$ assumes ∞ or $-\infty$.
Entropy of model (3.6) is (let log=ln) $H(t) = -\langle \ln f \rangle$.

$$\frac{dH(t)}{dt} = -\left\langle \frac{d}{dt} \ln f \right\rangle = -\left\langle \frac{1}{f} \left(\sum_{i=1}^{n} \frac{\partial f}{\partial y_i} \dot{y}_i + \frac{\partial f}{\partial t} \right) \right\rangle$$
$$= \int_{-\infty}^{\infty} \cdots \int_{-\infty}^{\infty} \left(\sum_{i=1}^{n} \frac{\partial f}{\partial y_i} \dot{y}_i \right) dy_1 \cdots dy_n - \int_{-\infty}^{\infty} \cdots \int_{-\infty}^{\infty} \frac{\partial f}{\partial t} dy_1 \cdots dy_n \tag{3.7}$$

Making use of the theorem on differentiation of integrands, we conclude that the second integral on the right-hand side is equal to zero. Substituting $\dot{y}_i = F_i$ $(i=1,2,\ldots,n)$ into (3.7) we have

$$\frac{dH(t)}{dt} = -\sum_{i=1}^{n} \int_{-\infty}^{\infty} \cdots \int_{-\infty}^{\infty} \frac{\partial f}{\partial y_i} F_i \, dy_1 \cdots dy_n \tag{3.8}$$

Due to the assumption on behaviour of fF_i at infinity we obtain (after integration by parts)

$$\int_{-\infty}^{\infty} \frac{\partial f}{\partial y_i} F_i \, dy_i = -\int_{-\infty}^{+\infty} f \frac{\partial F_i}{\partial y_i} \, dy_i \tag{3.9}$$

As a result we obtain the following differential equation for the entropy of the differential dynamical model (3.6)

$$\frac{dH(t)}{dt} = \sum_{i=1}^{n} \left\langle \frac{\partial F_i}{\partial y_i} \right\rangle , \quad H(t_0) = H(\underline{\overset{\circ}{Y}}) \tag{3.10}$$

Inthe case of linear differential model

$$\frac{dY_i^{m}(t)}{dt} + \sum_{k=1}^{n} a_{ik}(t) Y_k = 0 , \quad i = 1, \ldots, n \tag{3.11}$$

equation (3.10) is

$$\frac{dH(t)}{dt} = -\sum_{k=1}^{n} a_{ii}(t) , \quad H(t_0) = H_0 = H(\underline{\overset{\circ}{Y}}) \tag{3.12}$$

Example. Let us consider a harmonic oscillator with random initial conditions

$$\begin{aligned} &\ddot{Y}(t) + \beta(t)\dot{Y} + \omega_0^2 Y = 0 \\ &Y(t_0) = Y_0(\gamma) , \quad \dot{Y}(t_0) = Y_1(\gamma) \end{aligned} \tag{3.13}$$

Denoting: $Y=Y_1$, $\dot{Y}=Y_2$, $\underline{Y}=[Y_1, Y_2]$ we have

$$\begin{aligned} &\dot{Y}_1 - Y_2 = 0 , \\ &\dot{Y}_2 + \beta(t) Y_2 + \omega_0^2 Y_1 = 0. \end{aligned}$$

From (3.12) we obtain

$$\frac{dH_{\underline{Y}}(t)}{dt} = -\beta(t) , \qquad H_{\underline{Y}}(t_0) = H_0 = H\begin{bmatrix} Y_0(\gamma) \\ Y_1(\gamma) \end{bmatrix}$$

and finally

$$H_{\underline{Y}}(t) = H_{\underline{Y}}(t_0) - \int_{t_0}^{t} \beta(s) \, ds \tag{3.14}$$

It is seen that entropy $H_{\underline{Y}}(t)$ monotonically decreases as $t \to \infty$ if and only if

$$\sum_{i=1}^{n} a_{ii}(t) > 0 . \tag{3.15}$$

4. Signal processing

4.1. Maximum entropy spectral estimation

In the characterization of a second order weakly stationary stochastic process, use of the spectral density is often preffered to the autocorrelation function, because a spectral representation may reveal such useful information as hidden periodicities or close spectral peaks. In using the spectral density to characterize the process however, we have to construct a reliable estimator based on a finite length of data.

During long time most of the procedures used for estimating the spectral density of a stochastic process were based on the classical work of Blackman and Tukey [7] . According to this method, the available time series is first used to estimate the sample autocorrelation function for a number of lags, and then the estimate is multiplied by a window function that goes to zero beyond the largest available lag. Next, the Fourier transform of this product is determined to obtain an estimate of the spectral density. Statistical stability of this procedure and the results depend on the choice of the window function, and a significant effort has been made to determine a good window function.

Another procedure is based on the so-called periodogram, which is defined as the squared amplitude of the Fourier transform of the available time series. This approach has become rather popular especially after introducing the fast Fourier transform algoritm for performing discrete Fourier transformation (cf. [8]). However, use of the fast Fourier transform requires a periodic extension of the data, thereby inserting periodicities in the spectrum which may not exist in the data. Furthermore, as in the Blackman-Tuckey procedure, spectral density estimation based on the periodogram involve the use of a window functions which are independent of the properties of the stochastic process being analyzied. The windowing problem may be particularly accute if the available time series is very limited in length.

The windowing problem essential in the above linear procedures (linear - since they only involve the use of linear operations on the available data) may be overcome by using the maximum-likelihood method or maximum-entropy method (these methods are said to be nonlinear, since their construction is data-dependent). The first who introduced the concept of maximum entopy into the field of signal processing was Burg [9] . It seems, however, that the advantages of this approach have not sufficiently been put in use.

Suppose that we are given 2n+1 values of the autocorrelation function of a weakly stationary random process X(t) of zero mean.
We wish to obtain a spectral density estimate which corresponds to the most random (or most unpredictable) time series whose autocorrelation function is consistent with a set of known values. Of course, this condition is equivalent to an extrapolation of the autocorrelation function of the available time series by maximizing the entropy. Thus, this method avoids such assumptions as periodic extension of the data or that the data outside of the available record length is zero.

Let us introduce the entopy rate (cf. [10]) defined as

$$h = \lim_{n\to\infty} \frac{H}{n+1} \tag{4.1}$$

For Gaussian random process the entropy rate (or entropy density) is (cf. [10])

$$h = \frac{1}{4B} \int_{-B}^{B} \log g_x(\nu)\, d\nu + \log (2\pi e)^{1/2} \tag{4.2}$$

where $g_x(\omega)$ is the spectral density of the process and $B = \frac{1}{2\Delta t}$ is the bandwidth of the process; $\omega = 2\pi\nu$.
Expressing $g_x(\nu)$ in terms of the autocorrelation function of the process (exactly, of its discrete counterpart) $K_x(k)$ we have

$$h = \frac{1}{4B} \int_{-B}^{B} \log \left[\sum_{k=-\infty}^{+\infty} K_x(k) \exp(-i2\pi\nu k\Delta t) \right] d\nu + \log(2\pi e)^{1/2} \tag{4.3}$$

Following the principle of maximum entropy, h is now maximized subject to to the constraint that $g_x(\nu)$ is consistent with the known autocovariance $K_x(k)$, $|k| \geq n+1$. The variational problem to be solved reduces to

$$\frac{\partial h}{\partial K_x(k)} = 0 \quad , \qquad |k| \geq n+1 \tag{4.4}$$

Carrying out differentiation one finds that the conditions for the extremum are

$$\int_{-B}^{B} \frac{\exp(-i2\pi\nu k\Delta t)}{\hat{g}_x(\nu)}\, d\nu = 0 \quad , \qquad |k| \geq n+1 \tag{4.5}$$

where $\hat{g}_x(\nu)$ is the spectral density estimate constrained by (4.4). After appropriate transformations the final result is

$$\hat{g}_x(\nu) = \frac{P_n}{B\left|1 + \sum_{k=1}^{n} a_k \exp(-2\pi i\nu k\Delta t)\right|^2} \tag{4.6}$$

where P_n is a constant and the coefficients a_k are determined from the data. More exactly, P_n is the output power of a prediction-error

filter of order n, and a_k ,k=0,1,...,n are the corresponding filter coefficients, B is the bandwidth of the random signal X(t), and Δt is the sampling period equal to $\frac{1}{2B}$. Quantity (4.6) is termed as the maximum-entropy spectral density estimate.

It is clear that the value of a spectral estimate is dependent on the observations of a random signal; for new sets of measurements the numerical value of the estimate changes. It is important to find the mean and variance of the estimate and the covariance between values of the estimate at two different frequencies. These properties determine the degree of statistical stability of the particular estimator.
It is difficult to obtain general analytical expressions for the statistical properties of the maximum-entropy estimator. However, its asymptotic properties can be determined. It is found that the maximum-entropy estimate is asymptotically normal and asymptotically unbiased.

4.2. Optimal sampling of space-varying signals

If a random signal of interest depends both on the spatial and temporal variables (it is modelled as a random field) then an important problem is concerned with the best (according to the suitable criterion) distribution of sensors in the spatial domain. The use of an array of sensors for determining the properties of random fields is known in various applications. For example, in seismic applications the requirement is to use an array of sensors to facilitate the discrimination between earthquakes and underground nuclear explosions. In radio astronomy an array of some number of discrete antennas may be used to determine the intensity of radiation of some specific frequency reaching the earth from various regions of the sky.

Similar problem occurs in acoustical applications,especially in acoustic diagnostics of machines where the signals are the acoustic wave fields. In order to rationalize the diagnostic experiments it is important to study the problem of optimal spacing of microphones which register a random acoustic field generated by machine.
In stochastic structural dynamics we usually assume that random forces acting on structural element as well as random displacements, stresses etc. are spatially-temporal random fields. Important problem which arises is: how to design the experiment to obtain best knowledge on the random field under consideration on the basis of measurements in finite number of points. What should be a number of sensors which are necessary for obtaining sufficient information on random vibratory fields and - in particular - what should be their distribution in spatial domain.

The problem described above can be formulated with use of the information theary. It is reasonable to postulate that: among all possible ways of distribution of sensors (in the considered finite spatial domain) the best will be such which provides maximum entropy $H(\underline{r}_1, \underline{r}_2, \ldots, \underline{r}_N)$ of the field values at points $\underline{r}_1, \underline{r}_2, \ldots, \underline{r}_N$. Another possible criterion is the minimum of mutual information $I_{\underline{r}_i}(\underline{r}_j)$ between the indications of i-th and j-th sensors (i,j = 1,2,...,N).
In the case of the displacement field $u(\underline{r},t)$ of zero mean measured at N points $\underline{r}_1, \underline{r}_2, \ldots, \underline{r}_N$ the criterion of maximum entropy takes the form

$$H(u_1,u_2,\ldots,u_N) = -\int_{-\infty}^{\infty}\cdots\int_{-\infty}^{\infty} f(u_1,\ldots,u_N)\log f(u_1,\ldots,u_N)\,du_1\ldots du_N = \max_{\underline{r}_1,\ldots,\underline{r}_N} \tag{4.7}$$

where $f(u_1,u_2,\ldots,u_N)$ is the joint probability density function of $u_1 = u(\underline{r}_1,t)$, $u_2 = u(\underline{r}_2,t),\ldots,$ $u_N = u(\underline{r}_N,t)$.
If the field is Gaussian then the entropy is expressed in terms of the correlation function of the field. In general,

$$H(u_1,u_2,\ldots,u_N) = \log\sqrt{(2\pi e)^n |\underline{K}|} \tag{4.8}$$

where $|\underline{K}|$ is the determinant of the matrix $\underline{K}$. In the case of two measurement points we have

$$H(u_1,u_2) = \log 2\pi e\,(k_{11}k_{22} - k_{12}^2)^{\frac{1}{2}} \tag{4.9}$$

where

$$k_{ij} = \langle u(\underline{r}_i,t)\,u(\underline{r}_j,t)\rangle, \qquad i,j = 1,2. \tag{4.10}$$

It can be easily verified that in this case the criterion of minimum of mutual information is equivalent to the minimum of the correlation coefficient between u_1 and u_2.

Example. A beam vibrating under stochastic (Gaussian white noise) excitation.

governing equation and boundary conditions:
$$A_0 u_{tt} + B_0 u_{xxxx} + C_0 u_{xxxxt} = \xi(t,r)$$
$$u(0,t) = u_{xx}(0,t) = 0; \quad u(l,t) = u_{xx}(l,t) = 0$$

method: modal approach:
$$u(x,t) = \sum_{k=1}^{\infty} \varphi_k(t)\,\psi_k(x),$$
$$K_u(x_1,x_2,t) = \sum_{j,k=1}^{\infty} \psi_j(x_1)\psi_k(x_2)R_{jk}; \qquad R_{jk} = \langle \varphi_j(t)\varphi_k(t)\rangle$$

Since the solution $u(x_1,x_2,t)$ is a Gaussian process, expression (4.8) can be used and then maximized. In the case of two sensors, when two first vibration modes are accounted for we obtain the result saing that the sensors should be placed at $x = \frac{l}{5}$ and $x = \frac{l}{2}$ or, by the symmetry at $x = \frac{l}{2}$ and $x = \frac{4}{5}l$. More complex situations are recently under the author consideration.

References

1. Kullback S., Information Theory and Statistics, Chapman and Hall New York, 1959.

2. Poplavskij R.P., Thermodynamical models of information processes, Usp.Fiz.Nauk, Vol.115,Nr 3, 1975 (in Russian).

3. Csiszar I., Information measures: a critical survey, Seventh Prague Conf.on Inform.Theory, Statistical Decisions Functions and Stoch.Processes, Reidel, Dodrecht, 73-86, 1978.

4. Kerridge D.F., Inacuracy and inference, J.Roy.Statist.Soc., Ser.B Vol.23, 184-194, 1961.

5. Goodwin G.C., Payne R.I., Dynamic System Identification; Experiment Design and Data Analysis, Acad.Press, N.York, 1977.

6. Sobczyk K., On system identification, IFTR Reports, 26/1986

7. Blackman R.B., Tukey J.W., The Measurement of Power Spectra from the Point of View of Communication Engineering, Dover, N.York, 1959.

8. Oppenheim A.V., Schafer R.W., Digital Signal Processing, Prentice-Hall, N.York,1975.

9. Burg J.P., New concepts in power spectra estimation, 40-th Ann. Intern.Meeting, Soc.Exploration Geophysists, New Orleans, 1970.

10. Stratonovich R.L., Theory of Information (in Russian), Sov.Radio. Moskow,1975.

11. Bolotin V.V., Random Vibrations of Elastic Systems (in Russian), Nauka, Moskow, 1979.

INTEGRATED RELIABILITY-BASED OPTIMAL DESIGN OF STRUCTURES

J. D. Sørensen & P. Thoft-Christensen
University of Aalborg
Sohngaardsholmsvej 57
DK-9000 Aalborg, Denmark

1. INTRODUCTION

In conventional optimal design of structural systems the weight or the initial cost of the structure is usually used as objective function. Further, the constraints require that the stresses and/or strains at some critical points have to be less than some given values. Finally, all variables and parameters are assumed to be deterministic quantities. In this paper a probabilistic formulation is used. Some of the quantities specifying the load and the strength of the structure are modelled as random variables, and the constraints specify that the reliability of the structure has to exceed some given value. The reliability can be measured from an element and/or a systems point of view. A number of methods to solve reliability-based optimization problems has been suggested, see e.g. Frangopol [1], Murotsu et al. [2], Thoft-Christensen & Sørensen [3] and Sørensen [4].

For structures where the reliability decreases with time it is often necessary to design an inspection and repair programme. For example the reliability of offshore steel structures decreases with time due to corrosion and development of fatigue cracks. Until now most inspection and repair strategies are based on experience rather than on rational investigations, see e.g. Jubb [5] and Dunn [6]. As a result it can be expected that inspection and repair of the structure on the above-mentioned bases are not only uneconomic, but perhaps also unsatisfactory from a safety point of view.

In chapter 2 of this paper reliability-based optimal design is discussed. Next, an optimal inspection and repair strategy for existing structural systems is presented. An optimization problem is formulated, where the objective is to minimize the expected total future cost of inspection and repair subject to the constraint that the reliability at any time is acceptable (see Thoft-Christensen & Sørensen [7]). The reliability is estimated using first-order reliability methods, Thoft-Christensen & Murotsu [8] and Madsen et al. [9]. Finally, integration of the optimal inspection/repair strategy and the reliability-based optimal design problem is considered. A practically usable procedure to solve the described integrated optimization problem is presented and demonstrated on an offshore structure.

2. OPTIMAL DESIGN

From a classical, deterministic point of view optimal design of a structural system is usually formulated as an optimization problem where the structural weight is used an an objective function and where the constraints ensure that stresses, displacements, etc. do not exceed given critical values. The optimization variables are denoted $\bar{z} = (z_1, z_2, \ldots, z_m)$ and in most cases they are geometrical quantities, such as cross-sectional areas. However, instead of using the structural weight as an objective function the total or the initial cost of the structure can be used.

In reliability-based structural optimization some of the quantities describing the load and/or the strength of the system are modelled as random variables. The random variables are denoted $\bar{X} = (X_1, X_2, \ldots, X_n)$. A reliability model of the structural system is then formulated. The elements in this model are failure elements modelling potential failure modes of the elements of the structural system, e.g. fatigue failure of a tubular joint. Each failure element is described by a failure function

$$g(\bar{x}, \bar{z}) = 0 \tag{1}$$

Realizations $\bar{x}$ of $\bar{X}$ resulting in $g(\bar{x}, \bar{z}) \leq 0$ correspond to failure states, while $g(\bar{x}, \bar{z}) > 0$ correspond to safe states. In first-order reliability methods (FORM) a transformation $\bar{T}$ of the generally correlated and non-normally distributed variables $\bar{X}$ into standardized and normally distributed variables $\bar{U} = (U_1, U_2, \ldots, U_n)$ is defined. Let $\bar{X} = \bar{T}(\bar{U})$. In the u-space the reliability index β is defined as

$$\beta = \min_{g(\bar{T}(\bar{u}), \bar{z}) = 0} (\bar{u}^T \bar{u})^{1/2} \tag{2}$$

The solution point $\bar{u}^*$ to the optimization problem in (2) is called the design point. If the safety margin $M = g(\bar{T}(\bar{U}))$ is linearized in the design point we get

$$M \cong -\bar{\alpha}^T \bar{U} + \beta \tag{3}$$

where

$$\alpha_i = \frac{u_i^*}{\beta} = \frac{-1}{|\nabla_u g|} \frac{\partial g}{\partial u_i} \tag{4}$$

$\nabla_u g$ is the gradient of g with respect to $\bar{u}$ in the design point $\bar{u}^*$.

If the failure function is not severely non-linear then the probability of failure P_f can with good approximation be determined from

$$P_f \cong \Phi(-\beta) \tag{5}$$

where $\Phi(\cdot)$ is the standard normal distribution function.

Let the structural system be modelled by s failure elements and let failure of the system be defined as failure of one of these elements. Then a generalized reliability index β_S of this series system can be determined from

$$\beta_S = -\Phi^{-1}(P_f) = \Phi^{-1}(\Phi_s(\bar{\beta}; \bar{\bar{\rho}})) \tag{6}$$

where $\bar{\beta} = (\beta_1, \beta_2, \ldots, \beta_s)$ are the reliability indices of the failure elements and $\bar{\bar{\rho}}$ is a correlation coefficient matrix determined from the linearized safety margins. $\Phi_s(\cdot)$ is the s-dimensional standard normal distribution function. More sophisticated models of systems failure are described by Thoft-Christensen & Murotsu [8].

Let the systems reliability index β_S be used as a measure of the reliability. Then the reliability-based optimization problem can be formulated as, see Sørensen & Thoft-Christensen [10]

$$\min_{\bar{z}} \; C(\bar{z}) \tag{7}$$

$$\text{s.t.} \quad \beta_S(\bar{z}) \geq \beta_S^{\min} \tag{8}$$

$$\bar{z}^{\ell} \leq \bar{z} \leq \bar{z}^{u} \tag{9}$$

where $C(\bar{z})$ is the objective function (e.g. the initial cost of the structure), $\beta_S^{\min}$ is some target reliability index and $\bar{z}^{\ell}$ and $\bar{z}^{u}$ are lower and upper bounds of the optimization variables.

Alternatively, the reliability indices of the failure elements can be used as constraints. Then, instead of (8) the constraints are

$$\beta_i(\bar{z}) \geq \beta_i^{\min} \quad , \quad i = 1, \ldots, s \tag{10}$$

$\beta_i^{\min}$ is the lower bound of the acceptable reliability index of element i.

The reliability-based optimization problems are generally non-linear and non-convex. Most optimization algorithms require calculation of the gradients of the objective function and of the constraints. From (2) and (4) it is seen that

$$\frac{\partial \beta_i}{\partial z_j} = \frac{1}{|\nabla_u g_i|} \frac{\partial g_i(\bar{u}^*, \bar{z})}{\partial z_j} \tag{11}$$

(11) implies that gradients of (10) can be estimated effectively. Approximate methods to estimate quasi-analytical gradients of (8) are described in Sørensen [4]. A procedure by which the systems reliability optimization problem (7) - (9) is solved by using a sequence of element reliability constraint problems is also described in [4].

3. OPTIMAL INSPECTION AND REPAIR STRATEGIES

The purpose of an optimal inspection and repair strategy is to minimize the cost of inspection and repair of a given structure so that the structure in its expected service life has an acceptable reliability. The strategy is illustrated in figure 1, where T is the lifetime of the structure and β is the reliability index of the structure.

The reliability index β is assumed to be a non-increasing function with time t if no inspection and no repair are performed. T_i, i = 1, 2, . . . , N are the inspection times and β^{min} is the minimum acceptable reliability of the structure in its lifetime. The quality of inspection at the time T_i is measured by a variable q_i, i = 1, . . . , N. Depending on the magnitudes of the inspection qualities the reliability index function will increase at the inspection times.

It is further assumed that the structure is modelled by s failure elements and that the damage of each failure element can be modelled by an increasing function of time a(t) which is a realization of a time-dependent stochastic variable A(t). Failure of the element occurs when

$$a(t) \geq a_{cr} \tag{12}$$

where a_{cr} is a critical damage measure, e.g. a critical crack length.

Repair at the time T_i is assumed to be performed if

$$a_m \geq a_{in} \tag{13}$$

where a_m is the damage measured during the inspection and a_{in} is a critical damage measure. A repair is assumed to take place immediately and to be complete.

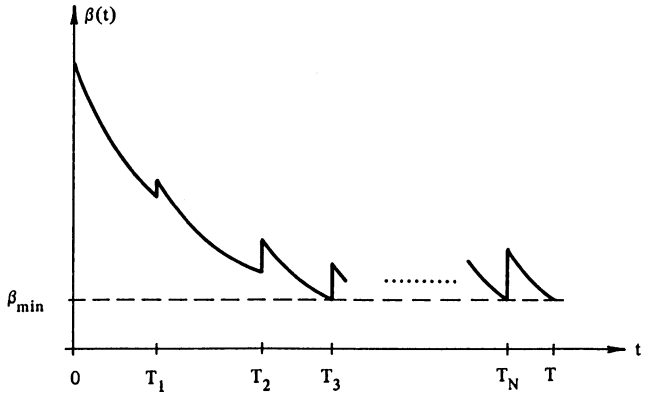

Figure 1. Reliability index β with inspection at the times $T_1, T_2, \ldots, T_N$.

The inspection uncertainty which is assumed to decrease with inspection quality q is divided into two groups: measurement uncertainty (e.g. measuring of crack length) and non-detection of critical damage (e.g. ignoring a critical crack). The measurement uncertainty is modelled as

$$A_m = A_1 A(t) \tag{14}$$

where A_1 is a random variable with parameters depending on q. Likewise, the non-detection of a critical damage is modelled by a random variable A_2 with parameters depending on the inspection quality q.

Generally, the cost of construction, inspection and repair has to be measured in real prices. The cost due to failure is neglected in this paper.

The cost of inspection C_{IN} is modelled as a function of the quality of inspections

$$C_{IN} = C_{IN}(q) \tag{15}$$

The cost of a repair C_R and of construction C_I are assumed only to be dependent on the design variables $\bar{z}$

$$C_R = C_R(\bar{z}) \tag{16}$$

$$C_I = C_I(\bar{z}) \tag{17}$$

If the number of inspections is N and the real rate of interest is constantly equal to r then the total real capitalized cost C is

$$C(\bar{q}, \bar{t}, \bar{z}) = C_I(\bar{z}) + \sum_{i=1}^{N} C_{IN,i}(q_i) e^{-rT_i} + \sum_{i=1}^{N} C_{R,i}(\bar{z}) E[R_i(\bar{q}, \bar{t})] e^{-rT_i} \tag{18}$$

where $E[R_i(\bar{q}, \bar{t})]$ is the expected number of repairs at the i^{th} inspection.

The reliability of the failure elements or of the system has to fulfil the following inequalities

$$\beta_i(t) \geqslant \beta_i^{min} \quad , \quad 0 \leqslant t \leqslant T, \; i = 1, 2, \ldots, s \tag{19}$$

$$\beta_S(t) \geqslant \beta_S^{min} \quad , \quad 0 \leqslant t \leqslant T \tag{20}$$

The minimum β-values are assumed to be at least of the order 3 - 4 so that the events of failure can be considered as rare events.

With the above assumptions the optimal inspection strategy for a single element in a given structure can be determined from the following optimization problem where the design variables are $\bar{q}, \bar{t}$ and N

$$\min_{\substack{q_1 \ldots q_N \\ t_1 \ldots t_N \\ N = 1, 2, \ldots}} C(\bar{q}, \bar{t}) = \sum_{i=1}^{N} C_{IN}(q_i) e^{-rT_i} + \sum_{i=1}^{N} C_R \, E[R_i(\bar{q}, \bar{t})] e^{-rT_i} \tag{21}$$

$$\text{s.t.} \quad \beta(T_i) \geqslant \beta^{min} \qquad i = 1, 2, \ldots, N, N+1 \tag{22}$$

$$0 \leqslant T - \sum_{i=1}^{N} t_i \leqslant t_{max} \tag{23}$$

$$t_{min} \leqslant t_i \leqslant t_{max} \qquad i = 1, 2, \ldots, N \tag{24}$$

$$q_{min} \leqslant q_i \leqslant q_{max} \qquad i = 1, 2, \ldots, N \tag{25}$$

where t_{min}, t_{max}, q_{min} and q_{max} are minimum and maximum time intervals and inspection qualities. $\beta(T_i)$ is the reliability index just before inspection at the time T_i or at the time T if i = N + 1.

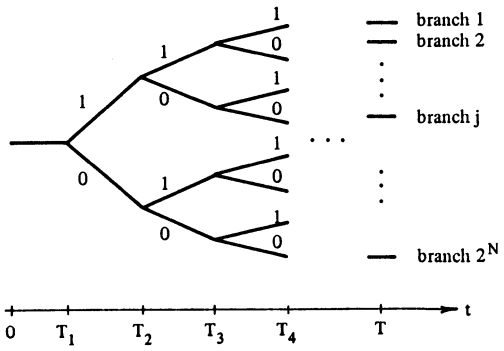

Figure 2. Repair realizations for a single element.

The total number of different repair courses (branches) is 2^N, see figure 2, where 0 and 1 signify non-repair and repair, respectively. Let $+R_i$ and $-R_i$ signify repair and non-repair at the time T_i and let B_j^i signify the event that branch j occurs at the time T_i. Then

$$E[R_i] = \sum_{j=1}^{2^{i-1}} P(+R_i \cap B_j^i) \tag{26}$$

If repair events are rare then approximately

$$E[R_i] \cong P(+R_i \cap -R_{i-1}) \tag{27}$$

A simple upper bound of (26) is

$$E[R_i] \leq 2^{i-1} P(+R_i \cap -R_1 \cap \cdots \cap -R_{i-1}) \tag{28}$$

(28) is expected to give reasonable estimates when the number of inspections is not too large and when the repair events cannot be considered as rare.

The reliability index $\beta(T_i)$ at the time T_i can be estimated using (6)

$$\beta(T_i) = -\Phi^{-1}[\sum_{j=1}^{2^{i-1}} P(F(T_i) \cap B_j^i)] \tag{29}$$

where $F(T_i)$ is the event that failure occurs at the time T_i. Corresponding to (27) and (28) an approximation and a simple lower bound can be estimated from

$$\beta(T_i) \cong -\Phi^{-1}[P(F(T_i) \cap -R_{i-1})] \tag{30}$$

and

$$\beta(T_i) \geq -\Phi^{-1}[\min\{1, 2^{i-1} P(F(T_i) \cap -R_1 \cap \cdots \cap -R_{i-1})\}] \tag{31}$$

In order to solve the optimization problem (21) - (25) effectively it is very important that the estimates and the gradients of $E[R_i]$ and $\beta(T_i)$ are not too complicated to calculate numerically. But even if approximate estimates are used it can be expected that the result of the optimization problem gives a reasonable distribution of inspection intervals and qualities.

Let a given structure be modelled by s failure elements in a series system and let all failure elements be inspected at the same times T_i and with the same inspection qualities q_i. Then an optimal inspection strategy can be determined from the following optimization problem

$$\min_{\substack{q_i \cdots q_N \\ t_i \cdots t_N \\ N = 1, 2, \ldots}} C(\bar{q}, \bar{t}) = \sum_{i=1}^{N} \sum_{j=1}^{s} C_{IN,j}(q_i) e^{-rT_i} + \sum_{i=1}^{N} \sum_{j=1}^{s} C_{R,j} E[R_{ij}(\bar{q}, \bar{t})] e^{-rT_i} \tag{32}$$

$$\text{s.t} \quad \beta_S(T_i) \geq \beta^{min} \qquad i = 1, 2, \ldots, N, N+1 \tag{33}$$

$$0 \leq T - \sum_{i=1}^{N} t_i \leq t_{max} \tag{34}$$

$$t_{min} \leq t_i \leq t_{max} \qquad i = 1, 2, \ldots, N \tag{35}$$

$$q_{min} \leq q_i \leq q_{max} \qquad 1 = 1, 2, \ldots, N \tag{36}$$

$C_{IN,j}$ and $C_{R,j}$ are the inspection and repair cost of element j. $E[R_{ij}]$ is the expected number of repairs at the time T_i in element j:

$$E[R_{ij}] = \sum_{k=1}^{2^{s(i-1)}} P(+R_{ij} \cap B_k^i) \tag{37}$$

The systems reliability index $\beta_S(T_i)$ is given by

$$\beta_S(T_i) = -\Phi^{-1}[\sum_{k=1}^{2^{s(i-1)}} P(\bigcup_{j=1}^{s} F_j(T_i) \cap B_k^i)] \tag{38}$$

$F_j(T_i)$ is the event that element j fails at the time T_i. If repair events are rare then simple approximations to (37) and (38) which include the essential features are

$$E[R_{ij}] \cong P(+R_{ij} \cap -R_{i-1\,j}) \tag{39}$$

$$\beta_S(T_i) \cong -\Phi^{-1}[P(\bigcup_{j=1}^{s} \{F_j(T_i) \cap -R_{i-1\,j}\})] \tag{40}$$

The two optimization problems (21) - (25) and (32) - (36) are a mixture of integer, non-linear and non-convex optimization problems, which can be solved sequentially for a fixed number of inspections N.

The probabilities in (26) - (40) can be estimated using first-order reliability methods, see example 2.

4. INTEGRATION OF OPTIMAL DESIGN AND OPTIMAL INSPECTION/REPAIR STRATEGIES

Let the design variables $\bar{z}$ and the inspection variables N, $\bar{t}$ and $\bar{q}$ be design variables in an integrated optimal design and optimal inspection strategy problem. Then the following optimization problem for a structural system modelled by s failure elements can be formulated

$$\min_{\substack{z_i \cdots z_m \\ q_i \cdots q_N \\ t_i \cdots t_N \\ N = 1, 2, \ldots}} C(\bar{z}, \bar{q}, \bar{t}) = C_I(\bar{z}) + \sum_{i=1}^{N} \sum_{j=1}^{s} C_{IN,j}(q_i) e^{-rT_i} + \sum_{i=1}^{N} \sum_{j=1}^{s} C_{R,j}(\bar{z}) E[R_{ij}(\bar{z}, \bar{q}, \bar{t})] e^{-rT_i} \tag{41}$$

$$\text{s.t.} \quad \beta_S(T_i) \geq \beta^{min} \qquad i = 1, 2, \ldots, N, N+1 \tag{42}$$

$$0 \leq T - \sum_{i=1}^{N} t_i \leq t_{max} \tag{43}$$

$$t_{min} \leq t_i \leq t_{max} \qquad i = 1, 2, \ldots, N \tag{44}$$

$$q_{min} \leq q_i \leq q_{max} \qquad i = 1, 2, \ldots, N \tag{45}$$

$$z_i^{\ell} \leq z_i \leq z_i^{u} \qquad i = 1, 2, \ldots, m \tag{46}$$

This second integer optimization problem is generally non-linear and non-convex. The optimization problem can alternatively be formulated as the problem to maximize the minimum systems reliability index during the lifetime of the structure with the constraints (43) - (46) and with the further constraint that the total cost of construction, inspection and repair must not exceed a maximum cost C_{max}. Another alternative is to formulate a multi-objective optimization problem where the solution can be chosen from the Pareto optimum set.

In this paper the formulation (41) - (46) is used. The optimization problem is solved sequentially for varying N using the NLPQL algorithm implemented by Schittkowski [11]. The algorithm is based on the method by Han [12], Powell [13] and Wilson [14]. Generally it is a very effective method where each iteration consists of two steps. The first step is determination of a search direction by solving a quadratic optimization problem formed by a quadratic approximation of the Lagrangian function of the non-linear problem and a linearization of the constraints at the current design point. The second step is a line search with an augmented Lagrangian merit function.

5. EXAMPLE 1. MODELLING OF FATIGUE CRACK FAILURE ELEMENTS

A simple fatigue crack failure element is considered in this example. In example 2 the same failure element is used to model the failure modes in a plane model of an offshore steel structure. Based on a linear elastic fracture mechanics approach, Paris' law and constant amplitude loading the following safety margin can be formulated corresponding to the failure event that the crack exceeds a critical crack length a_{cr}, see e.g. Madsen, Krenk & Lind [9].

$$M_F(t) = A_0^{\frac{2-M}{2}} - a_{cr}^{\frac{2-M}{2}} + \frac{2-M}{2} Y^M \left(\frac{B\Delta\sigma}{K}\right)^M \pi^{M/2} \nu t \tag{47}$$

where A_0 is the initial crack length, Y the stress intensity factor, B a load model uncertainty parameter, M and K material parameters, ν the stress cycle rate and t the time. $\Delta\sigma$ is the standard deviation of stress variations which is generally dependent on the design variables $\bar{z}$.

Following the assumptions stated above a safety margin corresponding to repair can be formulated as

$$M_R(t) = A_0^{\frac{2-M}{2}} - \left(\frac{a_{in}}{A_1}\right)^{\frac{2-M}{2}} + \frac{2-M}{2A_2} Y^M \left(\frac{B\Delta\sigma}{K}\right)^M \pi^{M/2} \nu t \tag{48}$$

where a_{in} is the critical repair crack length and A_1 and A_2 the stochastic variables modelling inspection uncertainty, see (13) - (14). In (47) and (48) A_0, Y, B, M and K are modelled as random variables.

From (48) it is seen that both A_1 and A_2 can be considered as inspection model uncertainty variables of the multiplication type. Therefore, it seems reasonable to model A_1 and A_2 as log-normally distributed variables. The following distribution parameters are used in this example

$$A_1 : LN(0.1\,\alpha(q), 0.02\,\alpha(q)) \quad , \quad 0 < q < 1 \tag{49}$$

$$A_2 : LN(\alpha(q), 0.2\,\alpha(q)) \quad , \quad 0 < q < 1 \tag{50}$$

where $LN(\mu, \sigma)$ is a log-normal distribution with the expected value μ and the standard deviation σ. In this example $\alpha(q)$ is

$$\alpha(q) = 0.14 \frac{1-q}{1-(1-q)^3} \quad , \quad 0 < q < 1 \tag{51}$$

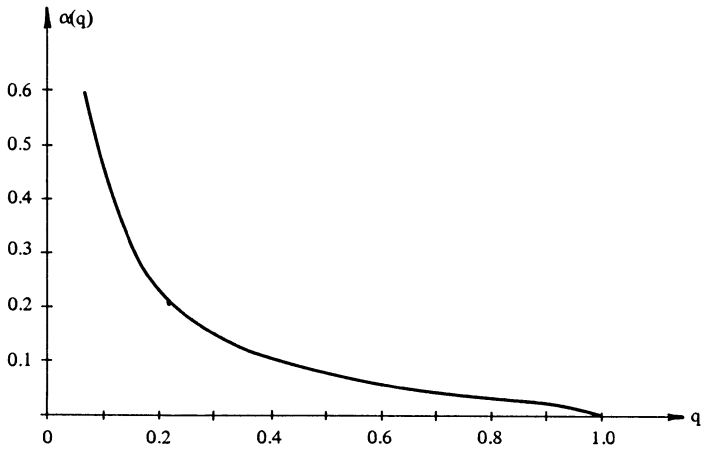

Figure 3. Example of model of inspection quality parameter $\alpha(q)$.

In a practical situation the constants in (49) - (51) should clearly be calibrated carefully to experimental data. The proposed model assumes that the inspection quality q is in the open interval from 0 to 1. The function $\alpha(q)$ in (51) is shown in figure 3. The slightly S-shaped form of $\alpha(q)$ implies that the probability of discovering a failure as a function of q will also be S-shaped. A consequence of this is that even a small inspection quality gives a relatively high probability of discovering a critical crack length. Contrary to this even a high inspection quality will not guarantee that a critical crack is discovered.

The other stochastic variables are modelled as follows

A_0: LN(1, 0.25) [mm]

Y: LN(1, 0.05)

B: LN(1, 0.25)

M: N(3.8, 0.095)

K: LN(6400, 1024) [10^6 N/m^2]

$N(\mu, \sigma)$ signifies that the variable is normally distributed with the expected value μ and the standard deviation σ. M and $\ln K$ are assumed to be correlated with the correlation coefficient $\rho = -0.44$ (see Karadeniz et al. [15]).

Following Wirshing [16] M and K are assumed to be independent. Further, the material variables A_0, M and K before and after a repair are assumed to be independent.

Using the first-order reliability method for a single element model (27) can be approximated by

$$E[R_i] \cong \Phi_2(-\beta_R(T_i), \beta(T_{i-1}); \rho) \tag{52}$$

where $\beta_R(T_i)$ is the reliability index corresponding to the safety margin (48) and ρ is the correlation coefficient between the safety margins at the time T_i and T_{i-1}. Only the time parameter changes in the safety margin M_R from the time T_{i-1} to T_i. Therefore, ρ can be expected to be close to -1 so that

$$\sum_{i=1}^{N} E[R_i] \cong \Phi(-\beta_R(T_N)) \tag{53}$$

A good approximation of (30) is

$$\beta(T_i) \cong -\Phi^{-1}[\Phi_2(-\beta_F(T_i), \beta_R(T_{i-1}); \rho)] \tag{54}$$

where $\beta_{i;}(T_i)$ is the reliability index corresponding to the safety margin (47) and ρ is the correlation coefficient between the linearized safety margins $M_F(T_i)$ and $M_R(T_{i-1})$. Again, due to no repair in the time interval between the two events, ρ can be expected to be close to -1. Therefore,

$$\beta(T_i) \cong -\Phi^{-1}[\max\{0, \Phi(\beta_R(T_{i-1})) - \Phi(\beta_F(T_i))\}] \tag{55}$$

For a series system model the above assumptions imply that the correlations between repair safety margins of a given failure element between repair events can be considered to be high. Further, the correlations between safety margins of different elements and between safety margins before and after repair can be considered close to 0. This implies that

$$E[R_i] \cong \sum_{j=1}^{s} \Phi(-\beta_{R_j}(T_N)) \tag{56}$$

and that $\beta_S(T_i)$ given by (40) can be approximated by

$$\beta_S(T_i) \cong -\Phi^{-1}[P(\bigcup_{j=1}^{s} \{F_j(T_i) \cap -R_{i-1\,j}\})] \geqslant -\Phi^{-1}[\min\{1, \sum_{j=1}^{s} P(F_j(T_i) \cap -R_{i-1\,j})\}]$$

$$\cong -\Phi^{-1}[\min\{1, \sum_{j=1}^{s} (\Phi(\beta_{R_j}(T_{i-1})) - \Phi(\beta_{F_j}(T_i)))\}] \tag{57}$$

or if the correlations between the safety margins of different elements are taken into account

$$\beta_S(T_i) \cong -\Phi^{-1}[\max\{0, \Phi_s(\bar{\beta}_R(T_{i-1}); \bar{\bar{\rho}}_R(T_{i-1})) - \Phi_s(\bar{\beta}_F(T_i); \bar{\bar{\rho}}_F(T_i))\}] \tag{58}$$

where $\bar{\bar{\rho}}_R$ and $\bar{\bar{\rho}}_F$ are the correlation coefficient matrices for safety margins of different elements for repair and failure events, respectively.

6. EXAMPLE 2. OPTIMAL INTEGRATED DESIGN OF A PLANE OFFSHORE STRUCTURE

In this example integration of optimal design and optimal inspection strategy for a plane model of a steel jacket platform with fatigue crack failure elements is considered. The structure shown in figure 4 is considered. The load modelling and the detailed geometrical description are described in Thoft-Christensen [17]. Due to symmetry only the 8 failure elements indicated by x in figure 4 are considered in this example, i.e. $s = 8$. The structural design variables are the tubular thicknesses of the 6 groups of elements indicated by o in figure 4, i.e. $m = 6$. Further, the following values of the constants in (47) and (48) are used: $\nu = 6.31 \cdot 10^6$ cycles/year, time t measured in years, $a_{cr} = 40$ mm, $a_{in} = 10$ mm. In this example a_{cr} is chosen to be constant. If the critical crack length is dependent on the tubular thickness then another possibility is to put a_{cr} equal to the design variable modelling the thickness of the actual structural element.

The standard deviation of stress variations is modelled as

$$\Delta\sigma = c\sigma(\mathrm{SCF}^a, \mathrm{SCF}^b, \text{influence coefficients, sectional area and modulus}) \tag{59}$$

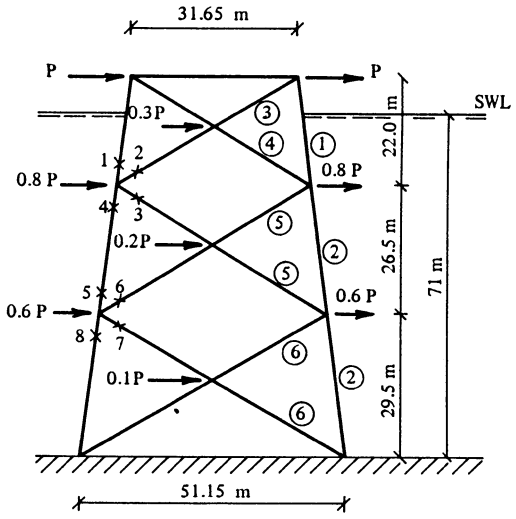

Figure 4. Offshore steel jacket structure.

where σ is the hot spot stress depending on the stress concentration factors for axial and bending load effects SCF^a and SCF^b (here the formulas by Kuang are used, see Almar-Næs [18]), the influence coefficients for unit loads and the sectional area and modulus. All these quantities are dependent on the design variables $\bar{z}$. c is a constant (in this paper $c = 25 \cdot 10^6$ N/m^2).

The cost functions in the objective function in (41) are modelled as

$$C_i(\bar{z}) = \text{weight } C_{IO} \quad , \quad C_{IO} = 35{,}000 \text{ kr/tons} \tag{60}$$

$$C_{IN,j}(q_i) = q_i^2 \, C_{INO} \quad , \quad C_{INO} = 200{,}000 \text{ kr.} \tag{61}$$

$$C_{R,j}(\bar{z}) = C_{RO} \quad , \quad C_{RO} = 25 \cdot 10^6 \text{ kr.} \tag{62}$$

The values of the constants are chosen on the basis of information of actual cost prices in the Danish part of the North Sea. The upper and lower bounds in (42) - (46) are chosen as

$t_{min} = 0.25$ year $\qquad t_{max} = 2$ years

$q_{min} = 0.1 \qquad q_{max} = 0.95$

$z_i^{\ell} = 30$ mm $\qquad z_i^u = 100$ mm $\quad , i = 1, 2, \ldots, 6$

$\beta^{min} = 3 \qquad T = 10$ years

$r = 0$

As mentioned above the NLPQL algorithm [11] is used to solve the optimization problem. The probability estimates are calculated using first-order reliability methods and derivatives are estimated using semi-analytical derivatives based on (11). Derivatives with respect to the design variables $\bar{z}$ are calculated using pseudo-load vectors formed by numerical differentiation of the stiffness matrix of the structural system with respect to the design variables $\bar{z}$.

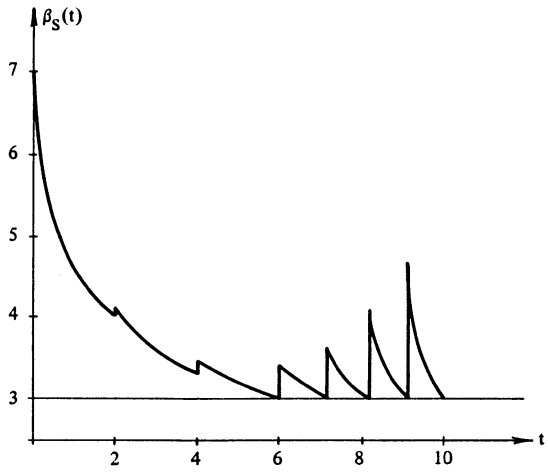

Figure 5. Systems reliability index β_S as a function of t for optimal values of design variables and inspection variables for N = 6.

For the number of inspections N = 6 the optimal values of the optimization variables are shown in table 1. The corresponding systems reliability index β_S as a function of t is shown in figure 5. In this example it is seen that the optimal time intervals between inspections decrease with time and that the inspection qualities increase with time so that at the end of the expected lifetime of the structure, when the reliability requirements become critical, the inspections should be performed more often and be of higher quality. Note that the increase in reliability after an inspection is growing with the time t.

In figure 6 the optimal value of the cost is shown for different values of the number of inspections N. It appears that the total cost has a minimum of about 6 - 7 inspections.

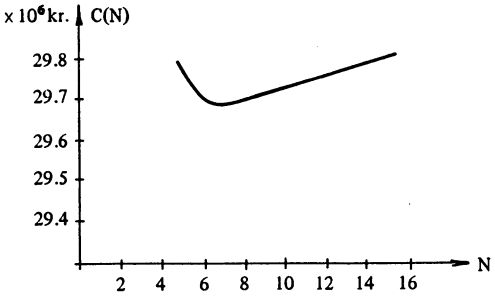

Figure 6. Optimal total cost as a function of the number of inspections.

In table 1 the optimization results for some simplified models of the general optimal strategy problem are also shown. In column 2 the results are shown if no inspection is performed. The increase in the total cost is about 9%. This indicates, at least in this example, that the total cost can be reduced considerably when inspection is included. In columns 3 and 4 the result of a sequential optimization is shown. First, optimization with respect to the design variables $\bar{z}$ with constant time intervals and inspection qualities is performed (column 3). Next, optimization with respect to $\bar{t}$ and $\bar{q}$ with $\bar{z}$ equal to the values from column 3 is performed. The optimal value of the cost by this sequential procedure is seen to be less than 1% greater than the result from column 1, although the optimal values of the variables differ somewhat. Use of the sequential procedure reduces the computer time by about 20% (full optimization on a VAX 8700 lasts about 1000 sec.).

In order to investigate the effect of the value of repair cost the same optimization problems are solved when C_{RO} is changed from $25 \cdot 10^6$ kr. to $2.5 \cdot 10^6$ kr. The results are shown in table 2. It is seen that the change of the repair cost has only small effect on the optimal values of $\bar{t}$, $\bar{q}$, $\bar{z}$ and the total cost. The reason for this is that the probability that repair takes place is extremely small.

	1 full optimization	2 no inspection	3 inspection at pre-determined times with given qualities	4 structural dimensions taken from 3
t_1 [year]	2		1.43	2
t_2 [year]	2		1.43	2
t_3 [year]	2		1.43	2
t_4 [year]	1.19		1.43	1.33
t_5 [year]	0.994		1.43	0.974
t_6 [year]	0.925		1.43	0.865
q_1	0.1		0.5	0.1
q_2	0.133		0.5	0.1
q_3	0.261		0.5	0.115
q_4	0.332		0.5	0.185
q_5	0.385		0.5	0.236
q_6	0.423		0.5	0.280
z_1 [mm]	68.9	76.2	70.6	70.6
z_2 [mm]	62.7	70.4	64.7	64.7
z_3 [mm]	30.0	30.0	30.0	30.0
z_4 [mm]	30.0	30.0	30.0	30.0
z_5 [mm]	50.4	59.2	52.4	52.4
z_6 [mm]	32.0	37.5	33.3	33.3
C [10^6 kr.]	29.7	32.3	32.1	29.9

Table 1. Optimal values of $\bar{t}$, $\bar{q}$ and $\bar{z}$ for N = 6 and $C_{RO} = 25 \cdot 10^6$ kr.

	1 full optimization	2 no inspection	3 inspection at pre-determined times with given qualities	4 structural dimensions taken from 3
t_1 [years]	2		1.43	2
t_2 [years]	2		1.43	2
t_3 [years]	2		1.43	2
t_4 [years]	1.18		1.43	1.33
t_5 [years]	0.987		1.43	0.973
t_6 [years]	0.916		1.43	0.865
q_1	0.1		0.5	0.1
q_2	0.144		0.5	0.1
q_3	0.277		0.5	0.115
q_4	0.343		0.5	0.185
q_5	0.392		0.5	0.236
q_6	0.442		0.5	0.280
z_1 [mm]	67.6	76.2	70.3	70.3
z_2 [mm]	62.6	70.4	64.7	64.7
z_3 [mm]	30.0	30.0	30.0	30.0
z_4 [mm]	30.0	30.0	30.0	30.0
z_5 [mm]	50.2	59.2	52.3	52.3
z_6 [mm]	32.5	37.5	33.4	33.4
C [10^6 kr.]	29.6	32.3	32.0	29.9

Table 2. Optimal values of $\bar{t}$, $\bar{q}$ and $\bar{z}$ for N = 6 and $C_{RO} = 2.5 \cdot 10^6$ kr.

7. CONCLUSIONS

A model by which the integrated optimal design and optimal inspection times and qualities can be determined has been formulated. The total cost of construction, inspection and repair in the expected lifetime of the structure is minimized in such a way that the reliability at any time is acceptable. The design variables are the time intervals between inspections, the quality of the inspections and some structural design variables. The reliability measures are estimated using first-order reliability methods.

A numerical example, where an offshore steel jacket structure modelled by fatigue crack failure elements is considered, indicates that the model works. The example shows that the total cost is reduced significantly by including inspection in the optimization. Further, the example indicates that the time intervals between inspections should decrease with time and the inspection qualities should increase with time.

In order to model the reliability of a more complex structure a system consisting of series and parallel systems of failure elements has to be used, see Thoft-Christensen & Murotsu [8]. Using such models the effects of redundancy can be more realistically modelled.

As can be seen from the optimization problems and figure 2 the number of possible branches becomes very large when the number of inspections increases and/or when the number of failure elements increases. Therefore, it is very important to be able to identify the most significant branches. The possibility of using expert systems for this purpose should be investigated.

After an inspection where the actual damage (crack length) has been measured the reliability estimates can be updated. Using the updated reliability measures new optimal inspection time intervals and qualities can be determined by solving the optimization problems (updated maintenance strategy).

8. REFERENCES

[1] Frangopol, D. M.: *Sensitivity of Reliability-Based Optimum Design.* ASCE, Journal of Structural Engineering, Vol. 111, No. 8, 1985.

[2] Murotsu, Y., M. Kishi, H. Okada, M. Yonezawa & K. Taguchi: *Probabilistic Optimum Design of Frame Structure.* In P. Thoft-Christensen (ed.): System Modelling and Optimization, Springer-Verlag, Berlin, 1984, pp. 545-554.

[3] Thoft-Christensen, P. & J. D. Sørensen: *Reliability Analysis of Tubular Joints in Offshore Structures.* To appear in Reliability Engineering, 1987.

[4] Sørensen, J. D.: *Reliability-Based Optimization of Structural Elements.* Structural Reliability Theory, Paper no. 18, The University of Aalborg, 1986.

[5] Jubb, J. E. M.: *Strategies for Assessing Design and Inspection Requirements for Redundant Structures.* In Proc. Int. Symp., Nov. 1983, Washington (Faulkner et al. (eds.)): The Role of Design, Inspection and Redundancy in Marine Structural Reliability), 1984, pp. 118-137.

[6] Dunn, F. P.: *Offshore Platform Inspection.* In Proc. Int. Symp., Nov. 1983, Washington (Faulkner et al. (eds.)): The Role of Design, Inspection and Redundancy in Marine Structural Reliability), 1984, pp. 199-219.

[7] Thoft-Christensen, P. & J. D. Sørensen: *Optimal Strategy for Inspection and Repair of Structural Systems.* Civil Engineering Systems, 1987.

[8] Thoft-Christensen, P. & Y. Murotsu: *Application of Structural Systems Reliability Theory.* Springer-Verlag, 1986.

[9] Madsen, H. O., S. Krenk & N. C. Lind: *Methods of Structural Safety.* Prentice-Hall, 1986.

[10] Sørensen, J. D. & P. Thoft-Christensen: *Structural Optimization with Reliability Constraints.* Proc. 12th IFIP Conf. on »System Modelling and Optimization», Springer-Verlag, 1986, pp. 876-885.

[11] Schittkowski, K.: *NLPQL: A FORTRAN Subroutine Solving Constrained Non-Linear Programming Problems.* Annals of Operations Research, 1986.

[12] Han, S. - P.: *A Globally Convergent Method for Non-Linear Programming.* Journal of Optimization Theory and Applications. Vol. 22, 1977, pp. 297-309.

[13] Powell, M. J. D.: *A Fast Algorithm for Non-Linearly Constrained Optimization Calculations.* In Numerical Analysis (ed. G. A. Watson): Lecture Notes in Mathematics, Vol. 630, Springer-Verlag, 1978.

[14] Wilson, R. B.: *A Simplicial Algorithm for Concave Programming.* Ph.D. thesis, Harvard University, Boston, 1963.

[15] Karadeniz, H., S. van Manen & A. Vrouwenvelder: *Probabilistic Reliability Analysis for the Fatigue Limit State of Off-Shore Structures.* Bulletin Technique du Bureau Veritas, July 1984, pp. 203-219.

[16] Wirshing, P. H.: *Fatigue Reliability for Offshore Structures.* ASCE, Journal of Structural Engineering, Vol. 110, No. 10, 1984, pp. 2340-2356.

[17] Thoft-Christensen, P.: *Structural Reliability Theory.* Proc. ESRA Pre-Launching Meeting, Ispra, Italy, 1985, pp. 82-99.

[18] Almar-Næs, A. (ed.): *Fatigue Handbook,* Tapir, Trondheim, 1985.

ON SOME GRAPH-THEORETIC CONCEPTS AND TECHNIQUES APPLICABLE IN THE RELIABILITY ANALYSIS OF STRUCTURAL SYSTEMS

Adrian Vulpe* & Alexandru Cărăusu**
* Department of Engineering Mechanics
** Department of Mathematics
Polytechnic Institute of Iasi
R-6600 Iasi-6, Romania

1. Introduction

Several recent papers on structural reliability, mainly due to Danish, Japanese and German authors, have brought to evidence that any failure analysis of multicomponent systems (subjected to combined / multiple loads) should be grounded on a consistent set-theoretic representation of system failure event in terms of component/ elementary failures ; see, e.g., P.Thoft-Christensen [1,...,4], P.Bjerager & S.Gravesen [5], M.Hohenbichler, R.Rackwitz et al. [6,...,10], Y.Murotsu et al. [11,...,16]. The theory of graphs not merely offers more explicit and convenient ways to visualize the structure of system failure events, but it is also involved as a rich source of concepts and efficient methods to be applied in the reliability analysis of structural systems.

A couple of attempts to reveal how some concepts and techniques from the field of graph theory are or can be applied in the area of reliability analysis of structures are presented. Section 2 deals with the concept of 'fault-tree'. A formal definition of this notion is proposed, together with an algorithm for the automatic generation of system failure event starting from a given fault tree. The minimal cut set / tie set representations [9] of the system failure event are characterized in terms of some parameters involved in this definition. Section 3 takes into account a couple of techniques for the search of stochastically dominant failure modes due to Y.Murotsu et al. It is briefly discussed the possibility to represent such failure modes by means of directed graphs and directed (labeled) hypergraphs. The final section of our paper includes a proposal for a branch and bound technique as a basis for the reliability evaluation of a framed or truss structure, conceived at the mechanism level. That is, the basic (elementary) failures there implied are not the potential plastic hinges but the fundamental failure mechanisms earlier considered by P. Thoft-Christensen & J.D.Sørensen in the framework of the 'β -unzipping method'.

2. Fault Trees and Their Representations

As we have already mentioned in the Introduction, the failure probability of a structural system can be evaluated only after the system failure event F has been represented in an appropriate way. It is well-known the set-theoretic representation

$$F = \bigcup_i \bigcap_j F_{ij} \tag{2.1}$$

where F_{ij} are elementary or basic failure events [1], [9], [15], a.o. For example, F_{ij} may represent the failure of a potential yield hinge j developed within the failure mode i, in the case of a frame structure. If the system is a truss structure, F_{ij} may be an element (member) j which is involved in the failure mode i. This general set-theoretic model is also appropriate to characterize the system failure event at the mechanism level [1], [2], [3]. In this case F_{ij} will be the event that the fundamental mechanism j occurs in the combined mechanism i which is one of the combined mechanisms that can lead to overall system failure. When dealing with larger structures, it is not a very simple task to find a set-theoretic representation of F like (2.1). On another hand, it is possible that not all the terms in the intersection-union decomposition of F are stochastically relevant, in the sense that some of the cut terms $\bigcap_j F_{ij}$ may have relatively small probabilities to develop in the system. As outlined in [9], one expects that only relatively few cuts will dominate the union, so that a large number of cuts can be sorted out without loosing much accuracy. Furthermore, the primary set-decomposition of the system failure event F could be more complex than the one in equation (2.1), which is a cut-set representation. It may be a more general combination of intersections and unions of failure events.

That is why an efficient reliability analysis of a structural system requires a preliminary reduction of the set-theoretic representation of F. Such a reduction may be accomplished in two ways. First of them is to find a minimal cut-set / tie-set representation of F. The CUTALG program of [9] renders such a decomposition. The second one is to further reduce the cut-set representation sorting out the non-relevant terms, after probabilities have been associated with the elementary events F_{ij}.

Since we are mainly concerned with the graph-theoretic aspects of the reliability analysis of structures, let us first remark that the set-theoretic structure of the system failure becomes more explicit

when a kind of logical diagram is employed. It looks like an arborescence rooted at a node that corresponds to the system failure event. This one and all the other branching nodes correspond to the so-called gates. Any gate may be either an "OR"- gate, or an "AND"- gate. The hanging nodes (leaves) correspond to basic failure events. As an example, we are taking from [9] such a logical diagram. However, it is represented in Figure 1 in a simpler way, which is closer to our formal definition of a fault arborescence that follows. A box-node is a gate with gate number and gate type inside (+ for "OR", * for "AND" following the gate number). A circlet-node is a leaf with basic failure event label inside.

Figure 1 :

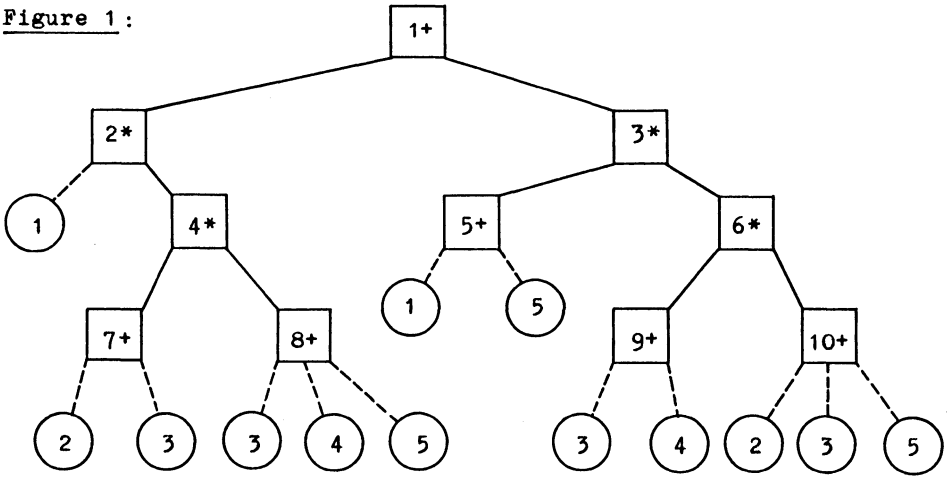

To state the formal definition of the fault arborescence, let k denote the level number, where k = 0, 1,..., K. The root is at the level k = 0. The lowest level of gate nodes corresponds to k = K.

Definition 2.1 A fault arborescence is a 5-tuple

$$T = (N, U, B, K, \lambda) \quad \text{where :} \tag{2.2}$$

N is the set of nodes, $N = N_G \cup N_L$ $(N_G \cap N_L = \emptyset)$; (2.3)

N_G is the set of gate nodes, $N_G = N_G^+ \cup N_G^*$; (2.4)
$(N_G^+ \cap N_G^* = \emptyset)$

$K + 1$ is the number of levels of gate nodes ;

N_G is level-partitioned by

$$N_G = \bigcup_{k=0}^{K} N_G^{(k)}, \qquad N_G^{(0)} = \{g_o^t\} \text{ with } t = +/* \tag{2.5}$$

U is the set of arcs, $U = U_n \cup U_t$ $(U_n \cap U_t = \emptyset)$ (2.6)

where

$$U_n \subset \bigcup_{k=1}^{K} \left[N_G^{(k-1)} \times N_G^{(k)} \right], \begin{cases} u = (g_1, g_2), \quad u' = (g_1', g_2') \\ \text{and} \quad u \neq u' \Longrightarrow g_2 \neq g_2' \end{cases} \tag{2.7}$$

is the set of nonterminal arcs, and

$$U_t \subset \bigcup_{k=0}^{K} \left[N_G^{(k)} \times N_L \right], \begin{cases} u = (g_1, l_1), \quad u' = (g_1', l_1') \\ \text{and} \quad u \neq u' \Longrightarrow l_1 \neq l_1' \end{cases} \tag{2.8}$$

is the set of terminal arcs. Note that a leaf may appear just under any of the levels of the arborescence, even under the root.

B is a (finite) set of basic failure events,

$$B = \{f_1, f_2, \ldots, f_m\} \quad ; \tag{2.9}$$

$$\lambda : N_L \longrightarrow B \quad \text{is the } \underline{\text{labeling function}}. \tag{2.10}$$

Although the definition is now complete, we have to define else another function — the "successor function" s — as it will be needed in formulating the algorithm which follows. If $u = (n_1, n_2) \in U$ is an arc of T, then $n_2 \in s(n_1)$. Thus, for any $n \in N_G$, $s(n)$ is the set of successors (or "sons", as they are sometimes termed in graph theory), immediately below n. It follows that s is a function of the form

$$s : \bigcup_{k=0}^{K} N_G^{(k)} \longrightarrow \left[\bigcup_{\ell=1}^{K} N_G^{(\ell)} \cup N_L \right]. \tag{2.11}$$

We have now the preliminaries necessary to state

<u>Proposition 2.1</u> Given a fault arborescence T (according to Definition 2.1) associated with a system failure event F, F can be represented in terms of set-theoretic operations (union and intersection) by means of the algorithm FSTR given below.

<u>Algorithm FSTR</u> (Failure Set-Theoretic Representation)

STEP 1 <u>L - clustering</u>

$$N_L = \bigcup_{k=1}^{K} N_L^{(k)} \quad \text{where} \tag{2.12}$$

$$N_L^{(k)} = \left\{ f \in N_L : \exists\, g \in N_G^{(k)} \text{ such that } f \in s(g) \right\} = \left\{ s(g) \cap N_L : g \in N_G^{(k)} \right\}. \tag{2.13}$$

Note that the +/* type of the gate is not specified in (2.13) since it is not essential at this step.

Set $p = 0$ (p is the cycle control variable).

N_L and $N_G^{(k)}$ are as in Definition 2.1 while s is defined by (2.11) with the foregoing specifications.

STEP 2 L-cluster Partitioning, Constructing Preterminal Events

(2.1) $p = p+1$ If $p \leq K$ GO TO (2.2) else GO TO Step 4

(2.2) $$I_p = \{ i \in \{1, \ldots, \text{card } N_G^{(K+1-p)}\} : \exists\ g_i \in N_G^{(K+1-p)} \text{ such that } s(g_i)(\ )N_L \neq \emptyset \}. \quad (2.14)$$

For every $i \in I_p$

$$N_{Li}^{(p)} = s(g_i) \cap N_L \ . \quad (2.15)$$

(2.3) For every $i \in I_p$

$$A_i^{(p)} = \begin{cases} \left(\bigcap_{f \in N_{Li}^{(p)}} \right) \{f\} & \text{if } g_i \in N_G^* \\ \left(\bigcup_{f \in N_{Li}^{(p)}} \right) \{f\} & \text{if } g_i \in N_G^+ \end{cases} \quad (2.16)$$

STEP 3 Constructing Compound Failure Events

(3.1) $$J_p = \{ j \in \{1, \ldots, \text{card } N_G^{(K+1-p)} : \exists\ g_j \in N_G^{(K+1-p)} \text{ such that } s(g_j) \cap N_G^{(K-p+2)} \underset{\text{not}}{=} m_j \neq \emptyset \} \quad (2.17)$$

(3.2) For every $j \in J_p$

$$A_j^{(p)} = \begin{cases} \left(\bigcap_{g_\ell \in m_j} \right) A_\ell^{(p-1)} & \text{if } g_\ell \in N_G^* \\ \left(\bigcup_{g_\ell \in m_j} \right) A_\ell^{(p-1)} & \text{if } g_\ell \in N_G^+ \end{cases} \quad (2.18)$$

(3.3) For every gate node $g \in N_G^{(K+1-p)}$ such that $\text{ind}(g) \in I_p \cap J_p$

$$A_{\text{ind}(g)}^{(p)} = \begin{cases} A_{\text{ind}(g)_i}^{(p)} \cap A_{\text{ind}(g)_j}^{(p)} & \text{if } g \in N_G^* \\ A_{\text{ind}(g)_i}^{(p)} \cup A_{\text{ind}(g)_j}^{(p)} & \text{if } g \in N_G^+ \end{cases} \quad (2.19)$$

the two terms of the intersection/union in the right hand side of the equation (2.19) have been constructed by (2.3) since the index of g, $\text{ind}(g) = \text{ind}(g)_i \in I_p$, and by (3.2), respectively, since the index $\text{ind}(g) \underset{\text{not}}{=} \text{ind}(g)_j \in J_p$.

At this stage, all the compound events corresponding to the gate nodes at the $(K+1-p)^{th}$ level of the arborescence are constructed.

GO TO Step 2 .

STEP 4 Terminating

This step is reached iff $p = K+1$ (see (2.1)) ; the system failure event has been constructed during the preceding cycle (when the value of p has been $p-1 = K$) :

$$F = A_o^{(p-1)} = A_o^{(K)} . \qquad (2.20)$$

$A_o^{(K)}$ is either a union or an intersection of events of the form $A^{(K-1)}$, depending on whether $g_o \in N_G^+$ or $g_o \in N_G^*$, respectively.

STOP

We do not give a formal proof of Proposition 2.1. Instead, we limit ourselves to a couple of remarks and comments.

1° At several substeps of the algorithm, the labeling function is involved but we have omitted it in order to avoid additional notational complexity. Thus, in equation (2.13) $f \in \lambda(N_L)$, $f \in \lambda(s(g))$ and λ should stand before the last set in this equation, since the set $N_L^{(k)}$ is essentially a set of basic failure events, hence a subset of B. Similarly, a λ should precede the set in the right hand side of equation (2.15).

2° The algorithm is convergent since the number K of the levels in arborescence T is finite and, for any k, card $N_G^{(K+1-p)}$ is also finite.

3° Step 1 of the algorithm could be omitted (except setting $p = 0$) as the sets $N_L^{(k)}$ are not involved at the subsequent steps. However, these subsets of "clusters" of leaves associated with each level of the abrorescence might be relevant, especially when the failure F of the system develops in time. In this case the control variable p becomes a discrete time parameter on the time axis directed from the bottom ($t = 0$) to the top ($t = K$) of the arborescence.

4° The algorithm FSTR is formally similar to some "bottom - up" parsing algorithms used in programming language compiling or in the theory of formal languages.

One more point we have to discuss would be its practical utility, the more so as the dimensions of the fault arborescence and the complexity of the set-theoretic representation of F (given by (2.20)) are expected to grow rapidly with the size of the structural system and with the number of its members / elementary failure events. The minimal cut-set / tie-set representations of F as considered in [9] are obviously more economic and have to be preferred. However, there may be two situations when a general representation like (2.20) could

be necessary or at least useful. The first of them has already been mentioned under 3° : the case when the failure of the system develops step by step, that is, sequentially along the time axis. The fault arborescence T and the representation (2.20) given by the algorithm reveal this temporal structure of F, while a cut-set representation – for instance – would destroy it. The second situation would be the one when the basic failure events are neither member failures nor (potential) plastic hinges developed within a failure mode, but fundamental failure mechanisms as considered by P.Thoft-Christensen in [1, ..., 4]. In this case the compound failure events $A_i^{(p)}$ given by (2.16) and $A_j^{(p)}$ given by (2.18) correspond to combined failure mechanisms and the dimension of the fault arborescence / the complexity of a representation like (2.20), respectively, will be much lower.

Coming back to the fault arborescences, it is clear that such an arborescence will look much simpler when the system failure event F is characterized by a minimal cut-set or by a minimal tie-set representation. To support this remark, we give in Figures 2 and 3 below the fault arborescences corresponding to the minimal cut-set representation and to the minimal tie-set representation of the failure event illustrated in Figure 1.

Figure 2 :

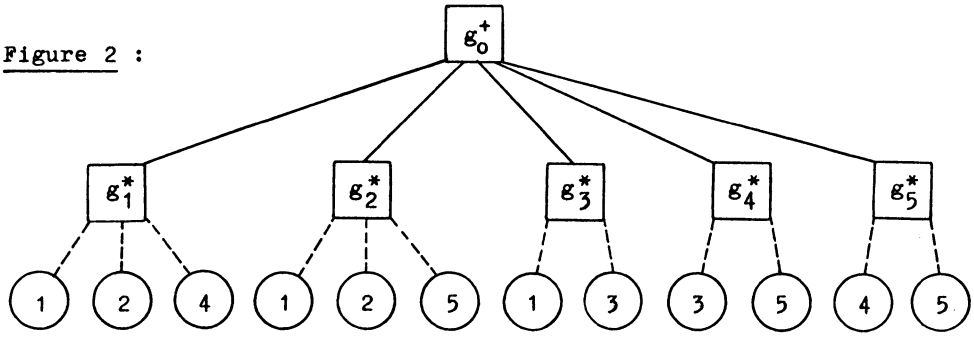

According to Definition 2.1, we find for this fault arborescence $K = 2$, $N_G^+ = N_G^{(0)} = \{g_0^+\}$, $N_G^* = N_G^{(1)} = \{g_1^*, g_2^*, g_3^*, g_4^*, g_5^*\}$. The minimal cut-set representation corresponding to this reduced arborescence (that we denote by T_{mc}) is

$$F = (f_1 \cap f_2 \cap f_4) \cup (f_1 \cap f_2 \cap f_3) \cup (f_3 \cap f_5) \cup (f_4 \cap f_5) \cup \cup (f_1 \cap f_3).$$

It can be found by the algorithm FSTR in a single application of Step 2 (with $p = 1$, $I_1 = \{1, 2, 3, 4, 5\}$, $J_1 = \emptyset$) and a single application of Step 3 (with $p = 2$, $I_2 = \emptyset$ and $J_2 = \{0\}$).

Figure 3 :

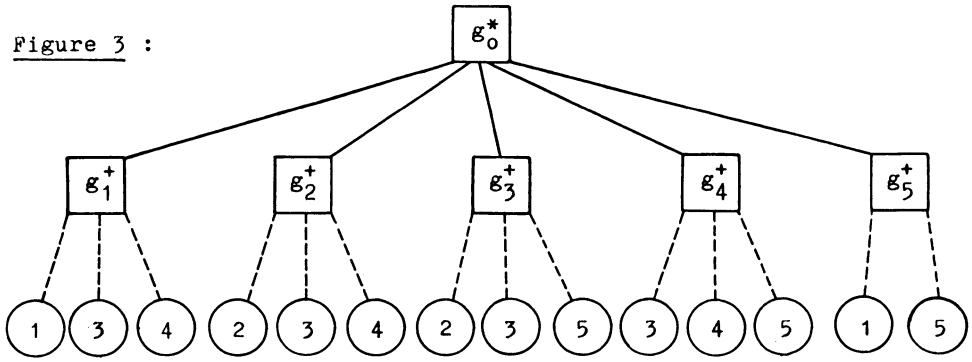

For this fault arborescence we have $K = 2$, $N_G^* = N_G^{(0)} = \{g_o^*\}$, $N_G^+ = N_G^{(1)} = \{g_1^+, g_2^+, g_3^+, g_4^+, g_5^+\}$. The corresponding minimal tie-set representation of F is obvious. Let us denote the fault arborescence generating such a tie-set decomposition by T_{mt}.

It can be readily verified that these two types of minimal fault arborescences are characterized by

Proposition 2.2 The fault arborescence T_{mc} generating the minimal cut-set representation satisfies the conditions :

$$K = 2, \quad N_G^+ = N_G^{(0)} = \{g_o^+\}, N_G^* = N_G^{(1)}, \quad U_n = \{g_o^+\} \times N_G^{(1)}$$
$$U_t \subset N_G^{(1)} \times N_L \, . \tag{2.21}$$

The fault arborescence T_{mt} generating the minimal tie-set representation of F satisfies the conditions :

$$K = 2, \quad N_G^* = N_G^{(0)} = \{g_o^*\}, N_G^+ = N_G^{(1)}, \quad U_n = \{g_o^*\} \times N_G^{(1)},$$
$$U_t \subset N_G^{(1)} \times N_L \, . \tag{2.22}$$

3. Searching Stochastically Dominant Failure Modes in Terms of Directed Graphs and Hypergraphs

In a series of recent papers, Y.Murotsu et al. have developed a family of efficient techniques for the selection of stochastically dominant failure modes and for the evaluation of structural reliability. They can be applied to (redundant) frame and truss structures under combined load effects and make use of stiffness matrices, of advanced methods for failure probability evaluation by use of lower and upper bounds on partial failure probabilities a.o. The kernel of the proposed methods for the automatic generation of failure modes

is a branch and bound algorithm which selects the stochastically dominant failure paths over the set of potential yield hinges [11,... ..., 16]. We shall take into account this technique, in more detail, in the next section. Here we are primarily interested in the graph-theoretic nature of these failure paths.

Plastic hinges are assumed to develop one by one up to some specific number p_k until a collapse mechanism is formed [13]. The sequence of those plastic hinges to form a collapse mechanism is symbolically denoted as

$$h_1 \longrightarrow h_2 \longrightarrow \ldots \longrightarrow h_p \longrightarrow \ldots \longrightarrow h_{p_k} \tag{3.1}$$

and it is referred to as a complete failure path. The partial sequence up to h_p, that is, $h_1 \longrightarrow h_2 \longrightarrow \ldots \longrightarrow h_p$ is said to be a partial failure path. The probability associated with a partial failure path is defined by

$$P_{fp(q)}^{(p)} = P\Big[\bigcap_{i=1}^{p} F_{h_i(q)}^{(i)}\Big] \tag{3.2}$$

where $F_{h_i(q)}^{(i)}$ is the failure event that plastic hinge h_i develops at the i-th order of sequence. Superscript p denotes the length of the failure path and q is used to denote a particular failure path. The combinatorial properties of identifying dominant failure paths are extensively investigated in [13]. The more difficult problem of evaluating the system failure probability on the basis of probabilities as those appearing in (3.2) is considered in all of the papers [11,..., 16], and various solutions are proposed, depending upon the type of the structure, the loading conditions and other assumptions.

From the graph-theoretic point of view, a failure path of the form (3.1) is effectively a path in a directed graph

$$G = (H, U) \quad \text{or} \quad G = (H, s) \tag{3.3}$$

where the finite set H of vertices (or nodes) corresponds, in this case, to the set of potential yield (plastic) hinges ; $\text{card}H = n$ is the order of G. U is the set of arcs. Alternatively, G can be defined by specifying the set H and the successor function s which has also been considered in the preceding section (see eq. (2.11)) . For a general graph $G = (H, s)$, the function s is defined on H and, for any $h \in H$, $s(h)$ is in 2^H (the set of subsets of H). A practical difficulty arises here in what concerns the possibility of actually constructing the failure graph G. Theoretically, the set U of the arcs is the set of all pairs (h_p, h_{p+1}) such that there

exists a failure path of the form (3.1) including $h_p \longrightarrow h_{p+1}$. But this cannot be accepted as a formal definition of U as it would be grounded on a rather heuristic basis. On the other hand, some restrictions should be imposed on actual failure paths in the failure graph G. Firstly, no failure path may be a circuit. Secondly, a node occurring in a particular failure path may not occur once again in the same path ; in other words, every failure path should be elementary.

The use of the successor function s in constructing a failure graph G = (H, s) could appear as more promising. Indeed, the failure path is constructed step by step. Once reached the node h_i in a partial failure path, the choice for the next node h_{i+1} to be selected is not free. It could be limited by imposing certain constraints on the successor function s. Thus, if $\mu_q^{(p)}$ is a (partial) failure path and if we denote by supp $\mu_q^{(p)}$ the set of distinct nodes occurring along this path of length p, then

$$h_i \in \text{supp } \mu_q^{(p)} \Longrightarrow h_{i+1} \in s(h_i) \setminus \text{supp } \mu_q^{(i)} \quad . \qquad (3.4)$$

But a constraint like (3.4) would in fact turn the successor function s into a path-dependent function : it is possible that a certain node h may not succeed h_i on the path $\mu_q^{(p)}$, but it may succeed h_i on another path $\mu_{q'}^{(p')}$ with $q \neq q'$.

Furthermore, the same nodes (plastic hinges) may occur on different failure paths, in different orders, of course. Theoretically, there may exist p! distinct failure paths over the same subset of p nodes. Even when the selection of the relevant failure paths is limited by means of probabilistic criteria (based on the use of probabilities of the form (3.2)), the number of possibilities can remain prohibitive.

Y.Murotsu et al. consider in [25] (Fig.5, page 87) a "search tree for evaluating upper and lower bounds of structural failure probability", involved in the reliability analysis of redundant truss structures. It looks like a forest of arborescences, and a probability is associated with every complete failure path in any of the arborescences. A partial failure graph could be constructed starting from a search tree of this kind, but it would be no more useful for distinguishing between different failure paths. Arguments of this nature as well as the difficulties outlined in the above discussion have led us to the idea that a formal model as a background for the reliability analysis of structural systems could be hardly based on the use of directed graphs.

Instead, we are going to propose another mathematical structure as a more suitable concept to be used for modelling the (dominant) failure modes of structural systems. It comes to directed (labeled) hypergraphs. Since this is a less usual mathematical structure, we recall its definition according to [24].

A directed hypergraph is a pair $DH = (N, A)$ in which N is a set (of nodes), and A is a set (of hyperarcs) defined by

$$A \subseteq \text{fam } TS(N) \quad \text{where} \quad \text{fam } M \text{ is the set of families over the set } M \text{ ;} \tag{3.5}$$

a family over M is a function $F : M \longrightarrow \mathbb{N}$.
$TS(N)$ is the set of tuples over N, hence $t \in TS(N)$ if $t = (n_1, n_2, \ldots, n_m)$ for some $m \geq 1$. A family can also be represented as a tuple, but for $F(t) = k$, F will include k successive occurrences of t. For our modelling purposes, it will suffice to restrict the range of families to the set $\{0, 1\}$ because we shall not accept repeated tuples in a hyperarc. Thus, a hyperarc will consist in a single tuple (ordered subset) of length $|t| \in \{2, \ldots, n\}$ where $n = \text{card } N$ (finite). Thus, the loops will be excluded. If $F(t) = 0$, then the tuple t won't be a hyperarc of DH.

A directed labeled hypergraph is a triple $DLH = (N, L, A)$ where N is also a set of nodes, L is a set of labels, and A is defined by

$$A \subseteq \text{fam } (TS(N) \times L) \ . \tag{3.6}$$

Here again we shall observe the above mentioned restrictions on the families. Therefore, a labeled (directed) hyperarc of DLH will be of the form

$$(t, \ell) = ((n_1, n_2, \ldots, n_k), \ell) \quad \text{with} \quad n_i \in N, \quad \ell \in L \ . \tag{3.7}$$

An arc of the form (3.7) can be graphically represented as follows :

Figure 4 :

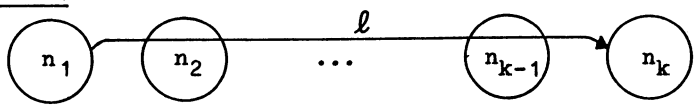

There exist equivalent representations for the directed labeled hypergraphs, namely CBT (class-bag-tuple) and RLS (relation list set) representations ; see [24] for details.

Let us now consider a structural system S with the (finite) set B of "basic" (elementary/ fundamental) potential failure events. If any possible failure mode (mechanism) develops sequentially over B, then the system failure event F can be modeled in terms of the di-

rected hypergraphs as follows.

The system failure event F can be represented by a directed hypergraph $DH_F = (B, A)$ in which B is the set of basic events and A is a set of directed hyperarcs, each $a \in A$ being a tuple whose length ranges between 2 and $m = \text{card } B$.

If probabilities can be associated with every basic failure event f and if there exists a procedure $\mathcal{P}$ to assign a probability $P(a)$ with every hyperarc $a \in A$, then the failure event F will be represented by a labeled directed hypergraph

$$DLH_F = (B, P(A), A) \tag{3.8}$$

where B and A are defined as above, while $P(A)$ is the set of labels. Therefore every hyperarc a (corresponding to a sequentially compound failure event) will be "labeled" or – in a more suitable language – weighted with its probability $P(a)$.

Finally, if another procedure $\mathcal{P}^*$ exists to select the stochastically dominant (or significant) failure modes among all the possible modes, then the set of selected failure modes will be modeled by a partial directed labeled / weighted graph of DLH_F, namely

$$DLH_F^* = (B, P(A^*), A^*) \quad \text{with} \quad A^* \subset A . \tag{3.9}$$

Then, the set $P(A^*)$ could be employed to evaluate the system failure probability $P_f = P(F)$ by means of appropriate techniques.

We suppose this model is general enough to encompass a wide range of methods for searching stochastically dominant failure modes and for evaluating the system failure probability.

4. A Branch and Bound Technique for Estimating System Reliability at the Mechanism Level

In a series of reports including [1,...,4], it is introduced the 'β - unzipping method' as an efficient and simple procedure to estimate the reliability of structural systems under specific assumptions. It can be applied either at the level of (single, pairs, triples,... of) failure elements, or at the mechanism level. The latter approach proved to be computationally more efficient.

On another hand, Y.Murotsu et al. have elaborated another method for evaluating the reliability of structural systems, based upon the automatic generation of stochastically dominant failure modes via a B & B technique [11,..., 16], [25].

Both the procedures share a more or less common mechanical and

probabilistic background. Differences emerge in what concerns the way to select stochastically dominant / significant failure modes. In this section we present an attempt to work out a B & B technique, similar to the one proposed by Y.Murotsu, with the difference that the failure modes are defined, like in [1,..., 4], as combined failure mechanisms over the set of fundamental failure mechanisms.

Let us consider a structural system, e.g. a framed one, with n potential failure elements. Let H be the set of these elements (for instance, potential yield hinges). Let F denote the set of fundamental failure mechanisms with card $F = m$. It is well known from the theory of plasticity that $m = n - r$, where r is the degree of redundancy. Let

$$F = \{f_1, f_2, \ldots, f_m\} \quad . \tag{4.1}$$

Denote by $L = \{P_1, P_2, \ldots, P_\ell\}$ the set of external applied loads. Then each fundamental mechanism f_i is assigned a linear safety margin [3]

$$M_i = \sum_{j=1}^{n} |a_{ij}| R_j - \sum_{k=1}^{\ell} b_{ik} P_k \tag{4.2}$$

where a_{ij} and b_{ik} are the influence coefficients, R_j is the yield strength of failure element j and P_k is load number k. The combined mechanism $f_i \pm f_j$ is the one with the safety margin

$$M_{i\pm j} = \sum_{r=1}^{n} |a_{ir} \pm a_{jr}| R_r - \sum_{k=1} (b_{ik} \pm b_{jk}) P_k \quad . \tag{4.3}$$

Equation (4.3) is recursively extended to combinations between an already combined mechanism and a (not therein involved) new fundamental mechanism. More precisely, let $m^{(p-1)}$ denote a combined failure mechanism, that is,

$$m^{(p-1)} = f_{i_1} \pm f_{i_2} \pm \ldots \pm f_{i_{p-1}} \quad . \tag{4.4}$$

Then, starting from $m^{(p-1)}$, a number of $m - (p-1)$ of new combined mechanisms, consisting of p fundamental mechanisms, can be obtained from $m^{(p-1)}$:

$$m_q^{(p)} = m^{(p-1)} \pm f_{i_p} = f_{i_1} \pm f_{i_2} \pm \ldots \pm f_{i_{p-1}} \pm f_{i_p} \tag{4.5}$$

where $i_p \in \{1, 2, \ldots, m\} \setminus \{i_1, i_2, \ldots, i_{p-1}\}$ and $q \in \{1, \ldots, Q_p\}$ with $Q_p = m - p + 1$. If $M^{(p-1)}$ denotes the safety margin of the combined mechanism $m^{(p-1)}$ in (4.4) with the influence coefficients $\bar{a}_r$ and $\bar{b}_k$, then the safety margin associated with the mechanism

$m_q^{(p)}$ of equation (4.5) will be

$$M_q^{(p)} = \sum_{r=1}^{n} |\bar{a}_r \pm a_{i_p r}| R_r - \sum_{k=1}^{\ell} (\bar{b}_k \pm b_{i_p k}) P_k \,. \tag{4.6}$$

The subscript q in equations (4.5) and (4.6) corresponds, in fact, to i_p ; that is, $i_p \in \{1, 2, \ldots, m\} \setminus \{i_1, i_2, \ldots, i_{p-1}\}$ $\Longleftrightarrow$ $q \in \{1, \ldots, Q_p\}$. The reliability index function

$$\beta : \bigcup_p \bigcup_q \{m_q^{(p)}\} \longrightarrow \mathbb{R} \tag{4.7}$$

can be calculated for every combined mechanism $m_q^{(p)}$ as in [3].

For increasing p, the set of possible combined failure mechanisms grows rapidly, even if p is bounded by m ($p \leq m$). Just this is the reason for applying the β - unzipping method in [1, ..., 4] in order to select only the stochastically significant failure mechanisms.

As a preliminary to our proposal of a B & B technique at the mechanism level, let us first remark that the probabilities associated with the failure mechanisms could be employed instead of the indices. A way to estimate these probabilities can be the one proposed in [8] by M.Hohenbichler. Another one could be based on the "exact" equation

$$P_{fm(q)}^{(p)} \underset{\text{not}}{=} P(m_q^{(p)}) \underset{\text{def}}{=} P\Big[\bigcap_{j=1}^{p} (M_{i_j} \leq 0) \Big] \tag{4.8}$$

To formulate a B & B algorithm to select stochastically dominant failure mechanisms as a basis for estimating the system failure probability, a couple of preliminary notations are necessary :

$\mathcal{M}_p$ = the set of (combined) failure mechanisms to be selected for branching at the p-th stage / cycle of the algorithm ;

$\mathcal{M}_1 = F$ = the set of fundamental failure mechanisms (see (4.1));

$\mathcal{D}_p$ = the set of discarded failure mechanisms at stage p ;

$\mathcal{M}_p^*$ = the set of selected failure mechanisms at stage p ;

supp $m_q^{(p)} = \{f_{i_1}, f_{i_2}, \ldots, f_{i_p}\}$ for $m_q^{(p)}$ as in equation (4.5).

P_{fmM} = the current value of the maximum probability of system failure by combined mechanisms ;

p = the stage (cycle) control variable, equal to the number of fundamental failure mechanisms involved in the combined mechanisms of $\mathcal{M}_p$.

A Branch and Bound Algorithm at the Mechanism Level

Step 1 Initializing

$\mathcal{M}_o = \emptyset$, $\mathcal{M}_o^* = \emptyset$, $\mathcal{D}_o = \emptyset$, $P_{fmM} = 0$, $p = 0$.

Step 2 Partitioning

(2.1) $p = p + 1$. If $p = 1$ set $\mathcal{M}_p = F$ and GO TO (2.3); else GO TO (2.2)

(2.2) If $p < m$ set $\mathcal{M}_p = \{m_*^{(p-1)} \pm f_{i_p} : f_{i_p} \in F \setminus \text{supp } m_*^{(p-1)}\}$, else GO TO (2.3)

(2.3) For every $m_q^{(p)} \in \mathcal{M}_p$, evaluate

$$P(m_q^{(p)}) = P\left[M_q^{(p)} \leqq 0 \right] \tag{4.9}$$

using equations (4.6) and (4.8).

Step 3 Branching

(3.1) Select

$$m_{q_o}^{(p)} : P_{fm(q_o)}^{(p)} = \max \{ P_{fm(q)}^{(p)} : m_q \in \mathcal{M}_p \} ; \tag{4.10}$$

denote $m_*^{(p)} = m_{q_o}^{(p)}$.

(3.2) Denote $P_{fmM}^{(p)} = P_{fm(q_o)}^{(p)}$ and GO TO Step 4.

Step 4 Bounding

(4.1) Update the maximum P_{fmM} of the probabilities of combined failure mechanisms as follows :

If $P_{fmM}^{(p)} > P_{fmM}$ then $P_{fmM} = P_{fmM}^{(p)}$ and GO TO (4.2); else P_{fmM} remains unchanged and GO TO (4.3) .

(4.2) $\mathcal{M}_p^* = \mathcal{M}_{p-1}^* \cup \{m_*^{(p)}\}$;

(4.3) $\mathcal{D}_p = \mathcal{D}_{p-1} \cup \{ m_q^{(p)} \in \mathcal{M}_p : P_{fm(q)} < 10^{-\gamma} P_{fmM} \}$ (4.11)

where γ is a bounding constant.

(4.4) $\mathcal{M}_p = \mathcal{M}_p \setminus (\mathcal{M}_p^* \cup \mathcal{D}_p)$. GO TO Step 5. (4.12)

Step 5 Terminating criterion

If $\mathcal{M}_p = \emptyset$ the search is completed ; STOP if $p = m$, else GO TO (2.1)

If $\mathcal{M}_p \neq \emptyset$ GO TO (3.1) .

Once the algorithm is terminating, it renders the set $\mathcal{M}_m^*$ as the set of stochastically dominant (most probable) combined failure mechanisms. On this basis, the system failure probability P_f could be estimated by using procedures similar to those of [11,..., 16] .

The algorithm is obviously more or less similar to the ones elaborated by Y.Murotsu et al. However, significant differences appear in what concerns, for instance, Step 3 (Branching) : when the failure events are already mechanisms, we have no more to check whether a collapse mechanism has been formed (Step 3.3 in [16]). Then, condition $p = m$ in our Terminating criterion must be imposed, while a similar condition is not explicitly stated in the above mentioned references. If $p < m$, the algorithm should go on with searching stochastically dominant failure mechanisms, even when $\mathcal{M}_p = \emptyset$. However, it is expected that the probabilities $P_{fmM}^{(p)}$ will decrease with increasing p, and therefore the size of the sets $\mathcal{D}_p$ will increase.

Although we have not yet compared our algorithm with the ones due to Y.Murotsu from the point of view of computational efficiency, it is likely to be less time-consuming since the number of possible combinations of fundamental mechanisms is limited.

5. Final Remarks

The extensive research work in the area of structural reliability analysis during the last decade has included a series of methods and models which involve graph-theoretic concepts or graph-based techniques, even though the mechanical and probabilistic backgrounds have naturally been dominating.

Our tentative consists in investigating some more ways to make use of graph-theoretic concepts and techniques in this field. Thus, a fault arborescence was defined in Section 2, and an algorithm was formulated to represent the system failure event in terms of basic failure events by set-theoretic operations. A general model for systems failing sequentially was proposed in Section 3, employing the concept of directed (labeled) hypergraph. A branch & bound technique for searching stochastically dominant failure mechanisms as combinations of fundamental failure mechanisms was constructed in Section 3 ; in a certain sense, it brings together elements from the models due to P.Thoft - Christensen and to Y.Murotsu.

The possible utility and specific adequacy of the models we proposed have also been discussed. Thus, the model of Section 3 would be applicable to time-dependent failing.

6. References

1. Thoft-Christensen, P. & Sørensen, J.D.: Reliability Analysis of Elasto-Plastic Structures. Structural Reliability Theory, Paper NO.2, December 1983, Instituttet for Bygningsteknik, Aalborg, IFB/A 8303.
2. Thoft-Christensen, P.: Reliability Analysis of Structural Systems by the - unzipping Method. Structural Reliability Theory, Paper No.3, March 1984, Instituttet for Bygningsteknik, Aalborg, R8401.
3. Thoft-Christensen, P.: Reliability of Structural Systems. Structural Reliability Theory, Paper No.5, June 1984, Instituttet for Bygningsteknik, Aalborg, R8403.
4. Thoft-Christensen, P. & Sørensen, J.D.: Optimization and Reliability of Structural Systems. Structural Reliability Theory, Paper No.6, July 1984, Instituttet for Bygningsteknik, Aalborg, R8404.
5. Bjerager, P. & Gravesen, S.: Lower Bound Reliability Analysis of Plastic Structures. Probabilistic Methods in the Mechanics of Solids and Structures (Proc. IUTAM Symposium, Stockholm, June 1984) Springer-Verlag 1985, 281-290.
6. Hohenbichler, M.: Mathematische Grundlagen der Zuverlässigkeitsmethode erster Ordnung, und einige Erweiterungen. SFB 96, Berichte zur Zuverlässigkeitstheorie der Bauwerke, Heft 72, München 1984.
7. Fiessler, B.: Das Programmsystem FORM zur Berechnung der Versagenwahrscheinlichkeit von Komponenten von Tragsystemen. SFB 96, Berichte zur Zuverlässigkeitstheorie der Bauwerke, Heft 43, München 1979.
8. Hohenbichler, M.: An Asymptotic Formula for the Probability of Intersections. SFB 96, Berichte zur Zuverlässigkeitstheorie der Bauwerke, Heft 69, München 1984.
9. L.K.I.- Techn.Univ.München : User's Manual for Structural Reliability Programs CUTALG - FORM - SORM - SYSREL. SFB 96, Berichte zur Zuverlässigkeitstheorie der Bauwerke, Heft 74, München 1985.
10. Hohenbichler, M. & Rackwitz, R.: First-Order Concepts in System Reliability. Structural Safety, Vol.1, No.3, April 1983, 177-188.
11. Murotsu, Y.: Reliability Analysis of Frame Structure through Automatic Generation of Failure Modes. Reliability Theory and Its Application in Structural and Soil Mechanics, P.Thoft-Christensen (ed.), Martinus Nijhof Publishers, 1983, 525-540.
12. Murotsu, Y., Okada, H., Yonezawa, M. & Kishi, M.: Identification of Stochastically Dominant Failure Modes in Frame Structure.Proc. Fourth International Conference on Applications of Statistics & Probability in Soil and Structural Engineering. Università di Firenze, Italy 1983, Pitagora Editrice, 1325-1338.
13. Murotsu, Y.: Combinatorial Properties of Identifying Dominant Failure Paths in Structural Systems. Bulletin University of Osaka Prefecture, Vol.32, No.2, 1983, 107-116.
14. Murotsu, Y., Okada, H. & Matsuzaki, S.: Reliability Analysis of Frame Structure under Combined Load Effects. Structural Safety & Reliability, Vol.1, ICOSSAR '85 (Fourth International Conference on Structural Safety and Reliability), 117-128.
15. Murotsu, Y.: Development in Structural Systems Reliability. Nuclear Engineering and Design 94 (1986), North-Holland Publ. Co., Amsterdam, 101-114.

16. Murotsu, Y., Matsuzaki, S. & Okada, H.: Automatic Generation of Stochastically Dominant Failure Modes for Large-scale Structures. JSME International Journal, Vol.30, No.260, 1987, 234-241.

17. Bartholomew, R.J. & Qualls, C.R.: A System Approach to Probabilistic Modelling of Fault Trees. Trans. Eighth International Conference on Structural Mechanics in Reactor Technology, Brussels, August 1985, Vol.M 2, 361-368.

18. Frutuoso e Melo, P.F., Lima, J.E. & Oliveira, L.F.: Some Insights on the Event Tree Methodology Used for the Ongoing Angra-1 PRA. Trans. Eighth International Conference on Structural Mechanics in Reactor Technology, Brussels, August 1985, Vol.M 2, 431-436.

19. Şesan, A. & Vulpe A.: Using the Theory of Graphs in the Formulation of Active Moment Method in terms of Matrices (in Romanian). Bulletin of the Polytechnic Institute of Iasi, Tome XIV(XVIII), Fasc.1-2, 1968, 515-522.

20. Negoiţă, A. & Vulpe, A.: On the Probability of Plastic Collapse in Safety Analysis of Frame Structures. Proc. Symposium on Plastic Analysis of Structures, Iasi, September 1972, 76-84.

21. Beineke, L.W. & Wilson, R.J. (ed.by): Selected Topics in Graph Theory. Academic Press, London - New York, 1978.

22. Minoux, M. & Bartnik, G.: Graphes, Algorithmes logiciels. Dunod, Paris 1986.

23. Gibbons, A.: Algorithmic Graph Theory. Cambridge University Press, Cambridge - London - New York, 1985.

24. Boley, H.: Directed Recursive Labelnode Hypergraphs and Their Use As Representation for Knowledge. Free session contribution to the Fourth International Joint Conference on Artificial Intelligence, September 1975, Tblisi.

25. Murotsu, Y., Okada, H., Niwa, K. & Miwa, S.: Reliability Analysis of Redundant Truss Structures. Reliability, Stress Analysis and Failure Prevention Methods in Mechanical Design (W.D.Milestone,ed.) ASME, 1980, 81-93.

Acknowledgements

The authors wish to express their sincere gratitude to Professor P.Thoft-Christensen of the University of Aalborg and to Professor Y. Murotsu of the University of Osaka Prefecture for sending them several papers which have been of essential importance in elaborating this communication.

RELIABILITY OF IDEAL PLASTIC SYSTEMS BASED ON LOWER-BOUND THEOREM

Henrik O. Madsen
A.S Veritas Research
P.O.Box 300, N-1322 HOVIK, Norway

Peter Bjerager
Technical University of Denmark
Building 118, DK-2800 LYNGBY, Denmark

ABSTRACT

Recent developments in system reliability analysis of structures based on ideal plastic analysis methods are presented. The lower-bound (static) theorem of ideal plasticity theory is applied in a probabilistic setting and upper and lower bounds on the system reliability are established. A comparison with the reliability for first member yielding provides a quantitative measurement of the system redundancy. The analysis is performed for static overloading with a probabilistic load model. Two example offshore jacket structures are used to demonstrate the analysis procedure.

1. INTRODUCTION

Present design practice focuses attention on assuring sufficient reliability of the structural elements individually rather than of the structural system as a whole. System effects due to redundancy and many failure modes can, however, be significant and should preferably be taken into account in a rational design procedure. This requires the availability of operational methods for assessing the reliability of a structural system.

Different approaches can be followed for reliability analysis of structural systems with system failure involving simultaneous failure of several elements. One approach is to formulate an ideal plastic model of the structure and define failure as plastic collapse (formation of a mechanism). Another possibility is to adopt a model in which the structural elements exhibit some deformation-load effect behavior and define failure of the structure as the event of a singular stiffness matrix or excessive deformations. A review of reliability models for structural systems is given in [1,2].

The ideal plastic model approach has been used in numerous works, see e.g. [3-8]. This is mainly because such systems are conveniently analyzed with respect to plastic collapse applying the lower and upper bound theorems of plasticity theory. In most reported work the analyses have been based on the upper bound theorem according to which an upper bound on the reliability can be evaluated on basis of a set of plastic mechanisms. If the set of mechanisms is complete, the upper bound coincides with the exact reliability with respect to plastic collapse. Typically, however, it is not practicable to take into account the complete set of mechanisms. In fact, even for simple structures the number of mechanisms can be infinite and the evaluation of the reliability is non-trivial. Methods for identifying a set of significant (most likely) mechanisms can be used for some types of structures. Based on these mechanisms a close upper bound on the reliability may be obtained. The formulation of the equation of virtual work for a given plastic mechanism can be rather involved, notably in the case of yield surfaces of random shape and when the geometry of the structure is random.

Recent developments for evaluating the reliability with respect to plastic collapse on basis of the lower bound theorem are presented. Both a lower and an upper bound on the reliability are obtained. The reliability model is formulated for a spatial truss structure, but the generalization to a spatial frame structure taking into account load-effect interaction in potential points of yielding is straight-forward, [9,10]. The analysis procedure is demonstrated on two example structures. Other example structures of up to 270 members have also been successfully analyzed.

2. STRUCTURAL MODEL

An n times redundant (statically indeterminate), plane or spatial truss structure of m bars is considered. The external loading is given in terms of a finite set of nodal forces $Q = (Q_1, Q_2, \cdots, Q_l)$ and the normal forces in the bars are denoted by $N = (N_1, N_2, \cdots, N_m)$. The bars are assumed to be of ideal plastic behavior. The yield load in tension is N_i^+ and the yield load in compression N_i^-, $i = 1,2,...,m$. The considered limit state of the structure is plastic collapse, i.e. formation of a mechanism.

3. LOWER BOUND THEOREM FORMULATION OF THE RELIABILITY

The lower bound theorem of limit analysis is valid for ideal plastic structures, i.e. the yield surface does not change during deformation, and the yield surface is convex and the plastic strain rates are derivable from the yield function through the flow rule (normality condition) under the assumption that changes in geometry of the structure at plastic collapse are insignificant. The lower bound theorem states that the structure is able to carry the external load if and only if there exists a statically admissible set of internal forces such that these nowhere violate the yield condition, see e.g. [11].

Focusing on equilibrium states of the structure it is convenient to apply a force method formulation. The complete set of statical conditions are expressed in terms of the normal forces N and the external nodal forces Q as

$$AN = Q \tag{1}$$

A is the equilibrium matrix given in terms of the geometry of the structure. By Gauss-Jordan elimination or an equivalent procedure within the force method, [12,13], the solutions to (1) can be expressed as

$$N = B_Q Q + B_Z z \tag{2}$$

where $z = (z_1, z_2, \cdots, z_n)$ is called the vector of redundants. If the elimination procedure is carried out such that each z-component corresponds to a normal force in a bar of the truss structure, (2) expresses a choice of a statically determinate primary system.

The state of the i th bar is described by two functions

$$\begin{aligned} g_{2i-1}(N_i^-, N_i) &= N_i^- + N_i \\ g_{2i}(N_i^+, N_i) &= N_i^+ - N_i \end{aligned} \tag{3}$$

corresponding to yielding of the bar in compression and tension respectively. If both functions are positive the i th bar behaves elastically. The behavior of the truss structure is thus described by $2m$ functions.

The physical basic variables in the formulation of the reliability comprise the nodal forces Q, the yield forces (N^-, N^+) and a number of geometrical variables. However, throughout this paper the geometry of the structure is assumed deterministic. If this is not the case, the equilibrium matrix in (1) is random and the analysis becomes significantly more complicated. The variables Q, N^-, N^+ are assumed to be random with continuous joint distribution. A transformation T exists such that

$$U = T(Q,N^-,N^+) \tag{4}$$

is a normalized Gaussian vector with independent components, see [14]. Let the dimension of this vector be q. The behavior of the truss structure is now described by $2m$ functions g_i in the q-dimensional u-space defined such that

$$\min_{i=1}^{2m} [g_i(u;z)] \begin{cases} > 0 & \textit{elastic behavior} \\ \leqslant 0 & \textit{yielding in some point } (s) \end{cases} \tag{5}$$

The reliability $1 - p_f$ with respect to plastic collapse can be expressed as

$$1 - p_f = P\{g(U) > 0\} \tag{6}$$

where

$$g(u) = \max_{z \in R^n} [\min_{i=1}^{2m} [g_i(u;z)]] \tag{7}$$

The max-operation expresses that an admissible equilibrium distribution of internal forces is sought for each set of values of the basic variables. The system representation by (7) may be referred to as a parallel system with an infinity of series subsystems.

For some of the considerations in the following it is necessary to recast the expression for the reliability. Noting that U can be expressed as $U = RA$ $(R \geqslant 0)$ where R^2 is a chi-square distributed random variable with q degrees of freedom and A is a q-dimensional vector uniformly distributed on the unit sphere Ω_q, the reliability can be given in the form

$$\begin{aligned} 1 - p_f &= \int_{\Omega_q} P\{g(RA) > 0 \mid A = a\} f_A(a) da \\ &= \int_{\Omega_q} P\{g(Ra) > 0\} f_A(a) da \end{aligned} \tag{8}$$

where $f_A(a) = \textit{constant}$ is the probability density on the unit sphere. If the safe set in u-space is star-shaped (e.g. convex) with respect to the origin, $P\{g(Ra) > 0\}$ is given in terms of the chi-square distribution function χ_q^2 as

$$P\{g(Ra) > 0\} = \chi_q^2(r(a)^2) \tag{9}$$

where $r(a)$ is the distance from the origin in u-space to the limit state surface in the direction defined by a. For fixed a, $r = r(a)$ is part of the solution to the optimization problem:

Determine $r \geqslant 0$ and $z \in R^n$ such that r is maximized subject to $\min_{i=1}^{2m} [g_i(ra;z)] > 0$.

If the transformation T is linear (normally distributed physical basic variables), the optimization problem reduces to a linear programming problem.

The formulation in this section is easily extended to cover load effect interaction in the yield function. Eq.(3) is then a function (linear or non-linear) of load effects and (7) still holds. If the yield function is piecewise linear and the transformation T is linear, the optimization problem remains a linear programming problem.

4. EVALUATION OF THE RELIABILITY

The evaluation of the reliability given by (6) or (8) is non-trivial for problems of high dimensionality. The following outlines how lower and upper bounds on the reliability can be calculated under certain assumptions. First and second order reliability methods FORM/SORM as well as Monte Carlo simulation methods are applied in the calculation. Besides the reliability measures, a FORM/SORM analysis directly provides parametric sensitivity measures for the reliability with respect to deterministic and distributional parameters, see [14]. These measures can be used in a search for an optimal design.

4.1 Lower Bound on the Reliability

If the considered equilibrium distributions of internal forces is restricted by substituting z in (7) by a finite number of vectors $z_1, z_2, \cdots, z_p$ the right side of (6) provides a lower bound on the reliability. The simplest case is to consider only one z-vector, z_0. The corresponding lower bound can be optimized by solving the non-linear optimization problem:

Determine $z_0 \in R^n$ such that the probability $P\{\min_{i=1}^{2m}[g_i(U;z_0)] > 0\}$ is maximized.

The amount of calculation can be reduced if the lower bound is sought maximized by solving the sub-optimization problem:

Determine $z_0 \in R^n$ such that $\min_{i=1}^{2m}[P\{g_i(U;z_0 > 0\}]$ is maximized.

If the transformation T is linear, this problem is a linear programming problem and a solution can be found efficiently. However, the lower bound on the reliability obtained in this way generally turns out to be considerably smaller than the exact reliability. Moreover, the result depends on the choice of the redundants, i.e. on the statically determinate primary system (B_Q and B_Z in (2)).

In [15,16] methods for improving the lower bound by considering more than one set of values for the redundant forces or by considering more than one choice of the statically determinate primary system are given. The improvements of the lower bound obtained by these approaches can be significant. However, no general and efficient procedure to assure this has been reported.

Here, improvements of the lower bound on the reliability by taking the set of redundants z as a random vector Z are considered. For any outcome u of U a value of z can be determined as the solution to the right hand side of (7). Let this solution be denoted by z=h(u). The reliability can thus be written as the reliability of a series system:

$$1 - p_f = P\{\min_{i=1}^{2m}[g_i(U;Z)] > 0\} \tag{10}$$

where

$$Z = h(U) = h(T(Q,N^-,N^+)) \tag{11}$$

Unfortunately, the function h is not known. However, the right hand side of (10) provides a lower bound on the reliability for any choice of the function h. Two choices are applied here.

First, Z is chosen as a linear function of the external loads Q, i.e.

$$Z = xQ + z_0 \tag{12}$$

and the lower bound based on this random z-vector is maximized by solving the optimization problem:

Determine x, z_0 such that $\min_{i=1}^{2m}[P\{g_i(U;Z) > 0\}]$ is maximized.

This non-linear optimization problem is solved by sequential linear programming. The solution has the advantage of being independent of the chosen redundants (see (2)).

Secondly, Z is chosen as a linear function of the external loads Q as well as the yield forces of the bars (N^-,N^+),

$$Z = xQ + y\begin{bmatrix} N^- \\ N^+ \end{bmatrix} + z_0 \tag{13}$$

and the optimization problem maximizing $\min_{i=1}^{2m}[P\{g_i(U;Z) > 0\}]$ is solved by sequential linear programming. This case includes the optimization problem formulation with deterministic safety margins in [7,17]. For the choice of Z in (13) also the following optimization problem is considered:

Determine x,y,z_0 such that $P\{\min_{i=1}^{2m}[g_i(U,Z)] > 0\}$ is minimized.

The problem is solved by a steepest ascent method. To improve the calculation efficiency the partial derivatives of the reliability with respect to the parameters x,y,z_0 are approximated by the asymptotic results for parametric sensitivity measures known from first and second order reliability methods, see [14].

The procedures are valid for yield functions with load effect interaction and for any joint distribution type of the physical basic variables. Some simplifications are achieved when the distributions are normal (linear transformation T). It turns out that the optimal z-solution determined for this situation is near optimal for a general distribution type situation.

The lower bound reliabilities from the ideal plastic analysis may be compared with a lower bound obtained by assuming a linear elastic distribution of internal forces in the structure. A measure of redundancy or reserve strength can thereby be defined.

4.2 Upper Bound on the Reliability

Two methods of plastic upper bound reliability analysis are considered, namely the *directional search method* [9,10], and the *linear combination method* [7,17]. An approximate evaluation of the reliability in (6) can be carried out by a first or second order reliability method provided the most likely failure points have been identified. Restricting the considerations to the cases where the transformation T is linear, the safe set in u-space is a polyhedral convex set. A close upper bound on the reliability corresponding to this set can be obtained by applying only the hyperplanes defining the faces of this polyhedral set with smallest distance to the origin of u-space. From experience it is known that within plastic system reliability analysis it is often necessary to apply several hyperplanes in order to get a close upper bound. Each hyperplane can be interpreted as representing a failure mode (plastic mechanism) of the structure.

The crucial point in calculating a close upper bound on the reliability is thus to identify the significant hyperplanes. One possibility is to apply the *directional search method* [9], describing the limit state surface in u-space by $r = r(\mathbf{a})$. A starting unit vector $\mathbf{a}^0$ is chosen. The distance to the limit state surface $r^0 = r(\mathbf{a}^0)$ is determined as the solution to a linear programming problem (see end of Section 3). Moreover, the unit normal vector $\boldsymbol{\alpha}_1$ to the limit state surface in $\mathbf{u}^1 = r^0\mathbf{a}^0$ is determined numerically. (Of course, attention should be paid to the possibility of having identified a singular point on the limit state surface). The safety margin corresponding to the face of the safe set in this point is then determined by the reliability index $\beta_1 = \boldsymbol{\alpha}_1^T\mathbf{a}^0 r^0$ and the unit normal vector $\boldsymbol{\alpha}_1$. With the new starting vector $\mathbf{a}^1 = \boldsymbol{\alpha}_1$ the same procedure is repeated resulting in $\beta_2 = \boldsymbol{\alpha}_2^T\boldsymbol{\alpha}_1 r^1$. The procedure is continued until a stop criterion ($\boldsymbol{\alpha}_l^T\boldsymbol{\alpha}_{l+1} \approx 1$) is fulfilled. The same scheme may now be repeated with a new starting vector $\mathbf{a}^0$. In each step of the algorithm the result $(\beta_l, \boldsymbol{\alpha}_l)$ is stored if the safety margin is not highly correlated ($\rho_{lj} = \boldsymbol{\alpha}_l^T\boldsymbol{\alpha}_j \approx 1$) with a previously identified safety margin.

Each sequence in the procedure is similar to the well-known Rackwitz and Fiessler algorithm of identifying a first order reliability index, see [14]. The deviations are, that only points on the limit state surface are considered, and that the result of each step in the algorithm is stored. The procedure is stopped by some convergence criterion based on the probability content of the identified polyhedral set. This probability is given by the multi-variate normal distribution function and can be evaluated approximately, e.g. in terms of upper and lower bounds [7,12]. The starting vector $\mathbf{a}^0$ in each sequence of the procedure is generated by simulation using a sampling density giving preference to directions corresponding to a lower fractile for a resistance variable and an upper fractile for a load variable. Alternatively, the starting vectors could be generated by some deterministic procedure, e.g. producing more or less uniformly spaced points on the unit sphere in u-space. The method can, in principle, easily be extended to load effect interaction in the

yield function. The extension, however, changes the optimization for $r(\mathbf{a})$ to a nonlinear optimization problem.

Another plasticity theoretical way of establishing an upper bound on the reliability is by the method of linear combination of lower bound safety margins [7,17]. This method, referred to as the *linear combination method*, can briefly be outlined as follows. Consider a linear combination of lower bound safety margins from (5) of the form

$$L = \sum_{i=1}^{m} \gamma_i \, g_{I(i)}(\mathbf{U}\,;\mathbf{z}) \tag{14}$$

where the index function $I(i)$ is equal to either $2i-1$ (compression safety margin for member i) or $2i$ (tension safety margin for member i). It can be shown that L is an upper bound safety margin corresponding to a plastic mechanism if L is independent of z, and the coefficients γ_i all are non-negative, [17]. The linear combination method uses this fact by establishing upper bound safety margins as linear combinations of the form in (14) using so-called *dominant* lower bound safety margins. The dominant lower bound safety margins are defined next.

A plastic lower bound analysis is performed considering deterministic redundants z_0. To each of the $2m$ lower bound safety margins in (5) is associated a reliability index $\beta_j = \Phi^{-1}(P[g_j(\mathbf{u}\,,\mathbf{z}_0) > 0])$. The lower bound is sought maximized by maximizing the smallest reliability index with respect to the deterministic redundants. The safety margins with reliability index equal to the smallest value in the solution are the dominant lower bound safety margins. It can be shown that for normally distributed basic variables a value of the redundants exists such that there are at least $n+1$ dominant lower bound safety margins [17].

Significant upper bound safety margins are searched by considering linear combinations of primarily the dominant lower bound safety margins. In other words, the dominant safety margins are taken as indicators for which members in the structure are likely to yield under plastic collapse. As opposed to failure tree reliability analyses based on successive elastic analyses, a *plastic analysis* is here used to identify members that are likely to be yielding in a significant mechanism. Details about the strategy for combining the lower bound safety margins can be found in [7,17]. The implementation in [7,17] is based on normally distributed physical basic variables. The set of significant upper bound safety margins determined in this way is expected to be representative also in the case of non-normally distributed physical basic variables. The linear combination method is presently being extended to handle load effect interaction in the yield function.

4.3 Reliability Calculation by Simulation

The reliability $1-p_f$ or the probability of failure p_f can be estimated by Monte Carlo simulation. In particular the method of directional simulation [18,19] seems appropriate using the expression for the reliability in (8). The simulation is carried out by generating N outcomes $\mathbf{a}_1, \mathbf{a}_2, \cdots, \mathbf{a}_i, \cdots, \mathbf{a}_N$ of the unit vector A. For each outcome $\mathbf{a}_i$ the distance $r(\mathbf{a}_i)$ is determined by solution of an optimization problem. With

$$p_i = 1 - \chi_q^2(r(\mathbf{a}_i)^2) \tag{15}$$

p_f is estimated by $\hat{P}$ with mean value and variance

$$E[\hat{P}] = \frac{1}{N}\sum_{i=1}^{N} p_i \tag{16}$$

$$Var[\hat{P}] = \frac{1}{N(N-1)}\sum_{i=1}^{N}(p_i - E[\hat{P}])^2 \tag{17}$$

Results from this type of simulation can be found in the examples in a later section. In [19] other examples are given and a method of reducing the variance of the estimator by importance sampling is proposed. Furthermore it is shown how parametric sensitivity measures can be simulated.

Example 1: Plane truss structure of 10 members

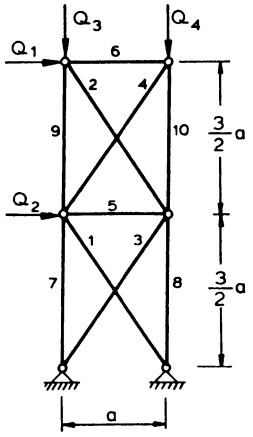

Fig. 1. Plane truss structure.

An $n=2$ times redundant plane truss structure of $m=10$ bars is considered, Fig. 1. The yield forces of the 10 bars are assumed to be normally distributed with the following representation:

$$E[N_i^-] = \begin{cases} 0.2\mu_N & \text{for } i = 1,2,3,4 \\ 1.0\mu_N & \text{for } i = 5,6 \\ 0.8\mu_N & \text{for } i = 7,8,9,10 \end{cases}$$

$$E[N_i^+] = \begin{cases} 0.4\mu_N & \text{for } i = 1,2,3,4 \\ 1.6\mu_N & \text{for } i = 5,6,7,8,9,10 \end{cases}$$

$$\frac{D[N_i^-]}{E[N_i^-]} = \frac{D[N_i^+]}{E[N_i^+]} = 0.15$$

All variables are assumed independent, except N_i^- and N_i^+, for which $\rho[N_i^-, N_i^+] = 0.90$ for all i. The stiffness of the bars no. 1-4 are assumed to be the equal and 20% of the stiffness of the remaining bars.

Three loading cases for the structure are considered. In load case *I* only the horizontal force Q_1 is acting, in load case *II* both horizontal forces Q_1 and Q_2 are acting, and in load case *III* the two vertical loads Q_3 and Q_4 are acting. The representation of the load variables are

$$E[Q_1] = 0.10\mu_N \ , \ D[Q_1] = 0.03\mu_N$$
$$E[Q_2] = 0.05\mu_N \ , \ D[Q_2] = 0.01\mu_N$$
$$E[Q_3] = 0.50\mu_N \ , \ D[Q_3] = 0.04\mu_N$$
$$E[Q_4] = 0.50\mu_N \ , \ D[Q_4] = 0.04\mu_N$$

The correlation coefficient between Q_1 and Q_2 is taken as 0.8, and the correlation coefficient between Q_3 and Q_4 as 0.5.

The reliability of the truss structure with respect to plastic collapse is calculated by the different methods. The results of the lower and upper bound analysis are given in Tables 1-4. The exact reliability for this small structure can be found by considering all plastic mechanisms, and for all three load cases the upper bound result coincides with the exact result.

Table 1. Results of lower bound analysis.
The numbers in parenthesis are the numbers of iterations in the non-linear programming problems.

Load case	*I* $[Q_1]$		*II* $[Q_1,Q_2]$		*III* $[Q_3,Q_4]$	
Type of analysis	β_{HL}	β_G	β_{HL}	β_G	β_{HL}	β_G
Elastic lower bound:	2.67	2.47	1.41	1.39	2.78	2.36
Plastic lower bound:						
max β_{HL} w.r.t. z	3.79	3.37	2.72	2.33	3.08	2.43
max β_{HL} w.r.t. x,z	3.91	3.55 (66)	2.91	2.54 (19)	3.10	2.45 (12)
max β_{HL} w.r.t. x,y,z	3.98	3.59 (19)	2.91	2.54 (8)	3.28	2.64 (40)
max β_G w.r.t. x,y,z	4.09	3.96 (219)	3.32	3.11 (117)	3.19	2.74 (64)
Exact result		4.34		3.36		3.20

Table 2. Results of upper bound analysis for load case *I*.

Mechanism no.	Linear combinations	Directional search	Bars in yielding
1	4.38	4.38	1^- 8^-
2	4.87	4.87	2^- 4^+
3	4.87	4.87	1^- 3^+
4	6.25		3^- 10^-
5		6.25	3^+ 7^+
6	6.49	6.49	7^+ 10^-
7	7.15	7.15	4^+ 8^+
8	8.22		4^+ 6^+ 10^-
9	8.55		1^- 7^-
β_G	4.34	4.34	

Table 3. Results of upper bound analysis for load case *II*.

Mechanism no.	Linear combinations	Directional search	Bars in yielding
1	3.44	3.44	1^- 3^+
2	3.71	3.71	1^- 10^-
3	4.87	4.87	2^- 4^+
4	5.87	5.87	3^+ 7^+
5		6.13	7^+ 10^-
6	7.15		4^+ 8^+
7	7.88		3^+ 4^+
8	8.36		3^+ 10^+
9	8.55		1^- 7^-
β_G	3.36	3.36	

The results of the lower bound analysis are given in terms of the Hasofer-Lind reliability index β_{HL} (equal to the reliability index corresponding to the reliability $\min_{i=1}^{2m}[P\{g_i(U;Z) > 0\}]$) and the system reliability index β_G. The only lower bounds close to the exact result are those obtained by optimizing the system reliability index. The elastic lower bound as well as the plastic lower bounds based on linear programming turn out to be significantly smaller than the exact reliability. Tables 2, 3 and 4 present results for the two independent upper bound methods. The methods yield the same and exact result on the system reliability index in all three load cases.

Table 4. Results of upper bound analysis for load case *III*.

Mechanism no.	Linear combinations	Directional search	Bars in yielding
1	3.62	3.62	2^- 8^-
2	3.62	3.62	4^- 8^-
3	3.62	3.62	1^- 7^-
4	3.62	3.62	3^- 7^-
5	3.76	3.76	1^- 10^-
6	3.76	3.76	4^- 9^-
7	3.76	3.76	3^- 10^-
8	3.76	3.76	2^- 9^-
9	7.08	7.08	5^+ 8^-
10	7.39		6^+ 7^- 8^-
11		7.45	6^+ 7^- 9^-
12		7.88	3^+ 6^+ 8^-
13		7.91	4^+ 6^+ 10^-
14	8.92		7^- 10^+
15	8.92		8^- 9^+
β_G	3.20	3.20	

Experience from other examples as well indicates that the upper bound analyses give close upper bounds, implying that the methods identify all significant mechanisms.

5. APPLICATION TO OFFSHORE JACKET STRUCTURES

The reliability analysis for the ideal plastic structural models has been used to evaluate a reliability measure for jacket-type offshore structures under extreme environmental loading [8,20]. In this context a computer analysis program RAPJAC (Reliability Analysis of Plastic Jackets) based on the reliability methods presented in the preceding sections has been developed, [21,22]. The program can be used within the SESAM program system for structural analysis. (SESAM is a trademark of A.S. Veritas Sesam Systems, Norway) In particular, the SESAM preprocessor for generating geometry and topology of a structure as well as a utility program for calculating water particle kinematics can be applied in connection with the reliability analysis program. Links to other commercial general purpose structural analysis program systems are straightforward to implement.

A first version of RAPJAC has been completed. The version handles spatial truss structures with the basic assumptions that the overall geometry of the structure is deterministic, and that the basic variables (yield forces of bars and nodal forces) are jointly normal. The latter assumption can be relaxed, since the present reliability analysis program can be coupled to general purpose probabilistic analysis programs handling any type of distributions like the PROBabilistic ANalysis Program PROBAN, [23] (PROBAN is a trademark of A.S. Veritas Research, Norway). In the reliability model all uncertainty is described by random variables and the program is aimed at reliability assessment with respect to an instantaneous overload.

An automatic generation of nodal forces from waves and current is available. The forces are established on basis of a deterministic water particle velocity field calculated from a discrete, plane wave applying a specified wave theory and using specified values for the wave height, period and direction as well as current velocity and direction. Given such a velocity field the joint distribution for the nodal forces is found using the Morison formula as follows. Consider a point on the axis of a tubular member below the water surface. Let the water particle velocity in the point be $v = (v_1, v_2, v_3)$ where the first two components are mutually orthogonal and orthogonal to the member axis, and the third component is parallel to it. Let the wave force intensity per unit

length of the tubular member at the considered point be $\mathbf{q} = (q_1, q_2, q_3)$, where q_1 and q_2 are orthogonal to the member axis and q_3 is parallel to it. $\mathbf{q}$ is then assumed given by

$$\begin{bmatrix} q_1 \\ q_2 \\ q_3 \end{bmatrix} = \frac{1}{2}\rho_W (D+2H) \begin{bmatrix} C_{D,11} & C_{D,12} & 0 \\ C_{D,21} & C_{D,22} & 0 \\ 0 & 0 & C_{D,33} \end{bmatrix} \begin{bmatrix} v_1\sqrt{v_1^2+v_2^2} \\ v_2\sqrt{v_1^2+v_2^2} \\ v_3|v_3| \end{bmatrix}$$

$$+ \frac{\pi}{4}\rho_W (D+2H)^2 \begin{bmatrix} C_{M,11} & C_{M,12} & 0 \\ C_{M,21} & C_{M,22} & 0 \\ 0 & 0 & C_{M,33} \end{bmatrix} \begin{bmatrix} \dot{v}_1 \\ \dot{v}_2 \\ \dot{v}_3 \end{bmatrix} \tag{18}$$

where ρ_W is the specific mass of the water, D is the diameter of the tubular member at the considered point, H is the excess radius of the member due to marine growth, the C_D parameters are drag coefficients, and the C_M parameters are inertia coefficients. For the sake of simplicity the off-diagonal elements as well as the third diagonal element in the two matrices are here taken as zero. Furthermore, the two diagonal elements in each matrix are assumed equal to C_D and C_M, respectively, since the structural member is tubular. However, it is noted that the more general formula in (18) is implemented in RAPJAC.

The coefficients C_D and C_M are assumed to be spatial Gaussian white noise processes over the structure. In a point, the two processes may be correlated and, typically, negative correlation originating from statistical uncertainty is expected. The white noise assumption has been introduced to reduce the computational effort when integrating the force intensities into nodal forces for which the second moment representation must be computed. Furthermore, the excess thickness H can be assumed to be a spatial white noise process. If this is the case, the second moment representation for the force intensities $\mathbf{q}$ is found approximately by a second order expansion in the mean point. This approximation is not fully consistent with a modern FORM/SORM analysis but has been introduced to reduce the computational effort, and to maintain the assumption of normally distributed nodal forces. The approximation can be avoided by coupling to PROBAN, but in that case the number of basic variables increases drastically. In summary, the uncertainty in the wave and current forces is modeled by random coefficients in the Morison equation together with a random diameter of the member. The mean value and standard deviation of the random variables at a given position can be specified as a piece-wise linear function of the elevation above the sea bed.

Gravity and buoyancy loads on the truss structure are generated automatically as well. Loads on the deck structure, e.g. gravity loads, live loads and wind loads, can not be generated by the present program, but load models in terms of nodal forces on the truss structure must be set up by the user.

The program provides lower and upper bounds on the reliability with respect to plastic collapse. A lower bound can be established as the reliability with respect to initial yielding under the assumption of elastic force distribution in the structure. Furthermore, the plasticity theoretical lower bounds can be calculated. The upper bound analysis is based on two different and completely independent plasticity theoretical approaches comprising the directional search procedure and the method of combining lower bound safety margins. Finally, the reliability can be checked by directional simulation. Results from such simulations are given as an estimate on the reliability together with an estimated coefficient of variation on the estimator.

The program has been applied for research purposes. It is planned to be available for practical purposes like comparisons between alternative design solutions, evaluation of the reliability of damaged structures, determination of the importance of the structural members and for identification of an optimal design under a complete load description. It is furthermore the

intention to continue the implementation of reliability methods for offshore jacket structures to the extent where real life sized structures modeled as spatial frameworks can be handled.

Example 2: Spatial truss structure of 48 members

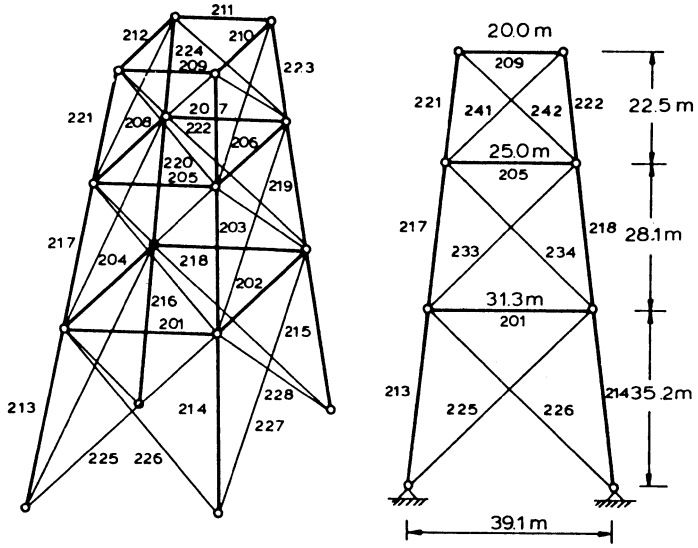

Fig. 2. Spatial truss tower of 48 tubular bars.

The model of a steel jacket offshore platform in Fig. 2 is considered. The structure is an $n=12$ times redundant spatial truss tower with $m=48$ tubular bars. All geometry variables, i.e. the dimensions of the structure given in Fig. 2 and the dimensions of the bars given in Table 5 are assumed to be deterministic.

Table 5. Dimensions and mean tension yield forces of bars. The ratio between the diameter d and the wall thickness t is assumed to be $d/t = 60$ for all bars.

Bar No.	d [m]	Area [m^2]	$E[N_i^+]$ [MN]
201-204	2.0	0.210	67.20
205-208	1.5	0.116	37.07
209-212	1.0	0.053	16.80
213-224	2.5	0.324	103.78
225-232	1.5	0.116	37.07
233-248	1.2	0.074	23.73

The yield forces and loads are assumed to be normally distributed with the following representation:

$$E[N_i^-] = 0.75E[N_i^+] \quad \textit{given in Table 5}$$
$$D[N_i^-] = 0.15E[N_i^-], \; D[N_i^+] = 0.10E[N_i^+]$$

Furthermore it is assumed that all yield forces are equi-correlated with correlation coefficient 0.5.

The external loading on the structure is due to gravity, live load, wind, wave and buoyancy. The following load models are applied:

Gravity and live loads: Gravity and live loads from the deck structure are modeled by four vertical loads, one in each of the four top level nodes of the truss structure. Each force has a mean value 20 MN, a coefficient of variation 0.10, and the four forces are equi-correlated with correlation coefficient 0.5. Gravity loads of the truss structure itself are referred to the nodes as single forces, and are calculated for a specific mass of the tubular members of $7.85 \cdot 10^3\, kg/m^3$. Furthermore, additional gravity loads are included (e.g. from inside stiffeners in the members and in the joints) by assuming that the specific mass of the interior of the members is $0.25 \cdot 10^3 kg/m^3$. The gravity forces on the truss structure are assumed deterministic.

Wind load: Wind load on the deck structure is modeled by a horizontal and a vertical force in each of the four top level nodes. The magnitude of these forces are all assumed proportional to a random variable of mean 1.0 MN and with coefficient of variation 0.30. The direction of the wind model forces and the coefficients of proportionality are given in Fig. 3. The model is based on the assumption that the wind acts in a direction of 30 degrees with one side of the truss structure. Wind loading on the jacket structure itself is neglected.

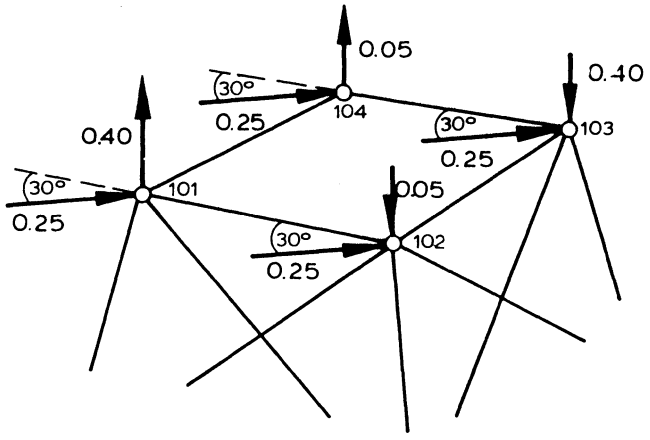

Fig. 3. Illustration of direction and magnitude of nodal forces from the wind loading on the deck structure.

Wave and buoyancy loads: The marine loading is calculated on basis of the water particle kinematics for a 5*th* order Stokes theory wave of height $h = 25m$ and period $T = 17s$. The water depth is assumed to be $d = 70m$, Fig. 4, and the direction of the wave is the same as the direction of the wind, Fig. 3. It is assumed that no current is present. A second moment representation for the nodal forces of the marine loading is determined under the assumption that the drag and inertia coefficients, C_D and C_M, in the Morison formula as well as the excess thickness of the tube walls due to marine growth, H, are spatial Gaussian white noise processes. The mean values and standard deviations as function of the position are given in Table 6. Finally, vertical deterministic buoyancy loads on the member parts under the sea surface are calculated and added to the respective nodal forces.

The position of the wave is defined by the wave phase angle θ. For $\theta = 0°$ the wave crest is above the first support of the structure (in the direction of the wave propagation). For $\theta \approx 20°$, the wave crest is in the middle of the structure. An elastic lower bound reliability analysis and a plastic upper bound reliability analysis based on the method of linear combination of lower bound

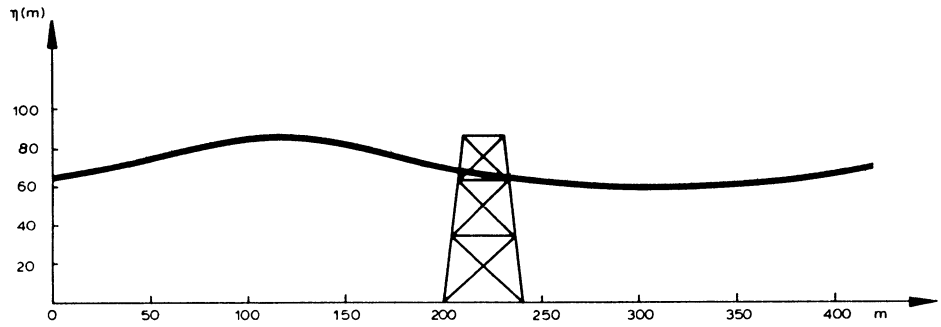

Fig. 4. Illustration of truss structure and the example Stokes 5th order wave. Wave length $L=392m$, wave period $T=17.5s$, and wave height $H=25m$.

Table 6. Mean value and standard deviation of C_D, C_M and H. Coefficients are a function of elevation above sea bed. Between the given levels the quantities vary linearly, and above 75m they are constant. At a given position the three variables are assumed uncorrelated.

Elevation z	$E[C_D]$	$D[C_D]$	$E[C_M]$	$D[C_M]$	$E[H]$	$D[H]$
00 m	1.0	0.4	2.0	0.3	0.00 m	0.000 m
30 m	1.0	0.4	2.0	0.3	0.01 m	0.002 m
65 m	1.0	0.4	2.0	0.3	0.05 m	0.010 m
75 m	1.0	0.4	2.0	0.3	0.10 m	0.030 m

safety margins are carried out for different values of the wave phase angle θ. Selected cases have been checked by directional simulation. The results are shown in Fig. 5.

The difference between the reliability with respect to initial yielding and the reliability with respect to total plastic collapse is seen. For different positions of the wave, different failure modes are dominating. The same holds for the most likely member to yield in the lower bound analysis. Only a small difference between the reliability of the most likely element to yield and yielding in any member is observed in the extreme loading situation. This is due to high correlation between element safety margins in this case. The same tendency is observed in the upper bound analysis with respect to plastic collapse, where the reliability index for the most likely mechanism is only slightly higher than the plastic system reliability index. Finally it is noted that the variation in θ of the reliability index with respect to plastic collapse in this case follows closely the variation of the elastic system reliability index.

6. CONCLUSIONS

Recent developments for evaluation of the system reliability with respect to plastic collapse of ideal plastic structures based on the lower bound theorem are presented. The reliability model is formulated for spatial truss structures and a lower and an upper bound on the reliability are obtained. A program for plastic reliability analysis of offshore jacket structures has been developed. The program can be applied within a larger commercial program package for structural analysis. In brief, the physical basic variables that can be modeled as random within the program are: compression and tension yield forces of bars (uncertainties in e.g. yield stress and cross sectional area, as well as model uncertainty), nodal forces describing external loading such as dead load, live load, wind load and wave and current load, parameters in the Morison equation,

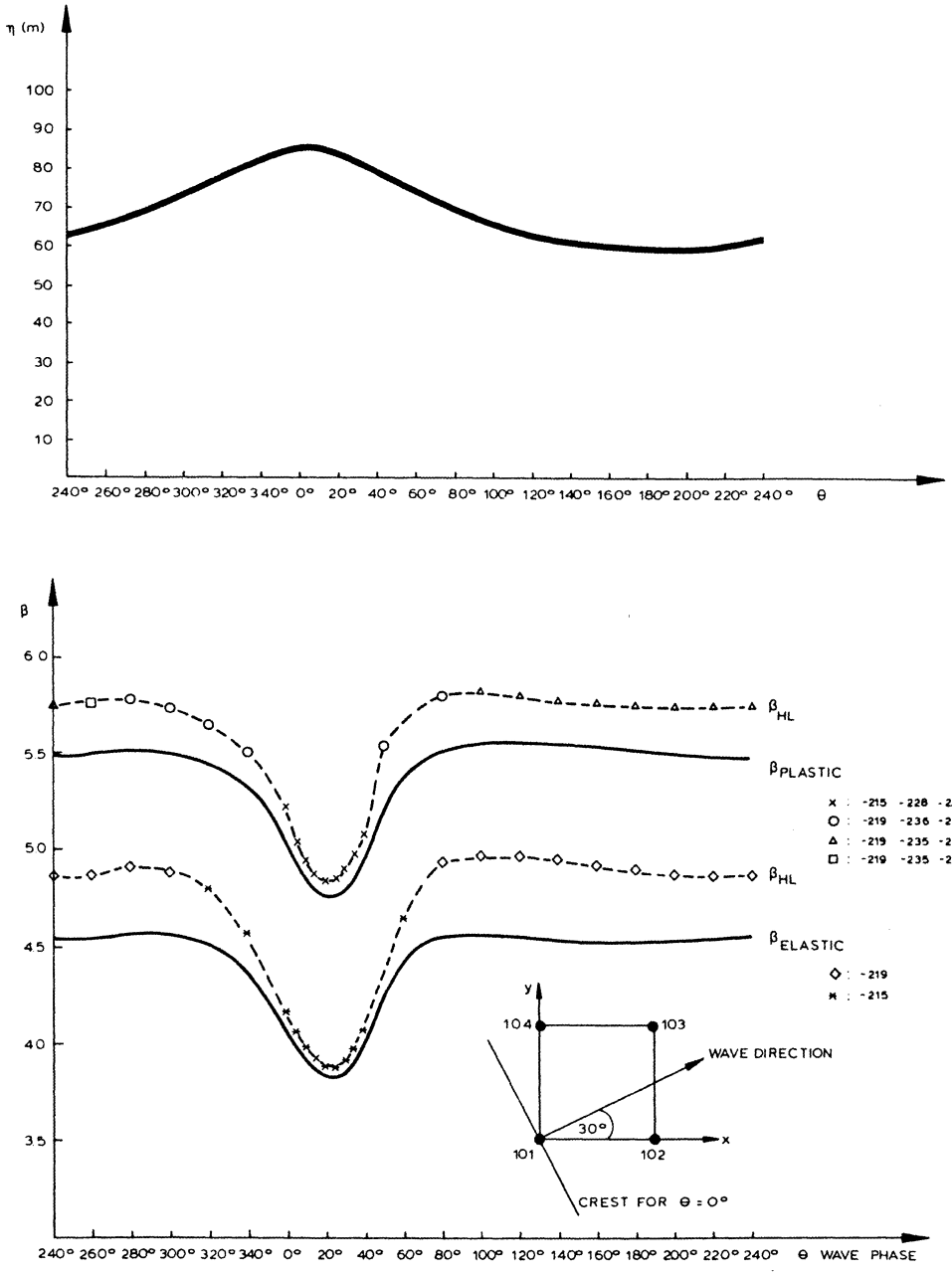

Fig. 5. Results of elastic reliability analysis with respect to initial yielding and plastic upper bound reliability analysis with respect to plastic collapse for different positions of the wave crest.

i.e. the normal and longitudinal drag and inertia coefficients (when wave and current forces are generated automatically), marine growth thickness (when wave and current forces are generated automatically), buoyancy and gravity forces, and model uncertainty in wave and current forces.

The following conclusions can be drawn:

- The reliability methods for ideal plastic systems provide a means of quantifying redundancy of structures. In common design practice such system effects are not accounted for. Furthermore, the system reliability method can be applied for evaluation of the reliability of damaged structures, and for development of reliability based optimal design.
- The upper bound on the reliability determined by a first order reliability method converges towards the exact reliability for increasing amount of calculation. Often a close upper bound on the reliability can be established with a manageable calculational effort even for real life sized structures.
- Simplifications must be introduced to make the calculation of a maximized lower bound on the reliability by a first or second order method practicable. Lower bounds based on one choice of the redundants are considered and three cases are undertaken: The vector of redundants is deterministic, linear in the nodal forces, or linear in the nodal forces and the yield forces. The lower bounds resulting from an optimization of these linear combinations do not in general converge towards the exact reliability for increasing calculational effort. Results from random redundants can be significantly closer to the exact reliability than results from deterministic redundants. Typically, however, the lower bounds turn out to be somewhat smaller than the exact reliability, at least for a practicable amount of calculation.
- The method of directional simulation provides a general and rather efficient means of establishing a confidence interval on the desired reliability.
- The plastic reliability methods considered herein are valid for truss structures under the assumptions that the geometry is assumed deterministic, and that the basic problem variables are normally distributed. The formulation of the reliability can be directly generalized to frame structures with load-effect interaction and the distributional assumptions above can be relaxed. However, the calculation methods based on linear programming in this paper then turns out to require non-linear programming. Alternatively, the optimization of the lower bounds and the identification of significant upper bound safety margins can be carried out using a representative Gaussian joint distribution, followed by a reliability computation using a general purpose probabilistic analysis program.
- The reliability models considered are formulated in terms of random variables. Generalizations to random process models should be considered.

ACKNOWLEDGEMENTS

The material is based on work supported by the joint Veritas Research and SAGA Petroleum research program "Reliability of Marine Structures".

REFERENCES

[1] O. Ditlevsen, and P.Bjerager, "Methods of Structural Systems Reliability", *Structural Safety*, Vol. 3, 1986, pp. 195-229.

[2] P. Bjerager, A. Karamchandani, and C. A. Cornell, "Failure Tree Analysis in Structural Systems Reliability", in *Proceedings* Int. Conf. on Appl. of Stat. and Prob. in Soil and Struct. Eng., ICASP5, (ed. N. C. Lind), May 25-29, 1987, Vancouver, Canada, Vol. II, pp. 985-996.

[3] G. Augusti, and A. Baratta, "Limit Analysis of Structures with Stochastic Strengths Variations", *Journal of Structural Mechanics*, Vol. 1., No. 1, 1972, pp. 43-62.

[4] M. R. Gorman, "Reliability of Structural Systems", Report No. 79-2, Department of Civil Engineering, Case Western Reserve University, Cleveland, Ohio, 1979.

[5] H.-F. Ma, and A. H.-S. Ang, "Reliability of Redundant Ductile Structural Systems", Report No. 81-2013, Department of Civil Engineering, University of Illinois, Urbana, 1981.

[6] P. Thoft-Christensen, and Y. Murotsu, *Application of Structural Systems Reliability Theory*, Springer Verlag, Berlin, 1986.

[7] P. Bjerager, "Reliability Analysis of Structural Systems", Report No. 183, Department of Structural Engineering, Technical University of Denmark, Denmark, 1984.

[8] Y. F. Guenard, "Application of System Reliability Analysis of Offshore Structures", Report No. 71, John A. Blume Earthquake Engineering Center, Stanford University, California, 1984.

[9] P. Bjerager, "System Reliability of Idealized Structures", in *Proceedings* 2nd International Workshop on Stochastic Methods in Structural Mechanics, (eds. Casciati & Faravelli), Pavia, Italy, August 24-27, 1985, pp. 255-270.

[10] P. Bjerager, "Plastic Systems Reliability by LP and FORM", to appear as DCAMM Report, Technical University of Denmark, 1987.

[11] L. E. Malvern, *Introduction to the Mechanics of a Continuous Medium*, Prentice-Hall Inc., 1969.

[12] J. Robinson, *Integrated Theory of Finite Element Methods*, John Wiley & Sons, New York, 1973.

[13] I. Kaneko, "On Computational Procedures for the Force Method", *International Journal for Numerical Methods in Engineering*, Vol. 18, 1982, pp. 1469-1495.

[14] H. O. Madsen, S. Krenk, and N. C. Lind, *Methods of Structural Safety*, Prentice-Hall Inc., 1986.

[15] H. O. Madsen, and R. Skjong, "Lower Bound Reliability Evaluation for Plastic Truss and Frame Structures", A.S Veritas Research Report No. 84-2043, Hovik, Norway, 1984.

[16] P. Bjerager, and S. Gravesen, "Lower Bound Reliability Analysis of Plastic Structures", in *Probabilistic Methods in the Mechanics of Solids and Structures*, (eds. S. Eggwertz and N. C. Lind), Springer Verlag, Berlin, 1984, pp. 281-290.

[17] O. Ditlevsen, and P. Bjerager, "Reliability of Highly Redundant Plastic Structures", *Journal of Engineering Mechanics, ASCE*, Vol. 110, No. 5, 1984, pp. 671-693.

[18] I. Deak, "Three Digit Accurate Multiple Normal Probabilities", *Numerische Mathematik*, Vol. 35, 1980, pp. 369-380.

[19] O. Ditlevsen, and P. Bjerager, "Plastic Reliability Analysis by Directional Simulation", to appear as DCAMM Report, Technical University of Denmark, 1987.

[20] H. Crohas, A.-A. Tai, V. Hachemi-Safai, and B. Barnouin, "Reliability Analysis of Offshore Structures Under Extreme Loading", in *Proceedings*, 16th Annual Offshore Technology Conference, Houston, Texas, May 1984, pp. 417-426.

[21] P. Bjerager, "RAPJAC Theoretical Manual", A.S Veritas Research Report No. 87-2013, Hovik, Norway, 1987.

[22] P. Bjerager, and R. Olesen, "RAPJAC User's Manual", A.S Veritas Research Report No. 87-2014, Hovik, Norway, 1987.

[23] H. O. Madsen, "PROBAN Theoretical Manual", A.S Veritas Research Report No. 86-2036, Hovik, Norway, 1987.

STRUCTURAL SYSTEM RELIABILITY ANALYSIS USING MULTI-DIMENSIONAL LIMIT STATE CRITERIA

R. C. Turner
W. S. Atkins Engineering Sciences, Epsom, UK, and Research Assistant
Imperial College of Science and Technology, London, UK

and

M. J. Baker
Reader in Structural Reliability
Imperial College of Science and Technology, London, UK

SYNOPSIS

In practice, the limit state criteria which are used to define the ultimate strength of structural components (i.e. members or joints) are often non-linear and multi-dimensional, and are associated with plastic flow.

This paper shows how the effects of plastic flow can be allowed for in determining the reliability of structural systems. The method is illustrated with the analysis of a simple structure.

NOTATION

$\bar{a}_{1j}$, $\bar{a}_{2j}$, $\bar{a}_{3j}$	elastic influence coefficients at position j
d	member outside diameter
E_i	the event of the i^{th} hinge forming
$f(\bar{Q})$	the limit state function
f_b	bending stress
f_v	shear stress
$\bar{F}$	set of axial forces at the hinges
F_y	yield stress in simple tension
F_{yi}	yield stress in simple tension at position i
I_y, I_z, I_{yz}	moment of inertia
k_1, k_2, k_3	constants
m_j^E	elastic influence coefficients of moment at positon j for the intact structure
m_{6j}, m_{6mj}, m_{6tj}	elastic influence coefficients of moment at position j for unit load, unit moment, and unit torque for the structure with a hinge at position 6
M_i	moment at position i
$\bar{M}$	set of moments at the hinges
M_i^E	moment at position i for the intact structures
M_p	plastic moment capacity
ΔM_i	change in moment at position i

δM_i	incremental change in moment at position i
M'_i	"corrected" moment at position i
p*	design value of the applied load
P	applied load
$\bar{P}^T$	total applied load
$\bar{P}$	set of applied loads
$\bar{P}^E$	set of applied loads such that the stress state just reaches the limit state surface at only one location
ΔP	load applied after the first hinge has formed
$P_f^{[0]}$, $P_f^{[1]}$	probability of failure at level 0, level 1 etc.
dq_i^p	plastic strain increment at position i
$\bar{Q}_i$	state of stress at position i
$\bar{Q}^T$	state of stress on the limit state surface
$\bar{\Delta s}$	set of self-equilibrating forces
t	tube wall thickness
t_j^E	elastic influence coefficients for torque at position j for the intact structure
t_{6i}, t_{6mj}, t_{6tj}	elastic influence coefficients for torque at position j for unit load, unit moment, and unit torque for a hinge at position 6
T_i	torque at position i
$\bar{T}$	set of torques at the hinges
T_i^E	torque at position i for the intact structure
ΔT_i	change in torque at position i
δT_i	incremental change in torque at position i
T'_i	"corrected" torque at position i
u	standard normal variable
$\bar{x}$	set of axial displacements at the hinges
Z	safety margin
β_{sys}, $\beta_{sys}^{[0]}$, $\beta_{sys}^{[1]}$	system reliability index at level 0, level 1,etc.
γ_i	torsional rotation at position i
γ_i^p, γ_i^m, γ_i^t	torsional rotation at position i for unit load, moment and torque
$d\gamma_i$	change in torsional rotation at position i after first hinge forms
$\bar{\delta}$	virtual displacements
λ	a non-negative unspecified scalar
θ_i	rotation at position i
θ_i^p, θ_i^m, θ_i^t	rotation at position i for unit load, moment and torque
$d\theta_i$	change in rotation at position i after first hinge forms

1. INTRODUCTION

Most of the published research concerning the system reliability of structures has assumed idealised structural behaviour with either pinned joints and axially-loaded members, or 2-dimensional rigid jointed frames in which the axial load effects have been ignored. Some reports and papers have considered multi-dimensional failure criteria, but in general they have either approximated the curved interaction surface by straight lines e.g. Edwards et al (1985), or they appear to have neglected the flow rule condition e.g. Crohas et al (1984).

Whilst it is not too difficult to include complex multi-dimensional failure criteria in a Level 2 type reliability program, it requires more effort to satisfy the associated flow rule. This paper explains an approach that can be followed for simple statically indeterminate structures subjected to time independent loads. The approach is illustrated with an example of a systems analysis of a simple structure using von Mises failure criterion.

One aim of this investigation is that the basic method should be capable of being extended to treat multi-dimensional limit state criteria in more complex structures, in particular the axial load/bending moment interaction in the bracing members of shallow water jacket structures.

2. BACKGROUND THEORY

2.1 Material Behaviour

Throughout this paper the structural material is assumed to be elastic-perfectly plastic. This assumption is used widely in general structural plastic analysis, and whilst the method explained in this paper for the successive elastic analysis approach does not specifically exclude the use of material with hardening behaviour the calculation becomes more complex.

Furthermore, the structural members are assumed to have bi-linear moment-curvature relationships. The main advantage of this assumption is that the initial yield surface (i.e. the surface bounding the elastic region in stress-space) coincides completely with the limit state surface. This means that within the limit state surface the behaviour is elastic, and plastic strain changes can only occur from flow when the stress state lies on the limit state surface. It is also important to note that the yield surface is independent of the loading history. This is not the case with material hardening or softening behaviour.

Unfortunately, the assumption that elastic moments are proportional to curvature until the limit state surface is reached (see Figs 1(a) and 1(b)) tends to underestimate deflections and leads to a calculated frame behaviour that is stiffer than it should be. For practical purposes, Heyman (1971) suggests that the effect of this assumption may largely be offset by the strain hardening of structural steel at high curvatures. This is an area for further research.

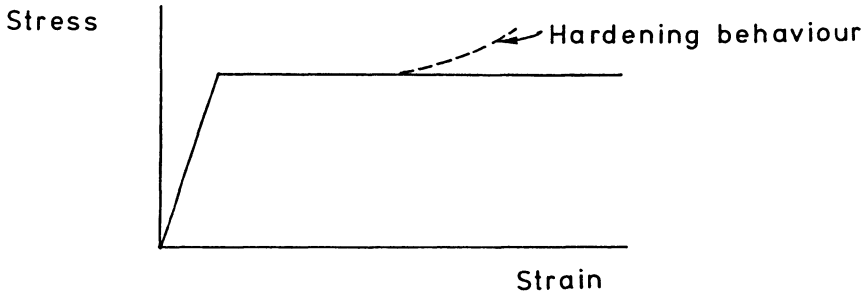

Figure 1(a): Idealised stress–strain behaviour.

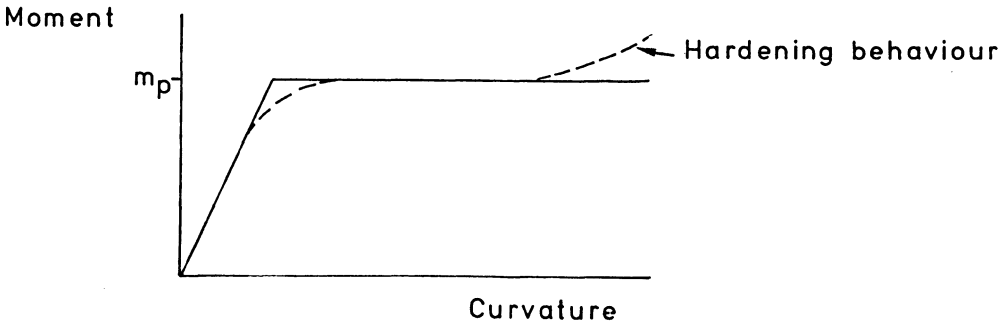

Figure 1(b): Idealised moment–curvature behaviour.

2.2 The Limit State Surface

The limit state surface is defined by the limit state function, $f(\bar{Q})$, and it marks the boundary between between elastic behaviour and plastic behaviour at the section under consideration: $f(\bar{Q}) > 0$ for elastic behaviour, and $f(\bar{Q}) = 0$ at the limit state surface. In a reliability analysis the limit state function is used within the definition of the safety margin Z.

The elastic region enclosed by the limit state surface is always convex in basic variable space, and typical failure functions include von Mises and Tresca, as well as the empirical formulae used for axial load/bending moment interaction in some codes of practice (e.g. AISC).

2.3 The Flow Rule

Consider a set of loads $\bar{P}^E$ such that the state of stress just reaches the limit state surface at only one location. A statically determinate structure will collapse at the application of loads $\bar{P}^E$ under the assumptions made in section 2.1. However, a statically indeterminate structure can carry increasing levels of loads $\bar{P} > \bar{P}^E$ up until a collapse mechanism forms.

For all sections i at which $f(\bar{Q}) = 0$ when $\bar{P} > \bar{P}^E$, plastic flow will occur. The plastic behaviour at the section is given by the flow rule or normality condition which is well covered in plastic theory literature (e.g. Martin, 1975).

The flow rule for section i may be stated as:

$$dq_i^p = \lambda \frac{\partial f}{\partial Q_i} \Bigg|_{\bar{Q}_i - \bar{Q}_i^T}$$

where dq_i^p is a plastic strain increment.

λ is a non-negative unspecified scalar

$\bar{Q}^T$ is the state of stress at a particular point on the limit state surface.

$$\frac{\partial f}{\partial Q_i} \Bigg|_{\bar{Q}_i - \bar{Q}_i^T}$$

is the partial derivative of the limit state function f evaluated at the stress state $\bar{Q}^T$.

The flow rule implies that the vector of plastic strain increments, $d\bar{q}^p$, has the direction of the outward normal to the limit state surface at stress state $\bar{Q}^T$.

Typical behaviour is illustrated in Figure 2. Until the limit state surface is reached the behaviour is piecewise-linear elastic. Plastic flow occurs at the section once the limit state surface is reached. Then the stress state satisfies the limit state function and alters according to the flow rule.

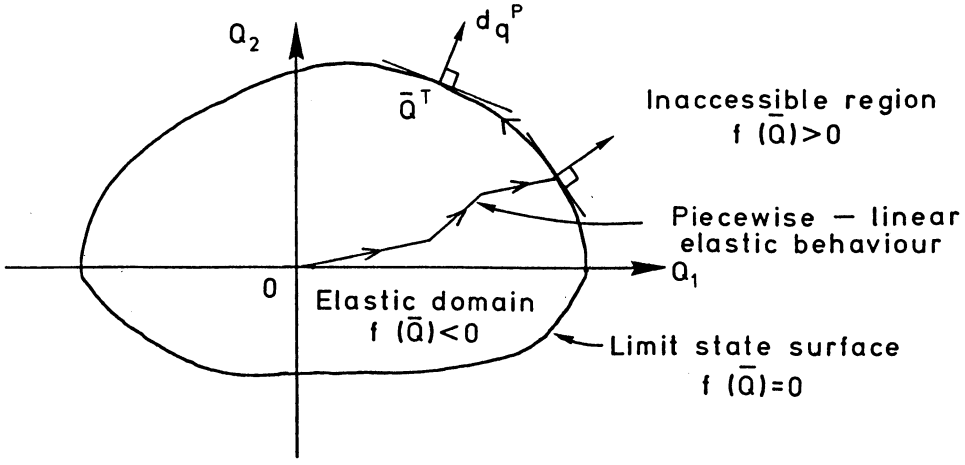

Figure 2: 2-Dimensional limit state surface in stress space.

3. SYSTEM RELIABILITY

3.1 The system reliability approach

In this paper all the variables are assumed to be time independent. The structure is loaded with a system of loads which are assumed to be random variables. The resistances at sections within the structure may be considered to have uncertain values which, according to circumstances, may be assumed to be:

(a) uniform throughout the structure,
(b) uniform throughout each member and independent between members,
(c) independent at discrete sections throughout the structure,
(d) obeying some complex correlation pattern.

As with a deterministic plastic analysis the positions of possible plastic hinges must be chosen. However, more positions must usually be considered within a reliability analysis since the possible hinge positions do not only depend on the structural form and type of loading, but also on how the resistances are assumed to vary within the structure. Thus possible hinges should be included at positions of peak moments for every independent resistance variable. The reliability of the structure is then based on the probabilities of forming plastic hinges at these positions.

Generally, the aim of a system reliability analysis is to determine the probability that a structure will collapse. This can be found directly by determining the probabilities of forming individual collapse mechanisms. A number of techniques have been developed to determine the most significant mechanisms, of which perhaps the most rigorous is a method developed by Ditlevsen and Bjerager (1984).

There are disadvantages to a direct collapse mechanism approach and a number of methods have been developed (reviewed in Baker, 1985) to identify the significant collapse mechanisms using a successive elastic analysis approach. All of these methods are very similar. Failure sequences leading to collapse are evaluated using successive elastic analyses as each hinge forms, and a failure tree of signifiant sequences is produced which is used to estimate the overall system reliability.

In Thoft-Christensen's β-unzipping method (1984) a system reliability can be evaluated after each level of successive analysis. Each successive result is a better estimate of the overall system reliability.

In this paper a successive elastic analysis approach and a direct collapse mechanism approach have been used to determine the system reliability. Both methods have been described by Thoft-Christensen (1984) but in this paper a more rigorous treatment of the multi-dimensional limit state surface has been undertaken.

3.2 System reliability using successive elastic analyses to identify collapse mechanisms

The intact structure is analysed with separate load cases for each independent set of loads, i.e. one load case for each independent loading variable. At each possible hinge position the member stresses are obtained for each load case, and the safety margins are formed from the limit state functions. The safety margins are used in a Level 2 reliability method to give probabilities for "first-failure" at each hinge.

The structural model is then modified by releasing freedoms at the position of one of the most likely hinges to form. The modified structure is re-analysed for a set of loads proportional to the original set, $(\overline{\Delta P})$, and separately for unit forces (or moments) at the hinge corresponding to each released freedom, $(\overline{\Delta s})$. Each of the above analyses for the modified structure has to be treated as a separate load case when using computer analysis.

Stresses $\bar{Q}$ at any position j in the structure are given by:

$$\bar{Q}_j = k_1 \bar{a}_{1j} \bar{P}^E + k_2 \bar{a}_{2j} \overline{\Delta P} + \bar{k}_3 \bar{a}_{3j} \overline{\Delta s}$$

where $\bar{a}_{1j}$ are elastic influence coefficients of stress obtained for the analysis of the intact structure with loads $\bar{P}^E$

$\bar{a}_{2j}$, $\bar{a}_{3j}$ are coefficients obtained from the successive analyses for loads $(\overline{\Delta P})$ and $(\overline{\Delta s})$ respectively

k_1, k_2, $\bar{k}_3$ are constants

At the plastic hinge, the limit state function and the flow rule must continue to be satisfied. Thus by considering the deformations, rotations and stresses at the hinge, expressions can be written for the constants k_1, k_2 and $\bar{k}_3$.

New safety margins can then be written for the onset of plasticity at other positions within the structure. They will in general be functions of the loading variables, the resistance property at the position in question and the resistance of the first hinge.

The procedure can then be repeated to consider the onset of plasticity at another section and this can be repeated until a collapse mechanism is formed.

3.3 The system reliability from the collapse mechanisms

In some situations it is much more efficient to determine the system reliability directly from the

collapse mechanisms.

Consider a collapse mechanism for the structure. Using the principles of virtual work, an equation can be written for the mechanism of the form:

$$\bar{P} \cdot \bar{\delta} = \bar{M} \cdot \bar{\theta} + \bar{T} \cdot \bar{\gamma} + \bar{F} \cdot \bar{x}$$

where $\bar{P}$, $\bar{M}$, $\bar{T}$, $\bar{F}$ are the applied loads and respective moments, torques and axial forces at the hinges,

$\bar{\delta}$ are the virtual displacements of the loads $\bar{P}$, and

$\bar{\theta}$, $\bar{\gamma}$, $\bar{x}$ are the corresponding rotations and axial deformations at the hinges.

The work equation can be rewritten with functions of the applied load and resistance variables using the following relationships.

Firstly, the geometry of the structure imposes constraints on the virtual displacements and provides relationships between θ's, γ's, x's and δ's. As with normal plastic analysis these relationships can either be found by inspection, by plotting the virtual displacements, or Watwood (1979) offers an analysis method.

Secondly, equilibrium conditions can be used to relate the applied loads to some of the hinge forces (or moments).

Thirdly, the limit state function must be satisfied at each hinge, so relationships can be written between M's, T's F's and the resistance variables.

Finally, the flow rule must also be satisfied at each hinge, i.e.

$$\theta_i = \lambda_i \frac{\partial f_i}{\partial M_i} \quad ; \quad \gamma_i = \lambda_i \frac{\partial f_i}{\partial T_i} \quad \text{etc.}$$

For simple examples the work equation can be written explicitly in terms of the applied loads and resistance variables. In general this will not be possible, but enough equations can usually be written so that a solution can be obtained.

The probability of failure for other collapse mechnisms are found in the same way, and the overall system probability for collapse of the structure is found by evaluating the union of events for all the individual mechanisms.

4. EXAMPLE: THE RIGHT ANGLE BENT

4.1 General

To illustrate the procedures discussed in the previous sections the structure shown in Figure 3 was analysed. Although it is only a simple two member structure it clearly demonstrates interaction in a two dimensional stress space, and it is well suited to a simple system analysis in which 2 or 3 hinges can form before collapse.

The structure was inspired by an example analysed by Thoft-Christensen (1984) in which the members were I-beam sections and for which the moment-torque interaction could be neglected. Most of the parameters and section properties have been retained in the example below except that the members are now tubular sections and interaction effects are properly considered. The equivalent dimensions for the tube are d = 0.3222m and t = 0.0046m. These dimensions are somewhat impractical but this is not important if local and overall buckling behaviour are neglected.

Although this structure is not directly relevant to offshore structures the principle of the analysis can be extended for use in more general situations.

4.2 Description of the structure

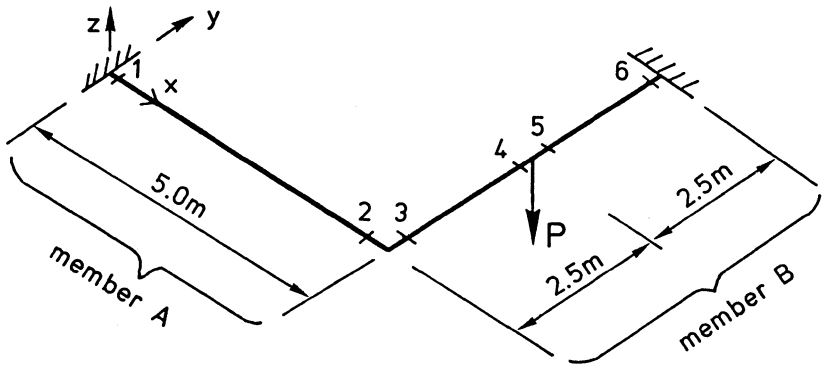

Figure 3: Sketch of the structure

The 2-D frame is acted upon by an out-of-plane point load P. All the joints and supports are rigid and both members consist of uniform tubular sections with the following deterministic properties:

X-sectional Area	=	4.59×10^{-3} m^2
$I_y = I_z$	=	57.9×10^{-6} m^4
Torsion, I_{yz}	=	115.8×10^{-6} m^4
Young's Modulus	=	2.1×10^{8} kN/m^2

The material is assumed to be elastic–perfectly plastic, and plastic hinges can only form according to von Mises criterion in the 6 positions shown:

$$f_b^2 + 3 f_v^2 = F_y^2$$

where $f_b = M/td^2$

$f_v = T/\frac{1}{2}\pi td^2$ (neglecting vertical shear)

F_y = yield stress in simple Tension

and where d is the tube diameter, and t is the wall thickness.

The following are considered as normally distributed random variables:

$E[P] = 60kN$ C of V for $[P] = 0.1$

$E[F_y] = 282.5 \times 10^3$ kN/m^2 C of V for $[F_y] = 0.1$

Three cases are to be considered:

a) F_y uniform throughout the structure

b) F_y uniform within members and independent between members A and B

c) F_y independent for all 6 possible hinge positions.

4.3 The reliability of the structure at level 1 (i.e. one hinge to form)

Using von Mises criterion the safety margin Z_j can be written for any position j (j = 1, 2 ... 6).

$$Z_j = F_{yj}^2 - \left[\frac{m_j^E P}{td^2}\right]^2 - 3\left[\frac{t_j^E P}{\pi td^2/2}\right]^2 \qquad (1)$$

where m^E_j and t^E_j are the elastic moment and torque at position j under a unit value of load P.

The results of the analysis at the corresponding failure boundaries have been mapped into standard normal space (u–space) and are plotted in Figure 4. For convenience the 5 failure surfaces have been superimposed in the one graph.

Case a) Yield stress uniform throughout the structure

In this case where all the yield stresses are equal, the event space can be represented in 2 dimensions (u_p and u_{Fy}). Figure 4 shows that plasticity must occur first at position 6. If a hinge were to develop first elsewhere it would violate the yield criterion at 6.

Therefore, the reliability of the structural system at Level 1 is $\beta[\frac{1}{S}]_{YS} = \beta_6 = 2.4698$

Case b) Yield stresses uniform within members and independent between members A and B

i.e. $F_{y1} = F_{y2}$ and $F_{y3} = F_{y4/5} = F_{y6}$; F_{y1} independent of F_{y3}

From Figure 4 (which should now be plotted in three dimensions as there are 3 independent random variables) it can be seen that plasticity would occur in member A at position 1 before position 2; and it would occur in member B at position 6 before positions 3 or 4/5. As the yield stresses are independent between the members plasticity can occur either at position 1 or position 6, although it is more likely to occur at 6.

Hence, the failure probability of the system at Level 1 is given by:

$$P_f^{[1]} = P\left[E_1 \cup E_6 \right] = \Phi \left\{ -\beta_1, -\beta_6 ; \rho_{16} \right\}$$

Therefore the reliability of the system at level 1 is:

$$\beta_{sys}^{[1]} = -\Phi^{-1} \left\{ P_f^{[1]} \right\} = 2.470$$

Case c) Yield stresses independent at all 6 positions

A hinge has a chance of occurring at any of the 6 positions, although it is most likely to occur first at position 6.

Therefore, at level 1 $P_f^{[1]} = P[E_1 \cup E_2 \cup E_3 \cup E_{4/5} \cup E_6]$

$$\beta_{sys}^{[1]} = -\Phi^{-1} \left\{ P_f^{[1]} \right\} = 2.470$$

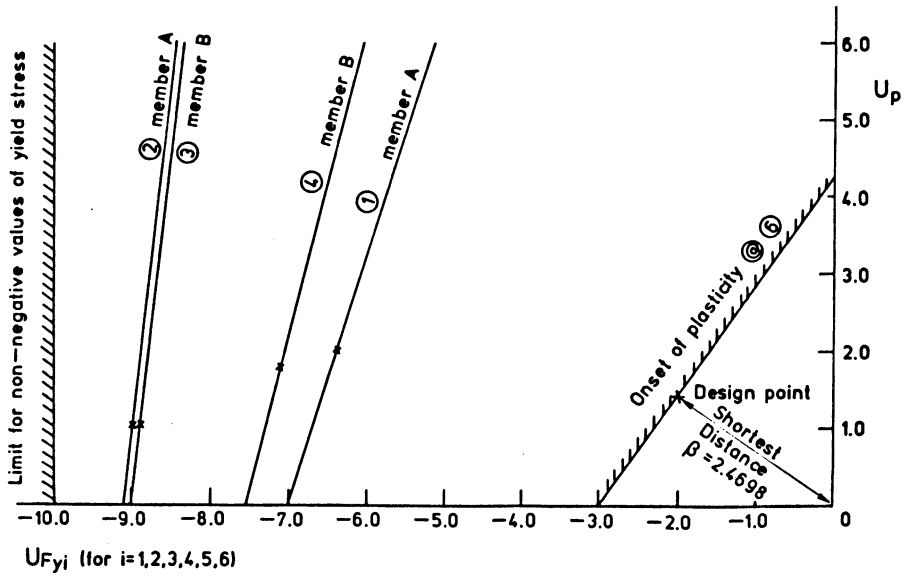

Figure 4: Plot in standard normal space for the onset of plasticity of the intact structure.

4.4 The Reliability of the Structure at level 2 (i.e. Two Hinges to Form)

Hinge first at Position 6

Consider the behaviour of the structure once the first hinge has formed, assuming that this is at position 6. When the hinge just forms it must obey von Mises criterion:

$$F_{y6}^{\ 2} = \left[\frac{m_6^E P^E}{td^2}\right]^2 + 3\left[\frac{t_6^E P^E}{\pi td^2/2}\right]^2 \qquad (2)$$

where m_6^E and t_6^E are elastic influence coefficients for the intact structure.
P^E is the load required to just form a hinge first at position 6.

For a further increase in load, the stress state at position 6 must still satisfy the limit state function, and the additional load will cause rotations at the hinge which must obey the flow rule. Plastic flow causes the stress state to move around the limit state surface, and the total change in stress state due to plastic flow depends on the total increase in load ΔP, where the total load $P^T = P^E + \Delta P$.

Unfortunately, there is no simple analytic method to evaluate the change in stress state resulting from plastic flow. However, there are a number of iterative and incremental methods which are suitable for use in system reliability analyses. Sloan (1987) outlines two of the methods currently used in non-linear finite element analysis programs. The method described here is based on the Euler integration scheme, although some of the results given later were evaluated using a different method.

For a small increment of load, δP, the stress state is assumed to move initially to some point along the tangent to the yield surface. The normal (and hence tangent) can be evaluated from the flow rule:

$$d\theta_6 = 2\lambda f_{b6} = 2\lambda\left[\frac{M_6 + \delta M_6}{td^2}\right] \; ; \; d\gamma_6 = 6\lambda f_{v6} = 6\lambda\left[\frac{T_6 + \delta T_6}{\pi td^2/2}\right] \qquad (3)$$

Where δM_6 and δT_6 are constraining forces applied to the hinge such that the flow rule is satisfied, and $d\theta_6$ and $d\gamma_6$ are incremental rotations at the hinge.

For a small increment

$$d\theta_6 = \theta_6^p\,\delta P + \theta_6^m\,\delta M_6 + \theta_6^t\,\delta T_6 \qquad (4a)$$

$$d\gamma_6 = \gamma_6^p\,\delta P + \gamma_6^m\,\delta M_6 + \gamma_6^t\,\delta T_6 \qquad (4b)$$

Equations 3 and 4 can be solved for δM_6 and δT_6.

Obviously, this new stress state lies outside the region bounded by the yield surface. Therefore, the stresses must be "corrected" to satisfy the yield condition. There is no unique method to scale the stresses, but the simplest is to assume that the correction is applied in a radial direction.

i.e.

$$T'_6 = \left[\frac{T_6 + \delta T_6}{M_6 + \delta M_6}\right] M'_6 \tag{5}$$

$$F_{y_6}^2 = \left[\frac{M'_6}{td^2}\right]^2 + \left[\frac{T'_6}{\pi td^2/2}\right]^2 \tag{6}$$

Equations 5 and 6 are then solved to determine the stress state after a load increment δP. The procedure can then be repeated for further increments δP. δP is usually chosen as a factor of ΔP, and obviously the accuracy of the method depends on the size of the sub-increments. One increment can be used although this will lead to a small over-estimation in the effect of plastic flow. 5 or 6 increments should in general produce reasonable accuracy for use in a system reliability analysis.

Once the stress state has been evaluated for the addition of the total load, the total change in moment and torque at the hinge due to plastic flow is:

$$\Delta M_6 = M'_6 - M_6^E$$
$$\Delta T_6 = T'_6 - T_6^E$$

The safety margin for any other position can then be written:

$$Z_j = F_{yj}^2 - \frac{1}{(td^2)^2}\left\{ m_j^E P^E + m_{6j}\Delta P + m_{6mj}\Delta M_6 + m_{6tj}\Delta T_6 \right\}^2$$
$$- \frac{3}{(\pi td^2/2)^2}\left\{ t_j^E P^E + t_{6j}\Delta P + t_{6mj}\Delta M_6 + t_{6tj}\Delta T_6 \right\}^2$$

where m_j^E, t_j^E are elastic influence coefficients for the undamaged structure.
m_{6j}, t_{6j}, m_{6mj}, t_{6mj}, m_{6tj}, t_{6tj} are elastic influence coefficients for the structure with a hinge at position 6.

Pos.	Case a) F_y Uniform	Case b) F_y independent between members	Case c) F_y independent
1	4.613	5.974	5.974
2	8.780	9.248	9.248
3	8.884	8.884	9.180
4/5	5.503	5.503	7.043

Table 1: Reliability indices at level 2 given a hinge has formed at position 6

Case a) Yield stress uniform through the structure (with hinge at position 6)

By inspection of the results in Table 1, plasticity can only occur at position 1 given that a hinge has already formed at position b. Therefore for level 2 the system reliability index if $\beta_{sys}^{[2]} = 4.613$

Case b) Yield Stresses uniform within members and independent between members A & B (with hinge at position 6)

By inspection of the results for case b) in Table 1, it can be seen that plasticity would occur in member A at position 1 before position 2; and it would occur in member B at position 4/5 before position 3. Therefore, a second hinge can form at either position 1 or position 4/5, and the corresponding reliability indices are:

Hinge at 6 followed by hinge at 1: $\beta = 5.974$
Hinge at 6 followed by hinge at 4/5: $\beta = 5.503$

Case c) Yield stresses independent (with hinge at position 6)

A hinge can form at any of the positions given in Table 1, although it is most likely to form at position 6 with $\beta = 5.9735$.

More detailed results are given in Turner (1986) and and results are also given for a hinge forming first at position 1 and also at position 4/5.

4.5 The enumeration method for collapse

The system reliability can be evaluated at level 3 in a similar manner to level 2 and the enumeration method can be followed up until structural collapse. The failure tree is shown for the 3 cases in Figs. 8a, 8b, and 8c.

Fig 5 is a part plot of the Moment–Torque interaction curve which shows the stress path from zero load to a collapse mechanism with hinges at positions 1 and 6. (The figure is drawn for $F_{y_1} = F_{y_6} = 161.9 \times 10^3$).

The stress path for position 6 is linear–elastic from O to C until it reaches the limit surface and a hinge forms. Then under plastic flow it moves from C around the limit surface to D when a hinge forms at postion 1. Then it moves from D to E when collapse occurs.

The stress path for position 1 is linear elastic from O to A when a hinge occurs at position 6. The stiffness of the structure changes and the stress path is linear elastic to B, when it reaches the limit surface. Then it moves under flow to E when collapse occurs.

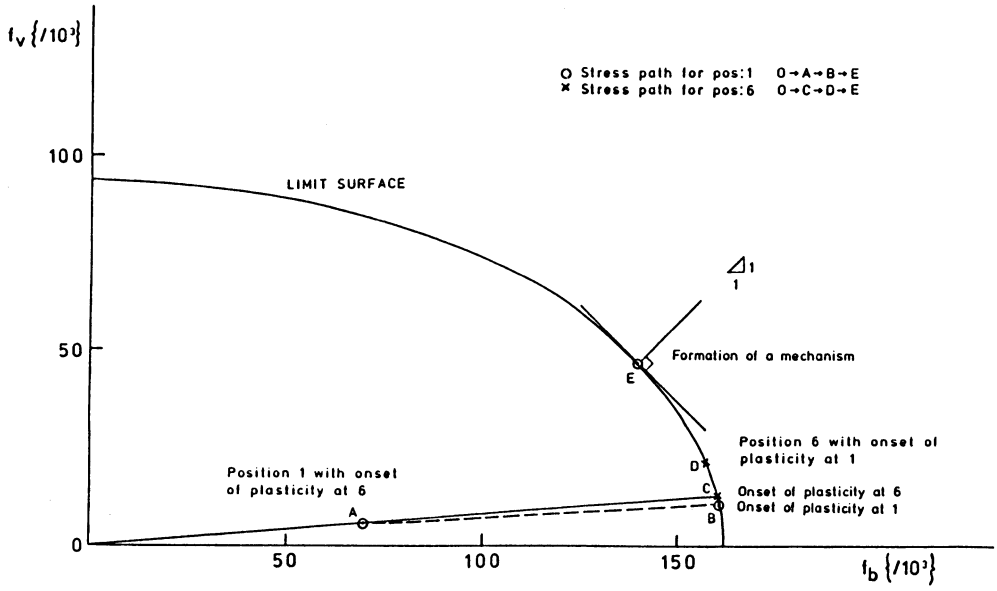

Figure 5: Torque stress/Bending stress interaction curve

4.6 The Mechanism Approach

Mechanism 1: Hinge formation at positions 1 and 6.

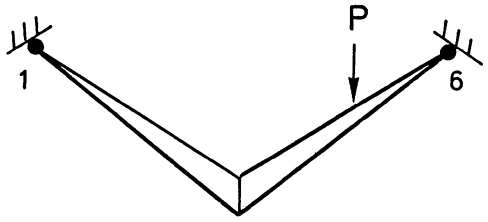

Figure 6: Mechanism 1.

From virtual work:

$$5P\theta/2 = M_1\theta_1 + T_1\gamma_1 + M_6\theta_6 + T_6\gamma_6 \qquad (7)$$

Now $\theta_1 = \gamma_6 = \theta_6 = \gamma_1 = \theta$

At each hinge the flow rule must be satisfied.

$$\theta_i = 2\lambda \frac{M_i}{(td^2)} \quad \text{and} \quad \gamma_i = 6\lambda_i \frac{T_i}{(\pi td^2/2)}$$

Also the stresses at each hinge must satisfy von Mises criterion.

$$F_{yi}^2 = \left[\frac{M_i}{td^2}\right]^2 + 3\left[\frac{T_i}{\pi td^2/2}\right]^2$$

After rearranging and substituting in equation (7) the safety margin can be written as:

$$Z = 1.31948\ td^2 F_{y_1} + 1.31948\ td^2 F_{y_6} - 2.500P$$

The results for this mechanism are given in Table 2.

Mechanism 2: Hinge formation at positions 1, 4 and 6.

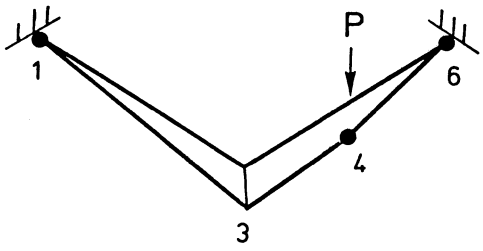

Figure 7(a): Mechanism 2

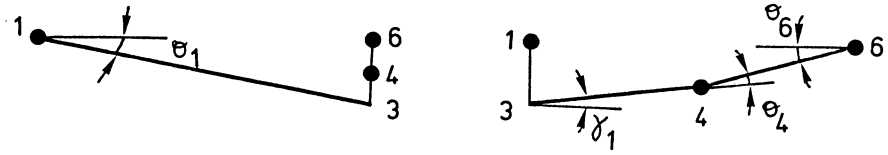

Figure 7(b): Rotations for mechanism 2

From virtual work:

$$2.5\ P\theta_6 = M_1\theta_1 + T_1\gamma_1 + M_4\theta_4 + T_4\gamma_4 + M_6\theta_6 + T_6\gamma_6 \quad (8)$$

Now $\theta_4 = \theta_6 - \gamma_1$

$\theta_1 \ell = \theta_6 \ell/2 + \gamma_1 \ell/2$ i.e. $2\theta_1 = \theta_6 + \gamma_1$

$\theta_1 = \gamma_6 + \gamma_4$

Also from the flow rule:

$$\frac{\theta_i}{\gamma_i} = \frac{M_i}{3T_i/(\pi/2)} = \frac{M_i}{1.90986T_i}$$

Using von Mises Criteria:

$$M_i = \frac{\theta_i t d^2 F_{yi}}{(\theta_i^2 + \gamma_i^2/3)^{\frac{1}{2}}} \quad ; \quad T_i = \frac{\gamma_i t d^2 F_{yi}}{1.90986(\theta_i^2 + \gamma_i^2/3)^{\frac{1}{2}}}$$

From equilibrium: $T_4 = T_6$

$$M_4 - T_1 = \tfrac{1}{2}(M_1 + T_4)$$

And $$0 = M_1 + T_1 + M_6 + T_6 - 2.5P \qquad (9)$$

Also the basic virtual work equation, equation (8), can be simplified by substitution of the geometric and equilibrium constraints to give:

$$0 = -T_1 + 2M_4 + M_6 - 2.5P \qquad (10)$$

The safety margin can then be written by adding 2 equations (9) and (10) together to give:

$$Z = M_1 + 2M_4 + 2M_6 + T_6 - 5.0P$$

Mechanism	Case a) F_y Uniform	Case b) F_y independent between members	Case c) F_y independent
Mechanism 1 Hinges at 1+6	5.333*	7.030	7.030
Mechanism 2 Hinges at 1, 4/5 + 6	5.080	6.018	7.550

Table 2: Reliability indices for mechanisms 1 and 2

* The results for mechanism 1 case a) are invalid because it can be shown that a further hinge would form at position 4 before collapse occurs.

4.7 The Results

No particular method has been used to truncate the branches of the failure tree; only obviously insignificant paths have been truncated. The system is dominated by one or two failure paths and any of the available truncation strategies would have reduced the computation and produced acceptable results.

Unfortunately the probabilities of failure for many of the events immediately prior to collapse could not be evaluated. The RELY program would only converge to design points in physically inadmissible regions if the initial starting values for the program were in the correct region of the event space, i.e. close to the design point. Satisfactory initial values could not be found for many of the events immediately prior to collapse.

Case a) Yield stress uniform throughout the structure

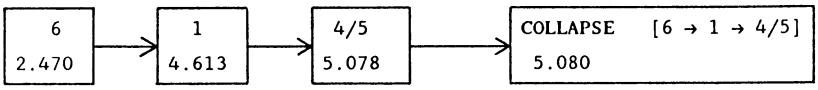

Figure 8(a): The failure tree for case a)

Case b) Yield stress uniform within members and independent between members A and B

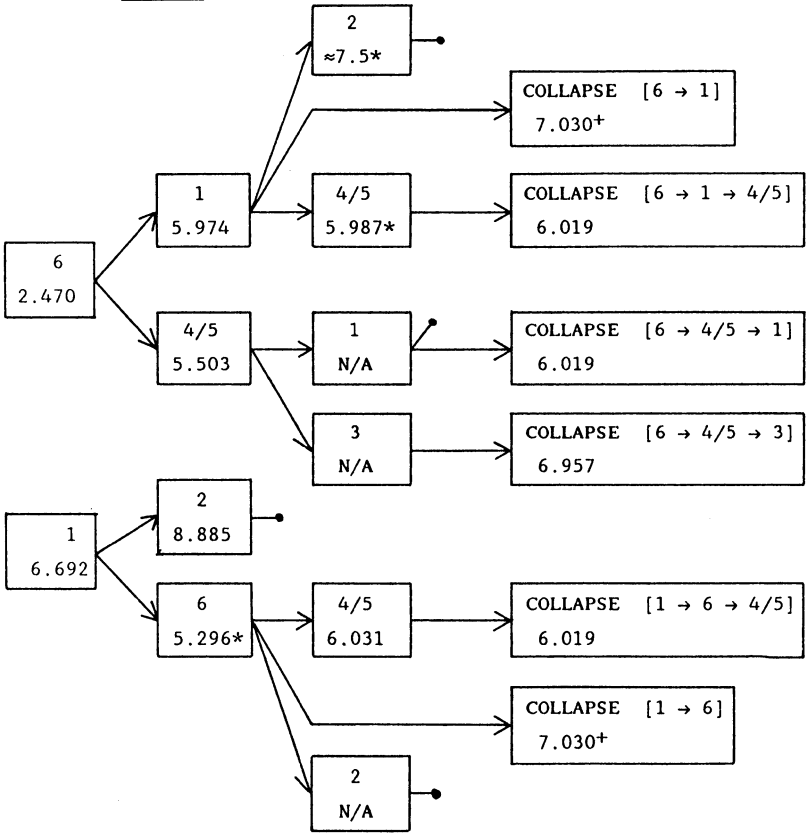

Figure 8(b): The failure tree for case b)

+ This mechanism cannot physically occur for values of yield stress at the design point.

* Design point is in a physically inadmissible region.

N/A Results not available

Case c) Yield stresses independent

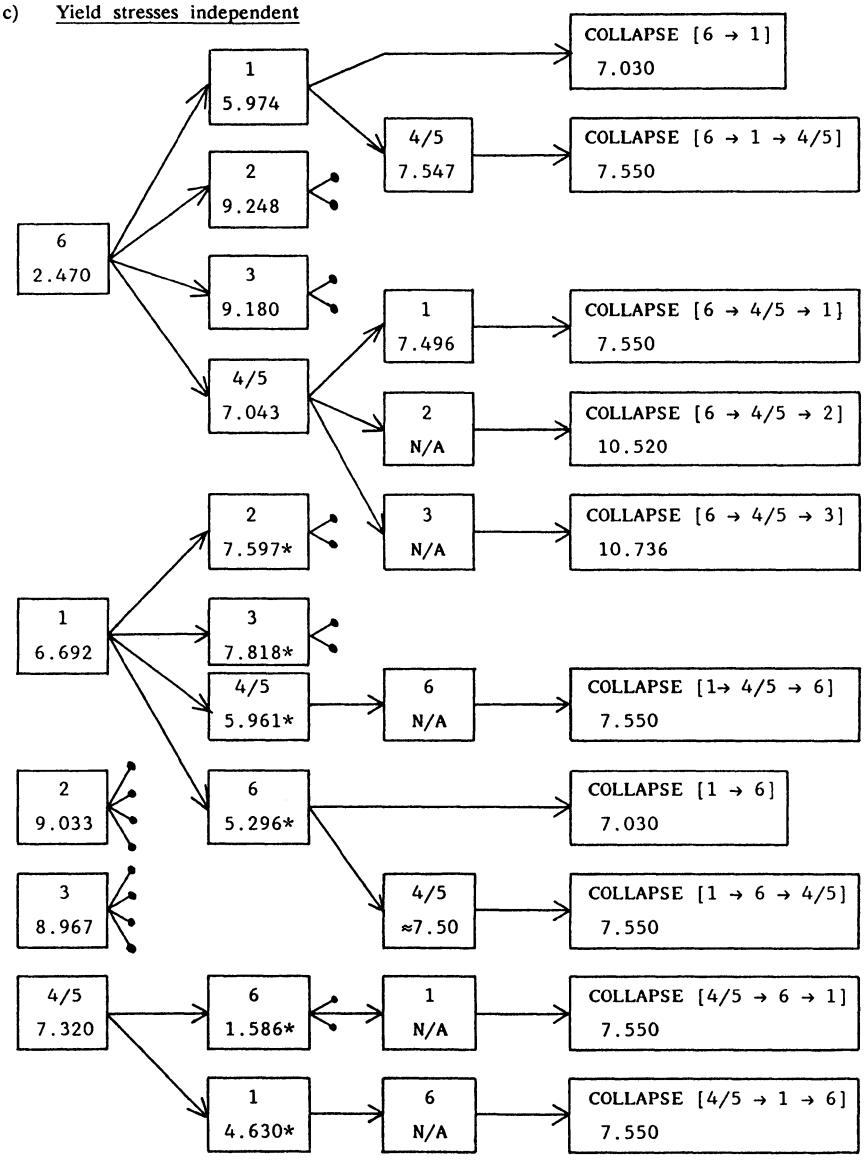

Figure 8(c): The failure tree for Case c)

---

* Design point in physically inadmissible region.

N/A Results not available

Tables 3a, 3b and 3c show the system reliabilities for the three cases. Probabilities of failure for the

Tables 3a, 3b and 3c show the system reliabilities for the three cases. Probabilities of failure for the significant failure paths have been evaluated at each level of analysis, (i.e. as each hinge forms) and the union of these has been evaluated to obtain the system reliability at each level. More detailed results are given in Turner (1986).

For case a) in which the yield stress is uniform throughout the structure, there is only one permissible path to failure. The probability that one hinge will form in the structure is approximately 0.0068, however, the structure can carry a considerable increase in load and the probability that the structure will go on to collapse is only 0.0020×10^{-3} (i.e. 2.0×10^{-6}).

For case b) in which the yield stresses within each member are uniform there are more possible failure paths. However, one is dominant. The probability that the structure will collapse is even less at 8.8×10^{-10}.

For case c) in which the yield stresses are independent throughout the structure there are many more possible failure paths. The dominant failure path to collapse is different from the previous cases, and the probability that the structure will collapse is 1.0×10^{-12}.

One interesting point is that if the structure had been designed elastically (using the AISC) with a nominal yield stress of 225 N/mm^2 (i.e. 2 standard deviations from the mean), the maximum allowable design load would be 34 kN. The collapse loads at the design points in the above cases are all over 72 kN.

It should just be mentioned that the system reliabilities at level 3 for cases b) and c) in Tables 3b and 3c are not lower bounds on the overall system reliability. This is because a full set of results was not evaluated.

Case a) Yield stress uniform throughout the structure

Level 1	Level 2	Level 3	Mechanism
$\beta^{[1]}_{sys} = 2.470$	$\beta^{[2]}_{sys} = 4.613$	$\beta^{[3]}_{sys} = 5.078$	$\beta_{sys} = 5.080$

Table 3a: The system reliability indices for case a)

Case b) Yield stresses uniform within members and independent between members A and B

Level 1	Level 2	Level 3	Mechanism
$\beta^{[1]}_{sys} = 2.470$	$\beta^{[2]}_{sys} = 5.493$	$\beta^{[3]}_{sys} = 6.350$	$\beta_{sys} = 6.019$

Table 3b: The system reliability indices for case b

Case c) Yield stresses independent

Level 1	Level 2	Level 3	Mechanism
$\beta^{[1]}_{sys} = 2.470$	$\beta^{[2]}_{sys} = 5.974$	$\beta^{[3]}_{sys} \approx 7.550$	$\beta_{sys} = 7.028$

Table 3c: The system reliability indices for case c)

DISCUSSION AND CONCLUSIONS

The purpose of this work was to investigate the use of multi-dimensional failure criteria with the system reliability analysis of structures. However, before concluding, a number of questions must be considered:

1. Is it necessary to use multi-dimensional criteria? This of course depends on the structure, the type of loading, and the failure function itself. Where interaction does occur its significance should be investigated, because the effect can be considerable. For instance, the effect of moment on an axial brace can seriously reduce the axial load capacity of the member. It is obvious that if interaction is ignored the strength of the member, and hence of the structure, will be overestimated, and the resulting probablity of failure will be unconservative.

2. If the failure surface is non-linear can it be linearized? Again this depends on the circumstances. Consider the formation of the first hinge in the structure analysed in this report. At the design point for position 6 a load of 68.5 kN is required for a hinge to form. If the failure surface had been linearized the load required would only be 51.2 kN. Thus the strength of the member and structure is underestimated, and the resulting probability of failure will be conservative.

3. Can the flow rule be ignored? The effect of plastic flow at the hinges can cause a significant redistribution of moments and forces within the structure. Again consider the structure analysed in the report. For case (c) with independent yield stress, the bending moment/torque ratio at position 6 when the first hinge forms is 8.36; this changes to 2.82 at collapse. The reliability index for the formation of a hinge at position 1 given that a hinge has already formed at position 6 is 5.974. If the flow rule had been ignored, so that the moment/torque ratio at position 6 remained constant at 8.36, the corresponding reliability index would have been 5.770. This may be considered to be an insignificant difference, except that the structure cannot carry any further increase in load, and so this must be considered to represent a collapse mechanism. The reliability for this system is also 5.770. There is a considerable difference between this value and the

corresponding value of 7.031 in Table 3c in which the flow rule is allowed for. It should also be noted that if the flow rule is neglected the sequence 6 → 1 → 4/5 could not form.

In this example the probability of failure is overestimated if the flow rule is ignored. In general this will usually be the case. However, if the flow rule is neglected, failure sequences that are derived may be incorrect, and mechanisms may be found which cannot physically occur. Thus any results for structural collapse from such an analysis should be carefully investigated.

The main advantage of the analysis method is that it is rigorous given the assumptions of perfectly-elastic plastic behaviour and bi-linear moment-curvature relationship. Hence, there is no additional concern over how conservative or unconservative the results are, as would be the case if the flow rule had been ignored. The method is flexible and can be used with both a successive elastic analysis approach and a direct mechanism approach to determine the probability of collapse. Both aproaches result in the same overall probability of collapse.

One apparent disadvantage of the method is the amount of calculation and equation manipulation that is required to determine the reliability of each event. However, the successive elastic analysis can be automated. The equations for the failure functions and plastic flow conditions can be easily generated using values for stresses and deflections obtained from successive elastic analyses. Unfortunately, the collapse mechanism approach is not so readily automated. Although, once the equations are determined, they can be readily solved.

The main disadvantage of the method is that it does not always converge for failure sequences that involve unloading, or that have design points in physically inadmissible regions. It has been shown that it is important to obtain all the values. However, approximate results can usually be obtained which are often good enough.

Therefore, considering all these points, since the method can be partly or fully automated, it is capable of being used to treat multi-dimensional failure criteria in more complex structures. The method is rigorous and can produce accurate results. Unfortunately, many of the approximate and simplified methods that can be used as an alternative to multi-dimensional failure criteria will produce inaccurate and misleading results.

Until now, the residual stresses have been assumed to be zero. Real structures are subjected to residual stresses which may be considerable. Their effect can be to greatly distort the component reliabilities at the earlier levels of a successive elastic analysis approach. Hence, the failure sequences can also be in error whether or not the flow rule

has been allowed for. Therefore, although each subsequent level of analysis is a better estimate to the overall system reliability at collapse, this point must always be borne in mind.

Finally, it is most important that the results of any reliabilty analysis are interpreted with care.

ACKNOWLEDGEMENTS

The work described in this paper has been carried out as part of the programme of the London Centre for Marine Technology on "System Reliability of Fixed Offshore Platforms", and has been jointly funded by SERC (MTD Ltd), Atkins Research and Development and Shell U.K. Exploration and Production.

REFERENCES

AISC, American Institute of Steel Construction (1980): Specifications for the design, fabrication and erection of structural steel for buildings.

Baker, M.J., (1985): The reliability concept as an aid to decision making in offshore structures. 4th BOSS Conference, Delft, The Netherlands.

Crohas, H., Ali-Asghar Tai, Hachemi-Safai & Barnouin, B. (1984): Reliability analysis of offshore structures under extreme environmental loading. Paper OTC 4826, 16th Offshore Technology Conference, Houston, Texas.

Ditlevsen, O. & Bjerager, P. (1984): Reliability of highly redundant plastic structures. Journal of Engineerng Mechanics, ASCE, Vol. 110, N0. 5.

Edwards, G.E., Heidweiller, A., Kerstens, J. & Vrouwenvelder, A. (1985): Methodologies for limit state reliability analysis of offshore jacket platforms. 4th BOSS Conference, Delft, The Netherlands.

Heyman, J. (1971): Plastic design of frames Vol. 2. Cambridge University Press.

Martin, J.B. (1975): Plasticity - fundamentals and general results. The MIT Press, Cambridge, Massachusetts.

Ramachandran, K. (1984): System bounds - a critical study. Civil Engineering Systems, Vol.

Sloan, S.W., (1987): Substepping schemes for the numerical integration of elasto-plastic stress strain relations. International J. of Numerical Methods in Engineering, Vol. 24.
Tang, L.K. & Melchers, R.E. (1984): Multinormal distribution function in structural reliability. Report No. 6/1984, Monash University, Melbourne.

Thoft-Christensen, P. (1984): Reliability analysis of structural systems by the β-unzipping method structural reliability theory. Paper No.3, Instituttet for Bygningsteknik, Aalborg University Centre, Denmark.

Thoft-Christensen, P. & Baker, M.J. (1982): Structural reliability theory and its applications. Springer-Verlag, Berlin.

Turner, R.C. & Baker, M.J. (1986): MULTIN user manual - approximate solutions to multivariate normal distribution functions. Report No. SSRG/1/86, Imperial College.

Turner, R.C. (1986): Structural system reliability analysis using multi-dimensional limit state criteria. Report No. SSRG/2/86, Imperial College.

Watwood, V.B. (1979): Mechanism generation for limit analysis of frames. J. of Struct. Div. ASCE. Vol. 105, No.1.

APPENDIX

Evaluating the change in stress state due to plastic flow

The evaluation of the change in stress state resulting from pl
problem which is being widely researched. The problem frequently occurs in non-linear finite element programs in which the stress state may have to be evaluated at many thousands of locations within a structure. Unfortunately, there is no simple analytic solution method.

However, there are a number of approximate iterative and incremental methods which are suitable for use in system reliability analyses. A simple method was used in this paper, but for the latest published research see Sloan (1987) who outlines two of the methods in current use, and suggests some improvements. Perhaps the most well-known and widely used method is the first-order Euler integration scheme.

The first step in the Euler scheme (and any other method) is to determine the initial stress state at which yielding begins. In the paper this corresponds to solving eq. 2 in section 4.4. The problem is then to determine the change of stress state that occurs for a further increase in load.

The enumeration approach to system reliability analysis discussed in this paper leads to a slightly different problem to that which is generally encountered in non-linear FE analysis programs. In this paper the structural model is modified when a hinge forms and is then re-analysed for separate load cases as discussed in section 3.2. Hence, with this method there is no prescribed strain increment. Instead, it is assumed here that for a small increment in load the stress state initially moves to some point along the tangent to the yield surface.

Obviously, for elastic perfectly plastic materials, another point along the tangent will lie outside the region bounded by the yield surface. Therefore, the stresses must be

"corrected" to satisfy the current yield condition. There is no unique method to scale the stresses. The simplest method is to assume that the correction is applied in a radial direction. This method leads to a small over-estimation in the effect of the plastic flow, and a better method is to assume that the correction is applied along a direction which is normal to the yield function. This method is usually done iteratively, and often only the first iteration is performed.

In the Euler scheme the load ΔP is divided into a number of smaller increments, or sub-increments, and the stress state is usually up-dated after each sub-increment. Obviously the accuracy of the scheme depends on the size of the sub-increments. In FE programs the number of sub-increments, n, is typically of the order:

$$n = 1 + 20\ \sigma_R/\sigma_y$$

where

σ_y is the yield stress

σ_R is the approximate change in stress caused by ΔP.

More general material behaviour assumptions are easily modelled in the Euler scheme. The yield condition can be up-dated after each sub-increment of load to allow for strain hardening, work hardening etc. The stress-state after each sub-increment is then "corrected" to satisfy the current yield condition.

SENSITIVITY MEASURES IN STRUCTURAL RELIABILITY ANALYSIS

Peter Bjerager & Steen Krenk
Department of Structural Engineering, Building 118
Technical University of Denmark, DK-2800 Lyngby, Denmark

ABSTRACT

Both reliability and sensitivity measures are important results of a structural reliability analysis. For reliability problems of the random variable type the measures can be computed approximately by first and asymptotic second order reliability methods. In this paper the parametric sensitivity of the most likely failure point is studied. A formula for the sensitivity of the unit normal vector to the failure surface in this point is derived. The parametric sensitivity of the first order reliability index is considered as well, and examples illustrating the results are given. Finally it is shown how parametric sensitivity factors for the probability of failure can be estimated by directional Monte Carlo simulation.

INTRODUCTION

A structural reliability analysis provides *reliability* measures and, often equally important, *sensitivity* measures. A set of useful sensitivity measures consists of the *parametric sensitivity factors*. Let the reliability be measured in terms of the reliability index $\beta_R = \Phi^{-1}(1-p_F)$, where p_F is the probability of failure and Φ^{-1} is the inverse standard normal distribution function. A parametric sensitivity factor with respect to the deterministic parameter θ is then equal to the derivative of the reliability index β_R with respect to this parameter, i.e. $d\beta_R/d\theta$. Typically, θ is a deterministic physical basic variables, e.g. a structural dimension, or a distributional parameter such as mean value or standard deviation. Usually more than one parameter enter a reliability problem. Each sensitivity factor is then defined as a partial derivative.

The parametric sensitivity factors for the reliability index have a number of important practical applications. The following can be mentioned:

- Within *reliability based design* a structure is designed by choosing the values of a set of design parameters θ such that the reliability of the structure is equal to a specified/codified value β_C. After the initial choice of the design parameters and a corresponding reliability analysis, guidance for the next choice $\theta+\Delta\theta$ can be obtained by the requirement that $\beta_R(\theta+\Delta\theta)$ should be equal to β_C using

$$\beta_R(\theta+\Delta\theta) \approx \beta_R(\theta) + \sum_i \frac{\partial\beta_R(\theta)}{\partial\theta_i}\Delta\theta_i \qquad (1)$$

- In *reliability based optimization* of structural design, construction, maintenance and inspection where the optimal solution, e.g. design or inspection strategy, is

found by solving a mathematical programming problem. The partial derivatives of the reliability with respect to the decision parameters are then needed in the computations.

- In a *parameter study* of the reliability where Eq. 1 can be applied to interpolate between parameter values for which a full reliability analysis is performed.
- Within *reliability updating* where the reliability is updated e.g. after inspection, probabilities conditioned on the new information must be calculated. For information that can be expressed as a function of a random vector being equal to zero, the conditional probability can be formulated as the ratio between parametric sensitivity factors, [7].

For a structural reliability problem of the continuous random vector type the reliability index β_R is efficiently, though approximately, computed by first or second order reliability methods, [5,6]. A parametric sensitivity factor $d\beta_R/d\theta$ can then be calculated numerically by repeated computations of the reliability index. However, without repeating the possibly expensive reliability analysis, the factors can be calculated more directly by use of asymptotic results derived in [4].

Part of the common results of a first order reliability analysis includes the unit directional vector $\boldsymbol{\alpha}$ to the most likely failure point on the failure surface. Also the parametric sensitivity of this vector turns out to have important practical applications of which two are mentioned here:

- In structural *system reliability* analysis where each component is described by a reliability index $\beta_{R,i}$ and a unit normal vector $\boldsymbol{\alpha}_i$. Dependence between component i and j can be described by the correlation coefficient given as the scalar product $\boldsymbol{\alpha}_i^T\boldsymbol{\alpha}_j$. The system reliability can be quite sensitive to the value of this correlation coefficient. This is for example the case for a series system of highly correlated components of equal or almost equal reliabilities. Thus, the change in $\boldsymbol{\alpha}_i$ caused by a change in a parameter θ may be significant in a system reliability analyses.
- In *outcrossing problems* where the failure surface is described in terms of a random vector. Such a problem may be dealt with by combining FORM/SORM and results from outcrossing analysis. For this task, the derivative of the unit normal vector with respect to a deterministic parameter is needed, [8].

In this paper an expression for $d\boldsymbol{\alpha}/d\theta$ is derived. This sensitivity factor can then be computed without numerical differentiation, i.e. without repeated reliability analyses. The result is based on an analysis of the derivative $d\mathbf{u}^*/d\theta$ of the most likely failure point. The results are valid for cases where the failure function is differentiable in this point. Also the known result for the sensitivity of the first order reliability index $d\beta/d\theta$ is obtained in the analysis. Finally, it is shown how a parametric sensitivity factor for the probability of failure can be estimated by directional Monte Carlo simulation.

FIRST ORDER RELIABILITY ANALYSIS

Consider a reliability problem defined in terms of the safety margin $G(\mathbf{X})$ where G is the failure function and $\mathbf{X}$ is the vector of physical basic variables with density $f_{\mathbf{X}}(\mathbf{x})$. Failure occurs when $G(\mathbf{X}) \leq 0$, whereas $G(\mathbf{X}) > 0$ identifies a safe state. Assuming that the probability distribution of $\mathbf{X}$ is continuous, a variable transformation $\mathbf{T}: \mathbf{X}=\mathbf{T}(\mathbf{U})$ exists such that $\mathbf{U}$ is a vector of n independent, standardized Gaussian variables, see [6]. The failure function in u-variables is $g(\mathbf{u}) = G(\mathbf{T}(\mathbf{u}))$, and the probability of failure p_F equals $P[g(\mathbf{U}) \leq 0]$.

Application of a first order reliability method implies that the failure surface in u-space, $\partial F = \{\mathbf{u} \mid g(\mathbf{u})=0\}$, is approximated by its tangent hyperplane in the point $\mathbf{u}^*$ closest to the origin. Here it is assumed that only one such point exists, i.e. that the surface is relatively flat, and that $g(\mathbf{u})$ is differentiable in this point.

The *first order reliability index*, β, is defined as the minimum distance from the origin to the failure surface in u-space. The most likely failure point $\mathbf{u}^*$ satisfies

$$\mathbf{u}^* = \beta\alpha, \quad \beta = \sqrt{\mathbf{u}^{*T}\mathbf{u}^*} \tag{2}$$

where α is the unit normal vector to the limit state surface in $\mathbf{u}^*$. In terms of the gradient vector

$$\nabla g(\mathbf{u}) = \left(\frac{\partial g(\mathbf{u})}{\partial u_1}, \frac{\partial g(\mathbf{u})}{\partial u_2}, \ldots, \frac{\partial g(\mathbf{u})}{\partial u_n}\right) \tag{3}$$

α can be expressed as

$$\alpha = -\frac{\nabla g(\mathbf{u}^*)}{|\nabla g(\mathbf{u}^*)|} \tag{4}$$

The first order approximation to the failure probability is $\Phi(-\beta)$. Improved approximations to the probability can be obtained by (asymptotic) second order reliability analysis, [5,6].

PARAMETRIC SENSITIVITY OF β AND α

Now, assume the reliability problem involves a deterministic parameter θ such that the failure surface in u-space can be written

$$g(\mathbf{u},\theta) = 0 \tag{5}$$

If θ is a deterministic physical variable, θ appears in the failure function $G = G(\mathbf{X},\theta)$, whereas, if θ is a distributional parameter it enters the problem in the variable transformation, i.e. $\mathbf{T} = \mathbf{T}(\mathbf{U},\theta)$. In the present analysis the problem is described solely in the general form in Eq. 5. In practical applications the origin of θ may be exploited and derivatives of $g(\mathbf{u},\theta)$ may conveniently be expressed in terms of G and $\mathbf{T}$ quantities and derivatives thereof.

The derivative of the first order reliability index β with respect to the parameter θ is

$$\frac{d\beta}{d\theta} = \alpha^T \frac{d\mathbf{u}^*}{d\theta} \tag{6}$$

using $\beta = \sqrt{\mathbf{u}^{*T}\mathbf{u}^*}$.

Correspondingly, the derivative of the unit normal vector $\alpha = \mathbf{u}^*/\beta$ in the most likely failure point can be written

$$\frac{d\alpha}{d\theta} = \frac{1}{\beta}\left(\frac{d\mathbf{u}^*}{d\theta} - \frac{d\beta}{d\theta}\alpha\right) = \frac{1}{\beta}\left(\frac{d\mathbf{u}^*}{d\theta} - \alpha^T\frac{d\mathbf{u}^*}{d\theta}\alpha\right) \tag{7}$$

using the result in Eq. 6.

Both derivatives are a function of the derivative $d\mathbf{u}^*/d\theta$ of the most likely failure point $\mathbf{u}^*$ with respect to θ. However, from Eq. 6 it is seen that $d\beta/d\theta$ only depends on the component of $d\mathbf{u}^*/d\theta$ in the direction of α. On the other hand, $d\alpha/d\theta$ is equal to the component of $d\mathbf{u}^*/d\theta$ orthogonal to α, scaled by $1/\beta$, Fig. 1. $d\mathbf{u}^*/d\theta$ is derived in the following section.

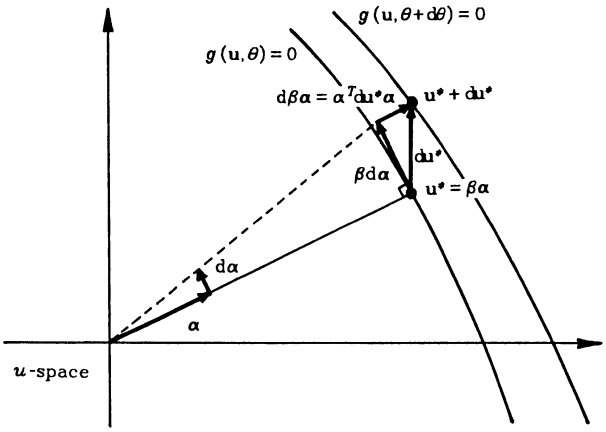

Fig. 1. Illustration of $d\mathbf{u}^*$, $d\beta$ and $d\boldsymbol{\alpha}$.

PARAMETRIC SENSITIVITY OF THE MOST LIKELY FAILURE POINT $\mathbf{u}^*$

The derivative of the most likely failure $\mathbf{u}^*$ with respect to the parameter θ is derived under the conditions that, *i)* $\mathbf{u}^*$ is a point on the failure surface, i.e. Eq. 5 is satisfied, and *ii)* $\mathbf{u}^*$ is the point closest to the origin, i.e., $\mathbf{u}^*$ is parallel to the gradient vector ∇g in the point,

$$\mathbf{u}^* = -\lambda \nabla g\,, \qquad \lambda = \frac{\beta}{|\nabla g|} \tag{8}$$

For the increment $d\theta$ in the parameter the most likely failure point is assumed to change by the amount $d\mathbf{u}^*$, Fig. 1. The new point, $\mathbf{u}^* + d\mathbf{u}^*$ must also satisfy the two conditions above. Differentiation of the first condition, Eq. 5, yields

$$\frac{dg}{d\theta} = \nabla g^T \frac{d\mathbf{u}^*}{d\theta} + \frac{\partial g}{\partial \theta} = 0 \tag{9}$$

Differentiation of the second condition, Eq. 8, gives

$$\frac{d\mathbf{u}^*}{d\theta} = -\frac{d\lambda}{d\theta}\nabla g - \lambda \frac{d\nabla g}{d\theta} \tag{10}$$

Let $\mathbf{D}$ be the matrix of second order derivatives of g in $\mathbf{u}$, i.e. $\mathbf{D} = \{\partial^2 g(\mathbf{u}^*)/\partial u_i \partial u_j\}$. Using that

$$\frac{d\nabla g}{d\theta} = \mathbf{D}\frac{d\mathbf{u}^*}{d\theta} + \frac{\partial \nabla g}{\partial \theta} \tag{11}$$

an expression for $d\mathbf{u}^*/d\theta$ is obtained from Eq. 10 and substituted into Eq. 8. From this equation, $d\lambda/d\theta$ is found and inserted into the expression for $d\mathbf{u}^*/d\theta$. After rearranging, the result for $d\mathbf{u}^*/d\theta$ can be expressed as

$$\frac{d\mathbf{u}^*}{d\theta} = \frac{1}{|\nabla g|}\frac{\partial g}{\partial \theta}\boldsymbol{\alpha} + \left[\frac{1}{|\nabla g|}\frac{\partial g}{\partial \theta}\left(\frac{\mathbf{A}\boldsymbol{\alpha}}{\boldsymbol{\alpha}^T\mathbf{A}\boldsymbol{\alpha}} - \boldsymbol{\alpha}\right) + \left(\mathbf{A}\boldsymbol{\eta} - \boldsymbol{\alpha}^T\mathbf{A}\boldsymbol{\eta}\frac{\mathbf{A}\boldsymbol{\alpha}}{\boldsymbol{\alpha}^T\mathbf{A}\boldsymbol{\alpha}}\right)\right] \tag{12}$$

where

$$\boldsymbol{\eta} = -\lambda\frac{\partial \nabla g}{\partial \theta}, \qquad \mathbf{A} = [\mathbf{I} + \lambda \mathbf{D}]^{-1} \tag{13}$$

and $\mathbf{I}$ is the identity matrix.

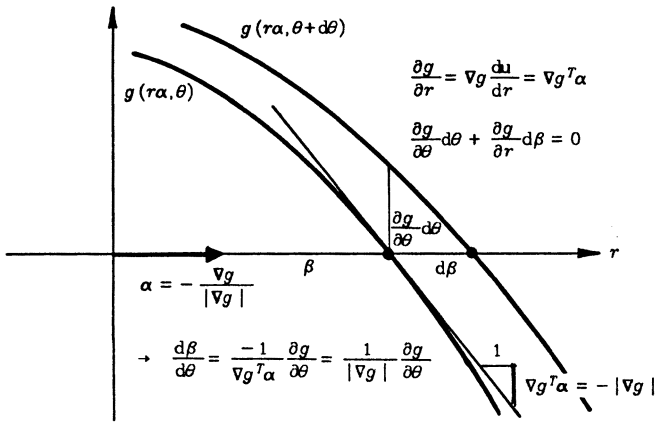

Fig. 2. Geometrical illustration of $d\beta/d\theta$. The parametric sensitivity factor for the first order reliability index can be derived by considering the change in distance from the origin in the direction of $\boldsymbol{\alpha}$. The same type of derivation is carried out in the section on directional simulation below.

The first term is a vector parallel to $\boldsymbol{\alpha}$. Furthermore, by multiplication with $\boldsymbol{\alpha}^T$ it is seen that the contribution in the bracket is orthogonal to $\boldsymbol{\alpha}$. Using Eqs. 6 and 7 together with Eq. 12 yields

$$\frac{d\beta}{d\theta} = \frac{1}{|\nabla g|}\frac{\partial g}{\partial \theta} \tag{14}$$

and

$$\frac{d\boldsymbol{\alpha}}{d\theta} = \frac{1}{\beta}\left[\frac{d\beta}{d\theta}\left(\frac{\mathbf{A}\boldsymbol{\alpha}}{\boldsymbol{\alpha}^T\mathbf{A}\boldsymbol{\alpha}} - \boldsymbol{\alpha}\right) + \left(\mathbf{A}\boldsymbol{\eta} - \boldsymbol{\alpha}^T\mathbf{A}\boldsymbol{\eta}\frac{\mathbf{A}\boldsymbol{\alpha}}{\boldsymbol{\alpha}^T\mathbf{A}\boldsymbol{\alpha}}\right)\right] \tag{15}$$

With Eqs. 14 and 15 inserted, Eq. 12 expresses the trivial result

$$\frac{d\mathbf{u}^*}{d\theta} = \frac{d\beta}{d\theta}\boldsymbol{\alpha} + \beta\frac{d\boldsymbol{\alpha}}{d\theta} \tag{16}$$

for $\mathbf{u}^* = \beta\boldsymbol{\alpha}$.

The result in Eq. 14 is the known asymptotic result from [4], see also [6]. A geometrical interpretation of the result is given in Fig. 2. The sensitivity factor for the first order reliability index is independent of $\mathbf{A}$, i.e. independent of the curvature of the failure surface in the most likely failure point.

The sensitivity factor for the unit normal vector $d\boldsymbol{\alpha}/d\theta$ depends on $\mathbf{A}$, i.e. on the curvatures in the point. If the curvatures are neglected (or the failure surface indeed is plane in the most likely failure point), that is $\mathbf{A} = \mathbf{I}$, the first parenthesis in the bracket in Eq. 12 (and Eq. 14) is equal to zero, and the expressions for $d\mathbf{u}^*/d\theta$ and $d\boldsymbol{\alpha}/d\theta$ reduces to

$$\frac{d\mathbf{u}^*}{d\theta} = \frac{d\beta}{d\theta}\boldsymbol{\alpha} + (\boldsymbol{\eta} - \boldsymbol{\alpha}^T\boldsymbol{\eta}\boldsymbol{\alpha}) \tag{17}$$

and

$$\frac{d\boldsymbol{\alpha}}{d\theta} = \frac{1}{\beta}(\boldsymbol{\eta} - \boldsymbol{\alpha}^T\boldsymbol{\eta}\boldsymbol{\alpha}) \tag{18}$$

Numerical examples indicate that the influence of the curvatures on $d\boldsymbol{\alpha}/d\theta$ may be

insignificant, and that $d\alpha/d\theta$ therefore for practical purposes can be calculated without computing the matrix of second order derivatives **D**. However, it is noted that the second order derivative in η, i.e. the derivatives of the gradient vector ∇g with respect to θ, must be calculated.

EXAMPLES

In this section two small examples illustrating the derived sensitivity factors are given. The basic variables in both examples are two normally distributed variables X_1 and X_2 of means μ_1 and μ_2, standard deviations σ_1 and σ_2 and mutually correlated with correlation coefficient ρ. The transformation to the standardized u-space is carried out by the transformation

$$x_1 = \sigma_1 u_1 + \mu_1 \tag{19a}$$

$$x_2 = \sigma_2(\rho u_1 + \sqrt{1-\rho^2}u_2) + \mu_2 \tag{19b}$$

The initial values of the distributional parameters from which the parametric sensitivity analyses are performed are

$$(\mu_1, \mu_2, \sigma_1, \sigma_2, \rho) = (2.0,\ 1.0,\ 0.3,\ 0.3,\ 0.5)$$

Example 1: Plane failure surface

For the linear safety margin

$$M = X_1 - X_2 \tag{20}$$

the failure function in the standard variables **u** is

$$g(u_1, u_2) = (\sigma_1 - \rho\sigma_2)u_1 - \sigma_2\sqrt{1-\rho^2}u_2 + \mu_1 - \mu_2 \tag{21}$$

First, the sensitivity to changes in σ_2 is studied, i.e. $\theta = \sigma_2$. From Eq. 21 it is seen that an increment in σ_2 decreases the positive coefficient to u_1 and increases numerically the negative coefficient to u_2, assuming the values for the parameters given above. It is therefore expected that changes in the value of σ_2 changes the unit normal vector α significantly. Since the limit state surface is plane, all second order derivative with respect to u_1 and u_2 are zero, and the simple formula in Eq. 18 is valid.

Approximations β_A and α_A to the exact results $\beta_E = \beta(\theta + \Delta\theta)$ and $\alpha_E = \alpha(\theta + \Delta\theta)$, respectively, are computed by

$$\beta_A = \beta_0 + \frac{d\beta}{d\theta}(\theta)\Delta\theta \tag{22}$$

and

$$\alpha_A = \frac{\alpha_0 + \frac{d\alpha}{d\theta}(\theta)\Delta\theta}{|\alpha_0 + \frac{d\alpha}{d\theta}(\theta)\Delta\theta|} \tag{23}$$

where β_0 and α_0 are the results for the initial parameter value θ.

The approximative results are compared to the exact results. In Fig. 3 results are shown for σ_2-values between 0 and 0.6, corresponding to reliability index values in the range 1.92 to 3.85 (the variation is not monotone in σ_2). The three quantities β_A/β_E, $\alpha_A{}^T\alpha_E$ and $\alpha_0{}^T\alpha_E$ are shown. The latter quantity describes how much the unit normal vector changes direction with the parameter. It is seen from the results that even for significant changes in α_E as compared to α_0, the approximation α_A is very good.

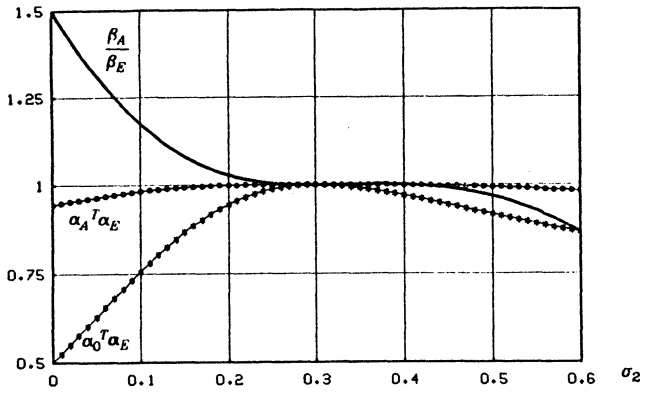

Fig. 3. Results from parametric sensitivity analysis with respect to the standard deviation σ_2. Plane failure surface.

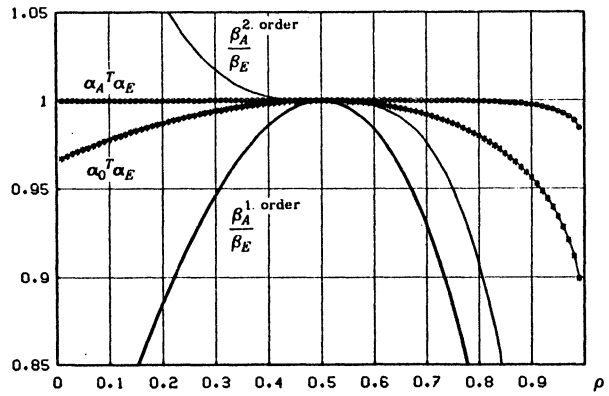

Fig. 4. Results from parametric sensitivity analysis with respect to the correlation coefficient ρ. Plane failure surface.

In Fig. 4 results for $\theta = \rho$ between 0.0 and 1.0 are shown. The corresponding range of the reliability index is 2.37 to 23.6 (monotone variation). The moderate variation in $\boldsymbol{\alpha}_0{}^T\boldsymbol{\alpha}_E$ shows that the unit normal vector in this case almost has the same direction for all considered values of ρ. Again, the approximation α_A turns out to be good in a large range.

It is seen that the approximation β_A to the (first order) reliability index β in this case is accurate only in a small range around the initial value $\rho = 0.50$. A reason for this is, of course, the very large (non-linear) changes in the value of the reliability index. A better approximation can be obtained by including the second order derivative of β with respect to θ, i.e.

$$\frac{d^2\beta}{d\theta} = \frac{d\boldsymbol{\alpha}}{d\theta}^T \frac{d\mathbf{u}^*}{d\theta} + \boldsymbol{\alpha}^T \frac{d^2\mathbf{u}^*}{d\theta^2} \tag{24}$$

and then use the second order approximation

$$\beta \approx \beta_0 + \frac{d\beta}{d\theta}(\theta)\Delta\theta + \frac{1}{2}\frac{d^2\beta}{d\theta}(\theta)(\Delta\theta)^2 \tag{25}$$

It is necessary to calculate the second order derivative of $\mathbf{u}^*$ with respect to θ. In general this is not likely to be practicable. For the simple example considered here the derivative can be found directly from a closed form expression for the reliability index. The thin solid line in Fig. 4 shows the ratio between the second order approximation in Eq. 25 and the exact result. Even though improvements are obtained as compared to the approximation in Eq. 22, a good approximation to the reliability index is still obtained only in a smaller range. This, together with the practical difficulties in obtaining the second order derivatives of $\mathbf{u}^*$ with respect to θ suggest not to follow this approximation further.

Example 2: Non-Flat Failure Surface

For the safety margin

$$M = 12 - X_1^2 - X_2^2 \tag{26}$$

the g-function in the standard variables $\mathbf{u}$ is

$$g(u_1,u_2) = 12 - (\sigma_1 u_1 + \mu_1)^2 - [\sigma_2(\rho u_1 + \sqrt{1-\rho^2}\,u_2) + \mu_2]^2 \tag{27}$$

With the initial parameter values given above the following results are obtained:

$$\mathbf{u} = \beta\boldsymbol{\alpha} = 3.4277\begin{bmatrix}0.9263\\0.3767\end{bmatrix}, \quad \nabla g = \begin{bmatrix}-2.3151\\-0.9414\end{bmatrix}, \quad \mathbf{D} = \begin{bmatrix}-0.2250 & -0.0779\\-0.0779 & -0.135\end{bmatrix}$$

For $\theta = \sigma_2$ we get

$$\boldsymbol{\eta} = \begin{bmatrix}8.9924\\15.5754\end{bmatrix}, \quad \mathbf{A} = \begin{bmatrix}1.4763 & 0.1937\\0.1937 & 1.2526\end{bmatrix}$$

and

$$\frac{d\mathbf{u}^*}{d\theta} = \begin{bmatrix}-5.4859\\3.0761\end{bmatrix}, \quad \frac{d\beta}{d\theta} = -3.9231, \quad \frac{d\boldsymbol{\alpha}}{d\theta} = \begin{bmatrix}-0.5403\\1.3286\end{bmatrix}$$

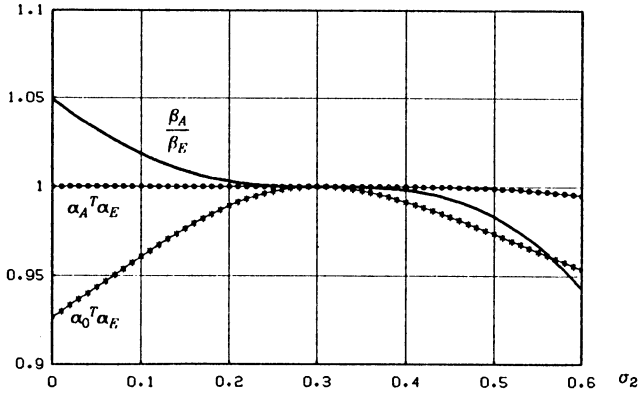

Fig. 5. Results from parametric sensitivity analysis with respect to the standard deviation σ_2. Non-flat failure surface.

Results for σ_2-values between 0.0 and 0.30 corresponding to values of the first order reliability index between 2.39 and 4.39 are shown in Fig. 5. As in Fig. 3, from the results on $\boldsymbol{\alpha}_0{}^T\boldsymbol{\alpha}_E$ a significant change in the unit normal vector is observed. The approximation to the unit normal vector based on the parametric sensitivity factor turns again out to be

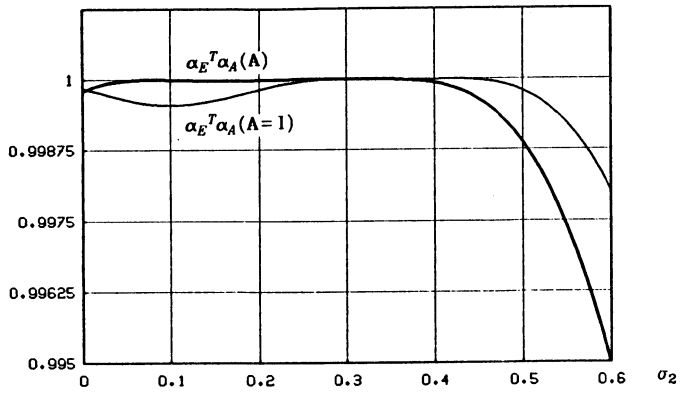

Fig. 6. Results from parametric sensitivity analysis with respect to the standard deviation σ_2. Comparison with results for the unit normal vector when the curvature of the non-flat failure surface is ignored.

very accurate in a larger range.

For comparison, results for $d\alpha/d\theta$ are calculated with $\mathbf{A}=\mathbf{I}$, i.e. the curvatures of the limit state surface are neglected. The result for $d\alpha/d\theta$ is

$$\frac{d\alpha}{d\theta}(\mathbf{A}=\mathbf{I}) = \begin{bmatrix} -0.4855 \\ 1.1939 \end{bmatrix}$$

and the results for α_A using this vector is practically the same as before. In fact, as seen in Fig. 6, in this case even (slightly) better results are observed for large σ_2-values. For practical purposes it may therefore not be worthwhile to calculate the matrix of second order derivatives $\mathbf{D}$ for the sole purpose of calculating the parametric sensitivity factor for the unit normal vector.

DIRECTIONAL SIMULATION OF PARAMETRIC SENSITIVITY FACTORS

Directional simulation is a conditional expectation Monte Carlo simulation method originally suggested for computing the multi-dimensional normal distribution function, [2]. The approach is directly applicable as a general simulation method for probability integration within structural reliability analysis, and the efficiency can be significantly improved by importance sampling based on results from FORM/SORM-analysis, [1,3]. In this section it is briefly outlined how parametric sensitivity factors $dp_F/d\theta$ for the probability of failure p_F can be estimated by directional simulation.

The basic idea in directional simulation is to express the standard normal vector $\mathbf{U}$ as $R\mathbf{C}$, where $\mathbf{C}$ is a unit vector uniformly distributed on the unit sphere Ω_n, and $R \geq 0$ is a chi-distributed variable. The probability of failure is expressed by the integral

$$p_F = \int_{\mathbf{c}\in\Omega_n} P[g(R\mathbf{C}) \leq 0 \mid \mathbf{C}=\mathbf{c}]\, f_{\mathbf{C}}(\mathbf{c})d\mathbf{c} = \int_{\mathbf{c}\in\Omega_n} p(\mathbf{c})\, f_{\mathbf{C}}(\mathbf{c})d\mathbf{c} \tag{28}$$

where $f_{\mathbf{C}}(\mathbf{c})$ is the constant density on the n-dimensional unit sphere. Provided the safe set is star-shaped with respect to the origin, the conditional probability $p(\mathbf{c})$ simply reads

$$p(\mathbf{c}) = 1 - \chi_n^2(r^2) \tag{29}$$

where $r = r(\mathbf{c})$ is the distance from the origin to the failure surface in the direction defined by $\mathbf{c}$, and χ_n^2 is the chi-square distribution function of n degrees of freedom. If the safe set in u-space is not star-shaped the probability $p(\mathbf{c})$ is equal to a sum of probabilities, each given in terms of the chi-square distribution function.

An estimate of p_F can be obtained by performing N simulations of the unit vector $\mathbf{C}$, calculate the distance r for each generated $\mathbf{c}$-vector, and then calculate the sample value $p(\mathbf{c})$ by Eq. 29. The average of the sample values is an unbiased estimator for p_F. An outcome $\mathbf{c}_i$ of $\mathbf{C}$ can be established by generating an outcome $\mathbf{u}_i$ of the standard Gaussian vector $\mathbf{U}$ and then use $\mathbf{c}_i = \mathbf{u}_i / |\mathbf{u}_i|$.

An expression for the parametric sensitivity factor $\mathrm{d}p_F/\mathrm{d}\theta$ can be obtained from Eqs. 28 and 29 as

$$\frac{\mathrm{d}p_F}{\mathrm{d}\theta} = \int_{\mathbf{c}\in\Omega_n} -2r\frac{\mathrm{d}r}{\mathrm{d}\theta} k_n(r^2) f_{\mathbf{C}}(\mathbf{c})\mathrm{d}\mathbf{c} \tag{30}$$

where k_n is the chi-square density function of n degrees of freedom. Using this expression $\mathrm{d}r/\mathrm{d}\theta$ can be estimated by directional simulation quite similarly to the simulation of p_F. In addition to determining $r = r(\mathbf{c})$ in each simulation, also the derivative $\mathrm{d}r/\mathrm{d}\theta$ must be computed.

The expression for $\mathrm{d}r/\mathrm{d}\theta$ is derived under the conditions that *i)* $\mathbf{u} = r\mathbf{c}$ is a point on the limit state surface, i.e. $g(r\mathbf{c}, \theta) = 0$, and *ii)* that $\mathrm{d}\mathbf{u} = \mathrm{d}r\mathbf{c}$ is parallel to $\mathbf{u}$, i.e. $\mathrm{d}\mathbf{u} = \mathrm{d}r\,\mathbf{u}$, Fig. 7. Substituting this expression for $\mathrm{d}\mathbf{u}$ into Eq. 9, solving for $\mathrm{d}r$, and inserting this result into $\mathrm{d}\mathbf{u} = \mathrm{d}r\,\mathbf{u}$, yields after rearranging

$$\frac{\mathrm{d}\mathbf{u}}{\mathrm{d}\theta} = -\frac{\mathbf{u}}{\nabla g^T \mathbf{u}}\frac{\partial g}{\partial \theta} \tag{31}$$

The derivative $\mathrm{d}r/\mathrm{d}\theta$ can then be expressed as

$$\frac{\mathrm{d}r}{\mathrm{d}\theta} = \mathbf{u}^T\frac{\mathrm{d}\mathbf{u}}{\mathrm{d}\theta} = -\frac{1}{\nabla g^T \mathbf{c}}\frac{\partial g}{\partial \theta} \tag{32}$$

It is seen that $\mathrm{d}r/\mathrm{d}\theta$ is equal to $\mathrm{d}\beta/\mathrm{d}\theta$ in Eq. 15 for $\mathbf{c} = -\nabla g / |\nabla g|$. Fig. 2 gives a geometrical interpretation of the result in Eq. 32.

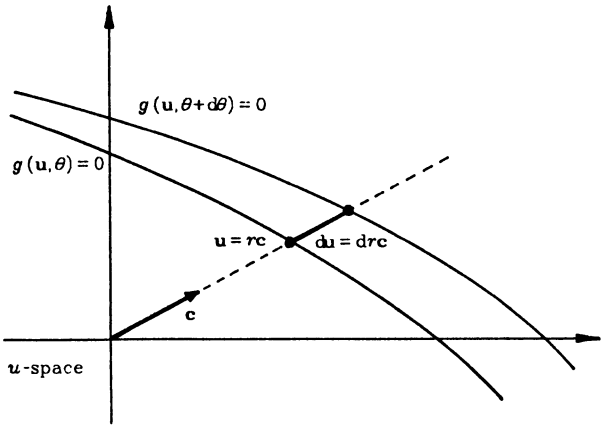

Fig. 7. Illustration of $\mathrm{d}r/\mathrm{d}\theta$ for directional simulation of parametric sensitivity factors.

A numerical example on directional simulation of parametric sensitivity factors can be found in [3], where the reliability with respect to plastic collapse of frame and truss structures is studied. The reliability is formulated on basis of the lower bound theorem of plasticity theory. The corresponding failure function is complicated in the sense that each evaluation of the function requires the solution of a linear programming problem. The same is required to determine the distance $r(\mathbf{c})$ for given direction $\mathbf{c}$, and $dr/d\theta$ must be computed by solving a set of linear equations. Since $dp_F/d\theta$ (as p_F) typically is of small order within structural reliability, large sample sizes are required to get a certain estimate on the sensitivity factor. Examples indicate that the *ratio* between different derivatives can be well estimated on basis of a smaller sample size. In many practical applications only the ratio between parametric sensitivity measures is needed.

CONCLUSION

Parametric sensitivity measures in structural reliability analysis are investigated. In particular, the derivative of the most likely failure point with respect to a deterministic parameter θ is derived. The following results and conclusions are reported:

- A parametric sensitivity factor $d\alpha/d\theta$ for the unit normal vector to the failure surface in the most likely failure point is derived. The factor has important applications in system reliability analysis and outcrossing problems.
- $d\alpha/d\theta$ is a function of the curvatures of the failure surface in the most likely failure point. However, numerical calculations indicate that this dependence may be neglected in practical applications, thereby saving the computation of the matrix of second order derivatives of the failure function. To determine $d\alpha/d\theta$ requires then only the computation of the derivatives of ∇g with respect to θ in excess of the standard output from a first order reliability analysis.
- Applications of $d\alpha/d\theta$ to estimate the change in the unit normal vector corresponding to a change $\Delta\theta$ in θ show accurate results.
- The known result for the parametric sensitivity factor $d\beta/d\theta$ for the first order reliability index is analyzed. The factor is used to estimate the change in the first order reliability index corresponding to a change $\Delta\theta$ in the parameter θ. An improved approximation can be obtained by including the second order derivative $d^2\beta/d\theta^2$ as well. Results are shown for a small example where the derivative is easily obtained. In general it seems not practicable, nor necessary for the practical applications to use this derivative.
- It is shown how parametric sensitivity factors for the probability of failure $dp_F/d\theta$ can be estimated by directional Monte Carlo simulation.

ACKNOWLEDGEMENTS

Thanks to Henrik O. Madsen for stimulating discussions.

REFERENCES

[1] Bjerager, P.: Probability Integration by Directional Simulation. Accepted for publication in *Journal of Engineering Mechanics*, ASCE, 1987.

[2] Deák, I.: Three Digit Accurate Multiple Normal Probabilities. *Numerische Mathematik*, Vol. 35, 1980, pp. 369-380.

[3] Ditlevsen, O. and Bjerager, P.: Plastic Reliability Analysis by Directional Simulation. Preprint: DCAMM Report No. 353, Technical University of Denmark, 1987. Submitted

to *Journal of Engineering Mechanics*, ASCE.

[4] Hohenbichler, M.: Mathematische Grundlagen der Zuverlässigkeitsmethode Erste Ordnung und Einige Erweiterungen. Doctoral Thesis, Technical University of Munich, Munich, West Germany, 1984.

[5] Hohenbichler, M., Gollwitzer, S., Kruse, W. and Rackwitz, R.: New Light on First- and Second-Order Reliability Methods. *Structural Safety*, Vol. 4, 1987, pp. 267-284.

[6] Madsen, H.O., Krenk, S. and Lind, N.C.: Methods of Structural Safety, Prentice Hall, Inc., Englewood Cliffs, New Jersey, 1986.

[7] Madsen, H.O.: Model Updating in Reliability Theory. In: Reliability and Risk Analysis in Civil Engineering 1, Proceedings of ICASP5 1987, ed. by N.C. Lind, Institute for Risk Research, University of Waterloo, Ontario, Canada, 1987, pp. 564-577.

[8] Madsen, H.O. and Moghtaderi-Zadeh, M.: Reliability of Plates under Combined Loading. In: Proceedings of the Marine Structural Reliability Symposium, SNAME, Arlington, Virginia, October 5-6, 1987.

INDEX OF AUTHORS

SUBJECT INDEX